UNIVERSITY OF
LINCOLN

SYNTHESIS OF TEIXOBACTIN ANALOGUES AND THEIR BIOLOGICAL EVALUATION

Anish Parmar

A thesis submitted in partial fulfilment of the requirements of the University of Lincoln for the degree of Doctor of Philosophy

September 2019

STATEMENT OF ORIGINALITY

"I, Anish Parmar, hereby declare that this submission is my own work and to the best of my knowledge it contains no materials previously published or written by another person, or substantial proportions of material which have been published or accepted for the award of any other degree or diploma at University of Lincoln or any other educational institution, except where references have been made in the thesis. Any contribution made to the research by others, with whom I have worked at the University of Lincoln or elsewhere, is explicitly acknowledged in the thesis. I also declare that the intellectual content of this thesis is the product of my own work, except to the extent that assistance from others in the project's design and conception or in style, presentation and linguistic expression is acknowledged."

All the work from Chapter 2 to 6 has been published (5 publications). In general, the work includes a highly efficient synthetic route to provide potent analogues and its SAR studies. My overall contributions to the publications have been provided below, however detailed contributions by all other authors will also be provided at the beginning of each chapter.

1. ***Parmar, A.*** *et al.* Efficient total syntheses and biological activities of two teixobactin analogues. *Chem. Commun.* **52**, 6060–6063 (2016).

2. ***Parmar, A.*** *et al.* Defining the molecular structure of teixobactin analogues and understanding their role in antibacterial activities. *Chemical communications* **53**, 2016–2019 (2017)

3. ***Parmar, A.*** *et al.* Syntheses of potent teixobactin analogues against methicillin-resistant Staphylococcus aureus (MRSA) through the replacement of L-allo-enduracididine with its isosteres. *Chemical Communications* **53**, 7788–7791 (2017)

4. ***Parmar, A.*** *et al.* Teixobactin analogues reveal enduracididine to be non-essential for highly potent antibacterial activity and lipid II binding. *Chemical Science* **8**, 8183–8192 (2017)

5. ***Parmar, A.*** *et al.* Design and Syntheses of Highly Potent Teixobactin Analogues against *Staphylococcus aureus*, Methicillin-Resistant *Staphylococcus aureus* (MRSA), and Vancomycin-Resistant Enterococci (VRE) *in Vitro* and *in Vivo*. *Journal of Medicinal Chemistry* **61**, 2009–2017 (2018).

All the building block synthesis, peptide synthesis for the analogues, optimisations, purifications and sample preparation for either mass analysis/NMR has been done by me. The initial drafting of the manuscript has been done by me with inputs from all authors.

For work in Chapter 6: All the animals used in this study were treated in accordance to the tenets of the Association for Research in Vision and Ophthalmology (ARVO) statement, and the protocol was approved by SingHealth Institutional Animal Care and Use Committee (IACUC) (AALACaccredited; protocol number 2012/SHS/775 for wound healing).

Signed ……  ……

Date …… 13/09/2019 …….

APPRECIATION AND ACKNOWLEDGEMENTS

It would be extremely selfish to believe that my entire PhD was solely earned by my effort and diligence. It will be nearly impossible to mention every single person here, but I would like to acknowledge those who have significantly supported me throughout my PhD, not only in terms of my scientific research, but morally and emotionally as well.

Firstly, I would like to thank my supervisor, Dr. Ishwar Singh, for his overwhelming support, motivation, tremendous patience and immense knowledge throughout my entire program. You granted the opportunity with your door always open for any questions and discussions. Because of that, you ensured that I was without any doubts during my research. I cannot thank you enough for believing in me even when I may have not shown the confidence in myself. The knowledge I have gained from you is invaluable and will be treasured forever.

I would like to now thank my immediate family. Pa, you left us early in life and, at times, I look up to the sky and say to myself, "I know you did that". Thank you for looking out for me and showering your blessings over me. This one is for you and I really miss you! Mum, you have been my pillar of strength and tenacity throughout this journey. You have sacrificed your life and dreams just to witness me achieve everything I set out to pursue. There are no words to describe how much I thank you for all the love, care and courage you have provided me. I owe you a lifetime! Reema, even though you are in Kenya, you have always been there and boosted my morale when I needed it the most. I am truly blessed to have you as my sister. Thank you for making Raunaav (my nephew) become certain that I am some sort of "super uncle" and trusting that I can be a good role model for him. This always makes me strive to be a better human being as I am aware that he is learning from my actions. I show high gratitude towards Hemil, who has always been my well wisher over the years and lifted my spirit when I was down.

Among my colleagues and friends in Lincoln, I show extreme appreciation to my friend Dr. Abhishek Iyer. Abhishek, I have always said "If you were not around I would really struggle with my PhD." Thank you for all the support you have given me. You've played a vital role in educating me with the relevant knowledge to kickstart my journey in the life of a PhD student. I am walking away with great memories like our late-night hours, jokes and adventures on campus. I would like to thank Aqssa and Ruba for always being compassionate, being by my side when I was down and sharing crazy little inside jokes over the years. I wish you both all the success in your respective PhD's. I would like to thank Maria, Keverne, Alex and Laura for the "heart to heart" discussions and our time spent in the labs. Paolo, Odera, Ranga and Ahmed, I thank you for creating the amazing atmosphere at Lincoln University and the sports we have played throughout our time together. I would like to thank Shreesha, Christian, Luke, Vincent and Louis for all the organic chemistry discussions we have had. I would like to express my special thanks for the whimsical NMR work of Dr. Stephen Prior and the excellent broad sample testing for biological activity of Prof. Rajamani Lakshminarayanan

at Singapore. I also thank Charlie, Dan and Edward for the initial biological tests carried out here at Lincoln. Without everyone's contributions, this PhD would be incomplete. A sincere thanks to all those whose names I may have missed herein and have played a significant part in my research.

There are notable people who played a significant part in educating me with the vital knowledge prior to starting my PhD. I would like to thank Kamal & Pinky Badiani for giving me beneficial advice and the opportunity to work at their company. I thank Hemal, Pawel, Rob and Andrew for their amazing support and always encouraging me that I could make it for a PhD position.

All work and no play can make a PhD life very dull. Throughout this journey, I was surrounded by those who stood by me through the wins and woes of my research. I thank all my cousins and friends outside university: Meenaben, Jayuben, Balraj, Peri, Jilan, Alpa, Kalpu, Deep, Rajin, Jasni, Nikita Supriya, Prayna, Sunny, Shyam, Brijesh, Nikky, Anika, Jheel, Tirth and Mica. You all know which category you belong to, but whether it was for late movie nights, advice, FIFA, music, singing or our quirky experiences, you all have happily given me the company to get through this program with the positive of attitudes. Thank you for always being by my side and supportive towards almost anything challenging I have attempted over the years. Please know that your positive vibes have played a significant role in any success I attain.

I would like to thank the members of the jury, Dr. Steven Cobb and Dr. Louis Adriaenssens, for taking out their valuable time to read, correct and be a part of my jury.

My PhD journey has been very enjoyable, and I've learned beyond my expectations. Most importantly, I have grown as a person. This process has broadened my perspective of life and has given me a terrific platform to contribute to science and help others less fortunate than myself. Not only will I cherish this opportunity, but I will always remain cognisant of this obligation.

Anish Parmar

Lincoln, 13th September 2019

LIST OF ABBREVIATIONS

^{13}C NMR	Carbon NMR
^{1}H NMR	Proton NMR
2-CTC	2-Chlorotrityl
Ac_2O	Acetic acid
Alloc	Allyloxycarbonyl (protecting group)
AMP	Antimicrobial peptide
B. subtilis	*Bacillus subtilis*
B.cereus	*Bacillus Cereus*
Boc	*tert*-Butyloxycarbonyl
C_{55}-P	Undecaprenyl phosphate
Cbz	Carboxylbenzyl
CDI	1,1'-Carbonyldiimidazole
CFU	Colony-forming unit
DCC	*N*, *N*'-Dicyclohexylcarbodiimide
DCM	Dichloromethane
DIC	N, N′-Diisopropylcarbodiimide
DIPEA	*N,N'*-diisopropylethyl amine
DMAP	4-Dimethylaminopyridine
DMF	N,N-Dimethylformamide
DMSO	Dimethyl sulfoxide
DNA	Deoxyribonucleic acid
E.coli	*Escherichia coli*
EDC	1-Ethyl-3-(3-dimethylaminopropyl)carbodiimide
End	Enduracididine
ESI	Electrospray Ionisation
Et_2O	Diethyl ether
Fmoc	9-fluorenylmethyloxycarbonyl
GlcNAc	*N*-acetyl glucosamine
HATU	N-[(dimethylamino-1H-1,2,3-triazolo[4,5-b]pyridin-1-ylmethylene]-N-methylmethanaminium hexafluorophosphate N-oxide
HCl	Hydrochloric Acid
hDFs	Human primary dermal fibroblasts

HGT	Horizontal gene transfer
HMBC	Heteronuclear Multiple Bond Correlation
HPLC	High-Performance Liquid Chromatography
HRMS	High resolution mass spectrometry
HSQC	Heteronuclear single quantum correlation
HTS	High-throughput screening
Ichip	Isolation chip
K_d	Dissociation constant
LCMS	Liquid Chromatography-Mass Spectrometry
$_L$-FDLA	1-fluoro-2,4-dinitrophenol-5-$_L$-Leucinamide
MBC	Minimum bactericidal concentration
MD	Molecular dynamics
MDR	Multi-drug-resistant
MeCN	Acetonitrile
MeOH	Methanol
MIC	Minimum Inhibitory Concentration
MNBA	2-Methyl-6-nitrobenzoic anhydride
MoeA	Moenomycin A
Mpp	PLP-Dependent enzyme
mRNA	Messenger ribonucleic acid
MRSA	Meticillin-resistant *Staphylococcus aureus*
MS	Mass spectrometry
MSSA	Methicillin-susceptible Staphylococcus aureus
Na_2SO_4	Sodium Sulphate
NAG	*N*-Acetylglucosamine
$NaHCO_3$	Sodium bicarbonate
NAM	*N*-Acetylmuramic acid
NMR	Nuclear Magnetic Resonance
NOESY	Nuclear Overhauser Effect Spectroscopy
Oxyma	Ethyl (hydroxyimino)cyanoacetate
P. aeruginosa	*Pseudomonas aeruginosa*
Pbf	2,2,4,6,7-Pentamethyldihydrobenzofuran-5-sulfonyl

PBPs	Penicillin-binding proteins
PBS	Phosphate-buffered saline
Pd(PPh3)	Tetrakis(triphenylphosphine)palladium(0)
PG	Peptidoglycan
$PhSiH_3$	Phenylsilane
PLP	Pyridoxal Phosphate
ppm	Parts per million
r.t	Retention Time
RMSD	Root-Mean-Square Deviation
RNA	Ribonucleic acid
RP-HPLC	Reverse-phase high performance liquid chromatography
rt	Room Temperature
S.Aureus	*Staphylococcus aureus*
S.epidermidis	*Staphylococcus epidermidis*
SAR	Structure-activity relationship
TB	Tuberculosis
*t*Bu	*Tert*-butyl
TES	Triethylsilyl ether
Tf_2O	Trifluoromethanesulfonic anhydride
TFA	Trifluoroacetic acid
THF	Tetrahydrofuran
TIS	Triisopropylsilane
TLC	Thin Layer Chromatography
TOCSY	Total Correlation Spectroscopy
Trt	Trityl
UDP	Uridine 5'-(trihydrogen diphosphate)
UTP	Uridine-5’-triphosphate
VRE	Vancomycin-resistant *enterococci*
WHO	World Health Organization
WTA	Wall teichoic acid

MESSAGE TO THE READER

The work herein is part of my PhD for four years (April 2015- October 2018) at Lincoln University, UK. I have had the opportunity to travel to Temple University, Philadelphia, the USA, to advance my techniques and work on other collaborated projects. Other projects have not been included in this thesis due to the relevancy of work and I had gained enough data on teixobactin to cover this entire thesis.

For convenience, I have split the descriptive and experimental sections and numbered tables, figures and references chapter-wise. Since all the work herein has been published by our group, me being the first author/co-joint first author, relevant texts have been directly taken from the articles and permissions have been granted from co-authors for the use of data.

The first chapter of the thesis covers - the introduction of bacteria, antibiotics, antimicrobial resistance and teixobactin. The later chapters focus on the efficient synthesis of the teixobactin analogue and the invention of more potent analogues, followed by the final overview of work from myself and others on teixobactin.

Please bear in mind, this thesis is a pinnacle of hard work, dedication and support not just by me and my supervisor but a range of collaborators from different research groups who have significantly contributed to the publications received. Happy reading!

ANISH PARMAR

TABLE OF CONTENTS

II CHAPTER-WISE EXPERIMENAL SECTIONS

PART I:
DESCRIPTIVE SECTION

CHAPTER 1

1 AN INTRODUCTION TO ANTIBIOTICS, ANTIBIOTIC RESISTANCE AND TEIXOBACTIN

1.1 Antibiotic discovery – a brief history

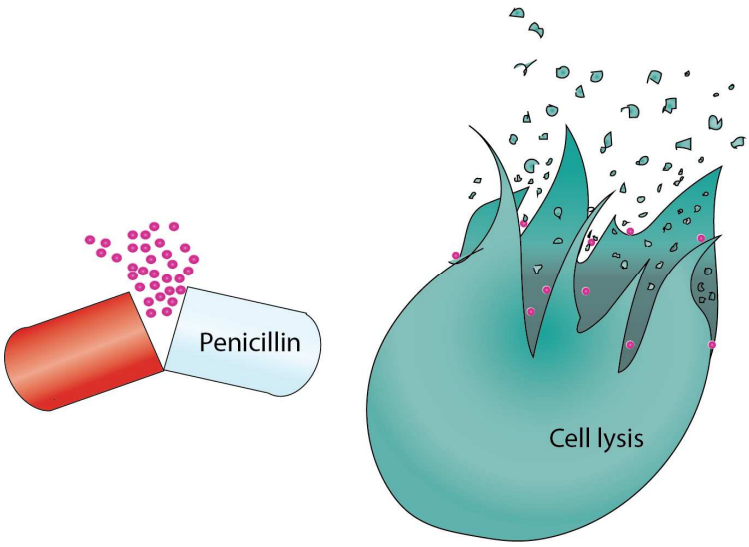

Paul Ehrlich in 1909 discovered Salvarsan[1], an antimicrobial to treat syphilis on his quest to find the 'magic bullet'. However, it was strictly not regarded as an antibiotic. The first true antibiotic to have come to light was penicillin in 1928, discovered by Sir Alexander Fleming for which he was awarded the Nobel prize in 1945[2]. Whilst examining Staphylococcus aureus, he noticed contaminations of mould (Penicillium notatum) on his petri dishes. His findings were phenomenal. He found that the mould was inhibiting the growth of a wide range of bacteria. Fleming struggled to isolate pure penicillin from the mould due to limited knowledge and resources at the time. However, other researchers such as Howard Florey and Ernst Chain from Oxford University with their ground-breaking research, turned several penicillins (Figure 1.1) into lifesaving drugs which cured previous untreatable infections[3].

Penicillin is within the sub-class of β-lactams, which also includes cephalosporins, monobactams and carbapenems. They all contain a β-lactam ring (a four membered ring with an amide bond, Figure 1.1) as part of their active core structure. B-lactams ability to bind to penicillin binding proteins (PBPs) results in bacterial cell lysis, due to the inhibition of the peptidoglycan synthesis[4]. Synthetic modifications (bulky side chains) of the 'R' group on the penicillins' provided higher stability against β-lactamase degradation and broadened the spectrum of activity, especially in gram-negative bacteria (Figure 1.1, compounds **1.5-1.9**) [5, 6].

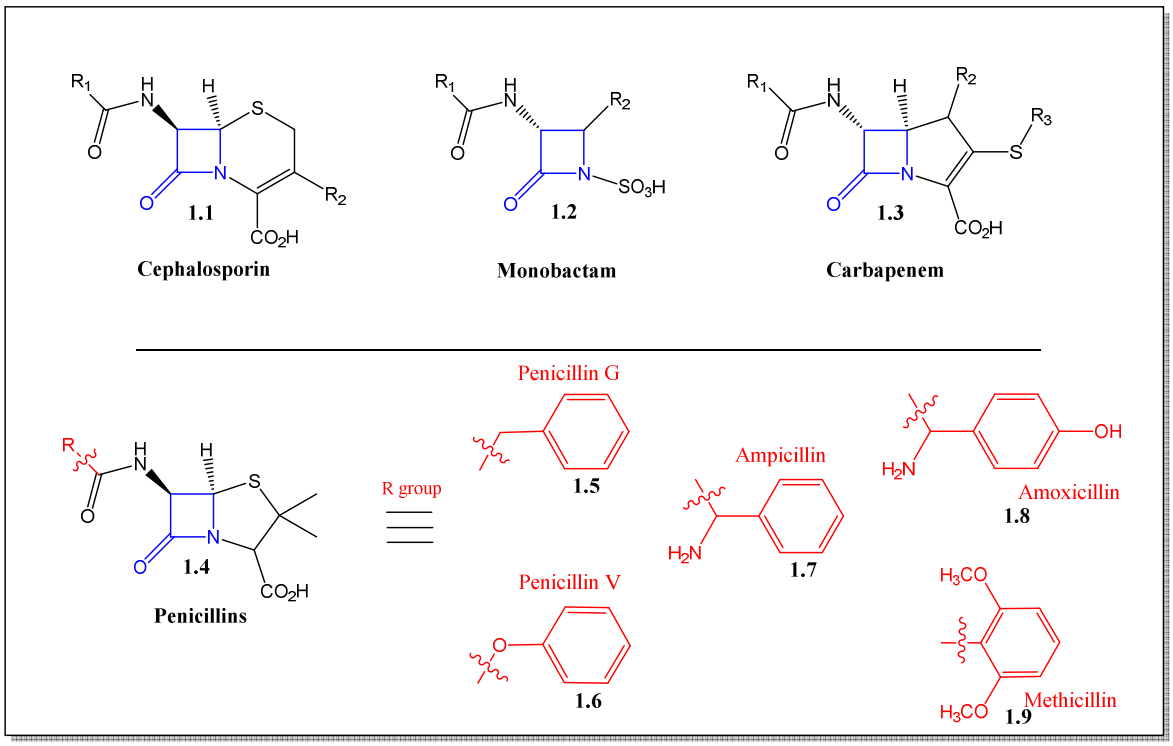

Figure 1.1: Class of antibiotics β-lactams (top) and variants of Penicillin (bottom).

Flemings work inspired many more scientists such as Selman Waksman and Albert Schatz to further explore new antibiotics. This led to the origin of Streptomycin: the first drug that was active in animal models against the pathogen *Mycobacterium tuberculosis* which caused tuberculosis (TB)[7]. Although the claim for the work was ambiguous[8], Waksman, in the end, was known to pioneer Actinomycetes to produce antibiotics and was awarded the name "Father of antibiotics". Streptomycin later faded the scene due to severe side effects, which led to patients becoming deaf during the treatment of tuberculosis[9].

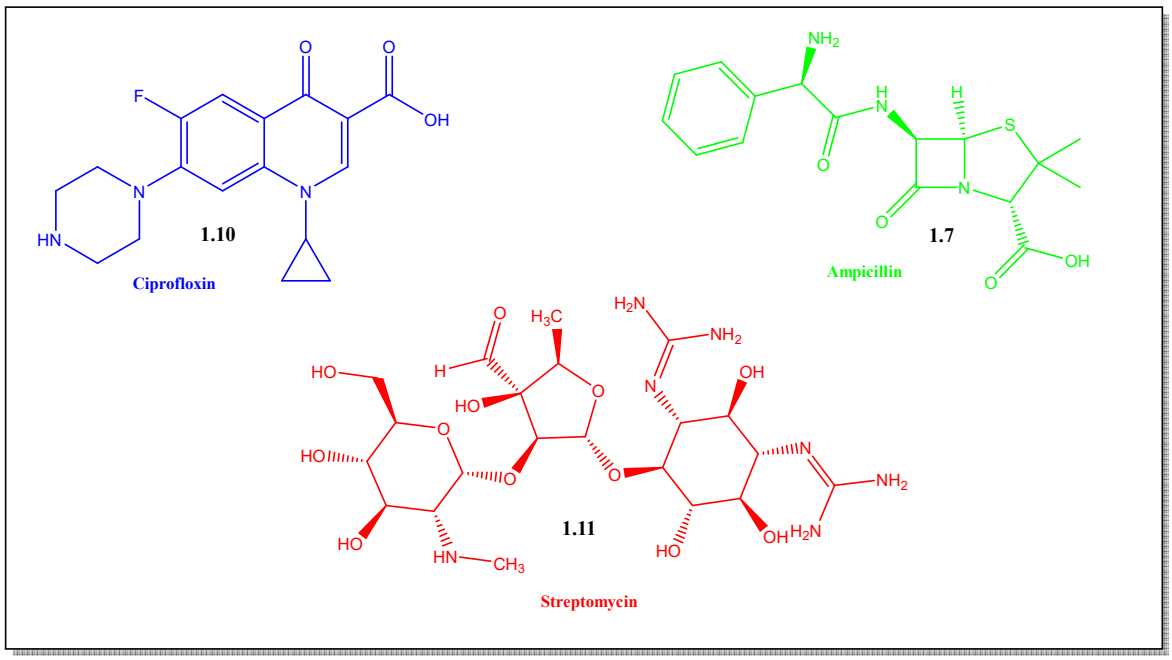

Figure 1.2: Structures of some of the most successful antibiotics the B-lactams (ampicillin **1.7**), fluoroquinolones (ciprofloxacin **1.10**) and aminoglycosides (streptomycin **1.11**).

Most of the commonly used antibiotics were discovered between 1950 through 1960 which became known as the 'golden age of antibiotics. The most successful classes were the β-lactams (**1.7**), aminoglycosides (**1.11**) and fluoroquinolones (**1.10**) (Figure 1.2). However, apart from the latest classes fluoroquinolones and the oxazolidinones, there has been a huge 'discovery void' in finding new classes for over 50 years (Figure 1.3)[10].

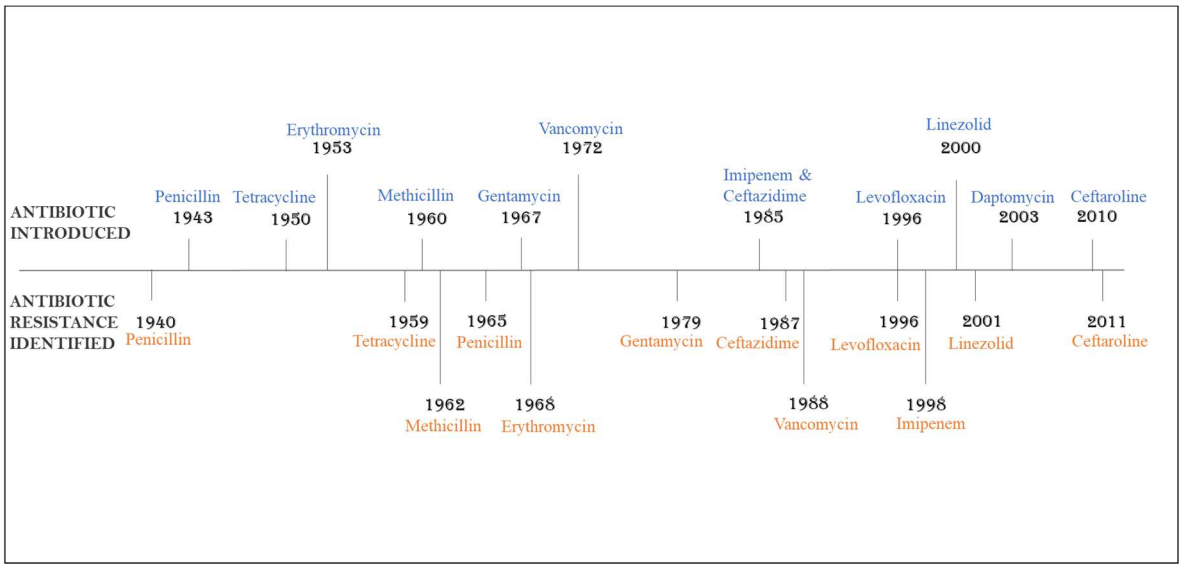

***Figure 1.3:** Timeline of most successful antibiotic discovery and evolution of antibiotic resistance[11].

* Image is original, concept derived from: Antibiotic Resistance Threats in the US. Centres for Disease Control and Prevention (CDC), 2013.

Even in the early days, resistance was observed after a few years for all new antibiotics discovered. Some of the drugs being discovered had resistance appearing simultaneously[10]. To understand how bacteria evolve to form resistance, we need to understand the modes of action antibiotics in the first place.

1.2 Antibiotics modes of action

The potency of antibiotics pinpoints certain features of the bacteria or their metabolic processes. The successful antibiotics only target just a few pathways out of approximately 200 conserved proteins[10]. There are important functions that are necessary for bacterial growth (Figure 1.4) and inhibition of these make good targets for antibiotics[12–14]. The most successful antibiotics are listed in (Figure 1.3).

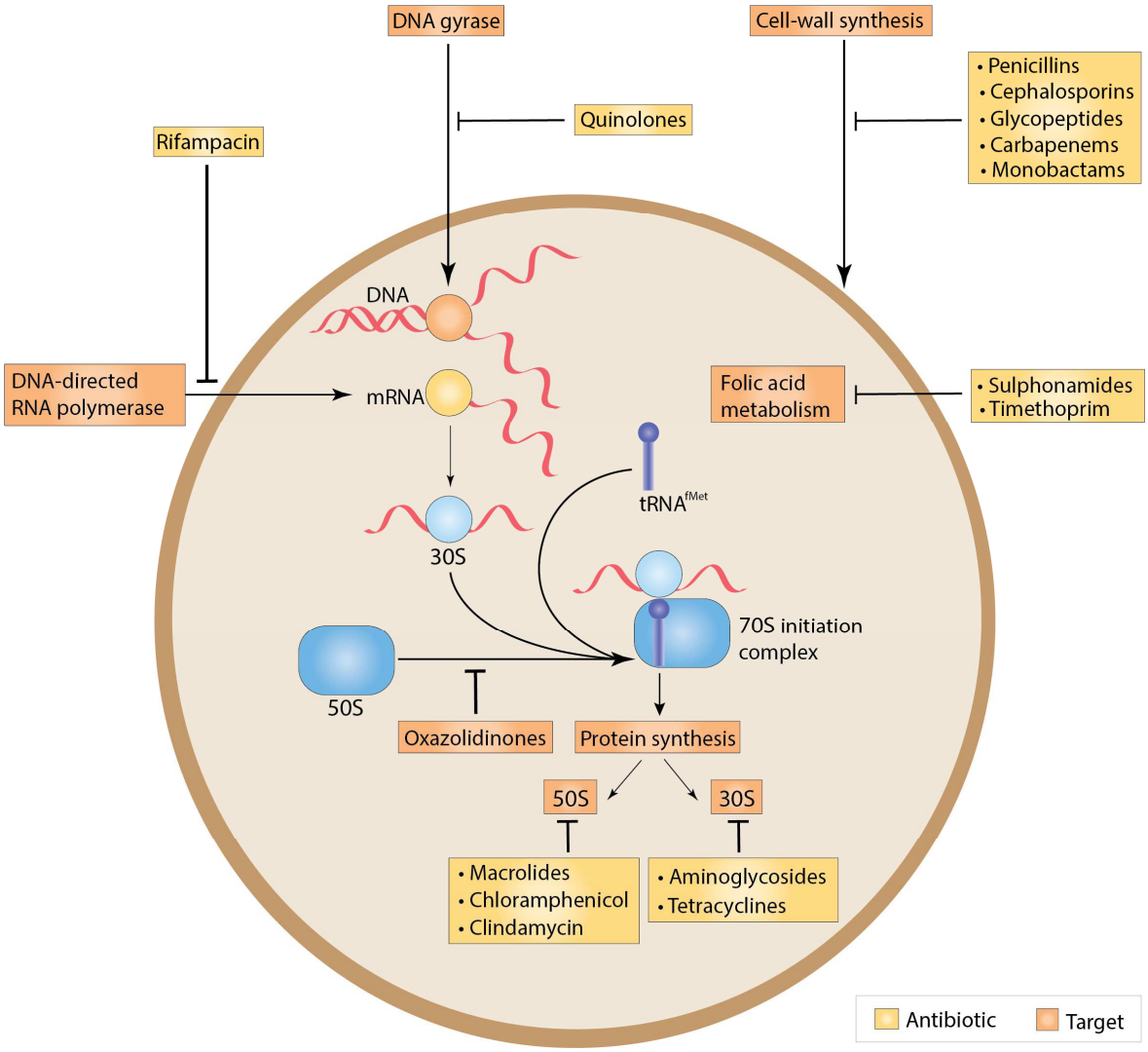

†‡**Figure 1.4:** Functions of bacterial growth and targets for its inhibition.

† Image is original, concept derived from: Lewis, K. Platforms for antibiotic discovery. *Nat. Rev. Drug Discov.* **12,** 371–87 (2013)

‡ Original article: Coates, A., Hu, Y., Bax, R. & Page, C. The future challenges facing the development of new antimicrobial drugs. *Nat. Rev. Drug Discov.* **1,** 895-910 (2002).

1.2.1 Inhibition of cell wall synthesis

Bacteria have a peptidoglycan (PG) layer which protects and supports the bacterial cell in harsh conditions in case of osmotic pressure. For bacteria to thrive, the clockwork must be very efficient to produce these penicillin binding proteins (PBPs)[15]. PBPs belong to the enzyme family of transpeptidases which are essential for incorporating disaccharide pentapeptides to elongate the already formed PG layer. The β-lactams (Penicillins **1.4**) work by inhibiting the peptide bond formation while glycopeptides (vancomycin **1.12**, Figure 1.5) bind directly to the pentapeptide part of the lipid II (D-Ala-D-Ala terminus) which in turn produces a damaged cell wall and leads to cell lysis[16].

1.2.2 Breakdown of cytoplasmic membrane

There are different specific classes of antibiotics that will cause damage to the cell membranes of the bacteria, which also depends on the specific type of lipids in their membranes. One such example is daptomycin **1.13**. Daptomycin **1.13** aggregates to the cell membrane which creates a distorted shape causing ions to leak through. The rapid depolarisation leads to the inhibition of cellular functions of the bacteria (Figure 1.5)[17].

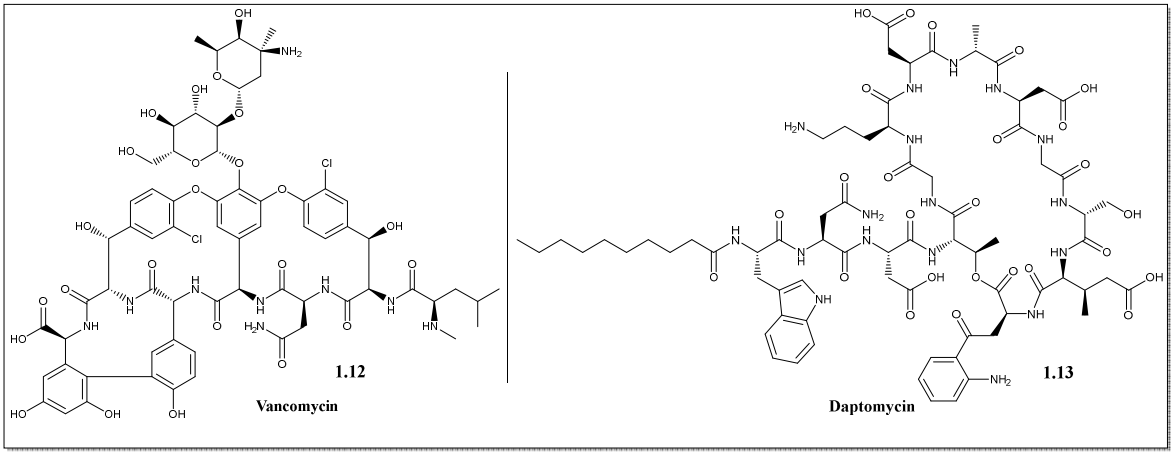

Figure 1.5: Structures of vancomycin **1.12** and daptomycin **1.13** that work well against Gram-positive pathogens.

1.2.3 Inhibition of nucleic acid structure and function

Nucleic acid synthesis is extremely essential for the survival of bacterial cells. Inhibition of the DNA synthesis comes conjointly with the inhibition of topoisomerase II and IV[18]. Quinolines inhibit the function of the helicase enzyme known for unwinding the DNA, thereby stopping replication. This also impacts the RNA synthesis of the bacteria[19].

1.2.4 Inhibition of protein synthesis

Ribosomes translate the mRNA into proteins. There is no doubt that protein is essential for the survival of bacteria, this makes it a great target for antibiotics. 30S or 50S subunit of the ribosome can be targeted, disrupting the mechanism to produce proteins[19].

1.2.5 Inhibition of metabolic pathways

For bacteria, tetrahydrofolic acid (derivative of folate/folic acid) is essential in the synthesis of nucleic acids. Bacteria metabolise *para*-amino benzoic acid (PABA) to folate. Sulphonamides are structurally very similar to folate and compete with the PABA precursor. This makes sulphonamides very selective to bacteria as humans do not produce folate[12].

1.3 Antibiotic resistance

Within the last few decades, antibiotic resistance has steadily risen and now become a critical issue in medical research, healthcare and society. A report from the World Health Organisation (WHO) has revealed that by 2050, antimicrobial resistance will cause more deaths per year than cancer. Inaction on the current issue fears a massive economic loss estimated at costing $100 trillion, globally[20].

Other treatments such as chemotherapy, surgery and transplants will be threatened and hampered due to the risk of patients being infected with serious resistant infections[21]. Most of the antibiotics prescribed today are either not needed or not as effective. Overuse of antibiotics in healthcare and agriculture has been the main source of bacteria developing resistance to some of the previous antibiotics. The alarming rate at which these resistance bacteria are appearing compared to the production of drugs, it is evident that there is still a significant amount of research to be pursued in antibacterial drug development[10].

Even with High-throughput Screening (HTS), there has been a decline in finding new reasonable, broad spectrum antibiotics in the clinic. The major issues for this being; penetration of antibiotics through the bacterial membranes and production being hampered by Lipinski's 'rule of five' guidelines[22, 23]. On the other hand, increasing the dosage for less potent drugs to give maximum efficacy compromises on the risk of toxicity. Antibiotics are short term treatments that hold the possibility of resistance occurring in the future, thus investment in chronic disease medications over antibiotics appeals more to pharmaceutical companies due to the longer shelf-life of the drugs[10].

Currently, the most serious multidrug resistant pathogens have been abbreviated 'ESKAPE,' globally. ESKAPE stands for *Enterococcus* spp., *Staphylococcus aureus*, *Klebsiella* spp., *Acinetobacter baumannii*, *Pseudomonas aeruginosa* and *Enterobacter* spp[24]. In some cases for example, A.*baumanni,* there are specific strains that are resistant to all available antibiotics[25]. WHO

released a priority list for the bacteria that we urgently need antibiotics, all ESKAPE pathogens are in a "critical" or "high" list of urgently required antibiotics.

Bacteria will inevitably acquire resistance to the antibiotics we discover; there is urgent action that is obligatory to avoid this scenario. Prevention of diseases and tracking of resistant bacteria should be high on the list. Development and improvement of antibiotics is a necessity, and to allow us to do that, we must first gain an understanding of the structure and the response of bacteria upon antibiotics.

Structurally, there are two main types of bacteria; the Gram-positive (G+) and the Gram-negative (G-) bacteria (Figure 1.6). A Danish microbiologist Hans Christian Gram in 1884 developed the Gram stain which consists of crystal violet and safranin[26]. Based on the thickness of the peptidoglycan layer, bacteria would stain differently allowing for rapid differentiation between G+ and G- bacteria. G+ bacteria with thick PG layer retained crystal violet dye and stained dark purple whereas G- bacteria with thin PG layer retained Safranin and stained red or pink[27].

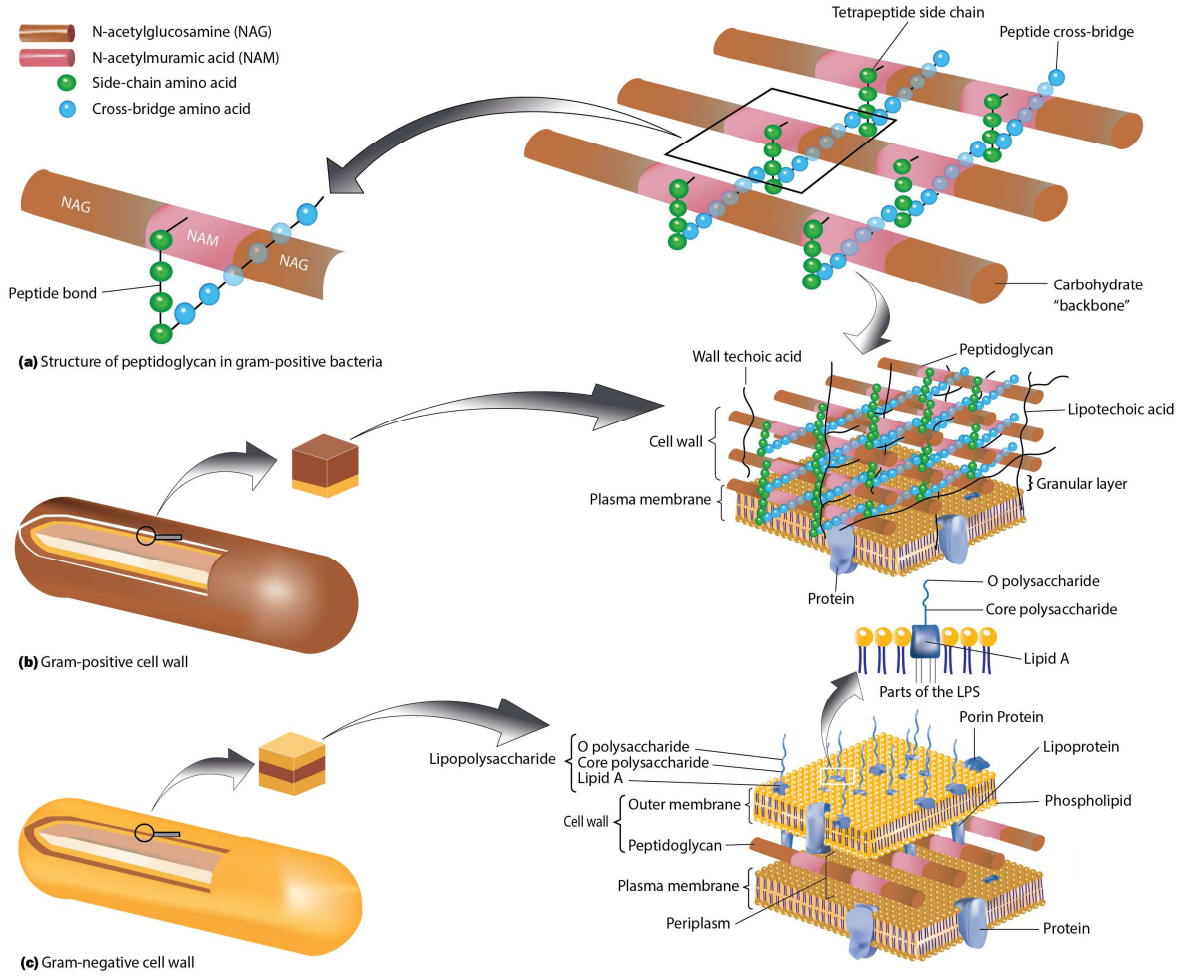

§**Figure 1.6***:* Structure of PG layer in Gram-positive (**a**) and comparison of the cell wall structures in Gram-positive (**b**) and Gram-negative (**c**) showing significant difference in the thickness of peptidoglycan layer and the presence of outer membrane in Gram-negative bacteria.

§ Image is original, concept derived from: Microbiology- an introduction Tortora et al. - Pearson – 2019, Figure 4.13

1.4 Mechanisms of antibiotic resistance

An antibiotic's main function is to neutralise or kill the bacteria by attacking its basic cellular functions. Bacteria use numerous mechanisms to counteract the function of antibiotics such as, decreased drug permeability, biofilm formation and active efflux pumps. Figure 1.7 shows some of the common ways that bacteria develop resistance and will be discussed further.

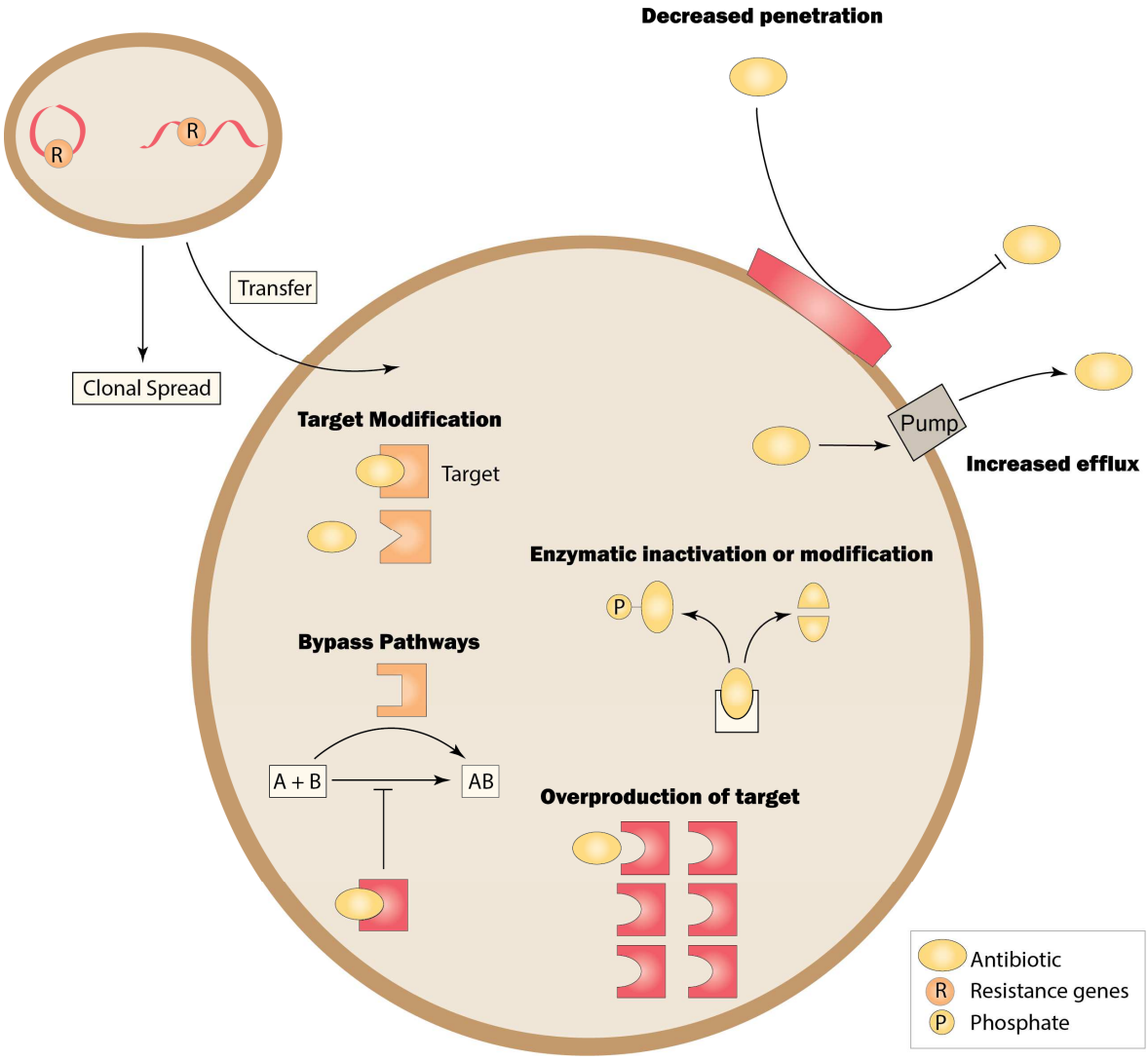

††Figure 1.7:** Some of the common ways by which bacteria overcome the antibiotic effect.

1.4.1 Intrinsic Resistance

It is known that bacteria adapt to many environmental changes[28, 29]. However, they also naturally inherit internal intrinsic resistance through which enzymes can detect and degrade the antibiotic preventing the drug binding to its target. Conserved proteins such as lipocalins are found in bacteria and are known to bind to hydrophobic compounds, causing claims of a role in resistance, although

** Image is original, concept derived from: Lewis, K. Platforms for antibiotic discovery. *Nat. Rev. Drug Discov.* **12,** 371-87 (2013)

†† Original article: Coates, A., Hu, Y., Bax, R. & Page, C. The future challenges facing the development of new antimicrobial drugs. *Nat. Rev. Drug Discov.* **1,** 895-910 (2002).

certain mechanisms of resistance are unclear. Recently, a study found *Pseudomonas aeruginosa* secreted a lipocalin (BCN) when exposed to antibiotic stress, provoking the naturally protective bacterial stress responses[30].

1.4.2 Mutation

Bacteria multiply rapidly and random point mutations are obvious to occur. Wild-type bacteria can mutate and alter the shape of its binding site, where the antibiotic targets. The antibiotic is unable to destroy the bacteria and proliferation causes new resistant strains to form. An example is the cell wall modification of vancomycin-resistant bacteria, which causes a decreased binding affinity of Vancomycin[31].

1.4.3 Inactivation of antibiotics

Bacteria possess enzymes that could basically modify or inactivate the antibiotic entirely. Structural properties within the antibiotics such as hydroxyl and amides are quite prone to hydrolysis and the addition of nucleotide, acetyl and phosphate groups[32]. The enzyme β-lactamases destroys a broad spectrum of β-lactam rings through hydrolysis of most β-lactam containing antibiotics, making it unusable[33].

1.4.4 Horizontal gene transfer

Bacteria not only transfer genes to their offspring but have the ability to also transfer genes between different species. This is known as horizontal gene transfer (HGT) (Figure 1.8). Resistant genes can be transferred by three main processes: I) Conjugation is the transfer of genetic material via a direct interaction between two bacterial species, II) Transformation is the uptake of floating genetic material from another deceased bacterium, and III) Transduction is the transfer of genes by a virus which previously infected another bacterium and hosted it's DNA[34].

It should be noted that there are several factors that contribute to the different mechanisms of HGT. Some of the common factors are competence levels of the recipient bacteria, environmental factors, and/or stabilised extracellular DNA. Out of the three mechanisms described above, conjugation is the most expected and frequently studied. Conjugation certainly provides a sufficient protective barrier, higher choice of species and an efficient route to transport genetic material, in comparison to utilising another medium to transport or capture genes[34].

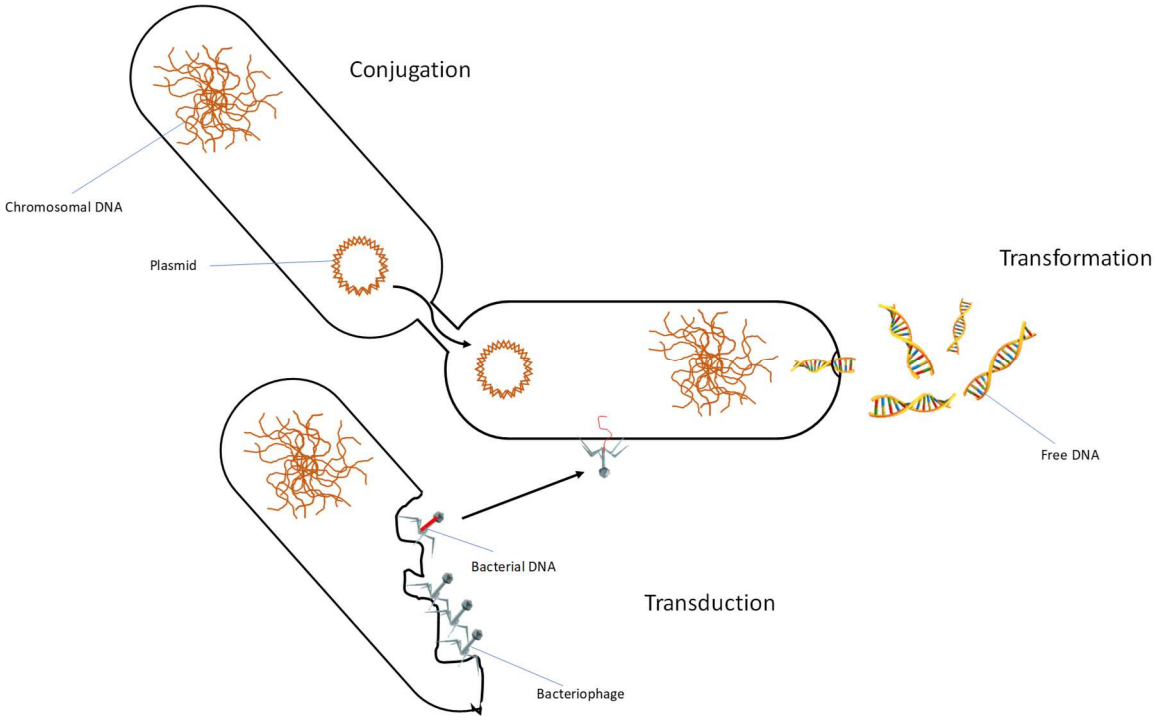

[‡‡]**Figure 1.8:** Diagram showing different mechanisms of horizontal gene transfer: - Conjugation, transformation and transduction.

1.4.5 Efflux pumps, Biofilm formation and quorum sensing

Quorum sensing is the ability of bacteria to communicate with each other through autoinducers releasing information of cell population (cell density), which enables bacteria to respond to expression of genes for survival. Biofilm formations are interconnected with quorum sensing considering the higher the cell density of bacteria, the easier for them to resist antibiotics. Bacteria require pumps to transport nutrients in and out of the cell. Bacteria can mutate and produce more of the specific pumps that flush the antibiotic out of the cell, lowering its concertation and increases its resistance. How efflux pumps promote biofilm formations is still insufficiently researched, however studies have shown that inhibiting the efflux pumps decreased biofilm production[35, 36].

1.5 Applications and solutions against AMR

It is obvious from the information gathered about AMR, optimum platforms and applications to tackle AMR are required. Investigating previous libraries may not be an adequate way in finding broad spectrum antibiotics. The main problem with most of the focused projects, is the Multi-drug resistant (MDR) pumps in the bacteria (especially Gram-negative), that limits the ligand-target binding. Therefore, drugs that focus on single targets may not be viable in the long run. Combination

[‡‡] Image is original, concept derived from: von Wintersdorff, C. J. H. *et al.* Dissemination of Antimicrobial Resistance in Microbial Ecosystems through Horizontal Gene Transfer. *Frontiers in Microbiology* **7**, 173 (2016).

therapies will be more advantageous in finding lead candidates through the revival of outdated, yet successful platforms. These new developed platforms should reliably find lead compounds[10].

There are many other additional platforms for the discovery of novel antibiotics, such as targeting virulence factors[37], phage therapy[38] and antimicrobial peptides (AMP)[39]. Although teixobactin **1.23** may not be regarded as a true AMP, AMPs will be discussed extensively below as my entire PhD was based on the design, synthesis and the biological evaluation of analogues of the peptide teixobactin **1.23** [40].

1.6 Antimicrobial peptides (AMP's)

AMPs are the first line of protection in multicellular organisms[39]. Peptides are short proteins consisting of circa 12-50 amino acids sequences. AMPs are abundant in marine life, mammals, insects, plants and soil bacteria[41]. Each AMP has its unique profile, ranging from structure (e.g. α-helical, β-sheet, coil (Figure 1.9))[42–44], net charge (+2 to +9), solubility (cationic) and other physical properties (amphipathic)[45]. Most of these properties correlate to its activity. The positive charge allows electrostatic interaction between negatively charged membranes of the bacteria and the hydrophobicity enables penetration through membranes causing leaks, eventually cell lysis. Due to the unique properties that AMPs possess, which are related to its activity, modification and design synthetically can play a huge role in developing new AMPs.

[§§]**Figure 1.9:** Structural varieties of major AMPs. Random/extended coils (indolicidin), B-sheets (human defensin 1) and α helix (magainin)[43, 44]. Regenerated using PDB id codes 1g89, 1kj5 and 2k6o respectively, utilising discovery studio.

1.6.1 Mode of action of AMPs

The mode of action of AMPs can be either direct killing or immune modulation. The direct killing mechanism is further divided into two categories, membrane targeting and non-membrane targeting[46]. The membrane targeting peptides can also be receptor-mediated or non-receptor

[§§] Images freely available in protein data bank Europe

mediated. Nisin for example has a receptor-mediated interaction binding to Lipid II, a cell wall precursor[47].

1.6.1.1 Direct killing: membrane targeting

Electrostatic interactions are critical in determining how strong the binding is between the cationic peptide and the negatively charged bacterial membrane. Both Gram-positive and Gram-negative bacteria possess negatively charged head groups (phospholipids) that can strongly interact with the positively charged peptides[48,49]. Moreover, hydrophobic peptides avoid the risk of selectivity and toxicity to mammalian membranes. Mammalian membranes contain cholesterol and are more zwitterionic which influences stabilisation of lipid layer and protects it from damage[50].

Once there is a certain accumulation of AMPs on the surface of the membrane, there are different models as to which of these peptides perform their action on the membranes. The transmembrane pore forming models: barrel stave and toroidal pore model and the non-transmembrane pore models: the carpet model and detergent-like model (Figure 1.10)[46].

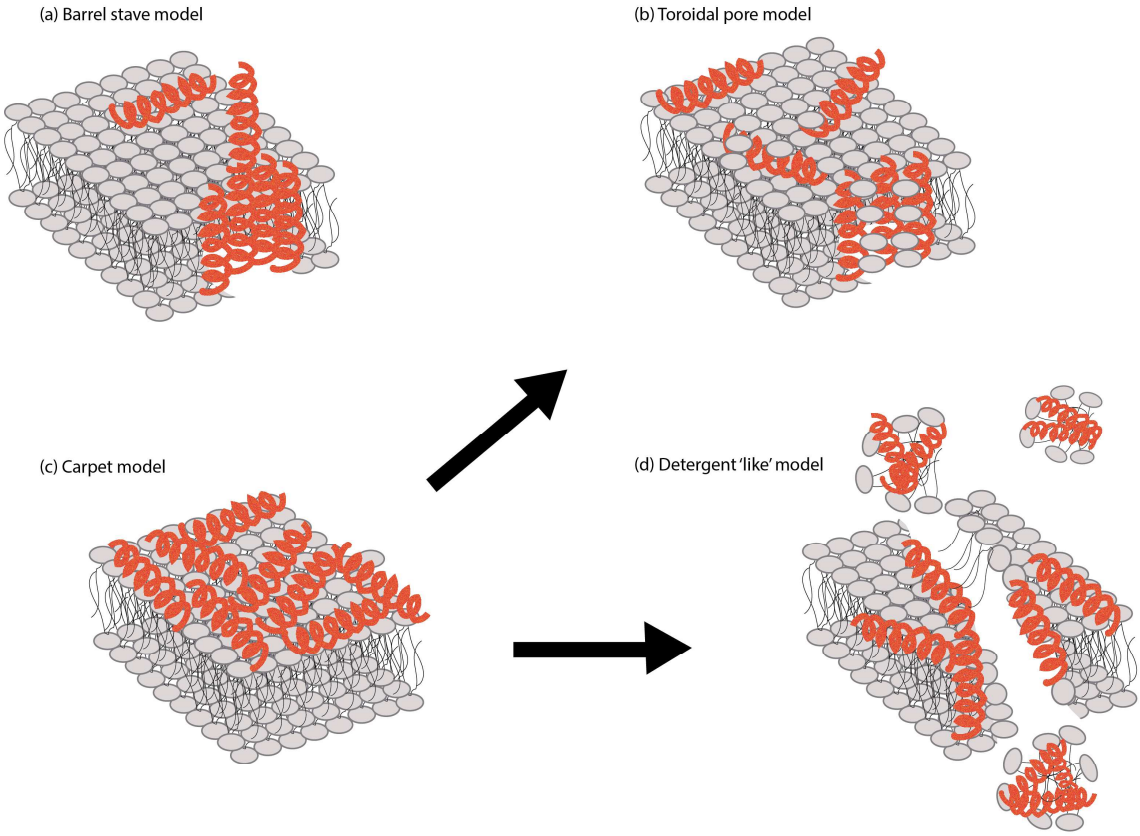

***Figure 1.10:** Different mechanism of action (models) of Antimicrobial peptides (AMPs)

In the barrel-stave model, first the AMPs are aligned parallel with the membrane surface and later forces its way vertically and into the membrane due to its amphipathic nature, creating pores[51] (Figure

*** Image is original, concept derived from: Kumar, P., Kizhakkedathu, J. & Straus, S. Antimicrobial Peptides: Diversity, Mechanism of Action and Strategies to Improve the Activity and Biocompatibility In Vivo. *Biomolecules* **8**, 4 (2018).

1.10a). Some examples of AMPs that form barrel stave are alamethicin,[52] pardaxin[53, 54] and protegrins[55].

In the toroidal model (Figure 1.10b), the AMPs again are aligned in parallel to the membrane surface; however, the aggregation of peptides forces the lipid bilayers to form a curve, causing the term "toroidal pores" mixed of peptide and lipid[52]. The difference between the barrel stave and toroidal model is that for the latter, the net arrangement of the hydrophobic and hydrophilic bilayer is disrupted, potentially allowing translocation of the AMP to further target intracellularly. Examples of some toroidal pore forming models include magainin 2 and melittin[56].

In the non-pore forming models like the carpet-like model (Figure 1.10c),[48, 56, 57] AMPs align at the membrane surface and causes a "carpet" effect that induces the membrane destabilisation. Before the membrane undergoes complete disintegration as shown in the detergent-like model (micelle formation) (Figure 1.10d), it briefly forms a transient pore like the toroidal model[56]. LL-37[57], indolicidin[58] and cecropin[59] are some of the AMPs which perform their action as carpet model.

1.6.1.2 Direct killing: non-membrane targeting

Initially, it was thought that AMPs were not targeting intracellular components. DNA and RNA are stereospecific targets. A study revealed that an alteration of $_{L}$-Amino acids to the $_{D}$ stereochemistry had similar potency, which confirmed no intracellular targets were involved[60]. However, it is now evident that AMPs at first engage at cytoplasmic membranes at low concentrations without initiating pore formation, to which it then accumulates intracellularly inhibiting several processes, triggering cell lysis[55]. A typical example is the action of burofin II, which passes the membrane and binds DNA and RNA of *E.coli*[61].

Other non-membrane targets of peptides are the bacterial cell wall precursors; Lipid II **1.25** (peptidoglycan precursor) and Lipid III **1.26** (wall teichoic acid (WTA) precursor) which are highly conserved in bacteria. Nisin, a lantibiotic binds to the Lipid II and creates a phosphate cage enabling pore formation[62].

Teixobactin **1.23**[40] on the other hand, specifically binds to the lipid II, lipid III and undecaprenyl pyrophosphate (C55-PP), which are essential for bacterial cell wall synthesis. Teixobactin and Lipid II will be extensively discussed later within the chapter.

1.6.1.3 Immune modulation

The production of AMPs is facilitated by certain immune cells such as neutrophils and macrophages. When an infection arises the first response is our immune system is to try and fight the foreign material. AMPs (LL-37, β defensins) attract and activate immune cells such as leukocytes, mast cells and dendritic cells, enhancing microbial death and inflammation control[63–65].

1.6.2 Challenges of AMPs and strategies to improve their therapeutic potential

Not many AMPs that have been discovered have passed through the United States Food and Drug administration (FDA) for clinical trials[66]. The ones that have been approved have been limited to topical treatment, of which cytotoxicity and protease degradation contributing to the main factors. Enzymes such as pepsin and trypsin in the digestive system break down peptides causing short half-lives for treatments. In many cases, rapid renal clearance is also an issue[67, 68].

The issue of proteolytic digestion of AMPs have been overcome by the chemical modification of AMPs to the $_{D}$-Amino acids. In many cases, modifications of the $_{L}$-amino acids to the $_{D}$-counterparts has prevented enzyme degradation without compromising the activity profile, due to enzymes being very stereospecific[46, 69–71]. Addition of non-proteogenic amino acids have also shown promise to proteolytic stability[72]. In some cases, the addition of an acetyl group also prevents degradation of AMPs by aminopeptidases, but the loss of charge compromises on activity[73, 74]. Different modes of cyclisation of peptides, such as disulphide bridges and head to tail cyclisation have also shown to improve serum stability[75, 76] and leads to better membrane permeation[77].

Delivery systems ranging from organic/inorganic molecules, polymers, surfactants and peptides have been used to improve AMPs[78, 79]. A former PhD student from our group, Abhishek Iyer, under the guidance of Dr. Ishwar Singh used peptides to improve the delivery of the Moenomycin A (MoeA) – a natural product with potent antibacterial activity against Gram positive bacteria but inactive against Gram negative bacteria. Specific 'delivery' peptides were designed, which contained residues Arg, Lys and/or Trp, known for their cell permeability[80–82]. The strategy involved the simple mixing of the cationic peptides with MoeA which resulted in the formation of non-covalent complexes, enabling the delivery of MoeA across the outer membrane of Gram-negative bacteria. This has resulted in a 30 times improvement in antimicrobial activity (PhD thesis, Abhishek Iyer, unpublished results).

1.7 Teixobactin: a new hope in antibiotic discovery

1.7.1 Ichip for the 'uncultivable'

As discussed previously, most of the antibiotics that have been produced during the golden age came from mining soils. Selman Waksman was the first to use such a platform. However, 99% of the soil bacteria cannot be grown under laboratory conditions. This has been a long problem in cultivating micro-organisms from the soil. "The great plate anomaly[83]" was first observed by Winterberg[84] an Austrian microbiologist where uncultured bacteria seen under a microscope cannot be grown on a petri dish. There have been efforts on trying to play with the media including different growth factors, but this limitation has stalled to find novel class of antibiotics and there is need to find new platforms to revive what Waksman had started.

Kim Lewis and his colleague Kaeberlein from Northeastern University had an idea which was very simple and efficient[85]. If we can't grow it in the lab lets send it back to its natural environment. They took a diluted sample from marine sediment and placed it onto a semipermeable membrane between an 'O' (Figure 1.11A). The polycarbonate membrane (0.03-µM pore-size) allows chemicals or nutrients exchange but restricts cell movement. This is then taken back to its natural environment.

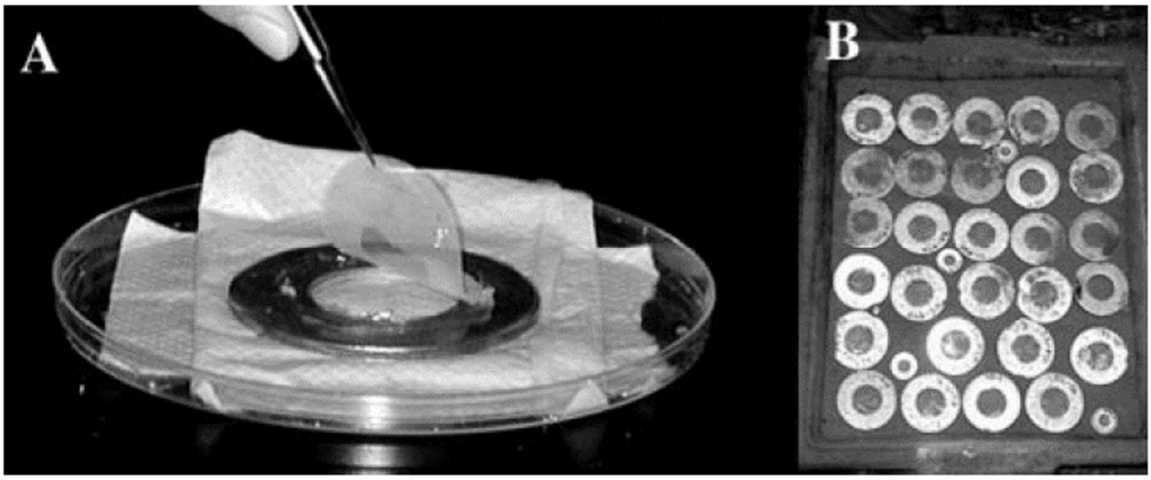

†††**Figure 1.11**: Diffusion growth chamber. (A) A semipermeable membrane between 2 'O' rings. (B) Growth chamber placed back to its original environment.

The authors found that a new species MSC1 could be grown as a pure culture in the chambers, but not on a petri dish. Their findings also revealed that bacteria do not like to grow in unfamiliar environment due to the signalling of growth factors with their neighbours. The authors further went on to study what these growth factors were and they happened to be siderophores[86]. Siderophores have a high binding affinity for Fe(III) which bacteria use to scavenge Fe(III) and then transport iron back to the cell when its low[87–89].

Having already established the design and knowledge of how to grow the 'uncultivables' a more sophisticated design was employed. The Isolation chip (Ichip)[90] which is very similar to the diffusion chamber is immersed in liquid-agar based medium containing mixed cells for cultivation(Figure 1.12A). Depending on the dilution, on average only a single cell is trapped in the tiny wells once the agar solidifies (Figure 1.12B). The membranes are then placed and screwed up (Figure 1.12C). The chip is then placed in its original environment for the colonies to form.

††† Reproduced from: Microorganisms in Pure Culture in a Simulated Natural Environment. *Science* **296**, (2002),

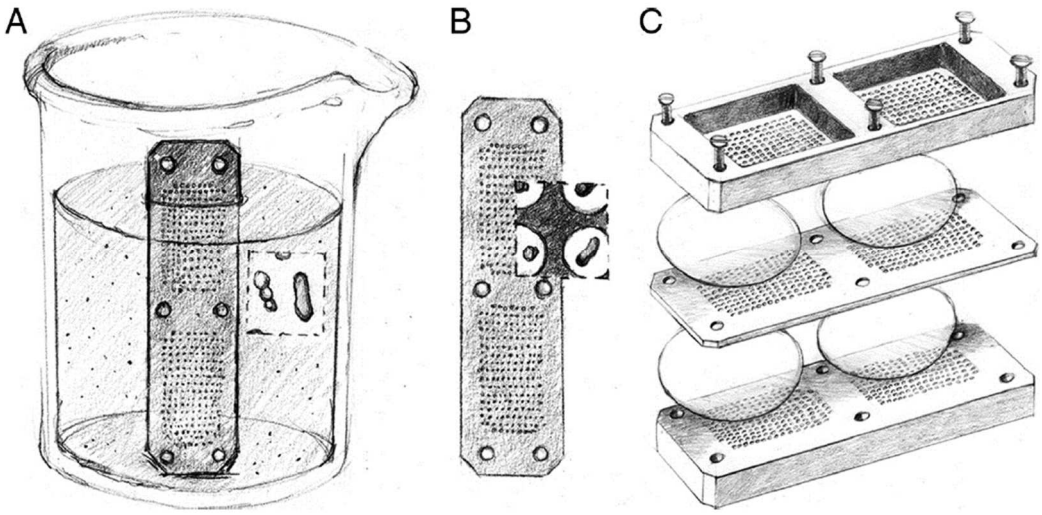

‡‡‡**Figure 1.12**: Ichip design and procedure for microbial cultivation in situ[40, 90].

1.8 Teixobactin (1.23) identification

Using the Ichip technique, microbial growths were screened and tested for antibacterial activity against *S. aureus*. A new species from the β-proteobacteria named *Eleftheria terrae*, was producing a compound that had high activity against Gram-positive bacteria. A partly purified analysis of the compound revealed a molecular weight of 1,242 Da, which was not reported in literature before. Further analysis was carried out by Selcia and Novobiotic pharmaceuticals to deduce the full structure of **1.23**[40].

1.8.1 NMR analysis

NMR 2D analysis data performed by NovoBiotic pharmaceuticals of Teixobactin revealed a 11 amino acid peptide, a 13 membered macrolactone ring and a rare unusual enduracididine amino acid **1.19**[40].

1.8.2 Marfey's analysis of amino acids

To determine the chirality of amino acids in the structure of teixobactin, advanced Marfey's analysis[91] was used in conjunction with liquid chromatography. A UV- active reagent $_L$-FDLA (1-fluoro-2,4-dinitrophenol-5-$_L$-Leucinamide) reacts with a racemic mixture of amino acids and forms separable diastereomers which can be detected by reverse-phase HPLC (RP-HPLC) (Figure 1.13). A combined advantage of UV detection and separation can reveal the stereochemistry of the amino acids[92, 93].

‡‡‡ Reproduced from: Use of ichip for high-throughput in situ cultivation of "uncultivable" microbial species. *Applied and environmental microbiology* **76**, 2445–50 (2010).

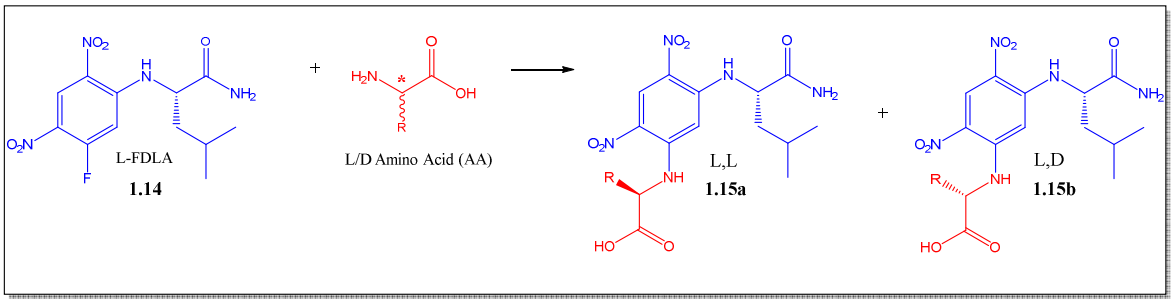

Figure 1.13: Figure showing Marfey's reagent **1.14** (blue) reacting with mixed stereoisomers (red) to give diastereoisomers **1.15a** and **1.15b** which can be analysed by RP-HPLC.

1.8.3 Synthesis of enduracididine (1.21)

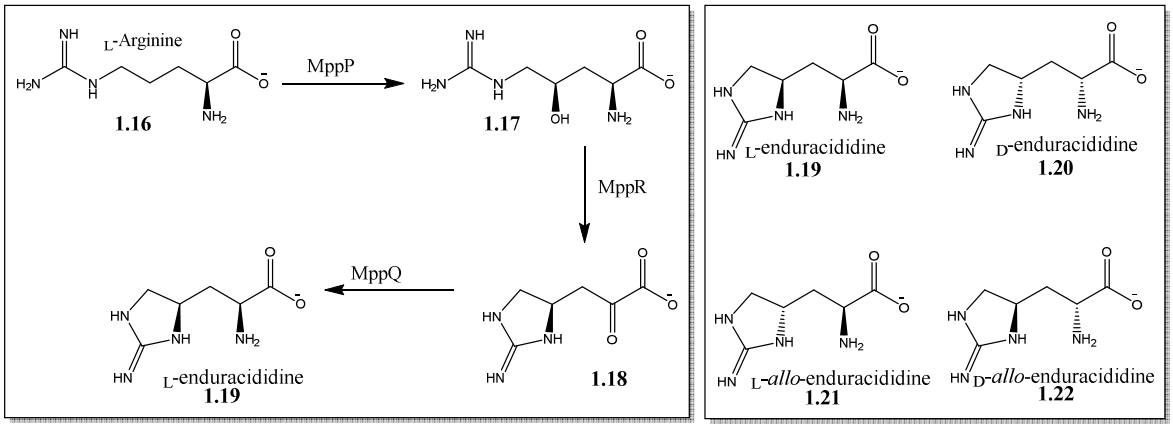

Figure 1.14: Biosynthetic pathway of L-enduracididne **1.19** (left) and stereoisomers of enduracididine **1.20-1.22**.

Biologically, **1.19** creation begins with the catalysation of L-arginine **1.16** by a PLP -dependent hydroxylase (mppP) to a guanidinovaleric acid **1.17**. The guaninidine acid undergoes cyclisation by the pyruvate aldose enzyme (mppR) to form **1.18**. The final transamination step by mppQ yields L-enduracididine **1.19**[94].

To determine the stereochemistry for the enduracididine amino acid all 4 diastereomers were synthesised by Selcia chemists. A few synthetic routes have been published for the rare amino acid, however most of them are inefficient and have tedious procedures[94]. Selcia chemists managed to synthesise all 4 diasteroemers of enduracididne and using the previously mentioned Marfey's analysis, teixobactin **1.23** adopts a L-*allo*-enduracididne **1.21** (L-*allo*-End). More on the chemical synthesis of enduracididine will be discussed in later sections of this chapter.

1.9 Structure of Teixobactin 1.23

Combining the NMR data and Marfey's analysis of amino acids and enduracididine, a full structure determination was possible (Figure 1.15). Teixobactin **1.23** is a cyclic depsipeptide and contains 11 amino acids, out of which 4 are D-aminoacids, namely *N*-Me-D-Phe$_1$, D-Gln$_4$, D-*allo*-Ile$_5$ and D-Thr$_8$. An ester bond in the 13 membered macrolactone ring is formed with D-Thr$_8$ and L-Ile$_{11}$. Other two L-

Ile come at position 2 and 7 and an Ala at position 9. Thus, structural complexity of **1.23** can been described as moderate to difficult.

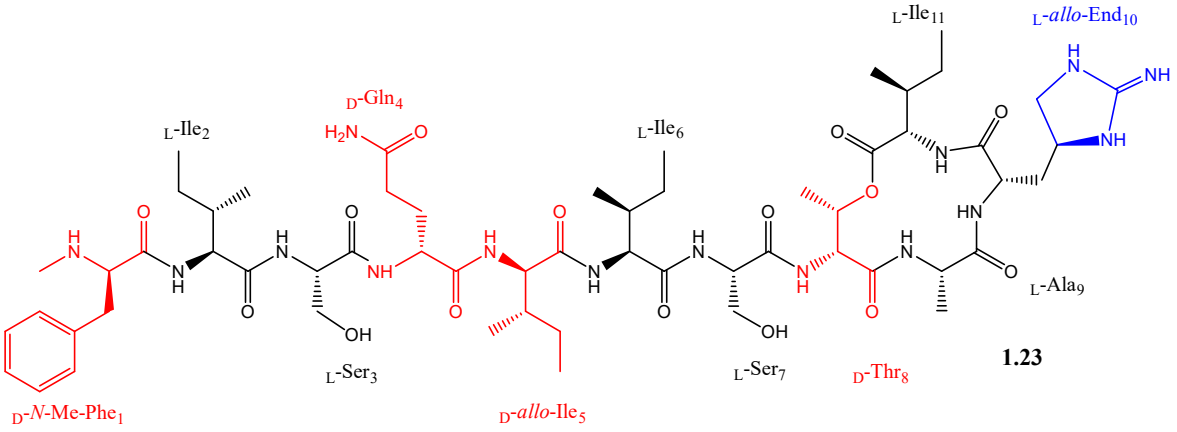

Figure 1.15: Structure and sequence numbering of teixobactin **1.23** with D-amino acids highlighted in red and the rare amino acid enduracididine marked in blue.

The gene cluster consists of Txo1 and Txo2, which are both large (~697kDa) nonribosomal peptide synthetases (NRPSs). Txo1 has a MT (methyltransferase) domain which is responsible for the methylation of phenylalanine and Txo2 has a unique two consecutive thioesterase domain which involves in the ligation of Thr_8 and Ile_{11}.

1.10 Resistance and mechanism of action of multidrug-resistant (MDR) pathogens

1.23 was tested against an extended panel for Minimum Inhibitory Concentration (MIC)[40] and it exhibited very high potency (low MIC) against very stubborn Gram-positive pathogens such as methicillin-resistant *Staphylococcus aureus* (MRSA), Penicillin-Resistant *streptococcus pneumonia* (PRSP) and vancomycin-resistant *Enterococcus* (VRE). It also has extremely high potency against *Mycobacterium tuberculosis* (Mtb) and *Clostridium difficile* (Table 1.1).

Organism	**Teixobactin (1.23) MIC (μg ml^{-1})**
S. aureus (MSSA)	0.25
S. aureus (MRSA)	0.25
Enterococcus faecalis (VRE)	0.5
Enterococcus faecium (VRE)	0.5
Streptococcus Pneumoniae (penicillinR)	≤0.03
B.anthracis	≤0.06
Clostridium difficile	0.005
Escherichia coli	25
Pseudomonas aeruginosa	>32
Klebsiella pneumoniae	>32

Table 1.1: MIC values of **1.23** tested against some important Gram-positive strains (blue) and Gram-negative (red).

Teixobactin **1.23** is effective against Gram-positive bacteria, however it not very effective against Gram-negative strains. This is most likely due to the outer membrane that Gram-negative possesses. To prove this concept a defected outer membrane strain of *E.coli asmB1* was tested and showed improved activity. **1.23** was not only nontoxic to mammalian cells, but no mutations in *S.aureus* or *M.tuberculosis* was observed under subminimum inhibitory concentrations (MIC). To check for resistant mutants a technique known as serial passage is employed[95]. A slightly lower dose is given initially that does not entirely kill the pathogen and can recover from the dose. Later a slightly higher dose than the previous is given, and this cycle is repeated until resistant mutants are observed.

The absence of detectable resistant mutants suggested that teixobactins' mode of action was clearly tracking towards something specific. Authors later discovered that it was a peptidoglycan synthesis inhibitor[40]. Proteins are more susceptible towards mutation and if no mutations were observed it couldn't be an enzyme or protein. Another molecule with similar characteristics was vancomycin **1.12**[96], a lipid II inhibitor, a peptidoglycan precursor.

1.10.1 Peptidoglycan bio-synthesis

Peptidoglycan layer (Murein) is the most important component of the bacterial cell wall allowing its structural rigidity and protects it against osmotic pressure[97]. As the name suggests, it's a combination of glycans (sugars) and peptide crosslinks. The two major alternating sugars to form the peptidoglycan layer involved are *N*-acetyl Muramic acid (MurNAc) and *N*-acetyl glucosamine (GlcNAc). There are three main stages involved in the synthesis if peptidoglycan synthesis. Cytoplasmic stage where GlcNAc and MurNAc are synthesised, membrane stage where the GlcNAc and MurNAc are attached and transferred to the cell membrane and the final extracellular stage where cross linking of the precursors occur[98] (Figure **1.16**).

1. In the cytoplasmic stage GlcNAc, initially made from glucose gets converted to UDP-GlcNAc with the help Uridine-5'-triphosphate (UTP). UDP-GlcNAc then undergoes another conversion to the second sugar UDP-MurNAc catalysed by enol pyruvate transferase. UDP- MurNAc is then conjugated to a tripeptide ($_{L}$-ala, $_{D}$-Glu, $_{L}$-Lys or *meso*-diaminopimelic acid (A_2pm)) and further converted to a pentapeptide (UDP-MurNAcpp) by addition of another two $_{D}$-Ala residues[99–101].
2. C_{55}-P (undecaprenyl phosphate or bacterprenol) is a key lipid known for the synthesis and transportation of the GlcNAc-MurNac from the cytoplasms to the external sites of the growing peptidoglycan layer. The UDP- MurNAcpp attaches to C_{55}-P which in turn triggers the conjugation of the UDP- GlcNAc to MurNAc. This forms a complex (Lipid II) and an enzyme peptidoglycan synthase (flippase[102]) transports lipid II to the growing cell wall. An enzyme phosphatase dephosphorylates C_{55}-P to be reused again, however this recycling step is not understood well[103–105].

3. The alternating MurNAc and GlcNAc which are polymerised by glycotransferase (GTase) are crosslinked with Transpeptidase (Penicillin binding protein or PBPs) with neighbouring pentapeptides hanging on the lipid II[106].

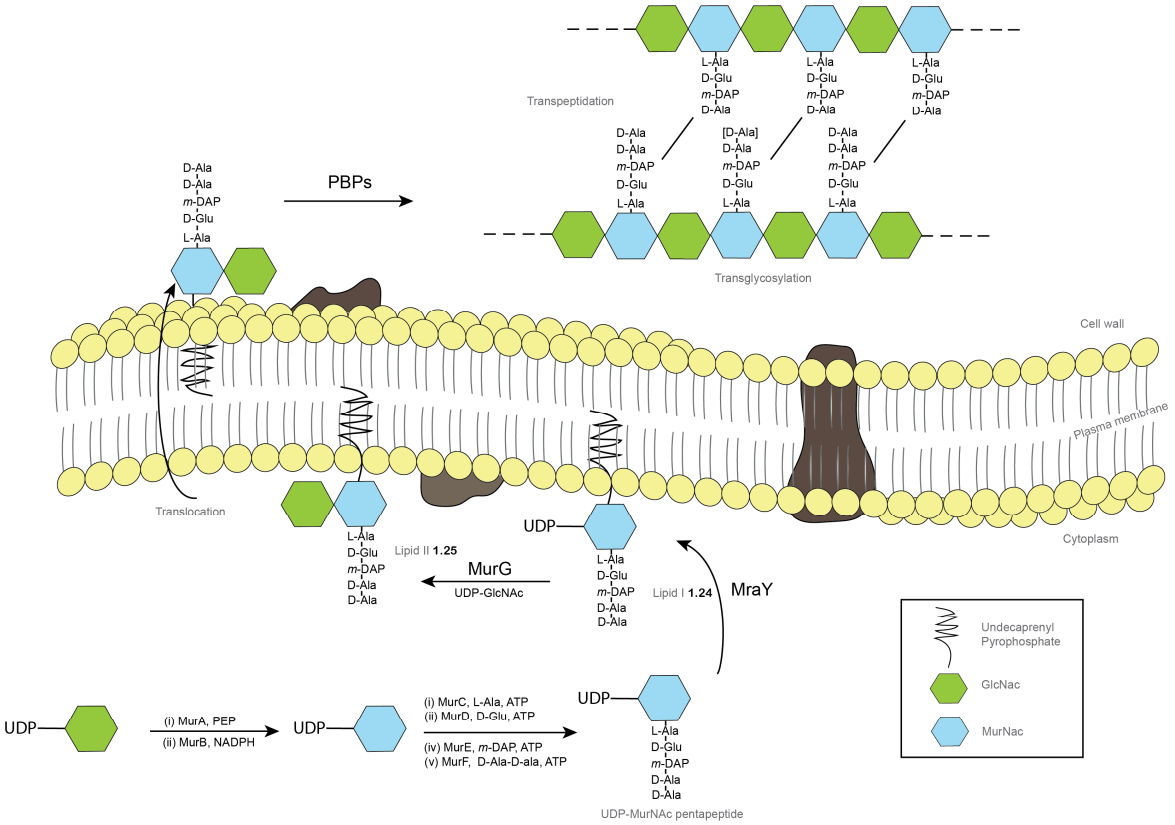

§§§**Figure 1.16**: Peptidoglycan synthesis stages and steps[107]**.**

1.10.2 Mode of action of teixobactin (1.23)

Both **1.12** and **1.23** inhibit the peptidoglycan synthesis, by binding to the lipid II precursor. **1.12** binds to the D-Ala-D-Ala terminus of the lipid II **1.25**, while **1.23** binds to the highly conserved phosphate moiety of both lipid II **1.25** and III **1.26** (Figure 1.17).

§§§Image is original, concept derived from: R. T. Gale, E. D. Brown, New chemical tools to probe cell wall biosynthesis in bacteria. *Current Opinion in Microbiology*. **27**, 69–77 (2015).

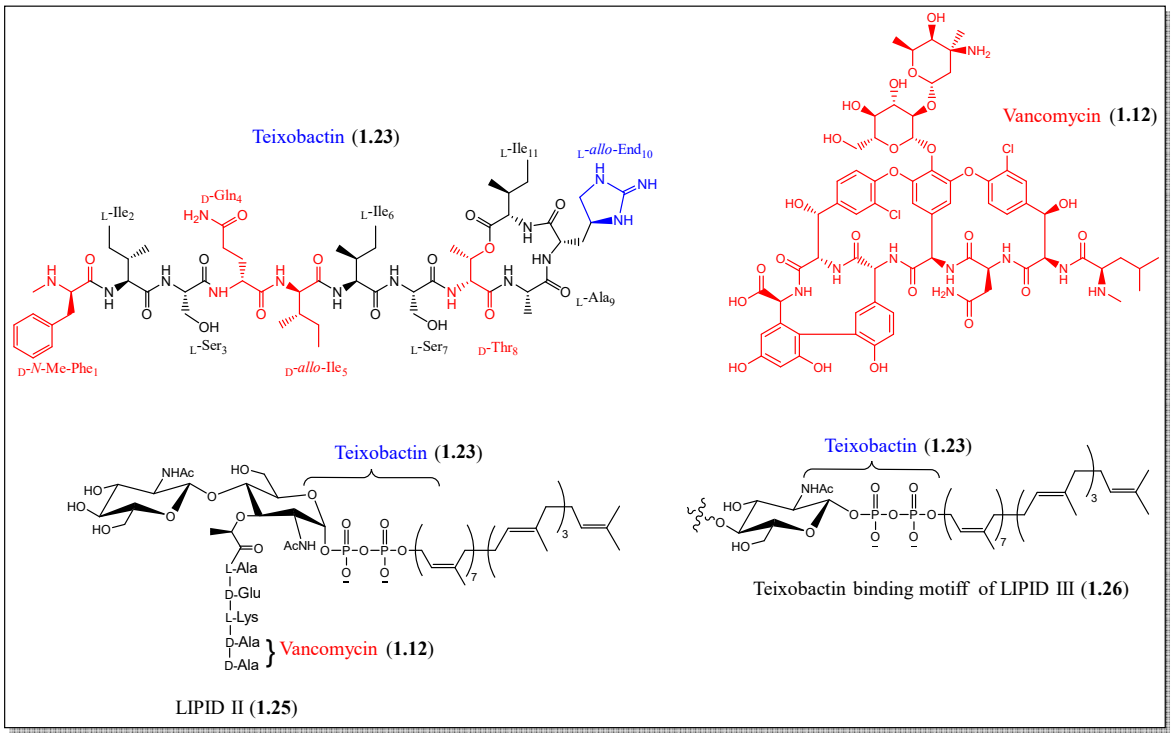

Figure 1.17: Figure showing Interactions of Teixobactin (**1.23**) and Vancomycin (**1.12**) with lipid II (**1.25**) and lipid III (**1.26**).

Vancomycin-Resistant bacteria mutate and change their lipid II D-Ala-D-Ala terminus to D-Ala-D-Lac. Since **1.12** binds via hydrogen bonding, the substitution of the NH to ester decreases the potency to 1000-fold[96, 108]. Efforts to redesign vancomycin **1.12** derivatives and the ability to bind to both the mutated and wild type lipid II **1.25** have been mentioned to enhance its activity[109].

Teixobactin **1.23** not only binds to lipid II but also lipid III, a precursor of wall teichoic acid (WTA), not surprising as the structures of both lipids are very similar (Figure 1.17, **1.25** & **1.26**). The binding of these highly conserved lipids in the bacteria inhibits the reprocessing of undecaprenyl pyrophosphate (C_{55}-PP), which is crucial in the biosynthesis of both lipid II and lipid III. Accumulation of UDP- MurNAcpp in the treatment of S.*aureus* determines the inhibition of the peptidoglycan synthesis, similar to those tested with Vancomycin **1.12**. Teixobactin **1.23** binds in a 2:1 (teixobactin/lipid) molar ratio with Lipid I, Lipid II, Lipid II (D-lac), lipid III and C_{55}-PP[40]. Due to the multiple binding non-protein sites, it is less likely for resistance developing in the near future.

In vivo studies of **1.23** on mouse models, showed high efficacy in antibacterial activity at a protective dose (PD_{50}) of 0.2mg/kg which contrasted positively to the 2.75mg/kg PD_{50} of **1.12**.

1.11 Total Synthesis of Teixobactin

Teixobactin **1.23** attracted a lot of media attention due to its high potency against MDR strains and the synergistic mode of action on non-protein targets (lipid II **1.25** and III **1.26**). This excited different groups including ours to pursue teixobactin research. The total synthesis of **1.23** would open attractive scaffolds for new antibiotic development and further analysis would be prime in

determining the structure-activity relationship (SAR) of teixobactin **1.23**. Our group initially also focused and attempted the total synthesis of **1.23**. Due to the laborious synthesis of L-*allo*-End **1.21**, our group decided to divert the focus more on designing simple and economical potent analogues, which will be discussed in later chapters.

1.11.1 Synthesis of Protected L-*allo*-Enduracididne (1.21)

To achieve the total synthesis of **1.23**, an appropriately protected, not commercially available L-*allo*-End **1.21** was compulsory to synthesise. A few procedures were already reported in literature[110–113], however these methods needed to be improvised to give access to a suitably protected enduracididne. One of the challenges was to establish the C4 chirality position of the L-*allo*-End **1.21**[40]. As mentioned previously, Selcia chemists had already prepared the building block for Marfey's analysis from a four-step synthesis starting from the nitro alcohol (Scheme 1.1, **1.27**). The nitro alcohol was synthesised from an optimised protocol by Rudolph *et al*[114]. The final synthesis yielded the production of both **1.19** and **1.21** in a 1:6 ratio respectively.

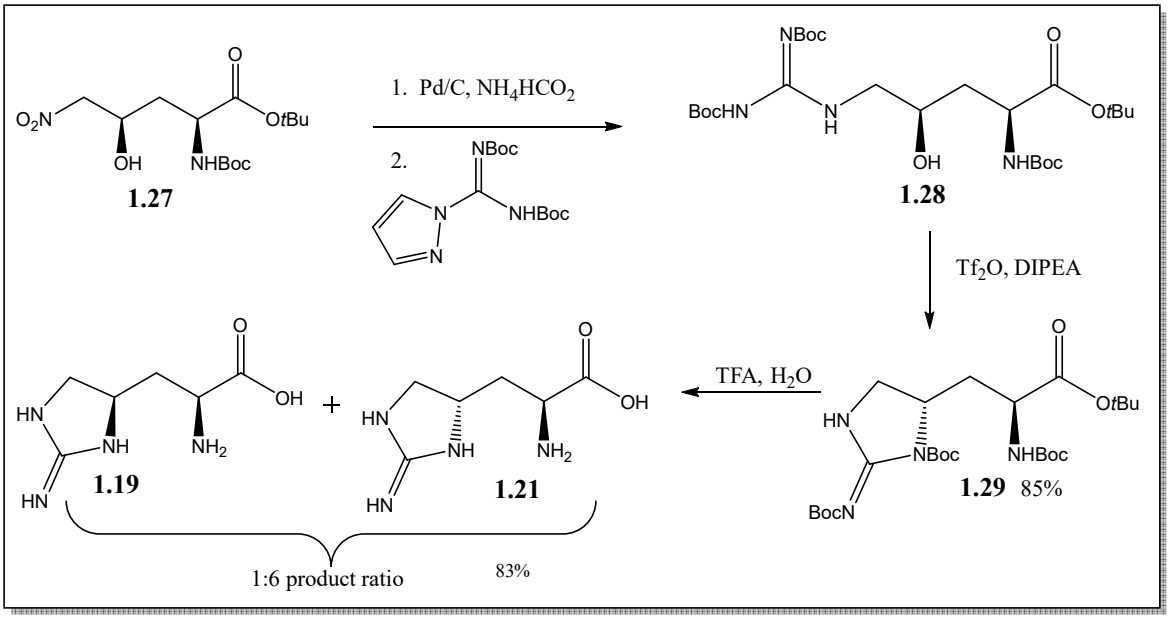

Scheme 1.1: Synthesis of L-*allo*-End **1.21** by Lewis et al.[40]

Using Rudolph's method of converting the protected aspartic acid **1.30** to nitro ketone **1.27**, Payne *et al.* then stereoselectively reduced the nitro ketone to the nitro alcohol using L-selectride achieving a diastereoisomeric product at a 5:1 ratio (Scheme 1.2, **1.31**)[115]. The minor stereomer was removed by flash column chromatography. The guanidine moiety was introduced using an improvised Goodman's reagent, and an intramolecular cyclisation resulted in the L-*allo*-End frame (Scheme 1.2, **1.33**). A simple Boc-removal step followed by a Fmoc coupling step on the α-amine produced the fully protected enduracididne, suitable for Fmoc solid phase synthesis (**1.34**).

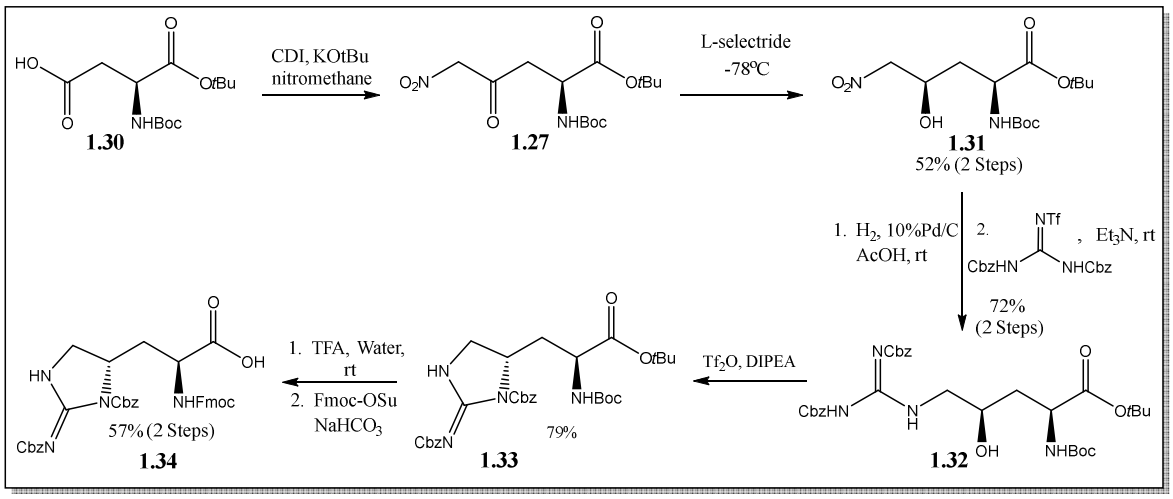

Scheme 1.2*:* L-*allo*-End synthesis by Payne et al[115].

Yuan *et al*. in 2015 published a highly stereoselective and scalable synthesis of L-*allo*-End (Scheme 1.3)[113]. The 10-step procedure started with the unique *trans*-hydroxy proline (**1.35**) obtaining a final product with high diastereoselectivity and an overall yield of 31%. A notable highlight was the use of bulky protection to cover the carboxylate (Scheme 1.3, **1.36**) which prevented the forming of both a lactone and a lactam, efficiently resulting in the L-*allo*-End **1.21** synthesis.

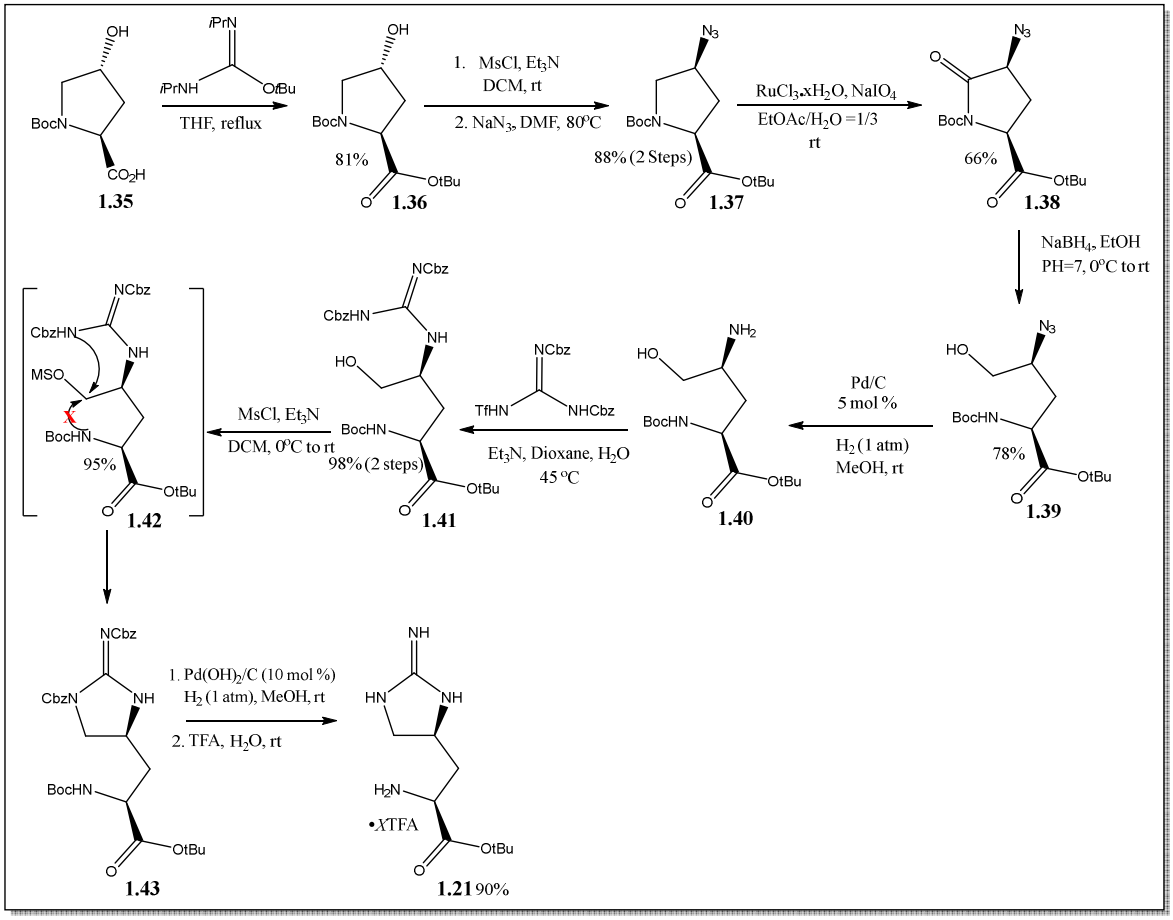

Scheme 1.3: L-*allo*-End synthesis by yuan et al[113]

1.11.2 Total synthesis of Teixobactin Schemes

Once the enduracididne synthesis had been optimised, a few groups delivered the total synthesis of teixobactin. Most of them employed the Fmoc-SPPS but had varying strategies[113, 115–117].

Payne group initially started their synthesis using the 2-chlorotrityl (2-CTC) resin, but they were not able to esterify the $_D$-Thr$_8$ to Ile$_{11}$[115]. Payne group believed it was due to the bulky 2-CTC resin that was hindering the hydroxy group of the Thr$_8$. As an alternative, a less, bulkier group (4-(hydroxymethyl)-3-methoxyphenoxy) acetic acid (HMPB), polyethylene glycol-based NovaPEG resin was selected[118]. A protected Fmoc-$_D$-Thr(TES)-OH was loaded to the resin followed by the esterification of Alloc-Ile-OH. The rest of the linear synthesis through Fmoc-SPPS was followed to achieve (Scheme 1.4, **1.45**).

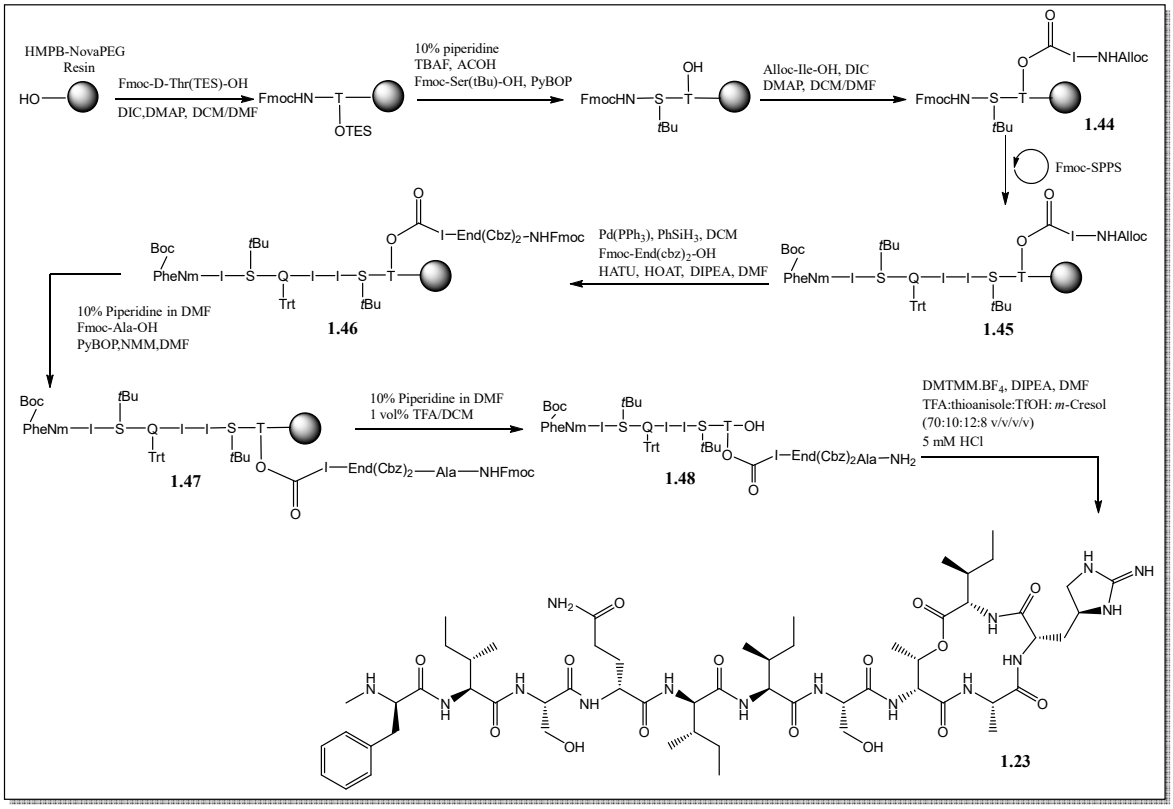

Scheme 1.4: Total synthesis of **1.23** by Payne group[115]

The protected Alloc from the Isoleucine group was then removed by palladium chemistry to free the amine and coupling of enduracididine (**1.46**). However, the conventional Fmoc deprotection was not successful due to the formation of diketopiperazine between the α-amine of the $_L$-*allo*-End and α-carboxylic acid of the $_L$-isoleucine. To minimise the diketopiperazine formation, the authors used a quick 30s deprotection solution (10% vol piperidine in DMF) and added a preactivated alanine coupling after rapidly washing the piperidine. The removal of Fmoc from the alanine provided the free amine to which the resin underwent partial cleave, leaving a fully protected depsipeptide (**1.48**). Cyclisation followed by full deprotection of the side chains provided **1.23** in an overall 24 step procedure at a 3.3% yield.

In 2016 Li *et al.* also reported the total synthesis of **1.23** (Scheme 1.5)[117]. They adopted a Ser/Thr ligation strategy adopted from their lab previously[119] by constructing the cyclic depsipeptide part of the teixobactin and conjugating it with the linear hexapeptide. The authors started off with a dimer synthesis in solution to obtain Alloc-$_D$-Thr-O(Fmoc-Ile)-OH **1.49** moiety and immobilising that onto the resin. Boc-Ser(*t*Bu)-OH coupling after removal of the alloc protecting group followed by Fmoc-SPPS of $_L$-*allo*-End and alanine yielded the pentapeptide (**1.50**). $_L$-*allo*-End was very slow requiring three repetitive 10h couplings to achieve completion. The mild resin cleavage followed by cyclisation produced the cyclic-depsi-pentapeptide moiety (**1.52**). The other linear hexapeptide salicylaldehyde ester was synthesised by conventional Boc-SPPS followed by ozonolysis (**1.51**). Ligation between the linear and the cyclic peptide in the presence of pyridine/AcOH (6:1) produced **1.23** in a 37% yield in the final step.

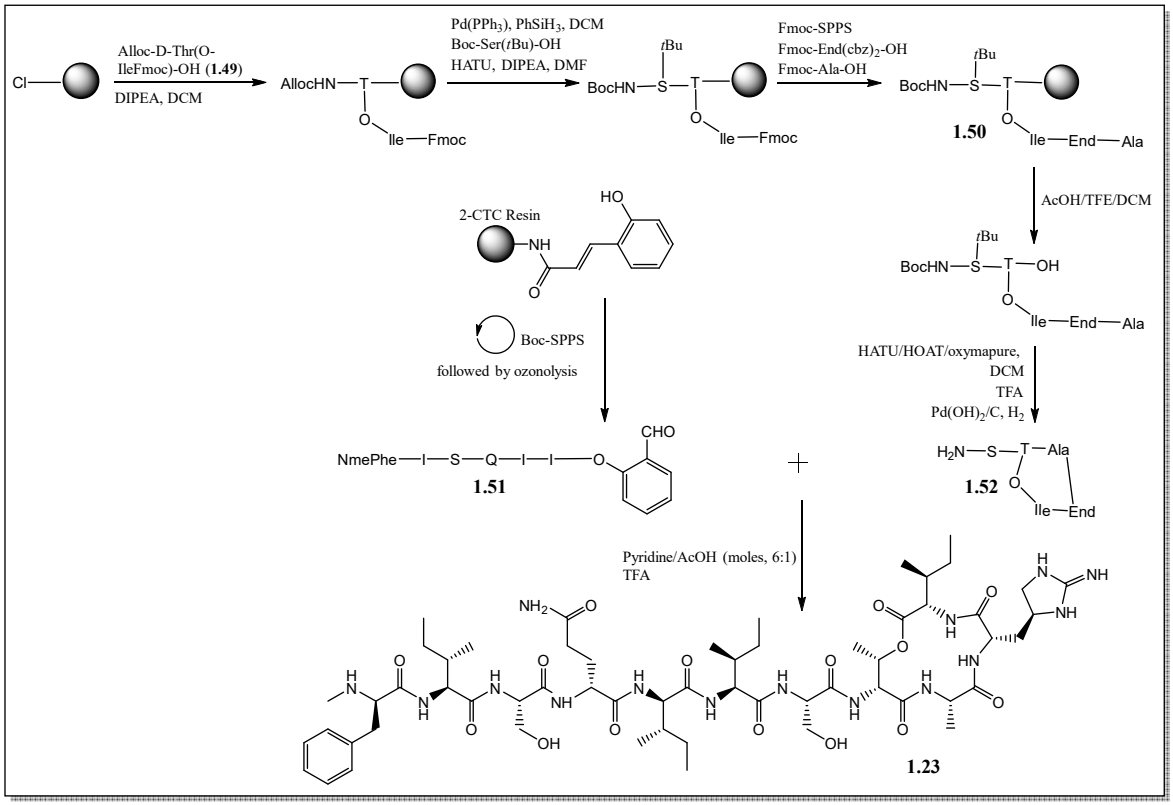

Scheme 1.5: Total synthesis of **1.23** by Li *et al.*[117]

Very recently another paper by Chen *et al.* reported the total synthesis of **1.23** and its stereoisomers[116]. They combined solution and solid phase synthesis to overcome racemisation and achieve an efficient convergent synthesis. Although the authors also reported a complete solid support synthesis of teixobactin, a half solution phase strategy was a better choice due to the racemisation between Thr_8 and Ile_{11}. Due to the distinctive nature of the synthesis in comparison to previous total syntheses, the convergent approach has been discussed.

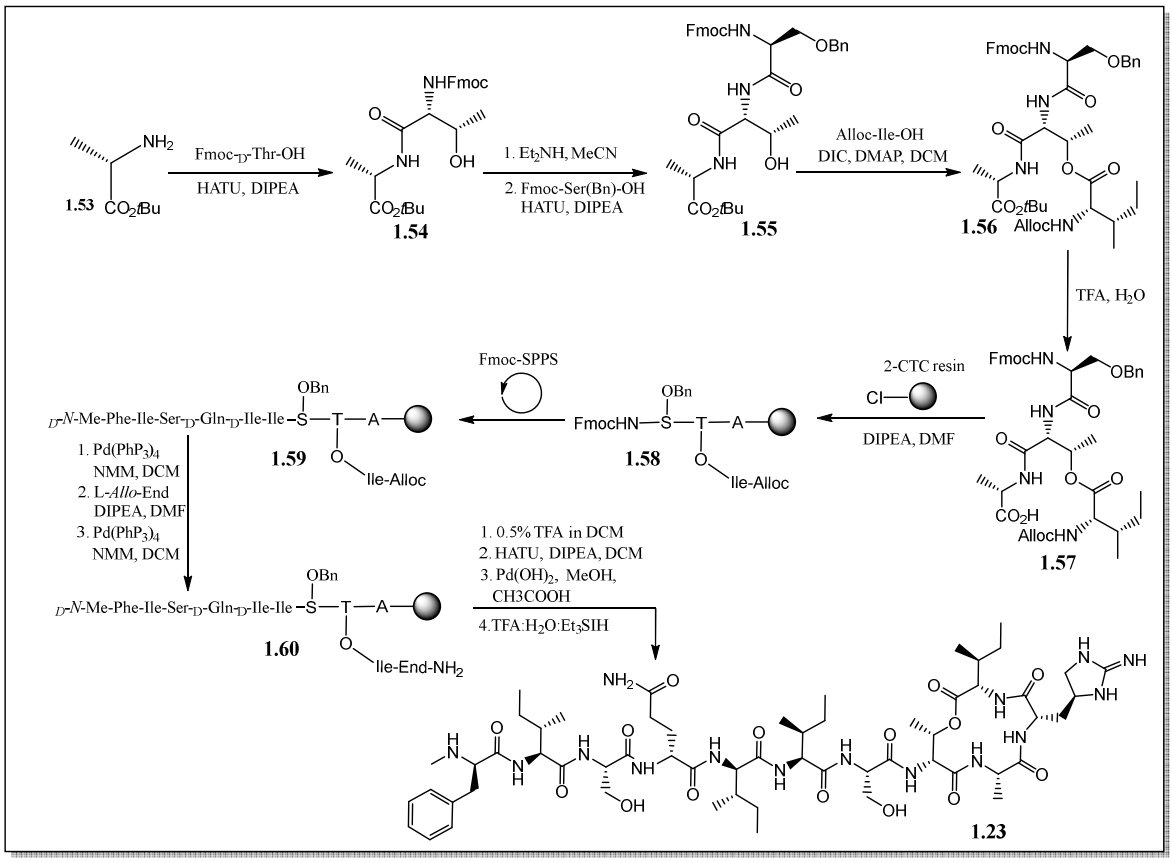

Scheme 1.6: Total synthesis of teixobactin by Chen et al[116]

The synthesis began in solution with the reaction of the carboxyl protected H-Alanine-O*t*Bu (Scheme 1.6, **1.53**) with Fmoc-D-Thr to form the dimer (**1.54**). Fmoc-Ser(Bn)-OH was then coupled prior to removal of Fmoc. Esterfication then proceeded to create the tetramer (**1.56**). Esterfication was also possible at the dimer stage to get the esterified trimer. However the further coupling of serine failed due to the facile O to N acyl transfer between the Ile and the Thr, during the removal of Fmoc on the Thr. Once the deprotected carboxyl tetramer was available, 2-CTC was reacted to attach the tetramer onto the resin followed by conventional Fmoc-SPPS. Alloc removal and coupling of enduracididine gave the complete on resin protected uncyclised teixobactin (**1.60**). Partial cleavage released the protected teixobactin and macrolactamisation by HATU produced the cyclised product to which full deprotection produced **1.23**.

Although it was not a fully synthesised teixobactin **1.23**, it is noteworthy to mention that Dhara *et al*[120]. synthesised a solution phase macrocyclic core of **1.23** with gram scale synthesis of **1.21** but were not able to attain full deprotection of the enduracididne. The present strategy might not be as advantageous to previous methods, but it can be used as a complementary one.

1.12 Project aims

This chapter comprises a brief overview highlighting the major challenges involved in overcoming antimicrobial resistance, the difference between multidrug resistant Gram-positive and Gram-negative bacteria, modes of action of antibiotics and resistant mechanisms with examples and additional details covering important aspects of antimicrobial peptides.

The last 30 years have been a colossal failure in terms of discovering new classes of antibiotics. AMR is continuing to grow at an alarming rate and the demand for new antibiotics is much higher than the current supply. Nonetheless, it does look that we are moving in the right direction with the recent technological advances in antibiotic research although there is still a significant amount of work to be completed. The issue of unculturable soil bacteria can now be circumvented using the novel ichip technique, which in the future is most likely to harbour new antibiotics.

AMPs have shown promise as future therapeutic agents. Developments of current AMPs aimed at therapeutic applications could reveal benefits in the next decade. The mode of action of several AMPs has not yet been fully understood. In addition to the models and mechanism of actions described earlier, it is possible that AMPs operate with other different modes. Understanding the modes of action of recently discovered antibiotics such as teixobactin (although may not be fully regarded as an AMP) and with the help of different imaging and assays, it is more likely that more modes of action will be revealed. Nonetheless, research and resistance must be kept on check and with novel studies, we should steadily be able to avoid the "post-antibiotic'' era.

Teixobactin falls under a new class of antibiotics and has emerged at a time when we urgently needed it. The 11-mer macrocyclic depsipeptide is produced by a soil bacterium named *Elefteria terrae*. It has shown better activity to vancomycin and oxacillin, which is our last defence against multi-drug resistant pathogens. The synergistic action of teixobactin on peptidoglycan and WTA biosynthesis inhibits cell wall synthesis. More importantly, due to this behaviour, resistance is less likely to be observed in the near future as the targets are non-protein based where mutations are not prone to form.

There is excellent potential for teixobactin to progress further to combat the resistance issue. There is also ample opportunity for researchers to study its structure-activity relationships by synthetically obtaining teixobactin, its analogues and understanding their mechanisms of action through modifiable residues in the teixobactin sequence. This will give rise to several analogues that will benefit the clinical industry by rewarding future antibiotic drug therapy.

Despite the encouraging results of teixobactin, which has shown very high promise against many multidrug Resistant bacteria, there are certain limitations that halts teixobactin being further developed as a potential candidate for drug development. Teixobactin is limited to a single molecule and there is a very rare chance that it reaches the regulatory approval due to the high dilapidation rate

in drug development. The production of teixobactin is also hampered by the synthetically challenging, expensive and low yielding $_{L}$-*allo*-End building block. It is therefore critical that we pursue in designing novel synthetic teixobactin analogues to generate libraries to address the challenges posed in drug development.

Keeping the current challenges in mind the current project aims at the development of a synthetic protocol which will aid in the total synthesis of teixobactin and its analogues. The role and importance of the $_{D}$-amino acids in teixobactin could uncover understanding of its mechanism of action along with providing insight into to its Structure-activity relationship (SAR). More potent analogues can then be synthesised with point modifications and an established synthetic route, which could in turn provide more potent analogues than native teixobactin. These analogues can be further tested in advanced biological models.

Our group during the past four years has worked extensively in designing potent analogues of teixobactin in order to better understand the SAR of the teixobactins.. There have been more than 700 citations of the original article since it was first published, therefore only relevant work has been discussed in the final chapter. The total synthesis described above has been mentioned earlier in this chapter, however several analogues of teixobactin were synthesised and evaluated for their activity prior to the total synthesis of native teixobactin. These molecules are relevant to our work and will be mentioned in the final chapter as an overview discussion.

1.13 References

1. K. J. Williams, The introduction of ‘chemotherapy’ using arsphenamine - the first magic bullet. *Journal of the Royal Society of Medicine*. **102**, 343–8 (2009).

2. A. Fleming, On the antibacterial action of cultures of a penicillium, with special reference to their use in the isolation of B. influenzae. 1929. *Bulletin of the World Health Organization*. **79**, 780–90 (2001).

3. E. Chain, H. W. Florey, A. D. Gardner, N. G. Heatley, M. A. Jennings, J. Orr-Ewing, A. G. Sanders, THE CLASSIC: penicillin as a chemotherapeutic agent. 1940. *Clinical orthopaedics and related research*. **439**, 23–6 (2005).

4. A. Tomasz, The Mechanism of the Irreversible Antimicrobial Effects of Penicillins: How the Beta-Lactam Antibiotics Kill and Lyse Bacteria. *Annual Review of Microbiology*. **33**, 113–137 (1979).

5. F. Adzitey, Antibiotic Classes and Antibiotic Susceptibility of Bacterial Isolates from Selected Poultry; A Mini Review. *World s Veterinary Journal*. **6**, 36 (2015).

6. R. Fernandes, P. Amador, C. Prudêncio, β-Lactams. *Reviews in Medical Microbiology*. **24**, 7–17 (2013).

7. S. A. Waksman, H. B. Woodruff, Actinomyces antibioticus, a New Soil Organism Antagonistic to Pathogenic and Non-pathogenic Bacteria. *Journal of bacteriology*. **42**, 231–49 (1941).

8. M. Wainwright, Streptomycin: discovery and resultant controversy. *History and philosophy of the life sciences*. **13**, 97–124 (1991).

9. F. Ryan, *The forgotten plague : how the battle against tuberculosis was won--and lost* (Little, Brown, 1993).

10. K. Lewis, Platforms for antibiotic discovery. *Nature Reviews Drug Discovery*. **12**, 371–387 (2013).

11. 'Antibiotic Resistant Threats' (USA, 2013), (available at https://www.cdc.gov/drugresistance/threat-report-2013/pdf/ar-threats-2013-508.pdf).

12. K. P. Talaro, B. Chess, *Foundations in microbiology*.

13. M. T. Madigan, T. D. Brock, *Brock biology of microorganisms* (Pearson, 2012).

14. G. D. Wright, Q&A: Antibiotic resistance: where does it come from and what can we do about it? *BMC Biology*. **8**, 123 (2010).

15. J. T. Park, T. Uehara, How Bacteria Consume Their Own Exoskeletons (Turnover and Recycling of Cell Wall Peptidoglycan). *Microbiology and Molecular Biology Reviews*. **72**, 211–227 (2008).

16. D. Kahne, C. Leimkuhler, W. Lu, C. Walsh, Glycopeptide and Lipoglycopeptide Antibiotics. *Chemical Reviews*. **105**, 425–448 (2005).

17. W. E. Alborn, N. E. Allen, D. A. Preston, Daptomycin disrupts membrane potential in growing Staphylococcus aureus. *Antimicrobial agents and chemotherapy*. **35**, 2282–7 (1991).

18. C.-R. Chen, M. Malik, M. Snyder, K. Drlica, DNA Gyrase and Topoisomerase IV on the Bacterial Chromosome: Quinolone-induced DNA Cleavage. *Journal of Molecular Biology*. **258**, 627–637 (1996).

19. E. Etebu, I. Arikekpar, Antibiotics : Classification and mechanisms of action with emphasis on molecular perspectives (2016), (available at https://www.semanti cscholar.org/paper/ Antibiotics-%3A-Classification-and-mechanisms-of-with-EtebuArikekpar/aebc84013852 9c147e54552205bf26ec8aa3ca2e).

20. http://amr-review.org/, Review on Antimicrobial Resistance. *2015*.

21. I. Chopra, C. Schofield, M. Everett, A. O'Neill, K. Miller, M. Wilcox, J.-M. Frère, M. Dawson, L. Czaplewski, U. Urleb, P. Courvalin, Treatment of health-care-associated infections caused by Gram-negative bacteria: a consensus statement. *The Lancet Infectious Diseases*. **8**, 133–139 (2008).

22. D. J. Payne, M. N. Gwynn, D. J. Holmes, D. L. Pompliano, Drugs for bad bugs: confronting the challenges of antibacterial discovery. *Nature Reviews Drug Discovery*. **6**, 29–40 (2007).

23. C. A. Lipinski, F. Lombardo, B. W. Dominy, P. J. Feeney, Experimental and computational approaches to estimate solubility and permeability in drug discovery and development settings. *Advanced drug delivery reviews*. **46**, 3–26 (2001).

24. H. W. Boucher, G. H. Talbot, J. S. Bradley, J. E. Edwards, D. Gilbert, L. B. Rice, M. Scheld, B. Spellberg, J. Bartlett, Bad Bugs, No Drugs: No ESKAPE! An Update from the Infectious Diseases Society of America. *Clinical Infectious Diseases*. **48**, 1–12 (2009).

25. P. G. Higgins, C. Dammhayn, M. Hackel, H. Seifert, Global spread of carbapenem-resistant Acinetobacter baumannii. *Journal of Antimicrobial Chemotherapy*. **65**, 233–238 (2010).

26. D. H. (David H. Bergey, J. G. Holt, *Bergey's manual of determinative bacteriology.* (9th ed., 1994;https://www.worldcat.org/title/bergeys-manual-of-determinativebacteriology/oclc /28183643).

27. S. Baron, *Medical microbiology* (University of Texas Medical Branch at Galveston, 1996).

28. J. L. Martinez, Environmental pollution by antibiotics and by antibiotic resistance determinants. *Environmental Pollution*. **157**, 2893–2902 (2009).

29. E. M. Wellington, A. B. Boxall, P. Cross, E. J. Feil, W. H. Gaze, P. M. Hawkey, A. S. Johnson-Rollings, D. L. Jones, N. M. Lee, W. Otten, C. M. Thomas, A. P. Williams, The role of the natural environment in the emergence of antibiotic resistance in Gram-negative bacteria. *The Lancet Infectious Diseases*. **13**, 155–165 (2013).

30. O. M. El-Halfawy, J. Klett, R. J. Ingram, S. A. Loutet, M. E. P. Murphy, S. Martín-Santamaría, M. A. Valvano, Antibiotic Capture by Bacterial Lipocalins Uncovers an Extracellular Mechanism of Intrinsic Antibiotic Resistance. *mBio*. **8** (2017), doi:10.1128/mBio.00225-17.

31. Y. Cetinkaya, P. Falk, C. G. Mayhall, Vancomycin-resistant enterococci. *Clinical microbiology reviews*. **13**, 686–707 (2000).

32. J. M. A. Blair, M. A. Webber, A. J. Baylay, D. O. Ogbolu, L. J. V. Piddock, Molecular mechanisms of antibiotic resistance. *Nature Reviews Microbiology*. **13**, 42–51 (2015).

33. G. Meletis, Carbapenem resistance: overview of the problem and future perspectives. *Therapeutic advances in infectious disease*. **3**, 15–21 (2016).

34. C. J. H. von Wintersdorff, J. Penders, J. M. van Niekerk, N. D. Mills, S. Majumder, L. B. van Alphen, P. H. M. Savelkoul, P. F. G. Wolffs, Dissemination of Antimicrobial Resistance in Microbial Ecosystems through Horizontal Gene Transfer. *Frontiers in Microbiology*. **7**, 173 (2016).

35. J. Ali, Q. A. Rafiq, E. Ratcliffe, Antimicrobial resistance mechanisms and potential synthetic treatments. *Future Science OA*. **4**, FSO290 (2018).

36. L. Zhang, T.-F. Mah, Involvement of a novel efflux system in biofilm-specific resistance to antibiotics. *Journal of bacteriology*. **190**, 4447–52 (2008).

37. D. T. Hung, E. A. Shakhnovich, E. Pierson, J. J. Mekalanos, Small-Molecule Inhibitor of Vibrio cholerae Virulence and Intestinal Colonization. *Science*. **310**, 670–674 (2005).

38. S. Ahiwale, N. Tamboli, K. Thorat, R. Kulkarni, H. Ackermann, B. Kapadnis, In Vitro Management of Hospital Pseudomonas aeruginosa Biofilm Using Indigenous T7-Like Lytic Phage. *Current Microbiology*. **62**, 335–340 (2011).

39. M. Zasloff, Antimicrobial peptides of multicellular organisms. *Nature*. **415**, 389–395 (2002).

40. L. L. Ling, T. Schneider, A. J. Peoples, A. L. Spoering, I. Engels, B. P. Conlon, A. Mueller, T. F. Schaberle, D. E. Hughes, S. Epstein, M. Jones, L. Lazarides, V. A. Steadman, D. R. Cohen, C. R. Felix, K. A. Fetterman, W. P. Millett, A. G. Nitti, A. M. Zullo, C. Chen, K. Lewis, A new antibiotic kills pathogens without detectable resistance. *Nature*. **517**, 455–459 (2015).

41. L. S. Biswaro, M. G. da Costa Sousa, T. M. B. Rezende, S. C. Dias, O. L. Franco, Antimicrobial Peptides and Nanotechnology, Recent Advances and Challenges. *Frontiers in microbiology*. **9**, 855 (2018).

42. M. Pasupuleti, A. Schmidtchen, M. Malmsten, Antimicrobial peptides: key components of the innate immune system. *Critical Reviews in Biotechnology*. **32**, 143–171 (2012).

43. L. T. Nguyen, E. F. Haney, H. J. Vogel, The expanding scope of antimicrobial peptide structures and their modes of action. *Trends in Biotechnology*. **29**, 464–472 (2011).

44. D. Takahashi, S. K. Shukla, O. Prakash, G. Zhang, Structural determinants of host defense peptides for antimicrobial activity and target cell selectivity. *Biochimie*. **92**, 1236–1241 (2010).

45. L. R. Sirtori, A. de S. da Motta, A. Brandelli, Mode of action of antimicrobial peptide P45 on *Listeria monocytogenes*. *Journal of Basic Microbiology*. **48**, 393–400 (2008).

46. P. Kumar, J. Kizhakkedathu, S. Straus, Antimicrobial Peptides: Diversity, Mechanism of Action and Strategies to Improve the Activity and Biocompatibility In Vivo. *Biomolecules*. **8**, 4 (2018).

47. E. Breukink, I. Wiedemann, C. van Kraaij, O. P. Kuipers, H. G. Sahl, B. de Kruijff, Use of the Cell Wall Precursor Lipid II by a Pore-Forming Peptide Antibiotic. *Science*. **286**, 2361–2364 (1999).

48. M. R. Yeaman, N. Y. Yount, Mechanisms of Antimicrobial Peptide Action and Resistance. *Pharmacological Reviews*. **55**, 27–55 (2003).

49. T. Ebenhan, O. Gheysens, H. G. Kruger, J. R. Zeevaart, M. M. Sathekge, Antimicrobial Peptides: Their Role as Infection-Selective Tracers for Molecular Imaging. *BioMed Research International*. **2014**, 1–15 (2014).

50. A. Giuliani, G. Pirri, S. Nicoletto, Antimicrobial peptides: an overview of a promising class of therapeutics. *Open Life Sciences*. **2**, 1–33 (2007).

51. G. Ehrenstein, H. Lecar, Electrically gated ionic channels in lipid bilayers. *Quarterly reviews of biophysics*. **10**, 1–34 (1977).

52. W. C. Wimley, Describing the Mechanism of Antimicrobial Peptide Action with the Interfacial Activity Model. *ACS Chemical Biology*. **5**, 905–917 (2010).

53. D. Rapaport, Y. Shai, Interaction of fluorescently labeled pardaxin and its analogues with lipid bilayers. *The Journal of biological chemistry*. **266**, 23769–75 (1991).

54. Y. Shai, D. Bach, A. Yanovsky, Channel formation properties of synthetic pardaxin and analogues. *The Journal of biological chemistry*. **265**, 20202–9 (1990).

55. K. A. Brogden, Antimicrobial peptides: pore formers or metabolic inhibitors in bacteria? *Nature Reviews Microbiology*. **3**, 238–250 (2005).

56. T.-H. Lee, K. N. Hall, M.-I. Aguilar, Antimicrobial Peptide Structure and Mechanism of Action: A Focus on the Role of Membrane Structure. *Current topics in medicinal chemistry*. **16**, 25–39 (2016).

57. Y. Shai, Mode of action of membrane active antimicrobial peptides. *Biopolymers*. **66**, 236–248 (2002).

58. A. Rozek, C. L. Friedrich, R. E. Hancock, Structure of the bovine antimicrobial peptide indolicidin bound to dodecylphosphocholine and sodium dodecyl sulfate micelles. *Biochemistry*. **39**, 15765–74 (2000).

59. N. Sitaram, R. Nagaraj, Interaction of antimicrobial peptides with biological and model membranes: structural and charge requirements for activity. *Biochimica et biophysica acta*. **1462**, 29–54 (1999).

60. D. Wade, A. Boman, B. Wåhlin, C. M. Drain, D. Andreu, H. G. Boman, R. B. Merrifield, All-D amino acid-containing channel-forming antibiotic peptides. *Proceedings of the National Academy of Sciences of the United States of America*. **87**, 4761–5 (1990).

61. C. B. Park, H. S. Kim, S. C. Kim, Mechanism of Action of the Antimicrobial Peptide Buforin II: Buforin II Kills Microorganisms by Penetrating the Cell Membrane and Inhibiting Cellular Functions. *Biochemical and Biophysical Research Communications*. **244**, 253–257 (1998).

62. D. Münch, H.-G. Sahl, Structural variations of the cell wall precursor lipid II in Gram-positive bacteria — Impact on binding and efficacy of antimicrobial peptides. *Biochimica et Biophysica Acta (BBA) - Biomembranes*. **1848**, 3062–3071 (2015).

63. A. L. Hilchie, K. Wuerth, R. E. W. Hancock, Immune modulation by multifaceted cationic host defense (antimicrobial) peptides. *Nature Chemical Biology*. **9**, 761–768 (2013).

64. N. J. Afacan, A. T. Y. Yeung, O. M. Pena, R. E. W. Hancock, Therapeutic potential of host defense peptides in antibiotic-resistant infections. *Current pharmaceutical design*. **18**, 807–19 (2012).

65. J. S. Mader, D. W. Hoskin, Cationic antimicrobial peptides as novel cytotoxic agents for cancer treatment. *Expert Opinion on Investigational Drugs*. **15**, 933–946 (2006).

66. H. Jenssen, P. Hamill, R. E. W. Hancock, Peptide Antimicrobial Agents. *Clinical Microbiology Reviews*. **19**, 491–511 (2006).

67. D. I. Andersson, D. Hughes, J. Z. Kubicek-Sutherland, Mechanisms and consequences of bacterial resistance to antimicrobial peptides. *Drug Resistance Updates*. **26**, 43–57 (2016).

68. M. Vaara, New approaches in peptide antibiotics. *Current Opinion in Pharmacology*. **9**, 571–576 (2009).

69. Y. Zhao, M. Zhang, S. Qiu, J. Wang, J. Peng, P. Zhao, R. Zhu, H. Wang, Y. Li, K. Wang, W. Yan, R. Wang, Antimicrobial activity and stability of the d-amino acid substituted derivatives of antimicrobial peptide polybia-MPI. *AMB Express*. **6**, 122 (2016).

70. J. Kindrachuk, E. Scruten, S. Attah-Poku, K. Bell, A. Potter, L. A. Babiuk, P. J. Griebel, S. Napper, Stability, toxicity, and biological activity of host defense peptide BMAP28 and its inversed and retro-inversed isomers. *Biopolymers*. **96**, 14–24 (2011).

71. C. Falciani, L. Lozzi, S. Pollini, V. Luca, V. Carnicelli, J. Brunetti, B. Lelli, S. Bindi, S. Scali, A. Di Giulio, G. M. Rossolini, M. L. Mangoni, L. Bracci, A. Pini, Isomerization of an Antimicrobial Peptide Broadens Antimicrobial Spectrum to Gram-Positive Bacterial Pathogens. *PLoS ONE*. **7**, e46259 (2012).

72. N. Berthold, P. Czihal, S. Fritsche, U. Sauer, G. Schiffer, D. Knappe, G. Alber, R. Hoffmann, Novel Apidaecin 1b Analogs with Superior Serum Stabilities for Treatment of Infections by Gram-Negative Pathogens. *Antimicrobial Agents and Chemotherapy*. **57**, 402–409 (2013).

73. E. A. Papanastasiou, Q. Hua, A. Sandouk, U. H. Son, A. J. Christenson, M. L. Van Hoek, B. M. Bishop, Role of acetylation and charge in antimicrobial peptides based on human β-defensin-3. *APMIS*. **117**, 492–499 (2009).

74. D. S. Jayawardene, C. Dass, The effect of N-terminal acetylation and the inhibition activity of acetylated enkephalins on the aminopeptidase M-catalyzed hydrolysis of enkephalins☆. *Peptides*. **20**, 963–970 (1999).

75. L. T. Nguyen, J. K. Chau, N. A. Perry, L. de Boer, S. A. J. Zaat, H. J. Vogel, Serum Stabilities of Short Tryptophan- and Arginine-Rich Antimicrobial Peptide Analogs. *PLoS ONE*. **5**, e12684 (2010).

76. B. Liu, W. Zhang, S. Gou, H. Huang, J. Yao, Z. Yang, H. Liu, C. Zhong, B. Liu, J. Ni, R. Wang, Intramolecular cyclization of the antimicrobial peptide Polybia-MPI with triazole stapling: influence on stability and bioactivity. *Journal of Peptide Science*. **23**, 824–832 (2017).

77. K. Andreev, M. W. Martynowycz, A. Ivankin, M. L. Huang, I. Kuzmenko, M. Meron, B. Lin, K. Kirshenbaum, D. Gidalevitz, Cyclization Improves Membrane Permeation by Antimicrobial Peptoids. *Langmuir*. **32**, 12905–12913 (2016).

78. R. Nordström, M. Malmsten, Delivery systems for antimicrobial peptides. *Advances in Colloid and Interface Science*. **242**, 17–34 (2017).

79. P. Urbán, J. J. Valle-Delgado, E. Moles, J. Marques, C. Díez, X. Fernàndez-Busquets, Nanotools for the delivery of antimicrobial peptides. *Current drug targets*. **13**, 1158–72 (2012).

80. F. Milletti, Cell-penetrating peptides: classes, origin, and current landscape. *Drug Discovery Today*. **17**, 850–860 (2012).

81. C. Bechara, M. Pallerla, Y. Zaltsman, F. Burlina, I. D. Alves, O. Lequin, S. Sagan, Tryptophan within basic peptide sequences triggers glycosaminoglycan-dependent endocytosis. *The FASEB Journal*. **27**, 738–749 (2013).

82. H. B. Albada, A.-I. Chiriac, M. Wenzel, M. Penkova, J. E. Bandow, H.-G. Sahl, N. Metzler-Nolte, Modulating the activity of short arginine-tryptophan containing antibacterial peptides with N-terminal metallocenoyl groups. *Beilstein Journal of Organic Chemistry*. **8**, 1753–1764 (2012).

83. J. T. Staley, A. Konopka, Measurement of in Situ Activities of Nonphotosynthetic Microorganisms in Aquatic and Terrestrial Habitats. *Annual Review of Microbiology*. **39**, 321–346 (1985).

84. H. Winterberg, Zur Methodik der Bakterienzählung. *Zeitschrift für Hygiene und Infectionskrankheiten*. **29**, 75–93 (1898).

85. T. Kaeberlein, K. Lewis, S. S. Epstein, Isolating "Uncultivable" Microorganisms in Pure Culture in a Simulated Natural Environment. *Science*. **296** (2002).

86. A. D'Onofrio, J. M. Crawford, E. J. Stewart, K. Witt, E. Gavrish, S. Epstein, J. Clardy, K. Lewis, Siderophores from neighboring organisms promote the growth of uncultured bacteria. *Chemistry & biology*. **17**, 254–64 (2010).

87. J. H. Crosa, C. T. Walsh, Genetics and assembly line enzymology of siderophore biosynthesis in bacteria. *Microbiology and molecular biology reviews : MMBR*. **66**, 223–49 (2002).

88. J. B. Neilands, Siderophores: structure and function of microbial iron transport compounds. *The Journal of biological chemistry*. **270**, 26723–6 (1995).

89. C. Wandersman, P. Delepelaire, Bacterial iron sources: from siderophores to hemophores. *Annual review of microbiology*. **58**, 611–47 (2004).

90. D. Nichols, N. Cahoon, E. M. Trakhtenberg, L. Pham, A. Mehta, A. Belanger, T. Kanigan, K. Lewis, S. S. Epstein, Use of ichip for high-throughput in situ cultivation of "uncultivable" microbial species. *Applied and environmental microbiology*. **76**, 2445–50 (2010).

91. P. Marfey, Determination ofD-amino acids. II. Use of a bifunctional reagent, 1,5-difluoro-2,4-dinitrobenzene. *Carlsberg Research Communications*. **49**, 591–596 (1984).

92. C. B'Hymer, M. Montes-Bayon, J. A. Caruso, Marfey's reagent: Past, present, and future uses of 1-fluoro-2,4-dinitrophenyl-5-L-alanine amide. *Journal of Separation Science*. **26**, 7–19 (2003).

93. R. Bhushan, H. Brückner, Use of Marfey's reagent and analogs for chiral amino acid analysis: Assessment and applications to natural products and biological systems. *Journal of Chromatography B*. **879**, 3148–3161 (2011).

94. D. J. Atkinson, B. J. Naysmith, D. P. Furkert, M. A. Brimble, Enduracididine, a rare amino acid component of peptide antibiotics: Natural products and synthesis. *Beilstein Journal of Organic Chemistry*. **12**, 2325–2342 (2016).

95. C. Rafaluk, G. Jansen, H. Schulenburg, G. Joop, When experimental selection for virulence leads to loss of virulence. *Trends in Parasitology*. **31**, 426–434 (2015).

96. C. Walsh, Vancomycin resistance: decoding the molecular logic. *Science*. **261**, 308–309 (1993).

97. T. D. H. Bugg, Bacterial Peptidoglycan Biosynthesis and its Inhibition. *Comprehensive Natural Products Chemistry*, 241–294 (1999).

98. A. L. Lovering, S. S. Safadi, N. C. J. Strynadka, Structural Perspective of Peptidoglycan Biosynthesis and Assembly. *Annual Review of Biochemistry*. **81**, 451–478 (2012).

99. E. Z. Baum, D. A. Montenegro, L. Licata, I. Turchi, G. C. Webb, B. D. Foleno, K. Bush, Identification and characterization of new inhibitors of the Escherichia coli MurA enzyme. *Antimicrobial agents and chemotherapy*. **45**, 3182–8 (2001).

100. W. Du, J. R. Brown, D. R. Sylvester, J. Huang, A. F. Chalker, C. Y. So, D. J. Holmes, D. J. Payne, N. G. Wallis, Two active forms of UDP-N-acetylglucosamine enolpyruvyl transferase in gram-positive bacteria. *Journal of bacteriology*. **182**, 4146–52 (2000).

101. T. D. H. Bugg, D. Braddick, C. G. Dowson, D. I. Roper, Bacterial cell wall assembly: still an attractive antibacterial target. *Trends in Biotechnology*. **29**, 167–173 (2011).

102. T. Mohammadi, V. van Dam, R. Sijbrandi, T. Vernet, A. Zapun, A. Bouhss, M. Diepeveen-de Bruin, M. Nguyen-Distèche, B. de Kruijff, E. Breukink, Identification of FtsW as a transporter of lipid-linked cell wall precursors across the membrane. *The EMBO Journal*. **30**, 1425–1432 (2011).

103. H. Barreteau, A. Kovač, A. Boniface, M. Sova, S. Gobec, D. Blanot, Cytoplasmic steps of peptidoglycan biosynthesis. *FEMS Microbiology Reviews*. **32**, 168–207 (2008).

104. A. Bouhss, A. E. Trunkfield, T. D. H. Bugg, D. Mengin-Lecreulx, The biosynthesis of peptidoglycan lipid-linked intermediates. *FEMS Microbiology Reviews*. **32**, 208–233 (2008).

105. K. Schirner, Y.-J. Eun, M. Dion, Y. Luo, J. D. Helmann, E. C. Garner, S. Walker, Lipid-linked cell wall precursors regulate membrane association of bacterial actin MreB. *Nature chemical biology*. **11**, 38–45 (2015).

106. W. Vollmer, U. Bertsche, Murein (peptidoglycan) structure, architecture and biosynthesis in Escherichia coli. *Biochimica et Biophysica Acta (BBA) - Biomembranes*. **1778**, 1714–1734 (2008).

107. R. T. Gale, E. D. Brown, New chemical tools to probe cell wall biosynthesis in bacteria. *Current Opinion in Microbiology*. **27**, 69–77 (2015).

108. T. D. H. Bugg, G. D. Wright, S. Dutka-Malen, M. Arthur, P. Courvalin, C. T. Walsh, Molecular basis for vancomycin resistance in Enterococcus faecium BM4147: biosynthesis of a depsipeptide peptidoglycan precursor by vancomycin resistance proteins VanH and VanA. *Biochemistry*. **30**, 10408–10415 (1991).

109. J. Xie, J. G. Pierce, R. C. James, A. Okano, D. L. Boger, A Redesigned Vancomycin Engineered for Dual d -Ala- d -Ala and d -Ala- d -Lac Binding Exhibits Potent Antimicrobial Activity Against Vancomycin-Resistant Bacteria. *Journal of the American Chemical Society*. **133**, 13946–13949 (2011).

110. S. Tsuji, S. Kusumoto, T. Shiba, Synthesis of enduracididine, a component amino acid of antibiotic enduracidin. *Chemistry Letters*. **4**, 1281–1284 (1975).

111. L. Sanière, L. Leman, J.-J. Bourguignon, P. Dauban, R. H. Dodd, Iminoiodane mediated aziridination of α-allylglycine: access to a novel rigid arginine derivative and to the natural amino acid enduracididine. *Tetrahedron*. **60**, 5889–5897 (2004).

112. D. E. Olson, J. Y. Su, D. A. Roberts, J. Du Bois, Vicinal Diamination of Alkenes under Rh-Catalysis. *Journal of the American Chemical Society*. **136**, 13506–13509 (2014).

113. W. Craig, J. Chen, D. Richardson, R. Thorpe, Y. Yuan, A Highly Stereoselective and Scalable Synthesis of l -allo-Enduracididine. *Organic Letters*. **17**, 4620–4623 (2015).

114. J. Rudolph, F. Hannig, H. Theis, R. Wischnat, Highly efficient chiral-pool synthesis of (2S,4R)-4-hydroxyornithine. *Organic Letters*. **3**, 3153–3155 (2001).

115. A. M. Giltrap, L. J. Dowman, G. Nagalingam, J. L. Ochoa, R. G. Linington, W. J. Britton, R. J. Payne, Total Synthesis of Teixobactin. *Organic Letters*. **18**, 2788–2791 (2016).

116. L. Liu, S. Wu, Q. Wang, M. Zhang, B. Wang, G. He, G. Chen, Total synthesis of teixobactin and its stereoisomers. *Organic Chemistry Frontiers*. **5**, 1431–1435 (2018).

117. K. Jin, I. H. Sam, K. H. L. Po, D. Lin, E. H. Ghazvini Zadeh, S. Chen, Y. Yuan, X. Li, Total synthesis of teixobactin. *Nature Communications*. **7**, 12394 (2016).

118. F. García-Martín, M. Quintanar-Audelo, Y. García-Ramos, L. J. Cruz, C. Gravel, R. Furic, S. Côté, A. Judit Tulla-Puche, F. Albericio, ChemMatrix, a Poly(ethylene glycol)-Based Support for the Solid-Phase Synthesis of Complex Peptides (2006), doi:10.1021/CC0600019.

119. Y. Zhang, C. Xu, H. Y. Lam, C. L. Lee, X. Li, Protein chemical synthesis by serine and threonine ligation. *Proceedings of the National Academy of Sciences of the United States of America*. **110**, 6657–62 (2013).

120. S. Dhara, V. B. Gunjal, K. L. Handore, D. Srinivasa Reddy, Solution-Phase Synthesis of the Macrocyclic Core of Teixobactin. *European Journal of Organic Chemistry*. **2016**, 4289–4293 (2016).

CHAPTER 2

2 Efficient total syntheses and biological activities of two teixobactin analogues

COMMUNICATION

View Article Online
View Journal | View Issue

CrossMark click for updates

Cite this: *Chem. Commun.*, 2016, 52, 6060

Received 13th December 2015,
Accepted 9th March 2016

DOI: 10.1039/c5cc10249a

Efficient total syntheses and biological activities of two teixobactin analogues†

Anish Parmar,[a] Abhishek Iyer,[ab] Charlotte S. Vincent,[c] Dorien Van Lysebetten,[b] Stephen H. Prior,[d] Annemieke Madder,[b] Edward J. Taylor*[c] and Ishwar Singh*[a]

Author contributions: All the building block synthesis, peptide synthesis for the analogues, optimisations, purifications and sample preparation for either mass analysis/NMR has been done by me. The initial drafting of the manuscript and supplementary information has been done by me with inputs from Abhishek Iyer. The antibacterial study has been carried out by Charlotte S. Vincent and Edward J. Taylor. Dorien Van Lysebetten and Annemieke Madder were responsible for running the mass analysis. Stephen H.Prior carried out and analysed the NMR experiments. Ishwar Singh conceived and designed the project.

2.1 Abstract

The discovery of the new antibiotic teixobactin has been timely in the race for unearthing novel antibiotics wherein the emergence of drug resistance bacteria poses a serious threat worldwide. Herein, we present the total syntheses and biological activities of two teixobactin analogues. This approach is simple, efficient and has several advantages: it uses commercially available building blocks, has a single purification step and a good recovery (22%). By using this approach we have synthesised two teixobactin analogues and established that the $_D$*-amino acids are critical for the antimicrobial activity of these analogues. With continuing high expectations from teixobactin, this work can be regarded as a stepping stone towards an in-depth study of teixobactin, its analogues and the quest for synthesising similar molecules.*

2.2 Brief Inroduction

The decreased potency of antibiotics such as penicillin **1.4**,[1] vancomycin **1.12**[2] and oxacillin[3] due to their excessive use is a consequence of the emergence of drug resistant bacteria. It has been predicted that antimicrobial resistance (AMR) will have disastrous consequences and it is estimated that by 2050 an additional 10 million people yearly could succumb to drug resistant infections.[4] The recently published article[5] describing the discovery of teixobactin **1.23** has provided a much needed breakthrough in the challenging field of antibiotic peptides. There has been no detectable resistance reported against **1.23**. Moreover, given the multiple mechanisms of attack by teixobactin **1.23** described by Süssmuth[6] resistance is less likely in the near future. Unfortunately, although teixobactin **1.23** provides some much needed answers, the problem is far from over. Organic chemists have worked round the clock to synthesise novel antibiotics and although progress has been steady, bacteria have time and again confounded even the best in this field.[7] This is where the multichannel device, iChip,[8] has made a considerable contribution enabling the identification of molecules like **1.23**, some of which could be active against drug resistant bacteria. However, the iChip device has its limitations. The probability of finding an antibiotic is extremely low (10^{-7} percent) and even with high-throughput screening, which takes considerable time and resources, there is no guarantee when the discovery of the next drug like teixobactin **1.23** will be. Undeniably, breakthroughs via organic synthesis have to be made to keep the drug resistance problem under check. The time for this is indeed now and teixobactin is a good starting point.

2.3 Aim of study

Teixobactin is a single potent molecule that has been produced by a bacterium and it is very rare a single molecule from the drug discovery phase will reach regulatory approval due to the high attrition rate in the drug development process. To realise the therapeutic potential of teixobactin, there is need for developing synthesis of teixobactin analogues. This study is aimed at a general approach through which, not only teixobactin but also other analogues can be synthesised. The synthetic approach will give access to analogues which nature cannot provide us with and therefore an organic synthesis approach to the bigger problem at hand should not be prematurely discarded. Moreover, the role of the $_{D}$-amino acids have not been proven.[9] Our work presents an efficient syntheses of both the D and L versions of the analogues of teixobactin (22% yield for **2.1**) and their role in antibacterial activity.

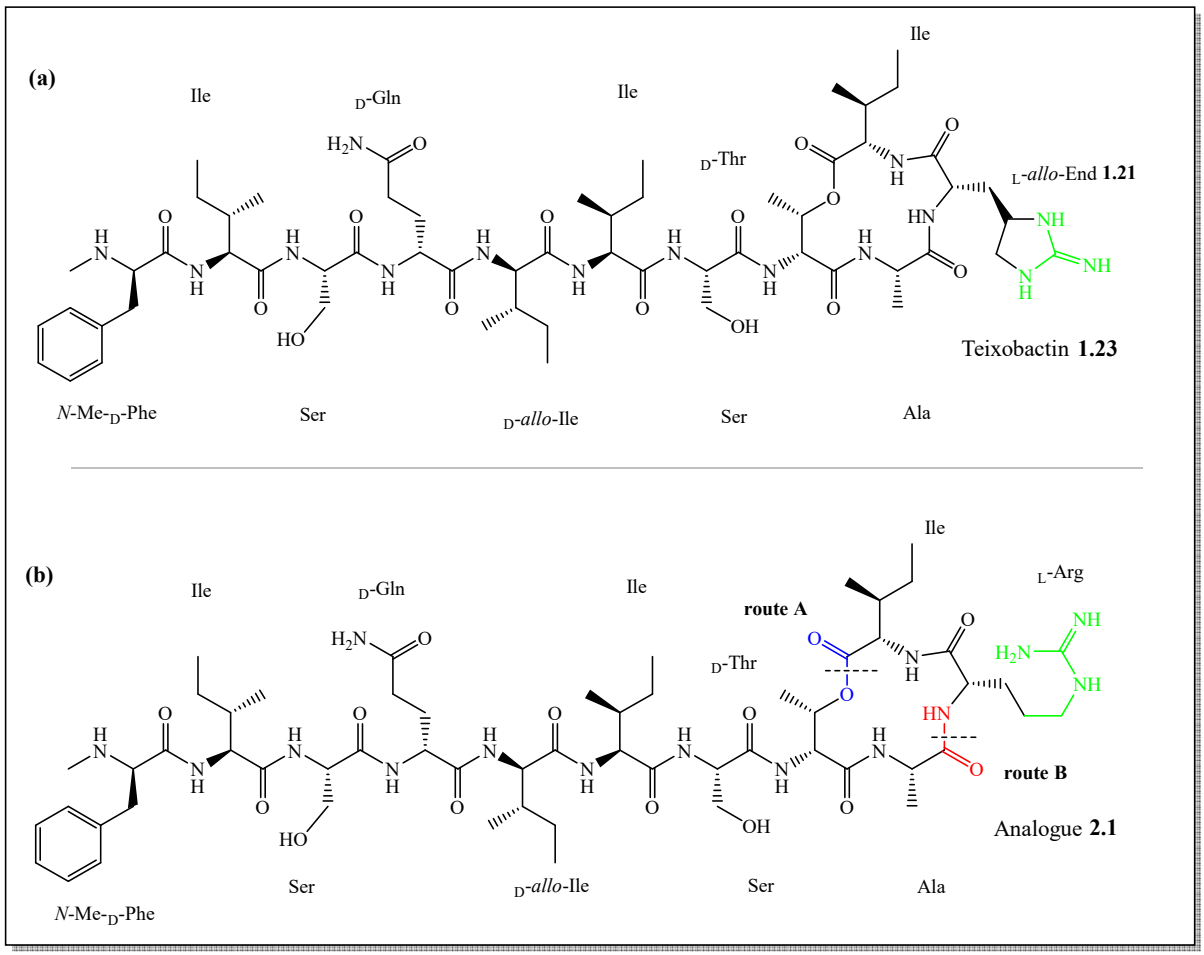

Figure 2.1: (**a**) (above) Structure of teixobactin **1.23**. (**b**) (below) Structure of the teixobactin analogue **2.1** showing the bonds to be cleaved for the synthesis routes A (in blue) and B (in red) and the structural differences (in green).

2.4 Results and discussion

Since teixobactin **1.23** has been fully characterised by NMR and LC-MS, the structural complexity of **1.23** can be described as moderate to difficult. It has also been described as an unusual depsipeptide due to the presence of the non-natural amino acids $_{L}$-*allo*-End$_{10}$ **1.21** and *N*-Me-$_{D}$-Phe$_{1}$ along with four $_{D}$-amino acids (Figure 2.1). Despite not possessing a lipid tail, the commercial unavailability of the amino acid **1.21** makes the total synthesis of **1.23** more time consuming than expected.[10]

The commercially available natural amino acid arginine (a linear guanidine) is the closest structural match suitable for the replacement of the **1.21** (a cyclic guanidine) as can be seen in Figure 2.1 (green). In this work, arginine was selected as a replacement of $_{L}$-*allo*-End$_{10}$ **1.21** for synthesis of Arg$_{10}$-teixobactin **2.1**.

2.4.1 Cyclisation *via* ester bond

A first approach towards tackling this molecule was to synthesise the complete peptide on solid phase and cyclise post-cleavage from the resin *via* an ester bond (Figure 2.2). This route has been previously used with success for the synthesis of the analogues of callipeltin B.[11]

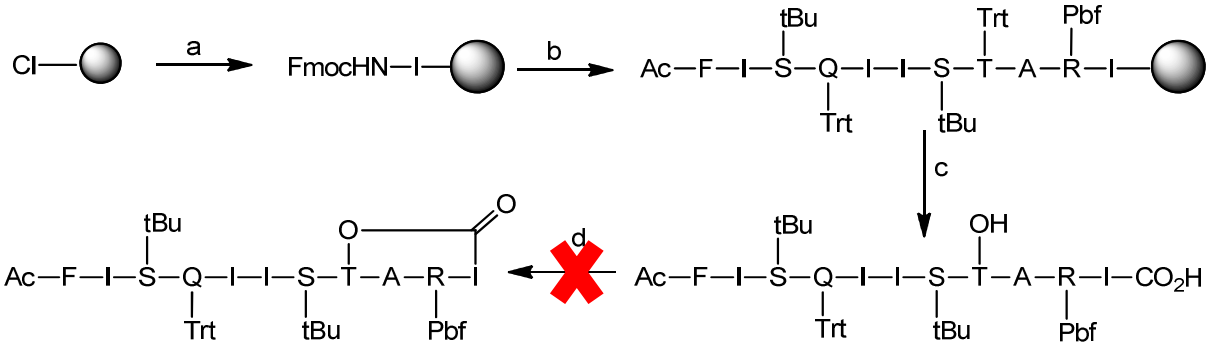

Figure 2.2: Scheme showing the attempted synthesis of the teixobactin analogue via route A

Briefly, commercially available 2-chlorotrityl (2-CTC) resin was loaded Fmoc-Ile OH (a). After loading determination, the Fmoc protecting group was removed by standard 20% piperidien in DMF and subsequent amino acids were successfully coupled using standard SPPS (b). Partial cleave with TFA:TIS:DCM (2:5:93) respectively released a fully protected peptide from the resin (c) and after solvent evaporation, several conditions for esterification (d) was tested as described in Table 2.1.

Sr. No.	Reagents	Solvent	Duration	Temperature
1.	1.2 eq. DCC/5 eq. DMAP	DMF	24h	r.t.
2.	2 eq. DCC + 1 eq. after 4h /5 eq. DMAP	DMF	24h	r.t.
3.	3 eq. DCC/20 mol% DMAP	DMF	2h	r.t
4.	1.2 eq. MNBA/2.4 eq. DMAP	DMF	12h	r.t.
5.	2.5 eq. EDCI/0.5 eq. DMAP	DMF	24h	r.t.
6.	18 eq. DCC/28 eq. DMAP	DMF	30 min, 6h	0-4 deg., r.t
7.	1.2 DCC/6 eq. DMAP	DMF	24h	60, heating
8.	1.2 eq. DIC/6 eq. DMAP	DMF	24h	60, heating

[*]**Table 2.1**: Esterfication conditions for cyclisation.

Unfortunately, none of them yielded the esterified product. This could be due to the steric bulk of protecting groups on the amino acids. This led to the conclusion that a direct and linear route is not the way to cyclisation.

[*]Diisoproplycarbodiimide (DIC), Dicyclohexylcarbodiimide (DCC) 2-methyl-6-nitrobenzoic anhydride (MNBA), 1-Ethyl-3-(3-dimethylaminopropyl)carbodiimide (EDC/EDCI) Hydrochloride, Diisopropylethylamine (DIPEA), Dimethyl-aminopyridine (DMAP)

2.4.2 Cyclisation *via* amide bond

2.4.2.1 Fragment (core ring) cyclisation

A new second synthetic route had been devised which involves cyclisation *via* amide bond formation (Figure 2.1, route B). For the total synthesis of **2.1**, an optimised pathway for the synthesis of the core ring structure (Figure 2.3, **2.2**) of teixobactin was required. Therefore, the initial efforts were focussed on obtaining this key fragment (Figure 2.3).

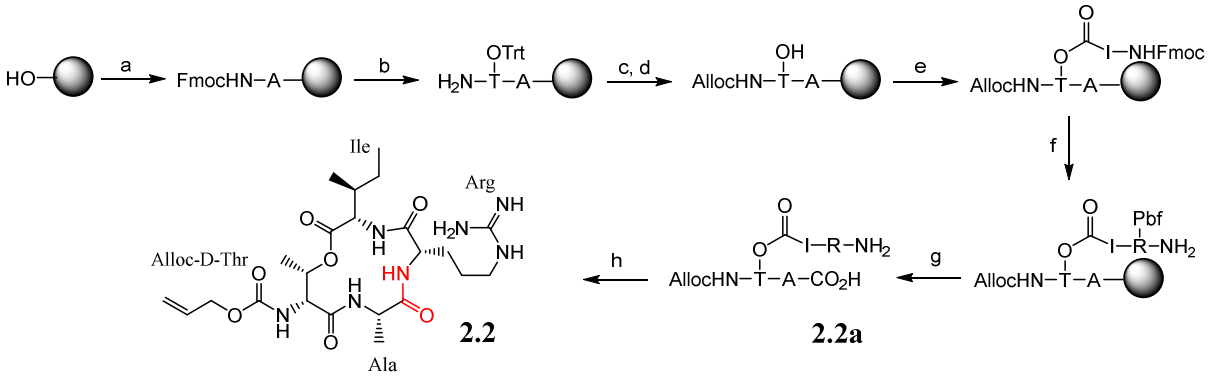

Figure 2.3: Synthesis scheme for the core teixobactin fragment 3 starting from Wang resin: a. 10 eq. Fmoc-Ala-OH, 10 eq. DIC, 1 eq. DMAP followed by 10% Ac_2O/DIPEA in DMF. b. 2.5 eq. Fmoc-D-Thr(Trt)-OH, 2.5 HATU/5 eq. DIPEA, 3h DMF followed by 20% piperidine in DMF. c. 4 eq. Allyl Chloroformate/8 eq. DIPEA in DCM, 1h. d. 1:5:96 TFA:TIS:DCM. 3 x 15 min. e. 10 eq. Fmoc-Ile-OH, 10 eq. DIC, 10 mol% DMAP in DCM, 2h followed by 10% Ac_2O/DIPEA in DMF, followed by 20% piperidine in DMF. f. 4 eq. Fmoc-Arg(Pbf)-OH, 4 eq. HATU/8 eq. DIPEA in DMF, 1h followed by 20% piperidine in DMF. g. TFA:TIS:H_2O = 95:2.5.2.5, 1h. h. 1 eq. HATU/10 eq. DIPEA in DMF, 1h, monitored on HPLC.

For optimisation of the synthesis, we chose Wang resin. Fmoc-Ala-OH was loaded onto this resin *via* ester bond formation. The unreacted resin was capped using 10% acetic anhydride/diisopropylethylamine (Ac_2O/DIPEA) followed by (*a*) the attachment of Fmoc-D-Thr(Trt)-OH *via* amide bond formation and subsequent (*b*) Fmoc removal. The orthogonal Alloc protecting group was installed on the amine (*c*) followed by (*d*) trityl group removal by 1:5:96 Trifluoroacetic acid/Triisopropylamine/Dichloromethane (TFA:TIS:DCM) and proceeded with (*e*) the challenging esterification reaction between Ile and Thr. It is to be noted that excess Ile and base were required to drive the reaction to completion.[12] This was succeeded by (*f*) amide bond formation using Arg and subsequent *(g)* cleavage from the resin using 95:2.5:2.5 TFA:TIS:H_2O to give **2.2a**. The final step was *(h)* the amide bond formation between Arg and Ala which proceeds smoothly yielding the desired cyclised fragment **2.2**.

2.4.2.2 Total synthesis of analogue 2.1

After the successful fragment cyclisation, the approach was then slightly modified and used for the total synthesis of **2.1** as described in Figure 2.4.

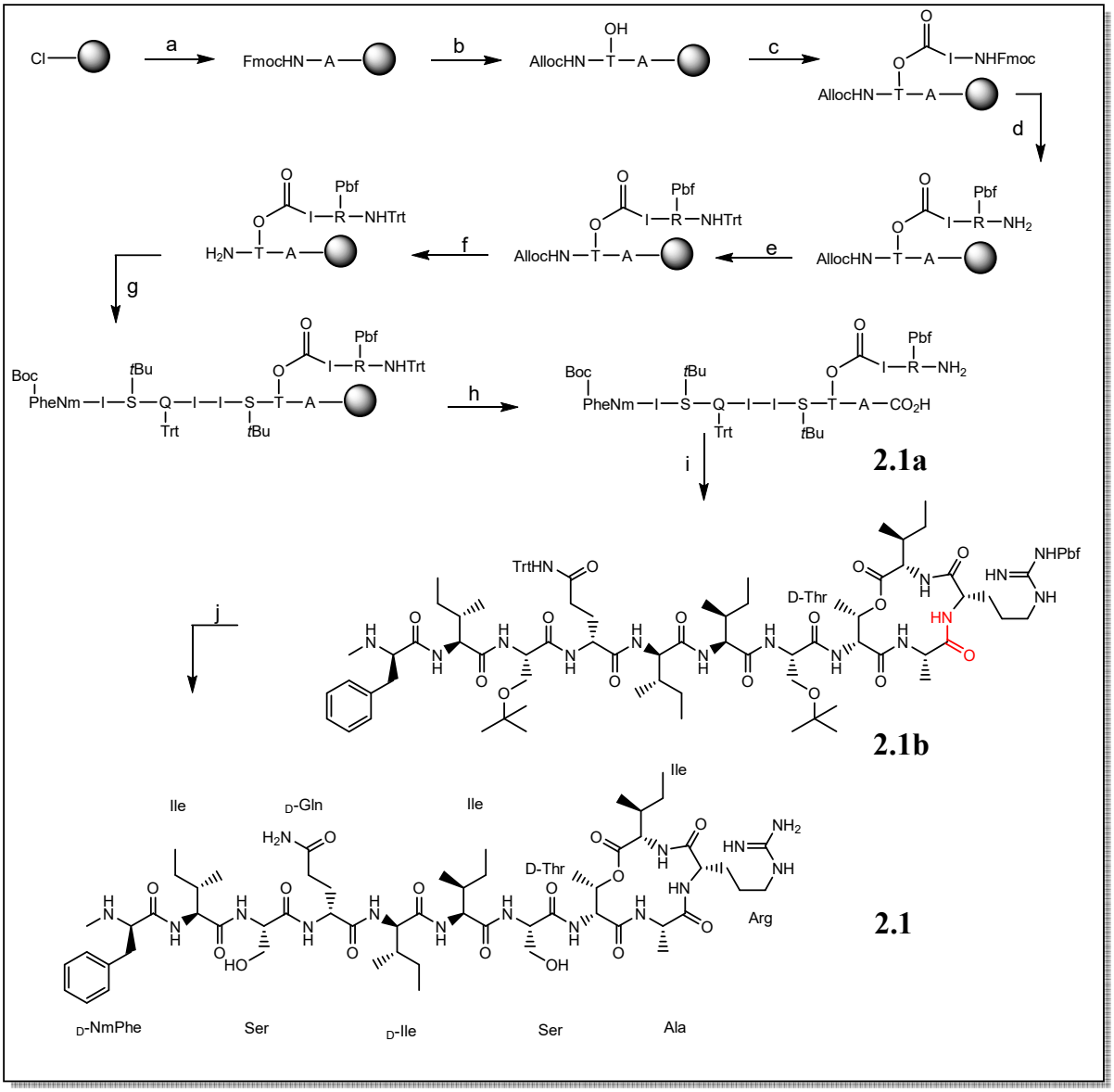

Figure 2.4: Total synthesis of **2.1** starting from 2-CTC resin: a. 4 eq. Fmoc-Ala-OH/8 eq. DIPEA in DCM, 3h. b. 20% piperidine in DMF followed by 3 eq. AllocHN-$_D$-Thr-OH **2.4**, 3 eq. HATU/6 eq. DIPEA. c. 10 eq. Fmoc-Ile-OH, 10 eq. DIC, 5 mol% DMAP in DCM, 2h followed by capping with Ac_2O/DIPEA 10% in DMF, 20% piperidine in DMF d. 4 eq. Fmoc-Arg(Pbf)-OH, 4 eq. HATU/8 eq. DIPEA in DMF, 1h followed by 20% piperidine in DMF e. 10 eq. Trt-Cl, 15% Et_3N in DCM, 1h. f. $[Pd(PPh_3)_4]^0$ (0.2 eq.) + 24 eq. $PhSiH_3$ in DCM, 2 x 1 h. g. Fmoc/Boc-AA(PG)-OH (AA = amino acid, PG = protecting group), HATU/DIPEA followed by 20% piperidine in DMF. h. TFA:TIS:DCM = 2:5:93, 2h. i. 1 eq. HATU/10 eq. DIPEA in DMF, 1h, monitored on HPLC. j. TFA:TIS:H_2O = 95:2.5:2.5, 1h.

(a) The first amino acid loaded on the resin in this case is Fmoc-Ala-OH followed by (b) an amide bond coupling with Alloc-$_D$-Thr-OH **2.4**. (c) Fmoc-Ile-OH is then coupled at this stage via an ester bond to the free –OH side chain of threonine. Next, (d) arginine was coupled *via* an amide bond, the Fmoc protecting group is removed and (e) the N-terminus is protected *via* a trityl protecting group[13] (combining cleavage and deprotection in a single step) to facilitate the cleavage and cyclisation as described in reactions h and i. (f) The alloc group protecting the N-terminus of the threonine is then removed[14] and (g) the peptide chain is built via standard Solid Phase Peptide Synthesis (SPPS). Partial cleavage was performed using 2:5:93 TFA:TIS:DCM followed by cyclization using 1-[Bis(dimethylamino) methylene]-1H-1,2,3-triazolo[4,5-b]pyridinium 3-oxid hexafluorophosphate (HATU) as a coupling reagent and DIPEA as a base in DMF for 1 hr. The protecting groups are then cleaved off using 95:2.5:2.5 TFA:TIS:H_2O yielding the desired peptide **2.1** (22% recovery).

2.4.2.3 Total synthesis of analogue 2.3

After successful synthesis of **2.1**, the general applicability of this approach was tested for the synthesis of analogue **2.3** (Figure 2.5). In **2.3**, the three $_D$-amino acids residues (Phe, Gln and Ile) were replaced by $_L$-amino acid residues. The synthesis of analogue **2.3** also worked efficiently (17% recovery).

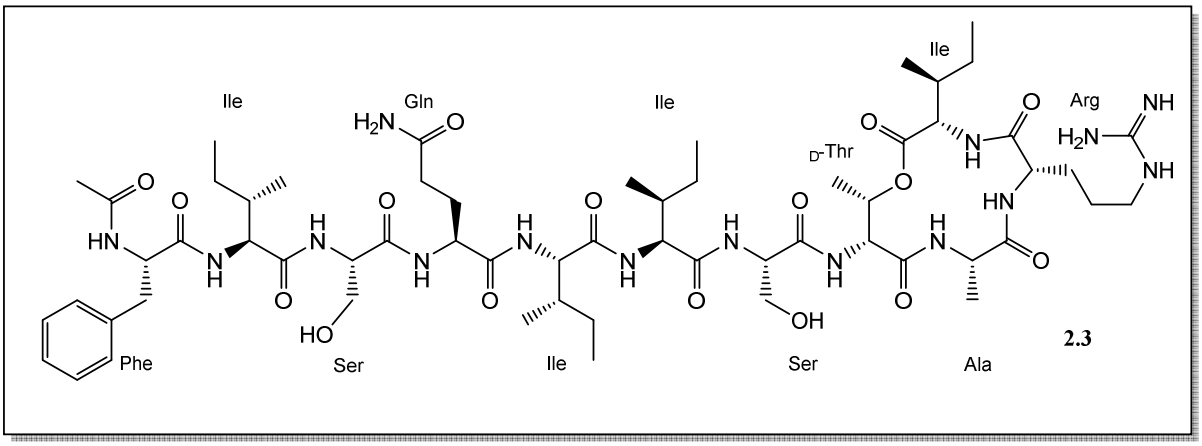

Figure 2.5: Structure of the aceytelated and $_L$-version of Arg_{10}-Teoxobactin (**2.3**).

2.4.3 Analysis and Activity

The detailed characterisation of **2.1** and **2.3** were performed using LC-MS and NMR. The NMR spectra of product **2.1** (Experimental chapter 2, section X) was shown to be identical as reported previously[5,9]. The NOEs of **2.1** were characteristic of a random coil, however, the NOEs of **2.3** suggested a considerable degree of structure.

The analogues **2.1** and **2.3** were evaluated for their antibacterial activity. MIC results showed a similar trend to teixobactin for analogue **2.1** against both Gram-positive and Gram-negative bacteria. Analogue **2.3** was not active against Gram-negative bacteria. Moreover, analogue **2.1** was 64 times more effective than analogue **2.3** (Table 2.2) against Gram-positive bacteria. This difference in

antibacterial activity has established that the three $_D$-amino acids residues of **2.1** are critical for the antibacterial activity.

Entry	Organism	2.1	2.3	Teixobactin (1.23)
1	*S. aureus* ATCC 25923	2	128	0.25*
2	*E. coli* ATCC 25922	64	GAW‡	25

Table 2.2: MIC (μg/ml) for **2.1** and **2.3** and teixobactin **1.23** (MICs from ref. 5, 0.25* were from a different strain of S. aureus). ‡Growth in all wells

2.5 Conclusion

In conclusion, this work reports efficient total syntheses of two teixobactin analogues (22% yield of teixobactin analogue **2.1**). Analogue **2.1** is identical to **1.23** in all aspects with the exception of the L-*allo*-End$_{10}$ amino acid. The methodology described here is not specific to only one molecule, but it can also be used as a general strategy for synthesis of other analogues of **1.23**. The role of three $_D$-amino acids had also been established. The three $_D$-amino acids present in the teixobactin analogue **2.1** but absent in analogue **2.3** are critical for antibacterial activity. This work also reports the synthesis of new AllocHN-$_D$-Thr-OH **2.4** building block (Experimental Chapter 2) and has incorporated it as such in the syntheses of teixobactin analogues **2.1** and **2.3**. We believe that this work to be pivotal for the synthesis of teixobactin and its analogues and therefore will be helpful to address the current challenges of antimicrobial resistance.

2.6 References

1. F. W. Goldstein, L. D. M. Médicale, F. H. Saint-joseph, R. Losserand, Leading articles. *Journal of Antimicrobial Chemotherapy*. **44**, 141–144 (1999).

2. P. Courvalin, Vancomycin Resistance in Gram-Positive Cocci. *Clinical Infectious Diseases*. **42**, 25–34 (2006).

3. J. H. Lee, Methicillin (Oxacillin)-resistant Staphylococcus aureus strains isolated from major food animals and their potential transmission to humans. *Applied and environmental microbiology*. **69**, 6489–94 (2003).

4. http://amr-review.org/, Review on Antimicrobial Resistance. *2015*.

5. L. L. Ling, T. Schneider, A. J. Peoples, A. L. Spoering, I. Engels, B. P. Conlon, A. Mueller, D. E. Hughes, S. Epstein, M. Jones, L. Lazarides, V. a Steadman, D. R. Cohen, C. R. Felix, K. A. Fetterman, W. P. Millett, A. G. Nitti, A. M. Zullo, C. Chen, K. Lewis, A new antibiotic kills pathogens without detectable resistance. *Nature*. **517**, 455–459 (2015).

6. F. von Nussbaum, R. D. Süssmuth, Multiple Attack on Bacteria by the New Antibiotic

Teixobactin. *Angewandte Chemie International Edition*. **54**, 6684–6686 (2015).

7. L. V. J. Blair, J. M. A., Webber, M. A., Baylay, A. J., Ogbolu, D. O, Piddock, Molecular mechanisms of antibiotic resistance. *Nature Reviews Microbiology*. **42**, 42–51 (2015).

8. D. Nichols, N. Cahoon, E. M. Trakhtenberg, L. Pham, a. Mehta, a. Belanger, T. Kanigan, K. Lewis, S. S. Epstein, Use of Ichip for High-Throughput In Situ Cultivation of 'Uncultivable' Microbial Species. *Applied and Environmental Microbiology*. **76**, 2445–2450 (2010).

9. Y. E. Jad, G. A. Acosta, T. Naicker, M. Ramtahal, A. El-Faham, T. Govender, H. G. Kruger, B. G. De La Torre, F. Albericio, Synthesis and Biological Evaluation of a Teixobactin Analogue. *Organic Letters*. **17**, 6182–6185 (2015).

10. W. Craig, J. Chen, D. Richardson, R. Thorpe, Y. Yuan, A Highly Stereoselective and Scalable Synthesis of l -allo-Enduracididine. *Organic Letters*. **17**, 4620–4623 (2015).

11. M. Kikuchi, Y. Watanabe, M. Tanaka, K. Akaji, H. Konno, Synthesis and cytotoxicity of the depsipeptides analogues of callipeltin B. *Bioorganic and Medicinal Chemistry Letters*. **21**, 4865–4868 (2011).

12. G. Yao, Z. Pan, C. Wu, W. Wang, L. Fang, W. Su, Efficient Synthesis and Stereochemical Revision of Coibamide A. *Journal of the American Chemical Society*. **137**, 13488–13491 (2015).

13. C. Gros, C. Boulègue, N. Galeotti, G. Niel, P. Jouin, Stereochemical control in the preparation of α-amino N-methylthiazolidine masked aldehydes used for peptide aldehydes synthesis. *Tetrahedron*. **58**, 2673–2680 (2002).

14. P. Grieco, P. M. Gitu, V. J. Hruby, Preparation of 'side-chain-to-side-chain' cyclic peptides by Allyl and Alloc strategy: Potential for library synthesis. *Journal of Peptide Research*. **57**, 250–256 (2001).

CHAPTER 3

3 Defining the molecular structure of teixobactin analogues and understanding their role in antibacterial activities

ChemComm

COMMUNICATION

View Article Online
View Journal | View Issue

Defining the molecular structure of teixobactin analogues and understanding their role in antibacterial activities†

Cite this: *Chem. Commun.*, 2017, 53, 2016

Received 29th November 2016,
Accepted 13th January 2017

DOI: 10.1039/c6cc09490b

Anish Parmar,[a] Stephen H. Prior,[b] Abhishek Iyer,[ac] Charlotte S. Vincent,[d] Dorien Van Lysebetten,[c] Eefjan Breukink,[e] Annemieke Madder,[c] Edward J. Taylor*[d] and Ishwar Singh*[a]

Author contributions: All the building block synthesis, peptide synthesis for the analogues, optimisations, purifications and sample preparation for either LC-MS analysis/NMR has been done by me. The initial drafting of the manuscript and supplementary information has been done by me with inputs from Abhishek Iyer. Stephen H. Prior carried out and analysed the NMR experiments. The antibacterial study has been carried out by Charlotte S. Vincent and Edward J. Taylor. Dorien Van Lysebetten and Annemieke Madder were responsible for the LC-MS analysis. Eefjan Breukink provided the Lipid II. The project was designed by Ishwar Singh.

3.1 Abstract

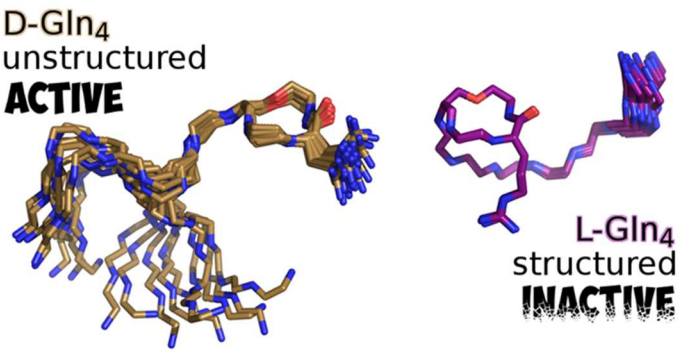

The discovery of the highly potent antibiotic teixobactin, which kills the bacteria without any detectable resistance, has stimulated interest in its structure activity relationship. While working in this project, a molecular structure-activity relationship had not yet been established so far for teixobactin. Moreover, the importance of the individual amino acids in terms of their L/D configuration and their contribution to molecular structure and biological activity was still unknown. For the first time, we have defined the molecular structure of seven teixobactin analogues through the variation of the D/L configuration of its key residues, namely N-Me-D-Phe, D-Gln, D-allo-Ile and D-Thr. Furthermore, we have established the role of the individual D-amino acids and correlated this to the molecular structure and biological activity. Through extensive NMR and structural calculations, including molecular dynamics simulations we have revealed the residues for maintaining a reasonably unstructured teixobactin which is imperative for biological activity.

3.2 Introduction

In Chapter 2, replacing the amino acid L-*allo*-End$_{10}$ **1.21** with its structurally closest natural amino acid arginine leads to an efficient Arg$_{10}$-teixobactin **2.1** synthesis. **2.1** follows a similar antibacterial activity trend as teixobactin **1.23** (Figure 3.1).[1,2,3,4] Therefore, conclusions drawn by synthesising analogues of **2.1** derivatives should hold true for teixobactin as well.

Teixobactin **1.23** contains 11 amino acids, out of which 4 are D-amino acids, namely *N*-Me-D-Phe$_1$, D-Gln$_4$, D-allo-Ile$_5$ and D-Thr$_8$ (Figure 3.1, marked in red). Peptides containing more D-amino acids are generally less susceptible to enzymatic degradation[5] which may well be applicable for teixobactin.[6] In my previous chapter,[3] we had already established the importance of the D-amino acids through the total synthesis of both D and L analogues of teixobactin (**2.1** and **2.3** respectively). Replacing the D-amino acids with their corresponding L-configurations (except D-Thr$_8$) results in a 64-times decrease in antibacterial activity against *S. aureus*.

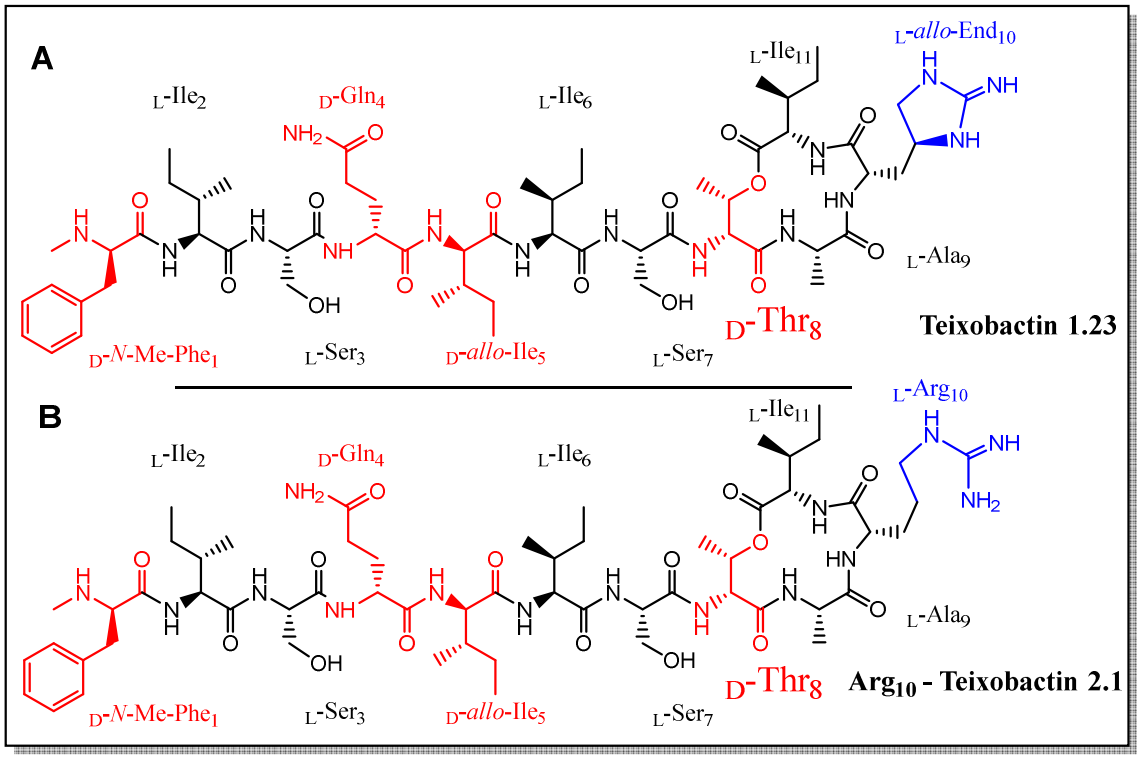

Figure 3.1: Structure of (**A**) Teixobactin (**1.23**) and (**B**) Teixobactin-Arg$_{10}$ (**2.1**) with the D-amino acids highlighted in *red* and the structural differences marked in *blue*.

3.3 †Aim of study

It is not yet known, however, if a molecular structure (three- dimensional structure)-activity relationship exists for teixobactin **1.23**. To date, except for the structural deduction of **1.23** published by Ling et. al.,[6] no molecular structural studies on teixobactin or its analogues have been reported. Moreover, the impact on the molecular structure and activity of teixobactin by varying individual amino acids in terms of their L/D configuration is still unknown. This study aims to explain why $_{L}$-analogues of teixobactin are not active. We have selected the systematic replacement of $_{D}$-amino acid residues with L configurations to understand the minimum number of $_{D}$-amino acid residues required for biological activity. Furthermore, the low cost of $_{L}$-amino acids was expected to lower the financial constraint on teixobactin development. For the first time, we have the determined molecular structures of seven teixobactin derivatives by changing D/L configurations from NMR, their antibacterial activity and lipid II binding. The results from our work will enable the better understanding of molecular structure-activity relationship of teixobactins and their further development as drug like molecules.

3.4 Results and discussion

Through this work, we investigate the role of each of the $_{D}$-amino acids, their impact on the molecular structure and activity of teixobactin and whether there exists a structure-activity relationship for the molecule. Through the syntheses of seven analogues of **2.1** (Table 3.1), followed by extensive NMR and structural calculations we have shown the importance of the $_{D}$-amino acids on the structure and activity of teixobactin analogues.

3.4.1 Structure-activity relationships (SAR) of LLLL and DDDD

Our initial efforts were focused towards understanding the pivotal role played by the stereochemistry of $_{D}$-Thr$_{8}$ upon the gross structure of **1.23**. This was achieved through the synthesis of analogue **2.1^{2}** (LLLL) and subsequent comparison with analogue **2.1^{1}** (DDDD, Figure 3.2). Outside the cyclic region encompassing residues 8 to 11 the peptide is largely unstructured (Figure 3.2A). The altered topological environment available to the analogue **2.1^{2}** (LLLL) makes it energetically favourable to adopt a well-defined hairpin structure (Figure 3.2B).

† When this work was conducted, no previous structure-activity relationship had been performed. All analogues in this chapter are derived from Arg$_{10}$-teixobactin (**2.1 or 2.1^{1}**). To avoid confusion to the reader, in most cases the code of the analogue (e.g. DDDD or LDDD) will also be heavily utilised in this chapter.

Analogue No.	Code	Configuration of Amino Acids				
		N-Me-Phe$_1$	Gln$_4$	Ile$_5$	Thr$_8$	MIC[†]
2.1 or 2.1[1]	DDDD	D	D	D	D	2
2.1[2]	LLLL	L	L	L	L	GAW[‡]
2.1[3]	DDLD	D	D	L	D	GAW
2.1[4]	DLDD	D	L	D	D	GAW
2.1[5]	LDDD	L	D	D	D	32-64
2.1[6]	LLDD	L	L	D	D	GAW
2.1[7]	LLLD*	L	L	L	D	128

Table 3.1: List of analogues of Arg10-teixobactin **2.1** synthesised by varying the D/L configuration of the key residues *N*-Me-$_D$-Phe$_1$, $_D$-Gln$_4$, $_D$-*allo*-Ile$_5$ and $_D$-Thr$_8$.[†] MIC values were measured against S. aureus and are given in µg/mL. [‡] Growth in all wells. *This analogue contains an acetylated Phe$_1$ instead of an *N*-Me-Phe$_1$ residue.

3.4.2 Root-Mean square deviation (RMSD) of teixobactin analogues to determine SAR

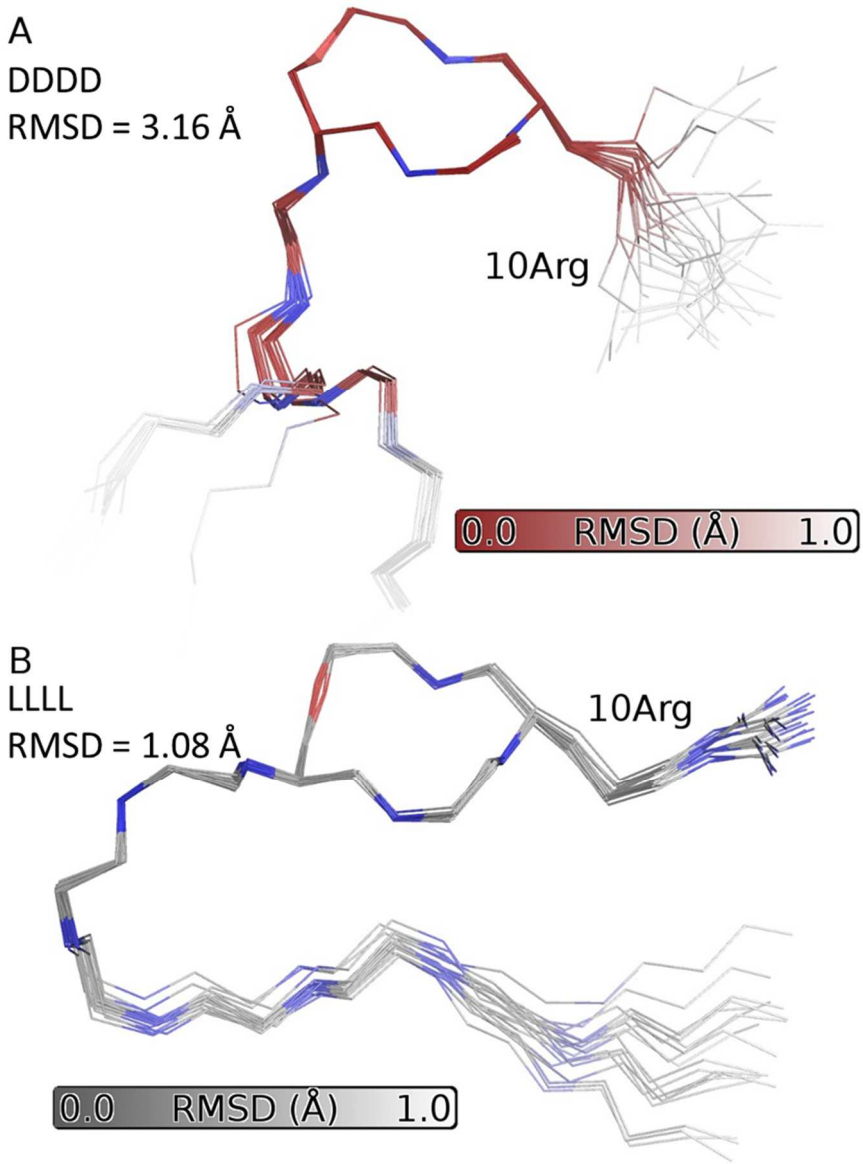

Figure 3.2: A. Structure of teixobactin analogue **2.1[1]** (DDDD) exhibiting native stereochemistry. B. Structure of analogue **2.1[2]** (LLLL) containing $_L$-Thr$_8$. Overlays of the 20 lowest energy structures aligned to the backbone atoms of the cyclic region are displayed. Atoms are colored according to their RMSD, fading to white at higher

RMSD. Atom transparency also increases with RMSD, with more highly disordered regions fading to invisibility. For clarity, only backbone atoms and the non-hydrogen atoms of Arg_{10} are displayed.

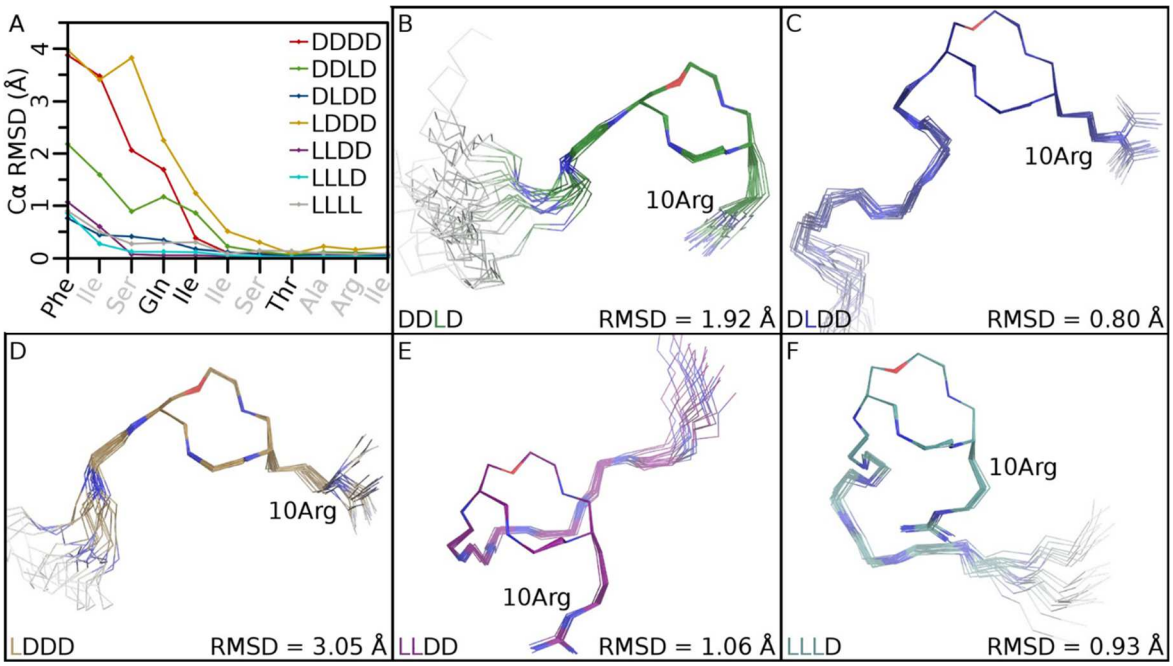

Figure 3.3: Effect of stereochemistry at different positions on the structure of teixobactin analogues. A. Majority of variation observed in structural ensembles accounted for by varying levels of disorder in the N-terminal residues. Positions labelled in black type have had their stereochemistry altered. The name of the analogues is as described in Table 3.1. (B-F) Backbone traces of 20 lowest energy structures aligned to the backbone atoms of the cyclic region. Atom colour and transparency as in Figure 3.2.

The teixobactin analogues routinely gave spectra of the highest quality (Figure S3.16), which made complete atomic assignment of each analogue possible (Table S3.2). Subsequent measurement of dipolar correlations allowed for full structural characterisation. The number of visible NOE cross-peaks (Figure S3.16) varied with different analogues: those with $_{D}$-Gln_4 (for example Figure S3.16 red contours) contained very few medium- and long-range correlations, which is typical for highly dynamic, unstructured peptides in which nuclei are seldom in close enough proximity for NOE build-up to occur. This flexibility is reflected in their high RMSD (Figure 3.2A, Figure 3.3, Table S3.3).

In contrast, analogues possessing $_{L}$-Gln_4 (**2.1^2, 2.1^4, 2.1^6, 2.1^7**) (for example Figure S3.16 *blue contours*) contained many more cross-peaks in their NOESY spectra, some of which are categorised as long-range (Table S3.3), a category entirely missing from the $_{D}$-Gln_4 containing analogues (**2.1^1, 2.1^3, 2.1^5**). Having numerous medium- to long-range NOEs is characteristic of peptides adopting a higher degree of structure, and this situation is reflected in their sub- to low Angstrom convergence (Figure 3.2B, Table S3.3).

Possessing an $_{L}$-Ile_5 imparts a slight tendency for the structure on the teixobactin analogues (Figure 3.3 A, B and F) but does not result in a high deviation from the original structure unlike that observed for $_{L}$-Gln_4. For instance, the RMSD of analogue **2.1^1** (native stereochemistry) is ~3 Å (Figure 3.2A,

Figure 3.3A) whereas that of **2.1**^{3} (DDLD), in which D-*allo*-Ile$_5$ has been replaced by $_{L}$-Ile$_5$, is reduced to ~2 Å (Table S3.3, Figure 3.3 A, B). A similar slight reduction in RMSD is observed in **2.1**^{7} (LLLD, 0.93 Å; Table S3.3, Figure 3.3 A, F) when compared to **2.1**^{6} (LLDD, 1.06 Å; Table S3.3, Figure 3.3 A, E) where again, the only difference between them is the stereochemistry at position 5. The stereochemistry of position 1 has little to no effect on overall structure, as can be seen when one compares the RMSDs of **2.1**^{1} (DDDD) to **2.1**^{5} (LDDD, both ~3 Å; Figure 3.2A, Figure 3.3A, D, Table S3.3). Although highly disordered, the N-terminal domains of both these analogues occupy a similar overall spatial region. Since the stereochemistry of position 1 is not important to the structure, it is likely that $_{D}$ configuration is important for slowing down enzyme degradation or for biological activity.

Taken together, these data allow us to conclude that the stereochemistry of position 4 is critical to structural stability. A ubiquitous structural characteristic of the $_{L}$-Gln$_4$ containing analogues absent from the $_{D}$-Gln$_4$ containing analogues is that Ile$_6$ packs against Ile$_{11}$. It is therefore possible that this long-range packing arrangement is made possible by the altered stereochemistry at position 4 and has the effect of stabilising the structures. We analysed the nature of this packing through extended molecular dynamics (MD) simulations on the microsecond time-scale. Trajectories were calculated for a total of 0.1 μs for analogue **2.1**^{1} and **2.1**^{7} in explicit solvent (Figure S3.17). It was immediately obvious from the simulations that the native analogue seldom visits this packing arrangement (Figure S3.17 B), and on the few occasions it does, it is very short-lived. However, the sidechains of Ile$_6$ and Ile$_{11}$ remain in constant hydrophobic contact throughout the entire simulation in the case of **2.1**^{7} (LLLD, Figure S3.17 B).

Functionally, it was important to discover how this increased stability through packing might explain the MICs observed in all analogues except **2.1**^{5} (LDDD, Table 3.1). A plausible mechanism was also revealed through MD, in that the sidechain of Arg$_{10}$ is less solvent exposed in **2.1**^{7} (LLLD, Figure S3.17 A). This interaction is stabilised through the formation of numerous transient intramolecular hydrogen bonds between Arg$_{10}$ and other residues (Figure S3.17, bottom panel), a situation almost entirely lacking in the native analogue.

Therefore, it is possible to surmise that if the hydrogen bond donors of the guanidine group of Arg$_{10}$ are spending a considerable proportion of their time in forming intra-molecular hydrogen bonds then they are unavailable for the formation of inter-molecular bonds. Thus, if Arg$_{10}$ is unavailable for involvement in intermolecular recognition events, this could help to explain the decrease in MIC in case of analogue **2.1**^{7} (LLLD) as compared to **2.1**^{1} (DDDD, Table 3.1). The frequency of unfavoured backbone torsion angles present in the teixobactin analogues (Table S3.3) correlates strongly with $_{D}$ amino acid content. This could be due to limitations with the analysis algorithms used.

Figure S3.17 reveals that native teixobactin analogue (Arg$_{10}$) is highly dynamic in solution, whereas an analogue containing $_{L}$-Gln$_4$ is both more tightly packed and structurally stable. This increased

burial (Figure S3.17 A) is probably a result of the formation of a number of transient hydrogen bonds between the guanidine group of Arg_{10} and other polar sidechains in the analogue (*teal bars*). In contrast, Arg_{10} only forms two short-lived hydrogen bonds (*red bars*) throughout the whole simulation in the native form.

Complex formation of teixobactin analogues **2.1[1]** (DDDD) and **2.1[2]** (LLLL) with lipid II and geranyl pyrophosphate were performed as described previously using TLC (Experimental VIII).[6] Both analogues bind to lipid II and geranyl pyrophosphate which is indicated by the reduction of lipid/phosphate visible on TLC (Figure S3.18 & S3.19). The binding of lipid II to LLLL analogue is unexpected as the LLLL is not biologically active. Therefore, it can be concluded that the binding assay on isolated lipid II does not necessarily reflect whole cell activities. A plausible explanation for this can be that lipid II is more freely available in solution than in the case of bacteria.

3.5 Conclusion

We have for the first time determined the 3D molecular structure of seven teixobactin analogues and established the importance of the individual amino acids in terms of their $_D$/$_L$ configurations in maintaining a relatively unstructured teixobactin. Furthermore, we can directly correlate this propensity for structure with antimicrobial activity and have identified a possible mechanism by which this disorder is maintained. We have shown that the $_D$- *N*-Me-Phe_{11} is not important from a structural standpoint. On the other hand, we have identified $_D$-Gln_4 as being very essential and $_D$-Ile_5 being important in maintaining the disordered structure of teixobactin imperative for its biological activity. We believe this work to be critical in understanding the structural-activity relationship and mechanism of teixobactin and its analogues and their further development as drug like molecules. The results presented in this work are of broad general interest and are expected to facilitate the future development of teixobactin derivatives and peptide-based antibiotics for addressing the serious challenges posed by AMR.

3.6 References

1. A. M. Giltrap, L. J. Dowman, G. Nagalingam, J. L. Ochoa, R. G. Linington, W. J. Britton, R. J. Payne, Total Synthesis of Teixobactin. *Organic Letters*. **18**, 2788–2791 (2016).

2. Y. E. Jad, G. A. Acosta, T. Naicker, M. Ramtahal, A. El-Faham, T. Govender, H. G. Kruger, B. G. De La Torre, F. Albericio, Synthesis and Biological Evaluation of a Teixobactin Analogue. *Organic Letters*. **17**, 6182–6185 (2015).

3. A. Parmar, A. Iyer, C. S. Vincent, D. Van Lysebetten, S. H. Prior, A. Madder, E. J. Taylor, I. Singh, Efficient total syntheses and biological activities of two teixobactin analogues. *Chem. Commun.* **52**, 6060–6063 (2016).

4. H. Yang, K. H. Chen, J. S. Nowick, Elucidation of the Teixobactin Pharmacophore. *ACS*

Chemical Biology. **11**, 1823–26 (2016).

5. R. Tugyi, K. Uray, D. Iván, E. Fellinger, A. Perkins, F. Hudecz, Partial D-amino acid substitution: Improved enzymatic stability and preserved Ab recognition of a MUC2 epitope peptide. *Proceedings of the National Academy of Sciences of the United States of America*. **102**, 413–418 (2005).

6. L. L. Ling, T. Schneider, A. J. Peoples, A. L. Spoering, I. Engels, B. P. Conlon, A. Mueller, D. E. Hughes, S. Epstein, M. Jones, L. Lazarides, V. a Steadman, D. R. Cohen, C. R. Felix, K. A. Fetterman, W. P. Millett, A. G. Nitti, A. M. Zullo, C. Chen, K. Lewis, A new antibiotic kills pathogens without detectable resistance. *Nature*. **517**, 455–459 (2015).

CHAPTER 4

4 Syntheses of potent teixobactin analogue against methicillin-resitant staphyococus (MRSA) through the replacement of L-*allo*-enduracididne with its isosteres

COMMUNICATION

View Article Online
View Journal | View Issue

Check for updates

Cite this: *Chem. Commun.*, 2017, 53, 7788

Received 24th May 2017,
Accepted 17th June 2017

DOI: 10.1039/c7cc04021k

rsc.li/chemcomm

Syntheses of potent teixobactin analogues against methicillin-resistant *Staphylococcus aureus* (MRSA) through the replacement of L-*allo*-enduracididine with its isosteres†

Anish Parmar,[a] Abhishek Iyer,[ab] Daniel G. Lloyd,[c] Charlotte S. Vincent,[c] Stephen H. Prior,[d] Annemieke Madder,[b] Edward J. Taylor[d] and Ishwar Singh*[a]

Author contributions: All the building block synthesis, peptide synthesis for the analogues, optimisations, purifications and sample preparation for either LC-MS analysis/NMR has been done by me. The initial drafting of the manuscript and supplementary information has been done by me with inputs from Abhishek Iyer. Stephen H. Prior carried out and analysed the NMR experiments. The antibacterial study has been carried out by Daniel G. Lloyd, Charlotte S. Vincent and Edward J. Taylor. Annemieke Madder was responsible for the LC-MS analysis. The project was designed by Ishwar Singh.

4.1 Abstract

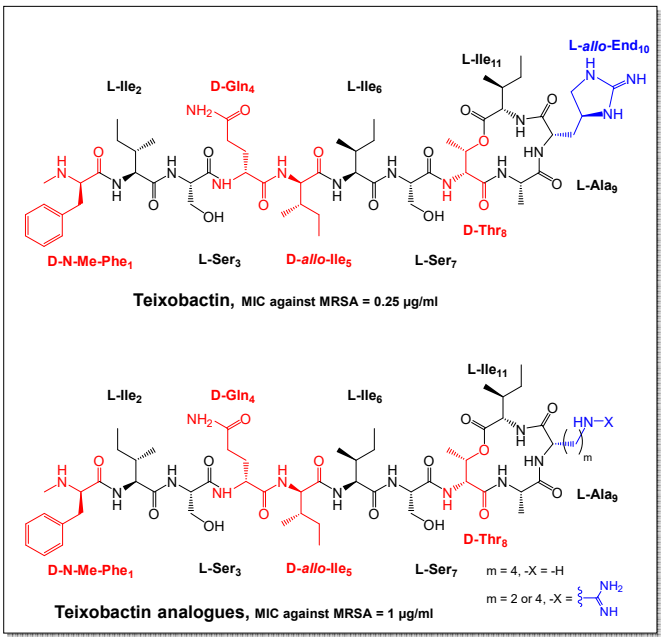

In this work, we have synthesised 8 analogues of teixobactin using commercially available building blocks by replacing the L-allo-enduracididine amino acid with its isosteres. Furthermore, we have tested all the compounds against a panel of Gram-positive bacteria including MRSA and explained the observed trend in biological activity. Although all the analogues were active, three analogues from this work, showed very promising activity against MRSA (MIC 1 μg/mL). We can conclude that amino acids which are the closest isosteres of L-allo-enduracididine are the key to synthesising simplified potent analogues of teixobactin using rapid syntheses and improved yields.

4.2 Brief Introduction

In the previous chapters, we have managed to develop a synthetic route to which many more analogues of teixobactin **1.23** can be synthesised and have performed a study to identify that D-amino acids are essential to maintain an unstructured teixobactin which correlates with its activity.

To further develop potent analogues of **1.23** against resistant bacteria such as MRSA, we are particularly interested in understanding the role of the polar amino acid residues at position 10 namely L-*allo*-End **1.21**, arginine and lysine. It has been suggested that **1.21** is important for the biological activity of **1.23**, however, as discussed previously, the synthesis of a properly protected **1.21** and its subsequent incorporation in **1.23** synthesis is complex and low yielding (3.3% overall yield).[1] Several research groups including us have already substituted this amino acid with commercially available building blocks such as Arginine,[2 3] Lysine[4] or Histidine.[5] The obtained analogues were less active than the natural product and will be discussed broadly in an overview chapter. However, the biological activity of teixobactin analogues suggests they are still suitable for further development as potential antibacterials. Therefore, it is important to synthesise new, potent derivatives with comparable biological activity to **1.23** which do not contain the L-*allo*-End **1.21**.

4.3 Aim of study

In this work, we have synthesised a total of eight analogues (seven new) of teixobactins using commercially available building blocks by replacing the L-*allo*- End **1.21** (Figure 4.1) with a series of amino acids that can be considered isosters thereof. We have tested all the analogues (**2.1, 4.1-4.7**) against a panel of Gram-positive bacteria including MRSA to compare the biological activity with teixobactin. This study is aimed at deciphering the most suited amino acids which can replace L-*allo*-End. We believe that the amino acids which possess a similar structure and functional group (isostere) as the L-*allo*-enduracididine amino acid are best suited for its replacement.

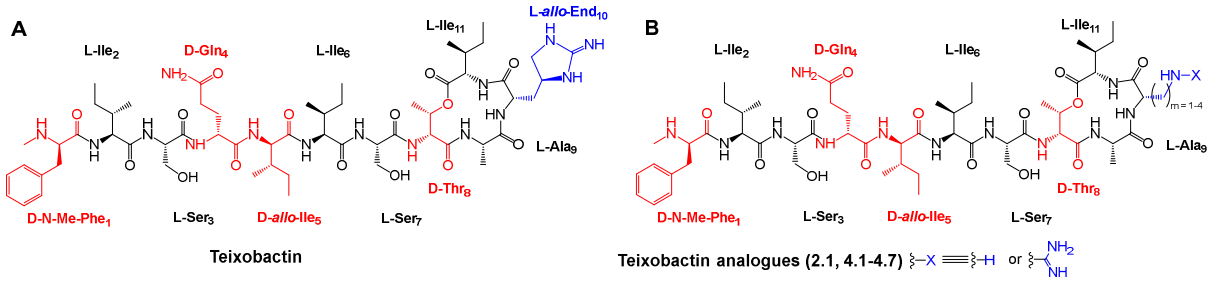

Figure 4.1: **A**. Teixobactin **B**. General structure of teixobactin analogues (**2.1, 4.1-4.7**) with the hydrophilic/charged residues shown in red, hydrophobic residues shown in black and structural differences shown in blue.

4.4 Results and Discussion

4.4.1 ‡Synthesis of analogues and their guanidines

The amino acids Lysine (Lys), Ornithine (Orn), L-2,4- Diaminobutyric acid (DAB) and L-1,3-Diaminopropionic acid (DAP) were chosen as these are the closest amine containing isosteres to **1.21**. Furthermore, through these amino acids we could sequentially shorten the side chain length by one methylene unit from 4 C atoms to 1 C atom. To further expand the number of teixobactin analogues and to reduce the overall cost and time taken by avoiding the re-syntheses of analogues containing non-natural guanidine side-chains, we have used a one-step route from our previous synthesis[3] and inspired by the results of Tor et. al.[6] to directly convert the deprotected amino-side chains into their corresponding guanidines (Figure 4.2).

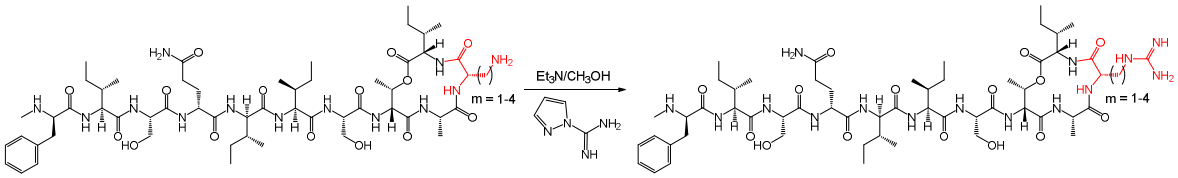

Figure 4.2*:* General scheme for the syntheses of teixobactin analogues **4.2**, **4.5** and **4.7** from their amino precursors **4.1**, **4.4** and **4.6** respectively.

For this purpose, the commercially available 1*H*-Pyrazole-carboxamidine hydrochloride in MeOH with Et_3N was used (Figure 4.2, Experimental Section III) followed by HPLC purification to remove any excess reagent present in the reaction mixture. By introducing Lys, Orn, DAB and DAP one at a time at position 10 we synthesised analogues Lys_{10}-teixobactin **4.1**, Orn_{10}-teixobactin **4.3**, DAB_{10}-teixobactin **4.4** and DAP_{10}-teixobactin **4.6** (Figure 4.3). We then directly converted Lys_{10}-teixobactin **4.1** to (Homoarginine) $HoArg_{10}$-teixobactin **4.2**, DAB_{10}-teixobactin **4.4** to $NorArg_{10}$-teixobactin **4.5** and DAP_{10}-teixobactin **4.6** to (L-2-amino-3-guanidinoaminopropionic acid) $GAPA_{10}$-teixobactin **4.7** using the aforementioned protocols (Figure 4.3). We thus synthesised 8 teixobactin analogues namely Lys_{10}-teixobactin **4.1**, $HoArg_{10}$-teixobactin **4.2**, Orn_{10}-teixobactin **4.3**, Arg_{10}-teixobactin **2.1**, DAB_{10}-teixobactin **4.4**, $NorArg_{10}$-teixobactin **4.5** DAP_{10}-teixobactin **4.6** and $GAPA_{10}$-teixobactin **4.7** (Figure 4.3).

‡ For simplicity, in most cases both the analogue name and **number** have been frequently used throughout the chapter.

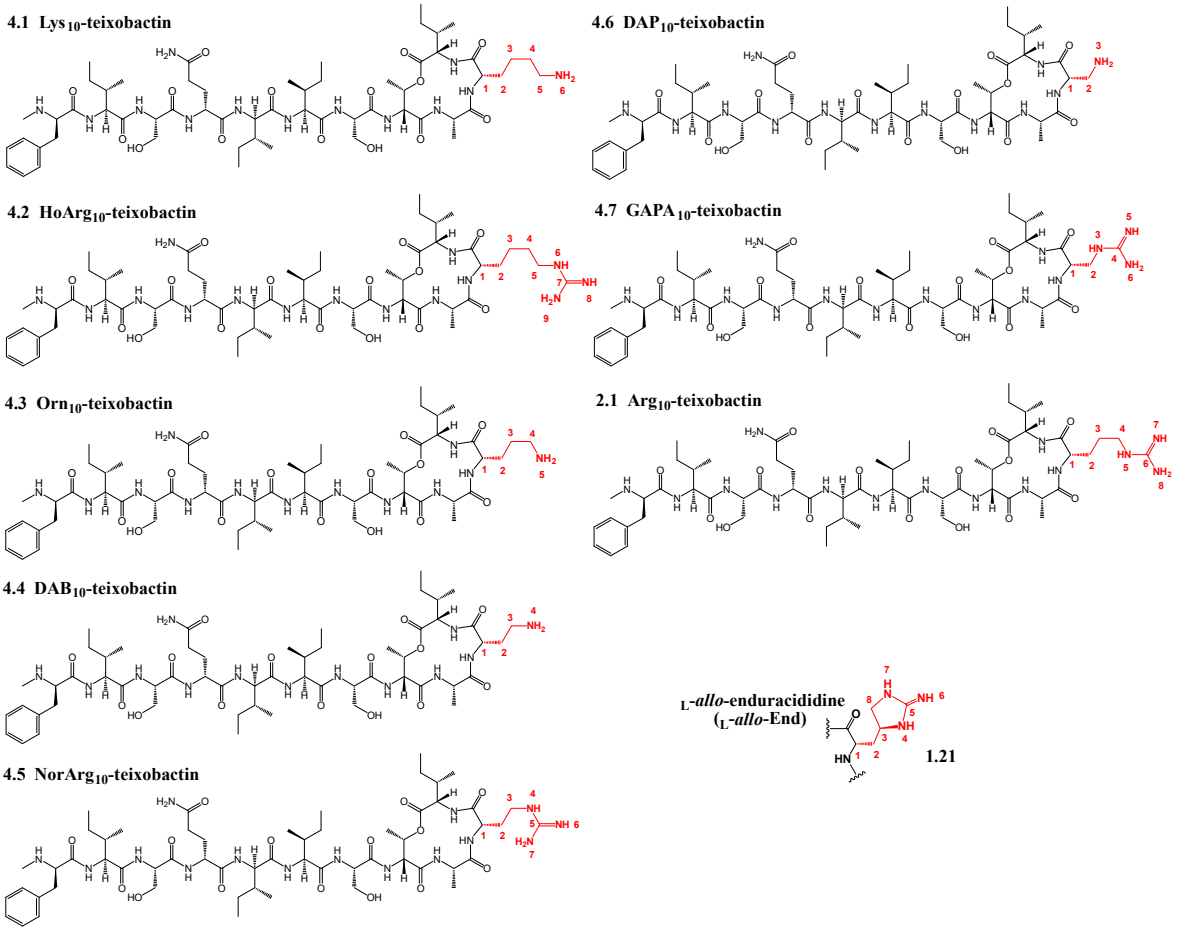

Figure 4.3: Complete structure of teixobactin analogues (**2.1, 4.1-4.7**) and structure of L-*allo*-End **1.21**. The amino acids at position 10 and L-*allo*-End **1.21** have been numbered and highlighted in red for clarity.

4.4.2 MIC evaluation on teixobactin analogues

Compound Number	Name	MIC against MRSA ATCC 33591 (μg/mL)	MIC against *Staphylococcus epidermidis* ATCC 12228 (μg/mL)	MIC against *Bacillus subtilis* 168 (μg/mL)
1.23	Teixobactin	0.25[7]	0.078-0.31[7]	0.02[7]
2.1	Arg_{10}-teixobactin	2	2	1
4.1	Lys_{10}-teixobactin	1	1	0.25
4.2	$HoArg_{10}$-teixobactin	1	0.25	0.125
4.3	Orn_{10}-teixobactin	2	1	0.25
4.4	DAB_{10}-teixobactin	2	2	1
4.5	$NorArg_{10}$-teixobactin	1	1	0.5
4.6	DAP_{10}-teixobactin	4	2	0.5
4.7	$GAPA_{10}$-teixobactin	4	4	1
1.12	Vancomycin	2	2	0.25-0.5

Table 4.1:Minimum Inhibitory Concentration (MIC) values of analogues against MRSA ATCC 33591, *Staphylococcus epidermidis* ATCC 12228 and *Bacillus subtilis* 168.

The syntheses and biological activity against *Staphylococcus aureus* of Lys_{10}-teixobactin **4.1**[4,5], Orn_{10}-teixobactin **4.3**[8], Arg_{10}-teixobactin **2.1**[2,3] and $NorArg_{10}$-teixobactin **4.5**[9] have already been reported. There has been very limited evaluation of teixobactin analogues against MRSA. Among the synthesised analogues, Orn_{10}-teixobactin (**4.3**) (MIC 2 μg/mL)[8] and $NorArg_{10}$-teixobactin **4.5** (MIC 16 μg/mL)[9] are the only ones tested against MRSA. However, a different strain of MRSA was used. To address this, we have evaluated the antibacterial activity of our eight teixobactin analogues (**2.1, 4.1**-**4.7**) against MRSA ATCC 33591 (identical to the strain reported in earlier[7]) to compare the biological activities with that of teixobactin **1.23** (Table 4.1). All the analogues were also screened against *Staphylococcus epidermidis* and *Bacillus subtilis* to provide a more comprehensive overview of the biological activities of these molecules. Vancomycin **1.12** was used as a control.

Herein we report for the first time the MIC of Lys_{10}-teixobactin **4.1** against MRSA which was found to be two times better than that of Arg_{10}-teixobactin **2.1** (Table 4.1) against the same species. $HoArg_{10}$-teixobactin **4.2** was found to have identical activity as Lys_{10}- teixobactin **4.1**. The MIC of Orn_{10}-teixobactin[8] **4.3** was found to be consistent with that reported in literature and identical to that of Arg_{10}-teixobactin **2.1**. The MIC of Dab_{10}-teixobactin **4.4** was found to be identical to Orn_{10}-teixobactin **4.3** (Table 4.1) which is expected as both DAB and Orn can be considered isosters of L-*allo*-Enduracididine (Figure 4.3). $NorArg_{10}$ teixobactin **4.5** showed two times better MIC than **2.1** (Table 4.1) although both Norarginine and Arginine are isosteric with L-*allo*-End. The difference can be potentially attributed to lower flexibility of **4.5** due to a reduced carbon chain length of NorArg and therefore being structurally more similar to L-*allo*-End. On further reducing the side-chain length of the amino acid at position 10 by one methylene group we obtained the analogues Dap_{10}-teixobactin (**4.6**) and $GAPA_{10}$-teixobactin **4.7** which were found to be less active than analogues (**2.1**, **4.1**-**4.5**) in MRSA. Both Dap_{10}-teixobactin **4.6** and $GAPA_{10}$-teixobactin **4.7** have an MIC two times higher than Arg_{10}-texiobactin **2.1**. The higher MICs in MRSA are probably because although both DAP and GAPA have structural similarities to L-*allo*-enduracididine (Figure 4.3), they have a shorter carbon chain thereby affording less flexibility. The MIC trend observed in *Staphylococcus epidermidis* and *Bacillus subtilis is* similar to that of MRSA. However, all compounds (**2.1, 4.1**-**4.7**) have shown 2-4 times better MICs in *B. subtilis* compared to MRSA and *S. epidermidis.* $HoArg_{10}$-teixobactin **4.2** was found to be the most potent analogue possessing the lowest MIC in all three species, followed by Lys_{10}-teixobactin **4.1** and Orn_{10}-teixobactin **4.3**. Overall, the MICs observed are consistent with the hypothesis that the closest isosteres of L-*allo*-End **1.21** are most suited for its replacement.

4.5 Conclusion

In conclusion, we have synthesised seven new teixobactin analogues and tested them against a panel of Gram-positive bacteria including MRSA to determine the most suited amino acids for replacing the synthetically challenging L-*allo*-End at position 10. Furthermore, for the rapid syntheses of guanidine containing teixobactin analogues from amines, we have used the direct conversion of amines to guanidines for completely deprotected teixobactin analogues. This method is compatible with secondary amines as well as other amino acid side chains and will therefore be suitable for diverse peptides. Based on the MICs against MRSA, we observe that all the synthesised compounds are active and therefore can be used as leads for further derivatisation. Lysine, homoarginine and norarginine are all equally suitable substitutions for L-*allo*-End. Furthermore, almost no difference in MIC was observed between the amino derivatives and their corresponding guanidine counterparts. This implies that there is a considerable tolerance for the substitution of L-*allo*-End with both proteogenic and non-proteogenic amino acids containing amine or guanidine side-chains. We have synthesised eight potent teixobactin analogues three of which show very promising activity against MRSA (MIC 1 μg/mL). The results from this work are expected to facilitate the development of teixobactin analogues against MRSA and have the potential to address the challenges posed by multi-drug resistant bacteria.

4.6 References

1. A. M. Giltrap, L. J. Dowman, G. Nagalingam, J. L. Ochoa, R. G. Linington, W. J. Britton, R. J. Payne, Total Synthesis of Teixobactin. *Organic Letters*. **18**, 2788–2791 (2016).

2. Y. E. Jad, G. A. Acosta, T. Naicker, M. Ramtahal, A. El-Faham, T. Govender, H. G. Kruger, B. G. De La Torre, F. Albericio, Synthesis and Biological Evaluation of a Teixobactin Analogue. *Organic Letters*. **17**, 6182–6185 (2015).

3. A. Parmar, A. Iyer, C. S. Vincent, D. Van Lysebetten, S. H. Prior, A. Madder, E. J. Taylor, I. Singh, Efficient total syntheses and biological activities of two teixobactin analogues. *Chem. Commun.* **52**, 6060–6063 (2016).

4. H. Yang, K. H. Chen, J. S. Nowick, Elucidation of the Teixobactin Pharmacophore. *ACS Chemical Biology*. **11**, 1823–26 (2016).

5. C. Wu, Z. Pan, G. Yao, W. Wang, L. Fang, W. Su, Synthesis and structure–activity relationship studies of teixobactin analogues. *RSC Adv.* **7**, 1923–1926 (2017).

6. K. M. Hamill, L. S. McCoy, E. Wexselblatt, J. D. Esko, Y. Tor, Polymyxins facilitate entry into mammalian cells. *Chem. Sci.* **7**, 5059–5068 (2016).

7. L. L. Ling, T. Schneider, A. J. Peoples, A. L. Spoering, I. Engels, B. P. Conlon, A. Mueller, D. E. Hughes, S. Epstein, M. Jones, L. Lazarides, V. a Steadman, D. R. Cohen, C. R. Felix, K. A. Fetterman, W. P. Millett, A. G. Nitti, A. M. Zullo, C. Chen, K. Lewis, A new antibiotic kills pathogens without detectable resistance. *Nature*. **517**, 455–459 (2015).

8. K. Jin, I. H. Sam, K. H. L. Po, D. Lin, E. H. Ghazvini Zadeh, S. Chen, Y. Yuan, X. Li, Total synthesis of teixobactin. *Nature Communications*. **7**, 12394 (2016).

9. K. Jin, K. H. L. Po, S. Wang, J. A. Reuven, C. N. Wai, H. T. Lau, T. H. Chan, S. Chen, X. Li, Synthesis and structure-activity relationship of teixobactin analogues via convergent Ser ligation. *Bioorganic & Medicinal Chemistry*. **25**, 4990–4995 (2017).

CHAPTER 5

5 Teixobactin analogues reveal enduracididne to be non-essential for highly potent activity and lipid II binding

EDGE ARTICLE

View Article Online
View Journal | View Issue

Check for updates

Cite this: *Chem. Sci.*, 2017, **8**, 8183

Teixobactin analogues reveal enduracididine to be non-essential for highly potent antibacterial activity and lipid II binding†

Anish Parmar,‡[a] Abhishek Iyer,‡[ab] Stephen H. Prior,[c] Daniel G. Lloyd,[d] Eunice Tze Leng Goh,[e] Charlotte S. Vincent,[d] Timea Palmai-Pallag,[d] Csanad Z. Bachrati,[d] Eefjan Breukink,[f] Annemieke Madder,[b] Rajamani Lakshminarayanan,[e] Edward J. Taylor[d] and Ishwar Singh*[a]

Author contributions: Myself and Abhishek Iyer contributed equally to this work. The project was conceived and designed by Ishwar Singh. The manuscript was written by Abhishek Iyer, Stephen H. Prior and Ishwar Singh through contributions from all authors. I carried out all the teixobactin analogues syntheses. Stephen H. Prior was responsible for the NMR analyses. Charlotte S. Vincent, Daniel G. Lloyd, and Edward J. Taylor have contributed to the antibacterial studies. Timea Palmai-Pallag and Csanad Z. Bachrati carried out the toxicity studies. Annemieke Madder was responsible for the LC-MS analyses. Eefjan Breukink was responsible for the syntheses and characterisation of lipid II. Eunice Tze Leng Goh and Rajamani Lakshminarayanan were responsible for the antibacterial studies and haemolytic assay.

5.1 Abstract

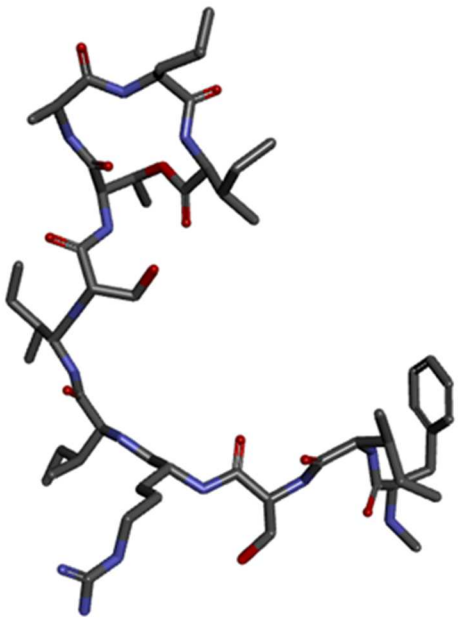

Due to many challenges in obtaining L-allo-End ***1.21****, the total synthesis of teixobactin* ***1.23*** *is laborious and low yielding (3.3%). In this work, we have identified a unique design and developed a rapid synthesis (10 min mwave assisted coupling per amino acid, 30 min cyclisation) of several highly potent analogues of teixobactin with yields of 10–24% by replacing the L-allo-End with commercially available non-polar residues such as leucine and isoleucine. Most importantly, the Leu_{10}-teixobactin* ***5.13*** *and Ile_{10}-teixobactin* ***5.12*** *analogues have shown highly potent antibacterial activity against a broader panel of MRSA and Enterococcus faecalis (VRE). Furthermore, these synthetic analogues displayed identical antibacterial activity to natural teixobactin (MIC 0.25 mg mL^{-1}) against MRSA ATCC*

33591 despite their simpler design and ease of synthesis. We have confirmed lipid II binding and measured the binding affinities of individual amino acid residues of Ala$_{10}$-teixobactin towards geranyl pyrophosphate by NMR to understand the nature and strength of binding interactions. Contrary to current understanding, we have shown that a cationic amino acid at position 10 is not essential for target (lipid II) binding and potent antibacterial activity of teixobactin. We thus provide strong evidence contrary to the many assumptions made about the mechanism of action of this exciting new antibiotic. Introduction of a non-cationic residue at position 10 allows for tremendous diversification in the design and synthesis of highly potent teixobactin analogues and lays the foundations for the development of teixobactin analogues as new drug-like molecules to target MRSA and Mycobacterium tuberculosis.

5.2 Brief Introduction

So far, all the analogues that have been described in previous chapters have all had lower potency in comparison to the natural product. Teixobactin scaffold contains 11 amino acids, with a mix of polar/non-polar residues with a cationic residue at position 10 known to be important for its activity. The insight of the role of each amino acid could provide better progress in the design and synthesis of simpler and more potent analogues against MDR bacterial pathogens, such as MRSA.

Alanine scanning is a technique that has been used has widely to determine the functions of different amino acids in proteins and peptides for its antibacterial studies. Since the simplest amino acid glycine is achiral, alanine is the next simplest amino acid which is chiral and can be used to retain the absolute conformation of the peptide. Because of its non-bulky nature, it does not enforce high electrostatic or steric effects[1]. Alanine is very abundant and frequently found in secondary structures of proteins. Due to the methyl group, it gives a structural understanding of the side chains of different amino acids in the sequence. Alanine-scanning has been utilised in several other antimicrobial compounds such as nisin[2] and feglimycin[3] which attributed to successfully synthesising novel peptides with increased activity.

5.3 Aim of study

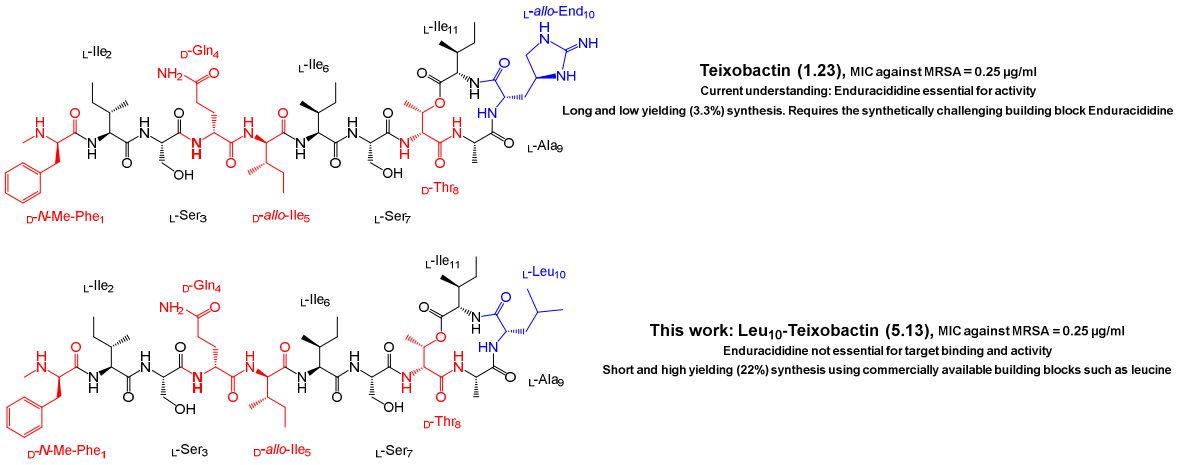

Figure 5.1: Structure of Teixobactin **1.23** and Leu_{10}-Teixobactin **5.13** with the D-amino acids highlighted in red and the L-*allo*-End **1.21** and replaced L-Leu residue highlighted in blue. MRSA ATCC 33591, Staphylococcus aureus ATCC 29213.

In this work, we describe a unique design and rapid synthesis of several highly potent analogues of teixobactin against *Staphylococcus aureus* (MSSA), Methicillin-resistant *Staphylococcus aureus* (MRSA) and *Enterococcus faecalis* (Vancomycin-resistant Enterococcus, VRE) by replacing the synthetically challenging L-*allo*-End with commercially available non-polar residues such as alanine, leucine and isoleucine. This study aims to answer two important questions. Firstly, is it essential to incorporate a residue with a positively charged side chain at position 10 for maintaining target binding (lipid II) and biological activity of teixobactin and its analogues? Secondly, what are the key residues involved and what are the target binding contributions of the individual amino acid residues in the teixobactin analogues? To evaluate both these questions and identify the key residues particularly with respect to position 10, an alanine scan was performed on Arg_{10}-teixobactin **2.1** (Figure 5.2, **5.1-5.8**). The alanine scanning technique has been used earlier on other antimicrobial peptides with success[4] but has not yet been performed on teixobactin or its analogues. In order to further improve the antibacterial activity of Arg_{10}-teixobactin by modifying the amino acid at position 10, new analogues of teixobactin were prepared by systematic replacement of Arg_{10} with D-Ala ($_D$-Ala_{10}-teixobactin, **5.9**), Gly (Gly_{10}-teixobactin, **5.10**), Val (Val_{10}-teixobactin **5.11**), Ile (Ile_{10}-teixobactin, **5.12**), Leu (Leu_{10}-teixobactin, **5.13**), Ser (Ser_{10}-teixobactin, **5.14**) and Phe (Phe_{10}-teixobactin, **5.15**) (Figure 5.2, **5.9-5.15**). We thus synthesised 15 analogues (Figure 5.2) of teixobactin using the conditions described in Figure 5.3, Figure S5.1.

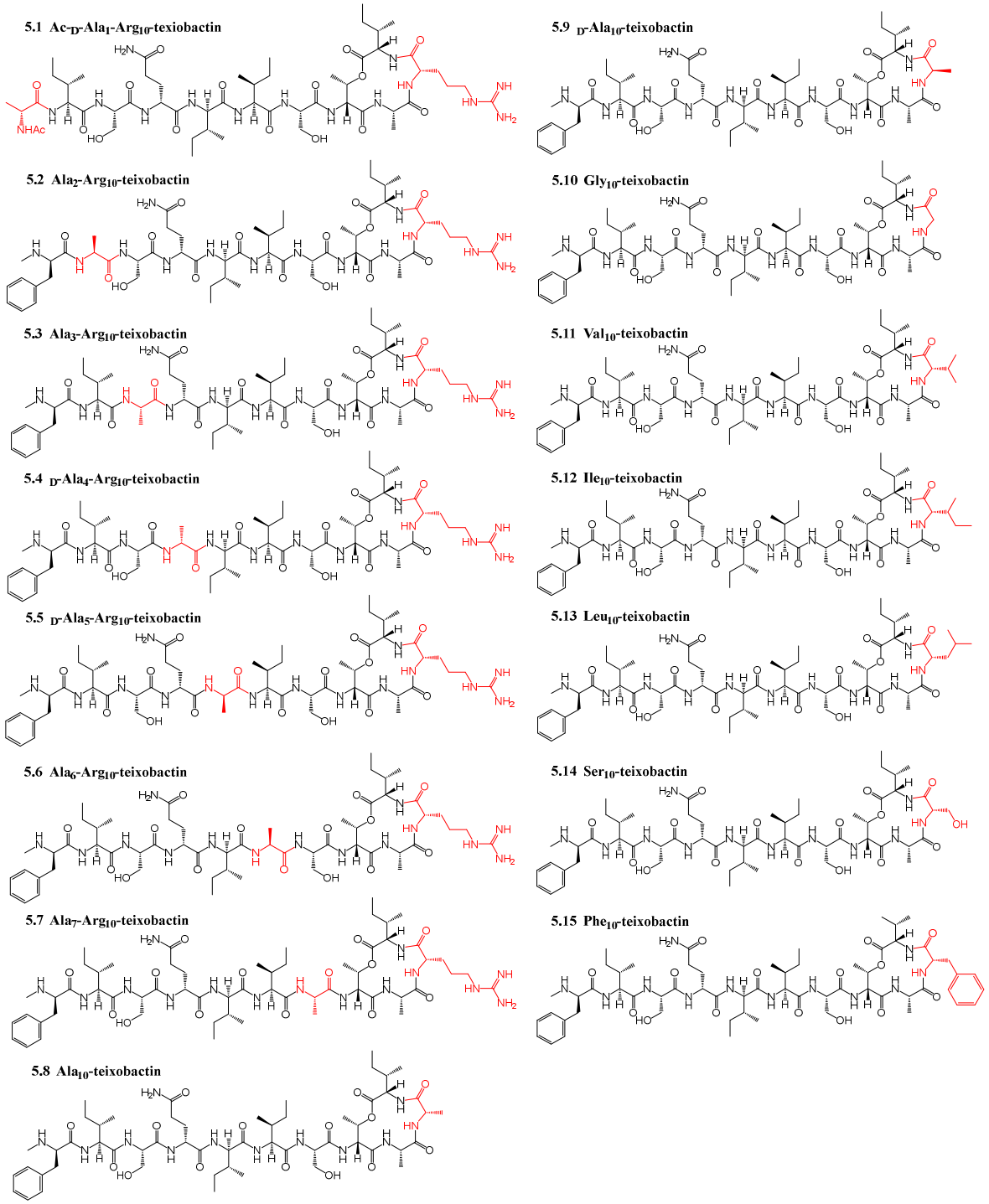

Figure 5.2: Structure of teixobactin analogues **5.1-5.15** synthesised with the replaced amino acids highlighted in *red*.

5.4 Results and discussion

5.4.1 Design and synthesis

The synthesis of all our analogues involved loading Fmoc-alanine-OH on the 2-CTC resin, followed by amide coupling with Alloc-NH-$_D$-Thr-OH, resin esterification with 10 eq. Fmoc-Ile-OH, and adding 10 eq. DIC and 5 mol% DMAP for 2h. The next amino acid (AA) was then coupled using 4 eq. AA with 4 eq. HATU/8 eq. DIPEA in DMF for 1h followed by Fmoc deprotection and trityl protection. Next, the N-terminal alloc protecting group was removed using $Pd(PPh_3)_4$ and phenylsilane (Figure 5.3). All other amino acids were coupled using 4 eq. AA with 4 eq. DIC/Oxyma using an automated microwave peptide synthesiser (coupling time of 10 min each). Fmoc deprotection was performed using 20% piperidine in DMF (Figure 5.3, Figure S5.1). Cyclisation was performed using 1 eq. HATU and 10 eq. DIPEA and was found to be complete within 30 min with complete conversion of the linear product into its cyclised counterpart (Experimental Figures S5.2 – S5.59). Yields after HPLC purification were found to be 10-24% (Table S5.1). We have identified a unique design in which the introduction of hydrophobic residues such as leucine at position 10 (Figure 5.1) has several advantages over the lengthy low-yielding (3.3%) synthesis of teixobactin, including overall yields of up to 24%, faster automated syntheses, and use of commercially available building blocks.

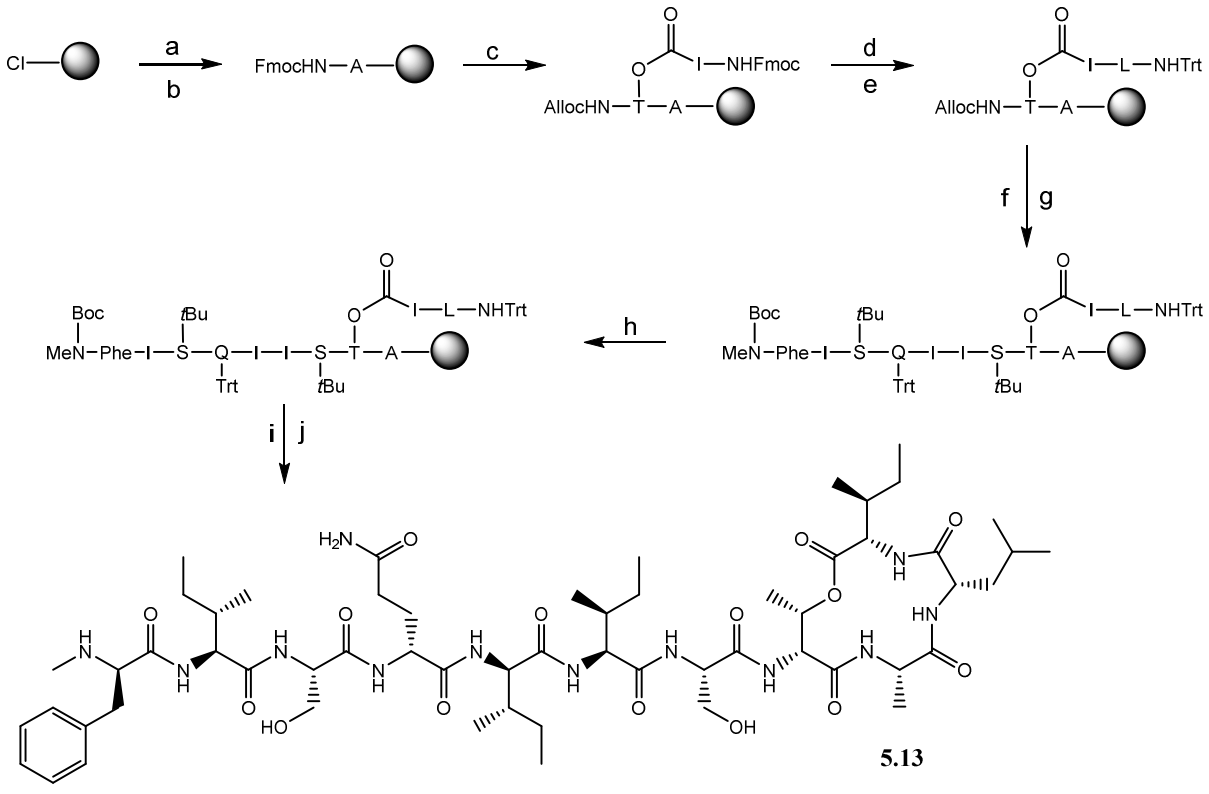

Figure 5.3: Synthesis of **5.13** starting from 2-CTC resin: a. 4 eq. Fmoc-Ala-OH/8 eq. DIPEA in DCM, 3h. b. 20% piperidine in DMF followed by 3 eq. AllocHN-D-Thr-OH, 3 eq. HATU/6 eq. DIPEA, 1.5h c. 10 eq. Fmoc-Ile-OH, 10 eq. DIC, 5 mol% DMAP in DCM, 2h followed by capping with Ac2O/DIPEA 10% in DMF, 20% piperidine in DMF d. 4 eq. Fmoc-Leu-OH, 4 eq. HATU/8 eq. DIPEA in DMF, 1h followed by 20%

piperidine in DMF e. 10 eq. Trt-Cl, 15% Et_3N in DCM, 1h. f. 0.2 eq. $[Pd(PPh_3)_4]^0$ + 24 eq. $PhSiH_3$ in dry DCM, 1x20 min, 1x45 min. g. 4 eq. Fmoc/Boc-AA(PG)-OH (AA = amino acid, PG = protecting group), 4 eq. DIC/Oxyma (µwave, 10 min) followed by 20% piperidine in DMF (3 min, 10 min). h. TFA:TIS:DCM = 2:5:93, 1h. i. 1 eq. HATU/10 eq. DIPEA in DMF, 30 min. j. TFA:TIS:H2O = 95:2.5:2.5, 1h.

Teixobactin and its active analogues such as Arg_{10}-teixobactin **2.1** and Lys_{10}-teixobactin **4.1** contain two positive charges. However, the analogues **5.1**, **5.8**-**5.15** contain only one positive charge and were therefore found to be more hydrophobic than the analogues **5.2-5.7**. All the compounds were found to be completely soluble in DMSO. Therefore, stock solutions of these compounds were prepared in DMSO for MIC testing. Upon dilution in the Mueller Hinton broth (Oxoid) culture media in which bacteria were grown (concentration ~256 µg/mL), no turbidity or precipitation was observed indicating that the compounds were soluble in the culture media.

5.4.2 Antibacterial studies

Analogues of teixobactin derived through an alanine scanning of teixobactin reveal that residues *N*-Me-Phe_1, Ile_2 $_D$-*allo*-Ile_5, L-Ile_6 and Ser_7 are important for antibacterial activity and their replacement by $_L$-Ala or $_D$-Ala results in decrease in biological activity (Table 5.1). Interestingly, replacement of $_L$-Ser_3 and $_D$-Gln_4 by $_L$-Ala and $_D$-Ala has no effect on antibacterial activity. Thus, the two residues $_L$-Ser_3 & $_D$-Gln_4 are ideal candidates for replacement in the case of teixobactin due to their more facile synthesis and minimal impact on biological activity. It has been suggested that replacement of any of the residues in the core ring structure of teixobactin negates all biological activity of the molecule.[5] In our case, however, the most interesting result was obtained through the replacement of $_L$-Arg_{10} by $_L$-Ala **5.8**.

The design and syntheses of potent teixobactin analogues published in the literature has thus far been limited to the substitution of $_L$-*allo*-End with amino acids such as Arg,[6 7] Lys[5] and Orn[8], all of which possess a cationic side chain. A positive charge is a common structural characteristic of depsipeptides which bind to lipid II[9]. $_L$-*allo*-End is thus reported to be important for potent antibacterial activity of teixobactin.[10] Therefore, it was expected that replacement of this residue with alanine, which is non-polar and uncharged, would completely abolish the biological activity of the molecule. Contrary to this, we observed that Ala_{10}-teixobactin was highly active against MRSA (Table 5.1) with an MIC of 1-2 µg/mL.

A plausible explanation could be that Ala_{10}-teixobactin binds to the pyrophosphate motif of lipid II using the amide backbone in a similar way to that proposed for the binding of nisin.[11] Superior results were obtained with Ile_{10}-teixobactin **5.12** and Leu_{10}-teixobactin **5.13**, which consistently gave identical MIC values of 0.25 µg/ml as compared to the reported MIC for teixobactin against MRSA (Table 5.1). Leu has a very similar hydrocarbon framework to $_L$-*allo*-End (Figure 5.1), followed very closely by Ile, which could explain the identical MIC value of these analogues **5.12** & **5.13** to teixobactin **1.23** against MRSA. In order to determine the effect of serum on antibacterial activity,

the MIC of compounds **5.12** and **5.13** were measured in presence of 10% human serum (Table S5.4). In both cases no change was observed in the MIC (Table 5.1) indicating that 10% human serum has no effect on the antibacterial activity.

Compound	Name	MIC[a] (µg/mL)
1.23	Teixobactin	0.25
2.1	Arg_{10}-teixobactin	2
5.1	Ac-$_D$-Ala_1-Arg_{10}-texiobactin	>128
5.2	Ala_2-Arg_{10}-teixobactin	>128
5.3	Ala_3-Arg_{10}-teixobactin	1-2
5.4	$_D$-Ala_4-Arg_{10}-teixobactin	2-4
5.5	$_D$-Ala_5-Arg_{10}-teixobactin	64-128
5.6	Ala_6-Arg_{10}-teixobactin	>128
5.7	Ala_7-Arg_{10}-teixobactin	16-32
5.8	Ala_{10}-teixobactin	1-2
5.9	$_D$-Ala_{10}-teixobactin	32
5.10	Gly_{10}-teixobactin	2
5.11	Val_{10}-teixobactin	0.5
5.12	Ile_{10}-teixobactin	0.25
5.12a	Ile_{10}-teixobactin + 10% human serum[b]	0.25
5.13	Leu_{10}-teixobactin	0.25
5.13a	Leu_{10}-teixobactin + 10% human serum[b]	0.25
5.14	Ser_{10}-teixobactin	16
5.16	Phe_{10}-teixobactin	2
1.12	Vancomycin	2

Table 5.1: List of teixobactin analogues (1-15). [a]MIC: Minimum Inhibitory Concentration. MRSA ATCC 33591 used. Culture Media: Mueller Hinton Broth (Oxoid). [b] 10% volume with human serum (SIGMA, H4522)

The fact that a cationic residue at position 10 is not essential for antibacterial activity represents a significant breakthrough in teixobactin research given the earlier stated importance of the $_L$-*allo*-End amino acid in the total synthesis of teixobactin.[10] Our design has considerably improved not only the antibacterial activity of teixobactin analogues but also the ease of synthesis. Our findings are of particular importance as MRSA is responsible for many infections worldwide.[12]

$_D$-Ala_{10}-teixobactin shows 16-times lower antibacterial activity than Arg_{10}-teixobactin which would be expected, as inversion of configuration of even a single amino acid in the core ring structure can significantly lower the MIC value of a teixobactin analogue.[5] Surprisingly, Gly_{10}-teixobactin **5.10** shows identical activity to Arg_{10}-teixobactin **2.1** showing that complete removal of the chiral center at position 10 is tolerated provided the configuration of the remaining residues is intact. Val_{10}-teixobactin **5.11** shows 4-times better antibacterial activity than Arg_{10}-teixobactin but Ser_{10}-teixobactin **5.14** shows 8-times lower activity, indicating that Ser at position 10 probably interferes with hydrogen bonding between the core ring structure of teixobactin and lipid II. Phe_{10}-teixobactin **5.15** gave an MIC of 2 µg/mL against MRSA indicating that an aromatic amino acid such as Phenylalanine at position 10 is also tolerated. Overall, from our work it appears that the claimed importance of a charged residue at position 10 in the form of an amine or guanidine group in texiobactin **1.23** has been overstated in the literature given that the most potent analogues obtained thus far are the Leu_{10}-teixobactin and Ile_{10}-teixobactin both of which are non-polar and non-charged.

This unexpected result facilitates the development of several highly potent teixobactin analogues against a broader panel of MRSA, MSSA and *Enterococcus faecalis* (VRE) including *Mycobacterium smegmatis* (Table 5.2) but with significantly higher yields compared to teixobactin. Although analogues of teixobactin with improved yields have been synthesised previously[6-13], none possess comparable activity to teixobactin and therefore the yields obtained for Ile_{10}-teixobactin and Leu_{10}- teixobactin (Table S5.1, S5.4, 10-20%) cannot be compared to those of the other less potent analogues of teixobactin described in literature.[6-13]

Based on the initial MIC results (Table 5.1), we identified Ala_{10}-teixobactin **5.8**, Val_{10}-teixobactin **5.11**, Ile_{10}-teixobactin **5.12** and Leu_{10}-teixobactin **5.13** as our lead compounds. These compounds along with Arg_{10}-teixobactin **2.1**, and vancomycin **1.21**/daptomycin **1.13** as controls, were tested against an extended panel of Gram positive bacteria (Table 5.2) to provide a more comprehensive overview of the biological activity of these molecules. A substancial difference in MIC was observed in the presence and absence of polysorbate 80 (Table S5.4).[14] Leu_{10}-teixobactin **5.13** showed potent activity against *M.smegmatis* (MIC ~ 1 µg/mL). Ala_{10}-teixobactin **5.8** and Arg_{10}-teixobactin **2.1** showed comparable activity against *M. smegmatis* with MICs in the range of 1-2 µg/mL. In general, the minimum bactericidal concentration (MBCs) of all compounds were found to be 2-4 times the MIC value. Ile_{10}-teixobactin **5.12** and Leu_{10}-teixobactin **5.13** were found to be the most potent compounds showing MICs ≤ 0.25 µg/mL in all strains.

The MICs and MBCs of both analogues against *Staphylococcus aureus* ATCC 29213 were found to be ≤ 0.0625 µg/mL and ≤ 0.125 µg/mL respectively, lower than the reported MIC of native teixobactin[14] against the same strains. Ile_{10}-teixobactin (**5.12**) in particular was found to be highly active against both VRE strains with MICs ≤ 0.0625 µg/mL and also an MIC 0.5 of µg/mL against *M. smegmatis*. We thus report, for the first time, two analogues of teixobactin showing highly potent antibacterial activity against a broader panel of resistant Gram-positive bacteria including clinical isolates. This is a very significant advancement in terms of teixobactin research and allows for the synthesis of a library of teixobactin derivatives based on Ile_{10}-teixobactin and Leu_{10}-teixobactin which can be simpler, highly potent and significantly more cost effective than the synthesis of teixobactin.

Strain ↓	Compound →	5.8	5.11	5.12	5.13	2.1	Vancomycin **1.12**	Daptomycin **1.13**
MRSA 1	MIC	4	1	0.25	0.25	1	2	0.5
	MBC	16	4	1	2	2	-	-
MRSA 2	MIC	1	0.5	≤ 0.0625	≤ 0.0625	0.125	2	0.5
	MBC	4	4	≤ 0.0625	≤ 0.0625	0.5	-	-
MRSA 3	MIC	1	0.25	≤ 0.0625	≤ 0.0625	0.5	2	0.5
	MBC	2	2	0.125	≤ 0.0625	1	-	-
Staphylococcus aureus	MIC	1	0.25	≤ 0.0625	≤ 0.0625	0.25	4	0.25
	MBC	2	1	0.125	0.125	1	-	
VRE 1	MIC	4	0.5	≤ 0.0625	0.25	2	>4	0.5
VRE 2	MIC	4	0.5	≤ 0.0625	0.25	2	>4	0.5
M. smegmatis	MIC	1-2	-	0.5	1	1-2	>64	-

Table 5.2: MIC and MBC (in µg/mL) of the teixobactin analogues **2.1**, **5.8**, **5.11-5.13** and daptomycin control against an extended panel of Gram positive bacteria. Strain information: MRSA 1: MRSA ATCC 700699, MRSA 2: MRSA DR 42412 (sputum), MRSA 3: MRSA DM21455 (eye). MRSA 2 and MRSA 3 are clinical isolates. *Staphylococcus aureus* ATCC 29213, *Enterococcus faecalis* (VRE 1: VRE ATCC 700802, VRE 2: VRE ATCC 29212). *M. smegmatis* ATCC 607. Culture Media: Mueller Hinton Broth.

5.4.3 Time -kill kinetics of analogues 5.12 and 5.13

Early stage time-kill kinetics for Ile_{10}-teixobactin **5.12** and Leu_{10}-teixobacitn **5.13** against MRSA ATCC 21455 using vancomycin as a control were carried out as described (Experimental section IX).[14] At 0.5 µg/ml, both **5.12** and **5.13** were found to elicit complete bactericidal activity within 8 h whereas substantial growth was observed in the presence of vancomycin (0.5 µg/ml, Figure 5.4A). The concentration of vancomycin needs to be increased to 8 µg/ml in order to have similar effects as the teixobactin analogues **5.12** & **5.13** (Figure 5.4B).

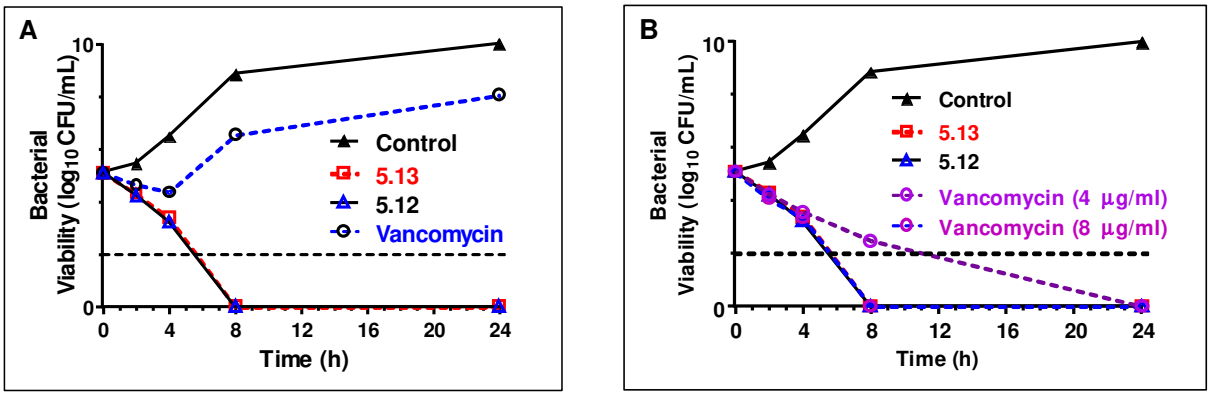

Figure 5.4: **A**. Time-kill kinetics of teixobactin analogues **5.12** & **5.13** with a comparative antibiotic (vancomycin) against MRSA 21455. The concentration of teixobactin analogues and vancomycin **1.12** are maintained at 0.5 µg/ml. **B**. Time-kill kinetics of teixobactin analogues with vancomycin against MRSA 21455 strains at elevated concentrations of the antibiotics. At 8 µg/ml concentration the kill kinetics profiles are similar for vancomycin & teixobactin analogues **5.12** & **5.13**. The horizontal dotted line represents the limit of detection.

5.4.4 Toxicity studies and haemolysis assay

The analogues Ala_{10}-teixobactin **5.8**, Val_{10}-texiobactin **5.11** and Leu_{10}-teixobactin **5.13** were tested on HeLa cell cultures and no significant toxicity was observed (relative survival 90-100%) up to a concentration of 100 µM (Figure S5.79) which is well above the MIC values (0.2-0.8 µM, 125-500 times). Additionally, a haemolytic assay using Leu_{10}-teixobactin and Ile_{10}-teixobactin against rabbit erythrocytes using Melittin as a control (Figure 5.5) indicated that peptides **5.13** and **5.12** did not show any discernible haemolytic activity, even at concentrations that exceed >500x the mean MIC values whereas substantial haemolytic activity was observed for melittin (Figure 5.5). These results establish the non-haemolytic properties of the designed teixobactin analogues.

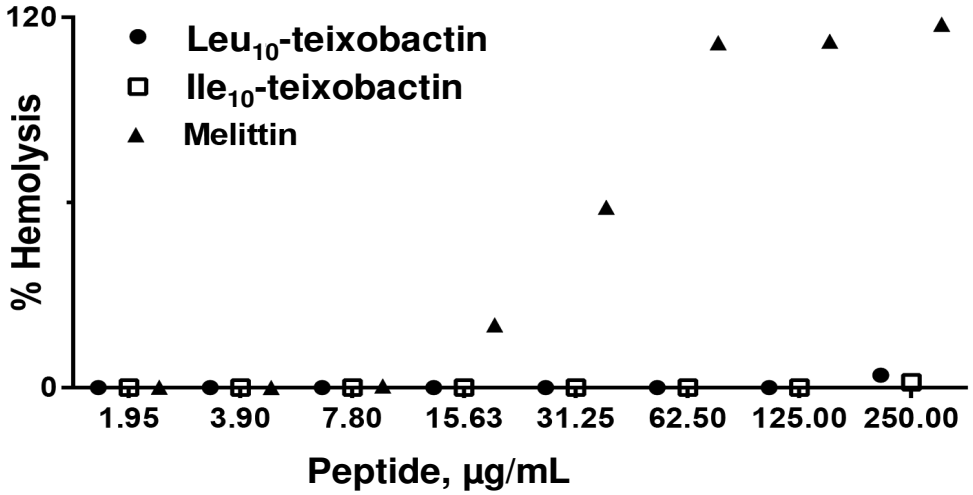

Figure 5.5: Hemolytic activity of teixobactin analogues for rabbit erythrocytes. The blood cells were exposed to various concentrations of peptides for 1 h and the release of haemoglobin was determined spectrophotometrically. Each value represents an average of triplicate experiments.

5.4.5 Lipid II binding assay

To better understand the potent antibacterial activity of Ala_{10}-teixobactin we have performed the lipid II TLC binding assay as reported earlier for teixobactin.[14] Teixobactin and Arg_{10}-teixobactin bind to lipid II in a 2:1 ratio resulting in the complete disappearance of the lipid II spot on TLC (Figure S5.76). Although Ala_{10}-teixobactin also shows binding with lipid II in a 2:1 ratio, a small amount of lipid II was still visible on TLC. The lipid II spot, however, completely disappears by increasing the concentration of Ala_{10}-teixobactin (Figure S5.76). TLC binding studies with Leu_{10}-teixobactin also showed complete disappearance of the lipid II spot when a ratio of 2:1 was used (Figure S5.78). It is very interesting that Ala_{10}-teixobactin and Leu_{10}-teixobactin were able to bind to lipid II without having a cationic amino acid residue like $_{L}$-*allo*-End/arginine off the cyclic peptide ring.

5.4.6 Geranyl Pyrophosphate (lipid II mimic) binding studies

In order to evaluate target binding, we have performed the lipid II TLC binding assay[14] with Ala_{10}-teixobactin. This assay provides qualitative binding data of Ala_{10}-teixobactin **5.8** with lipid II. Although the technique is fast and effective, the results obtained via this method do not necessarily reflect whole cell activities. This has been reported previously by us where both D and L derivatives of teixobactin were found to bind to lipid II but only the former was biologically active.[15] Therefore, in order better understand the target binding of teixobactin analogues in a quantitative manner, extensive NMR studies (Figure 5.6) on **5.8** and geranyl pyrophosphate were performed. Geranyl pyrophosphate possesses a pyrophosphate and isoprenyl chain similar to lipid II making it suitable for solution phase NMR studies.

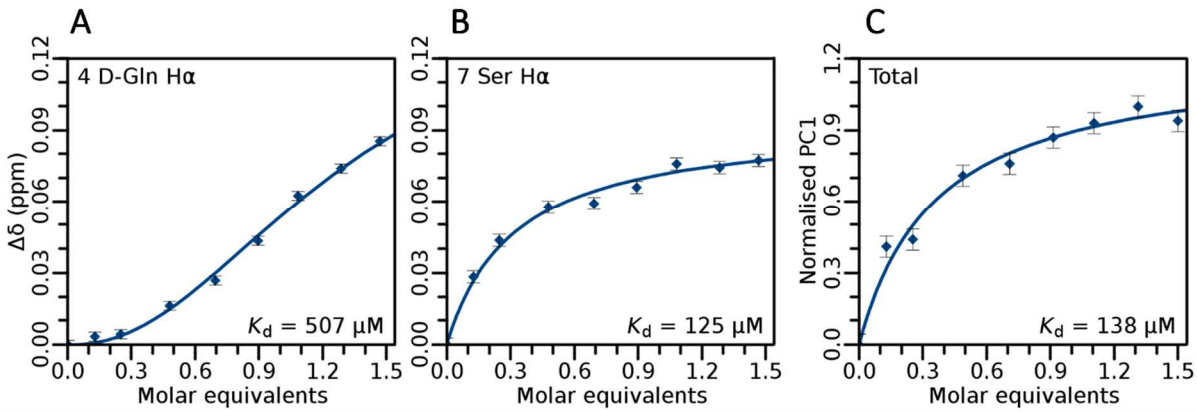

Figure 5.6: Selected binding isotherms obtained from titrations of geranyl pyrophosphate into Ala_{10}-teixobactin demonstrating residue-specific binding behavior with cooperative characteristics. Error bars show RMS of function fit. PC: Principal Component.

Both TLC (Figure S5.77) and NMR (Figure 5.6, Table 5.3) suggest a 2:1 binding between Ala_{10}-teixobactin **5.8** and geranyl pyrophosphate. When titrating geranyl pyrophosphate into **5.8** certain residues such as Ser_7 were found to bind with classic Michaelis-Menton binding kinetics (Figure 5.6**B**). However, some isotherms exhibited a sigmoidal shape (Figure 5.6A). This can occur due to intermediate exchange on the NMR time-scale, and therefore cooperative binding is not an obvious choice. However, given our initial TLC data which shows a binding of 2:1 we have fitted the sigmoidal data using the Hill coefficient. It was found that all *N*-terminal residues weakly bound (K_D ~0.5mM) geranyl pyrophosphate in a highly cooperative (Hill coefficient ~2) manner, whereas ring-proximal residues bound significantly tighter but less cooperatively. Tightest binding was observed for Ser_7 (K_D ~125µM), which in a recently published teixobactin X-ray structure[12] points its hydroxyl directly towards a bound anion. Analysing the overall binding using PCA (Figure 5.6**C**), which removes any influence of intermediate exchange from the isotherms,[16] gave a net K_D of ~138 µM.

Entry	K_D (μM)	Hill coefficient
1 Me-D-Phe Hα	n.d.	n.d.
2 Ile Hα	348 ± 18	2.1
3 Ser Hα	503 ± 8	2.0
4 D-Gln Hα	507 ± 2	2.2
5 D-Ile Hα	483 ± 4	1.7
6 Ile Hα	n.d.	n.d.
7 Ser Hα	125 ± 3	
8 D-Thr Hα	204 ± 3	
9 Ala Hα	394 ± 4	2.1
10 Ala Hα	314 ± 3	
11 Ile Hα	391 ± 4	1.5
Net	**138 ± 5**	

Table 5.3: Dissociation constants between Ala_{10}-teixobactin **5.8** and geranyl pyrophosphate at residue resolution, as determined by NMR titration. A blank Hill coefficient indicates Michaelis-Menton binding kinetics was sufficient to satisfactorily describe the titration data.

In order to determine if teixobactins aggregate in the presence of geranyl pyrophosphate ^{1}H DOSY (diffusion ordered spectroscopy) spectra were recorded at each titration point and the diffusion coefficients calculated for both geranyl pyrophosphate and **5.8** (Figure 5.7). Over the course of the titration the diffusion coefficient obtained from **5.8** remained constant, indicating no aggregation occurred. The diffusion coefficient observed for geranyl pyrophosphate increased slightly over the course of the titration, indicating that it may have adopted a more compact structure upon association with the teixobactin analogue.

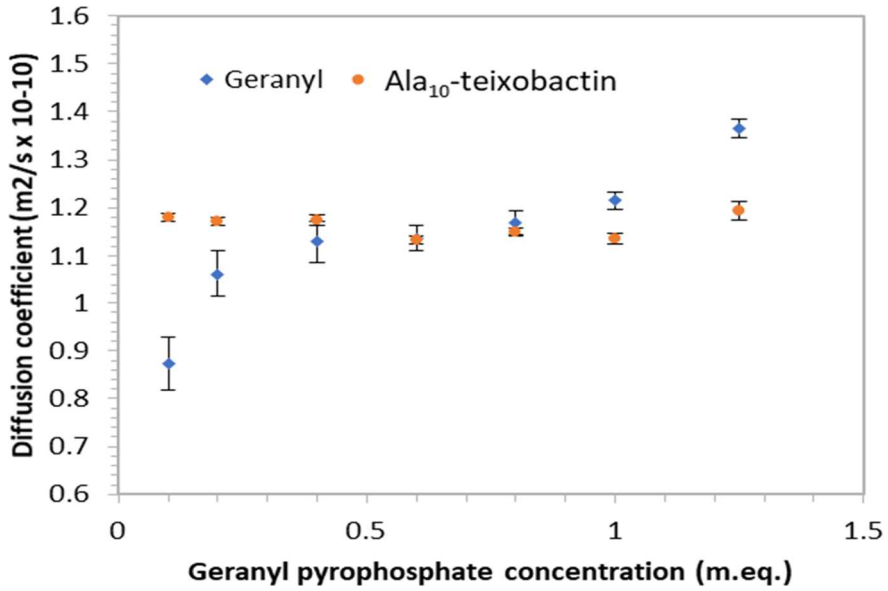

Figure 5.7: Graph of Diffusion co-efficient vs concentration of geranyl pyrophosphate indicating teixobactin does not aggregate when exposed to increasing geranyl pyrophosphate concentrations. Error bars indicate standard deviation of the fitting function.

5.4.7 Antagonization Assay

In order to further prove a lipid II mediated mode of action, an antagonization assay was performed using Leu_{10}-teixobactin **5.13** with lipid II as described in literature.[14] The ratios of **5.13** to lipid II tested were 1:0.5, 1:1, 1:2 and 1:5 and growth was observed. These results are consistent with the 2:1 binding ratio observed using the TLC assay (Table S5.3). However, in case of Leu_{10}-teixobactin **5.13** (control) no growth was observed.

5.4.8 NMR Structural Studies

NMR analysis of teixobactin analogues (Figure 5.8) reveals common structural characteristics between those analogues which retain some residual antibacterial activity. Analogue **5.8** was chosen for NMR studies as it provides the most direct comparison with other analogues. All analogues retain most of the NOEs observed in the Arg_{10}-teixobactin **2.1**, despite some differences in amide chemical shift (Figure 5.8**A**). From Figure 5.8**B** and Figure 5.8**C** it can be observed that α proton chemical shifts show little variation between analogues at both termini: *N*-terminal similarities are likely due to these residues existing in a random coil environment; *C*-terminal similarities are likely due to the restraints placed upon these residues by the ring structure. Amide chemical shifts are more variable, particularly for residues 7 and 8, in which the chemical shift of these protons is ~1 ppm downfield in Ala_{10}-teixobactin **5.8**. This is likely due to the loss of the guanidinium group and suggests proximity between these residues and Arg_{10}. The *N*-terminus again shows little variation, characteristic of a random coil. The mutated residue chemical shifts were excluded from the statistics. Figure 5.8D shows that in all three mutants Ala_3-Arg_{10}-teixobactin **5.3**, Ala_4-Arg_{10}-teixobactin **5.4** and Ala_{10}-teixobactin **5.8** the *N*-termini were unstructured but were showing evidence of structure starting approximately from residue 5, where in all cases the RMSD had dropped by ~50% from that observed at their termini. The RMSDs observed at the *C* termini are low, as this area is highly constrained in structure by the ring.

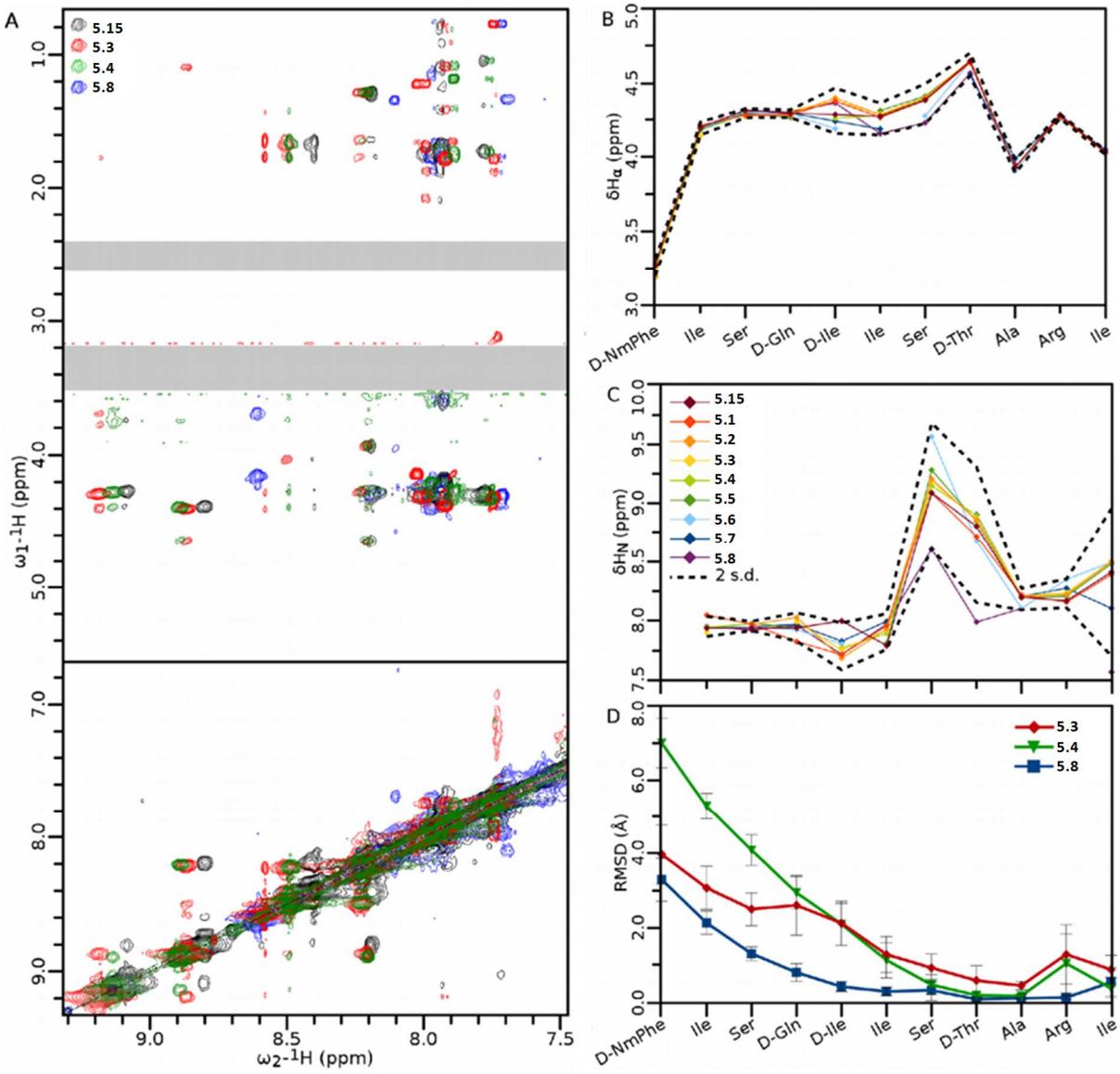

Figure 5.8: (**A**) Overlay of the amide fingerprint regions of the 1H-1H NOESY spectra of wild type (Arg_{10}-teixobactin) and active teixobactin analogues. (**B** and **C**) Chemical shift data obtained from α (**B**) and amide (**C**) protons. (**D**) Statistics of structures calculated using the NOEs obtained from panel (**A**). For clarity, the DMSO (~3.3 ppm) and residual water (~2.5 ppm) signals have been obscured with grey boxes. Data show the average RMSD of each atom in the residue from all 20 members of the ensemble. Error bars are standard deviation in the RMSDs of each residue's atoms. Standard deviations were calculated including the chemical shifts for 16.[7] Ensembles of 20 structures generated by Cyana 2.1[17] and refined in Gromacs[18]. Error bars indicate standard deviation amongst all the atoms of that residue. Spectra were recorded on 1 mM teixobactin samples dissolved in DMSO-d_6 on a 500 MHz spectrometer at 300 K. Legends for Figure 5.8**B** and Figure 5.8**C** are the same, and are shown in panel (**C**).

5.5 Conclusion

In conclusion, we have described a unique design and rapid synthesis of several highly potent teixobactin analogues by replacing the synthetically challenging amino acid L-*allo*-End with the commercially available non-polar residues such as leucine **5.13** and isoleucine **5.12**. The teixobactin analogues from this work have shown highly potent antibacterial activity against a broad panel of MRSA, MSSA and VRE, despite their simpler design. Early stage kill kinetics data suggests Leu_{10}-teixobactin and Ile_{10}-teixobactin to be superior to vancomycin against MRSA. An antagonization assay suggests a lipid II mediated mode of action for Leu_{10}-teixobactin. Most importantly, contrary to the current understanding we have demonstrated that cationic amino acids such as L-*allo*-End, arginine or lysine at position 10 are not essential for target (lipid II) binding and antibacterial activity. This surprising finding opens the door to the design and syntheses of several highly simplified potent teixobactin analogues and challenges many of the current assumptions about the mechanism of action of teixobactin. Our design of highly potent teixobactin analogues has several advantages such as improved yields ~10-20%, ease of synthesis (including 10 min μwave assisted coupling steps and a 30 min cyclisation step) and uses commercially available building blocks.

NMR studies reveal that the analogues Ala_3-Arg_{10}-teixobactin **5.3**, Ala_4-Arg_{10}-teixobactin **5.4** and Ala_{10}-teixobactin **5.8** are more unstructured towards the *N*-termini but highly structured towards the *C* termini due to the close-by ring. We have performed qualitative lipid II binding experiments and measured the binding affinities of individual amino acid residues of Ala_{10}-teixobactin and geranyl pyrophosphate (lipid II mimic) by NMR to understand the role of amino acid residues in binding. Ser_7 was found to have the tightest binding with an experimental K_D of 125 μM.

To the best of our knowledge, Ile_{10}-teixobactin **5.12** and Leu_{10}-teixobactin **5.13** are the only reported teixobactin analogues which have shown superior potency against resistant Gram-positive bacteria. The results from this work represent a significant advancement in our current understanding of the residues critical to the biological activity of teixobactin and associated analogues. We anticipate that our design and relatively rapid synthesis will help overcome current challenges in the field. As it stands, our work herein provides ready access to highly potent teixobactin analogues and will enable the development of teixobactin analogues with drug like properties against resistant bacterial strains. The findings presented in this work have broad implications and are expected to facilitate the development of peptide-based antibiotics for combatting the serious global challenges posed by AMR.

5.6 References

1. B. C. Cunningham, J. A. Wells, High-Resolution Epitope Mapping of hGH-Receptor Interactions by Alanine-Scanning Mutagenesis. *Science*. **244**, pp. 1081–1085.

2. X. Ge, K. Teng, J. Wang, F. Zhao, F. Wang, J. Zhang, J. Zhong, Ligand determinants of nisin for its induction activity. *Journal of Dairy Science*. **99**, 5022–5031 (2016).

3. A. Hänchen, S. Rausch, B. Landmann, L. Toti, A. Nusser, R. D. Süssmuth, Alanine Scan of the Peptide Antibiotic Feglymycin: Assessment of Amino Acid Side Chains Contributing to Antimicrobial Activity. *ChemBioChem*. **14**, 625–632 (2013).

4. S. M. Simonsen, L. Sando, K. J. Rosengren, C. K. Wang, M. L. Colgrave, N. L. Daly, D. J. Craik, Alanine scanning mutagenesis of the prototypic cyclotide reveals a cluster of residues essential for bioactivity. *Journal of Biological Chemistry*. **283**, 9805–9813 (2008).

5. H. Yang, K. H. Chen, J. S. Nowick, Elucidation of the Teixobactin Pharmacophore. *ACS Chemical Biology*. **11**, 1823–26 (2016).

6. Y. E. Jad, G. A. Acosta, T. Naicker, M. Ramtahal, A. El-Faham, T. Govender, H. G. Kruger, B. G. De La Torre, F. Albericio, Synthesis and Biological Evaluation of a Teixobactin Analogue. *Organic Letters*. **17**, 6182–6185 (2015).

7. A. Parmar, A. Iyer, C. S. Vincent, D. Van Lysebetten, S. H. Prior, A. Madder, E. J. Taylor, I. Singh, Efficient total syntheses and biological activities of two teixobactin analogues. *Chem. Commun.* **52**, 6060–6063 (2016).

8. K. Jin, I. H. Sam, K. H. L. Po, D. Lin, E. H. Ghazvini Zadeh, S. Chen, Y. Yuan, X. Li, Total synthesis of teixobactin. *Nature Communications*. **7**, 12394 (2016).

9. F. von Nussbaum, R. D. Süssmuth, Multiple Attack on Bacteria by the New Antibiotic Teixobactin. *Angewandte Chemie International Edition*. **54**, 6684–6686 (2015).

10. A. M. Giltrap, L. J. Dowman, G. Nagalingam, J. L. Ochoa, R. G. Linington, W. J. Britton, R. J. Payne, Total Synthesis of Teixobactin. *Organic Letters*. **18**, 2788–2791 (2016).

11. S.-T. D. Hsu, E. Breukink, E. Tischenko, M. A. G. Lutters, B. de Kruijff, R. Kaptein, A. M. J. J. Bonvin, N. A. J. van Nuland, The nisin-lipid II complex reveals a pyrophosphate cage that provides a blueprint for novel antibiotics. *Nature structural & molecular biology*. **11**, 963–7 (2004).

12. R. V Rasmussen, V. G. Fowler Jr, R. Skov, N. E. Bruun, Future challenges and treatment of Staphylococcus aureus bacteremia with emphasis on MRSA. *Future Microbiology*. **6**, 43–56 (2011).

13. C. Wu, Z. Pan, G. Yao, W. Wang, L. Fang, W. Su, Synthesis and structure–activity relationship studies of teixobactin analogues. *RSC Adv.* **7**, 1923–1926 (2017).

14. L. L. Ling, T. Schneider, A. J. Peoples, A. L. Spoering, I. Engels, B. P. Conlon, A. Mueller, D. E. Hughes, S. Epstein, M. Jones, L. Lazarides, V. a Steadman, D. R. Cohen, C. R. Felix, K. A. Fetterman, W. P. Millett, A. G. Nitti, A. M. Zullo, C. Chen, K. Lewis, A new antibiotic kills pathogens without detectable resistance. *Nature*. **517**, 455–459 (2015).

15. A. Parmar, S. H. Prior, A. Iyer, C. S. Vincent, D. Van Lysebetten, E. Breukink, A. Madder, E. J. Taylor, I. Singh, Defining the molecular structure of teixobactin analogues and understanding their role in antibacterial activities. *Chemical communications*. **53**, 2016–2019 (2017).

16. J. Xu, D. Van, Tracking Equilibrium and Nonequilibrium Shifts in Data with TREND. *Biophysical Journal*. **112**, 224–233 (2017).

17. P. Guntert, L. Buchner, Combined automated NOE assignment and structure calculation with CYANA. *Journal of Biomolecular NMR*. **62**, 453–471 (2015).

18. M. J. Abraham, T. Murtola, R. Schulz, S. Pall, J. C. Smith, B. Hess, E. Lindah, Gromacs: High performance molecular simulations through multi-level parallelism from laptops to supercomputers. *SoftwareX*. **1–2**, 19–25 (2015).

CHAPTER 6

6 Design and Syntheses of Highly Potent Teixobactin Analogues against *Staphylococcus aureus*, Methicillin-Resistant *Staphylococcus aureus* (MRSA), and Vancomycin-Resistant Enterococci (VRE) *in Vitro* and *in Vivo*

Journal of Medicinal Chemistry

Article

Cite This: *J. Med. Chem.* 2018, 61, 2009−2017

pubs.acs.org/jmc

Design and Syntheses of Highly Potent Teixobactin Analogues against *Staphylococcus aureus*, Methicillin-Resistant *Staphylococcus aureus* (MRSA), and Vancomycin-Resistant Enterococci (VRE) *in Vitro* and *in Vivo*

Anish Parmar,[†,¶] Rajamani Lakshminarayanan,[‡,¶] Abhishek Iyer,[†,§] Venkatesh Mayandi,[‡] Eunice Tze Leng Goh,[‡] Daniel G. Lloyd,[∥] Madhavi Latha S. Chalasani,[⊥] Navin K. Verma,[⊥,‡] Stephen H. Prior,[#] Roger W. Beuerman,[‡] Annemieke Madder,[§] Edward J. Taylor,[∥] and Ishwar Singh*[,†]

Author contributions: Myself and Rajamani Lakshminarayanan contributed equally to this work. The project was conceived and designed by Ishwar Singh. The manuscript was written by Me, Abhishek Iyer, Rajamani Lakshminarayanan and Ishwar Singh through contributions from all authors. All teixobactin analogues herein were synthesised by me. Daniel G. Lloyd, and Edward J. Taylor have contributed to the antibacterial studies. Madhavi Latha S. Chalasani and Navin K. Verma carried out the in vitro toxicity studies. Annemieke Madder was responsible for the LC-MS analyses. Venkatesh Mayandi, Eunice Tze Leng Goh, Roger W. Beuerman and Rajamani Lakshminarayanan were responsible for the in vitro antibacterial studies and in vivo toxicity and antibacterial studies.

6.1 Abstract

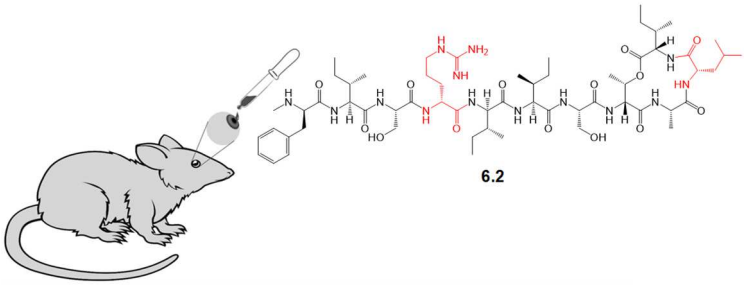

The cyclic depsipeptide, teixobactin kills a number of Gram-positive bacteria including Methicillin-resistant Staphylococcus aureus (MRSA) and Mycobacterium tuberculosis without detectable resistance. To date, teixobactin ***1.23*** *is the only molecule in its class which has shown in vivo antibacterial efficacy. In this work, we designed and synthesised 10 new in vivo ready teixobactin analogues. These analogues showed highly potent antibacterial activity against Staphylococcus aureus, MRSA, and vancomycin-resistant Enterococci (VRE) in vitro. One analogue,* $_D$*-Arg4-Leu10-teixobactin* ***6.2*** *was found to be non-cytotoxic in vitro and in vivo. Moreover, topical instillation of peptide* ***6.2*** *in a mouse model of S. aureus keratitis decreased the bacterial bioburden (>99.0% reduction) and corneal edema significantly as compared to untreated mouse corneas. Collectively, our results have established the high therapeutic potential of teixobactin analogue in attenuating bacterial infections and the associated severities.*

6.2 Breif Introducion

From the previous chapter, to expedite access to highly potent teixobactin analogues, a new design was reported by which we replaced the synthetically challenging enduracididine with commercially available hydrophobic residues such as as leucine and isoleucine.[1] Leu_{10}- teixobactin (**5.13**) and Ile_{10}-teixobactin (**5.12**) showed identical activities against MRSA *in vitro* that were identical to teixobactin. However, increased hydrophobicity may have an adverse influence on the *in vivo* capacity to be further developed as therapeutic drugs. Teixobactin **1.23** and key teixobactin analogues and their antibacterial activities are summarised in Figure 6.1.

Teixobactin **1.23** has shown antibacterial efficacy *in vivo* in three mouse models of infection. Although these results are encouraging, a significant amount of work remains in developing **1.23** as a therapeutic antibiotic for human use.[2] The translation of molecules from a discovery phase to that of useful therapeutic antibiotics is prone to high failure rates due to numerous challenges, such as balancing high efficacy *in vivo* against a broad spectrum of pathogens with minimal liabilities against human targets and the balancing of hydrophobicity with hydrophilicity to address water solubility issues.[3] There is a pressing need for highly potent analogues of **1.23** to address common drug-development challenges. To date, there have been no *in vivo* evaluation studies of teixobactin analogues.

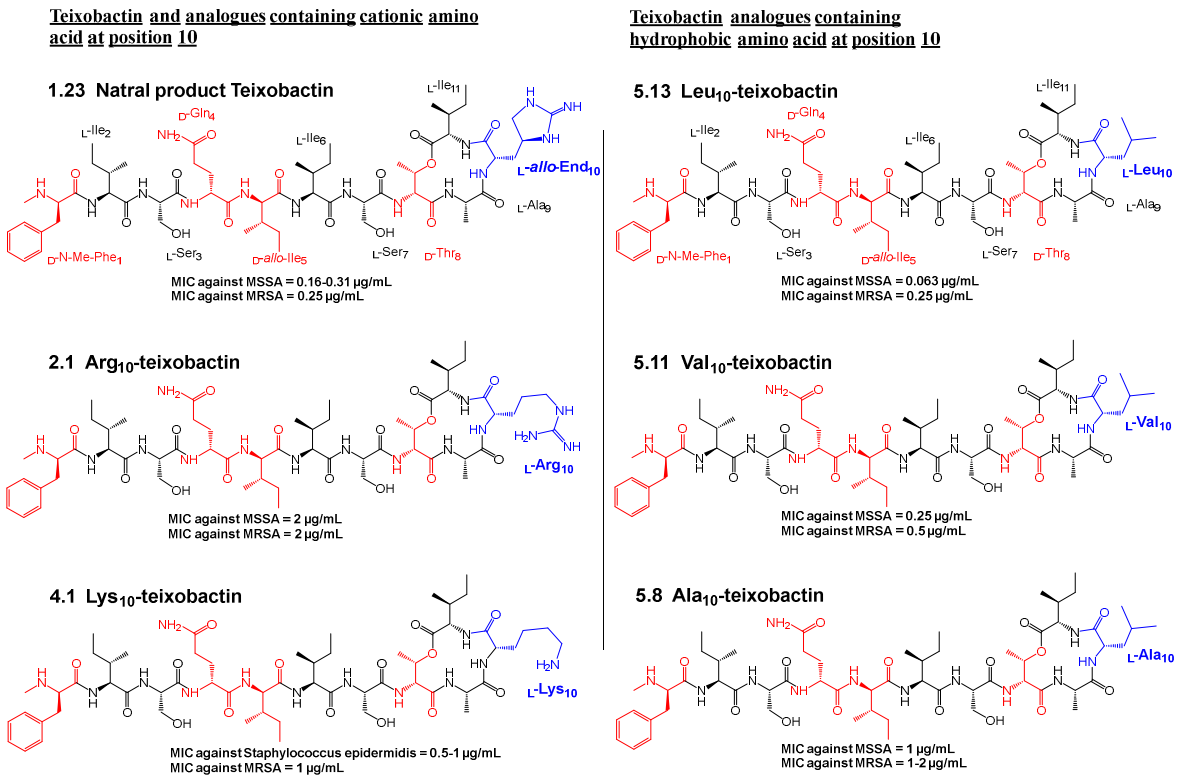

Figure 6.1: Teixobactin and its analogues containing cationic and hydrophobic amino acids. Cationic analogues **1.23**[1, 4, 5], **2.1**[6–8], **4.1**[8, 9] and hydrophobic analogues **5.13**[1], **5.11**[1], **5.8**[1, 10] with the (D-amino acids highlighted in red and the position 10 amino acids are highlighted in blue).

6.3 Aim of study

To address teixobactin development challenges, we report herein the design and synthesis of 10 highly potent teixobactin analogues (Figure 6.2) and their antibacterial evaluations aganist *S. aureus* (SA), MRSA, VRE; and the *in vivo* evaluation of one analogue in a mice model of *S. aureus* keratitis. This work lays the foundation for the development of *in vivo* ready teixobactin analogues.

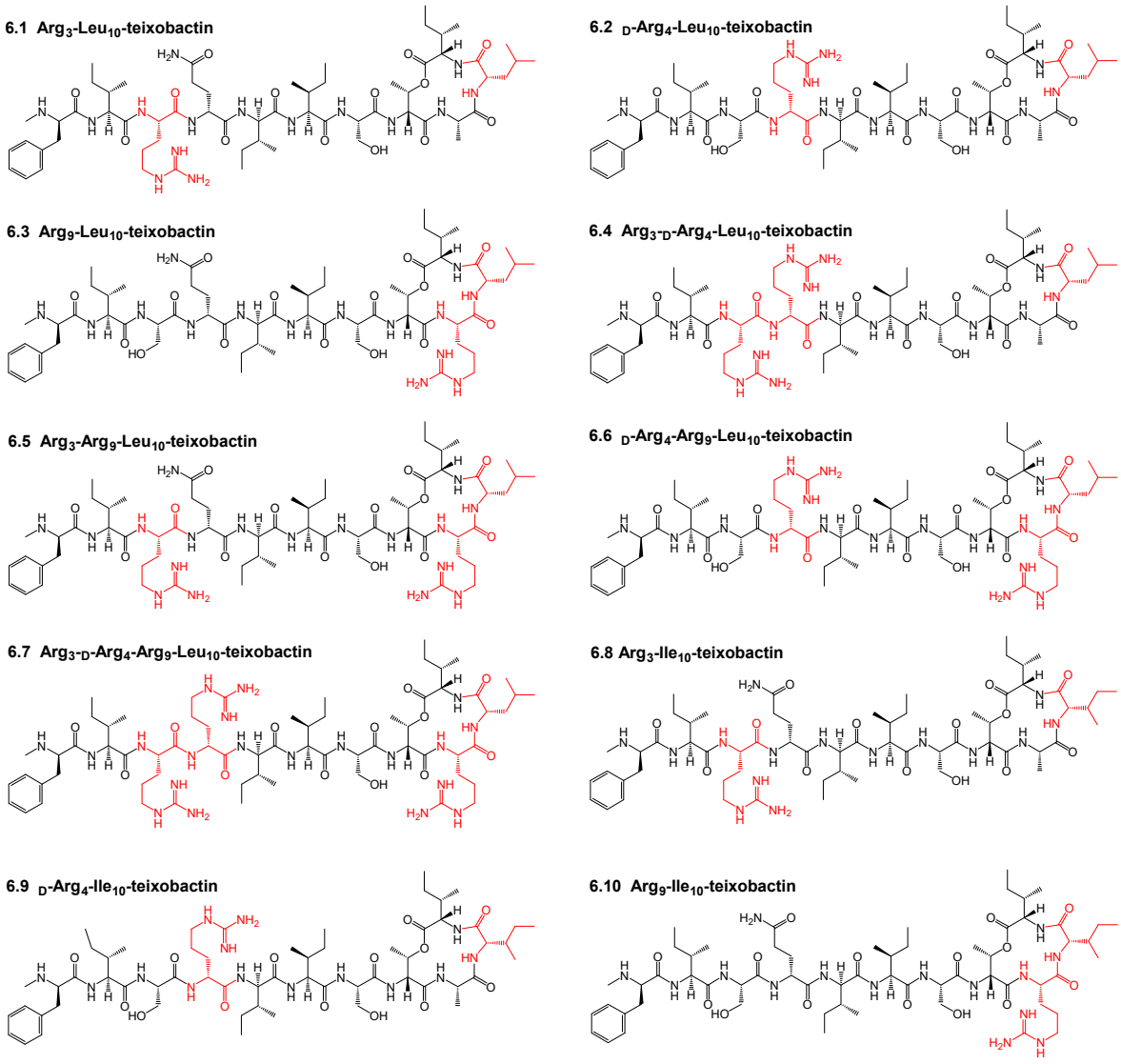

Figure 6.2: Structure of teixobactin analogues **6.1-6.10**

6.4 Results and discussion

6.4.1 Design and synthesis

To date, teixobactin **1.23** is the only molecule in its class which has shown *in vivo* antibacterial efficacy. To realise the therapeutic potential of molecules based on the teixobactin scaffold, there is a pressing need for *in vivo* ready simplified teixobactin analogues with ease of access to address the current challenges associated due to the lengthy and daunting total synthesis of teixobactins.

In this work, to address such teixobactin development challenges, we speculated that the replacement of Ser_3, $_D$ -Gln_4 and Ala_9 of Leu_{10}-teixobactin and Ile_{10}-teixobactin with cationic arginine would mimic the suitable balance of hyrophobicity and hydrophilicity of natural teixobactin. We thus replaced the Ser_3, $_D$ -Gln_4 and Ala_9 of Leu_{10}-teixobactin and Ile_{10}-teixobactin with arginine in a systematic fashion (**6.1**-**6.10**, Figure 6.2). In this way, we realised an optimal balance between hyrophobicity with hydrophilicity. Six of these analogues (**6.1**-**6.3** and **6.8**-**6.10**, Figure 6.2) have hyrophobic-hydrophilic profiles (two positive charges at physiological pH) similar to that of natural teixobactin. Three analogues (**6.4**-**6.6**, Figure 6.2) feature three positive charges and one analogue (**6.7**, Figure 6.2) bears four positive charges. In total, we synthesised 10 new and highly potent teixobactin analogues (**6.1-6.10**, Figure 6.2) in a smilar fashion to our recently reported highly efficient strategy (Scheme 6.1 and experimental section III, Scheme S6.1).[1]

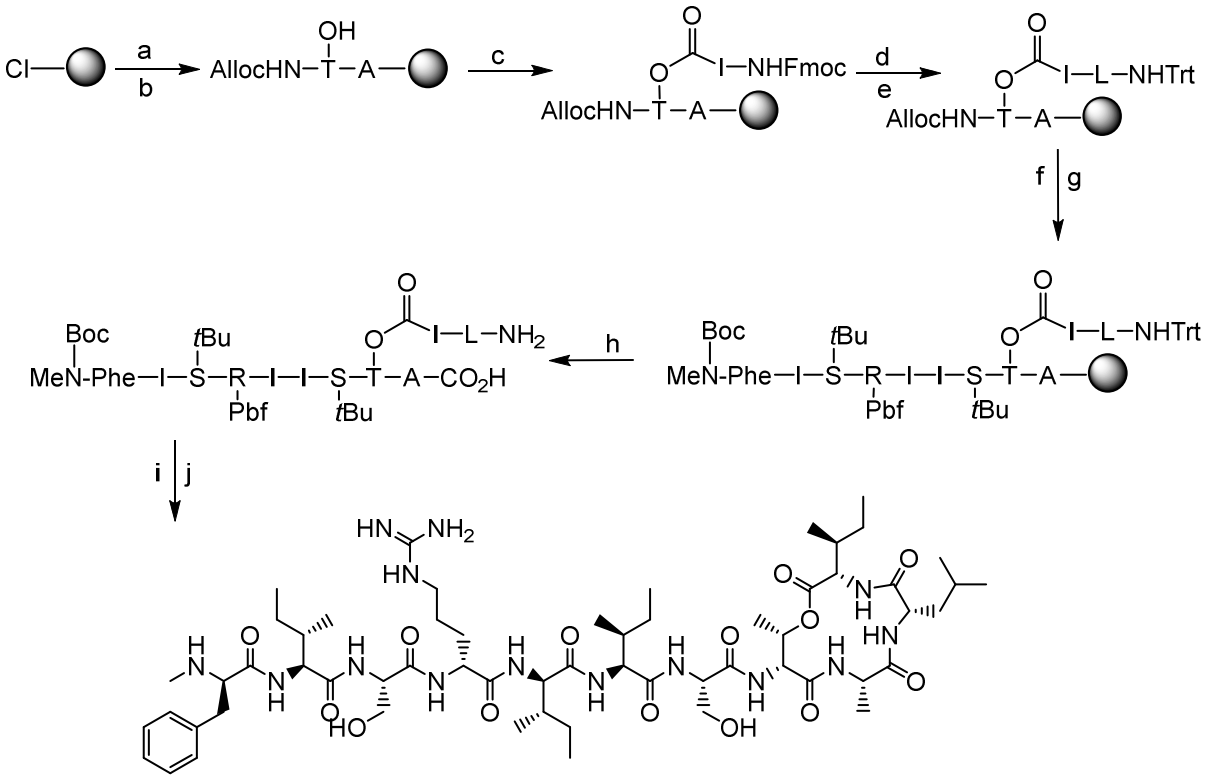

Scheme 6.1: Synthesis of **6.2** starting from 2-chlorotritylchloride resin: a. 4 eq. Fmoc-Ala-OH/8 eq. DIPEA in DCM, 3h. b. 20% piperidine in DMF followed by 3 eq. AllocHN-$_D$-Thr-OH, 3 eq. HATU/6 eq. DIPEA, 1.5h c. 10 eq. Fmoc-Ile-OH, 10 eq. DIC, 5 mol% DMAP in DCM, 2h followed by capping with Ac_2O/DIPEA 10%

in DMF, 20% piperidine in DMF d. 4 eq. Fmoc-Leu-OH, 4 eq. HATU/8 eq. DIPEA in DMF, 1h followed by 20% piperidine in DMF e. 10 eq. Trt-Cl, 15% Et_3N in DCM, 1h. f. 0.2 eq. $[Pd(PPh_3)_4]^0$ + 24 eq. $PhSiH_3$ in dry DCM, 1 x 20 min, 1 x 45 min. g. 4 eq. Fmoc/Boc-AA(PG)-OH (AA = amino acid, PG = protecting group), 4 eq. DIC/Oxyma (µwave, 10 min) followed by 20% piperidine in DMF (3 min, 10 min). h. TFA:TIS:DCM = 2:5:93, 1h. i. 1 eq. HATU/10 eq. DIPEA in DMF, 30 min. j. TFA:TIS:H2O = 95:2.5:2.5, 1h.

6.4.2 *In vitro* Antibacterial studies

The antimicrobial potencies of teixobactin analogues **6.1-6.10** were assessed against MRSA ATCC 33591. Leu_{10}-teixobactin **5.13** and natural teixobactin **1.23** were included as benchmark for activity. The six analogues **6.1**-**6.3** and **6.8**-**6.10** with two cationic charges have hydrophobic-hydrophilic balances like that of **1.23** (two cationic charges). These analogues showed comparable potencies (MIC 0.125 - 0.25µg/ ml) to **1.23** (MIC 0.25µg/ ml, Table 6.1). Analogues **6.4**-**6.6** each possess three cationic charges. Interestingly, analogue **6.4** showed comparable antimicrobial activity (MIC 0.25µg/ ml) to natural teixobactin. However, analogues **6.5** and **6.6** showed 4 times reduced antibacterial activities (MIC 1µg/ ml) than **1.23** or **5.13**. The analogue **6.7** with four cationic charges, also showed reduced antibacterial activity (MIC 1µg/ ml).

Compound	Name	[a]MIC (µg/mL)
1.23	Teixobactin	0.25
5.13	Leu_{10}-teixobactin	0.25
6.1	Arg_3-Leu_{10}-texiobactin	0.125
6.2	$_D$-Arg_4-Leu_{10}-texiobactin	0.125
6.3	Arg_9-Leu_{10}-texiobactin	0.125
6.4	Arg_3-$_D$-Arg_4-Leu_{10}-teixobactin	0.25
6.5	Arg_3-Arg_9-Leu_{10}-teixobactin	1
6.6	$_D$ -Arg_4-Arg_9-Leu_{10}-teixobactin	1
6.7	Arg_3-$_D$-Arg_4-Arg_9-Leu_{10}-teixobactin	1
6.8	Arg_3-Ile_{10}-texiobactin	0.25
6.9	$_D$ -Arg_4-Ile_{10}-texiobactin	0.125
6.10	Arg_9-Leu_{10}-texiobactin	0.25

Table 6.1: List of Teixobactin and Teixobactin analogues (**1.23, 5.13, 6.1-6.10**). [a]MIC: Minimum Inhibitory Concentration. MRSA ATCC 33591 was used.

Teixobactin analogues **6.1-6.10** were further assessed against an extended panel of antibiotic-resistant and antibiotic susceptible Gram-positive pathogens and compared to the antibiotic daptomycin (Figure 6.3). The MIC results indicate that the synthetic analogues are potent against the various strains tested, but their MIC distribution differs significantly. Interestingly, we observed a wider distribution of MIC values as the overall net charge of the peptide was increased (Table 6.1 and Table 6.2).

Notably, the MIC values for *Staphylococcus* were not altered, whereas significant increases in the *Enterococcus* MIC values were observed for the analogue with four cationic charges (**6.7**, MIC 2-8µg/ ml). Similar trends have been reported for teixobactin analogues whereby increases in positive charges, confer increases in MICs against *Staphylococcus* aureus ATCC 29213[11]. Herein, for example, Lys_{3}-$_{D}$-Lys_{4}-Lys_{10}-teixobactin, which has four cationic charges (Figure 6.1E), has reported MIC 8µg/ ml against *Staphylococcus* aureus ATCC 29213[11], were as we observed an MIC of 1µg/ ml (an 8 times improvement) for Arg_{3}-$_{D}$-Arg_{4}-Arg_{9}-Leu_{10}-teixobactin (7, four cationic charges, Figure 6.2) against the same bacterial strain.

The inclusion of 3 arginines in the above case likely perturbs the amphiphilic character of teixobactin, resulting in a decrease in activity. The six analogues with two cationic charges, **6.1**-**6.3** and **6.8**-**6.10** showed comparable antibacterial potencies to that of Leu_{10}-teixobactin. Importantly, the hydrophobic-hydrophilic balances of these analogues were like that of natural teixobactin (two cationic charges). The analogues with three cationic charges, **6.4**-**6.6** also showed comparable antibacterial potencies to that of Leu_{10}-teixobactin **5.13**. All synthesized analogues showed good potency against a broad panel of bacteria including clinical isolates. Nine analogues, **6.1**-**6.6**, and **6.8**-**6.10** showed drug-like profiles, such as high antibacterial potencies and optimal balances of hydrophobicity and hydrophilicity. We have further determined the minimum bactericidal concentrations (MBC) of teixobactin analogues against *S. aureus*/MRSA strains (Table S6.4). Compound **6.2** displayed highly potent bactericidal properties, as its MBC values did not increase above 4 times its MICs against the tested strains. Compound **6.2** was found to be inactive against *Pseudomonas aeruginosa,* a Gram-negative bacterium (Table S6.3). In view of narrow MIC-distribution values and bactericidal properties, we focused our attention on compound **6.2** and further investigated its biological properties.

Strain	Compd 6.1	Compd 6.2	Compd 6.3	Compd 6.4	Compd 6.5	Compd 6.6	Compd 6.7	Compd 6.8	Compd 6.9	Compd 6.10	Compd 5.13
Staphylococcus saprophyticus ATCC BAA 750	<0.0625	<0.0625	<0.0625	<0.0625	<0.0625	<0.0625	<0.0625	<0.0625	<0.0625	<0.0625	-
Staphylococcus saprophyticus ATCC 15305	<0.0625	<0.0625	<0.0625	<0.0625	<0.0625	<0.0625	0.25	<0.0625	<0.0625	<0.0625	-
Staphylococcus saprophyticus ATCC 49453	<0.0625	<0.0625	<0.0625	<0.0625	<0.0625	<0.0625	<0.0625	<0.0625	<0.0625	<0.0625	-
Staphylococcus saprophyticus ATCC 49907	<0.0625	<0.0625	<0.0625	<0.0625	<0.0625	<0.0625	<0.0625	<0.0625	<0.0625	<0.0625	-
VRE 1001	0.25	0.5	0.5	1	0.5	1	2	1	0.5	1	-
VRE 1002	0.5	1	1	1	1	1	8	1	1	1	-
VRE 1004	<0.0625	0.25	0.25	0.5	0.5	1	4	1	0.5	1	-
VRE 1008	0.125	0.5	0.25	0.5	0.5	1	8	1	0.5	1	-
VRE ATCC 700802	0.5	0.5	0.5	2	1	1	4	1	0.25	1	0.25
VRE ATCC 29212	0.5	0.5	1	1	1	1	4	1	0.25	1	0.25
MRSA ATCC 700699	0.5	0.25	0.5	0.5	1	1	2	1	0.25	1	0.25
MRSA 42412	<0.0625	0.0313	<0.0625	0.25	0.25	1	2	0.125	<0.0625	0.125	<0.0625
MRSA 21455	0.03125	0.0313	0.25	0.5	1	1	2	0.25	0.03125	0.5	<0.0625
MRSA 1003	<0.0625	0.5	0.25	1	2	0.5	2	0.125	<0.0625	0.5	-
S. aureus 29213	0.25	<0.0625	0.5	0.25	1	1	1	0.5	0.0625	1	-
S. aureus 4299	0.125	-	0.25	0.25	0.5	0.5	1	0.125	<0.0625	1	-
S. epidermidis 12228	<0.0625	<0.0625	<0.0625	<0.0625	<0.0625	<0.0625	<0.0625	<0.0625	<0.0625	<0.0625	-
Bacillus Cereus ATCC 11788	<0.0625	0.5	0.25	1	1	1	1	0.125	<0.0625	0.5	-
Bacillus Subtilis ATCC 6633	<0.0625	0.125	<0.0625	<0.0625	<0.0625	<0.0625	<0.0625	<0.0625	<0.0625	0.125	-

Table 6.2: MIC values of compounds **5.13**, **6.1-6.10** against a broad panel of bacteria[a]. [a]*Enterococcus faecalis*, VRE 1001-1002, 1004, 1008 are clinical isolates. MRSA 42412, MRSA 21455 and MRSA 1003 are clinical isolates.

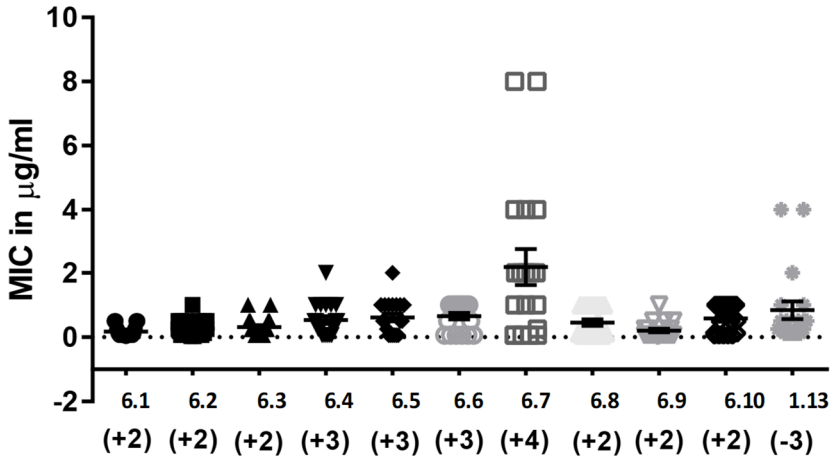

Figure 6.3: MIC distribution of various analogues of teixobactin (**6.1-6.10**) against 19 different Gram-positive pathogens (Table S6.3). Daptomycin **1.13** was included for comparison. Note the increase in MIC distribution as the overall net charge on the teixobactin analogues was increased. The number in parenthesis indicates the overall net charge of the peptides.

6.4.3 Resistance studies and time depenadat killing of bacteria using teixobactin analogue 6.2

$_D$-Arg$_4$-Leu$_{10}$-teixobactin (**6.2**) was evaluated for single step resistance in *S. aureus* ATCC 29213 and MRSA ATCC 33591. We were unable to obtain mutants of *S. aureus* ATCC 29213 or MRSA ATCC 33591 resistant to teixobactin analogue **6.2** (5, 10, and 20x MIC). The calculated frequency of resistance to teixobactin analogue **6.2** was found to be $<10^{-10}$ (SI section V), which is comparable to that of teixobactin **1.23**.[4] A lack of resistance in preliminary studies against **6.2** is promising in the development of drug like molecules against resistant bacteria.

Time-kill kinetics studies of $_D$-Arg$_4$-Leu$_{10}$-teixobactin, **6.2**, against *S. aureus* ATCC 29213 were investigated to ascertain if the chemical modifications retained the bactericidal properties. The exposure of bacterial inoculum to 0.5 µg/ml or 1 µg/ml of compound **6.2** resulted in ≥ 2 log10 decrease in bacterial viability at 8 h (Figure S6.23), which is comparable to those in previous reports of teixobactin analogues and teixobactin.[1, 4]

6.4.4 *In vitro* cytotoxicity studies

It was important to evaluate the cytotoxicity of compound **6.2** on mammalian cells prior to *in vivo* studies. We determined the cytotoxicity of **6.2** in human-lung-epithelial-cell line A549 and primary dermal fibroblasts (hDFs). Both of these cell culture models are already established for the evaluation of cytotoxicity of antimicrobial peptides.[12,13] An MTS assay indicated that both mammalian cell-types exposed to various concentrations of the peptide retained significant metabolic activity (≥ 80% viability, Figure 6.4 a,b), even at a concentration that was ~900 times (250 µg/ml) higher than the average MIC (0.27 µg/ml) values, indicating excellent cell selectivity of the teixobactin analogues. High-content images indicated the absence of any cytoskeletal and nuclear disruptions upon exposure of both epithelial and fibroblasts cells to compound **6.2** (Figure 6.4 c,d), establishing its non-cytotoxic properties. The morphology of mammalian cells exposed to **6.2** appeared similar to that of the untreated cells. However, exposure of cells to an antineoplastic agent (nocodazole, used as a control) resulted in substantial loss of adhered cells, confirming its cytotoxicity.

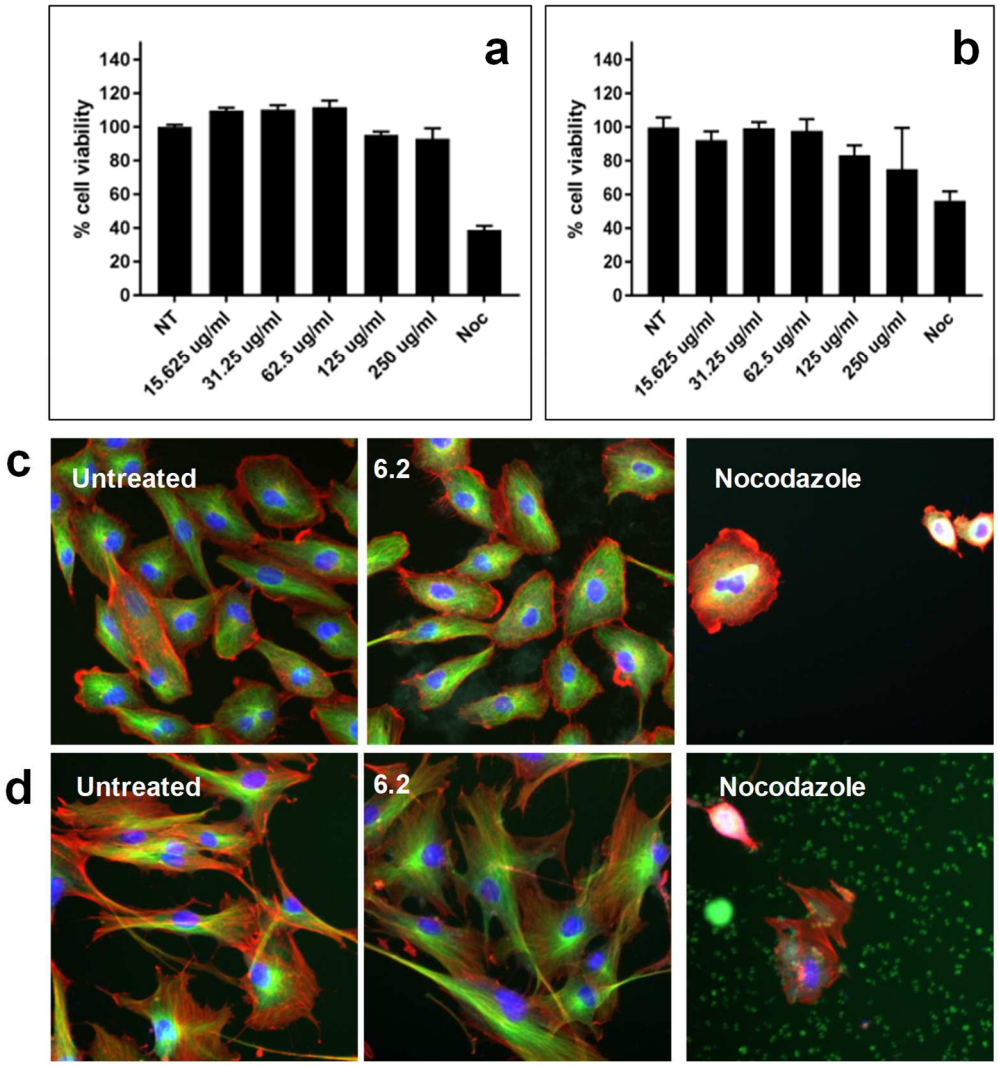

Figure 6.4: Cytotoxicity evaluation of **6.2** in A549 lung epithelial cell line and human primary dermal fibroblasts (hDFs). Both A549 cells (**a**) and hDFs () were **b** treated with increasing concentrations of **6.2** (ranging from 15.62 µg/ml to 250 µg/ml) for 24 h. The stock solution of **6.2** (500 µg/ml) was prepared fresh by directly dissolving **6.2** in cell culture medium just before use. Cells were treated with dimethyl sulfoxide (DMSO, 0.1% v/v) or nocodazole (5 µg/ml dissolved in DMSO) as controls. At the end of the treatment period, metabolic activities of cells were quantified by MTS-based cell viability assay. Data represents mean ± the standard errors of the means (SEM) of three independent triplicate experiments, (*p>0.05). After 24 h treatment with **6.2**, A549 cells (**c**) and hDFs (**d**) were fixed; fluorescently stained with rhodamine-phalloidin (red), alexa fluor 488 conjugated anti-α-tubulin (green) and Hoechst 33342 (blue); and imaged using IN Cell Analyzer 2200 automated microscope. Representative images of cells treated with **6.2** (62.5 µg/ml for 24 h) or nocodazole (10 µg/ml, toxicity control) are shown.

6.4.5 *In vivo* Toxicity Studies

We examined the *in vivo* toxicity of **6.2** in a rabbit corneal-damage model. A 0.3% (w/v) solution (50µL) was applied topically (4 times/day) to the circularly debrided cornea, and re-epithelialization was monitored by fluorescein staining. The vehicle alone served as a control. Figure 6.5 shows the decrease in fluorescein staining with time for both control wounds and wounds treated with **6.2**.

There was no significant difference in wound closure between PBS-treated wounds or wounds treated with 29 (Figure S6.24). The lack of any delay in the re-epithelialization and wound closure for the injured corneas treated with **6.2** suggests good biocompatibility of the peptide.

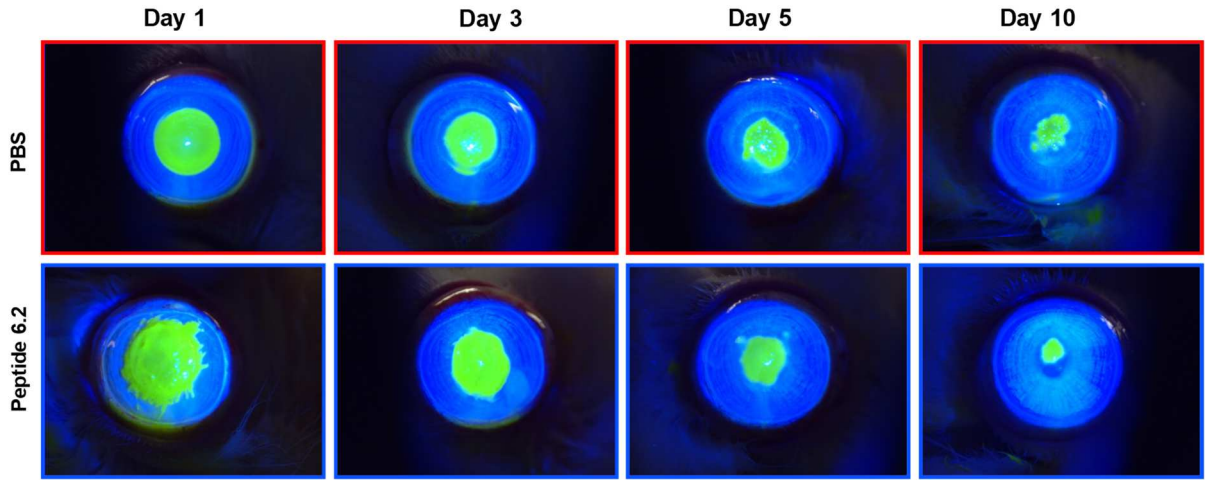

Figure 6.5: Representative slit lamp fluorescence images showing the time-dependent changes in wound closure of corneas after the application of PBS (2 eyes) or 0.3% peptide **6.2** (4 eyes). The wounded corneas were stained with fluorescein to observe epithelial defects and imaged by slit-lamp biomicroscopy.

6.4.6 *In vivo* antibacterial efficacy of $_D$-Arg$_4$-Leu$_{10}$-teixobactin 6.2 in bacterial keratitis model

We examined the *in vivo* efficacy of peptide **6.2** in a mouse-eye model of *S.aureus* keratitis. *S. aureus* is one of the major etiological agents for bacterial keratitis, and the toxic secretions produced by this microorganism have been implicated in corneal melt, leading to significant morbidity and vision loss[14, 15]. Scarified cornea of the mice was infected with *S. aureus* ATCC 29213 inocula (15 µL of 6×10^6 CFU/ml). At 6 h post infections (p.i.), the infected cornea were treated with vehicle (PBS), peptide **6.2** (0.3% w/v in PBS) or moxifloxacin (0.3%). A total of 8 doses was applied and the progression of the infection was monitored by slit lamp examination, anterior segment optical coherent tomography (AS-OCT), and microbiological enumeration of the bacterial bioburden. Mouse corneas treated with PBS had severe clinical presentations indicated by chemosis, the significant presence of hypopyonlike materials and corneal infiltrates (Figure 6.6).

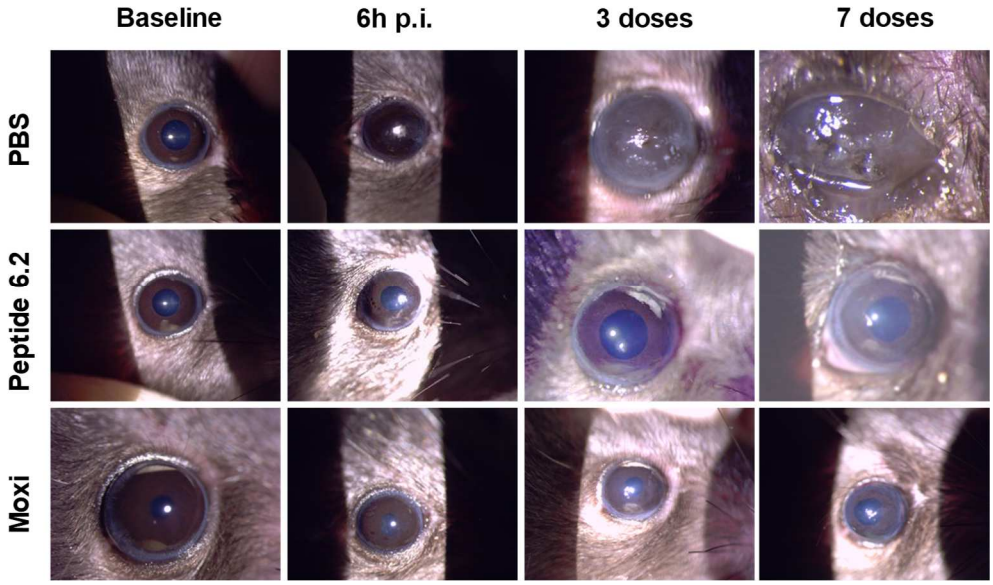

Figure 6.6: Slit lamp examination of mice infected with S. aureus ATCC 29213 strains. After scratching the corneal epithelium with scalpel blade, the scarified cornea was infected with a bacterial inoculum of 6 x 10^6 CFU/ml (15 µL/cornea). At 6 h post infections, the infected corneas were treated with 15 µL of PBS, peptide **6.2** (0.3% w/v in PBS) or moxifloxacin (0.3% w/v in PBS). Note the significant presence of corneal haze and mucopurulent discharge in PBS-treated cornea whereas peptide **6.2** and moxifloxacin treated cornea remained clear and no signs of corneal defects.

Notably, infected cornea treated with peptide **6.2** or a fluoroquinalone antibiotic, had similar clinical-appearance presentations, as indicated by lack of any conjunctival chemosis and corneal infiltrates. These results indicate that peptide **6.2** halted the progression of *S. aureus* infections and the activity was comparable to that of moxifloxacin. To determine the effect of treatments on tissue severity, we determined the corneal thickness for various groups (Figure 6.7a, Figure S6.25). The baseline corneal thickness of mice (93.8±2.9 µm) decreased moderately (79.0±3.4 µm) after de-epithelialization followed by the *S. aureus* infection (6h p.i.). Treatment of the infected cornea with vehicle alone (PBS) resulted in substantial increases in corneal thicknesses after 24 h (151.7±12.7 µm) and 48 h (186.2±17.5 µm), indicating corneal edemas after infection. Infected corneas treated with peptide **6.2** had a mean corneal thickness of 92.3±12.5 and 121.7 ± 3.2 µm 24 h and 48 h post treatment (p.t.), respectively. For the moxifloxacin-treated corneas the mean corneal thickness was 124.2±9.4 µm after 24 h p.t. and 140.3±10.3 µm after 48 h p.t. These results suggested that peptide **6.2** treatment resulted in significant decrease in corneal edemas after *S. aureus* infections as compared with those PBS-treated or moxifloxacin-treated groups.

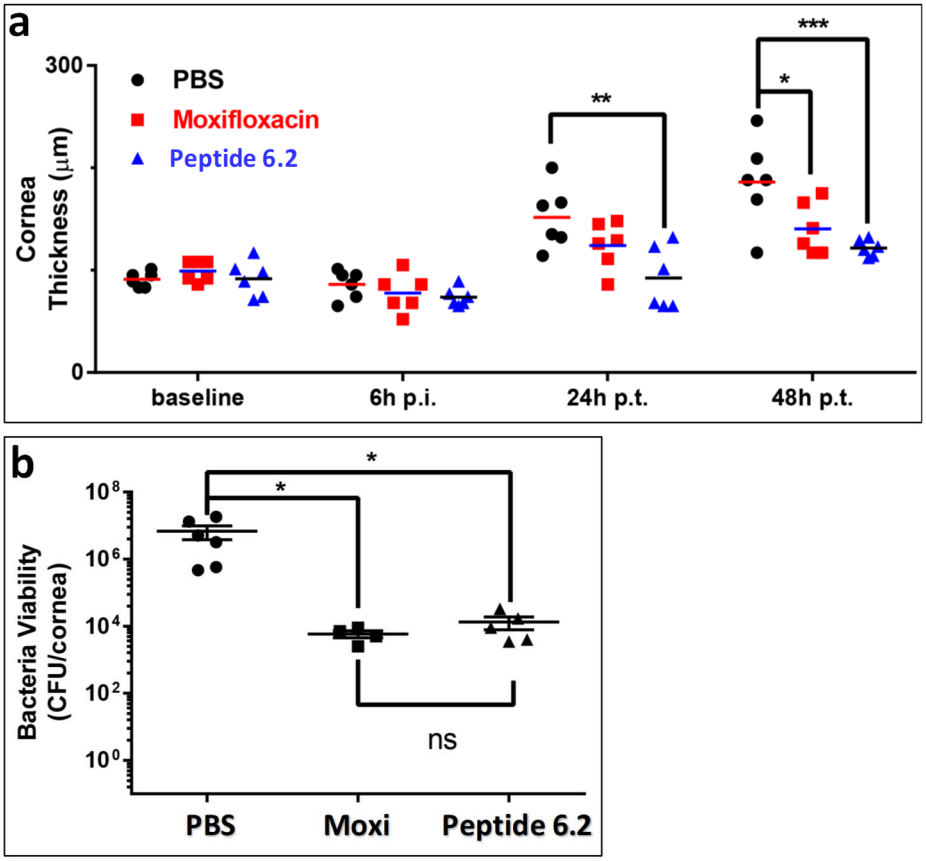

Figure 6.7: (**a**) Changes in corneal thickness (CT) of mice before and after infections and treatment with various groups. Note that the CT values for peptide **6.2** treated cornea approached the baseline values 48 h p.t., which did not happen in the cases of PBS- and Moxifloxacin-treated corneas. Note that a significant decrease in corneal edemas was observed for infected cornea treated with peptide **6.2** compared with those in the untreated corneas (p, 0.01 two-way ANOVA) as early as after 3 doses, and the edemas decreased further after 8 doses (p, 0.001). The results indicated a marked decrease in the severity of the infections after treatment with **6.2** when compared to standard antibiotic treatment. (**b**) Bacterial bioburden in the infected corneas 48 h after treatment in the various groups. The values represent colony counts from individual cornea, and bars represent mean CFU/tissue ± standard errors of the mean.

Bacterial enumeration of the corneal tissues harvested after 8 dosages confirmed the *in vivo* efficacy of peptide **6.2** (Figure 6.7b). All the infected cornea that received PBS treatment contained significant amounts of bacteria, varying from 4.7×10^5 – 1.3×10^7 CFU/tissue. The mean $\log_{10}$ CFU/tissue ± standard error of the mean for PBS treated cornea was 6.51±0.27. Five out of six cornea treated with peptide **6.2** had detectable bacterial colonies. The mean $\log_{10}$ CFU/tissue for the peptide **6.2** treated cornea was 3.97±0.19. Four infected corneas treated with moxifloxacin contained detectable bacterial colonies with a mean $\log_{10}$ CFU/tissue of 3.7±0.24. These results confirmed that peptide **6.2** had a similar antibacterial effect to that of an established antibiotic in decreasing the bacterial bioburden, thus demonstrating its potential as a safe therapeutic for topical applications.

6.5 Conclusion

In conclusion, we have designed and synthesised 10 novel analogues of teixobactin through the selective replacement of Ser_3, $_D$-Gln_4 and Ala_9 residues by $_D$ and $_L$ arginines in Leu_{10}-teixobactin and Ile_{10}-teixobacin. We have successfully achieved a fine balance of hyrophobicity-hydrophilicity while maintaining a high antibacterial potency both *in vitro* and *in vivo*. Importantly, most of these teixobactin analogues showed highly potent antibacterial activity against *S. aureus*, MRSA and VRE, comparable to that of Leu_{10}-teixobactin **5.13** and Ile_{10}-teixobactin **5.12**. The MIC values on a broad panel of Gram-positive bacteria indicate a direct correlation between overall net charge and a narrow distribution of MIC values; for example, as the overall net charge of the peptide increases, a wider distribution of MIC values results.

The teixobactin-based peptide analogue **6.2** was found to be noncytotoxic *in vitro* and *in vivo*. In a mouse model of infectious keratitis, the topical instillation of **6.2** resulted in >99.0% reduction in bacterial bioburden, and the efficacy was comparable to that of moxifloxacin. Notably, *S. aureus* is one of the major etiological agents for bacterial keratitis and has been implicated in corneal melt, leading to significant morbidity and vision loss[14,15]. Furthermore, in our keratitis mouse models, synthetic teixobactin analogue **6.2** decreased the severities of corneal edemas substantially when compared with those in untreated corneas or moxifloxacin-treated corneas. To the best of our knowledge, this is the first *in vivo* demonstration of the excellent therapeutic potential of a teixobactin analogue in attenuating bacterial infections and the associated severities. We believe this work represents a significant advancement in the development of *in vivo* ready simplified teixobactin analogues. Thus, the design of safe and highly potent synthetic peptide analogues of teixobactin presented here will enable the development of drug like analogues against antibiotic-resistant bacterial strains. The findings presented in this work have broad implications and are expected to facilitate the development of peptide-based therapies to combat the serious global challenges posed by AMR.

6.6 References

1. A. Parmar, A. Iyer, S. H. Prior, D. G. Lloyd, E. T. Leng Goh, C. S. Vincent, T. Palmai-Pallag, C. Z. Bachrati, E. Breukink, A. Madder, R. Lakshminarayanan, E. J. Taylor, I. Singh, Teixobactin analogues reveal enduracididine to be non-essential for highly potent antibacterial activity and lipid II binding. *Chemical Science*. **8**, 8183–8192 (2017).

2. W. D. Fiers, M. Craighead, I. Singh, Teixobactin and Its Analogues: A New Hope in Antibiotic Discovery. *ACS Infectious Diseases*. **3**, 688–690 (2017).

3. D. Hughes, A. Karlén, Discovery and preclinical development of new antibiotics. *Upsala Journal of Medical Sciences*. **119**, 162–169 (2014).

4. L. L. Ling, T. Schneider, A. J. Peoples, A. L. Spoering, I. Engels, B. P. Conlon, A. Mueller, D. E. Hughes, S. Epstein, M. Jones, L. Lazarides, V. a Steadman, D. R. Cohen, C. R. Felix, K. A. Fetterman, W. P. Millett, A. G. Nitti, A. M. Zullo, C. Chen, K. Lewis, A new antibiotic kills pathogens without detectable resistance. *Nature*. **517**, 455–459 (2015).

5. A. M. Giltrap, L. J. Dowman, G. Nagalingam, J. L. Ochoa, R. G. Linington, W. J. Britton, R. J. Payne, Total Synthesis of Teixobactin. *Organic Letters*. **18**, 2788–2791 (2016).

6. Y. E. Jad, G. A. Acosta, T. Naicker, M. Ramtahal, A. El-Faham, T. Govender, H. G. Kruger, B. G. De La Torre, F. Albericio, Synthesis and Biological Evaluation of a Teixobactin Analogue. *Organic Letters*. **17**, 6182–6185 (2015).

7. A. Parmar, A. Iyer, C. S. Vincent, D. Van Lysebetten, S. H. Prior, A. Madder, E. J. Taylor, I. Singh, Efficient total syntheses and biological activities of two teixobactin analogues. *Chem. Commun.* **52**, 6060–6063 (2016).

8. A. Parmar, A. Iyer, D. G. Lloyd, C. S. Vincent, S. H. Prior, A. Madder, E. J. Taylor, I. Singh, Syntheses of potent teixobactin analogues against methicillin-resistant Staphylococcus aureus (MRSA) through the replacement of l -allo-enduracididine with its isosteres. *Chemical Communications*. **53**, 7788–7791 (2017).

9. H. Yang, K. H. Chen, J. S. Nowick, Elucidation of the Teixobactin Pharmacophore. *ACS Chemical Biology*. **11**, 1823–26 (2016).

10. K. H. Chen, S. P. Le, X. Han, J. M. Frias, J. S. Nowick, Alanine scan reveals modifiable residues in teixobactin. *Chem. Commun.* **53**, 11357–11359 (2017).

11. S. A. H. Abdel Monaim, E. J. Ramchuran, A. El-Faham, F. Albericio, B. G. de la Torre, Converting Teixobactin into a Cationic Antimicrobial Peptide (AMP). *Journal of Medicinal Chemistry*. **60**, 7476–7482 (2017).

12. C. F. Le, M. Y. M. Yusof, H. Hassan, S. D. Sekaran, In vitro properties of designed

antimicrobial peptides that exhibit potent antipneumococcal activity and produces synergism in combination with penicillin. *Scientific Reports*. **5**, 1–8 (2015).

13. X. Wu, Z. Wang, X. Li, Y. Fan, G. He, Y. Wan, C. Yu, J. Tang, M. Li, X. Zhang, H. Zhang, R. Xiang, Y. Pan, Y. Liu, L. Lu, L. Yang, In vitro and in vivo activities of antimicrobial peptides developed using an amino acid-based activity prediction method. *Antimicrobial Agents and Chemotherapy*. **58**, 5342–5349 (2014).

14. S. F. Mah, R. Davidson, E. J. Holland, J. Hovanesian, J. Kanellopoulos, N. Shamie, C. Starr, D. Vroman, T. Kim, Current knowledge about and recommendations for ocular methicillin-resistant Staphylococcus aureus. *Journal of Cataract & Refractive Surgery*. **40**, 1894–1908 (2014).

15. C. R. Henry, H. W. Flynn, D. Miller, R. K. Forster, E. C. Alfonso, Infectious keratitis progressing to endophthalmitis: A 15-year study of microbiology, associated factors, and clinical outcomes. *Ophthalmology*. **119**, 2443–2449 (2012).

CHAPTER 7

7 OVERVIEW OF TEIXOBACTINS, SUMMARY, CONCLUSIONS AND PERSPECTIVES

7.1 Overview of teixobactin analogues

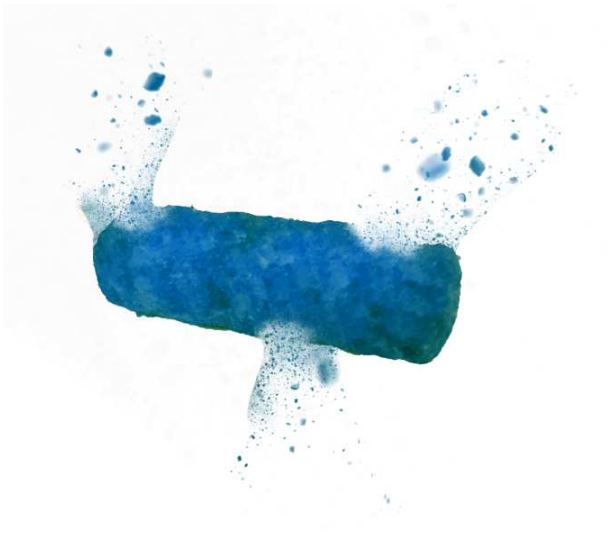

During the last 4 years, since the first publication of teixobactin ***1.23****, it has merited more than 700 citations. It would be almost impossible to review every single work that has been published on teixobactin, however this section aims to provide a generous review of work that is very relevant to this thesis. Total synthesis of teixobactin and the unusual rare amino acid* $_L$*-allo-End* ***1.21*** *has been discussed broadly in Chapter 1 and therefore more details about analogues, synthetic strategies, and the structure-activity relationship will be addressed herein.*

7.1.1 Synthesis of teixobactin analogues

$_L$-*allo*-End **1.21** is not commercially available and very laborious to synthesise[1], due to this, many efforts utilized commercially available amino acids, especially arginine, which is a linear guanidine moiety compared to **1.21**.

Our group efficiently synthesised Arg_{10}-teixobactin **2.1** that is covered in chapter 2 with an overall 22% yield[2]. Other groups such as Albericio[3, 4], Nowick[5] and Su[6], have also contributed significantly to the synthetic strategies of teixobactin analogues[7]. Among these routes, Su, Fang group (Scheme 7.1, Route 4) uniquely utilised an aryl hydrazine solid support. An advantageous feature of this resin is the stability under acidic and basic conditions that is cleaved by a mild oxidative reaction. Other noteworthy features in this scheme were, the release of the final cyclic peptide *in situ* upon cleavage, and the suppressed racemisation on the final macrocyclisation step[6]. The other routes in the schemes all utilised the 2-CTC resin. Albericio group provided two different synthetic routes (Scheme 7.1, Routes 1&2), one with Arg_{10}-teixobactin **2.1** and the other with Lys_{10}-teixobactin **4.1** respectively[3, 4]. Route 2 employed an efficient (>95% yield) on-resin cyclisation and then an elongation of the peptide, before finally releasing the peptide from the solid support. In route 1, the orthogonal allyl protection is utilised twice, and the final cyclisation is formed between residues Ala_9 and Arg_{10}, same ring closure to our route (chapter 2) and route 4. Nowick group[5] (Scheme 7.1, Route 3) had a very similar scheme to route 4. However they initially elongated the first 10 amino acids with the

conventional Fmoc SPPS, followed by the incorporation of Ile_{11} through esterification with the final ring closure between Arg_{10} and Ile_{11}. It should be noted that the synthesis schemes covered in chapter 1 for the total synthesis of **1.23** have also been used to synthesise analogues of **1.23**.

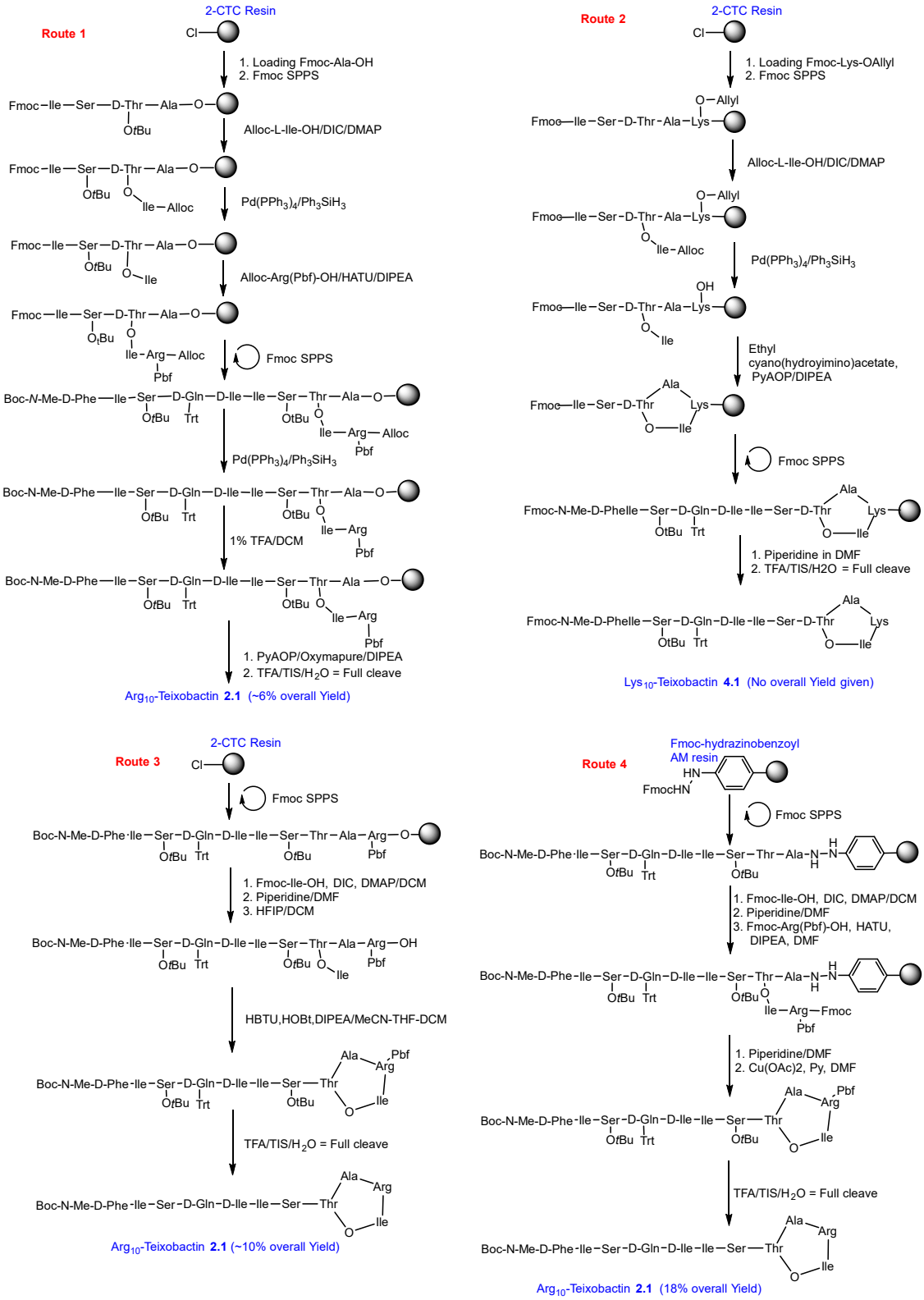

Scheme 7.1: Synthetic routes for the teixobactin analogues. Routes 1 and 2 were employed by Albericio group[3, 4] and Routes 3 and 4 were employed by Nowick group[5] and Su, Fang group[6] respectively[7].

7.1.2 Structure-activity relationship (SAR)

As observed above, quite a number of groups, including ours have provided the synthetic routes to several analogues, such as Arg_{10}-Teixobactin **2.1** which further opened avenues for the synthesis of unique analogues and SAR to be determined.

2.1 showed a 10-fold decreased activity compared to the native product **1.23**. The results were consistent with our observations previously. Our group has shown that any modification to the $_D$-amino acids to their $_L$-versions leads to a significant decrease in activity and NMR studies confirmed that a disordered structure is essential for antibacterial activity (covered in chapters 2 and 3)[8, 9]. Nowick group reported the minimum pharmacophore of teixobactin[5]. In this study, analogue **2.1** experienced an enantiomeric change (a mirror image), where all the $_D$-amino acids were interchanged with $_L$, and vice versa and similar activity was observed. This study indicated that the relative configurations of amino acids are essential, and not the absolute configuration, also revealing that teixobactin must bind to an achiral membrane.

Interestingly, replacement of arginine with lysine showed increased activity in some strains[5, 6, 10], providing an insight that the guanidine group is not essential in maintaining activity. In the same study, residues 1- 5 of teixobactin was shortened by just the addition of Arg, which resulted in a total loss of activity. The analysis was further tested in which residues 1-5 were replaced with a dodecanoyl group. The compound given the name lipobactin **7.2** (Figure 7.1) showed minimal decrease in activity in comparison to **2.1**. These findings established that the hydrophobic tail of teixobactin was notable for its activity and is most likely involved in membrane anchoring. A mutated teixobactin **7.1**, where the lactone is replaced by a lactam ring, by substituting $_D$-Thr to $_D$-Dap exhibited similar activity, again indicating that the cyclic portion together with its configuration plays prime importance to maintain activity. Jamieson group also reported analogues, where residues 1-7 were replaced with a farnesyl isoprenoid **7.3** (Figure 7.1) and descent antibacterial activity was observed[11].

The replacement of *N*-Me-$_D$-Phe to *N*-Me-$_L$-Phe shows decreased activity[9], perhaps due to proteolysis degradation, however removal of methyl group showed no change in activity[6], but interestingly, a slight decrease in activity was observed when a second methyl was introduced[12]. A diminished activity was observed when *N*-Me-$_D$-Phe was replaced with *N*-Me-$_D$-Lys[4].

A lysine scan by Albericio group[13], alanine scans by our group[14] and Nowick group[13, 15] were performed to decode the role of each amino acid. A lysine scan revealed that the hydrophobic residues especially the four Ile's present in teixobactin are critical for activity. The replacement of these with lysine lead to the total loss of antibacterial activity. Furthermore, no significant change was observed when Ser_3 and Gln_4 were replaced with Lys, suggesting these positions were tolerated for substitution[13]. All analogues that were previously synthesised were less active than the natural product **1.23**. To determine suitable positions for modifications an alanine scan was performed to

discover more potent analogues with identical activity. Alanine scans by ours and the Nowick group revealed enduracididine to be non-essential for activity. Our group further went to establish that substituting the complicated L-*allo*-End$_{10}$ **1.21** by simple hydrophobic amino acids such as Ala, Leu and Ile does not hamper activity and in fact, some data showed superior potency than natural teixobactin **1.23**, further confirming that a cationic residue at position 10 is not essential for activity. These findings were later on confirmed by Xuenchen Li *et al.*, who also reported the same analogues with their bactericidal activity[16].

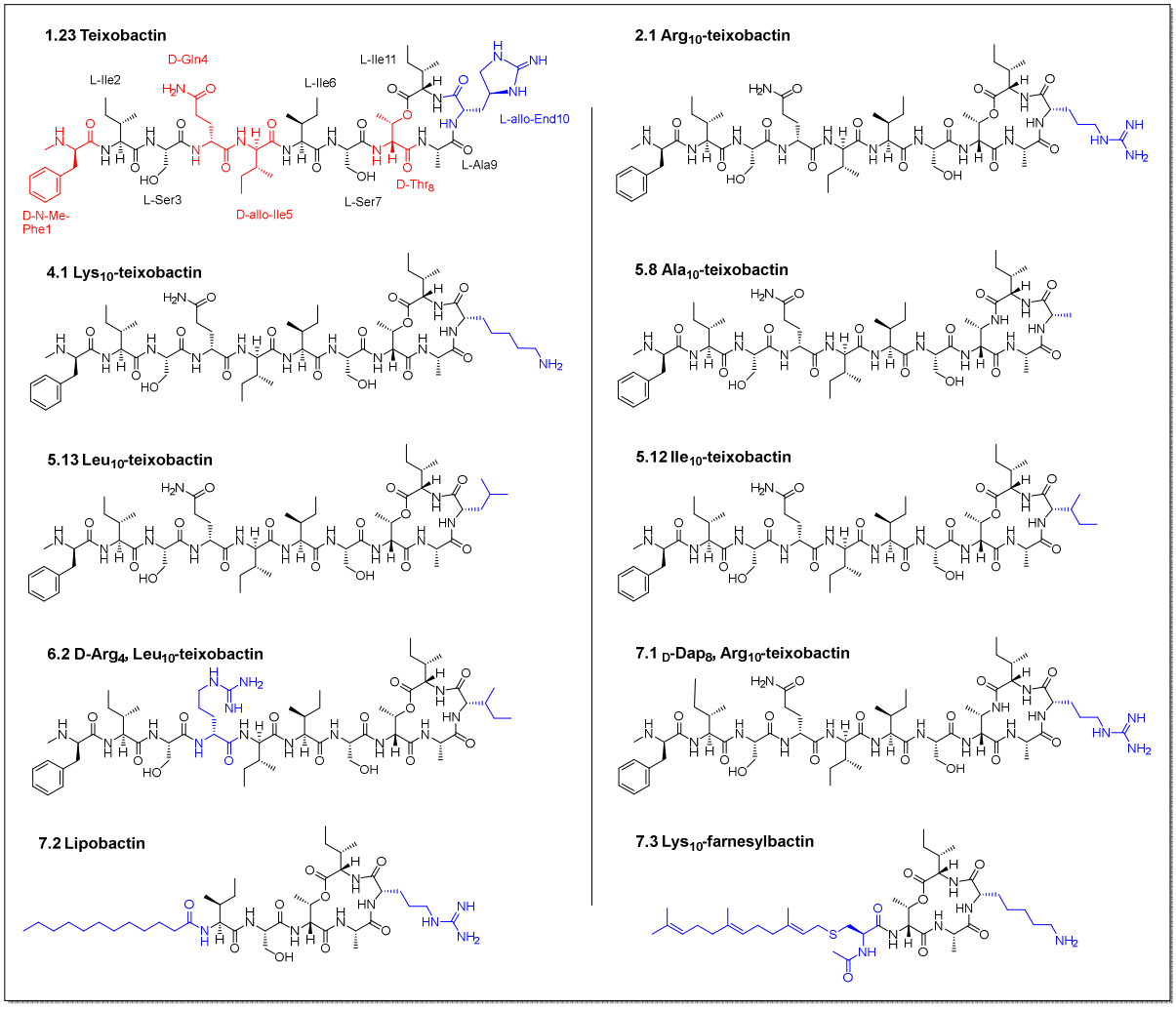

Figure 7.1: Relevant or unique teixobactin analogues showing structure comparison. Alteration of positions shown in blue. D-aminoacids of native teixobactin shown in red.

	Staphylococcus aureus	*Bacillus Subtilis*	*MRSA*
Teixobactin	0.25	0.02-0.06	0.25
Arg_{10}-teixobactn	1.6	0.4	2
Lys_{10}-teixobactin	2	0.5	1
Lipobactin	-	4	-
Lys_{10} -Farnesylbactin	8	-	-
$_{D}$-Dap_8, Arg_{10} -teixobactin	-	1	4
Ala_{10}-teixobactn	1	-	1
Leu_{10}-teixobactn	0.0625	-	0.25
Ile_{10}-teixobactn	0.0625	-	0.25
$_{D}$-Arg_4, Leu_{10}-teixobactn	0.0625	0.125	-

*__Table 7.1__: Minimum Inhibitory concentration (MIC) in μgmL^{-1} of various analogues for the determination of SAR of teixobactin.

Quite a few studies on the Lipid II binding/mechanism studies have been performed with teixobactin and its analogues[14, 17–19]. Through NMR studies on various analogues such as Ala_{10}-teixobactin, we revealed that the N-termini of the teixobactin to be highly structured in contrast to the unstructured C-termini. In the same study, we found that Ser_7 had the tightest binding affinity with a lipid II mimic (geranyl pyrophosphate)[14]. Consistently Ser_7 was also found to be involved in lipid binding in a study by Tajkhorshid *et al*[18]. By the use of molecular modelling and microsecond-scale molecular dynamic simulations, the authors were able to capture teixobactin-lipid II complexes[18]. In this study it was proposed that teixobactin most likely stops cell wall synthesis by inhibition of the transglycosylation step while not affecting the transpeptidation step. Recently, by the use of solid state NMR, a full complex of native teixobactin with lipid II was also reported by Lewandowski *et al*[19]. Upon binding to lipid II, a conformational change (coil to β-conformation) in residues 2-6 was observed. β-conformations are highly prone to aggregations, and it is envisaged this is a plausible mechanism for action. A more recent study by Nowick group confirmed a β-sheet formation behaviour and proposed this being the mode of action[17].

Our group has also reported highly potent analogues against various strains both *in vitro* and *in vivo*[20]. One analogue $_{D}$-Arg_4-Leu_{10}-teixobactin showed a good balance between hydrophobicity and hydrophilicity while maintaining high potency. The analogue is found to be not only noncytotoxic, but *in vivo* studies showed >99% reduction in the bacterial bioburden of an infected S. *aureus* keratitis mouse model. Moreover, corneal edemas were reduced substantially in comparison to untreated mouse models and very similar data to the currently used antibiotic moxifloxacin.

So far, there is relevant progress been made in understanding SAR of teixobactins, but several challenges need to be answered to make teixobactin as a viable drug. The resistance mechanism and the binding of teixobactin with lipid II in the native membrane setting is not still well understood. There is also lack of a thorough study of teixobacins *in vivo*. Gaining an understanding of these

* These data have been taken from various publications and therefore it is most likely the bacterial strains may be different. Data above is only meant for a general comparison of activity.

ambiguities could unlock the door to the production of many valuable, next generation highly potent analogues.

7.2 Summary of work

This section provides the summary of work done towards my PhD at the University of Lincoln. When I arrived in Lincoln May 2015, I had previously gained some experience in peptide synthesis. Coincidently the same year, the first publication of teixobactin[21] had gained much interest by Ishwar Singh group. My project was based on the synthesis and development of teixobactin analogues to discover its structure-activity relationships (SAR).

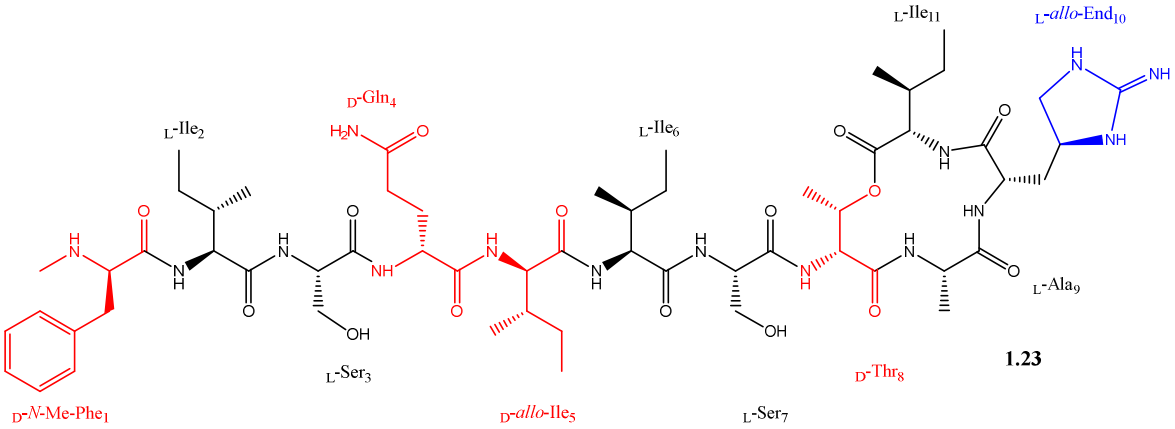

Figure 7.2: Structure of native teixobactin

Initially, the first part of the project was to design a synthetic route for the total synthesis of teixobactin and its analogues. To obtain total synthesis, the compulsory building block L-*allo*-End **1.21** is quite time consuming and expensive. Therefore, efforts to design the analogue was probably the better choice.

Chapters 1 is based on literature review. All the work from Chapter 2 to 6 has been published, which includes a highly efficient synthetic route to provide potent analogues and its SAR studies. A short description of work carried out in each publication is provided below.

1. ***Parmar, A.*** *et al.* Efficient total syntheses and biological activities of two teixobactin analogues. *Chem. Commun.* **52**, 6060–6063 (2016).

An efficient synthetic route was established that can be used broadly to deliver a variety of analogues. Two Arg_{10}-teixobactin analogues were synthesised, and the role of the D-amino acids was determined (chapter 2).

2. ***Parmar, A.*** *et al.* Defining the molecular structure of teixobactin analogues and understanding their role in antibacterial activities. *Chemical communications* **53**, 2016–2019 (2017)

For the first time, 3D molecular structures of teixobactin analogues were povided and the role of each $_D$-amino acid was determined. Through NMR studies the essential of $_D$-Gln$_4$ and importance of $_D$-Ile$_5$ for the maintenance of an unstructured teixobactin was identified (chapter 3).

3. ***Parmar, A.*** *et al.* Syntheses of potent teixobactin analogues against methicillin-resistant Staphylococcus aureus (MRSA) through the replacement of $_L$-allo-enduracididine with its isosteres. *Chemical Communications* **53**, 7788–7791 (2017)

In this study the $_L$-*allo*-End **1.21** was replaced with its isosteres. A rapid one-step conversion of a deprotected amino side to a guanidine moiety was used to expand the number of teixobactins. It was further reasoned that the closest isosteres to $_L$-*allo*-End are key to improved activity (chapter 4).

4. ***Parmar, A.*** *et al.* Teixobactin analogues reveal enduracididine to be non-essential for highly potent antibacterial activity and lipid II binding. *Chemical Science* **8**, 8183–8192 (2017)

In this work, a rapid synthetic route for potent analogues was established utilising μwave assisted couplings. Contrary to previous reports, that a cationic residue at position 10, including the synthetically challenging and expensive amino acid $_L$-*allo*-End **1.21** was confirmed to be non-essential for activity and target binding. With the new and novel design, A substituted $_L$-*allo*-End$_{10}$ with simple commercially available uncharged and nonpolar residues such as Leu$_{10}$ and Ile$_{10}$ showed identical or superior activity to natural teixobatin against MRSA. Individual binding affinities were also confirmed and measured in the presence of geranyl pyrophosphate (lipid II mimic) by NMR to understand the binding modes (chapter 5).

5. ***Parmar, A.*** *et al.* Design and Syntheses of Highly Potent Teixobactin Analogues against *Staphylococcus aureus*, Methicillin-Resistant *Staphylococcus aureus* (MRSA), and Vancomycin-Resistant Enterococci (VRE) *in Vitro* and *in Vivo*. *Journal of Medicinal Chemistry* **61**, 2009–2017 (2018).

In this study, novel analogues were synthesised having a good balance between hydrophobicity and hydrophilicity. For the first time, the therapeutic potential of simple teixobactin analogues was demonstrated by treating bacterial eye infection in mice. These analogues showed substantial reduction in bacterial burden and edema in a synergistic fashion (chapter 6).

7.3 Conclusions

For the past four years, my work has been involved in the designing of potent analogues of teixobactins, which is a natural cyclic depsipeptide that has potent activity against Gram-positive pathogens.

The total synthesis of teixobactin was also attempted by us, however we later turned our interest to synthesise simpler analogues of teixobactin due to the laborious, time consuming and expensive $_L$-*allo*-End.

To conclude the work in this thesis, we have established a synthetic route that has been used very extensively in the broad diversification of teixobactin analogues. We have later optimised the same synthesis further utilising μwave assisted 10min coupling and a 30min cyclisation step, obtaining yields in a range of 10-24%. Initially we determined that the role of $_{D}$-amino acids was very important for its activity and further went on to test the role of each $_{D}$-amino acid, through which we provided 3D molecular structures of teixobactin analogues. We discovered that the any changes from the $_{D}$-amino acid to the $_{L}$-version leads to decreased activity that correlated with the degree of unstructured peptide. We further identified the importance of $_{D}$-Gln$_4$ and $_{D}$-Ile$_5$ for the maintenance of an unstructured teixobactin.

We further reasoned that the closest isosteres to $_{L}$-*allo*-End are key to improved activity. Our procedure utilised a rapid one-step conversion of a deprotected amino side chain to a guanidine moiety to expand the number of teixobactins. To develop analogues with identical or superior potency to natural teixobactin, we established a novel design and through alanine scanning, we determined that Ala$_{10}$-teixobactin possessed similar activity to Arg$_{10}$-teixobactin. This further contributed to the development of more potent analogues by replacing $_{L}$-*allo*-End with hydrophobic amino acids such as Leu$_{10}$ and Ile$_{10}$ that showed better activity in some strains in comparison to the natural product. Individual binding affinities were confirmed and measured in the presence of geranyl pyrophosphate (lipid II mimic) by NMR to understand the binding modes. Contrary to previous reports, we confirmed that a cationic residue at position 10 is non-essential for highly potent activity and target binding.

The hydrophobic residues at position 10 proved to be highly potent against pathogens such as MRSA, but there was a loss of positive charge. The aim was then to find a good balance between hydrophobic and hydrophilic analogues. We successfully synthesised 10 new *in vivo* active compounds. For the first time we have treated mice eye infections by using simplified teixobactin analogues based on our novel design. $_{D}$-Arg4 -Leu$_{10}$ teixobactin showed >99% reduction of bacterial bioburden in a mouse keratitis model, similar to the current drug moxifloxacin. The analogue also showed a substantial decrease in corneal edema in comparison to untreated or moxifloxacin-treated mice, with good safety.

We believe that the work that has been mentioned above will be pivotal for not only synthesising more analogues efficiently but will also provide a good understanding of teixobactin SAR and further deduce the mechanism of action. The discoveries offered in this work have broader implications and are expected to facilitate the development of peptide-based therapies to combat the severe global challenges posed by AMR.

7.4 Perspectives

A heavy load of work has already been conducted on teixobactin, majority of the work being a suitable synthesis route to achieve the native or analogue form of teixobactin with its SAR. Our group and others have significantly contributed to the development of many synthetic strategies and analogues which have showed higher yields in comparison to the synthesis of native teixobactin. Some analogues that we developed have even shown superior potency than the native compound. Although native teixobactin has showed excellent antibacterial efficacy, it is limited to a single molecule and may call for a more sophisticated biosynthetic approach to produce the native compound. The chemical synthesis of the native compound is not a viable option due the challenging and expensive building block L-*allo*-End and its incorporation in the total synthesis of teixobactin. In any case, relying on a single molecule is less likely to reach regulatory approval, due to a high attrition rate involved in the drug development process.

Analogues of teixobactin, on the other hand, have shown encouraging results. It is therefore crucial to pursue the development of novel analogues based on teixobactin scaffolds, to generate a library of molecules, which addresses the challenges of drug development.

A considerate amount of work has been done to understand SAR but research on teixobactin is still in its infancy. Several limitations need to be overcome to make teixobactins' as a viable drug. Broader screenings of teixobactin analogues is needed against MDR strains such as VRE and MRSA, including clinical isolates, to further advance SAR studies, which will aid in finding future potent analogues. Advanced *in vivo* studies are also lacking and could potentially identify lead molecules for the future. Since the discovery of teixobactin, no detectable resistance has been reported. It is therefore obvious to state that there is apparently a high resistant barrier that the natural product possesses. A range of teixobactin analogues could enhance the barrier even further, since bacteria are not known to cope with such diversity. Lipid II interactions with teixobactin in native membrane and understanding resistance mechanisms will also be valuable in discovering more potent analogues. Pharmacokinetics (PK) properties are currently lacking and it is essential to investigate these properties to identify future lead molecules.

Without doubt as mentioned, there are synthetic resources available to produce analogues, even simpler synthetic strategies could be useful to bulk up the production of many unique analogues to further the therapeutic advantage. Addressing these limitations can make a virtuous platform for developing many more robust new classes of antibiotics that will combat MDR bacterial infections.

Currently our group is working towards resolving this using various non-proteogenic amino acids for the replacement of L-*allo*-End. These analogues have shown promising results both *in vitro* and *in vivo*.

7.5 References

1. W. Craig, J. Chen, D. Richardson, R. Thorpe, Y. Yuan, A Highly Stereoselective and Scalable Synthesis of l -allo-Enduracididine. *Organic Letters*. **17**, 4620–4623 (2015).

2. A. Parmar, A. Iyer, C. S. Vincent, D. Van Lysebetten, S. H. Prior, A. Madder, E. J. Taylor, I. Singh, Efficient total syntheses and biological activities of two teixobactin analogues. *Chem. Commun.* **52**, 6060–6063 (2016).

3. Y. E. Jad, G. A. Acosta, T. Naicker, M. Ramtahal, A. El-Faham, T. Govender, H. G. Kruger, B. G. De La Torre, F. Albericio, Synthesis and Biological Evaluation of a Teixobactin Analogue. *Organic Letters*. **17**, 6182–6185 (2015).

4. S. A. H. Abdel Monaim, E. J. Ramchuran, A. El-Faham, F. Albericio, B. G. de la Torre, Converting Teixobactin into a Cationic Antimicrobial Peptide (AMP). *Journal of Medicinal Chemistry*. **60**, 7476–7482 (2017).

5. H. Yang, K. H. Chen, J. S. Nowick, Elucidation of the Teixobactin Pharmacophore. *ACS Chemical Biology*. **11**, 1823–26 (2016).

6. C. Wu, Z. Pan, G. Yao, W. Wang, L. Fang, W. Su, Synthesis and structure–activity relationship studies of teixobactin analogues. *RSC Adv.* **7**, 1923–1926 (2017).

7. C. Guo, D. Mandalapu, X. Ji, J. Gao, Q. Zhang, Chemistry and Biology of Teixobactin. *Chemistry - A European Journal*. **24**, 5406–5422 (2018).

8. A. Parmar, A. Iyer, C. S. Vincent, D. Van Lysebetten, S. H. Prior, A. Madder, E. J. Taylor, I. Singh, Efficient total syntheses and biological activities of two teixobactin analogues. *Chem. Commun.* **52**, 6060–6063 (2016).

9. A. Parmar, S. H. Prior, A. Iyer, C. S. Vincent, D. Van Lysebetten, E. Breukink, A. Madder, E. J. Taylor, I. Singh, Defining the molecular structure of teixobactin analogues and understanding their role in antibacterial activities. *Chemical communications*. **53**, 2016–2019 (2017).

10. A. Parmar, A. Iyer, D. G. Lloyd, C. S. Vincent, S. H. Prior, A. Madder, E. J. Taylor, I. Singh, Syntheses of potent teixobactin analogues against methicillin-resistant Staphylococcus aureus (MRSA) through the replacement of l -allo-enduracididine with its isosteres. *Chemical Communications*. **53**, 7788–7791 (2017).

11. G. C. Girt, A. Mahindra, Z. J. H. Al Jabri, M. De Ste Croix, M. R. Oggioni, A. G. Jamieson, Lipopeptidomimetics derived from teixobactin have potent antibacterial activity against *Staphylococcus aureus*. *Chemical Communications*. **54**, 2767–2770 (2018).

12. S. A. H. A. Monaim, S. Noki, E. J. Ramchuran, A. El-Faham, F. Albericio, B. G. de la Torre, Investigation of the N-Terminus Amino Function of Arg10-Teixobactin. *Molecules*. **22**, 1632 (2017).

13. S. A. H. Abdel Monaim, Y. E. Jad, E. J. Ramchuran, A. El-Faham, T. Govender, H. G. Kruger, B. G. de la Torre, F. Albericio, Lysine Scanning of Arg $_{10}$ –Teixobactin: Deciphering the Role of Hydrophobic and Hydrophilic Residues. *ACS Omega*. **1**, 1262–1265 (2016).

14. A. Parmar, A. Iyer, S. H. Prior, D. G. Lloyd, E. T. Leng Goh, C. S. Vincent, T. Palmai-Pallag, C. Z. Bachrati, E. Breukink, A. Madder, R. Lakshminarayanan, E. J. Taylor, I. Singh, Teixobactin analogues reveal enduracididine to be non-essential for highly potent antibacterial activity and lipid II binding. *Chemical Science*. **8**, 8183–8192 (2017).

15. K. H. Chen, S. P. Le, X. Han, J. M. Frias, J. S. Nowick, Alanine scan reveals modifiable residues in teixobactin. *Chem. Commun.* **53**, 11357–11359 (2017).

16. K. Jin, K. H. L. Po, W. Y. Kong, C. H. Lo, C. W. Lo, H. Y. Lam, A. Sirinimal, J. A. Reuven, S. Chen, X. Li, Synthesis and antibacterial studies of teixobactin analogues with non-isostere substitution of enduracididine. *Bioorganic & Medicinal Chemistry*. **26**, 1062–1068 (2018).

17. H. Yang, M. Wierzbicki, D. R. Du Bois, J. S. Nowick, X-ray Crystallographic Structure of a Teixobactin Derivative Reveals Amyloid-like Assembly. *Journal of the American Chemical Society*. **140**, 14028–14032 (2018).

18. P.-C. Wen, J. M. Vanegas, S. B. Rempe, E. Tajkhorshid, Probing key elements of teixobactin–lipid II interactions in membranes. *Chemical Science*. **9**, 6997–7008 (2018).

19. C. Öster, G. P. Walkowiak, D. E. Hughes, A. L. Spoering, A. J. Peoples, A. C. Catherwood, J. A. Tod, A. J. Lloyd, T. Herrmann, K. Lewis, C. G. Dowson, J. R. Lewandowski, Structural studies suggest aggregation as one of the modes of action for teixobactin. *Chemical Science*. **9**, 8850–8859 (2018).

20. A. Parmar, R. Lakshminarayanan, A. Iyer, V. Mayandi, E. T. Leng Goh, D. G. Lloyd, M. L. S. Chalasani, N. K. Verma, S. H. Prior, R. W. Beuerman, A. Madder, E. J. Taylor, I. Singh, Design and Syntheses of Highly Potent Teixobactin Analogues against *Staphylococcus aureus* , Methicillin-Resistant *Staphylococcus aureus* (MRSA), and Vancomycin-Resistant Enterococci (VRE) *in Vitro* and *in Vivo*. *Journal of Medicinal Chemistry*. **61**, 2009–2017 (2018).

21. L. L. Ling, T. Schneider, A. J. Peoples, A. L. Spoering, I. Engels, B. P. Conlon, A. Mueller, T. F. Schaberle, D. E. Hughes, S. Epstein, M. Jones, L. Lazarides, V. A. Steadman, D. R. Cohen, C. R. Felix, K. A. Fetterman, W. P. Millett, A. G. Nitti, A. M. Zullo, C. Chen, K. Lewis, A new antibiotic kills pathogens without detectable resistance. *Nature*. **517**, 455–459 (2015).

PART II:
CHAPTER-WISE EXPERIMENTAL SECTION

EXPERIMENTAL SECTION FOR CHAPTER 2

I. Materials

All L amino acids, Fmoc-$_D$-Ile-OH, Fmoc-$_D$-Thr(Trt)-OH and oxyma pure were purchased from Merck Millipore. 1-[Bis(dimethylamino)methylene]-1H-1,2,3-triazolo[4,5-b]pyridinium 3-oxid hexafluorophosphate (HATU), Fmoc-$_D$-Gln(Trt)-OH, Boc-$_D$-Nmethylphenyl-OH, H2N-$_D$-Thr-OH, Phenylsilane (PhSiH3), Tetrakis(triphenylphosphine)palladium(0) [Pd(PPh3)], 2-methyl-6-nitrobenzoic anhydride (MNBA), 1-Ethyl-3-(3-dimethylaminopropyl)carbodiimide (EDC/EDCI) Hydrochloride, Diisoproplycarbodiimide (DIC) and Triisopropylsilane (TIS) were purchased from Fluorochem, UK. The protecting groups for the amino acids are tBu for Ser, Pbf for Arg and Trt for Gln and Thr unless specified otherwise. Diisopropylethylamine (DIPEA), supplied as extra dry, redistilled, 99.5 % pure, Acetic anhydride, allyl chloroformate and CDCl3 and were purchased from Sigma Aldrich. Tritylchloride and 4-(Dimethylamino)pyridine were purchased from Alfa Aesar. Dimmethylformamide (DMF) peptide synthesis grade and Trifluoroacetic acid (TFA) was purchased from Rathburn chemicals. Triethylamine, Diethyl ether, Dimethylsulfoxide, Dichloromethane, Tetrahydrofuran (extra dry with molecular sieves), Formic acid 98-100% purity and Acetonitrile (HPLC grade) were purchased from Fisher Scientific. Water with the Milli-Q grade standard was obtained in-house from an ELGA Purelab Flex system. 2-Chlorotritylchloride resin (manufacturer's loading: 1.20 mmol/g) was purchased from Fluorochem. Wang Resin (manufacturer's loading: 0.7 mmol/g) was obtained from NovaBioChem. All chemicals were used without further purification.

II. Equipment used for the analysis and purification of compounds:

All peptides were analysed on a Thermo Scientific Dionex Ultimate 3000 RP-HPLC equipped with a Phenomenex Gemini NX C18 110 Å (150 x 4.6 mm) column using the following buffer systems: A: 0.1% HCOOH in milliQ water. B: ACN using a flow rate of 1 ml/min. The column was flushed with 95% A for 5 min prior to an injection and was flushed for 5 min with 95% B and 5% A after the run was finished.

Peptides were analysed using the following gradient: 95% A for 2 min. 5-95% B in 25 min. 95% B for 5 min. 5% A for 4 min.

Peptides were purified using the same gradient as mentioned above, on a Thermo Scientific Dionex Ultimate 3000 RP-HPLC with a flow rate of 5 mL/min using a Phenomenex Gemini NX C18 110 Å (150 x 10 mm) semi-prep column.

LC-MS data were collected on an Agilent 1100 Series instrument with a Phenomenex Kinetex C18 100Å column (150 x 4.6 mm, 5 μm at 35 °C) connected to an ESMSD type VL mass detector with a flow rate

of 1.5 ml/min was used with the following solvent systems: (A): 0.1% HCOOH in H_2O and (B) MeCN. The column was flushed with 100% A for 2 min, then a gradient from 0 to 100% B over 6 min was used, followed by 2 min of flushing with 100% B. Alternatively, LC-MS/HRMS were performed using a Xevo QTof mass spectrometer (Waters) coupled to an Acquity LC system (Waters) using an Acquity UPLC BEH C18 column (2.1 x 50 mm, Waters).

NMR spectra were recorded on a Bruker 500 MHz Avance III HD spectrometer equipped with a broadband probe.

III. Attempted synthesis of the teixobactin analogue 2.1 via route A:

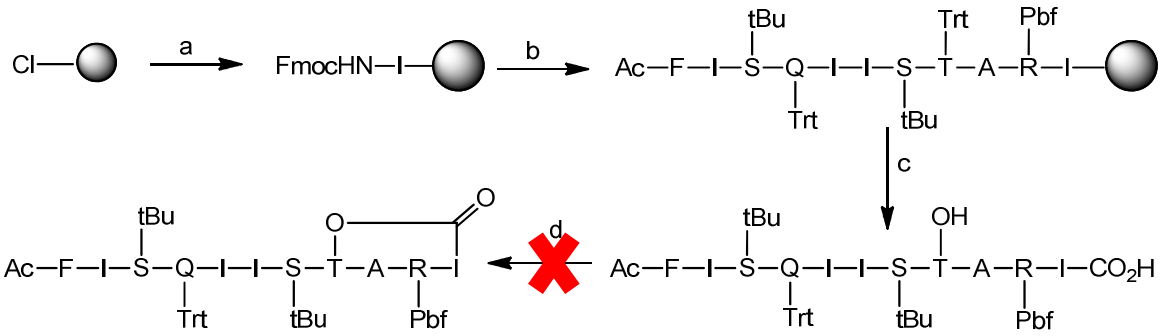

Figure S2.1: Scheme showing the attempted synthesis of the teixobactin analogue **2.1** via route A.

(step *a*) Commercially available 2-Chlorortritylchloride resin (manufacturer's loading = 1.2 mmol/g) was pre-swelled in DCM in a reactor. To it was added 4 eq. Fmoc-Ile-OH, 8 eq. DIPEA in DCM and the reaction was shaken for 3h. The resin was then washed 3 x DCM, 3 x DMF. Any unreacted resin was capped with MeOH:DIPEA:DCM = 1:2:7 by shaking for 1h. The loading determined by UV absorption of the piperidine-dibenzofulvene adduct was calculated to be 0.6 mmol/g. (step *b*) The Fmoc protecting group was deprotected using 20% piperdine in DMF by shaking for 3 min, followed by draining and shaking again with 20% piperidine in DMF for 10 min. The subsequent amino acids were successively coupled (except the Fmoc-$_D$-Thr(Trt)-OH) using the following protocol: 4 eq. FmocHN-AA(P.G.)-OH (AA = Amino Acid, PG = Protecting Group), 4 eq. DIC/Oxyma in DMF using a microwave peptide synthesizer by irradiating for 10 min. Fmoc deprotection was performed using the procedure described in step *a* above. Washing steps were performed using DMF as follows: 4 x 45s after every deprotection step and 6 x 45s after every coupling step. Fmoc-$_D$-Thr(Trt)-OH was coupled using 3 eq. Amino acid, 3 eq. HATU and 6 eq. DIPEA in DMF and shaking for 1h at r.t. The N terminus was capped using 10% DIPEA/Ac_2O in DMF and shaking for 30 min. (step c) The peptide was cleaved off the resin keeping the side chain protecting groups on using: TFA:TIS:DCM = 2:5:93 and shaking for 2h. (step d) The solvent was evaporated and the following conditions were used for esterification:

Sr. No.	Reagents	Solvent	Duration	Temperature
1.	1.2 eq. DCC/5 eq. DMAP	DMF	24h	r.t.
2.	2 eq. DCC + 1 eq. after 4h /5 eq. DMAP	DMF	24h	r.t.
3.	3 eq. DCC/20 mol% DMAP	DMF	2h	r.t
4.	1.2 eq. MNBA/2.4 eq. DMAP	DMF	12h	r.t.
5.	2.5 eq. EDCI/0.5 eq. DMAP	DMF	24h	r.t.
6.	18 eq. DCC/28 eq. DMAP	DMF	30 min, 6h	0-4 deg., r.t
7.	1.2 DCC/6 eq. DMAP	DMF	24h	60, heating
8.	1.2 eq. DIC/6 eq. DMAP	DMF	24h	60, heating

Table S2.1: List of conditions used for cyclisation via esterification

IV. Synthesis of teixobactin core ring structure (2.2):

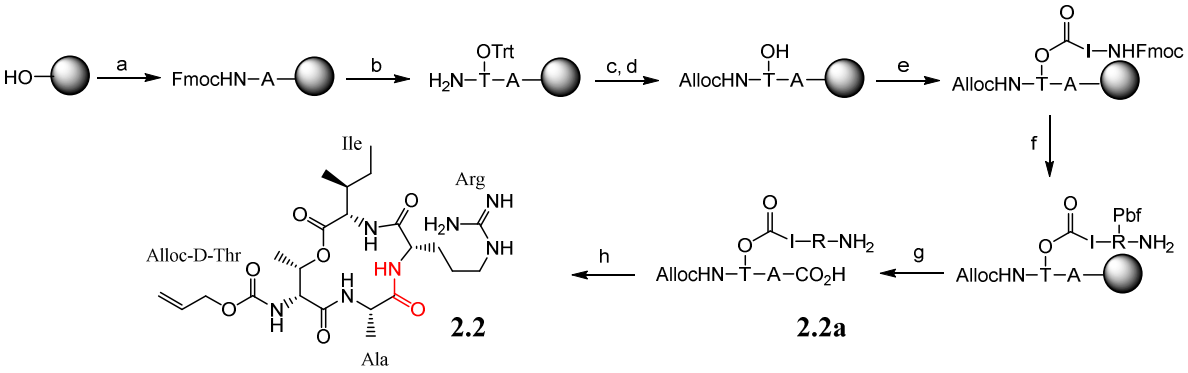

Figure S2.2: Synthesis scheme for the teixobactin core ring (**2.2**)

(step a) Wang resin (manufacturer's loading = 0.7 mmol/g) was weighed out in a clean dry reactor. To the resin, pre-swelled in DMF, was added 10 eq. Fmoc-Ala-OH, 10 eq. DIC and 1 eq. DMAP and the reactor was shaken for 3h. The unreacted alcohol was then capped using 10% Ac2O/DIPEA in DMF. The loading determined by UV absorption of the piperidine-dibenzofulvene adduct was calculated to be 0.47 mmol/g. (step b) 2.5 eq. Fmoc-$_D$-Thr(Trt)-OH, 2.5 eq. HATU and 5 eq. DIPEA in DMF were added on the resin and the reactor was shaken for 3h at room temperature. The coupling of Fmoc-$_D$-Thr(Trt)-OH was verified using the Ninhydrin color test. The Fmoc protecting group was then removed using the protocol described in section III step (b) earlier. (step c) The free amine was protected by adding 4 eq. Allyl Chloroformate/8 eq. DIPEA in DCM to the resin pre-swelled in DCM and shaking for 1h. (step d) The trityl protecting group was removed using TFA:TIS:DCM = 1:5:94 by performing 3 x 15 min cycles and washing with DCM. (step e) Esterification was performed using 10 eq. Fmoc-Ile-OH, 10 eq. DIC, 10 mol% DMAP in DCM and shaking for 2h followed by capping with 10%

Ac_2O/DIPEA in DMF. (step f) Fmoc-Arg(Pbf)-OH was coupled using 4 eq. of AA, 4 eq. HATU and 8 eq. DIPEA in DMF and shaking for 1h followed by Fmoc deprotection using 20% piperidine in DMF using the protocol described in section III step (b) earlier. (step g) The fragment was cleaved off the resin using TFA:TIS:H_2O = 95:2.5.2.5 and shaking for 1h. (step h) Cyclization was performed using 1 eq. HATU/10 eq. DIPEA in DMF by stirring for 1h. HPLC trace of crude **2.2** (Figure S2.9). ESI-HRMS mass calcd. for compound **2.2**: $C_{23}H_{39}N_7O_7$ = 525.2911, found $M+H^+$ = 526.3010 (Figure S2.10).

V. Synthesis and characterisation of AllocHN-$_D$-Thr-OH (2.4)

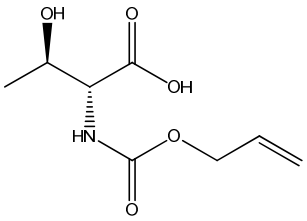

Figure S2.3: Structure of AllocHN-$_D$-Thr-OH (**2.4**)

2 g, 16.8 mmol, H_2N-$_D$-Thr-OH was dissolved in water containing 2 eq. $NaHCO_3$: THF = 2:1, 40 mL and the reaction was cooled to 0°C. Water was then added dropwise till all the H_2N-$_D$-Thr-OH dissolved. Ally chloroformate, 1.2 eq., 2.1 mL, was then added slowly to the reaction and was left stirring for 3 days at r.t. The reaction was monitored by TLC after 24h intervals. The reaction was then acidified to pH = 2 using 6N HCl. The product was extracted using Et_2O (3x). The organic layer was then dried using Na_2SO_4 and the solvent was evaporated under reduced pressure. The reaction mixture was purified using silica gel column chromatography DCM/MeOH = 9:1 to obtain a colourless oil. 82% yield. ^{1}H NMR (500 MHz, DMSO-d_6) δ 1.10 (d, *J* = 6.41 Hz, 3 H), 3.94 (dd, *J* = 9.00, 3.51 Hz, 1 H), 4.02 - 4.13 (m, 1 H), 4.50 (d, *J* = 5.19 Hz, 2 H), 5.19 (dd, *J* = 10.68, 1.22 Hz, 1 H), 5.32 (dd, *J* = 17.40, 1.53 Hz, 1 H), 5.84 - 5.98 (m, 1 H), 6.85 (d, *J* = 8.85 Hz, 1 H), (Figure S2.4); ^{13}C NMR (125 MHz, DMSO-d_6) δ ppm 20.8, 60.3, 65.0, 66.9, 117.4, 134.0, 156.7, 172.7, (Figure S2.5)**;** ESI-HRMS calcd. for $C_8H_{14}NO_5$ = 203.0794 found: M+ H^+ = 204.0864, M+Na^+ = 226.0704. Cald. for [M – CO2 + H^+] = [203.0794 – 43.9898 + 1.0072] = 160.0968, found 160.0968, (Figure S2.6)

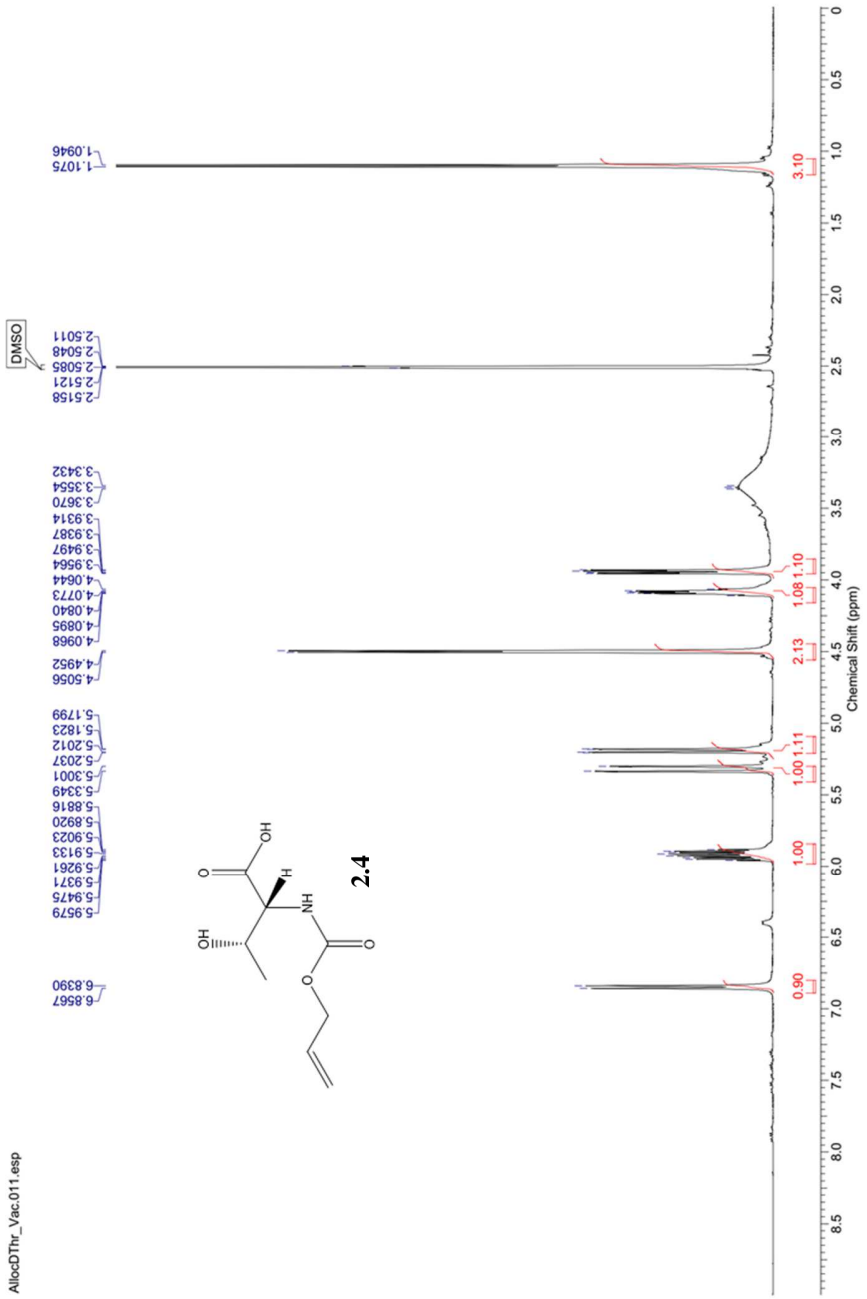

Figure S2.4: 1H NMR Spectrum for compound **2.4**

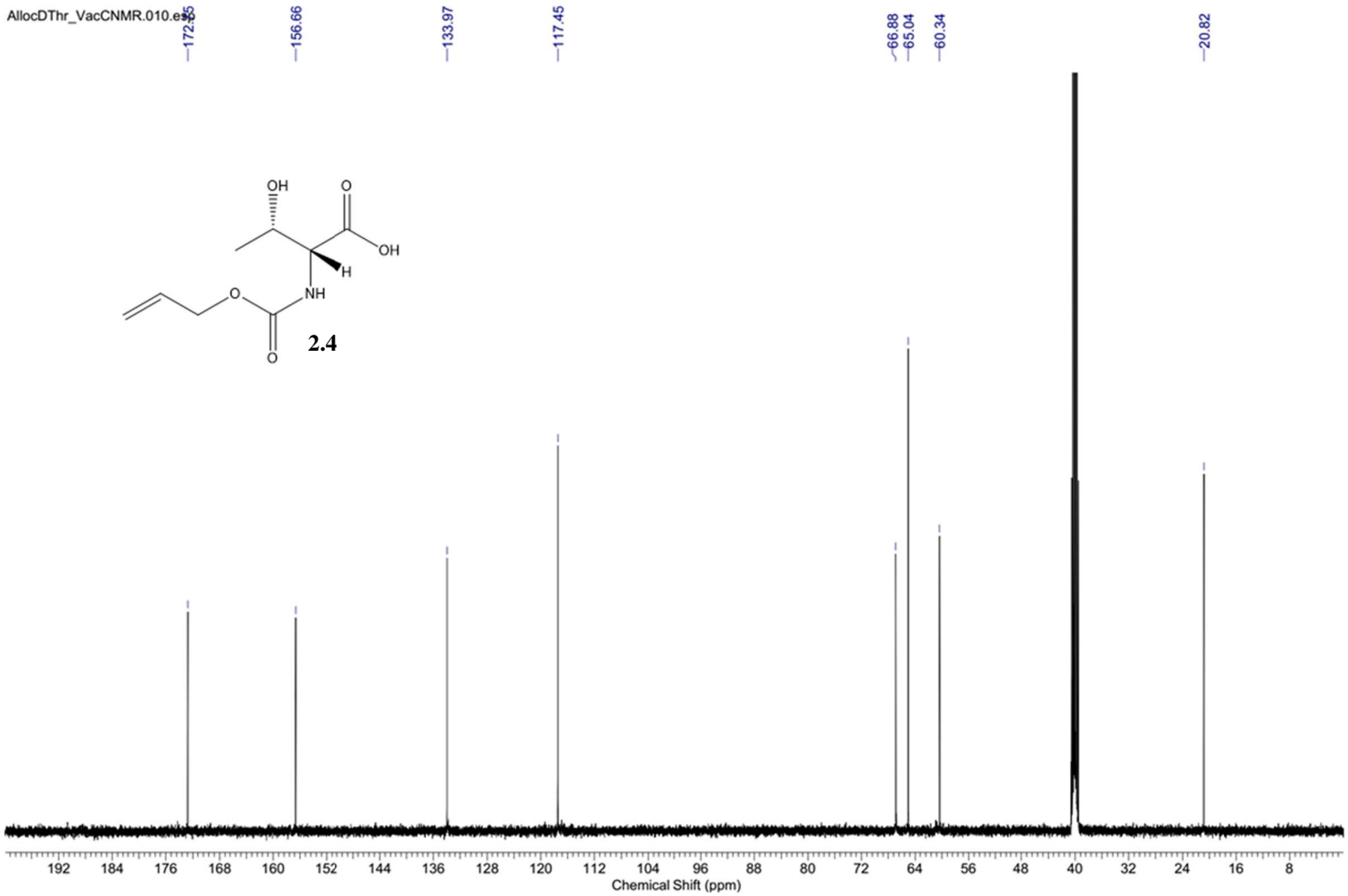

Figure S2.5: ^{13}C NMR Spectrum for compound **2.4**

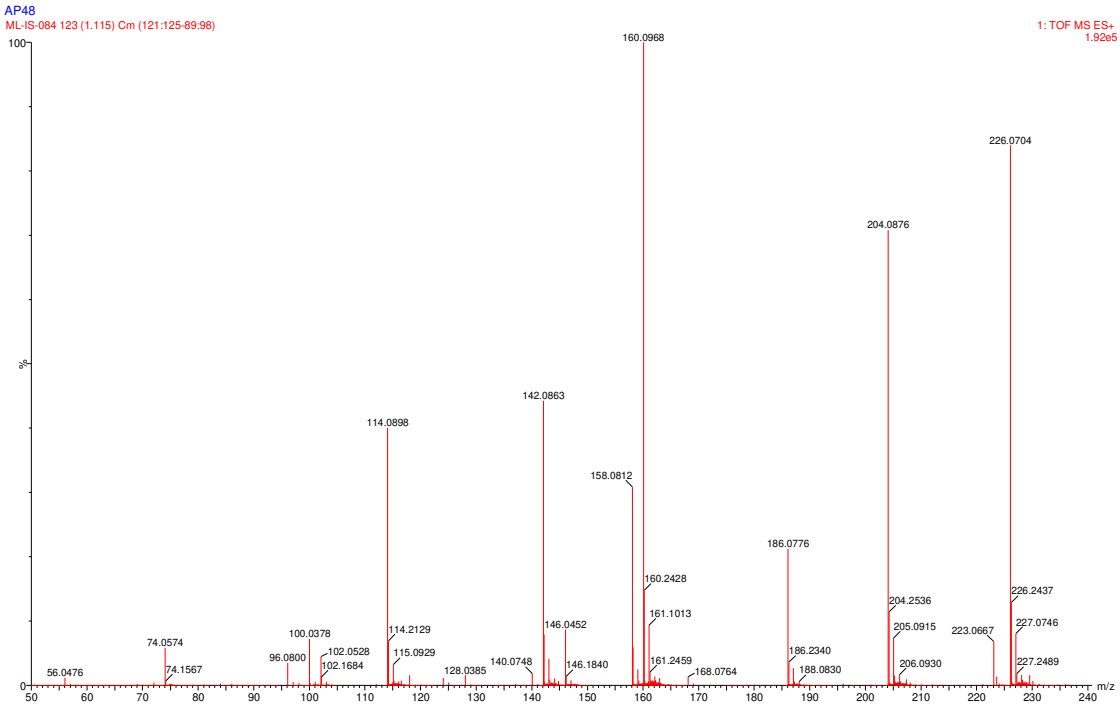

Figure S2.6: HRMS spectrum of AllocHN-$_D$-Thr-OH (**2.4**). HRMS calcd. for $C_8H_{14}NO_5$ = 203.0794 found: M+ H^+ = 204.0864, M+Na^+ = 226.0704. Cald. for [M – CO_2 + H^+] = [203.0794 – 43.9898 + 1.0072] = 160.0968, found 160.0968.

VI. Synthesis of the Teixobactin analogue 2.1 via route B:

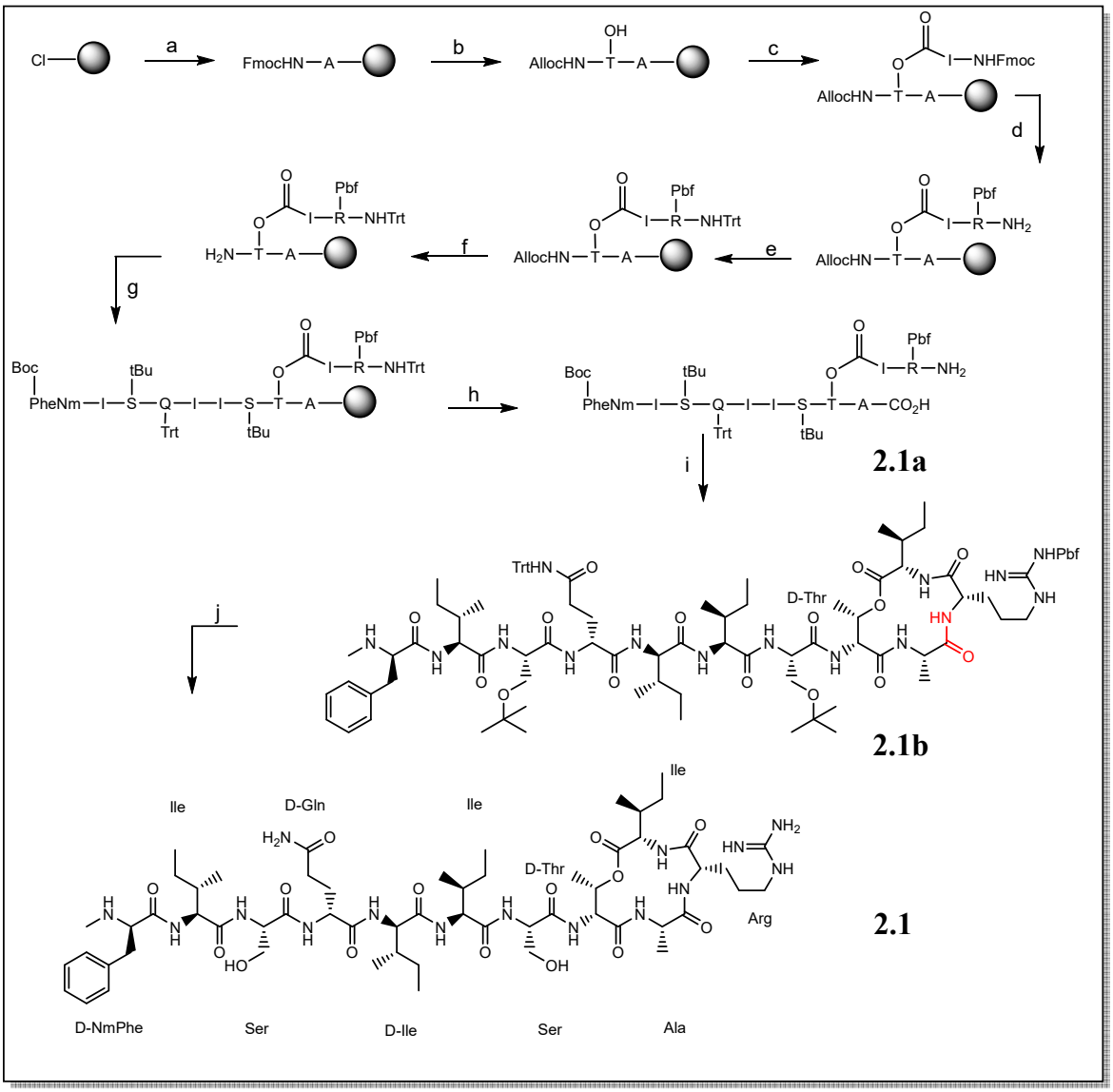

Figure S2.7: Synthesis scheme for the Teixobactin analogue **2.1**

(step a) Commercially available 2-Chlorotrityl chloride resin (manufacturer's loading = 1.2 mmol/g, 170 mg resin) was swelled in DCM in a reactor. To this resin was added 4 eq. Fmoc-Ala-OH/8 eq. DIPEA in DCM and the reactor was shaken for 3h. The loading determined by UV absorption of the piperidine-dibenzofulvene adduct was calculated to be 0.6 mmol/g, (170mg resin, 0.102mmol). Any unreacted resin was capped with MeOH:DIPEA:DCM = 1:2:7 by shaking for 1h. (step b) The fmoc protecting group was removed using 20% piperidine in DMF following the protocol described earlier in section III. (step b) The previously synthesized AllocHN-D-Thr-OH (**2.4**) was then coupled to the resin by adding 3 eq. of the AA, 3 eq. HATU and 6 eq. DIPEA in DMF and shaking for 3h at room temperature. (step c) Esterification was performed using 10 eq. of Fmoc-Ile-OH, 10 eq. DIC and 5 mol% DMAP in DCM and

shaking the reaction for 2h. This was followed by capping the unreacted alcohol using 10% Ac_2O/DIPEA in DMF shaking for 30 min and Fmoc was removed using protocol described earlier in section III. (step d) Fmoc-Arg(Pbf)-OH was coupled using 4 eq. of AA, 4 eq. HATU and 8 eq. DIPEA in DMF and shaking for 1h followed by Fmoc deprotection using 20% piperidine in DMF as described earlier. (step e) The N terminus of Arg was protected using 10 eq. Trt-Cl and 15% Et_3N in DCM and shaking for 1h. The protection was verified by the Ninhydrin colour test. (step f) The Alloc protecting group of $_D$-Thr was removed using 0.2 eq. $[Pd(PPh^3)]^0$ and 24 eq. $PhSiH_3$ in dry DCM under argon for 1 h. This procedure was repeated twice and the resin was washed thoroughly with DCM and DMF to remove any Pd stuck to the resin. (step g) All amino acids were coupled using 4 eq. AA, 4 eq. HATU and 8 eq. DIPEA. Deprotection cycles were performed as described earlier. Each coupling and deprotection cycle were checked by the Ninhydrin colour test. (step h) The peptide was cleaved off from the resin without cleaving off the protecting groups for the amino acid side chains using TFA:TIS:DCM = 2:5:93 and shaking for 2h. (step i) The solvent was evaporated and the peptide was redissolved in DMF to which 1 eq. HATU and 10 eq. DIPEA were added and the reaction was stirred for 1h to perform the cyclization. The reaction was monitored on HPLC till all starting material had been consumed (Fig. S13). (step j) The side-chain protecting groups were then cleaved off using TFA:TIS:H_2O = 95:2.5:2.5 by stirring for 1h. The peptide was precipitated using cold Et_2O (-20°C) and centrifuging at 7000 rpm to obtain a white solid. This solid was further purified using RPHPLC using protocols as described in the section II. Fractions were collected, concentrated and lyophilised to obtain a white solid (28 mg, 22% yield). HRMS mass calcd for **2.1**: $C_{58}H_{98}N_{15}O_{15}$ = 1243.7289, found M+ H^+ = 1244.7336 HRMS. HPLC trace of crude and purified **2.1** (Figure S2.12Figure S2.13), HRMS of **2.1** (Figure S2.14).

VII. Synthesis of the Teixobactin analogue 2.3 via route B:

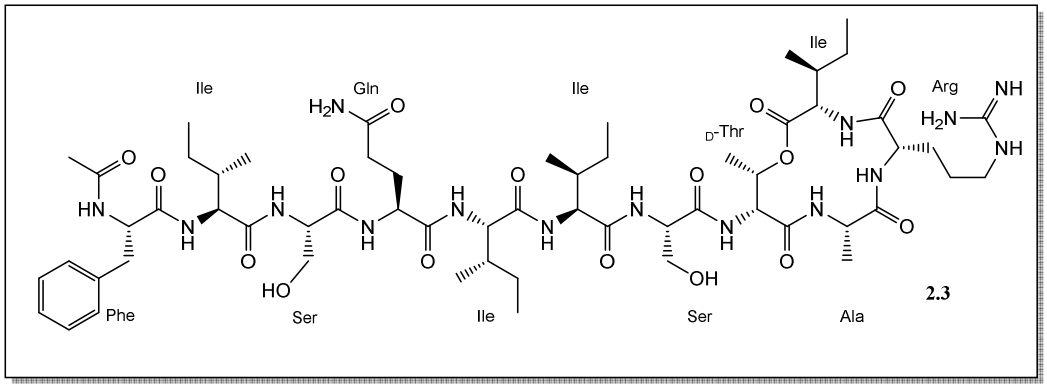

Figure S2.8: Complete structure of teixobactin analogue **2.3**

The synthesis of analogue **2.3** (Figure S2.8) was achieved (200 mg resin, 0.12 mmol scale) using the same procedure as analogue **2.1** except for the final acetylation. Fmoc removal of the L-phenyl alanine

was performed using the protocol described previously (in section III) and acetylation of the amine was achieved by using 10% Ac2O/DIPEA in DMF and shaking for 30 min. TFA cleavage was performed as described in IV. *step j* above. The solvent was evaporated and the peptide was redissolved in DMF to which 1 eq. HATU and 10 eq. DIPEA were added and the reaction was stirred for 1h to perform the cyclization. The reaction was monitored on HPLC till all starting material had been consumed (Figure S2.15). The side-chain protecting groups were then cleaved off using TFA:TIS:H_2O = 95:2.5:2.5 by stirring for 1h. The peptide was precipitated using cold Et_2O (-20°C) and centrifuging at 7000 rpm to obtain a white solid. This solid was further purified using RPHPLC using protocols as described in the section II. Fractions were collected, concentrated and lyophilised to obtain a white solid (24 mg, 17% yield). ESI-HRMS mass calcd for **2.3** $C_{59}H_{98}N_{15}O_{16}$: 1272.7316, found 1272.7379. HPLC trace of crude and purified **2.3** (Figure S2.16 and Figure S2.17), ESI- HRMS of **2.3** (Figure S2.18).

VIII. Antimicrobial Activity.

The "Dilution Susceptibility" test[1] was used to determine the Minimum inhibitory concentration (MIC) in 96 well plate format. The test used cation adjusted Mueller-Hinton broth (OXOID) medium and was performed in triplicate. Plates were incubated at 37°C for 24hrs. The MIC was defined as the lowest concentration of antibiotic which resulted in no visible growth.

IX. HPLC/LC-MS analysis

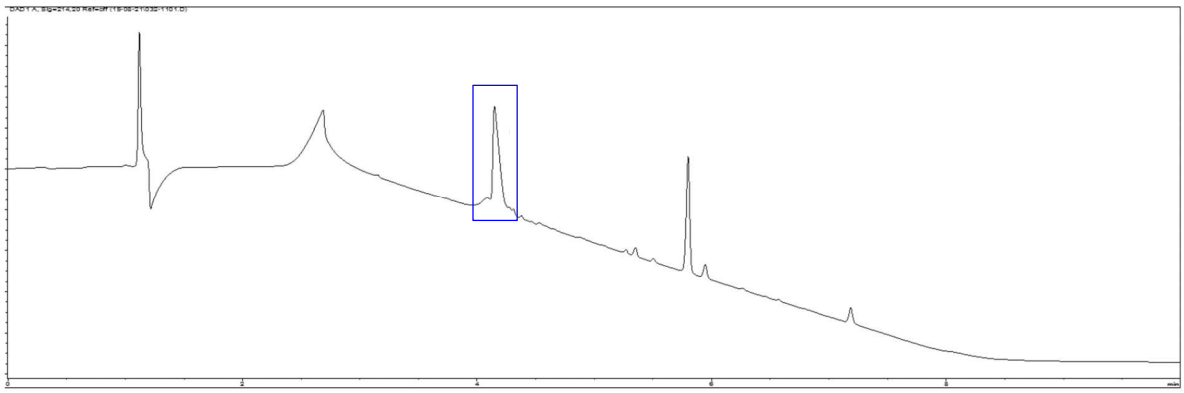

Figure S2.9: HPLC trace of the crude compound **2.2** (gradient: 0-100% ACN in 6 min using A: 0.1% HCOOH in water, B: ACN)

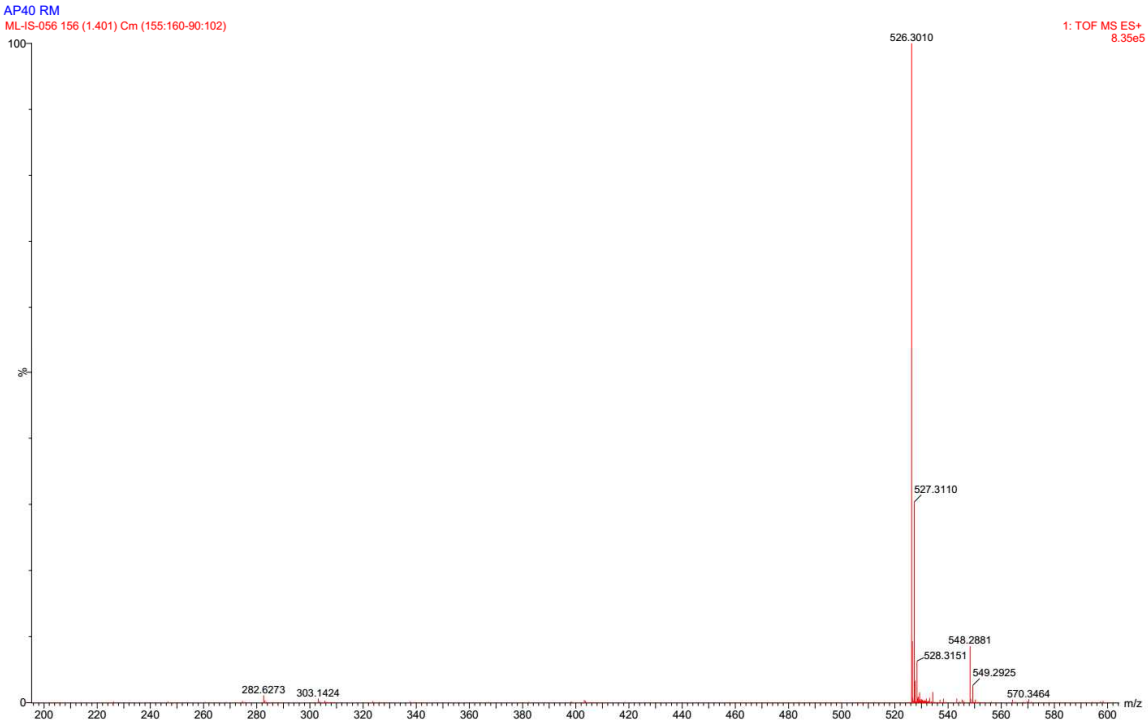

Figure S2.10: HRMS of compound **2.2**. Mass calcd for $C_{23}H_{39}N_7O_7$: 525.2911, found $M+H^+$ = 526.3010.

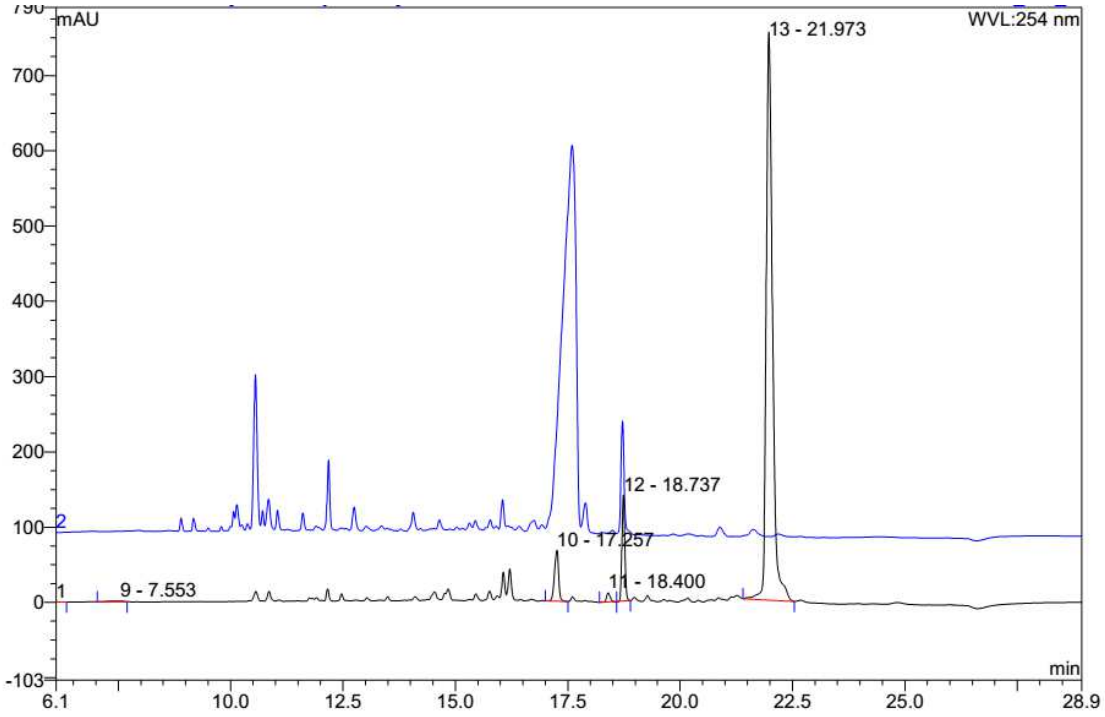

Figure S2.11: HPLC trace showing the progress of cyclisation reaction (i): conversion of the uncyclized protected teixobactin analogue **2.1a** t_R= 17.257 min (shown in blue) to the cyclized protected teixobactin analogue **2.1b** t_R = 21.973 min (shown in black) (Gradient: 5-95% in 25 min)

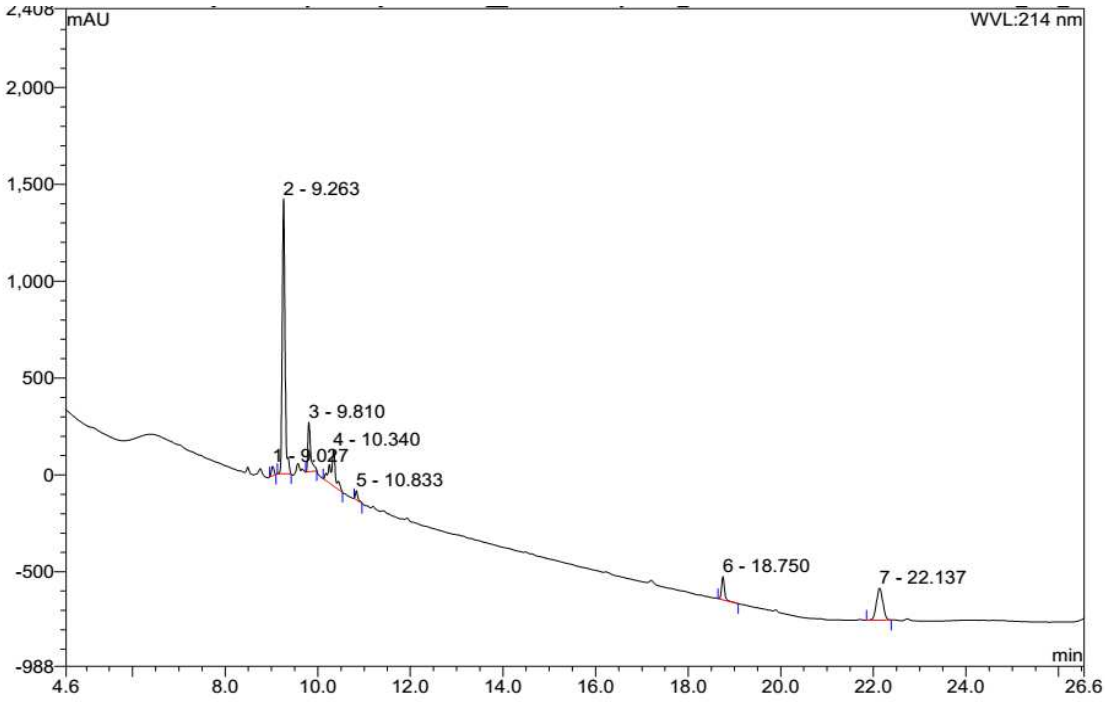

Figure S2.12: HPLC trace of crude teixobactin analogue **2.1** t_R = 9.263 min (gradient: 5-95% ACN in 25 min using A: 0.1% HCOOH in water, B: ACN)

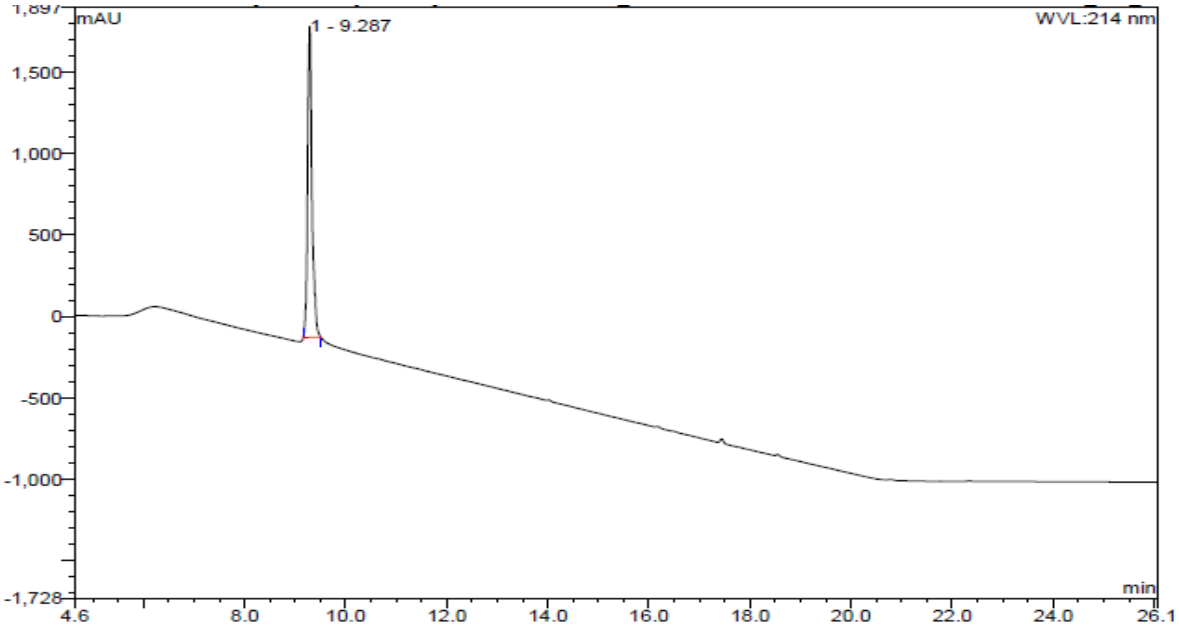

Figure S2.13: HPLC trace of HPLC purified teixobactin analogue **2.1** t_R = 9.287 min (gradient: 5-95% ACN in 25 min using A: 0.1% HCOOH in water, B: ACN)

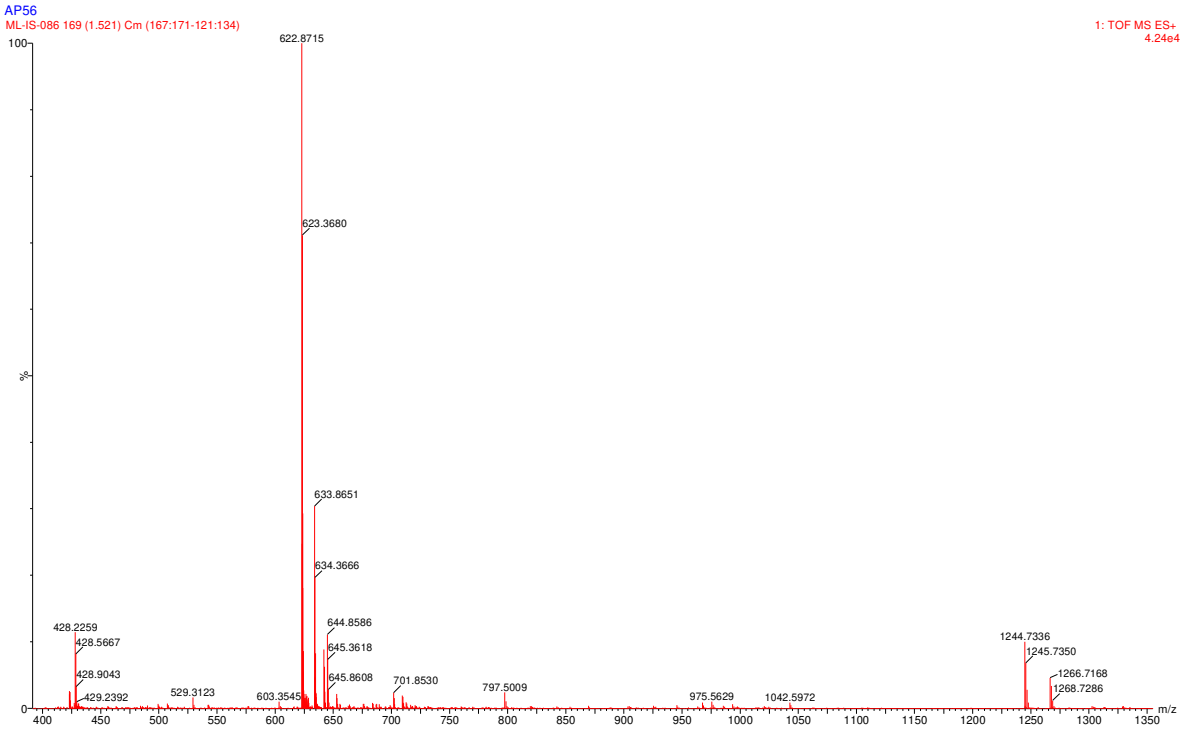

Figure S2.14: HRMS of teixobactin analogue **2.1**. Mass calcd for $C_{58}H_{98}N_{15}O_{15}$: 1243.7289, found M+H$^+$ = 1244.7336, M/2 + H$^+$ = 622.8715

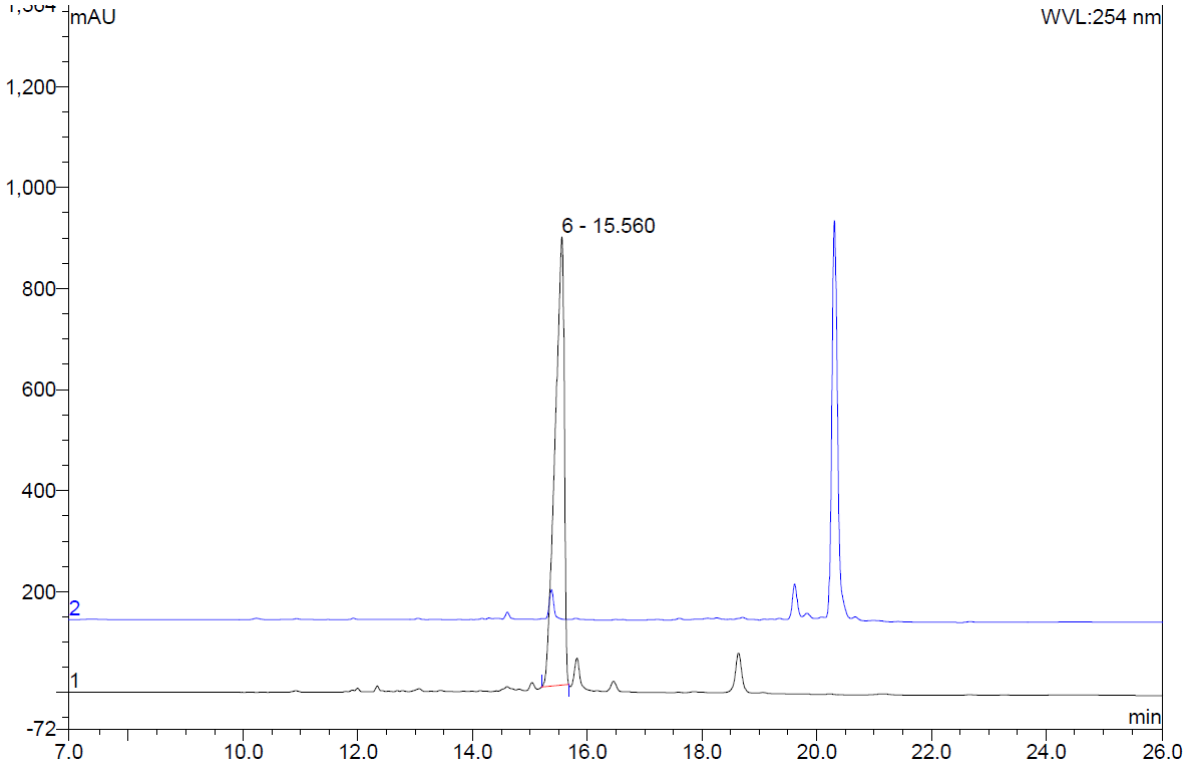

Figure S2.15: HPLC trace showing the progress of reaction of teixobactin analogue **2.3**: conversion of the uncyclized protected teixobactin analogue **2.3a** t_R= 15.560 min (shown in black) to the cyclized protected teixobactin analogue **2.3b** t_R = 20.310 min (shown in blue) (Gradient: 5-95% in 25 min)

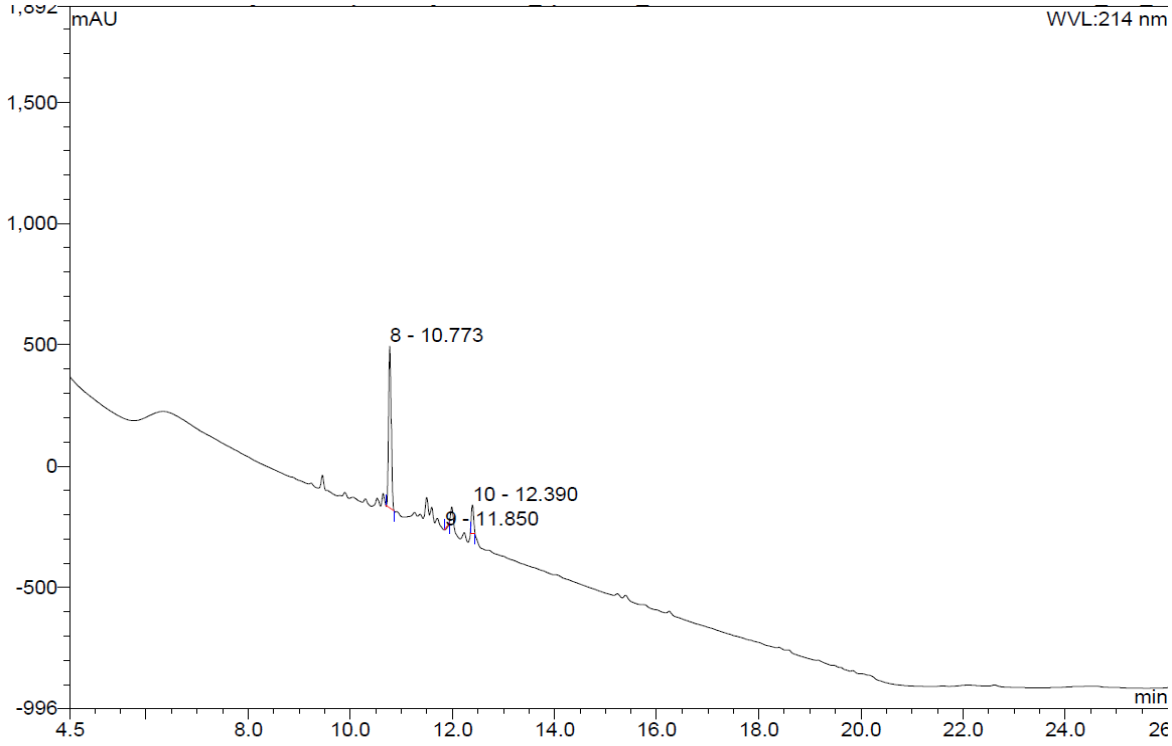

Figure S2.16: HPLC trace of crude teixobactin analogue **2.3** t_R = 10.773 min (gradient: 5-95% ACN in 25 min using A: 0.1% HCOOH in water, B: ACN)

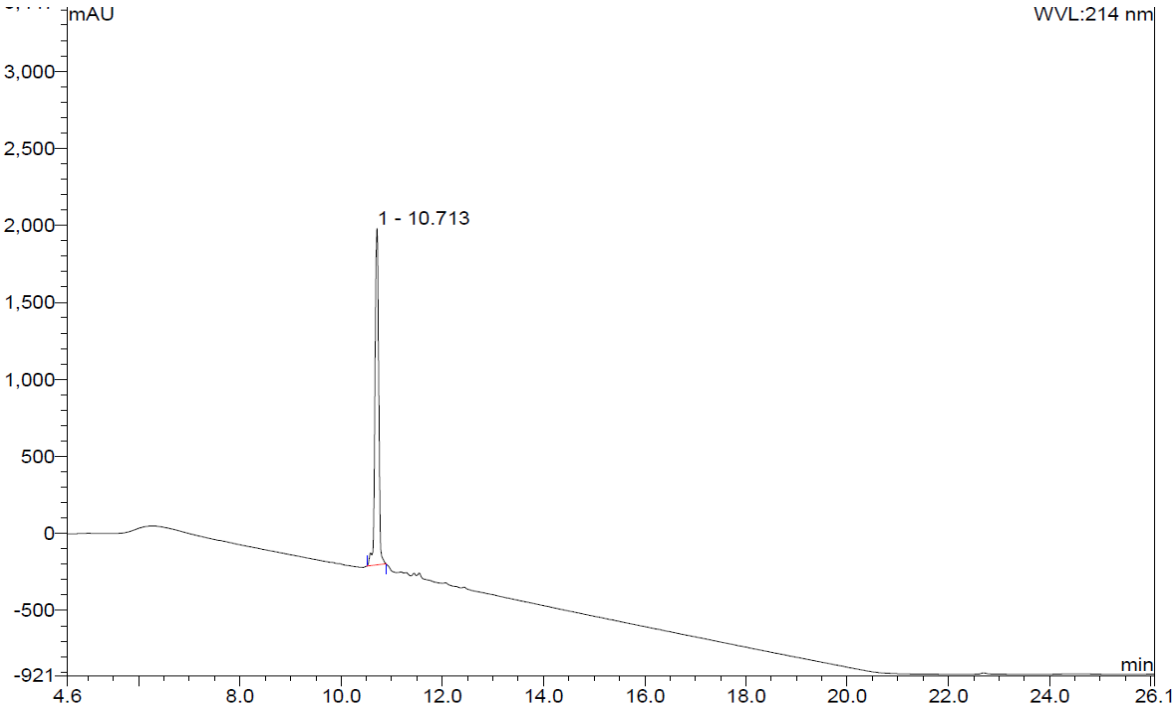

Figure S2.17: HPLC trace of purified teixobactin analogue **2.3** t_R = 10.713 min (gradient: 5-95% ACN in 25 min using A: 0.1% HCOOH in water, B: ACN)

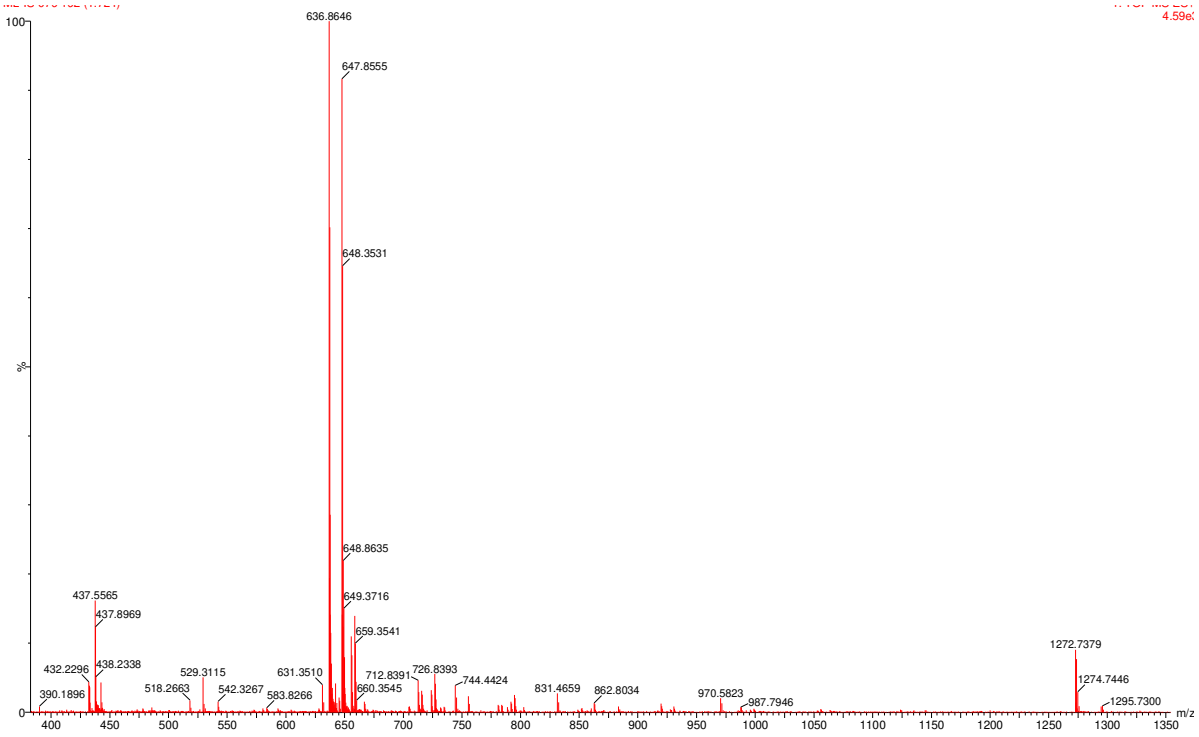

Figure S2.18: ESI-HRMS of purified teixobactin analogue **2.3**. ESI-HRMS mass calcd for $C_{59}H_{98}N_{15}O_{16}$: 1271.7238, found $M+H^+$ = 1272.7379, $M/2 +H^+$ = 636.8646, $(M+ Na^+ + H^+)/2$ = 647.8555

X. Detailed NMR Analysis of Compounds 2.1 and 2.3

NMR was performed at 303.15°K on 1mM solutions of **2.1** and **2.3** dissolved in DMSO-d_6 on a Bruker 500 MHz Avance III HD spectrometer equipped with a broadband probe. Proton spectra were recorded with 128 transients and 64k points. Two dimensional spectra (H-H NOESY, H-H TOCSY, H-C HSQC, H-C HMBC) were recorded with 16 transients and 4k and 196 complex points in the direct and indirect dimensions, respectively. Data processing and analysis were performed using Bruker TopSpin and CcpNmr Analysis.

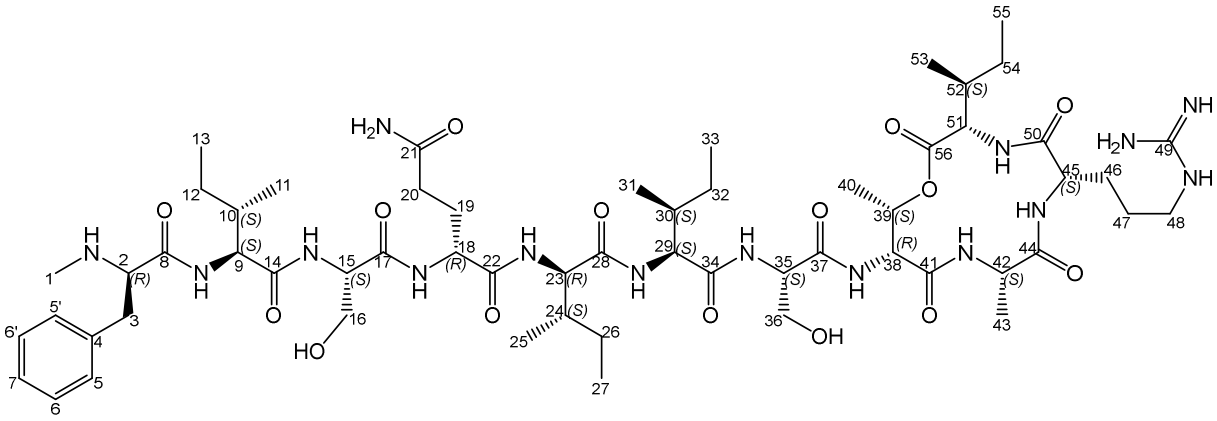

Figure S2.19: Structure of teixobactin analogue **2.1** with numbering. NMR assignments are shown in Table S2.2

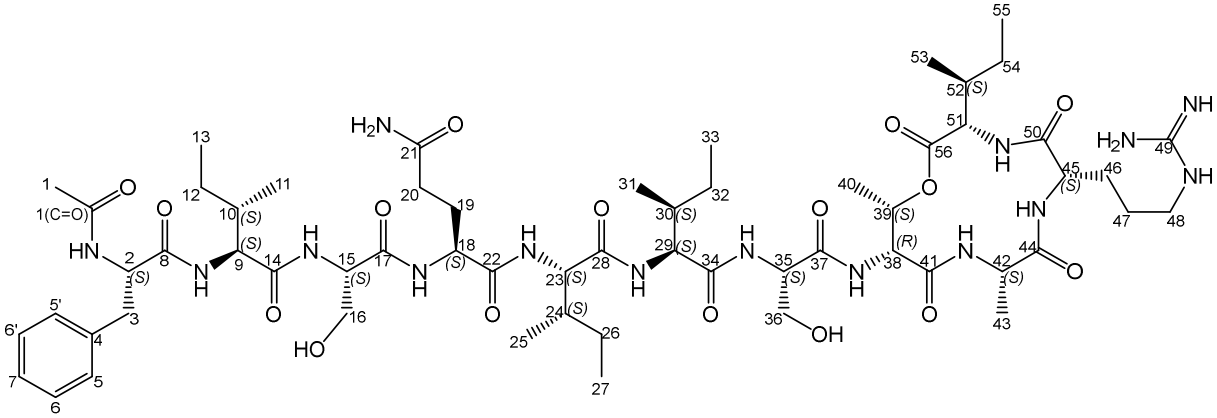

Figure S2.20: Structure of teixobactin analogue **2.3** with numbering. NMR assignments are shown in Table S2.3

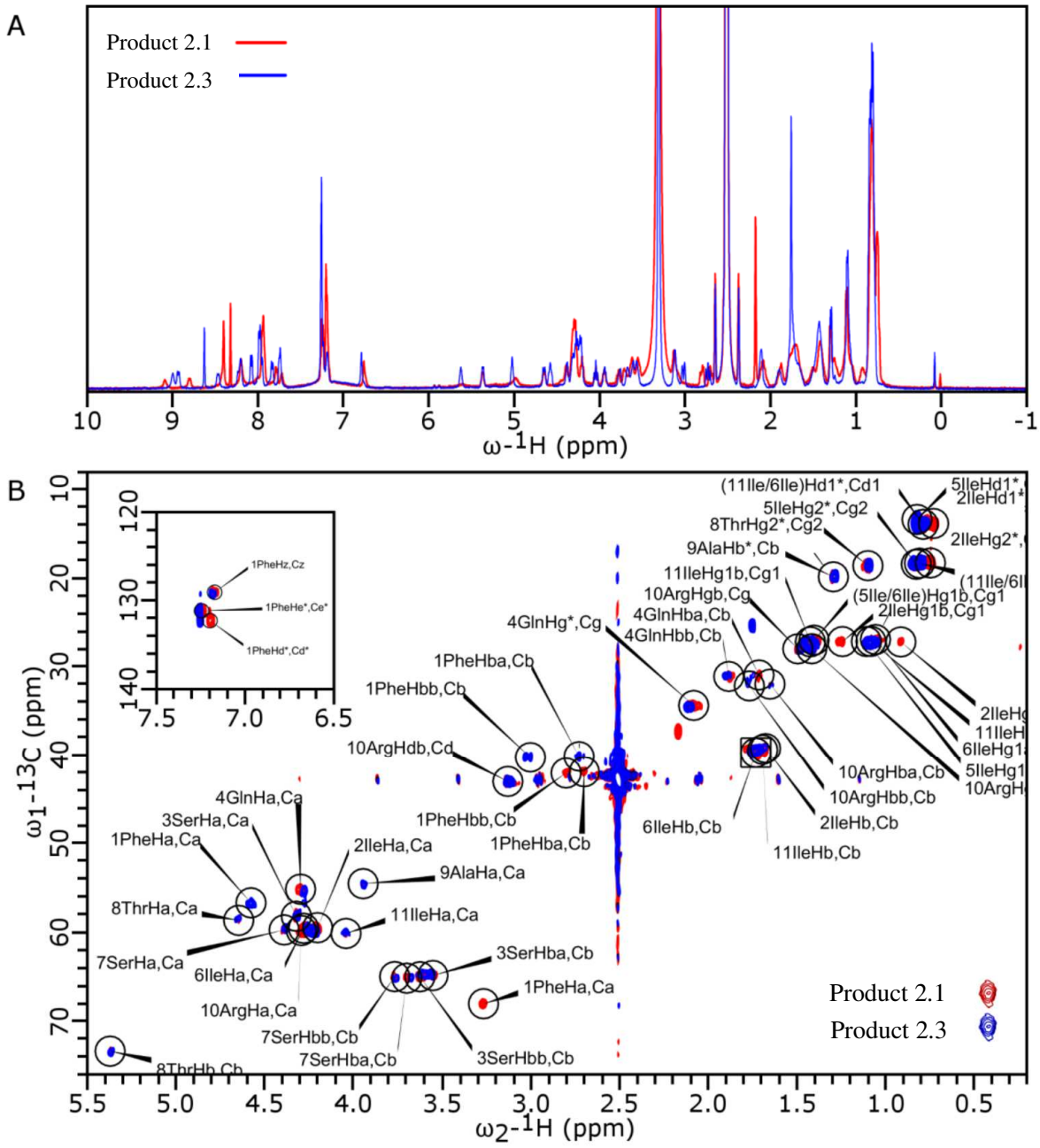

Figure S2.21: NMR spectra obtained from product **2.1** (*red*) and product **2.3** (*blue*). A. Overlaid proton spectra. B. Overlaid ^{1}H-^{13}C HSQC spectra, showing complete assignment. Inset shows aromatic correlations. Samples were 1mM teixobactin analogue in DMSO-d_6, and spectra were recorded on 500 MHz Bruker Avance III HD at 303.15 K.

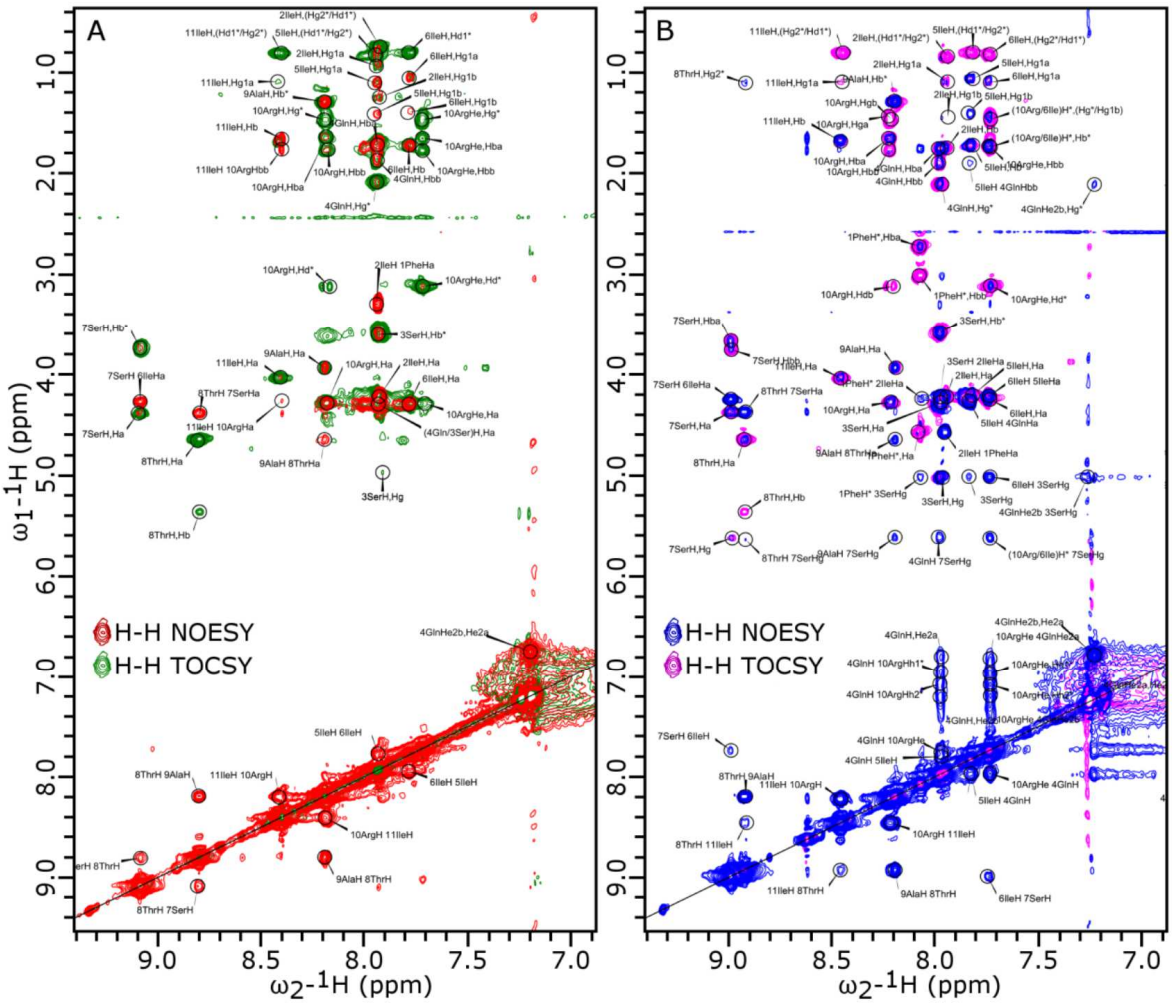

Figure S2.22: Through-space and through-bond proton-proton correlation spectra of product **2.1** and product **2.3** showing complete spectral assignment. A. Fingerprint region of product **2.1** showing ^{1}H-^{1}H NOESY (*red contours*) and ^{1}H-^{1}H TOCSY (*green contours*). The presence of only intra-residue and sequential NOEs is characteristic of an unstructured peptide. B. Fingerprint region of product 3 showing ^{1}H-^{1}H NOESY (*blue contours*) and ^{1}H-^{1}H TOCSY (*magenta contours*). The presence of mid-range NOEs in addition to short-range NOEs suggests that this peptide has adopted a certain degree of structure. Samples were 1mM teixobactin analogue in DMSO-d_6, and spectra were recorded on 500 MHz Bruker Avance III HD at 303.15 K. The extremely broad resonance at ~7.1 ppm is the guanidinium group of Arg_{10}.

	Product 2.1 from [ref. 2]		Product 2.1		
Position	Carbon	Proton	Carbon	Proton	Notes
1	31.9	2.48	34.79	2.169	Δδ[1] 1.01 ppm. Confirmed by NOE to 2-NH
2	61.8	4.17	65.45	3.275 (t, 7.0 Hz)	Δδ 1.51 ppm. Confirmed by NOE to 9-NH
2-NH		9.06			
3	36.5	3.00	39.50	2.696 (dd, 13.5, 6.5 Hz)	Δδ 1.04 ppm. Confirmed by TOCSY to 2.
3'		3.14		2.795	
4	135.0		138.89		Δδ 1.30 ppm. Confirmed by HMBC to 6, 3
5, 5'	129.7	7.24	129.61	7.192 (d, 7.0 Hz)	
6, 6'	129.0	7.33	128.50	7.244 (t, 7.5 Hz)	
7	127.6	7.27	126.41	7.170 (t, 7.0 Hz)	
8	167.0		173.69		Δδ 2.23 ppm. Confirmed by HMBC to 3
9	57.8	4.16	56.92	4.202 (t, 7.4 Hz)	
9-NH		8.49		7.932	
10	36.6	1.55	36.73	1.681	

[1] Difference from chemical shift published in [ref. 2] of greater than 1 ppm. Calculated using the equation

$$\Delta\delta_{H,C} = \sqrt{\left[(\Delta\delta_H)^2 + \frac{(\Delta\delta_C)^2}{3}\right]}$$

11	15.5	0.62	15.80	0.746	
12	24.3	0.74	24.69	0.921	
12'		1.05		1.249	
13	11.3	0.66	11.35	0.741	
14	170.6		171.39		
15	55.5	4.35	55.64	4.316	
15-NH		7.92		7.928	
16	62.4	3.55	62.35	3.570 (q, 5.7 Hz)	
16'				3.599 (q, 6.3 Hz)	
16-OH				4.974	
17	170.1		170.15		
18	57.2	4.35	52.60	4.294	Δδ 1.54 ppm. Confirmed by HSQC
18-NH		8.03		7.939	
19	28.6	1.72	28.51	1.721	
19'		1.88		1.880	
20	31.9	2.10	31.87	2.074	
20'				2.080	
21	174.4		174.14		
21-NH2		6.76		6.751	
21-NH2'		7.21		7.197	
22	171.3		171.55		Overlapped
23	54.1	4.29		4.278	

23-NH		8.23		7.949	
24	37.5	1.82			Overlapped
25	14.7	0.82	15.94	0.823	
26	26.2	1.11	24.58	1.107	
26'		1.31		1.413	
27	10.5	0.82	10.88	0.822	
28	171.6				
29	56.4	4.39	56.98	4.282	
29-NH		7.77		7.785	
30	36.6	1.82	37.24	1.731	
31	15.5	0.88	15.82	0.812	
32	25.3	1.44	24.46	1.068	
32'		1.55		1.408	
33	11.3	0.82	11.44	0.806	
34	171.6				Broad signal
35	52.6	4.35	57.17	4.387	Δδ 1.52 ppm. Confirmed by NOE to 38-NH. Minor form[3] at 4.444 ppm
35-NH		8.03		9.087	Δδ 1.06 ppm. Confirmed by NOEs to 29 and 38-NH. Minor form[3] at 8.189 ppm
36	62.4	3.62	62.49	3.724 (q, 4.0 Hz)	Minor form[3] at 3.616 ppm
36'		3.84		3.759 (q, 5.7 Hz)	Minor form[3] at 3.642 ppm

37	169.5		172.17		
38	56.4	4.50	56.10	4.649 (d, 8.5 Hz)	Minor form[3] at 4.741 ppm
38-NH		8.76		8.800	Minor form[3] at 8.548 ppm
39	71.0	5.38	70.76	5.634 (q, 7.2 Hz)	
40	15.8	1.11	16.10	1.105 (d, 6.1 Hz)	Minor form[3] at 1.166 ppm
41	158.4				Broad signal
42	52.1	3.93	51.98	3.939 (quint, 7.1)	Minor form[3] at 3.942 ppm
42-NH		8.13		8.197	Minor form[3] at 8.548 ppm
43	17.3	1.31	17.36	1.295 (d, 7.5 Hz)	Minor form[3] at 1.202 ppm
44	172.8		172.90		
45	52.1	3.60	57.23	4.290	Δδ 1.84 ppm. Confirmed by HSQC
45-NH				8.185	
46	25.7	1.44	29.57	1.661	Δδ 1.31 ppm. Confirmed by NOE intensity
46'				1.765	
47	29.4	1.26	25.48	1.429	Δδ 1.32 ppm. Confirmed by NOE intensity
47'				1.475	
48, 48'	43.9	3.17	40.51	3.119 (q, 6.6 Hz)	Δδ 1.13 ppm. Confirmed by TOCSY to 45, 46, 47, 48, 45-NH and 48-NH
48-NH				7.719	

49	157.2				Broad Signal
49-NH2				7.036	
49-NH2'				7.036	
50	171.9				Broad Signal
51	57.5	4.05	57.56	4.039 (t, 9.9 Hz)	Minor form[3] at 4.295 ppm
51-NH		8.18		8.411	Minor form[3] at 7.995 ppm
52	37.0	1.82	36.90	1.693	Minor form[3] at 1.767 ppm
53	16.0	0.82	15.82	0.808	Minor form[3] at 0.833 ppm
54	24.7	1.16	24.66	1.809	
54'		1.44		1.428	
55	11.9	0.82	11.44	0.801	Minor form[3] at 0.833 ppm
56	168.7		166.27		

Table S2.2: Complete NMR assignment for product **2.1**

Position	Carbon	Proton	Position	Carbon	Proton
1	22.88	1.752[2]	29	57.00	4.248
1-C=O	169.67		29-NH		7.737
2	54.12	4.576[1]	30	37.05	1.736
2-NH		8.075	31	15.81	0.825
3	37.67	2.727	32	24.78	1.087
3'		3.013	32'		1.431
4	138.50		33	11.35	0.822
5, 5'	129.59	7.252	34		
6, 6'	128.37	7.253	35	57.01	4.376
7	126.60	7.181	35-NH		8.989
8	169.66[1]		36	62.56	3.672
9	57.32	4.229	36'		3.757
9-NH		7.950	36-OH		5.622
10	37.05	1.740	37	171.86	
11	15.81	0.827	38	55.84	4.645
12	24.79	1.086	38-NH		8.922
12'		1.430	39	70.87	5.361

[2] Chemical shift difference from **2.1** due to presence of *N*-terminal acetyl group

[3] The small number of differences observed to previously published chemical shifts were attributable to the cyclic portion of **2.1** existing in equilibrium between two unevenly distributed populations. The chemical shifts match those described in ref. 2. However, there exists an additional minor form of the cyclic portion of **2.1** whose chemical shifts are reported here.

13	11.28	0.827	40	16.05	1.097
14	171.52		41		
15	55.59	4.312	42	52.05	3.935
15-NH		7.976	42-NH		8.198
16	62.09	3.568	43	17.29	1.290
16'		3.588	44	172.85	
16-OH		5.020	45	54.23	4.270
17	170.34		45-NH		8.219
18	52.75	4.269	46	29.45	1.667
18-NH		7.977	46'		1.757
19	28.45	1.756	47	25.58	1.433
19'		1.896	47'		1.472
20	32.05	2.103	48, 48'	40.57	3.114
20'		2.103	48-NH		7.732
21			49		
21-NH2		6.788	49-NH2		6.959
21-NH2'		7.228	49-NH2'		7.075
22	171.55		50	171.43	
23	57.32	4.218	51	57.44	4.043
23-NH		7.827	51-NH		8.458
24	36.89	1.726	52	36.64	1.681
25	15.72	0.805	53	15.81	0.814
26	24.77	1.064	54	24.77	1.098

26'		1.414	54'		1.421
27	11.35	0.802	55	11.35	0.803
28	171.53		56	168.22	

Table S2.3: Complete NMR assignment for product **2.3**

XI. References:

1. J. H. Jorgensen, M. J. Ferraro, Antimicrobial susceptibility testing: a review of general principles and contemporary practices. *Clinical infectious diseases : an official publication of the Infectious Diseases Society of America*. **49**, 1749–55 (2009).

2. Y. E. Jad, G. A. Acosta, T. Naicker, M. Ramtahal, A. El-Faham, T. Govender, H. G. Kruger, B. G. De La Torre, F. Albericio, Synthesis and Biological Evaluation of a Teixobactin Analogue. *Organic Letters*. **17**, 6182–6185 (2015).

EXPERIMENTAL SECTION FOR CHAPTER 3

I. Materials

All L amino acids, Fmoc-$_D$-Ala-OH Fmoc-$_D$-Gln(Trt)-OH, Boc-N-methyl-D-phenylalanine, 1-[Bis(dimethylamino)methylene]-1H-1,2,3-triazolo[4,5-b]pyridinium3-oxidhexafluorophosphate (HATU), Phenylsilane ($PhSiH_3$), Tetrakis(triphenylphosphine)palladium(0) [$Pd(PPh_3)$], Diisoproplycarbodiimide (DIC) and Triisopropylsilane (TIS) were purchased from Fluorochem, UK. Fmoc-D-*allo*-Ile-OH and oxyma pure were purchased from Merck Millipore. The side chain protecting groups for the amino acids are ^{t}Bu for Ser, Pbf for Arg and Trt for Gln and Thr unless specified otherwise. Diisopropylethylamine (DIPEA), supplied as extra dry, redistilled, 99.5 % pure, Acetic anhydride, allyl chloroformate and $CDCl_3$ and were purchased from Sigma Aldrich. Tritylchloride and 4-(Dimethylamino)pyridine were purchased from Alfa Aesar. Dimmethylformamide (DMF) peptide synthesis grade was purchased from Rathburn chemicals. Triethylamine, Diethyl ether (Et_2O), Dimethylsulfoxide (DMSO), Dichloromethane (DCM), Tetrahydrofuran (extra dry with molecular sieves), Formic acid 98-100% purity and Acetonitrile (HPLC grade) were purchased from Fisher Scientific. Water with the Milli-Q grade standard was obtained in-house from an ELGA Purelab Flex system. 2-Chlorotritylchloride resin (manufacturer's loading: 1.20 mmol/g) was purchased from Fluorochem. All chemicals were used without further purification.

II. Equipment used for the analysis and purification of compounds

All peptides were analysed on a Thermo Scientific Dionex Ultimate 3000 RP-HPLC equipped with a Phenomenex Gemini NX C18 110 Å (150 x 4.6 mm) column using the following buffer systems: A: 0.1% HCOOH in milliQ water. B: ACN using a flow rate of 1 ml/min. The column was flushed with 95% A for 5 min prior to an injection and was flushed for 5 min with 95% B and 5% A after the run was finished.

Peptides were analysed using the following gradient: 95% A for 2 min. 5-95% B in 25 min. 95% B for 5 min. 5% A for 4 min.

Peptides were purified using the same gradient as mentioned above, on a Thermo Scientific Dionex Ultimate 3000 RP-HPLC with a flow rate of 5 mL/min using a Phenomenex Gemini NX C18 110 Å (150 x 10 mm) semi-prep column.

LC-MS data were collected on an Agilent 1100 Series instrument with a Phenomenex Kinetex C18 100Å column (150 x 4.6 mm, 5 µm at 35 °C) connected to an ESMSD type VL mass detector with a flow rate of 1.5 ml/min was used with the following solvent systems: (A): 0.1% HCOOH in H_2O and (B) MeCN. The column was flushed with 100% A for 2 min, then a gradient from 0 to 100% B over 6 min was used, followed by 2 min of flushing with 100% B.

NMR spectra were recorded on a Bruker AV 500 NMR.

III. Syntheses and HPLC/LC-MS analysis

Sr No.	Compound Number	Code	Exact Mass	Mass found [M + H$^+$]	Overall yield
1	**2.1^2**	LLLL	1243.73	1244.4	16%
2	**2.1^3**	DDLD	1243.73	1244.4	17%
3	**2.1^4**	DLDD	1243.73	1244.4	9%
4	**2.1^5**	LDDD	1243.73	1244.4	13%
5	**2.1^6**	LLDD	1243.73	1244.4	14%

Table S3.1: Mass analysis and overall yields for compounds **2.1^2**-**2.1^6**. Analysis and overall yields for compounds **2.1^1** & **2.1^7** have been published previously (See Chapter 2).[1]

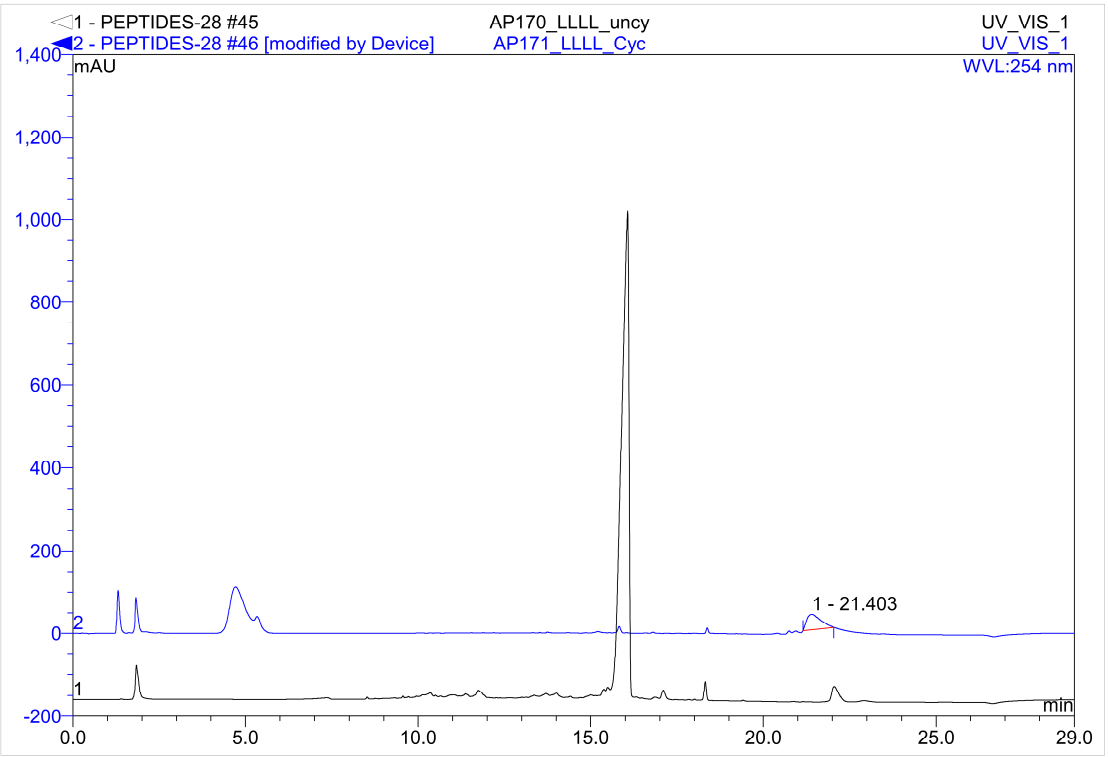

Figure S3.1: HPLC trace showing the progress of cyclisation reaction for **2.1^2** (LLLL) (i): conversion of the uncyclized protected teixobactin analogue t_R= 16.067 min (shown in black) to the cyclized protected teixobactin analogue t_R = 21.403 min (shown in blue) (Gradient: 5-95% in 25 min)

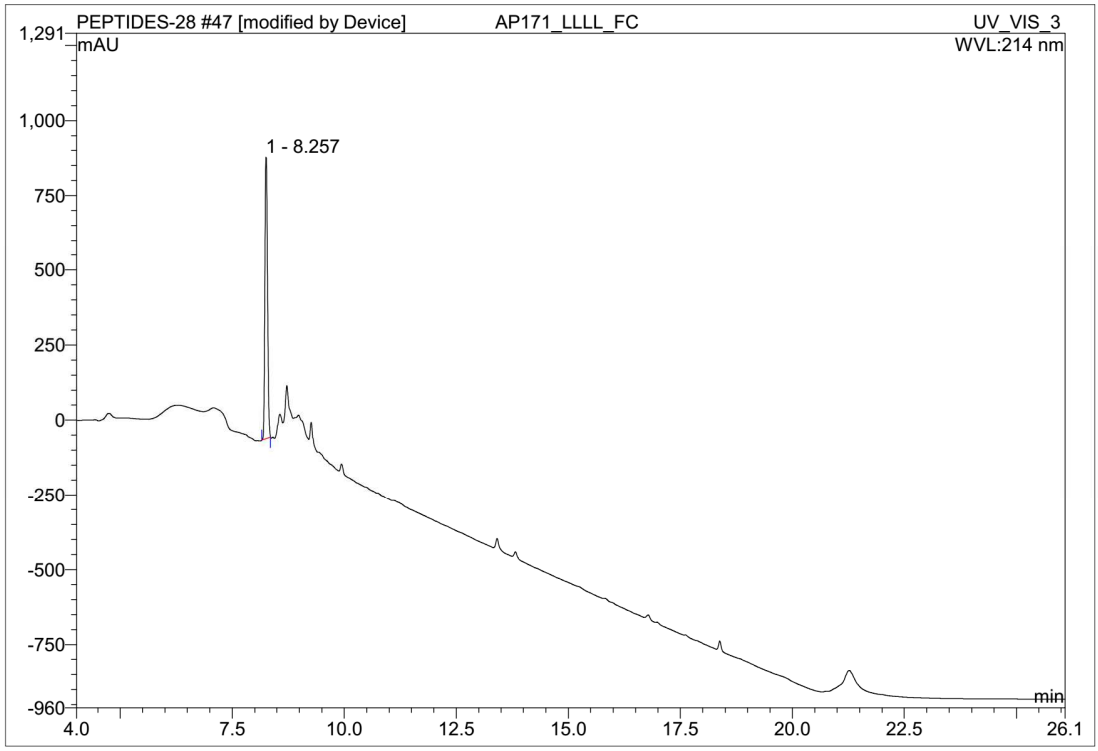

Figure S3.2: HPLC trace of crude teixobactin analogue **2.1**[2] (LLLL) t_R = 8.257 min (gradient: 5-95% ACN in 25 min using A: 0.1% HCOOH in water, B: ACN)

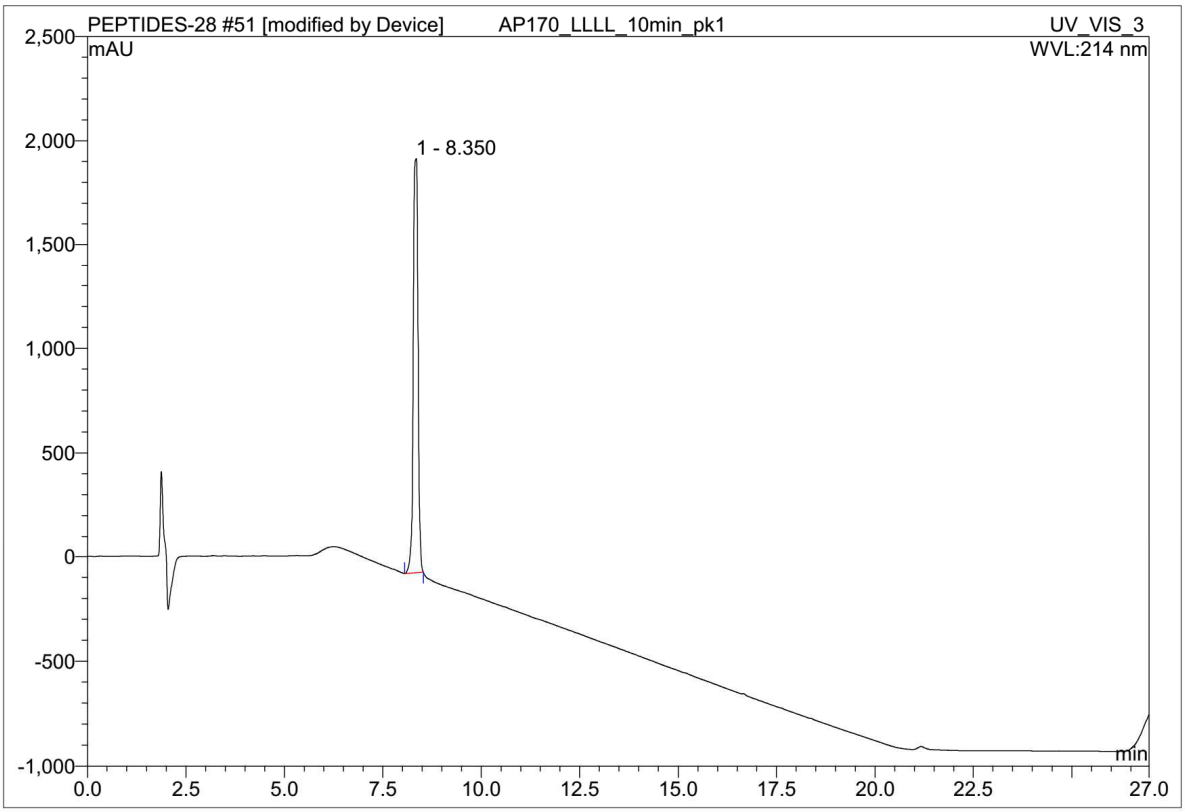

Figure S3.3: HPLC trace of HPLC purified teixobactin analogue **2.1**[2] (LLLL) (gradient: 5-95% ACN in 25 min using A: 0.1% HCOOH in water, B: ACN)

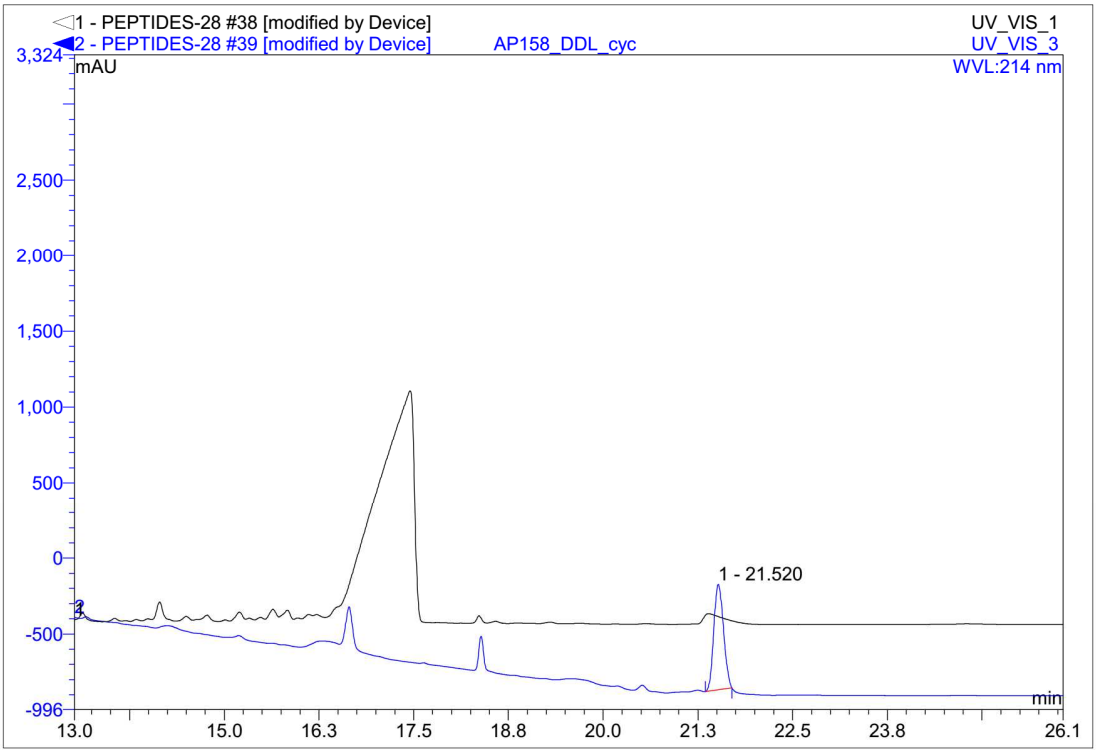

Figure S3.4: HPLC trace showing the progress of cyclisation reaction for **2.1**[3] (DDLD) (i): conversion of the uncyclized protected teixobactin analogue t_R= 17.457 min (shown in black) to the cyclized protected teixobactin analogue t_R = 21.520 min (shown in blue) (Gradient: 5-95% in 25 min)

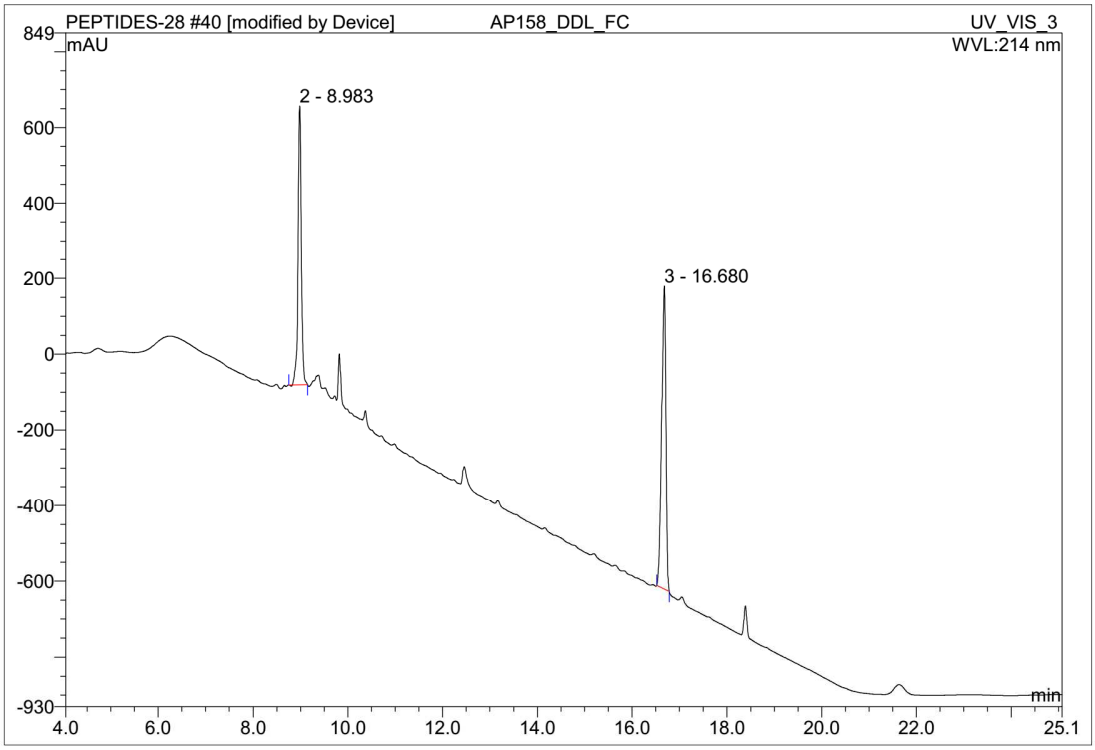

Figure S3.5: HPLC trace of crude teixobactin analogue **2.1**[3] (DDLD) t_R = 8.983 min (gradient: 5-95% ACN in 25 min using A: 0.1% HCOOH in water, B: ACN)

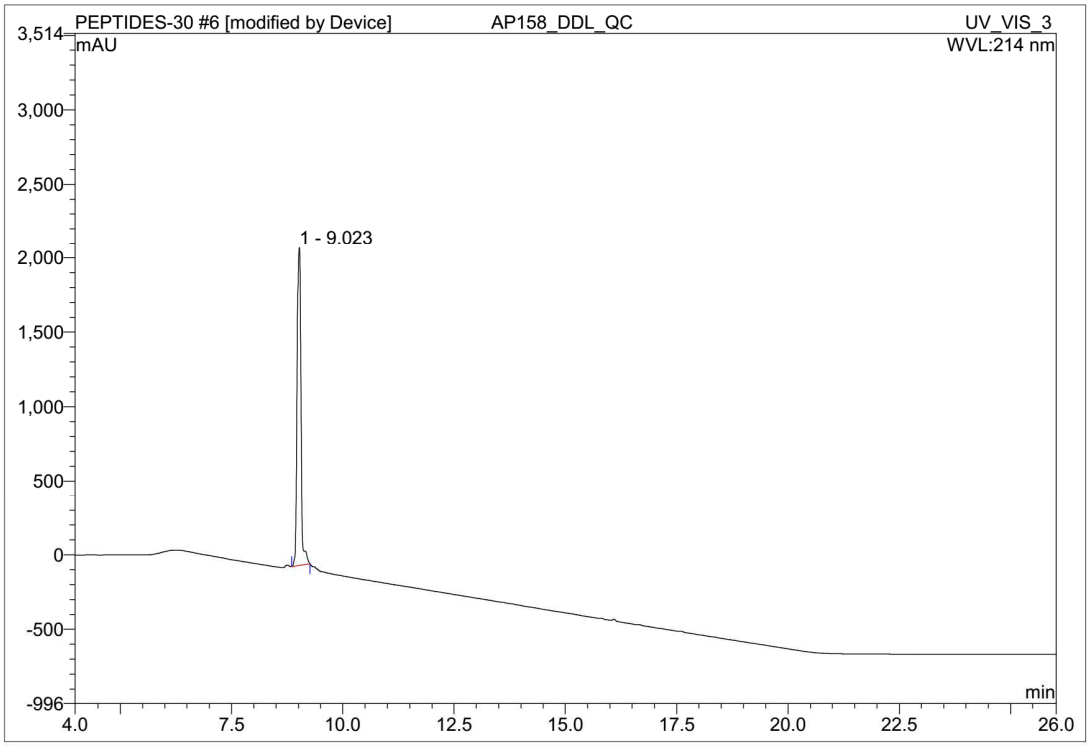

Figure S3.6: HPLC trace of HPLC purified teixobactin analogue **2.1**[3] (DDLD) (gradient: 5-95% ACN in 25 min using A: 0.1% HCOOH in water, B: ACN)

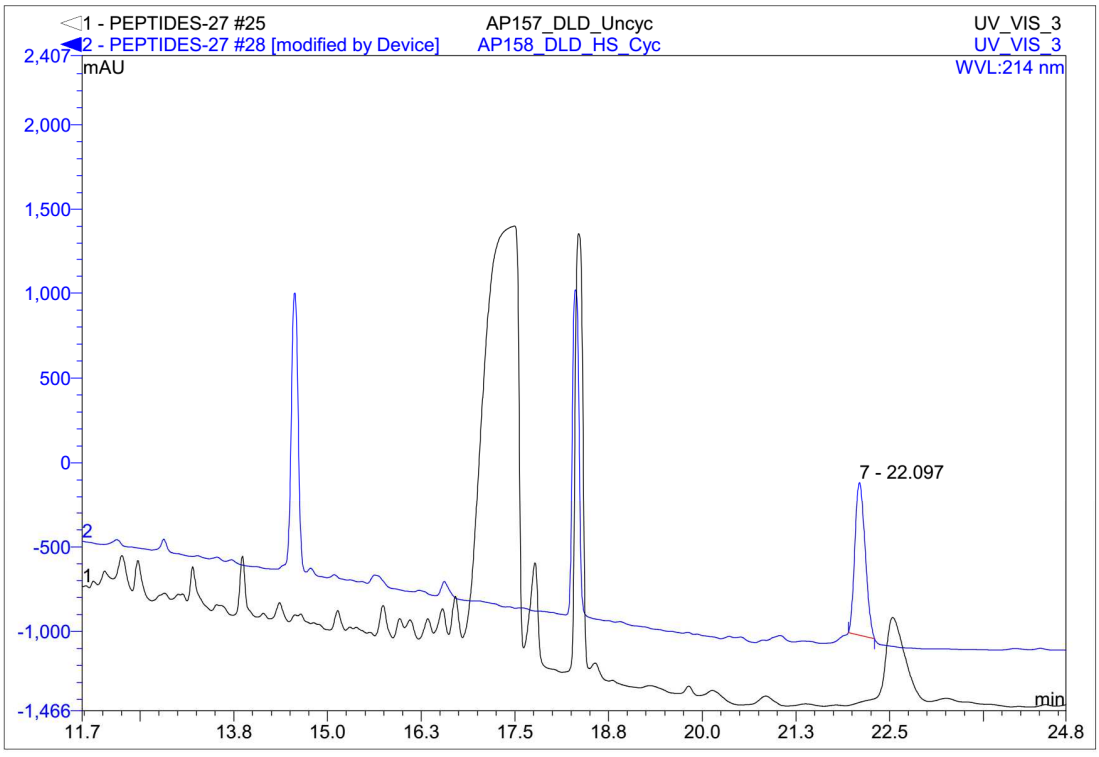

Figure S3.7: HPLC trace showing the progress of cyclisation reaction for **2.1**[4] (DLDD) (i): conversion of the uncyclized protected teixobactin analogue t_R= 17.493 min (shown in black) to the cyclized protected teixobactin analogue t_R = 22.097 min (shown in blue) (Gradient: 5-95% in 25 min)

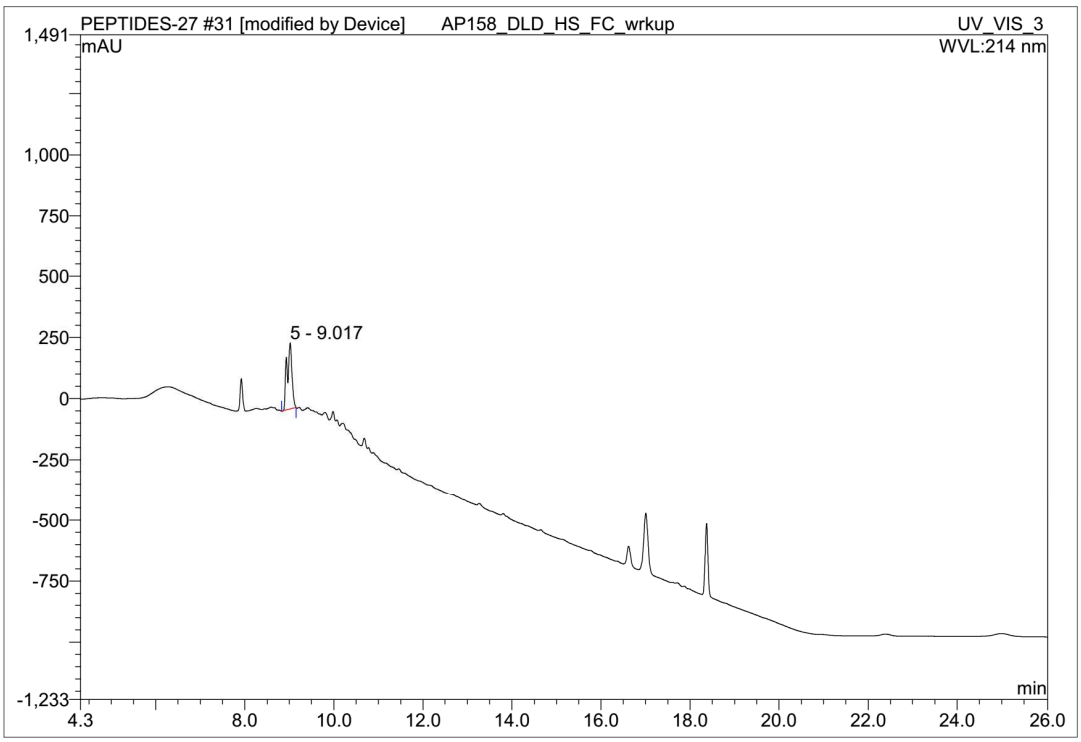

Figure S3.8: HPLC trace of crude teixobactin analogue **2.1**[4] (DLDD) t_R = 9.017 min (gradient: 5-95% ACN in 25 min using A: 0.1% HCOOH in water, B: ACN)

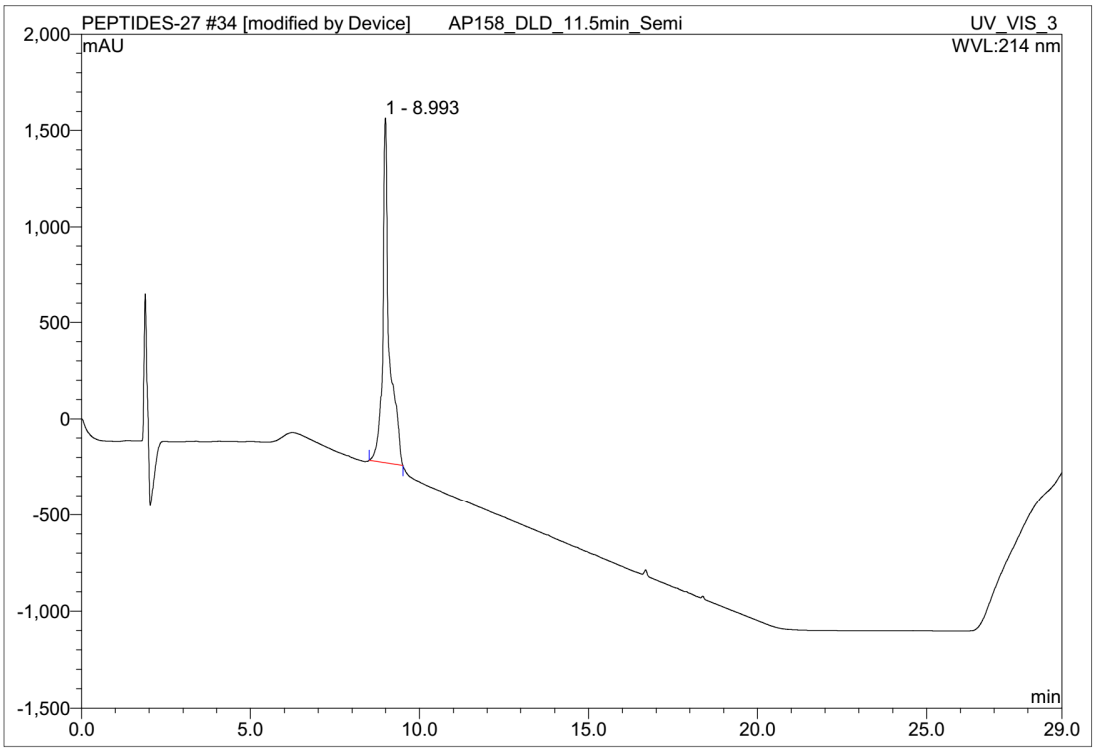

Figure S3.9: HPLC trace of HPLC purified teixobactin analogue **2.1**[4] (DLDD) (gradient: 5-95% ACN in 25 min using A: 0.1% HCOOH in water, B: ACN)

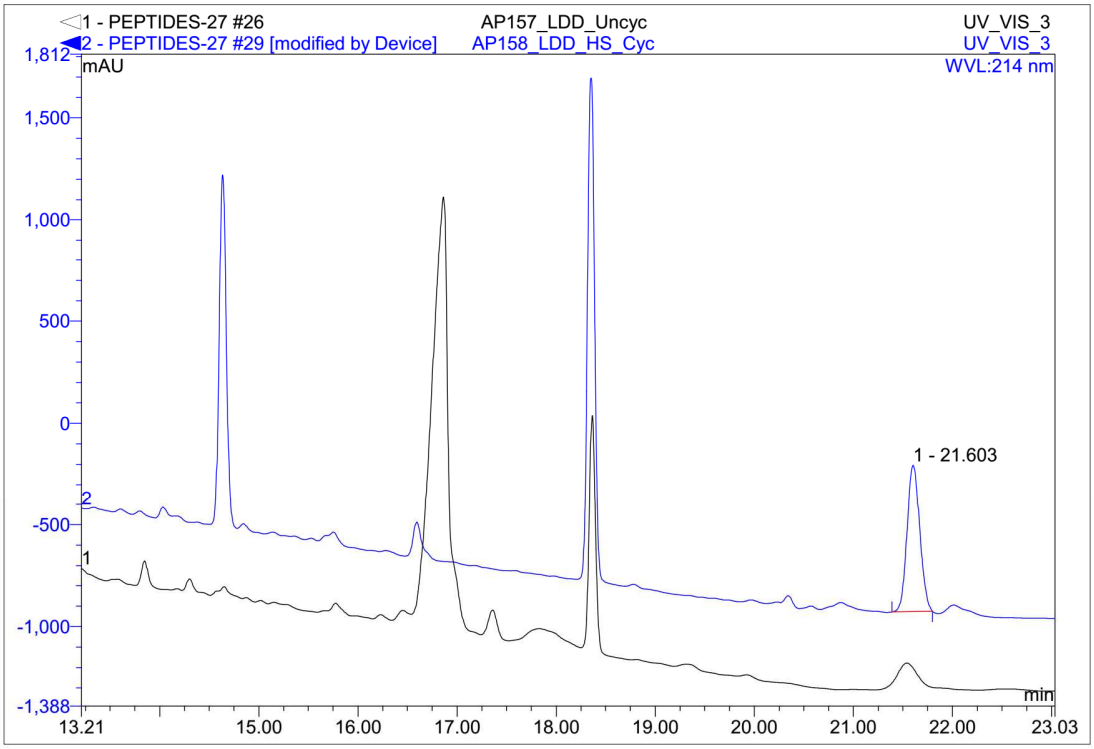

Figure S3.10: HPLC trace showing the progress of cyclisation reaction for **2.1**[5] (LDDD) (i): conversion of the uncyclized protected teixobactin analogue t_R= 16.863 min (shown in black) to the cyclized protected teixobactin analogue t_R = 21.603 min (shown in blue) (Gradient: 5-95% in 25 min)

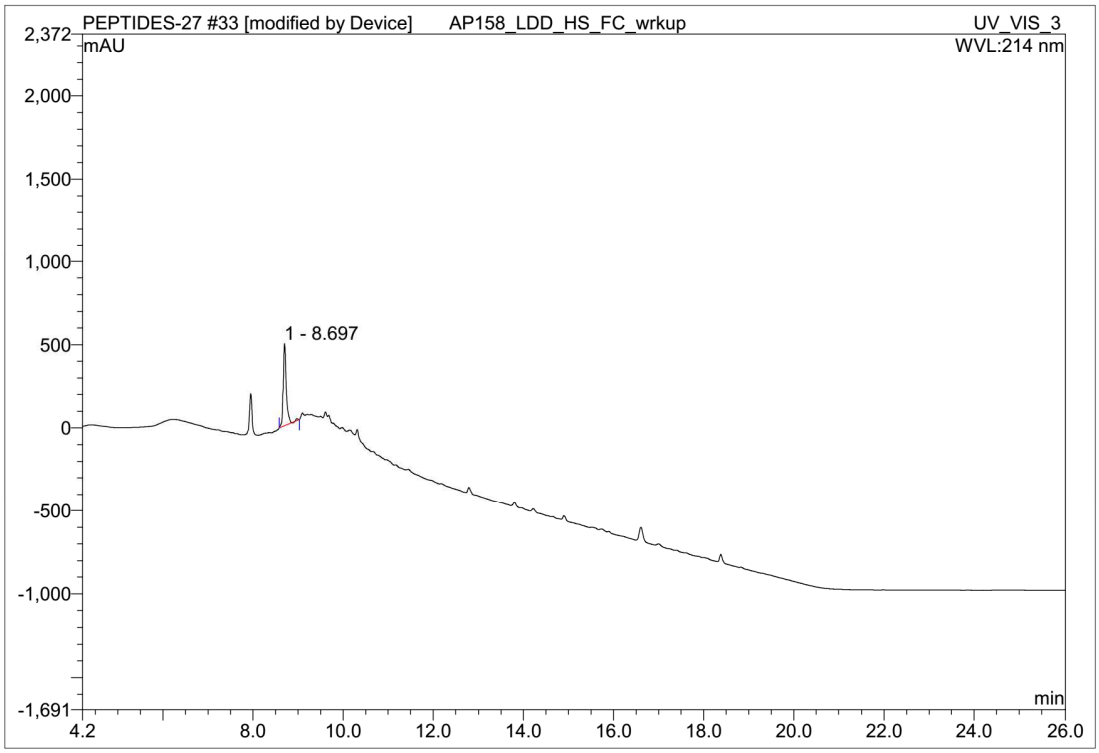

Figure S3.11: HPLC trace of crude teixobactin analogue **2.1**[5] (LDDD) t_R = 8.697 min (gradient: 5-95% ACN in 25 min using A: 0.1% HCOOH in water, B: ACN)

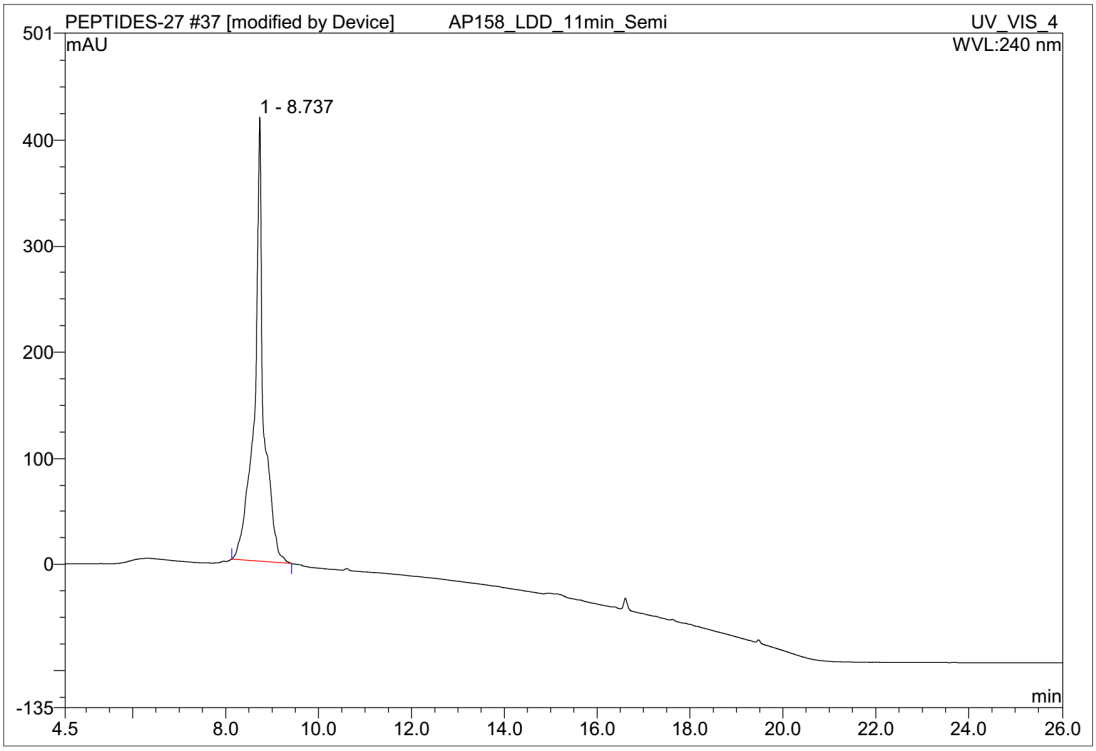

Figure S3.12: HPLC trace of HPLC purified teixobactin analogue **2.1**[5] (LDDD) (gradient: 5-95% ACN in 25 min using A: 0.1% HCOOH in water, B: ACN)

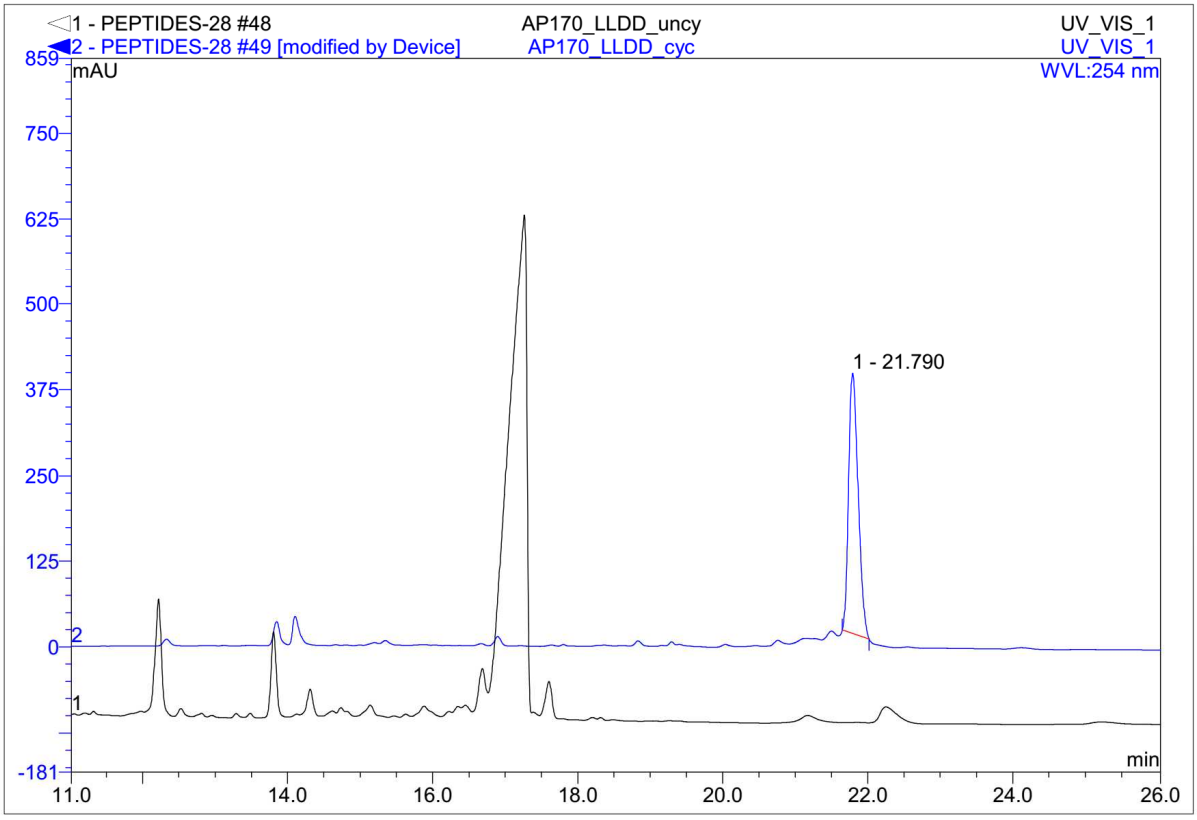

Figure S3.13: HPLC trace showing the progress of cyclisation reaction of **2.1**[6] (LLDD) (i): conversion of the uncyclized protected teixobactin analogue t_R= 17.263 min (shown in black) to the cyclized protected teixobactin analogue t_R = 21.790 min (shown in blue) (Gradient: 5-95% in 25 min)

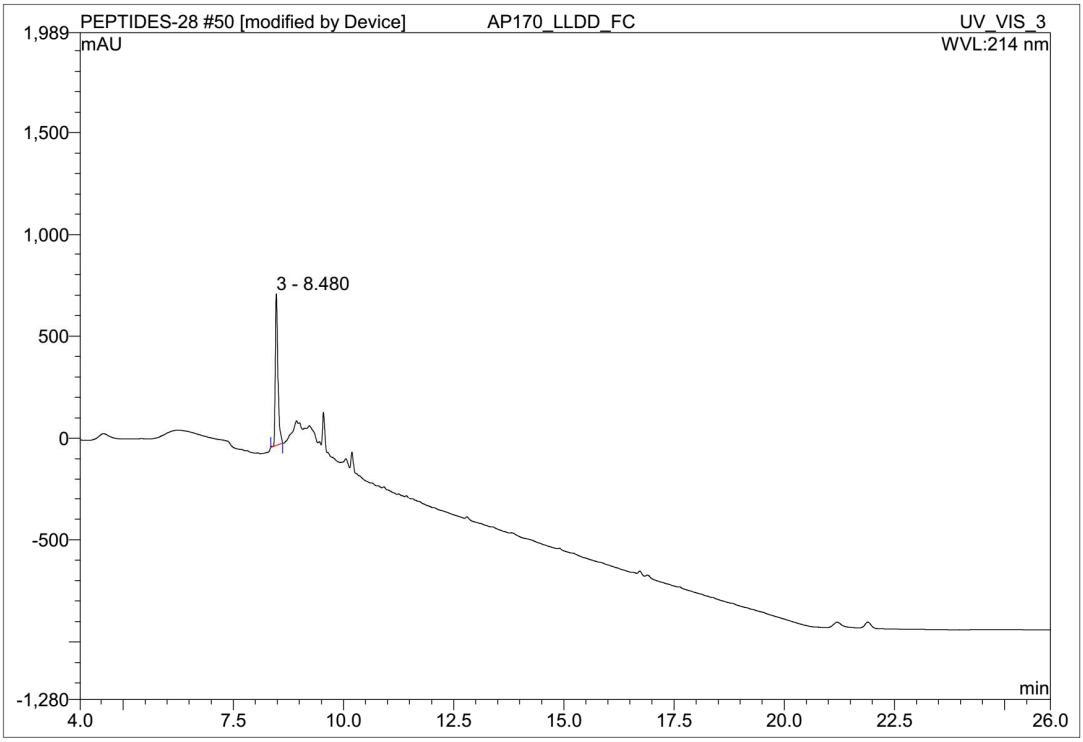

Figure S3.14: HPLC trace of crude teixobactin analogue **2.1**[6] LLDD t_R = 8.480 min (gradient: 5-95% ACN in 25 min using A: 0.1% HCOOH in water, B: ACN)

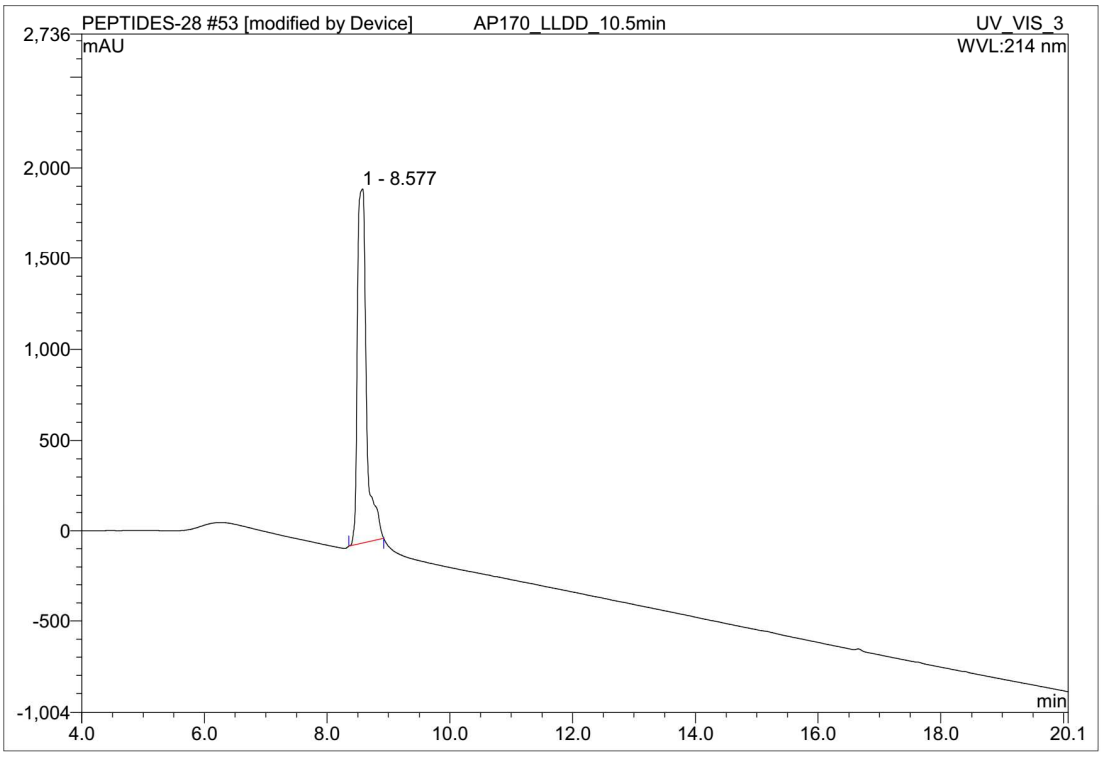

Figure S3.15: HPLC trace of HPLC purified teixobactin analogue **2.1**[6] LLDD (gradient: 5-95% ACN in 25 min using A: 0.1% HCOOH in water, B: ACN)

IV. NMR Analysis

Spectra were recorded using 1 mM teixobactin analogues dissolved in DMSO-d_6 at 298.2 K on a Bruker Avance III 500 MHz spectrometer. Assignments were made using ^{1}H-^{1}H TOCSY, ^{1}H-^{13}C HSQC and ^{1}H-^{13}C HMBC. Through-space dipolar correlations were measured using ^{1}H-^{1}H NOESY with 200 ms mixing time. Spectra were acquired with 2048 complex points, and either 196 (TOCSY, NOESY, HSQC) or 512 (HMBC) complex points in the direct and indirect dimensions, respectively. Spectra were processed using Bruker TopSpin and analysed using CcpNmr Analysis.[2] Structures of the homologues were obtained via the process of iterative NOE assignment, with the structural calculations carried out using Cyana 2.1.[3] A final round of energy minimisation in explicit solvent was carried out using Gromacs 5.1.2[4] and the RSFF2 forcefield,[5] which has been shown to perform favourably with cyclic peptides.[6] Structures were visualised and analysed using PyMOL.

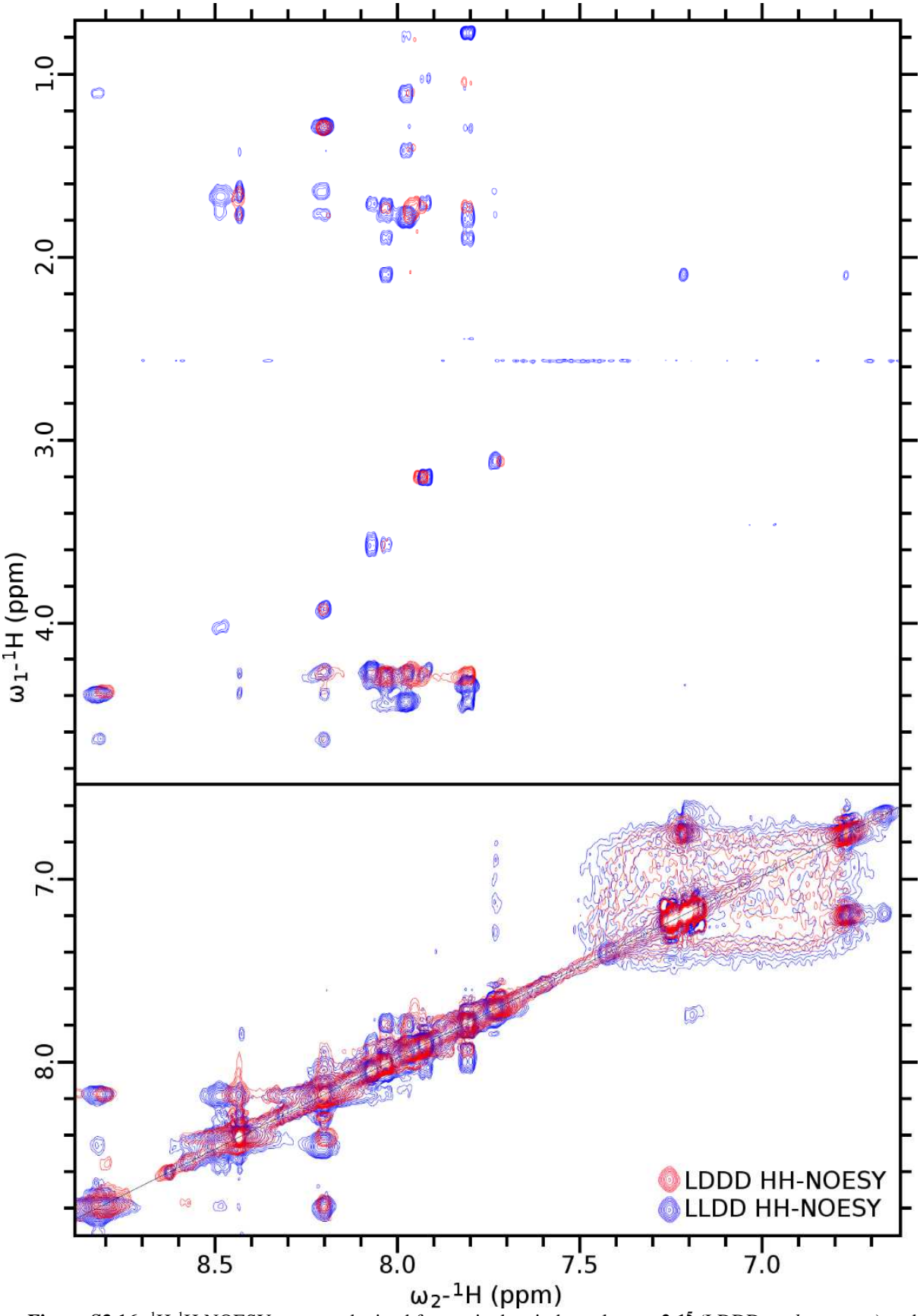

Figure S3.16: ^{1}H-^{1}H NOESY spectra obtained from teixobactin homologues **2.1**^{5} (LDDD, *red contours*) and LLDD (*blue contours*), which only differ from each other in the stereochemistry of position 4. There are many more crosspeaks visible in the spectrum of **2.1**^{6} (LLDD) when compared to **2.1**^{5} (LDDD), some of which are due to medium- to long-range interactions. These differences are borne out by the RMSDs of the structural

ensembles generated using these crosspeaks: **2.1[5]** (LDDD) with few crosspeaks resulted in an unstructured peptide with an RMSD of ~3 Å (Table 3.1; Figure 3.3A,D), whereas **2.1[6]** (LLDD) with many crosspeaks of different classes resulted in a structured peptide of ~1 Å (Table 3.1; Figure 3.3A,E). Samples were prepared identically and spectra were acquired under identical conditions. Contours for each spectrum were set to identical levels, which was set at one level above noise.

	2.1[3] (DDLD)	**2.1[4] (DLDD)**	**2.1[5] (LDDD)**	**2.1[6] (LLDD)**	**2.1[2] (LLLL)**
1Phe H*					
1Phe Hα	3.263	3.263	3.205	3.208	3.206
1Phe Hβ	2.789	2.688	2.676	2.677	2.688
	2.691	2.775	2.869	2.877	2.875
1Phe Hδ*	7.193	7.195	7.180	7.198	7.197
1Phe Hε*	7.193	7.234	7.248	7.214	7.246
1Phe Hζ	7.191	7.173	7.190	7.239	7.193
2Ile H	7.926	7.928	7.930	7.914	7.910
2Ile Hα	4.210	4.167	4.294	4.279	4.281
2Ile Hβ	1.674	1.642	1.723	1.702	1.714
2Ile Hγ1	0.898	0.907	1.026	1.026	1.033
	1.244	1.235	1.377	1.376	1.387
2Ile Hγ2*	0.734	0.726	0.804	0.800	0.802
2Ile Hδ1*	0.734	0.726	0.804	0.800	0.802
3Ser H	7.980	7.955	8.031	8.065	8.084
3Ser Hα	4.300	4.313	4.311	4.313	4.306
3Ser Hβ	3.553	3.507	3.569	3.564	3.557
	3.598	3.600	3.589	3.586	3.557
3Ser Hγ	5.009	5.073	4.998	5.041	5.007
4Gln H	7.909	8.059	7.946	8.023	7.976
4Gln Hα	4.326	4.308	4.302	4.352	4.269
4Gln Hβ	1.697	1.899	1.872	1.900	1.876
	1.888	1.726	1.714	1.730	1.714
4Gln Hγ	2.056	2.089	2.073	2.098	2.086
	2.056	2.088	2.073	2.098	2.086
4Gln Hε2	6.747	6.766	6.776	6.768	6.758
	7.198	7.221	7.220	7.214	7.195
5Ile H	7.851	7.819	7.804	7.799	7.888
5Ile Hα	4.254	4.326	4.281	4.444	4.195
5Ile Hβ	1.732	1.730	1.772	1.798	1.712
5Ile Hγ1	1.058	1.036	1.098	1.071	1.048
	1.369	1.378	1.400	1.293	1.405
5Ile Hγ2*	0.788	0.807	0.798	0.773	0.796
5Ile Hδ1*	0.788	0.807	0.798	0.773	0.799
6Ile H	7.851	8.010	7.958	7.963	7.887
6Ile Hα	4.229	4.265	4.282	4.284	4.239
6Ile Hβ	1.731	1.761	1.728	1.775	1.723
6Ile Hγ1	1.065	1.113	1.106	1.106	1.073

	1.438	1.407	1.377	1.413	1.402
6Ile Hγ2*	0.809	0.815	0.822	0.815	0.805
6Ile Hδ1*	0.809	0.815	0.822	0.815	0.806
7Ser H	8.965	9.124	9.124	9.202	8.079
7Ser Hα	4.378	4.380	4.385	4.404	4.352
7Ser Hβ	3.667	3.738	3.700	3.708	3.537
	3.756	3.736	3.769	3.770	3.567
7Ser Hγ	5.655	5.592	5.616	5.643	4.918
8Thr H	8.953	8.763	8.798	8.820	7.759
8Thr Hα	4.644	4.638	4.642	4.645	4.796
8Thr Hβ	5.361	5.359	5.361	5.361	4.482
8Thr Hγ2*	1.091	1.091	1.095	1.092	1.075
9Ala H	8.211	8.185	8.202	8.197	9.454
9Ala Hα	3.932	3.930	3.928	3.929	4.466
9Ala Hβ*	1.290	1.288	1.287	1.279	1.339
10Arg H	8.211	8.159	8.190	8.205	9.168
10Arg Hα	4.274	4.276	4.281	4.279	4.052
10Arg Hβ	1.654	1.636	1.652	1.642	1.731
	1.768	1.765	1.771	1.769	1.731
10Arg Hγ	1.486	1.494	1.491	1.491	1.545
	1.430	1.412	1.417	1.413	1.522
10Arg Hδ	3.108	3.118	3.119	3.116	3.111
	3.108	3.118	3.119	3.116	3.111
10Arg Hε	7.742	7.731	7.714	7.734	7.801
10Arg Hη1	6.918	7.101		6.913	6.984
	7.067	7.101		7.013	6.984
10Arg Hη2	7.194	7.302		7.308	7.165
	7.281	7.302		7.144	7.165
11Ile H	8.471	8.415	8.434	8.481	7.972
11Ile Hα	4.035	4.028	4.032	4.031	4.412
11Ile Hβ	1.670	1.671	1.693	1.685	1.942
11Ile Hγ1	1.088	1.099	1.103	1.091	1.154
	1.423	1.418	1.422	1.415	1.346
11Ile Hγ2*	0.811	0.813	0.801	0.801	0.848
11Ile Hδ1*	0.811	0.808	0.801	0.801	0.849

Table S3.2: Chemical shift assignments of the teixobactin homologues. *Underlined values* are more than 2 standard deviations away from the average values. Chemical shifts for analogues **2**.1[1] (DDDD) and **2**.1[7] (LLLD) have been published previously[1].

V. Structural Statistics for teixobactin analogues

	2.1[1] (DDDD)	2.1[3] (DDLD)	2.1[4] (DLDD)	2.1[5] (LDDD)	2.1[6] (LLDD)	2.1[7] (LLLD)	2.1[2] (LLLL)
NMR distance restraints							
Intra-residue	38	56	55	43	57	50	44
Sequential ($\|i-j\| = 1$)	11	18	18	14	21	19	18
Med range ($\|i-j\| < 5$)	5	7	1	6	6	6	1
Long range ($\|i-j\| > 4$)	0	0	2	0	8	2	1
TOTAL	54	81	76	63	92	77	64
Statistics of overall structural quality							
Ensemble pairwise RMSD							
Heavy atom (Å)	3.16 ± 1.44	1.83 ± 0.55	0.76 ± 0.20	2.96 ± 1.26	1.06 ± 0.45	0.93 ± 0.44	1.08 ± 0.32
Backbone (Å)	1.83 ± 1.10	0.93 ± 0.37	0.37 ± 0.15	1.92 ± 0.93	0.59 ± 0.30	0.53 ± 0.28	0.50 ± 0.20
Restr violations > 0.1 Å	0	0	0	0	0	0	0
RMSD from idealised covalent geometry[7]							
Bond lengths (Å)	0.013	0.013	0.013	0.013	0.013	0.011	0.013
Bond angles (°)	2.1	1.9	1.9	2.0	2.1	1.8	1.9
Ramachandran analysis[8]							
Allowed (%)	58.8 ± 6.3	95.6 ± 5.6	77.7 ± 0.0	88.9 ± 0.0	88.8 ± 0.0	98.3 ± 4.1	98.9 ± 3.4
Gen allowed (%)	20.5 ± 6.7	4.4 ± 5.6	22.2 ± 0.0	2.2 ± 4.5	0.0 ± 0.0	1.7 ± 4.0	1.1 ± 3.4
Disallowed (%)	20.5 ± 6.5	0.0 ± 0.0	0.0 ± 0.0	8.9 ± 4.5	11.1 ± 0.0	0.0 ± 0.0	0.0 ± 0.0
ProCheck *G*-factor	-0.58 ± 0.1	-0.37 ± 0.1	-0.31 ± 0.1	-0.25 ± 0.1	-0.32 ± 0.1	-0.12 ± 0.1	-0.27 ± 0.1
MolProbity clash score[9]	0.27 ± 1.20	1.06 ± 2.18	0.00 ± 0.00	0.00 ± 0.00	0.00 ± 0.00	1.06 ± 2.18	5.85 ± 1.64

Table S3.3: Structural statistics for teixobactin analogues.

VI. Molecular Dynamic simulations

Molecular dynamics simulations were carried out using Gromacs 5.1.2 and RSFF2. The lowest energy structure from each ensemble was solvated in TIP3P water and neutralised with chloride ions. This system was subjected to 100 ps of NVT and NPT equilibration. 100 ns of simulation was carried out with periodic boundary conditions at 298.2 K, and the trajectory analysed with VMD.[10]

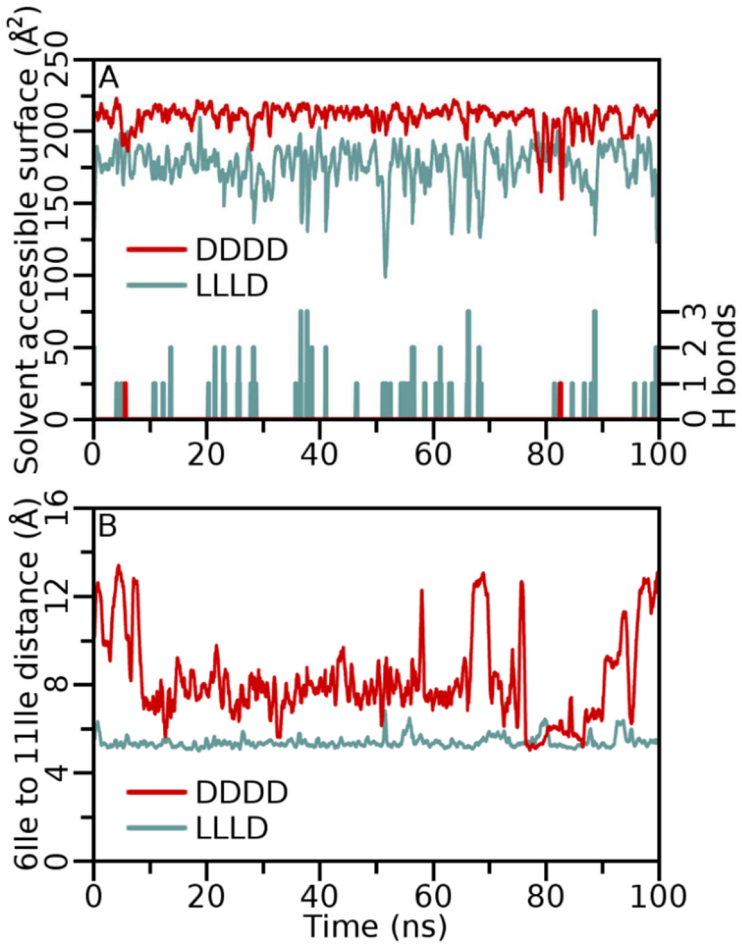

Figure S3.17: Molecular dynamics simulations of teixobactin stereochemical analogues. A. The sidechain of Arg_{10} consistently presents ~15% less surface area to the solvent in non-native teixobactin **2.1**[7] (LLLD, *teal line*) when compared to the native **2.1**[1] (DDDD, *red line*) over the course of the simulation. B. Hydrophobic packing between the sidechains of Ile_6 and Ile_{11} is consistent over the course of the simulation in the analogue (*teal line*), whereas this packing is only infrequently visited in the native form (*red line*). Simulations were performed using Gromacs 5.1.2 and the RSFF2 forcefield. Surface area, hydrogen bonds and interatomic distances were calculated using the Gromacs modules *sasa*, *hbond* and *distance*, respectively. Data were recorded every 10 ps and were plotted as a rolling average over 50 data points.

VII. MIC testing

For MIC testing all peptides were dissolved in DMSO. Bacteria were grown on Mueller Hinton broth (oxoid). All incubations were at 37°C. Dilutions were carried out using Mueller Hinton. 100 µl of autoclaved Mueller Hinton broth was added to wells 2-12 on a 96-well plate. 200 µl of the peptide was added to well one at a concentration of 512 µg/ml. 100µl of peptide in well one was taken up and pipetted into well two. The mixture was then mixed via pipetting before 100µl was taken up and pipetted into well three. This process was repeated up to well 11. Once peptide was added to well 11 100 µl was taken up and then discarded ensuring the well 12 had no peptide present. Each well was then inoculated with 100µl of bacteria that had been diluted to an OD600nm of 0.1. This was repeated three times. The 96-well plates were then incubated for 24 hours. The MIC was determined to be the lowest concentration at which there was no growth visible.

VIII. Complex formation of teixobactin with lipid II and geranyl pyrophosphate

Complex formation of teixobactin analogues **2**^{1} (DDDD) and **2**^{2} (LLLL) with lipid II and geranyl pyrophosphate was performed using TLC as described previously[11]. Binding of teixobactin to lipid II and geranyl pyrophosphate was analysed by incubating 30 µL of 2 nmol of each precursor with 2 or 4 nmoles of teixobactin in 50 mM Tris/HCl, pH 7.5, for 30 min at room temperature. Complex formation was analysed by extracting unbound precursors from the reaction mixture with 30 µL n-butanol/6M pyridine acetate (pH 4.2) (2:1; vol/vol) followed by TLC analysis of the organic layer using chloroform/methanol/water/ammonia (88:48:10:1, v/v/v/v) as the solvent and detection of lipid/phosphate containing precursors by phosphomolybdic acid staining[12]. The TLC figures represent the results obtained through three independent experiments.

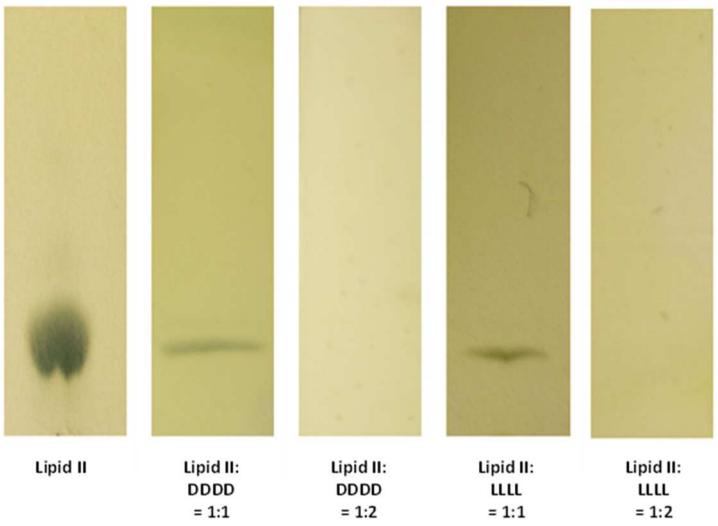

Figure S3.18: Binding of teixobactin analogues **2**^{1} (DDDD) and **2**^{2} (LLLL) with lipid II using the protocols described in literature[11]. Partial binding is observed when the ratio of lipid II to the analogue is 1:1 (indicated by lighter spots on the TLC) and complete binding is observed when the ratio of lipid II to the analogue is 1:2 (indicated by no spots on TLC).

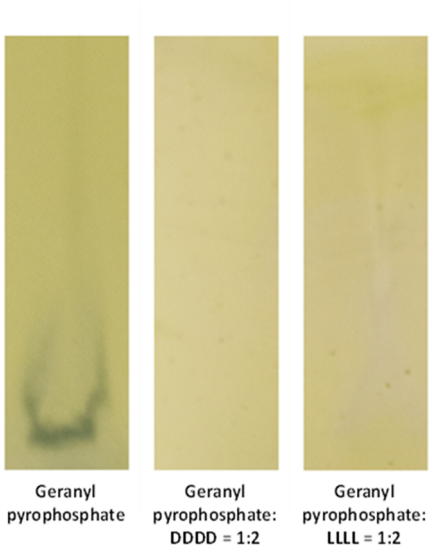

Figure S3.19: Binding of teixobactin analogues **2**[1] (DDDD) and **2**[2] (LLLL) with geranyl pyrophosphate using the protocols described in literature[11]. No binding is observed when the ratio of the phosphate to the analogue is 1:2 (indicated by no spots on the TLC).

IX. References

1. A. Parmar, A. Iyer, C. S. Vincent, D. Van Lysebetten, S. H. Prior, A. Madder, E. J. Taylor, I. Singh, Efficient total syntheses and biological activities of two teixobactin analogues. *Chem. Commun.* **52**, 6060–6063 (2016).

2. W. F. Vranken, W. Boucher, T. J. Stevens, R. H. Fogh, A. Pajon, M. Llinas, E. L. Ulrich, J. L. Markley, J. Ionides, E. D. Laue, The CCPN data model for NMR spectroscopy: Development of a software pipeline. *Proteins: Structure, Function and Genetics*. **59**, 687–696 (2005).

3. P. Guntert, L. Buchner, Combined automated NOE assignment and structure calculation with CYANA. *Journal of Biomolecular NMR*. **62**, 453–471 (2015).

4. M. J. Abraham, T. Murtola, R. Schulz, S. Pall, J. C. Smith, B. Hess, E. Lindah, Gromacs: High performance molecular simulations through multi-level parallelism from laptops to supercomputers. *SoftwareX*. **1–2**, 19–25 (2015).

5. S. Li, A. H. Elcock, Residue-Specific Force Field (RSFF2) Improves the Modeling of Conformational Behavior of Peptides and Proteins. *The Journal of Physical Chemistry Letters*. **13**, 2127–2133 (2015).

6. H. Geng, F. Jiang, Y.-D. Wu, Accurate Structure Prediction and Conformational Analysis of Cyclic Peptides with Residue-Specific Force Fields. *The Journal of Physical Chemistry Letters*. **7**, 1805–10 (2016).

7. Aneerban Bhattacharya, Roberto Tejero, Gaetano T. Montelione, Evaluating Protein Structures Determined by Structural Genomics Consortia. *Proteins*. **66**, 778–795 (2007).

8. R. Laskowski, J. A. Rullmann, M. MacArthur, R. Kaptein, J. Thornton, AQUA and PROCHECK-NMR: Programs for checking the quality of protein structures solved by NMR. *Journal of Biomolecular NMR*. **8**, 477–486 (1996).

9. S. C. Lovell, I. W. Davis, W. B. Adrendall, P. I. W. de Bakker, J. M. Word, M. G. Prisant, J. S. Richardson, D. C. Richardson, Structure validation by C alpha geometry: phi,psi and C beta deviation. *Proteins-Structure Function and Genetics*. **50**, 437–450 (2003).

10. W. Humphrey, A. Dalke, K. Schulten, VMD: visual molecular dynamics. *Journal of molecular graphics*. **14**, 33–8, 27–8 (1996).

11. L. L. Ling, T. Schneider, A. J. Peoples, A. L. Spoering, I. Engels, B. P. Conlon, A. Mueller, D. E. Hughes, S. Epstein, M. Jones, L. Lazarides, V. a Steadman, D. R. Cohen, C. R. Felix, K. A. Fetterman, W. P. Millett, A. G. Nitti, A. M. Zullo, C. Chen, K. Lewis, A new antibiotic kills pathogens without detectable resistance. *Nature*. **517**, 455–459 (2015).

12. L.-T. Sham, E. K. Butler, M. D. Lebar, D. E. Kahne, T. G. Bernhardt, N. Ruiz, MurJ is the flippase of lipid-linked precursors for peptidoglycan biogenesis. *Science*. **719**, 220–222 (2014).

EXPERIMENTAL SECTION FOR CHAPTER 4

I. Materials

All L amino acids including Fmoc-Orn(Boc)-OH, Fmoc-Dab(Boc)-OH and Fmoc-Dap(Boc)-OH and D amino acids Fmoc-D-Ala-OH Fmoc-D-Gln(Trt)-OH, Boc-N-methyl-D-phenylalanine and 1-[Bis(dimethylamino)methylene]-1H-1,2,3-triazolo[4,5-b]pyridinium3-oxidhexafluorophosphate (HATU), Phenylsilane ($PhSiH_3$), Tetrakis(triphenylphosphine)palladium(0) [$Pd(PPh_3)$], Diisoproplycarbodiimide (DIC), Triisopropylsilane (TIS) and and 1*H*-Pyrazole-carboxamidine hydrochloride were purchased from Fluorochem, UK. Fmoc-D-*allo*-Ile-OH and oxyma pure were purchased from Merck Millipore. The side chain protecting groups for the amino acids are ^{t}Bu for Ser, Pbf for Arg and Trt for Gln and Thr unless specified otherwise. Diisopropylethylamine (DIPEA), supplied as extra dry, redistilled, 99.5 % pure, Acetic anhydride, allyl chloroformate, $CDCl_3$ and polysorbate 80 and were purchased from Sigma Aldrich. Tritylchloride and 4-(Dimethylamino)pyridine were purchased from Alfa Aesar. Dimmethylformamide (DMF) peptide synthesis grade was purchased from Rathburn chemicals. Triethylamine, Diethyl ether (Et_2O), Dimethylsulfoxide (DMSO), Dichloromethane (DCM), Tetrahydrofuran (extra dry with molecular sieves), Formic acid 98-100% purity and Acetonitrile (HPLC grade) were purchased from Fisher Scientific. Water with the Milli-Q grade standard was obtained in-house from an ELGA Purelab Flex system. 2-Chlorotritylchloride resin (manufacturer's loading: 1.20 mmol/g) was purchased from Fluorochem, UK. All chemicals were used without further purification.

II. Equipment used for the analysis and purification of compounds

All peptides were analysed on a Thermo Scientific Dionex Ultimate 3000 RP-HPLC equipped with a Phenomenex Gemini NX C18 110 Å (150 x 4.6 mm) column using the following buffer systems: A: 0.1% HCOOH in milliQ water. B: ACN using a flow rate of 1 ml/min. The column was flushed with 95% A for 5 min prior to an injection and was flushed for 5 min with 95% B and 5% A after the run was finished.

Peptides were analysed using the following gradient: 95% A for 2 min. 5-95% B in 25 min. 95% B for 5 min. 5% A for 4 min.

Peptides were purified using the same gradient as mentioned above, on a Thermo Scientific Dionex Ultimate 3000 RP-HPLC with a flow rate of 5 mL/min using a Phenomenex Gemini NX C18 110 Å (150 x 10 mm) semi-prep column.

HRMS spectra were recorded on a Thermo Scientific Q Exactive Plus Orbitrap Mass Spectrometer in the positive ion mode.

III. Syntheses of teixobactin analogues

Teixobactin analogues **2.1, 4.1**, **4.3**, **4.4** & **4.6** were synthesized according to our previously described protocol.[1]

Procedure for Guanidation: 5 mg of the amino precursor for the corresponding guanidine teixobactin was dissolved in 200 µL of MeOH. 15 eq. of Et_3N was then added to it and the solution was stirred till all the teixobactin analogue dissolved. 1.5 eq. of 1*H*-Pyrazole-carboxamidine hydrochloride was then added and stirred vigorously. MeOH was added dropwise (if necessary) till all the reagent dissolved and the reaction mixture was stirred for 8h at r.t. The reaction mixture was then analysed on RP-HPLC followed by RP-HPLC purification and freeze dried to yield the corresponding guanidine teixobactin.

IV. HPLC/LC-MS analysis

Compound Number	Name	Chemical formula	Calculated Exact Mass	Mass found [M + H^+]	Overall yield [%]
4.1	Lys_{10}-teixobactin	$C_{58}H_{97}N_{13}O_{15}$	1215.7227	1216.7314	19 [a]
4.2	$HoArg_{10}$-teixobactin	$C_{59}H_{99}N_{15}O_{15}$	1257.7445	1258.7533	64 [b]
4.3	Orn_{10}-teixobactin	$C_{57}H_{95}N_{13}O_{15}$	1201.7071	1202.7153	16 [a]
4.4	Dab_{10}-teixobactin	$C_{56}H_{93}N_{13}O_{15}$	1187.6914	1188.7009	20 [a]
4.5	$NorArg_{10}$-teixobactin	$C_{57}H_{95}N_{15}O_{15}$	1229.7132	1230.7216	50 [b]
4.6	Dap_{10}-teixobactin	$C_{55}H_{91}N_{13}O_{15}$	1173.6758	1174.6852	13 [a]
4.7	$GAPA_{10}$-teixobactin	$C_{56}H_{93}N_{15}O_{15}$	1215.6976	1216.7057	48 [b]

Table S4.1: Compound number, name, chemical formula, exact mass, mass found and overall yield for compounds **4.1, 4.3, 4.6** & **4.2, 4.5, 4.7**.

[a] isolated yield.

[b] isolated yields for guanidation step.

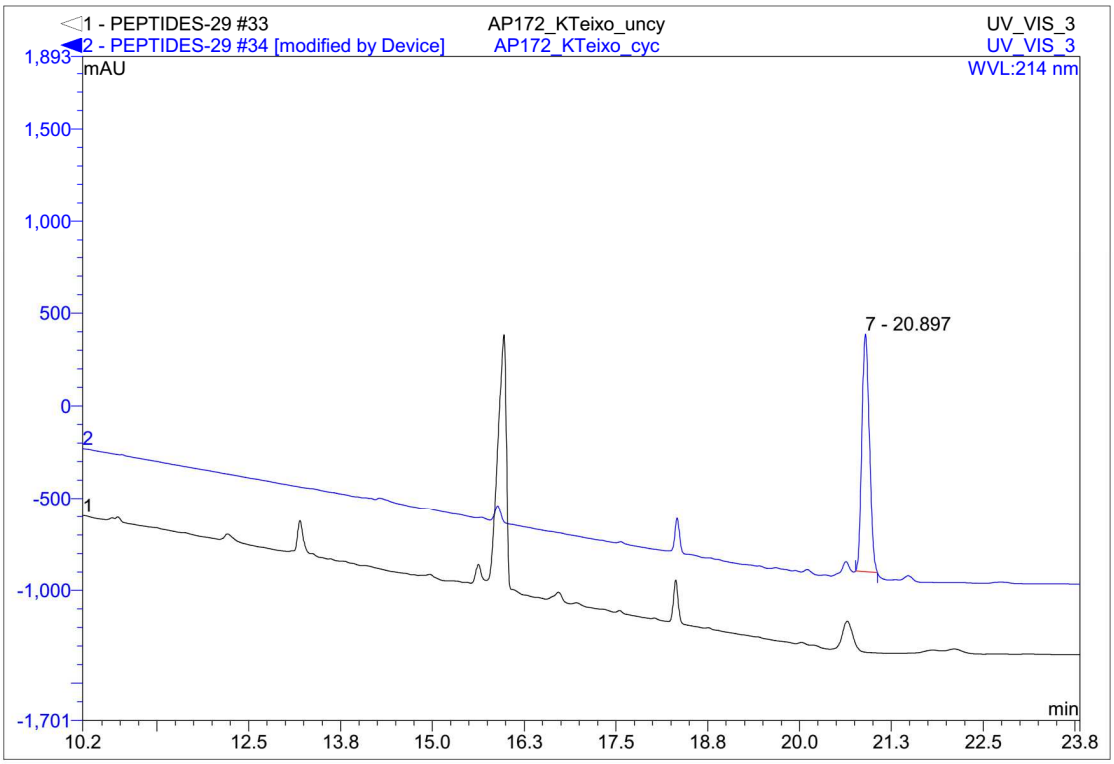

Figure S4.1: HPLC trace showing the progress of the cyclisation reaction for analogue **4.1**: conversion of the uncyclized protected teixobactin analogue tR= 15.977 min (shown in black) to the cyclized protected teixobactin analogue tR = 20.897 min (shown in blue) (Gradient: 5-95% in 25 min)

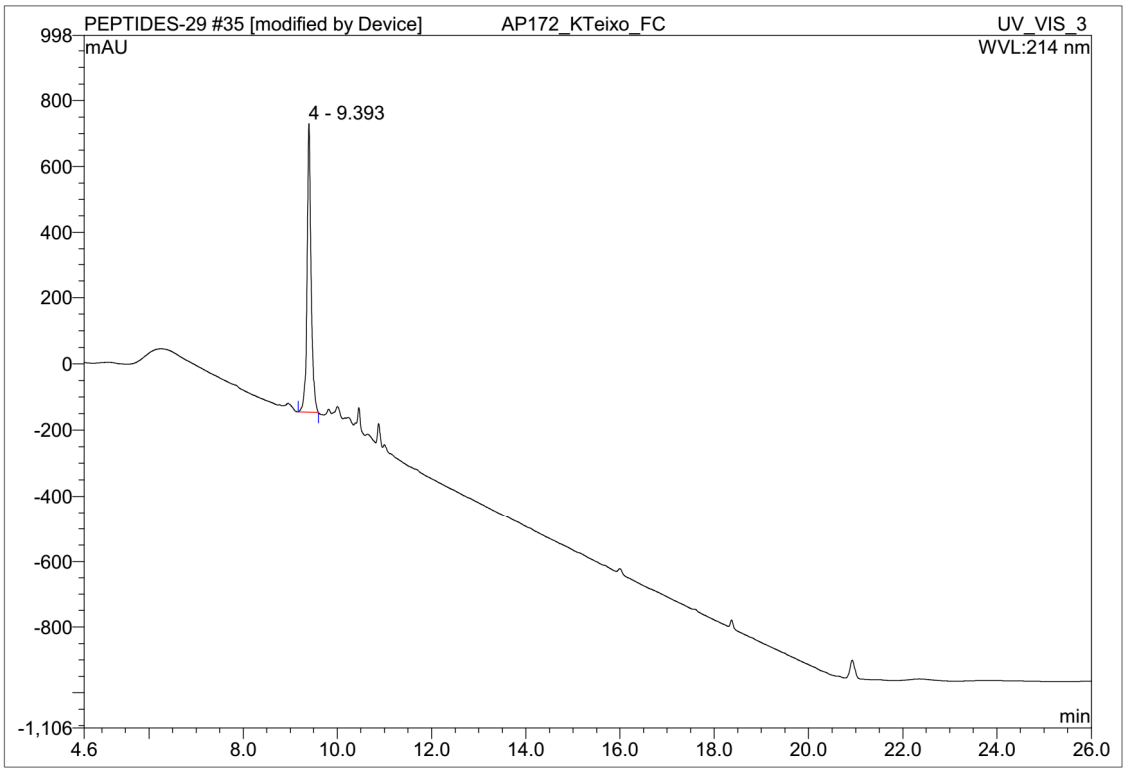

Figure S4.2: HPLC trace of crude teixobactin analogue **4.1** t_R = 9.393 min (gradient: 5-95% ACN in 25 min using A: 0.1% HCOOH in water, B: ACN)

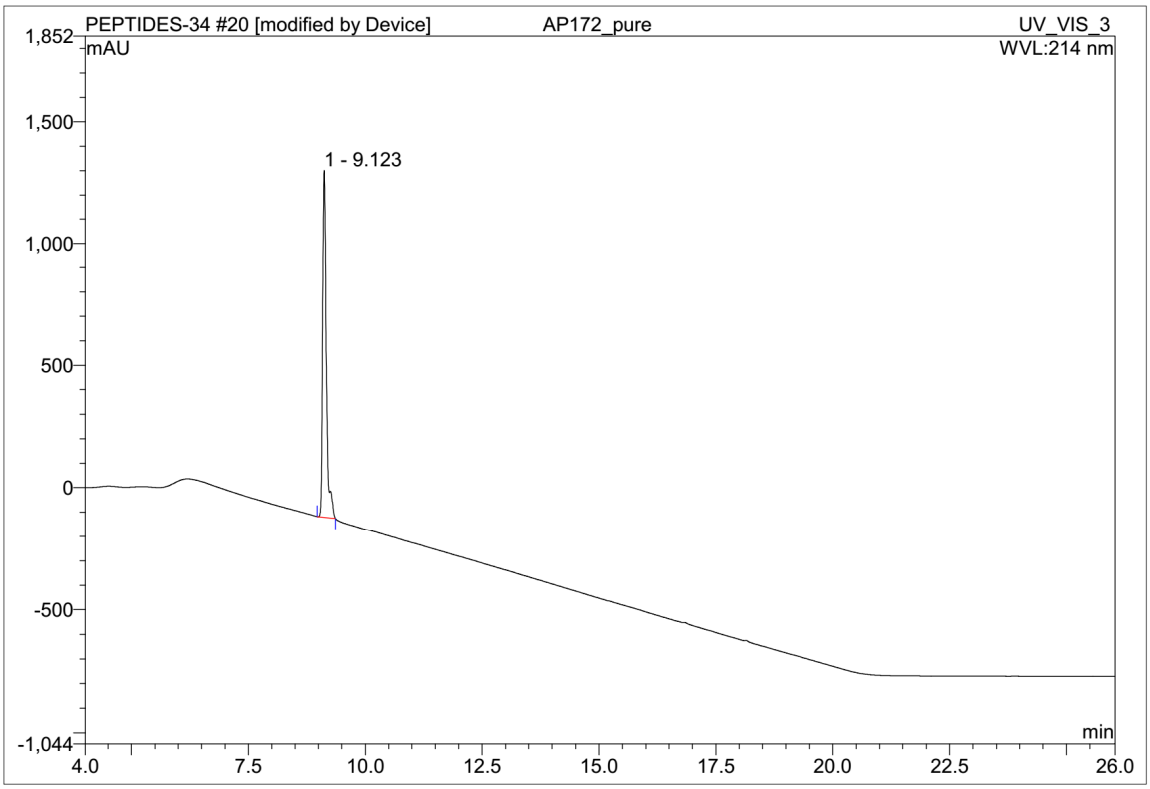

Figure S4.3: HPLC trace of HPLC purified teixobactin analogue **4.1** (gradient: 5-95% ACN in 25 min using A: 0.1% HCOOH in water, B: ACN)

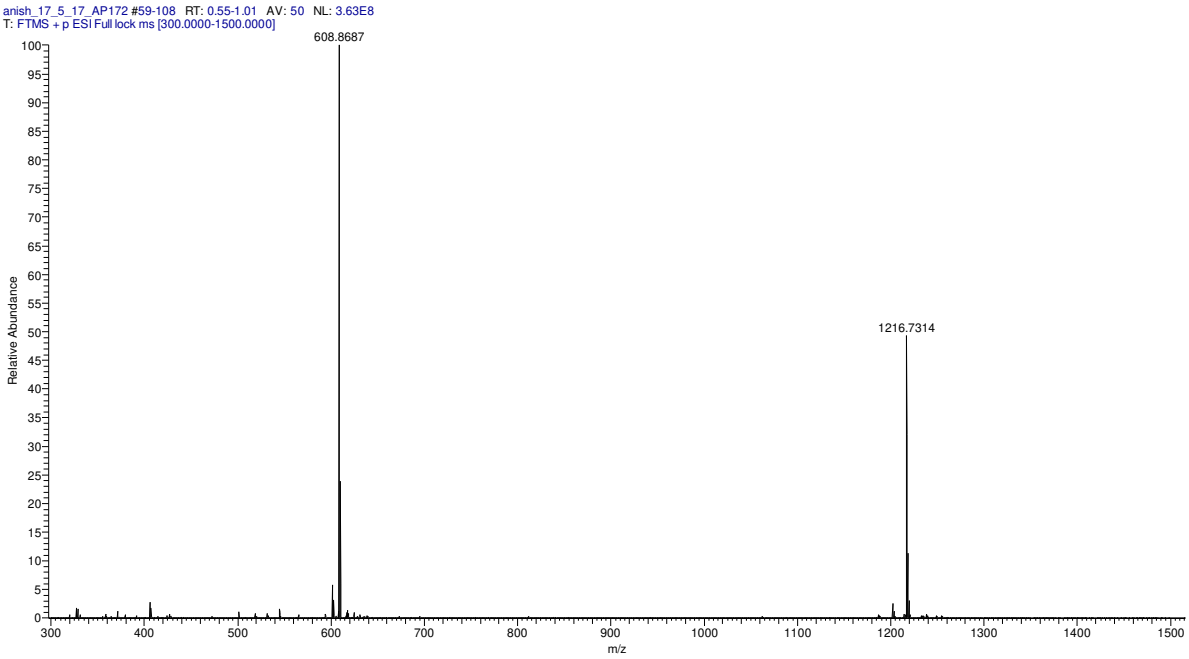

Figure S4.4: HRMS spectra from of HPLC purified teixobactin analogue **4.1**. Exact Mass calcd. for $C_{58}H_{97}N_{13}O_{15}$ = 1215.7227, found $M+H^+$ = 1216.7314 and $M/2 + H^+$ = 608.8687

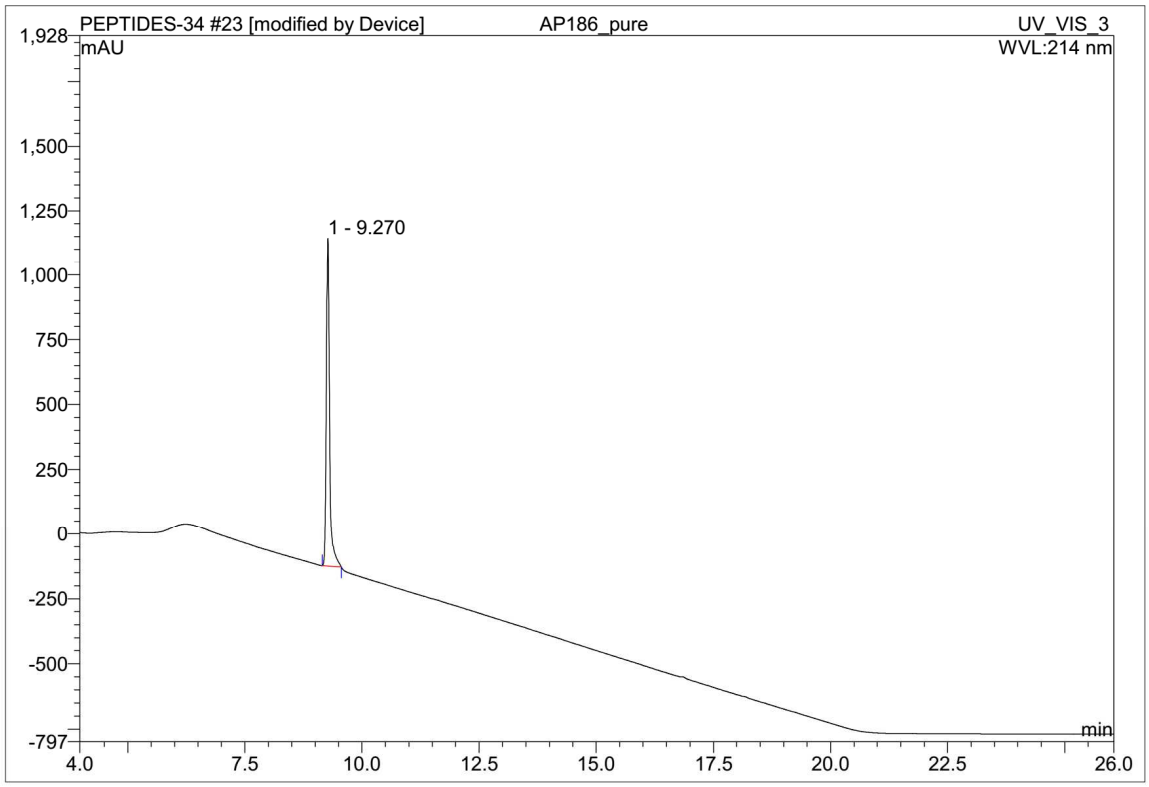

Figure S4.5: HPLC trace of HPLC purified teixobactin analogue **4.2** (gradient: 5-95% ACN in 25 min using A: 0.1% HCOOH in water, B: ACN)

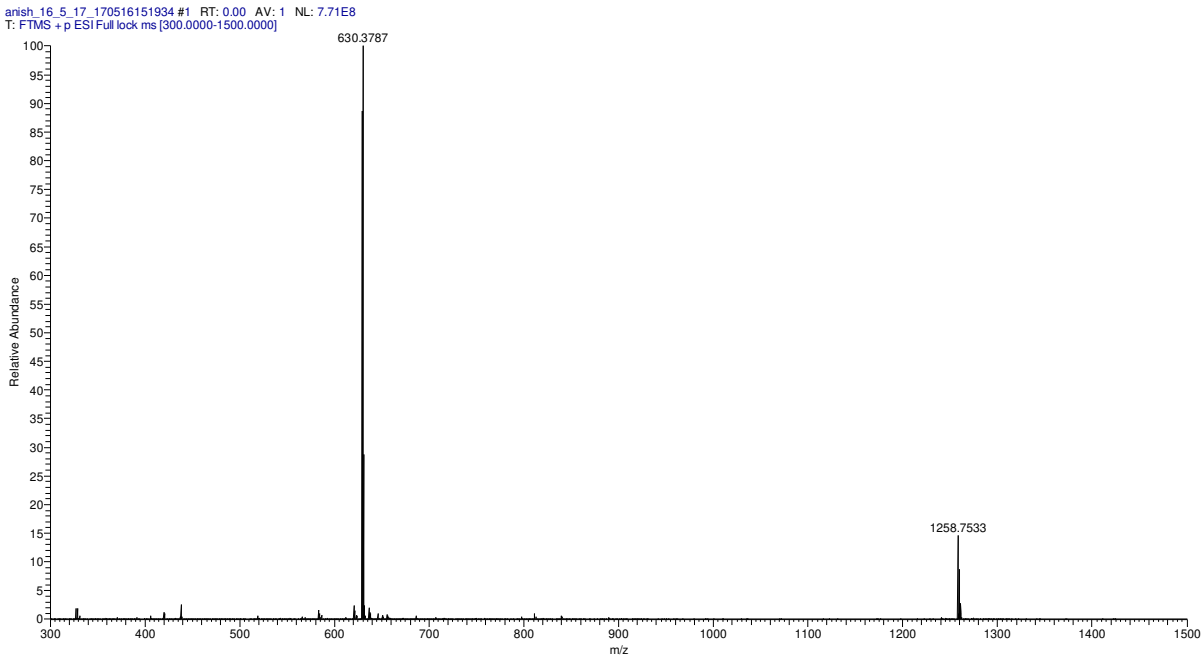

Figure S4.6: HRMS spectra of HPLC purified teixobactin analogue **4.2**. Exact Mass calcd. for $C_{59}H_{99}N_{15}O_{15}$ = 1257.7445, found $M+H^+$ = 1258.7533 and $M/2 + H^+$ = 630.3787

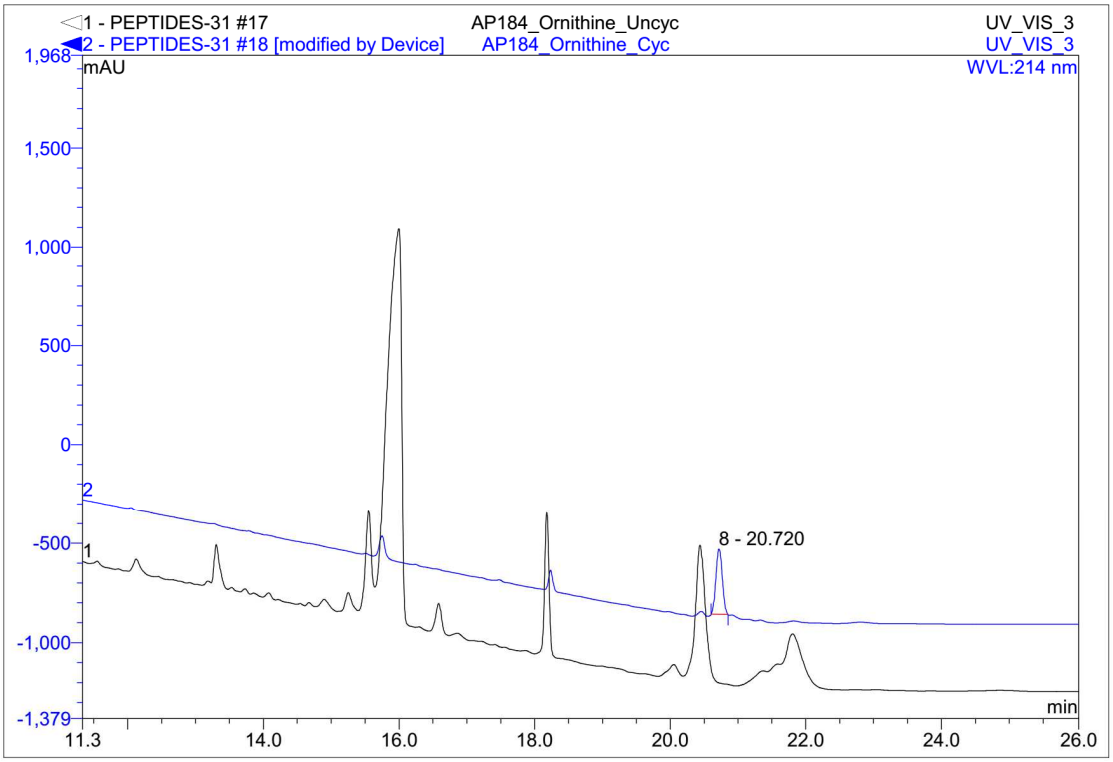

Figure S4.7: HPLC trace showing the progress of the cyclisation reaction for analogue **4.3**: conversion of the uncyclized protected teixobactin analogue tR= 16.000 min (shown in black) to the cyclised protected teixobactin analogue tR = 20.720 min (shown in blue) (Gradient: 5-95% in 25 min)

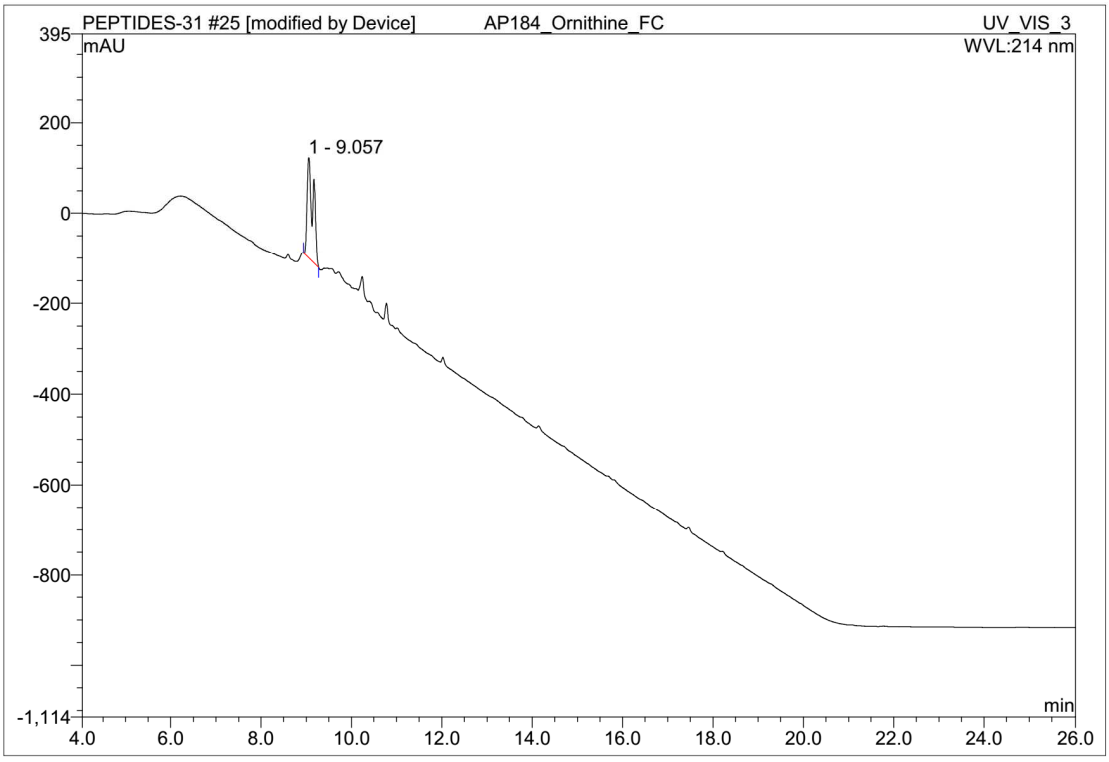

Figure S4.8: HPLC trace of crude teixobactin analogue **4.3** t_R = 9.057 min (gradient: 5-95% ACN in 25 min using A: 0.1% HCOOH in water, B: ACN)

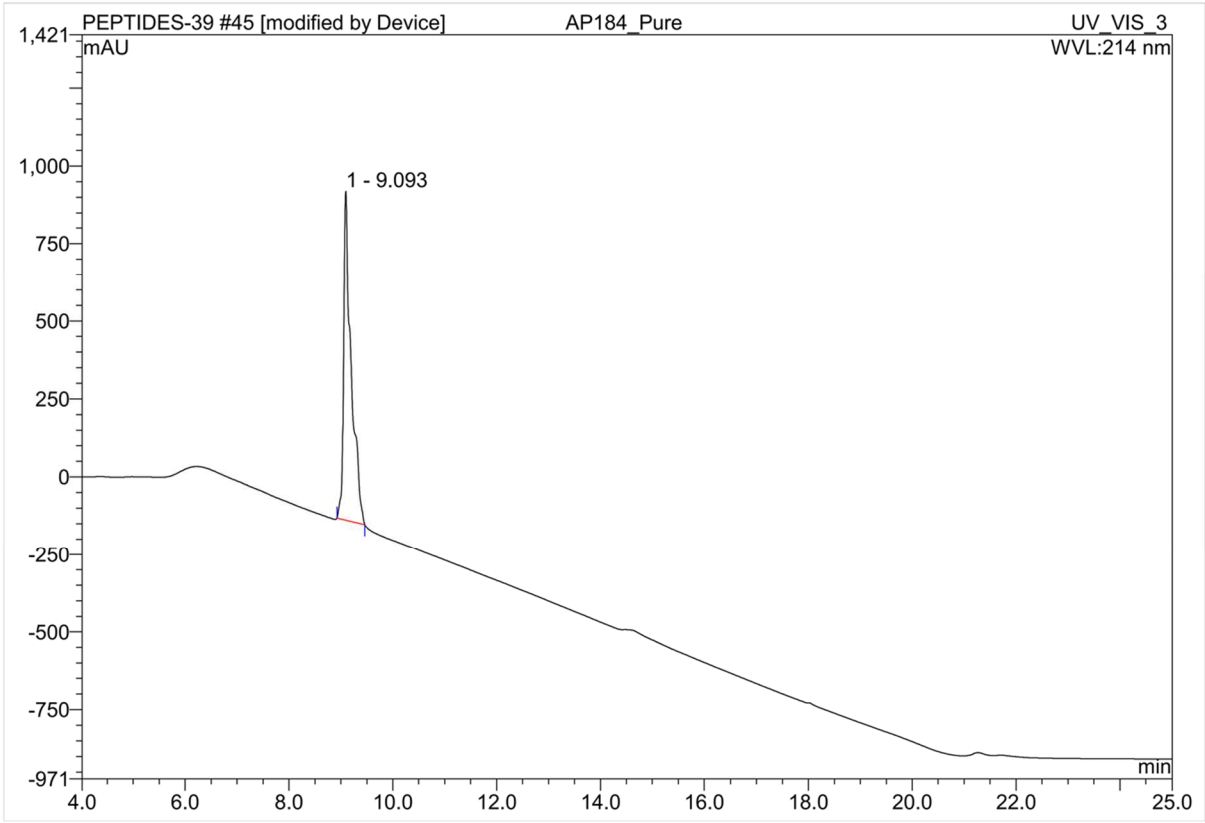

Figure S4.9: Ornithine HPLC trace of HPLC purified teixobactin analogue **4.3** (gradient: 5-95% ACN in 25 min using A: 0.1% HCOOH in water, B: ACN)

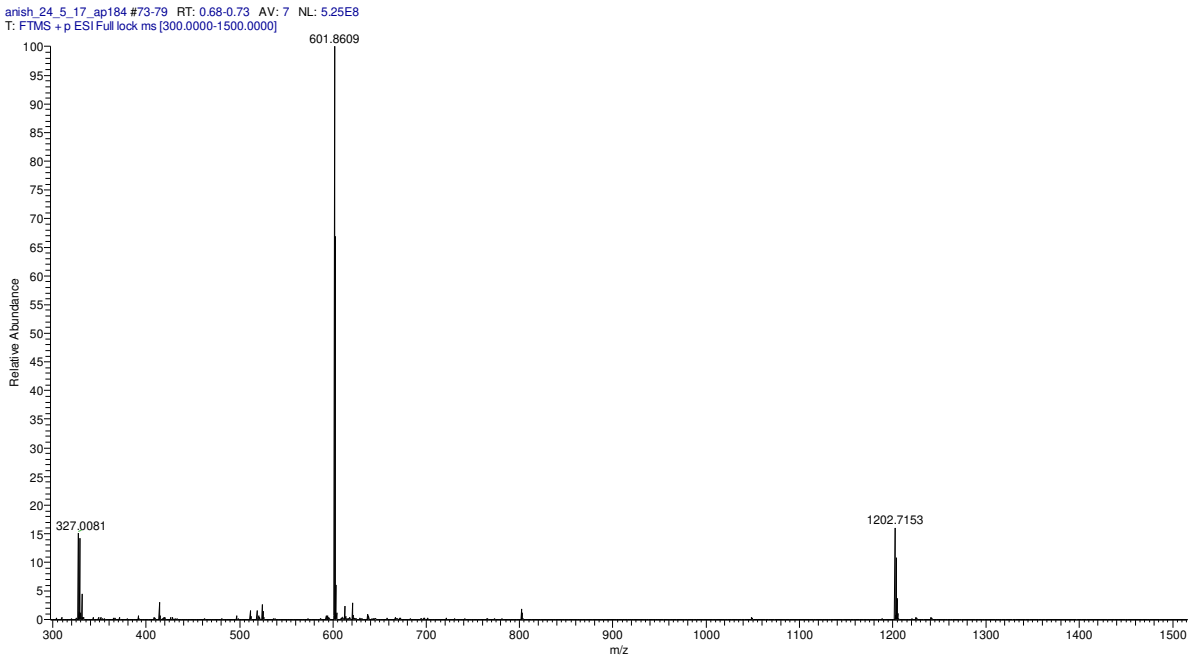

Figure S4.10: ESI-MS spectra from LC-MS of HPLC purified teixobactin analogue **4.3**. Exact Mass calcd. for $C_{57}H_{95}N_{13}O_{15}$ = 1201.71, found $M+H^+$ = 1202.7153 and $M/2 + H^+$ = 601.8609

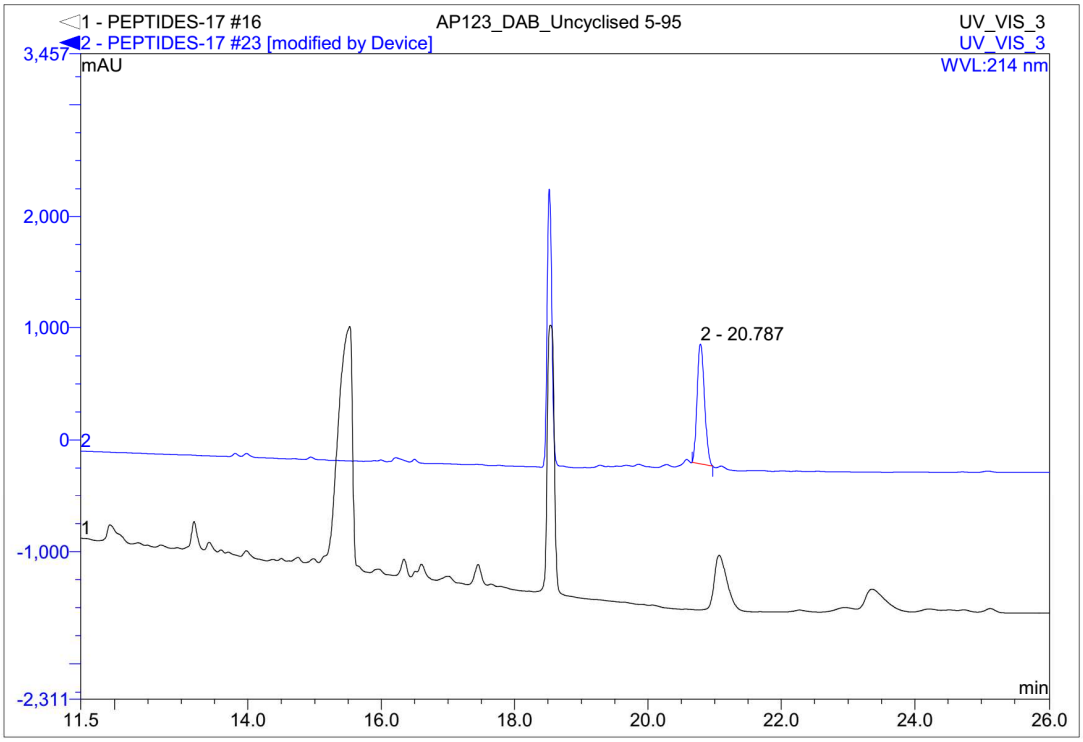

Figure S4.11: HPLC trace showing the progress of cyclisation reaction for analogue **4.4**: conversion of the uncyclized protected teixobactin analogue t_R= 15.527 min (shown in black) to the cyclized protected teixobactin analogue t_R = 20.787 min (shown in blue) (Gradient: 5-95% in 25 min)

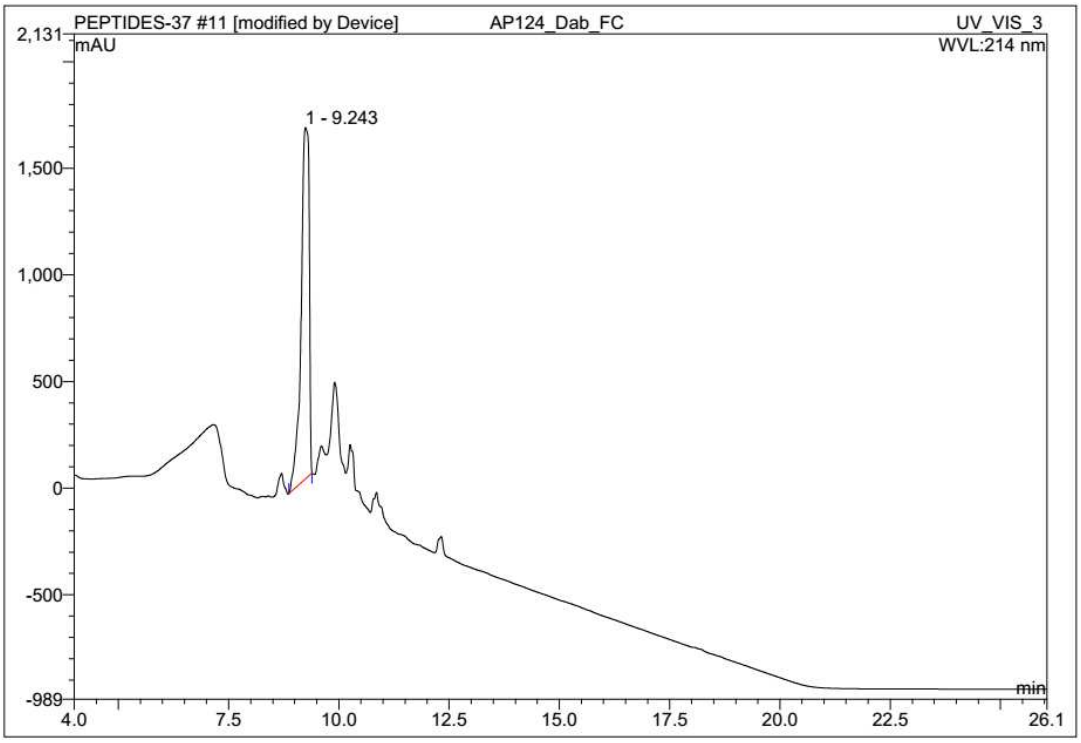

Figure S4.12: HPLC trace of crude teixobactin analogue **4.4** t_R = 9.243 min (gradient: 5-95% ACN in 25 min using A: 0.1% HCOOH in water, B: ACN)

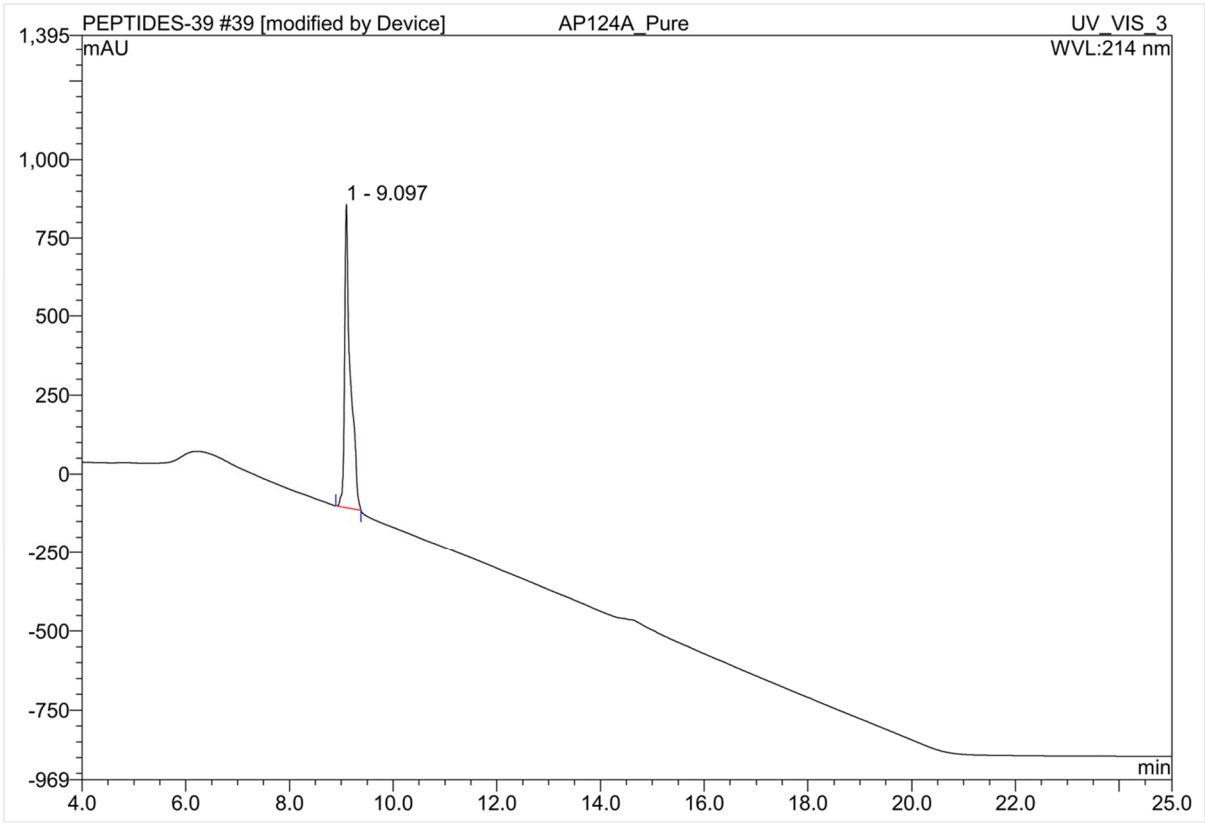

Figure S4.13: HPLC trace of HPLC purified teixobactin analogue **4.4** (gradient: 5-95% ACN in 25 min using A: 0.1% HCOOH in water, B: ACN)

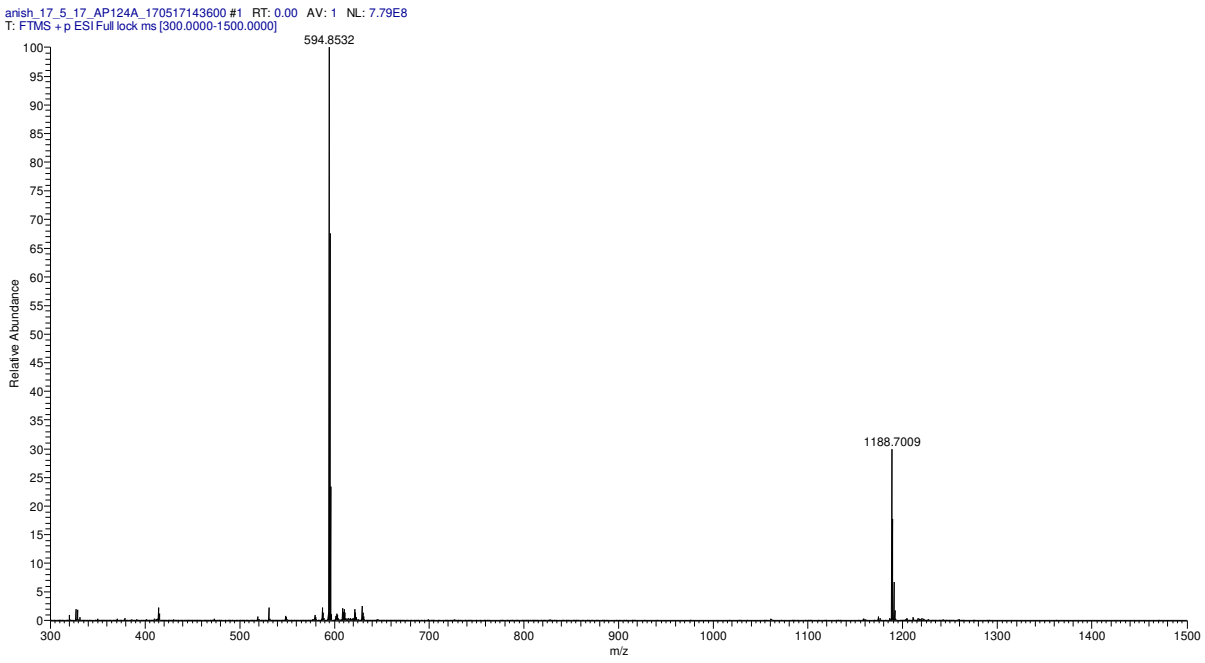

Figure S4.14: HRMS spectra from LC-MS of HPLC purified teixobactin analogue **4.4**. Exact Mass calcd. for $C_{56}H_{93}N_{13}O_{15}$ = 1187.6914, found M+H$^+$ = 1188.7009 and M/2 + H$^+$ = 594.8532

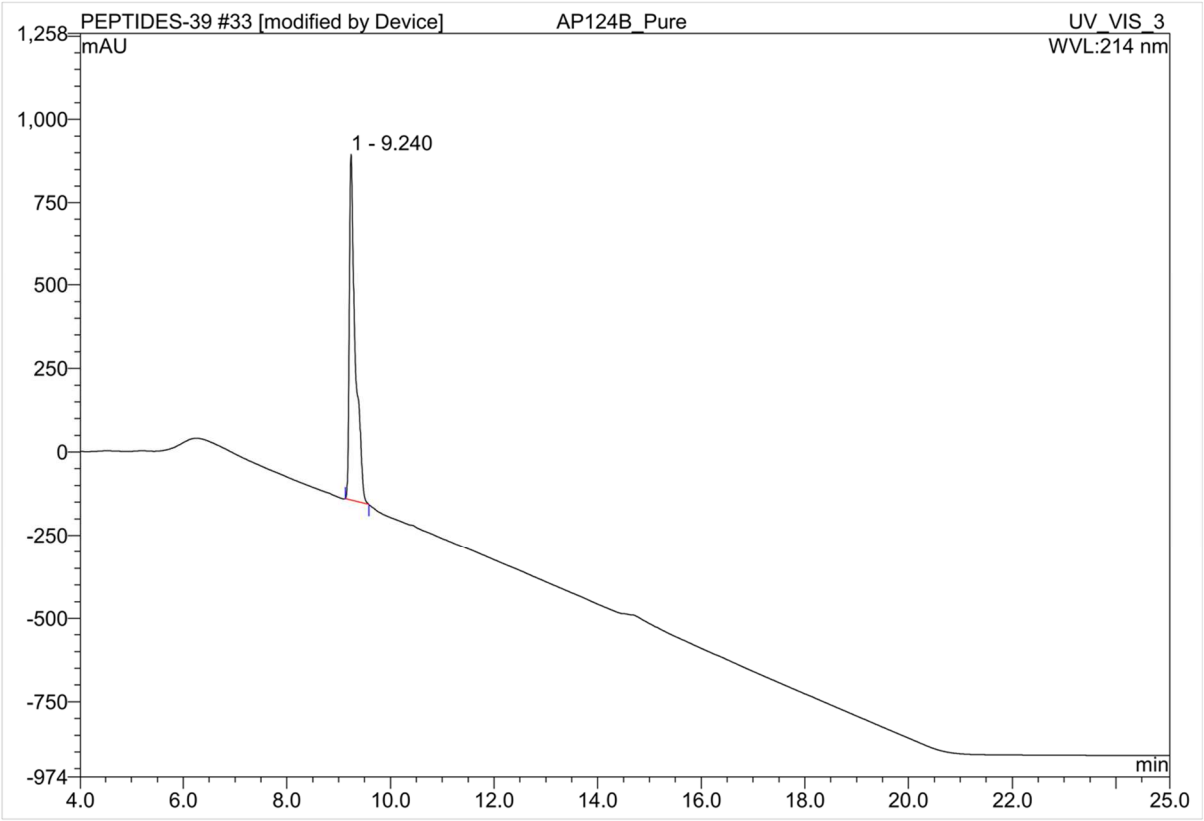

Figure S4.15: HPLC trace of HPLC purified teixobactin analogue **4.5** (gradient: 5-95% ACN in 25 min using A: 0.1% HCOOH in water, B: ACN)

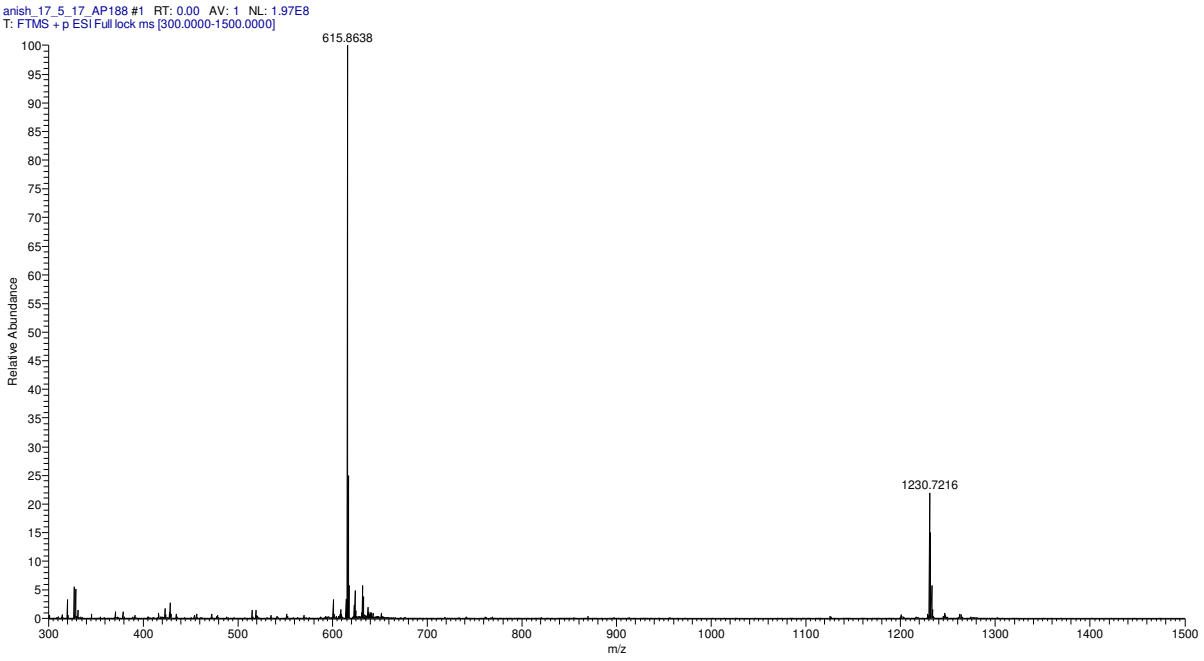

Figure S4.16: ESI-MS spectra from LC-MS of HPLC purified teixobactin analogue **4.5**. Exact Mass calcd. for $C_{57}H_{95}N_{15}O_{15}$ = 1229.7132, found $M+H^+$ = 1230.7216 and $M/2 + H^+$ = 615.8638

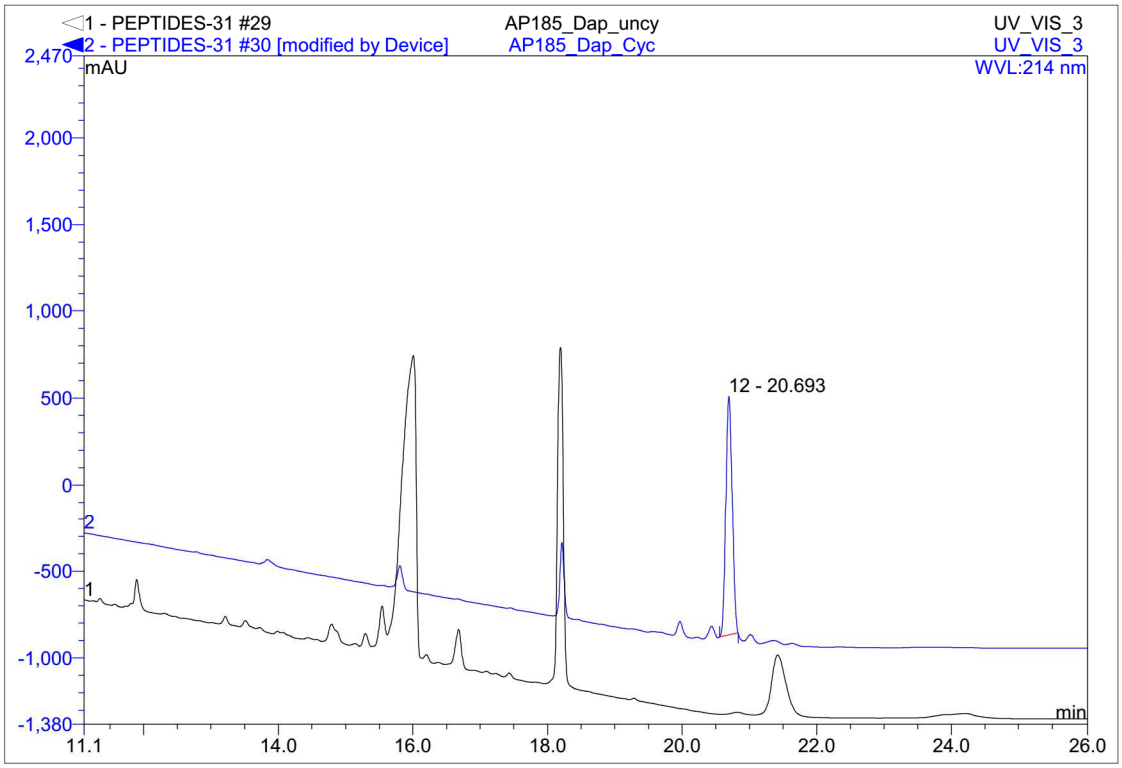

Figure S4.17: HPLC trace showing the progress of cyclisation reaction of analogue **4.6**: conversion of the uncyclized protected teixobactin analogue t_R= 16.010 min (shown in black) to the cyclized protected teixobactin analogue t_R = 20.693 min (shown in blue) (Gradient: 5-95% in 25 min)

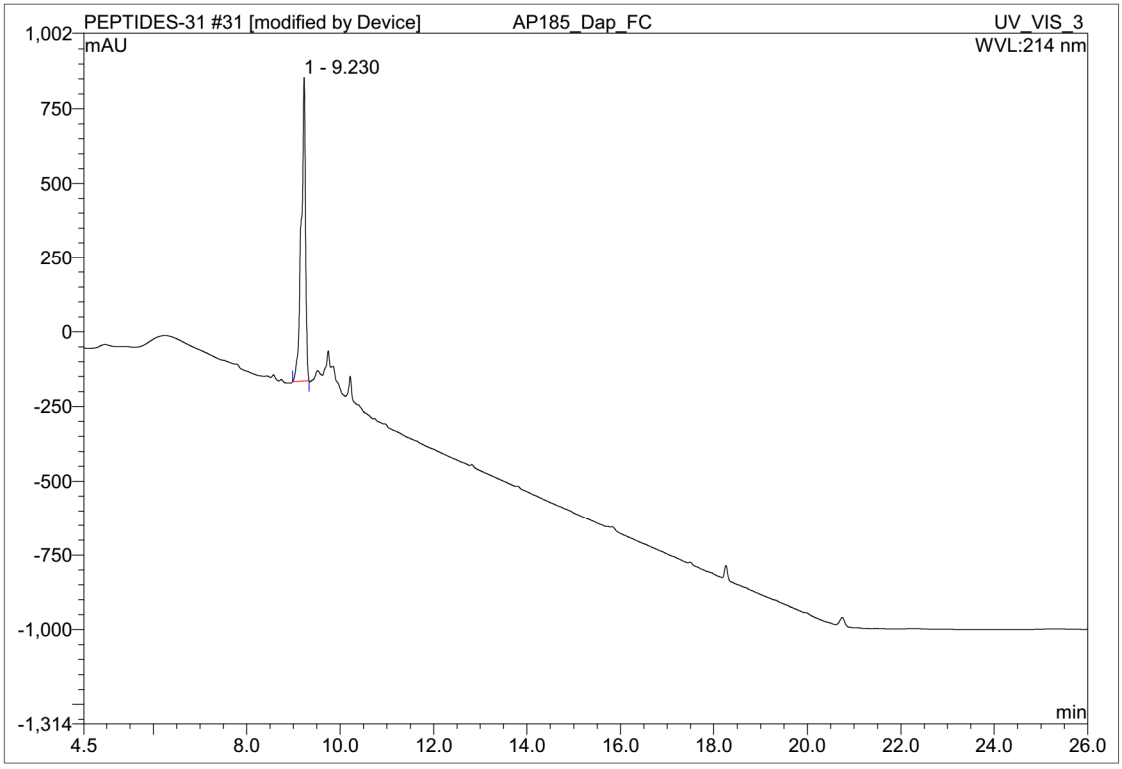

Figure S4.18: HPLC trace of crude teixobactin analogue **4.6** t_R = 9.230 min (gradient: 5-95% ACN in 25 min using A: 0.1% HCOOH in water, B: ACN)

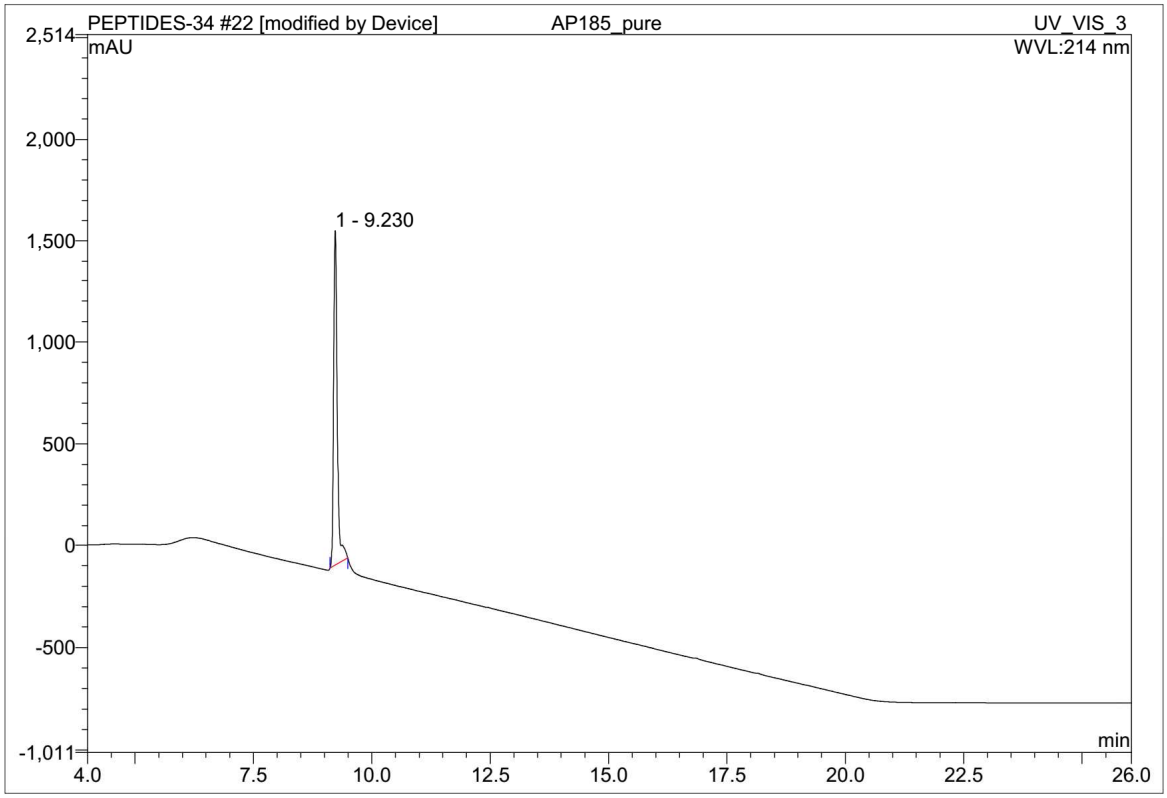

Figure S4.19: HPLC trace of HPLC purified teixobactin analogue **4.6** (gradient: 5-95% ACN in 25 min using A: 0.1% HCOOH in water, B: ACN)

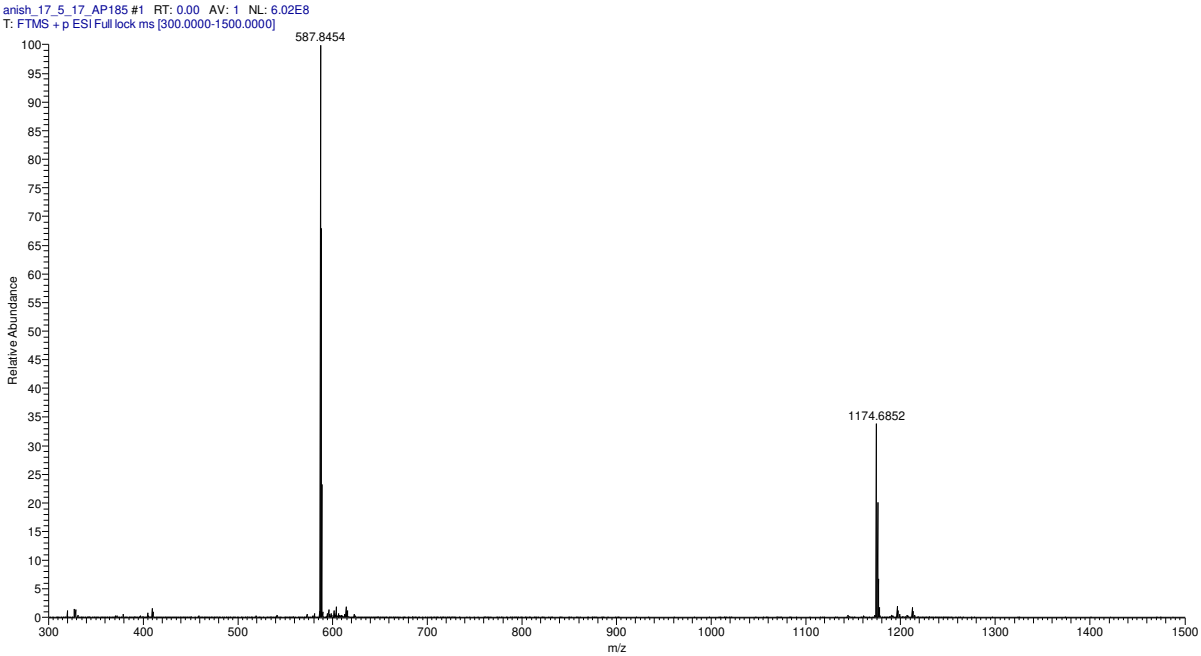

Figure S4.20: ESI-MS spectra from LC-MS of HPLC purified teixobactin analogue **4.6**. Exact Mass calcd. for $C_{55}H_{91}N_{13}O_{15}$ = 1173.6758, found $M+H^+$ = 1174.6852 and $M/2 + H^+$ = 587.8454

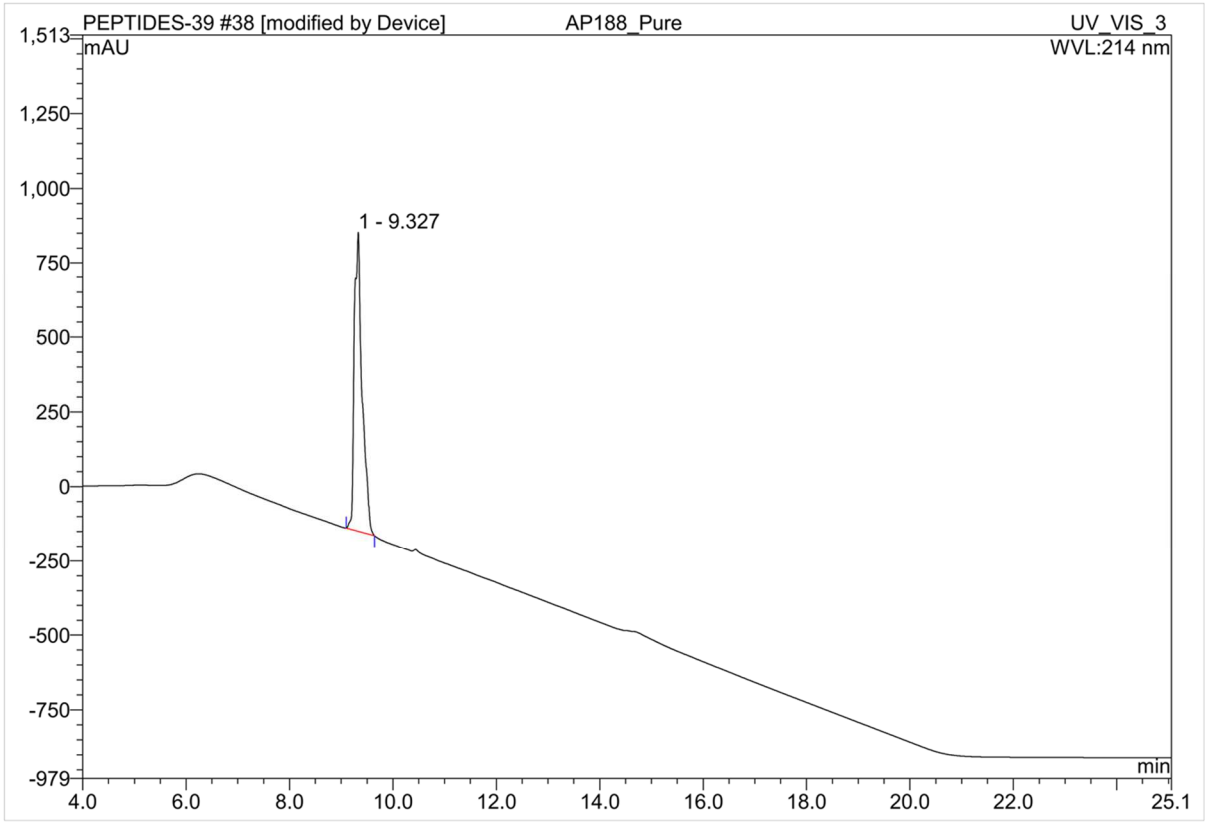

Figure S4.21: HPLC trace of HPLC purified teixobactin analogue **4.7** (gradient: 5-95% ACN in 25 min using A: 0.1% HCOOH in water, B: ACN)

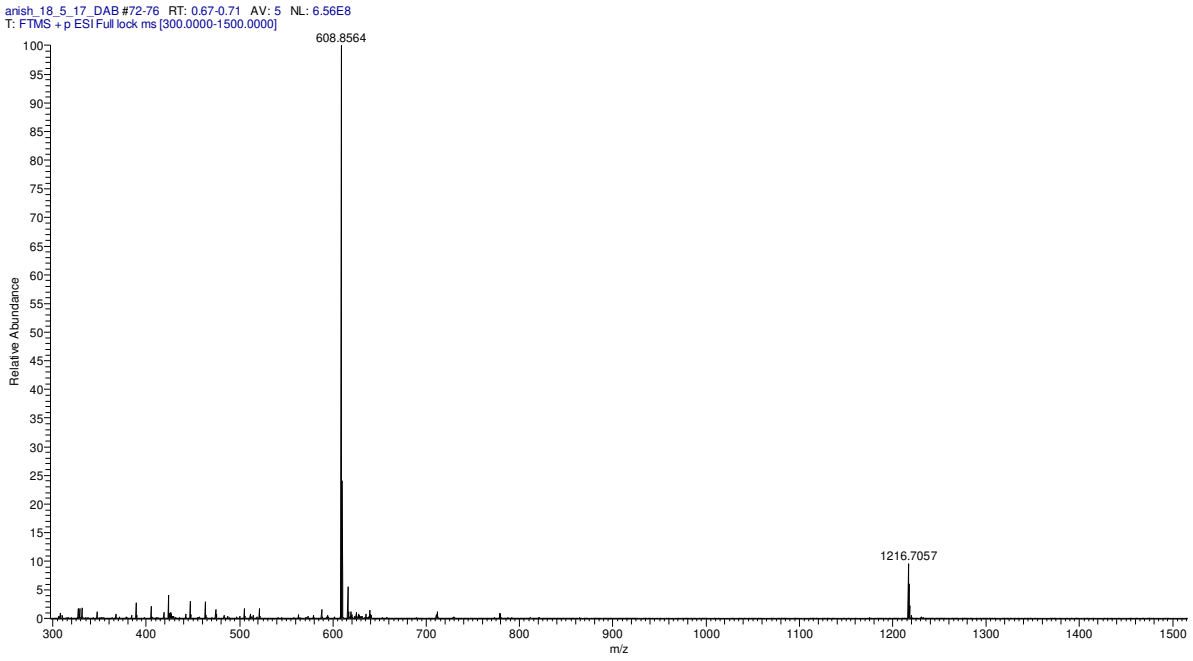

Figure S4.22: ESI-MS spectra from LC-MS of HPLC purified teixobactin analogue **4.7**. Exact Mass calcd. for $C_{56}H_{93}N_{15}O_{15}$ = 1215.6976, found $M+H^+$ = 1216.7057

V. MIC testing

For MIC assays all peptides were dissolved in DMSO containing 0.002% polysorbate 80[2]. All bacteria were grown in Mueller Hinton broth (Oxoid). All incubations were at 37°C. Dilutions were carried out in triplicate. 100 µl of autoclaved Mueller Hinton broth was added to wells 2-12 on a 96-well plate. 200 µl of the peptide was added to well one at a concentration of 512 µg/mL. 100µl of peptide in well one was taken up and pipetted into well two. The mixture was then mixed via pipetting before 100µl was taken up and pipetted into well three. This process was repeated up to well 11. Once peptide was added to well 11 100 µl was taken up and then discarded ensuring the well 12 had no peptide present. Thus, the concentrations (in µg/mL) were: 512, 256, 128, 64, 32, 16, 8, 4, 2, 1, 0.5 and no peptide present. Each well was then inoculated with 100µl of bacteria that had been diluted to an OD600nm of 0.1. This was repeated three times. The 96-well plates were then incubated for 24 hours. The MIC was determined to be the lowest concentration at which there was no growth visible.

For all the compounds in which the MIC lower than 1 µg/ml for the initial test, the above procedure was repeated at an altered initial concentration of 64 µg/ml. Therefore, the new concentrations for MIC were: 64, 32, 16, 8, 4, 2, 1, 0.5, 0.25, 0.125, 0.0625 and no peptide present. Vancomycin was used as a control.

VI. References

1 A. Parmar, A. Iyer, C. S. Vincent, D. Van Lysebetten, S. H. Prior, A. Madder, E. J. Taylor and I. Singh, *Chem. Commun.*, 2016, **52**, 6060–6063.

2 L. L. Ling, T. Schneider, A. J. Peoples, A. L. Spoering, I. Engels, B. P. Conlon, A. Mueller, D. E. Hughes, S. Epstein, M. Jones, L. Lazarides, V. A. Steadman, D. R. Cohen, C. R. Felix, K. A. Fetterman, W. P. Millett, A. G. Nitti, A. M. Zullo, C. Chen and K. Lewis, *Nature*, 2015, **517**, 455–459.

EXPERIMENTAL SECTION FOR CHAPTER 5

I. Materials

All $_{L}$-amino acids, Fmoc-D-Ala-OH Fmoc-D-Gln(Trt)-OH, Boc-*N*-methyl-$_{D}$-phenylalanine, 1-[Bis(dimethylamino)methylene]-1H-1,2,3-triazolo[4,5-b]pyridinium3-oxidhexafluorophosphate (HATU), Phenylsilane ($PhSiH_3$), Tetrakis(triphenylphosphine)palladium(0) [$Pd(PPh_3)$], Diisoproplycarbodiimide (DIC) and Triisopropylsilane (TIS) were purchased from Fluorochem, UK. Fmoc-D-*allo*-Ile-OH and oxyma pure were purchased from Merck Millipore. The side chain protecting groups for the amino acids are ^{t}Bu for Ser, Pbf for Arg and Trt for Gln and Thr unless specified otherwise. Diisopropylethylamine (DIPEA), supplied as extra dry, redistilled, 99.5 % pure, Acetic anhydride, allyl chloroformate, $CDCl_3$ and polysorbate 80 and were purchased from Sigma Aldrich. Tritylchloride and 4-(Dimethylamino)pyridine were purchased from Alfa Aesar. Dimmethylformamide (DMF) peptide synthesis grade was purchased from Rathburn chemicals. Triethylamine, Diethyl ether (Et_2O), Dimethylsulfoxide (DMSO), Dichloromethane (DCM), Tetrahydrofuran (extra dry with molecular sieves), Formic acid 98-100% purity and Acetonitrile (HPLC grade) were purchased from Fisher Scientific. Water with the Milli-Q grade standard was obtained in-house from an ELGA Purelab Flex system. 2-Chlorotritylchloride resin (manufacturer's loading: 1.20 mmol/g) was purchased from Fluorochem. All chemicals were used without further purification. Geranyl pyrophosphate ammonium salt, 1 mg/mL in MeOH was purchased from Sigma Aldrich.

II. Equipment used for the analysis and purification of compounds

All peptides were analysed on a Thermo Scientific Dionex Ultimate 3000 RP-HPLC equipped with a Phenomenex Gemini NX C18 110 Å (150 x 4.6 mm) column using the following buffer systems: A: 0.1% HCOOH in milliQ water. B: ACN using a flow rate of 1 ml/min. The column was flushed with 95% A for 5 min prior to an injection and was flushed for 5 min with 95% B and 5% A after the run was finished.

Peptides were dissolved in (1:1) 0.1% HCOOH buffer in water and acetonitrile (ACN) and analysed using the following gradient: 95% A for 2 min. 5-95% B in 25 min. 95% B for 5 min. 5% A for 4 min.

Peptides were dissolved in 0.1% HCOOH buffer in water and in ACN (10-30% ACN) and purified using the same gradient as mentioned above, on a Thermo Scientific Dionex Ultimate 3000 RP-HPLC with a flow rate of 5 mL/min using a Phenomenex Gemini NX C18 110 Å (150 x 10 mm) semi-prep column.

LC-MS data were collected on an Agilent 1100 Series instrument with a Phenomenex Kinetex C18 100Å column (150 x 4.6 mm, 5 µm at 35 °C) connected to an ESMSD type VL mass detector with a flow rate of 1.5 ml/min was used with the following solvent systems: (A): 0.1% HCOOH in H_2O and (B) MeCN. The column was flushed with 100% A for 2 min, then a gradient from 0 to 100% B over 6 min was used, followed by 2 min of flushing with 100% B.

NMR spectra were recorded on a Bruker AV 500 NMR. HRMS spectra were recorded on a Thermo Scientific Q Exactive Plus Orbitrap Mass Spectrometer in the positive ion mode.

III. Syntheses of teixobactin analogues

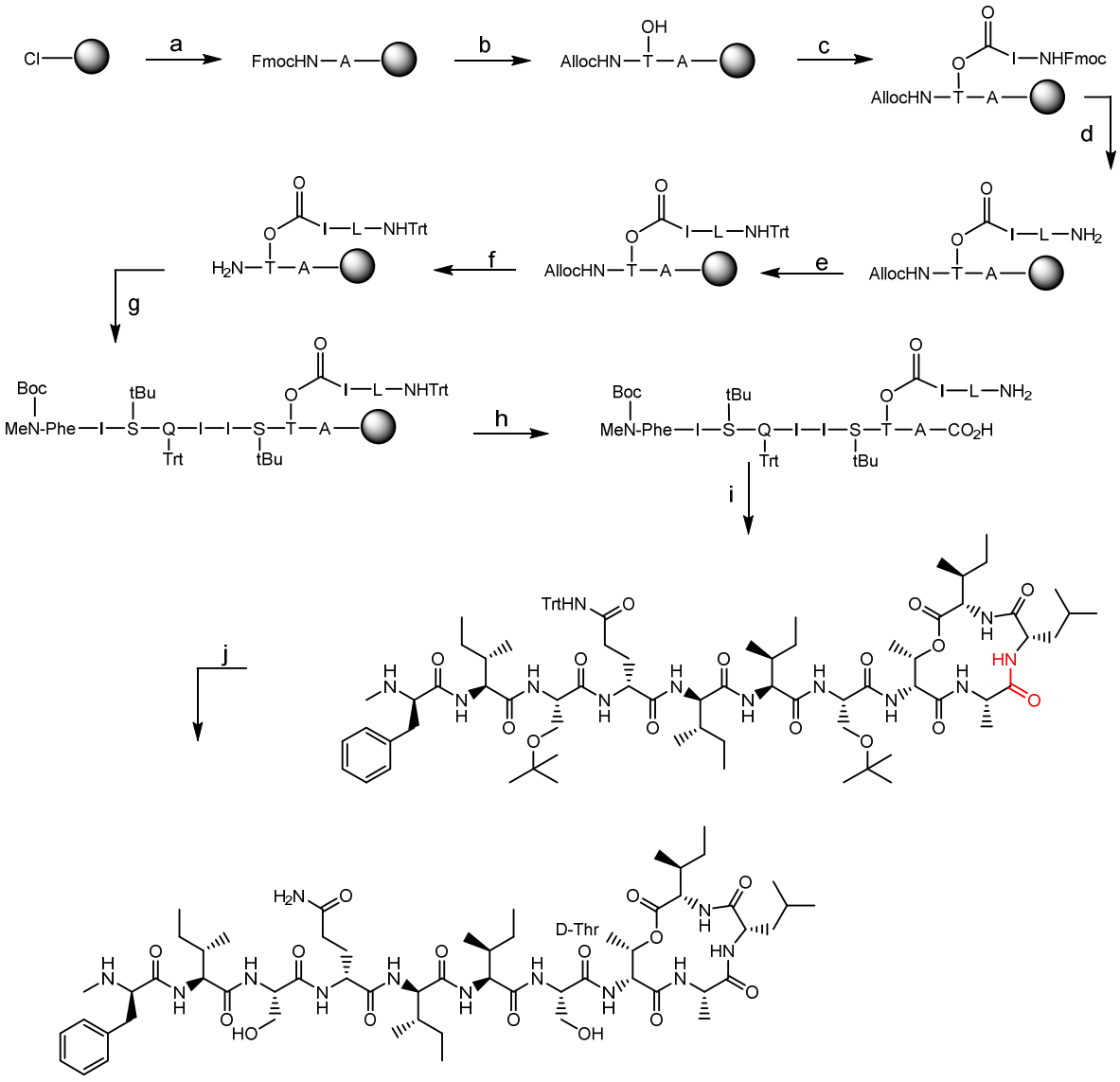

Figure S5.1: Synthesis of Leu10-teixobactin **5.13**

(step a) Commercially available 2-Chlorotrityl chloride resin (manufacturer's loading = 1.2 mmol/g, 170 mg resin) was swelled in DCM in a reactor. To this resin was added 4 eq. Fmoc-Ala-OH/8 eq. DIPEA in DCM and the reactor was shaken for 3h. The loading determined by UV absorption of the

piperidine-dibenzofulvene adduct was calculated to be 0.6 mmol/g, (170mg resin, 0.102 mmol). Any unreacted resin was capped with MeOH:DIPEA:DCM = 1:2:7 by shaking for 1h. (step b) The Fmoc protecting group was deprotected using 20% piperdine in DMF by shaking for 3 min, followed by draining and shaking again with 20% piperidine in DMF for 10 min. AllocHN-D-Thr-OH was then coupled to the resin by adding 3 eq. of the AA, 3 eq. HATU and 6 eq. DIPEA in DMF and shaking for 1.5h at room temperature. (step c) Esterification was performed using 10 eq. of Fmoc-Ile-OH, 10 eq. DIC and 5 mol% DMAP in DCM and shaking the reaction for 2h. This was followed by capping the unreacted alcohol using 10% Ac_2O/DIPEA in DMF shaking for 30 min and Fmoc was removed using protocol described earlier in step (b). (step d) Fmoc-Leu-OH was coupled using 4 eq. of AA, 4 eq. HATU and 8 eq. DIPEA in DMF and shaking for 1h followed by Fmoc deprotection using 20% piperidine in DMF as described earlier. (step e) The N terminus of Leu was protected using 10 eq. Trt-Cl and 15% Et_3N in DCM and shaking for 1h. The protection was verified by the Ninhydrin colour test. (step f) The Alloc protecting group of D-Thr was removed using 0.2 eq. $[Pd(PPh^3)]^0$ and 24 eq. $PhSiH_3$ in dry DCM under argon for 20 min. This procedure was repeated again increasing the time to 45 min and the resin was washed thoroughly with DCM and DMF to remove any Pd stuck to the resin. (step g) All amino acids were coupled using 4 eq. Amino Acid, 4 eq. DIC/Oxyma using a microwave peptide synthesizer. Coupling time was 10 min. Deprotection cycles were performed as described earlier. (step h) The peptide was cleaved from the resin without cleaving off the protecting groups of the amino acid side chains using TFA:TIS:DCM = 2:5:93 and shaking for 1h. (step i) The solvent was evaporated and the peptide was redissolved in DMF to which 1 eq. HATU and 10 eq. DIPEA were added and the reaction was stirred for 30 min to perform the cyclization. (step j) The side-chain protecting groups were then cleaved off using TFA:TIS:H_2O = 95:2.5:2.5 by stirring for 1h. The peptide was precipitated using cold Et_2O (-20°C) and centrifuging at 7000 rpm to obtain a white solid. This solid was further purified using RP-HPLC using the protocols described previously[1].

All other teixobactin analogues were synthesised according to the above procedure.

Sr No.	Compound Number	Name	Chemical formula	Exact Mass	Mass found [M + H^+]	Overall yield [%]
1	5.1	Ac-D-Ala_1-Arg_{10}-texiobactin	$C_{53}H_{93}N_{15}O_{16}$	1195.69	1196.4	12
2	5.2	Ala_2-Arg_{10}-teixobactin	$C_{55}H_{91}N_{15}O_{15}$	1201.68	1202.4	10
3	5.3	Ala_3-Arg_{10}-teixobactin	$C_{58}H_{97}N_{15}O_{14}$	1227.73	1228.5	11
4	5.4	D-Ala_4-Arg_{10}-teixobactin	$C_{56}H_{94}N_{14}O_{14}$	1186.71	1187.4	12
5	5.5	D-Ala_5-Arg_{10}-teixobactin	$C_{55}H_{91}N_{15}O_{15}$	1201.68	1202.4	11
6	5.6	Ala_6-Arg_{10}-teixobactin	$C_{55}H_{91}N_{15}O_{15}$	1201.68	1202.4	12
7	5.7	Ala_7-Arg_{10}-teixobactin	$C_{58}H_{97}N_{15}O_{14}$	1227.73	1228.5	12
8	5.8	Ala_{10}-teixobactin	$C_{55}H_{90}N_{12}O_{15}$	1158.66	1159.5	13
9	5.9	D-Ala_{10}-teixobactin	$C_{55}H_{90}N_{12}O_{15}$	1158.66	1159.5	10
10	5.10	Gly_{10}-teixobactin	$C_{54}H_{88}N_{12}O_{15}$	1144.65	1145.6	18*
11	5.11	Val_{10}-teixobactin	$C_{57}H_{94}N_{12}O_{15}$	1186.70	1187.6	24
12	5.12	Ile_{10}-teixobactin	$C_{58}H_{96}N_{12}O_{15}$	1200.71	1201.5	10
13	5.13	Leu_{10}-teixobactin	$C_{58}H_{96}N_{12}O_{15}$	1200.71	1201.5	20
14	5.14	Ser_{10}-teixobactin	$C_{55}H_{90}N_{12}O_{16}$	1174.66	1175.6	21
15	5.15	Phe_{10}-teixobactin	$C_{61}H_{94}N_{12}O_{15}$	1235.6962	1235.7040	12

Table S5.1: Compound number, code, exact mass, chemical formula, mass found and overall yields for compounds **5.1-5.15**.

***** Gly_{10}-teixobactin afforded a yield of 2% when synthesised for the first time possibly due to deletion sequences. Since the yield was unusually low, therefore, the synthesis was repeated a second time thereby affording a yield of 18%.

IV. HPLC/LC-MS analysis

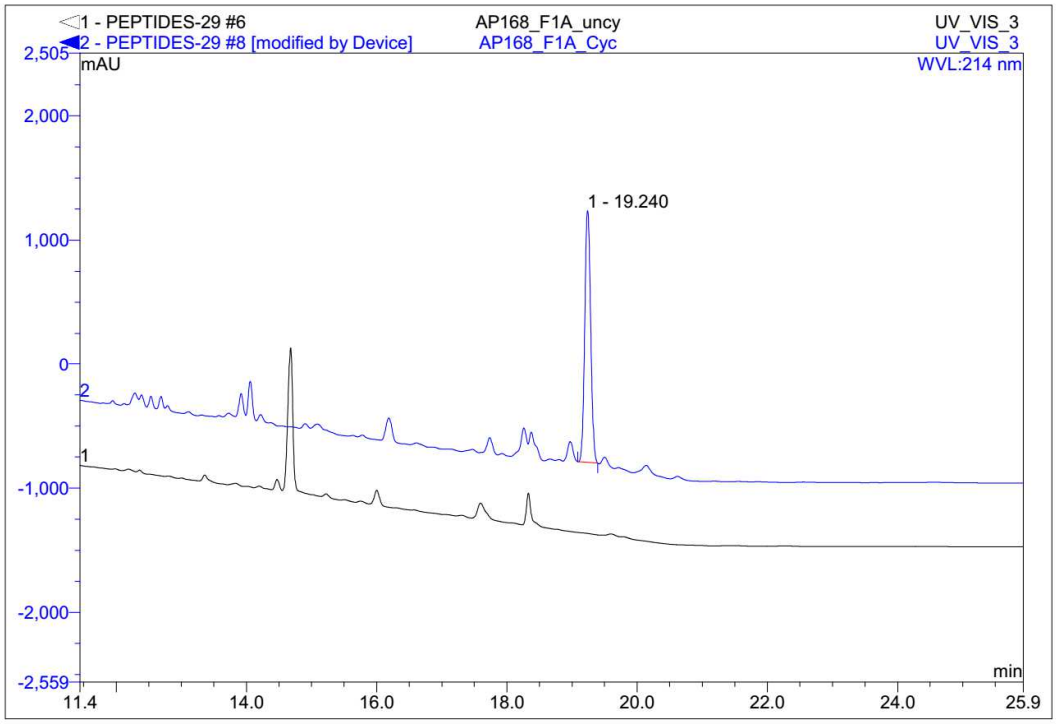

Figure S5.2: HPLC trace showing the progress of cyclisation reaction for the synthesis of analogue **5.1** (i): conversion of the uncyclized protected teixobactin analogue t_R= 14.677 min (shown in black) to the cyclized protected teixobactin analogue t_R = 19.240 min (shown in blue) (Gradient: 5-95% in 25 min)

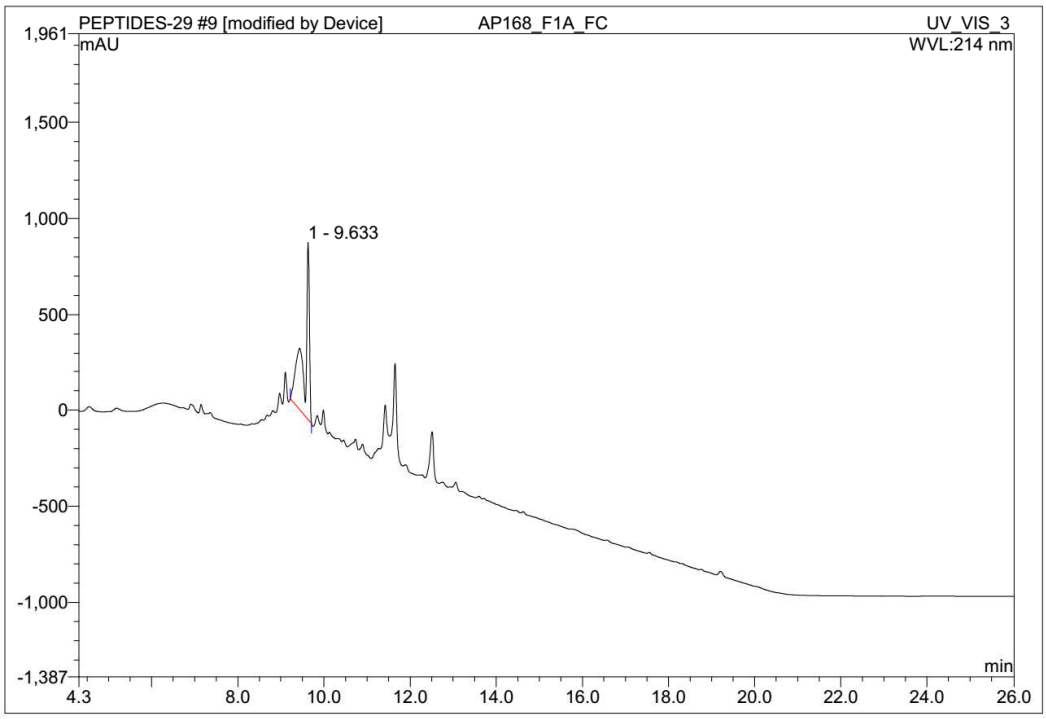

Figure S5.3: HPLC trace of crude teixobactin analogue **5.1** t_R = 9.633 min (gradient: 5-95% ACN in 25 min using A: 0.1% HCOOH in water, B: ACN)

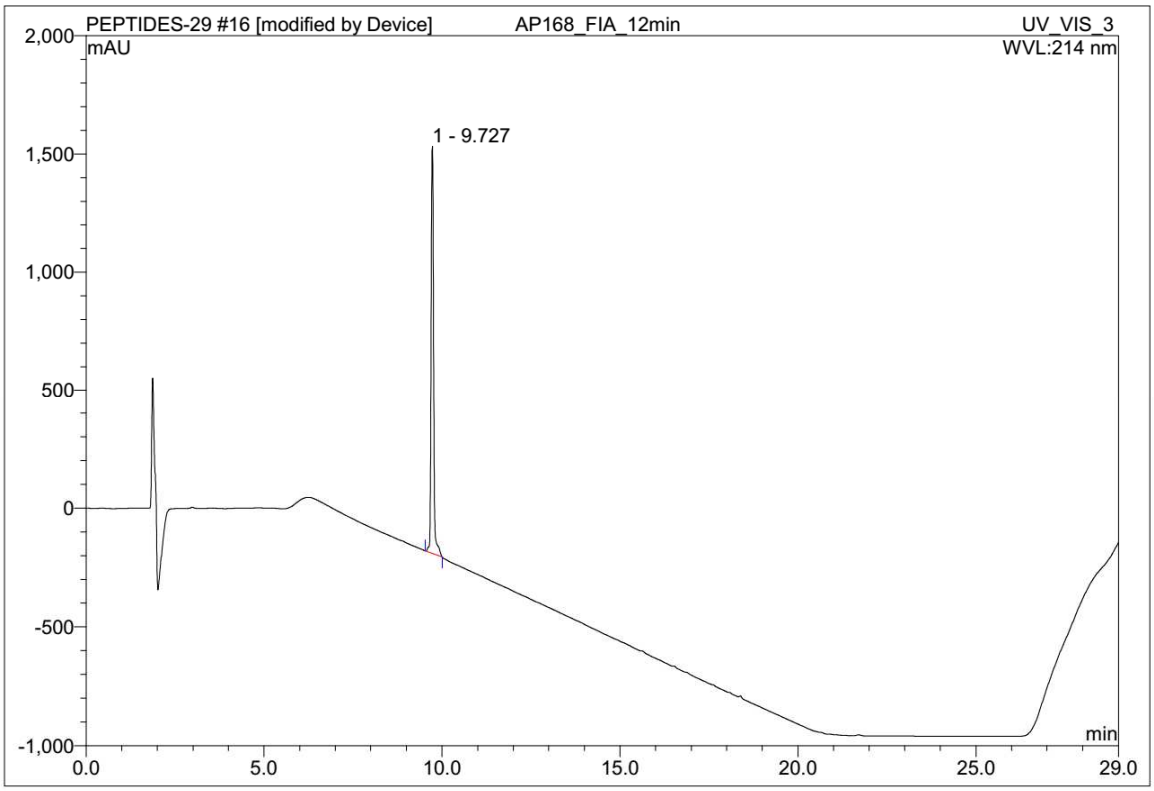

Figure S5.4: HPLC trace of HPLC purified teixobactin analogue **5.1** (gradient: 5-95% ACN in 25 min using A: 0.1% HCOOH in water, B: ACN)

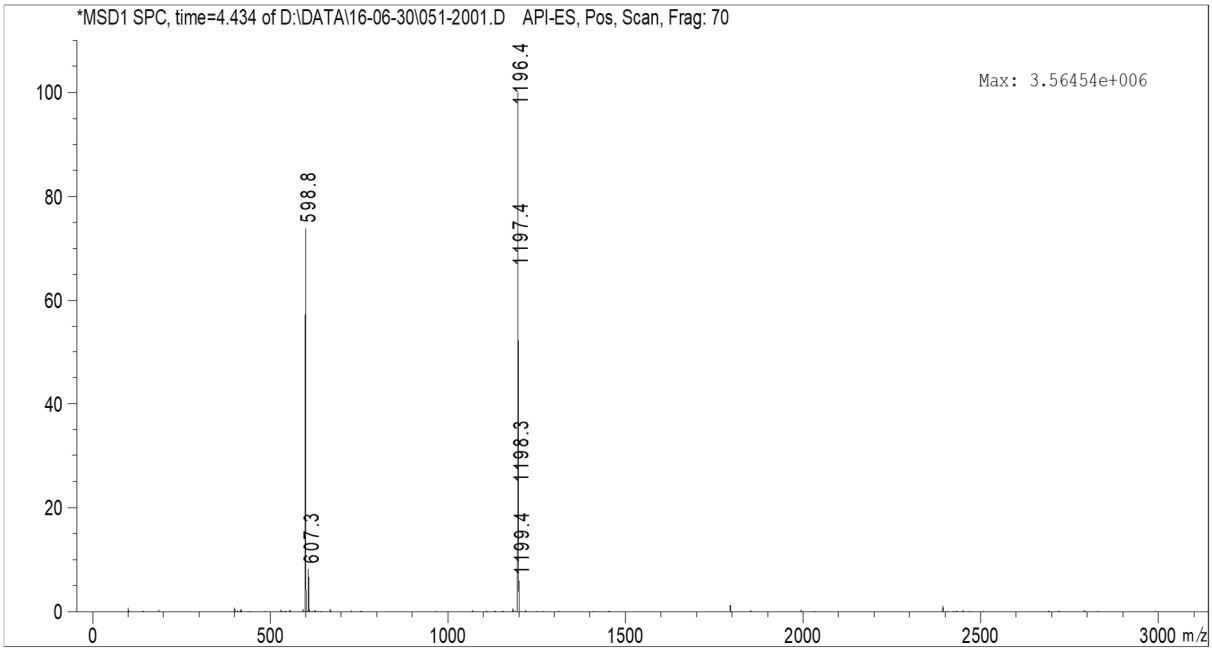

Figure S5.5: ESI-MS from LC-MS of HPLC purified teixobactin analogue **5.1**. Exact mass calcd. for $C_{53}H_{93}N_{15}O_{16}$ = 1195.69, found M + H^+ = 1196.4, M/2 + H^+ = 598.8.

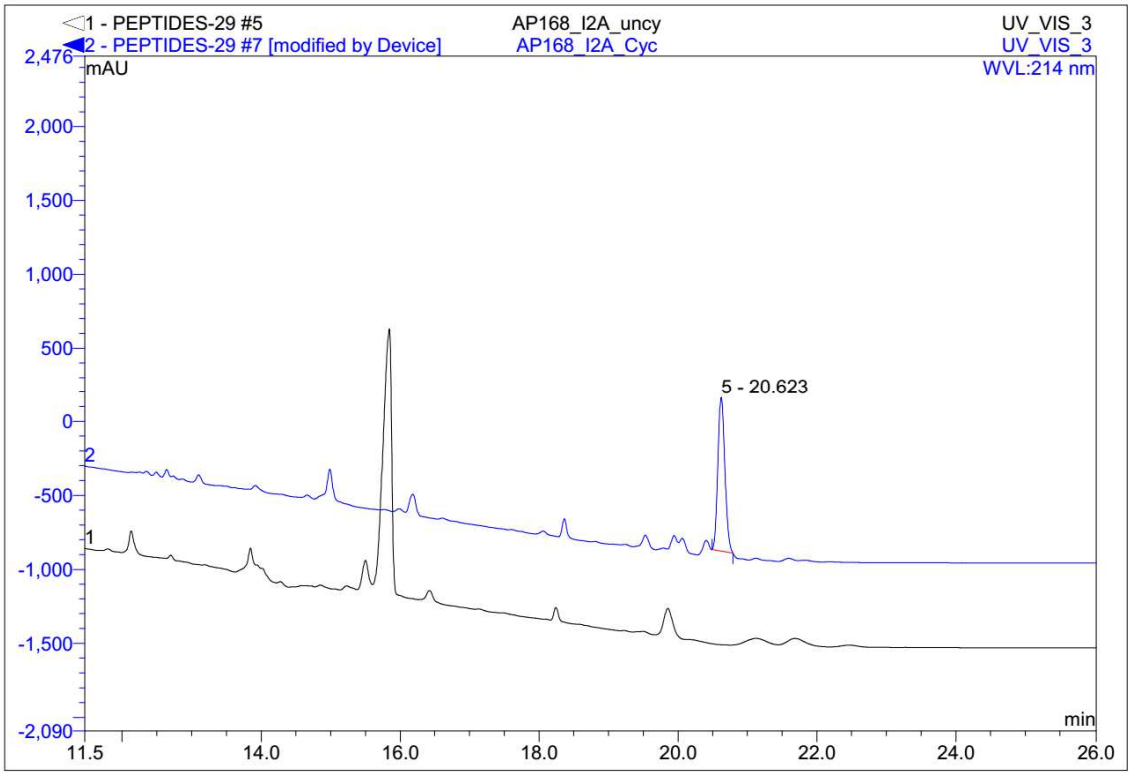

Figure S5.6: HPLC trace showing the progress of cyclisation reaction for the synthesis of analogue **5.2** (i): conversion of the uncyclized protected teixobactin analogue t_R= 15.843 min (shown in black) to the cyclized protected teixobactin analogue t_R = 20.623 min (shown in blue) (Gradient: 5-95% in 25 min)

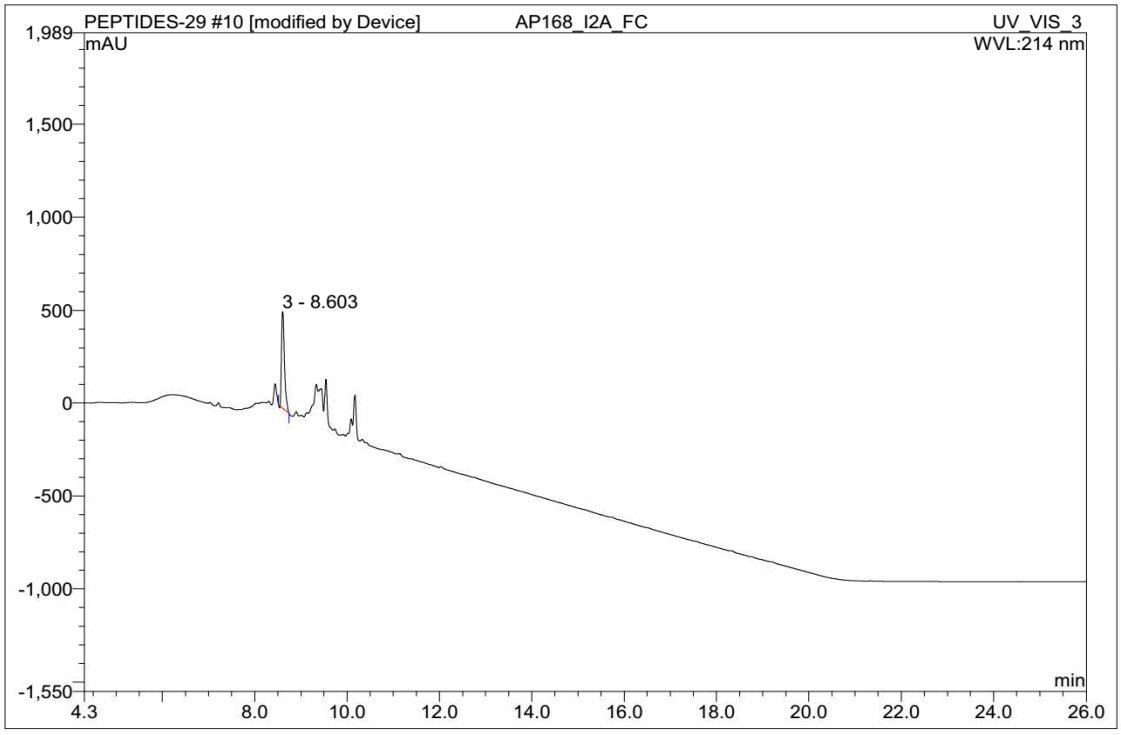

Figure S5.7: HPLC trace of crude teixobactin analogue **5.2** t_R = 8.603 min (gradient: 5-95% ACN in 25 min using A: 0.1% HCOOH in water, B: ACN)

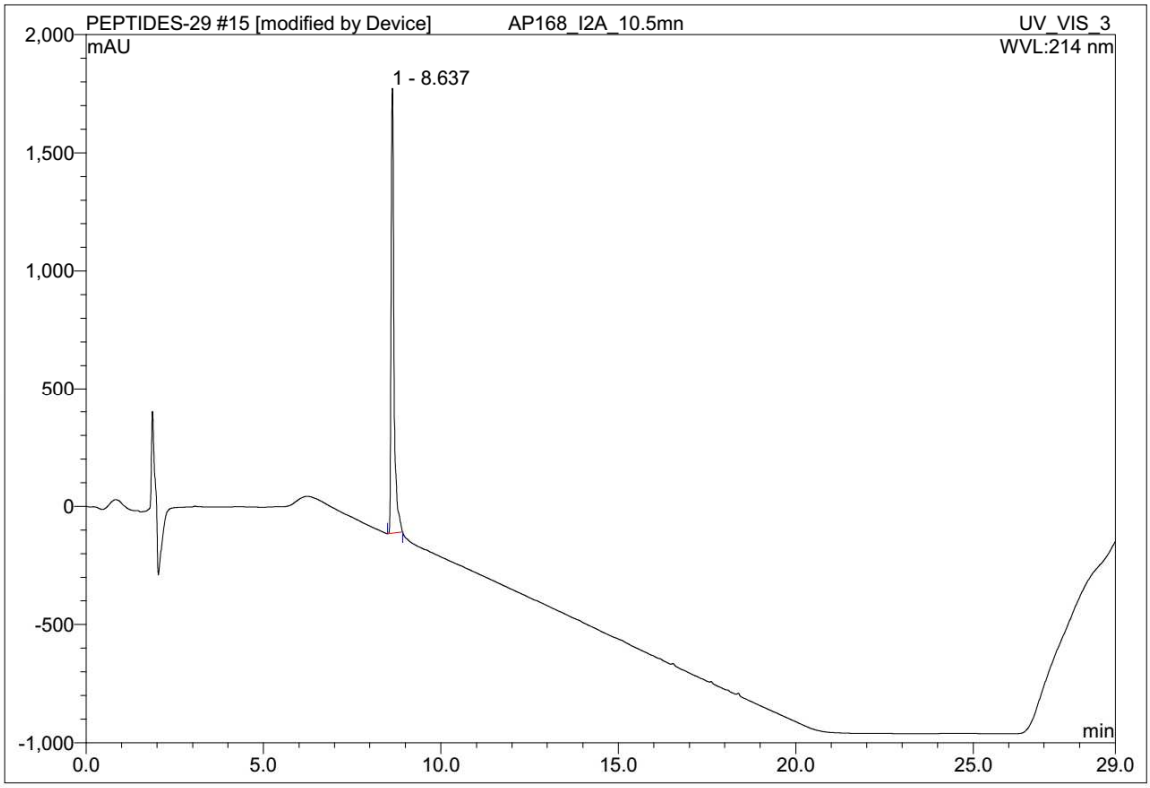

Figure S5.8: HPLC trace of HPLC purified teixobactin analogue **5.2** (gradient: 5-95% ACN in 25 min using A: 0.1% HCOOH in water, B: ACN)

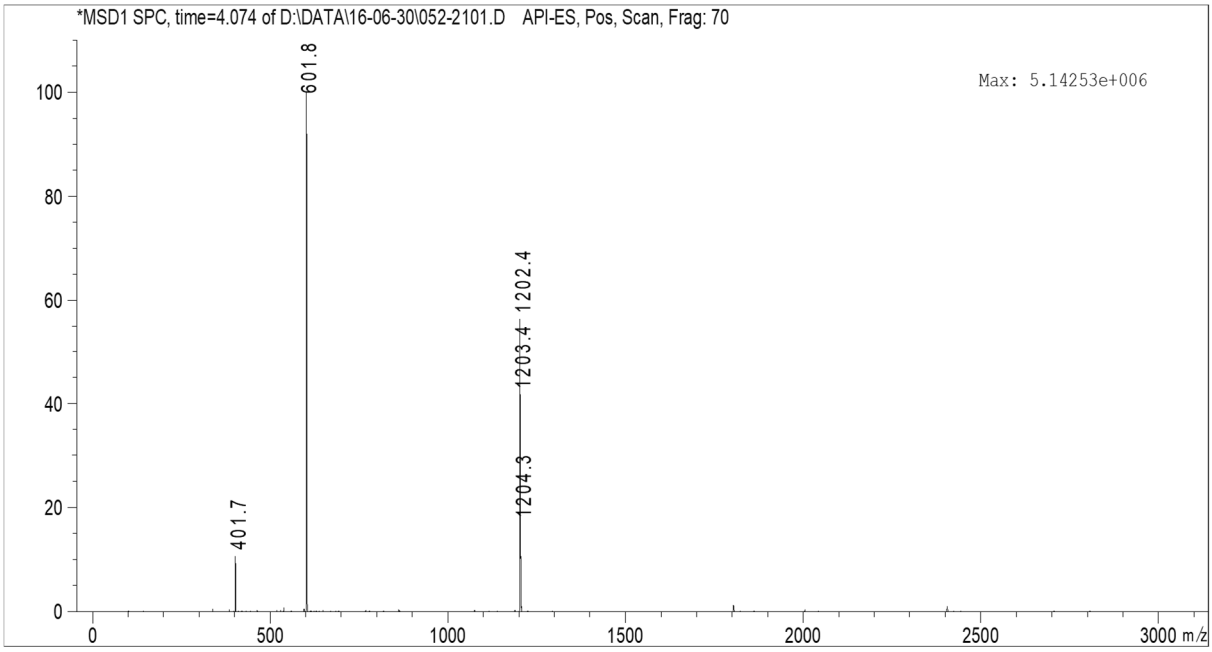

Figure S5.9: ESI-MS from LC-MS of HPLC purified teixobactin analogue **5.2**. Exact mass calcd. for $C_{55}H_{91}N_{15}O_{15}$ = 1201.68, found M + H^+ = 1202.4, M/2 + H^+ = 601.8, M/3 + H^+ = 401.7.

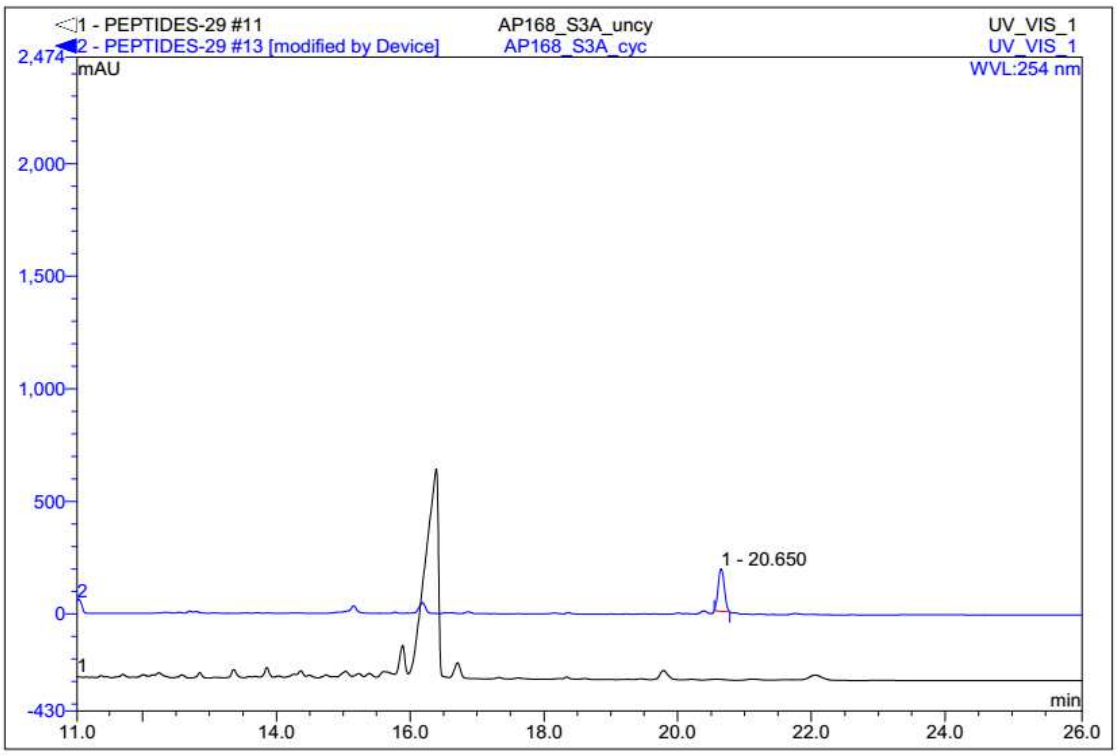

Figure S5.10: HPLC trace showing the progress of cyclisation reaction for the synthesis of analogue **5.3** (i): conversion of the uncyclized protected teixobactin analogue t_R= 16.390 min (shown in black) to the cyclized protected teixobactin analogue t_R = 20.650 min (shown in blue) (Gradient: 5-95% in 25 min)

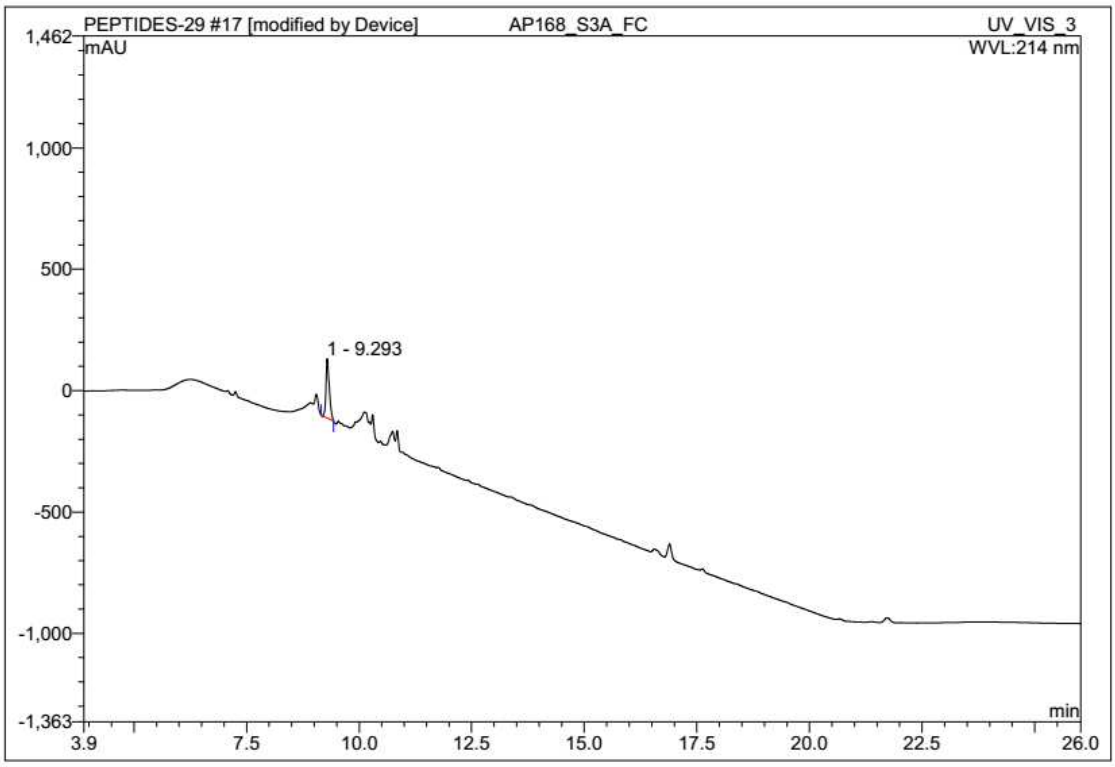

Figure S5.11: HPLC trace of crude teixobactin analogue **5.3** t_R = 9.293 min (gradient: 5-95% ACN in 25 min using A: 0.1% HCOOH in water, B: ACN)

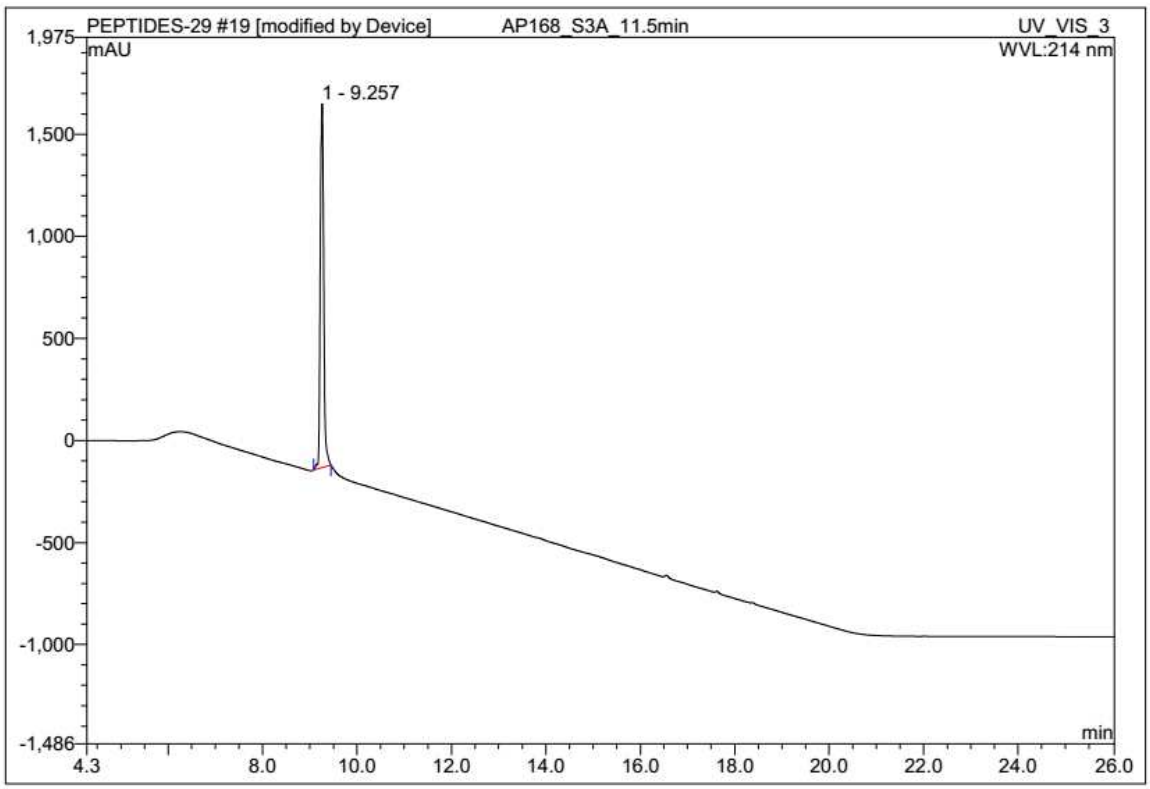

Figure S5.12: HPLC trace of HPLC purified teixobactin analogue **5.3** (gradient: 5-95% ACN in 25 min using A: 0.1% HCOOH in water, B: ACN)

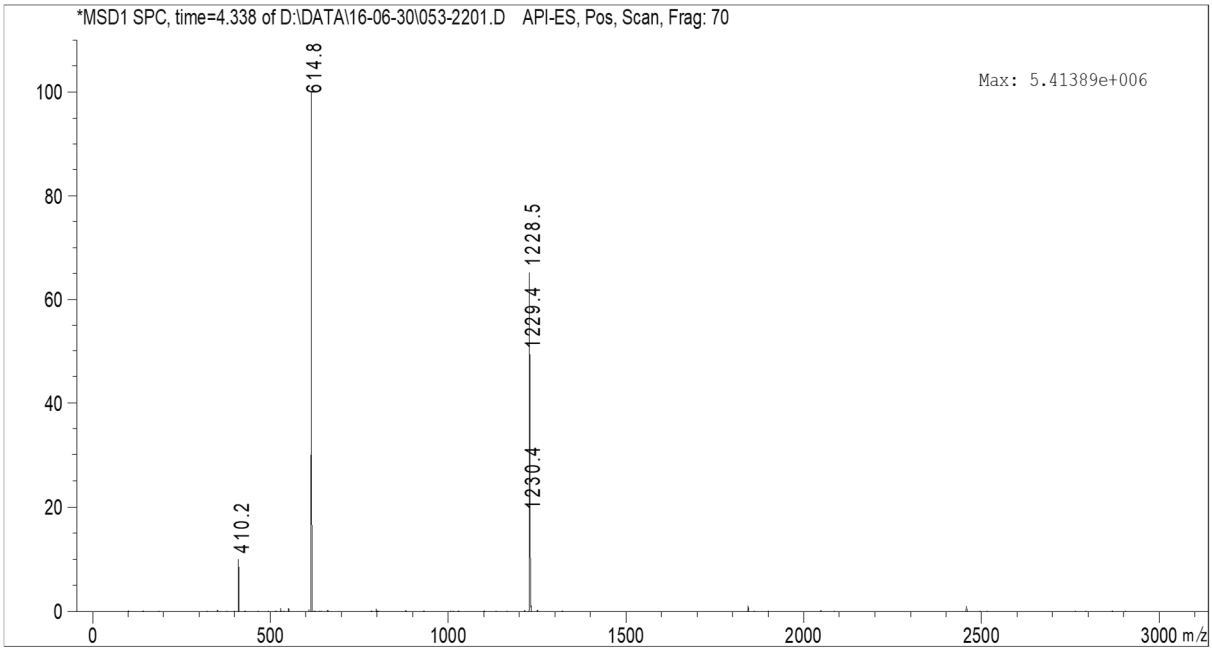

Figure S5.13: ESI-MS from LC-MS of HPLC purified teixobactin analogue **5.3**. Exact mass calcd. for $C_{58}H_{97}N_{15}O_{14}$ = 1227.73, found M + H^+ = 1228.5, M/2 + H^+ = 614.8, M/3 + H^+ = 410.2.

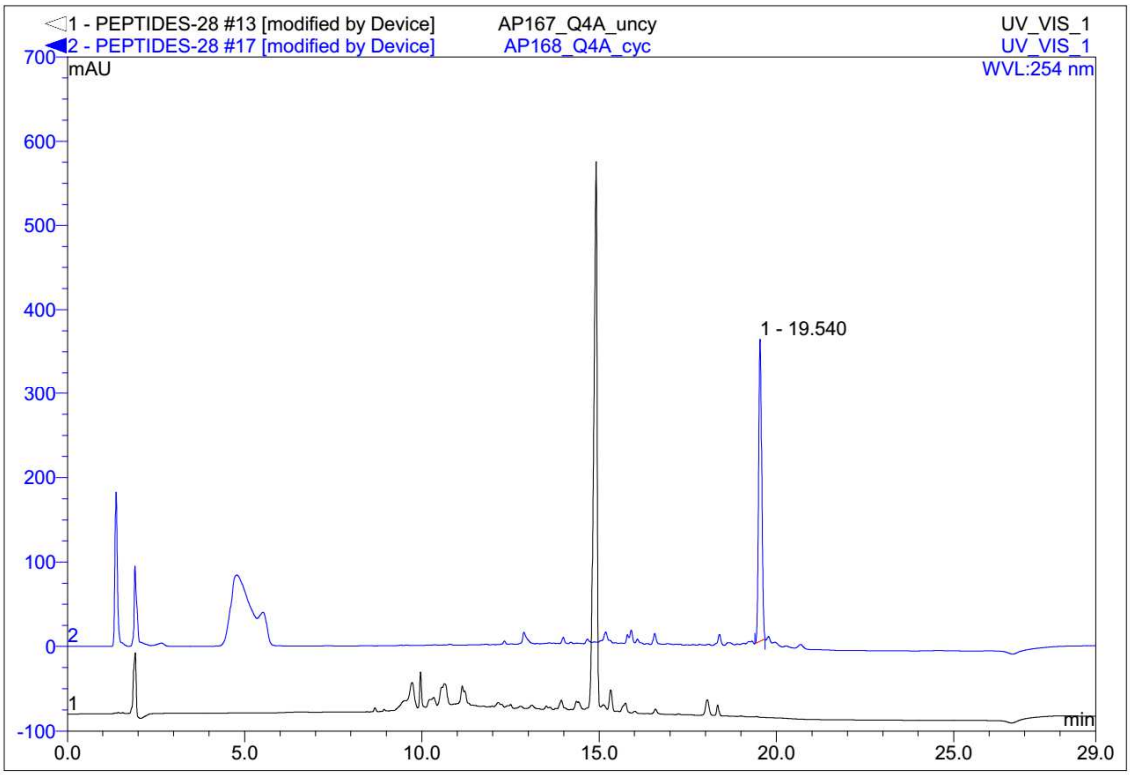

Figure S5.14: HPLC trace showing the progress of cyclisation reaction for the synthesis of analogue **5.4** (i): conversion of the uncyclized protected teixobactin analogue t_R= 14.917 min (shown in black) to the cyclized protected teixobactin analogue t_R = 19.540 min (shown in blue) (Gradient: 5-95% in 25 min)

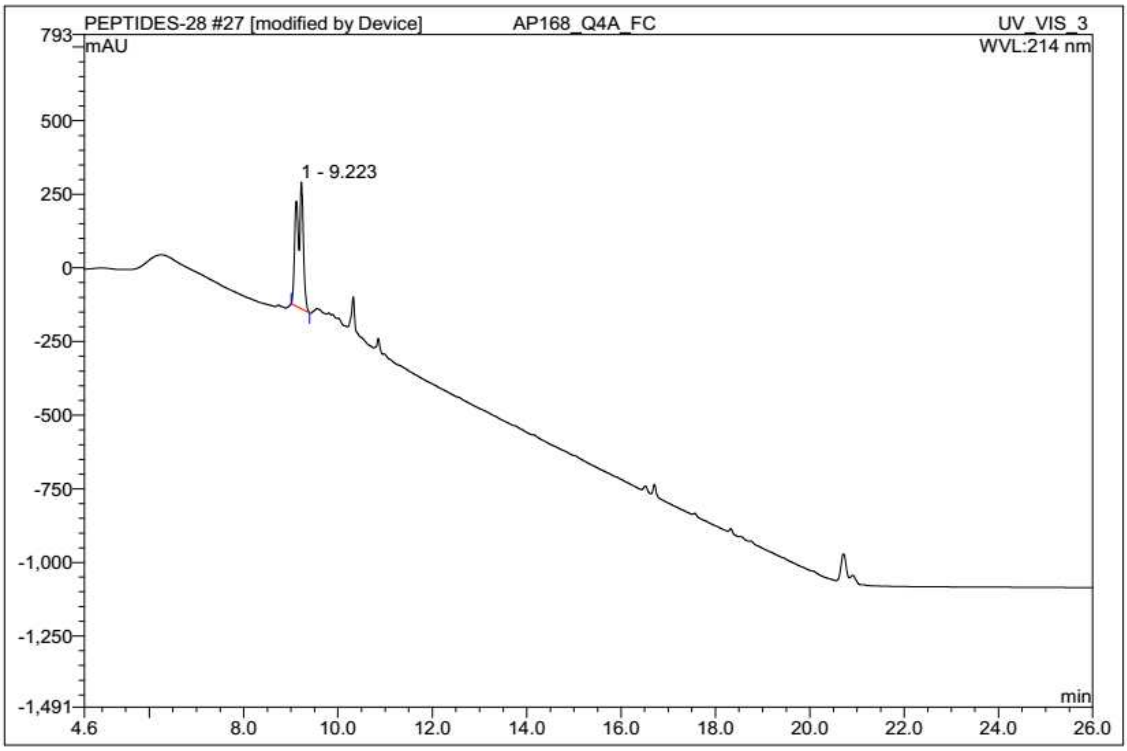

Figure S5.15: HPLC trace of crude teixobactin analogue **5.4** t_R = 9.223 min (gradient: 5-95% ACN in 25 min using A: 0.1% HCOOH in water, B: ACN)

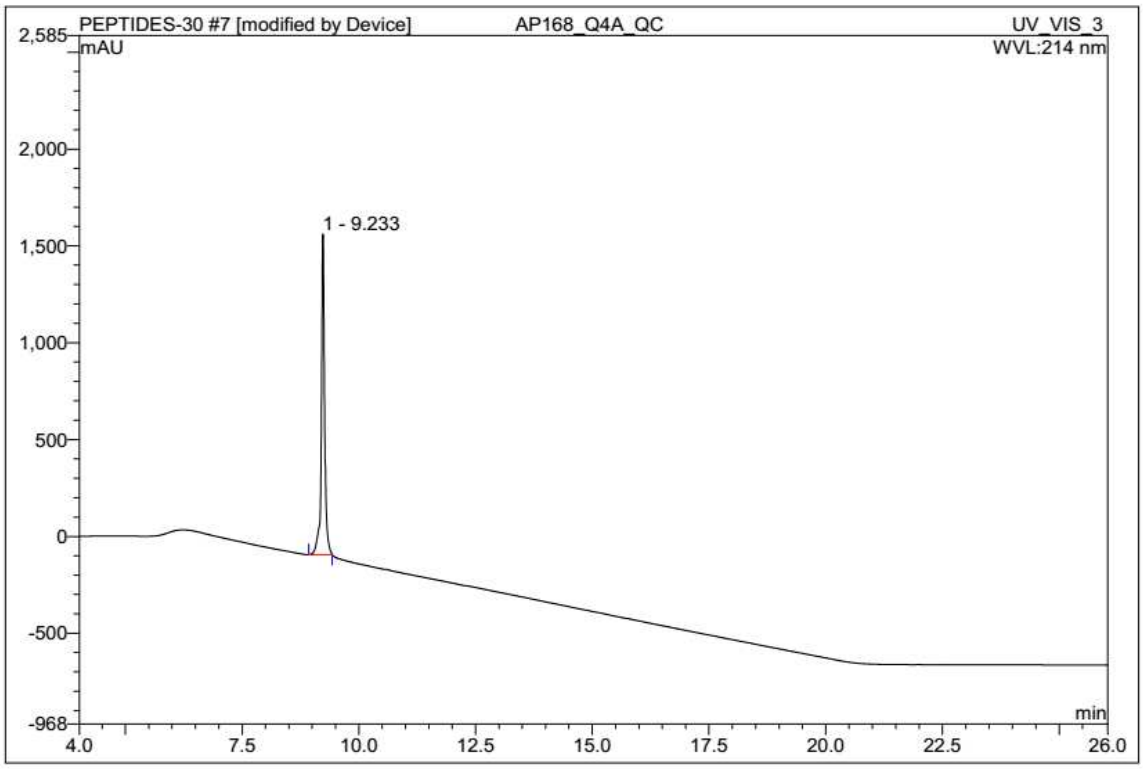

Figure S5.16: HPLC trace of HPLC purified teixobactin analogue **5.4** (gradient: 5-95% ACN in 25 min using A: 0.1% HCOOH in water, B: ACN)

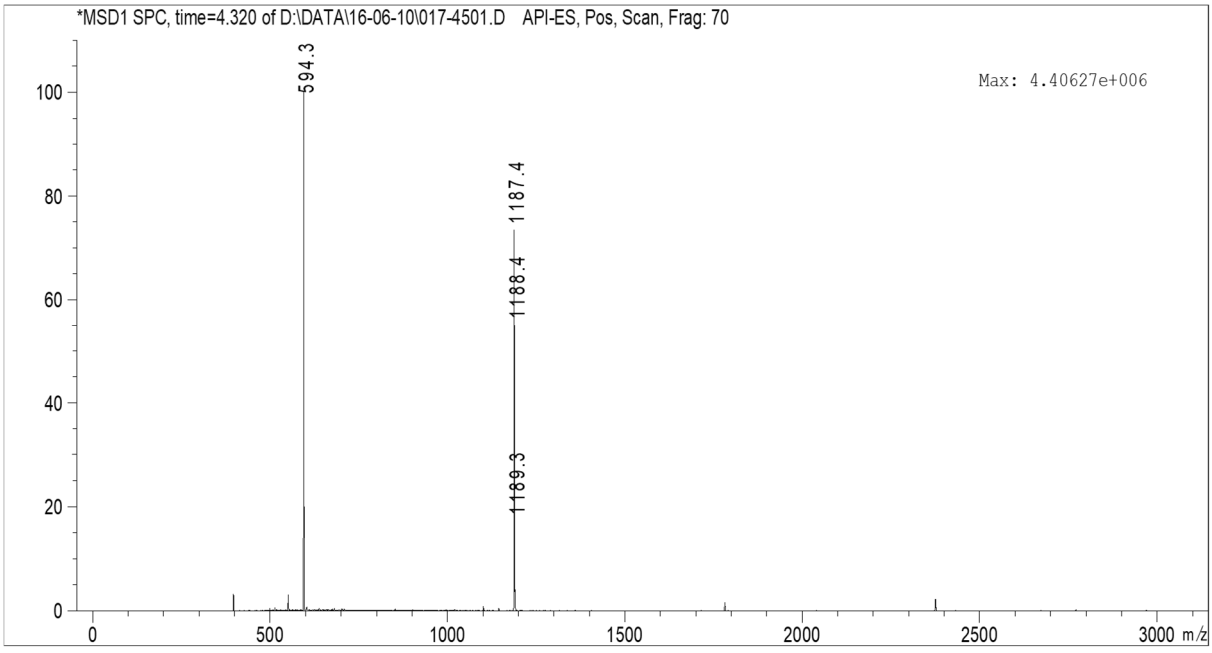

Figure S5.17: ESI-MS from LC-MS of HPLC purified teixobactin analogue **5.4**. Exact mass calcd. for $C_{56}H_{94}N_{14}O_{14}$ = 1186.71, found M + H^+ = 1187.4, M/2 + H^+ = 594.3.

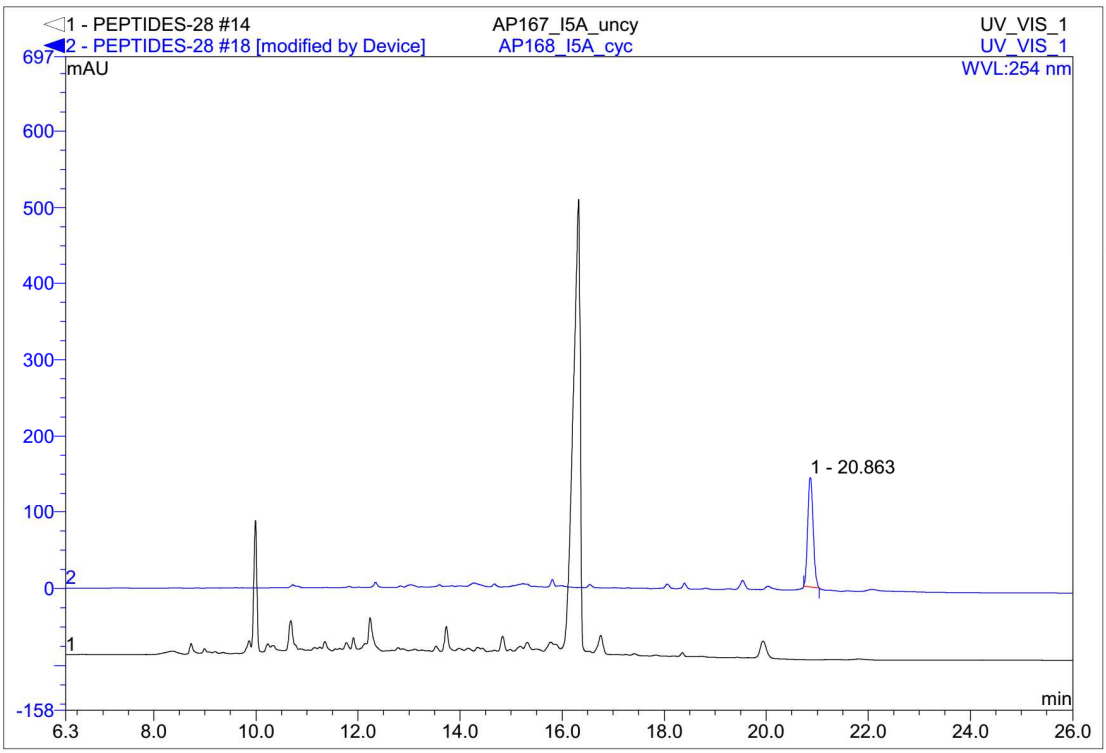

Figure S5.18: HPLC trace showing the progress of cyclisation reaction for the synthesis of analogue **5.5** (i): conversion of the uncyclized protected teixobactin analogue t_R= 16.323 min (shown in black) to the cyclized protected teixobactin analogue t_R = 20.863 min (shown in blue) (Gradient: 5-95% in 25 min)

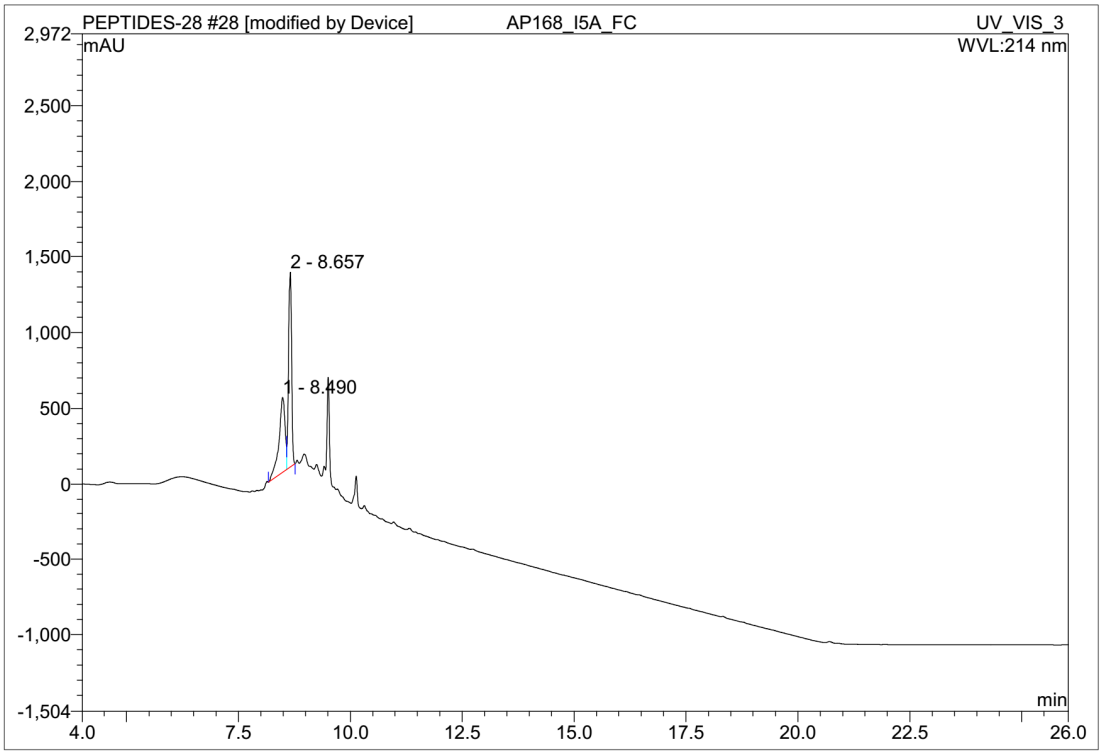

Figure S5.19: HPLC trace of crude teixobactin analogue **5.5** t_R = 8.657 min (gradient: 5-95% ACN in 25 min using A: 0.1% HCOOH in water, B: ACN)

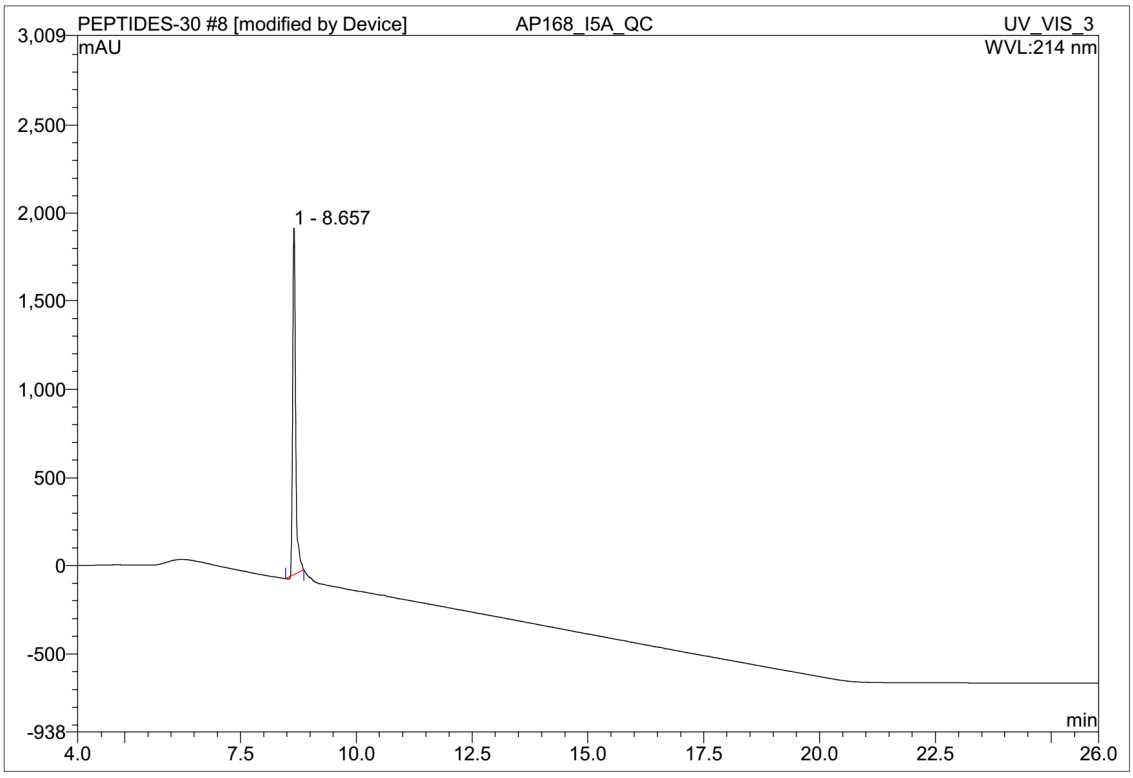

Figure S5.20: HPLC trace of HPLC purified teixobactin analogue **5.5** (gradient: 5-95% ACN in 25 min using A: 0.1% HCOOH in water, B: ACN)

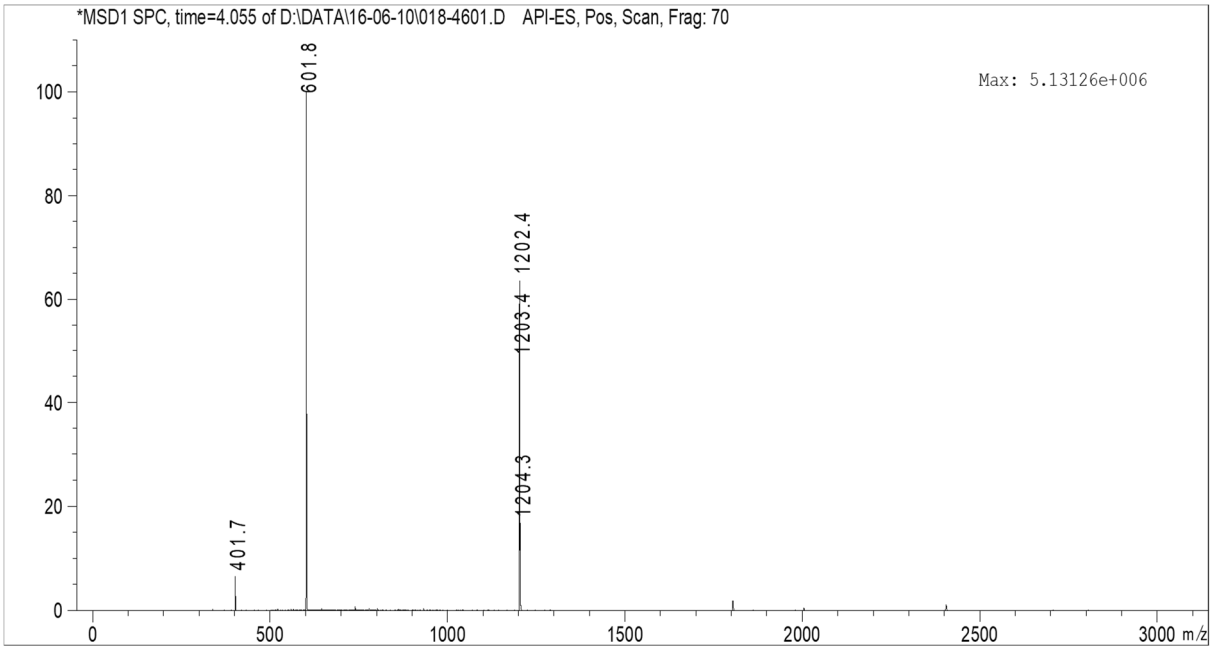

Figure S5.21: ESI-MS from LC-MS of HPLC purified teixobactin analogue **5.5**. Exact mass calcd. for $C_{55}H_{91}N_{15}O_{15}$ = 1201.68, found M + H^+ = 1202.4, M/2 + H^+ = 601.8, M/3 + H^+ = 401.7.

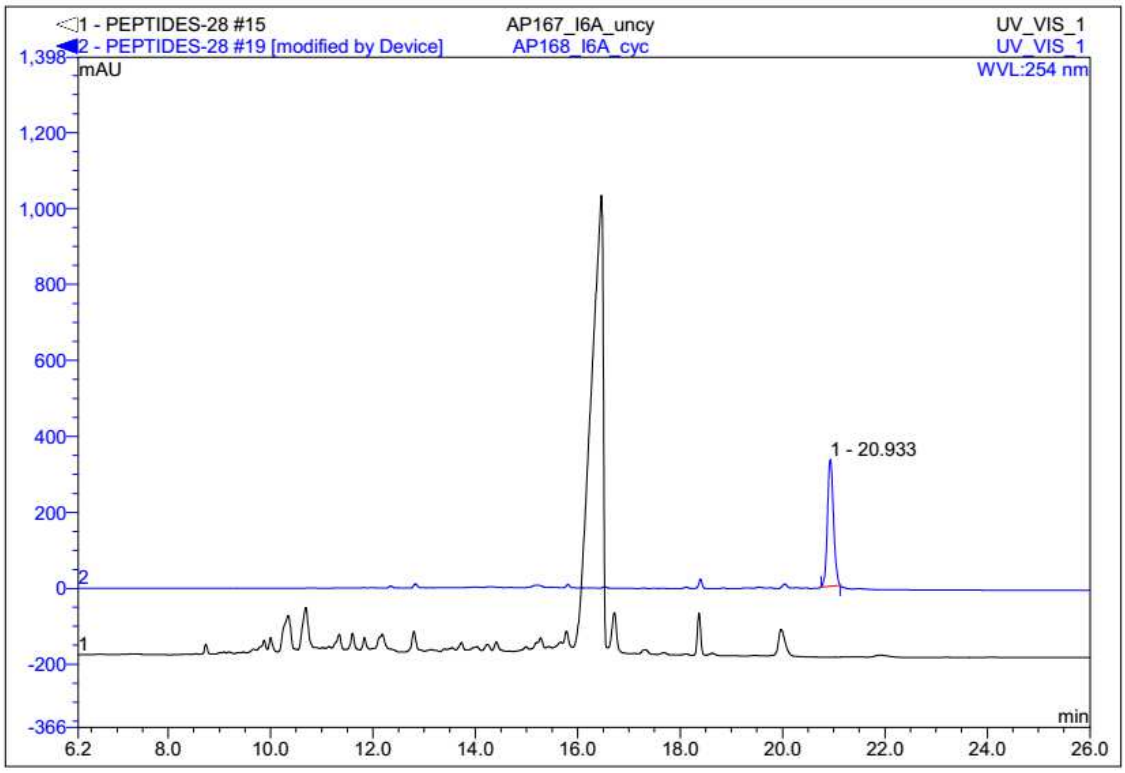

Figure S5.22: HPLC trace showing the progress of cyclisation reaction for the synthesis of analogue **5.6** (i): conversion of the uncyclized protected teixobactin analogue t_R= 16.467 min (shown in black) to the cyclized protected teixobactin analogue t_R = 20.933 min (shown in blue) (Gradient: 5-95% in 25 min)

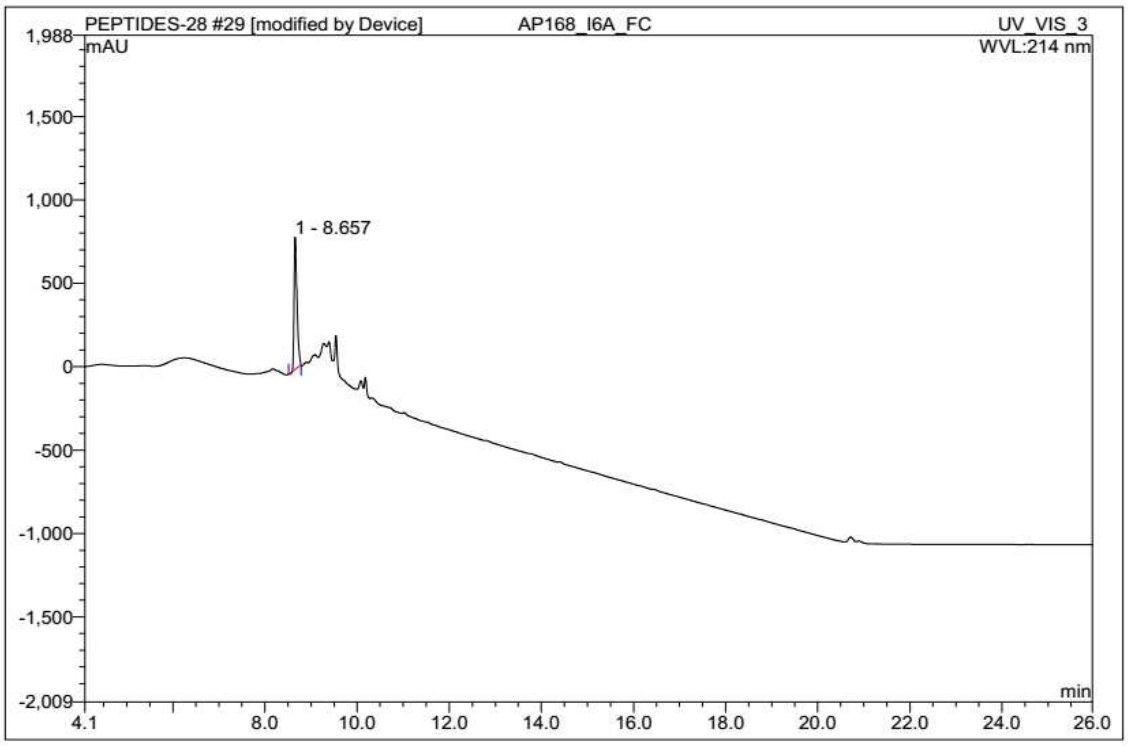

Figure S5.23: HPLC trace of crude teixobactin analogue **5.6** t_R = 8.657 min (gradient: 5-95% ACN in 25 min using A: 0.1% HCOOH in water, B: ACN)

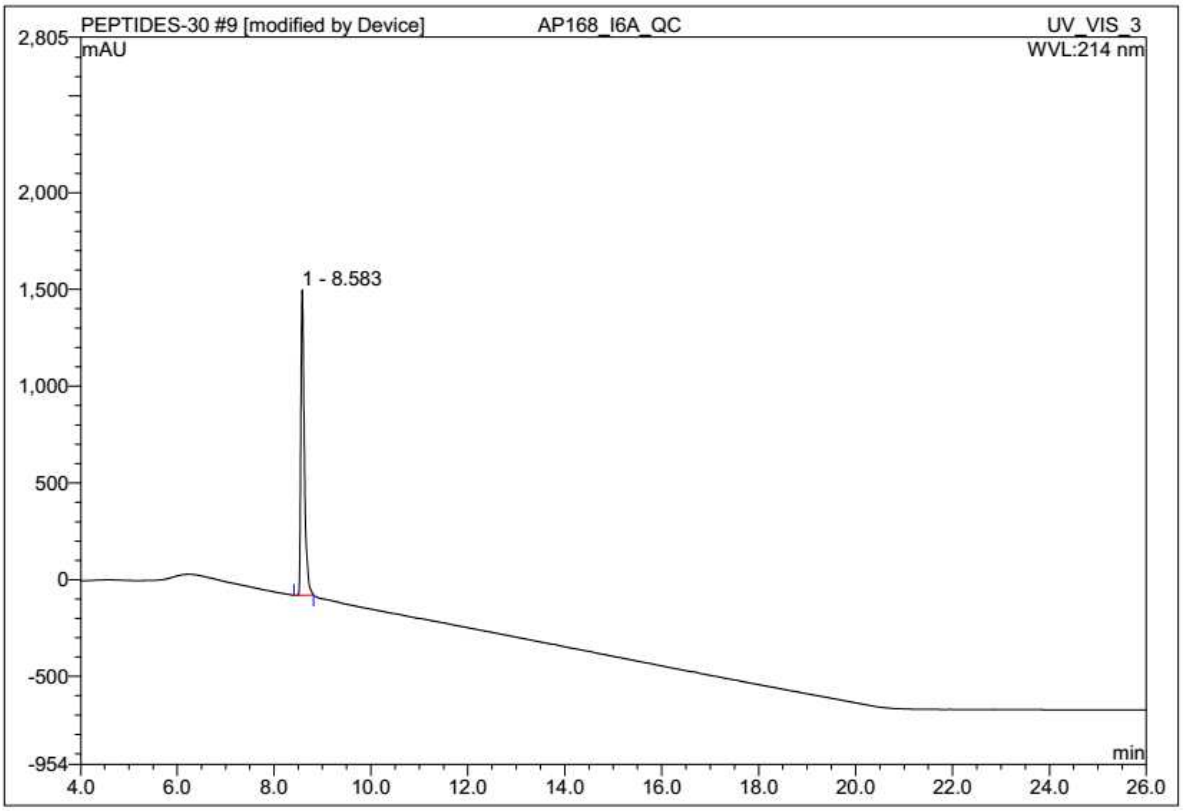

Figure S5.24: HPLC trace of HPLC purified teixobactin analogue **5.6** (gradient: 5-95% ACN in 25 min using A: 0.1% HCOOH in water, B: ACN)

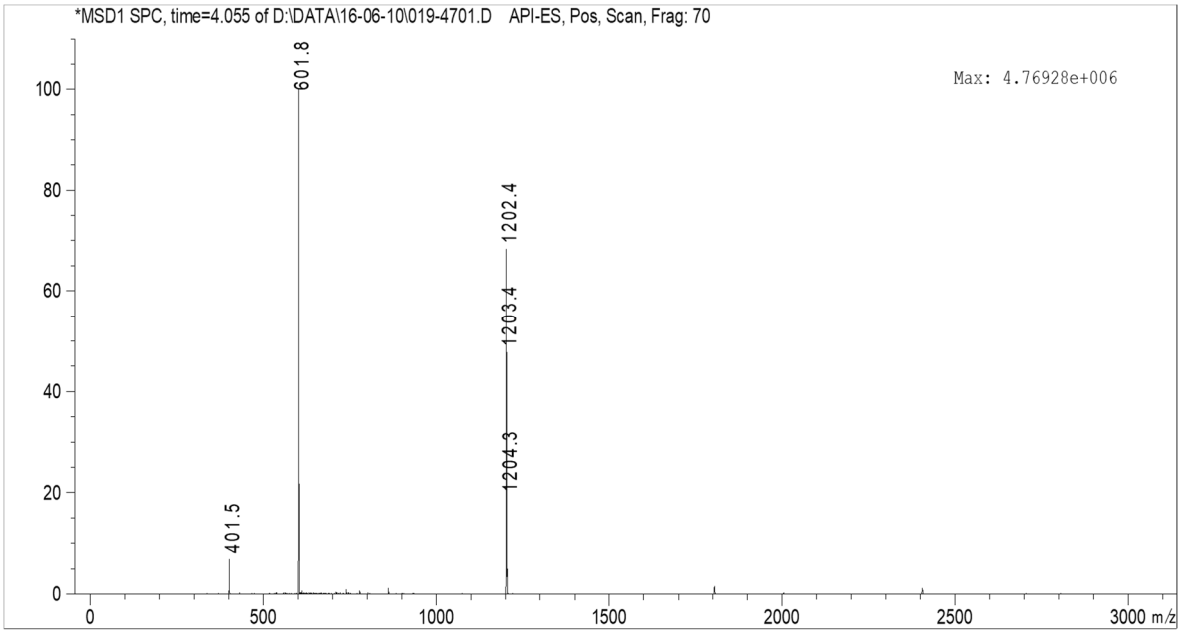

Figure S5.25: ESI-MS from LC-MS of HPLC purified teixobactin analogue **5.6**. Exact mass calcd. for $C_{55}H_{91}N_{15}O_{15}$ = 1201.68, found M + H^+ = 1202.4, M/2 + H^+ = 601.8, M/3 + H^+ = 401.7.

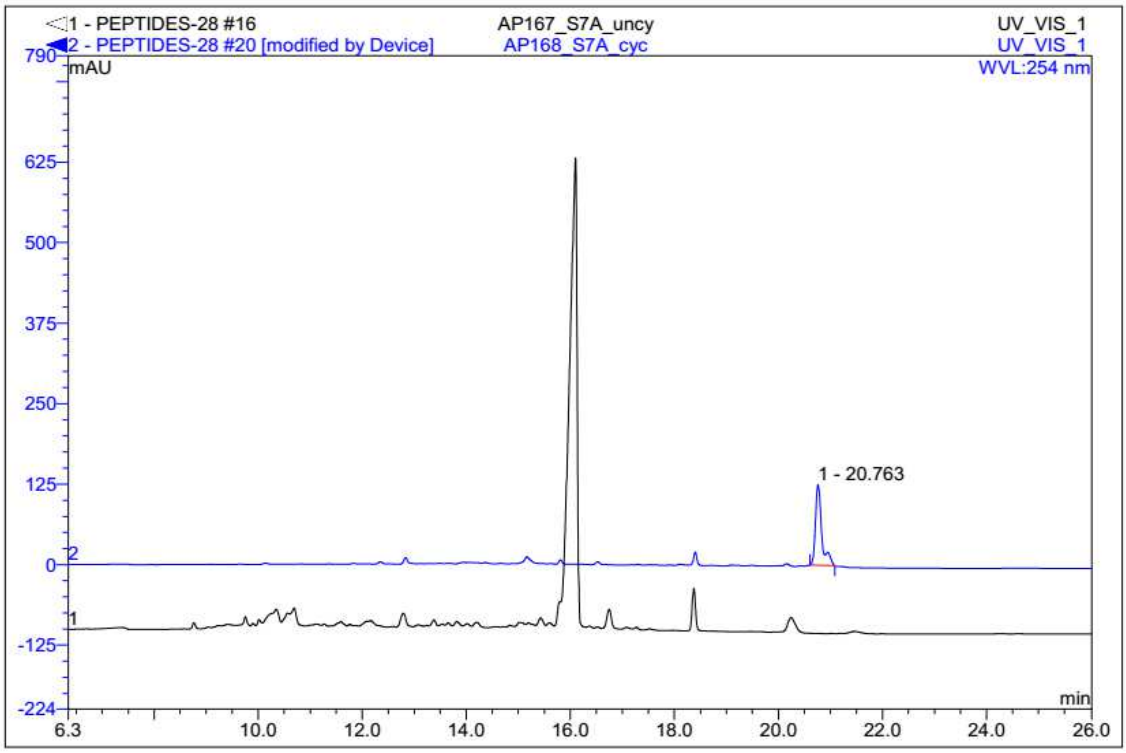

Figure S5.26: HPLC trace showing the progress of cyclisation reaction for the synthesis of analogue **5.7** (i): conversion of the uncyclized protected teixobactin analogue t_R= 16.100 min (shown in black) to the cyclized protected teixobactin analogue t_R = 20.763 min (shown in blue) (Gradient: 5-95% in 25 min)

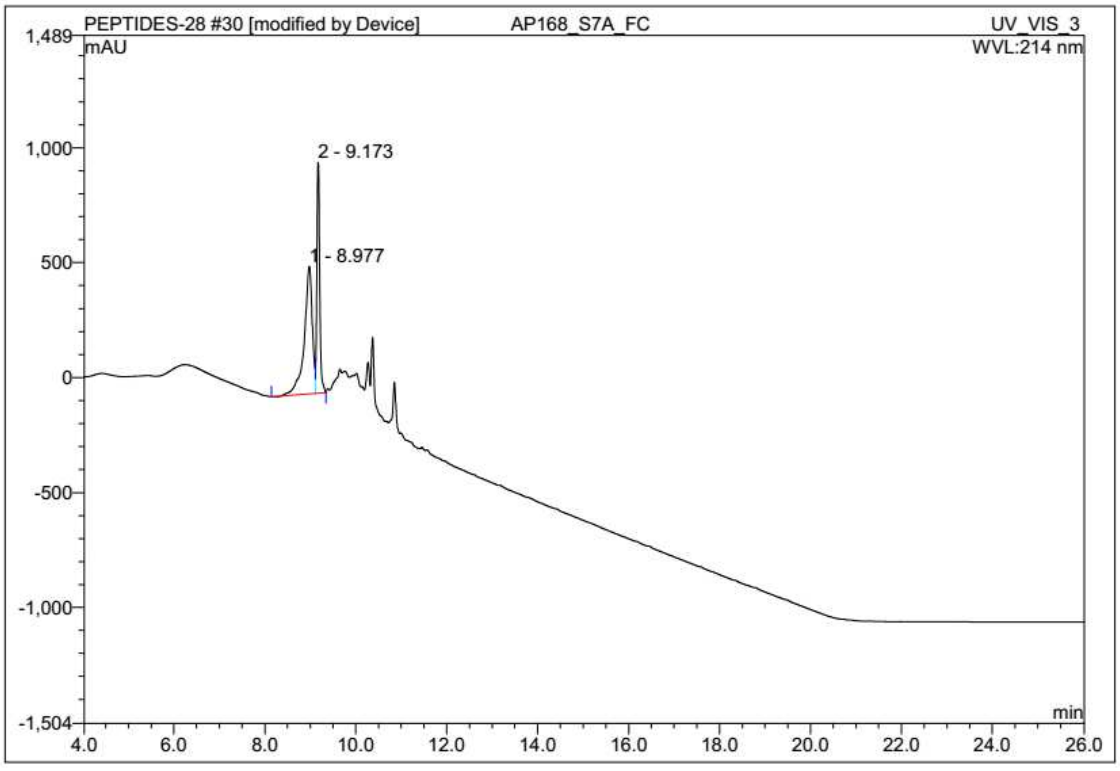

Figure S5.27: HPLC trace of crude teixobactin analogue **5.7** t_R = 9.173 min (gradient: 5-95% ACN in 25 min using A: 0.1% HCOOH in water, B: ACN)

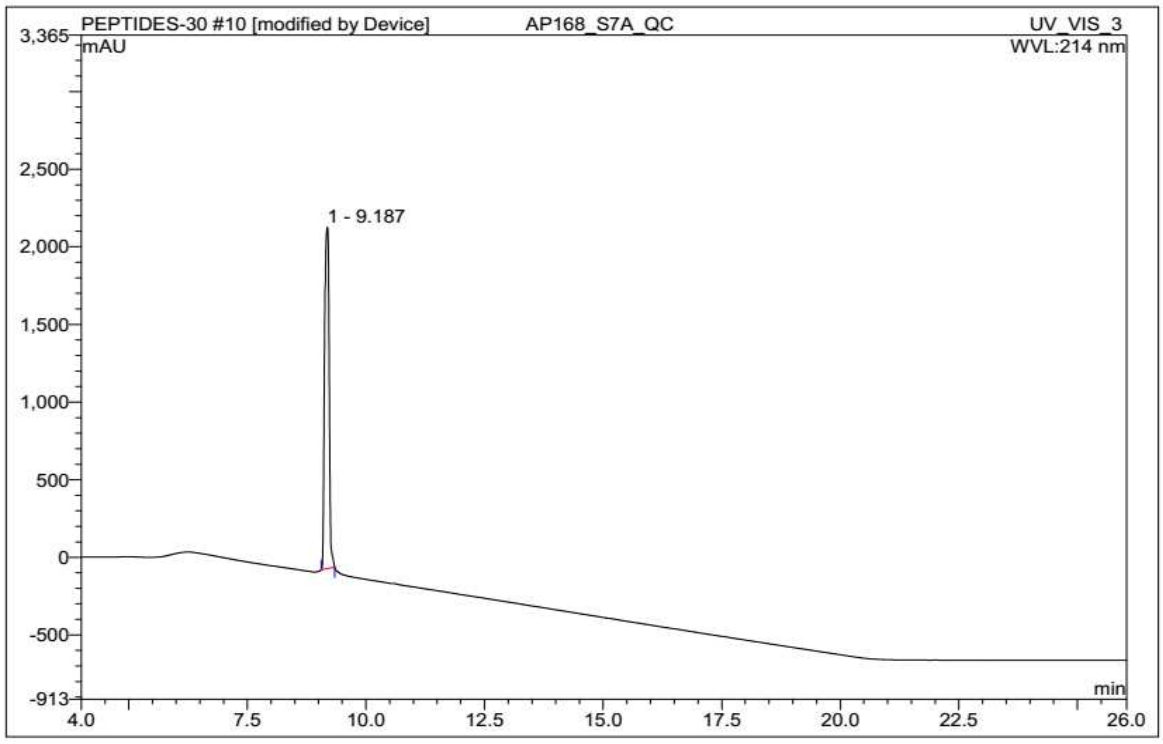

Figure S5.28: HPLC trace of HPLC purified teixobactin analogue **5.7** (gradient: 5-95% ACN in 25 min using A: 0.1% HCOOH in water, B: ACN)

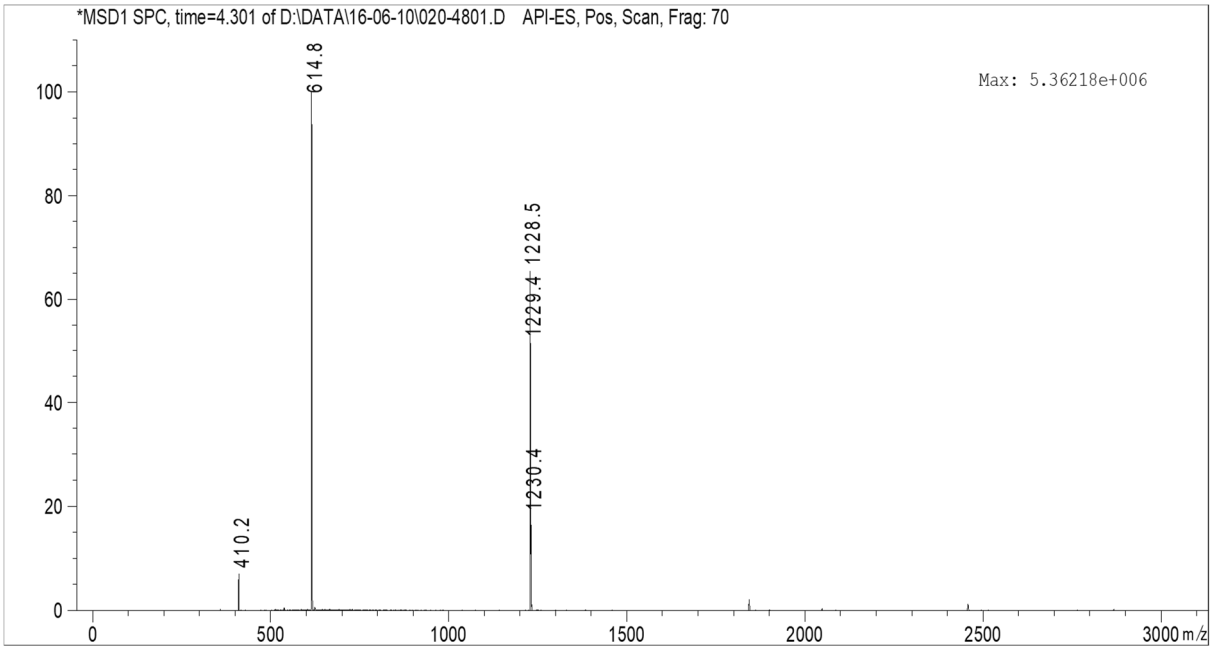

Figure S5.29: ESI-MS from LC-MS of HPLC purified teixobactin analogue **5.7**. Exact mass calcd. for $C_{58}H_{97}N_{15}O_{14}$ = 1227.73, found M + H^+ = 1228.5, M/2 + H^+ = 614.8, M/3 + H^+ = 410.2.

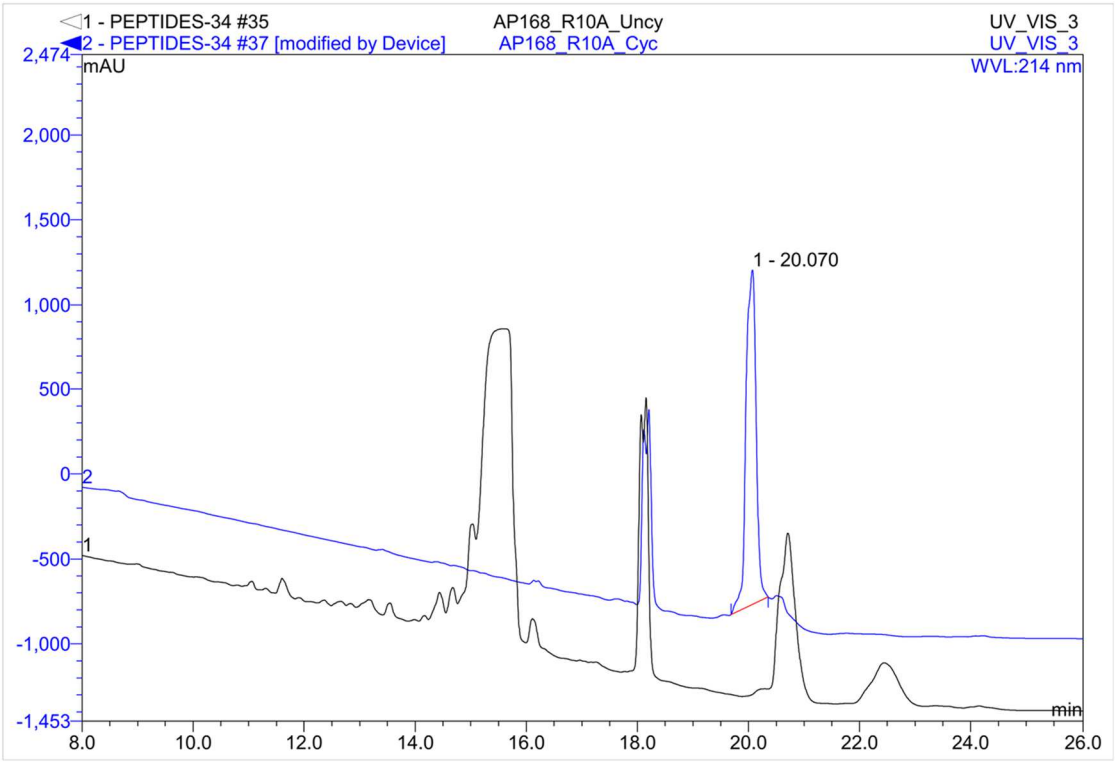

Figure S5.30: HPLC trace showing the progress of cyclisation reaction for the synthesis of analogue **5.8** (i): conversion of the uncyclised protected teixobactin analogue t_R= 15.640 min (shown in black) to the cyclized protected teixobactin analogue t_R = 20.763 min (shown in blue) (Gradient: 5-95% in 25 min)

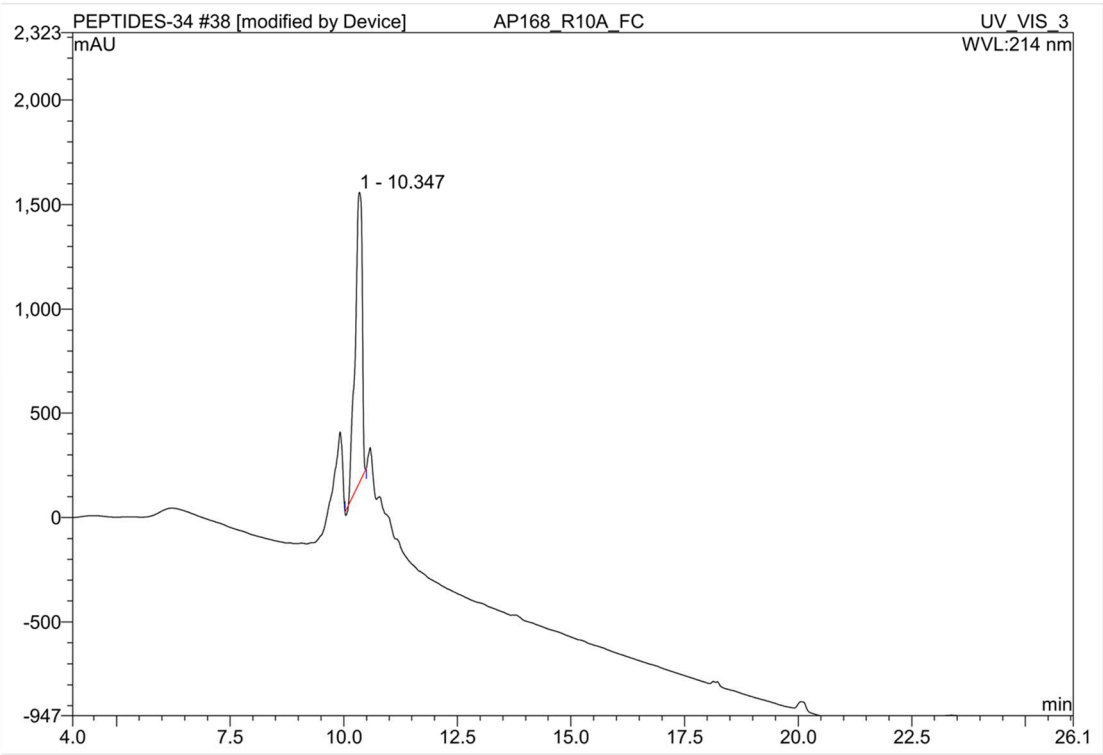

Figure S5.31: HPLC trace of crude teixobactin analogue **5.8** t_R = 10.347 min (gradient: 5-95% ACN in 25 min using A: 0.1% HCOOH in water, B: ACN)

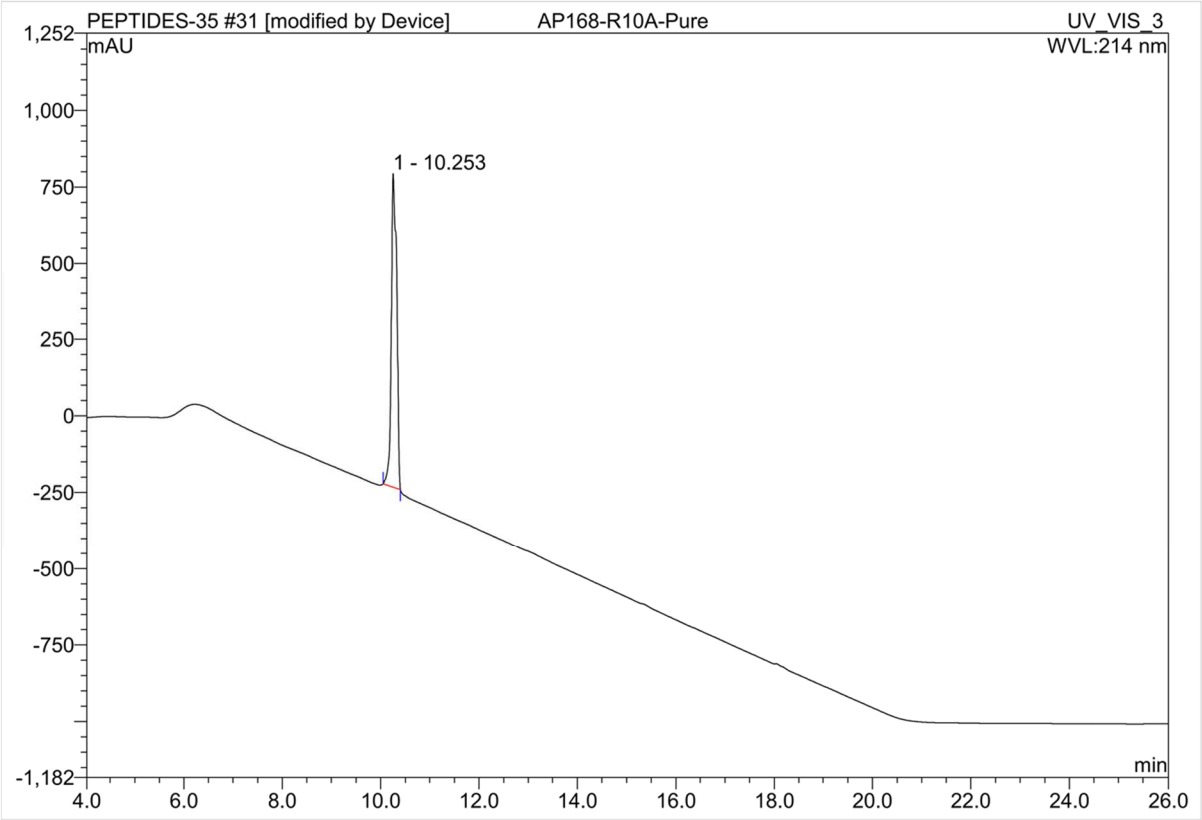

Figure S5.32: HPLC trace of HPLC purified teixobactin analogue **5.8** (gradient: 5-95% ACN in 25 min using A: 0.1% HCOOH in water, B: ACN)

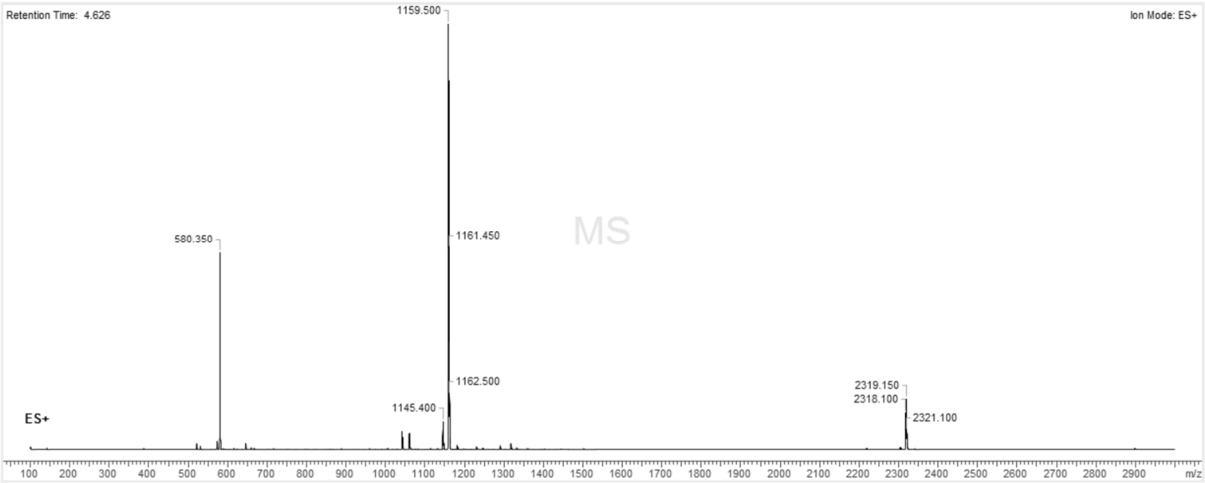

Figure S5.33: ESI-MS from LC-MS of HPLC purified teixobactin analogue **5.8**. Exact mass calcd. for $C_{55}H_{90}N_{12}O_{15}$ = 1158.66, found M + H^+ = 1159.50, M/2 + H^+ = 580.35.

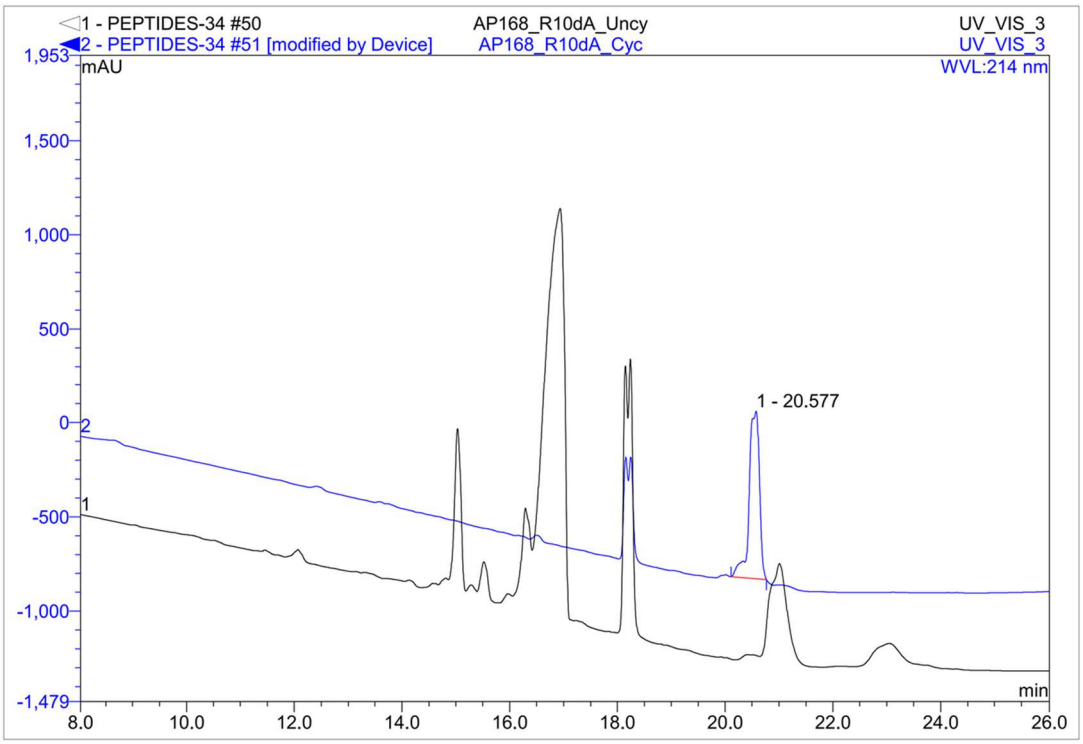

Figure S5.34: HPLC trace showing the progress of cyclisation reaction for the synthesis of analogue **5.9** (i): conversion of the uncyclized protected teixobactin analogue t_R= 16.940 min (shown in black) to the cyclized protected teixobactin analogue t_R = 20.577 min (shown in blue) (Gradient: 5-95% in 25 min)

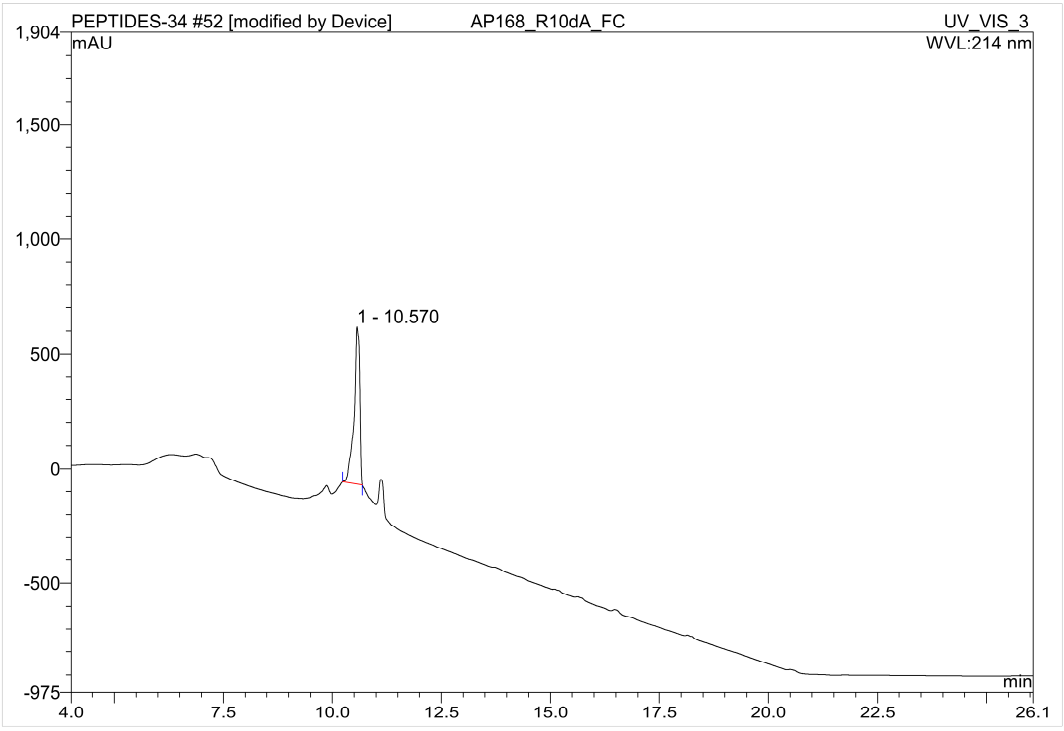

Figure S5.35: HPLC trace of crude teixobactin analogue **5.9** t_R = 10.570 min (gradient: 5-95% ACN in 25 min using A: 0.1% HCOOH in water, B: ACN)

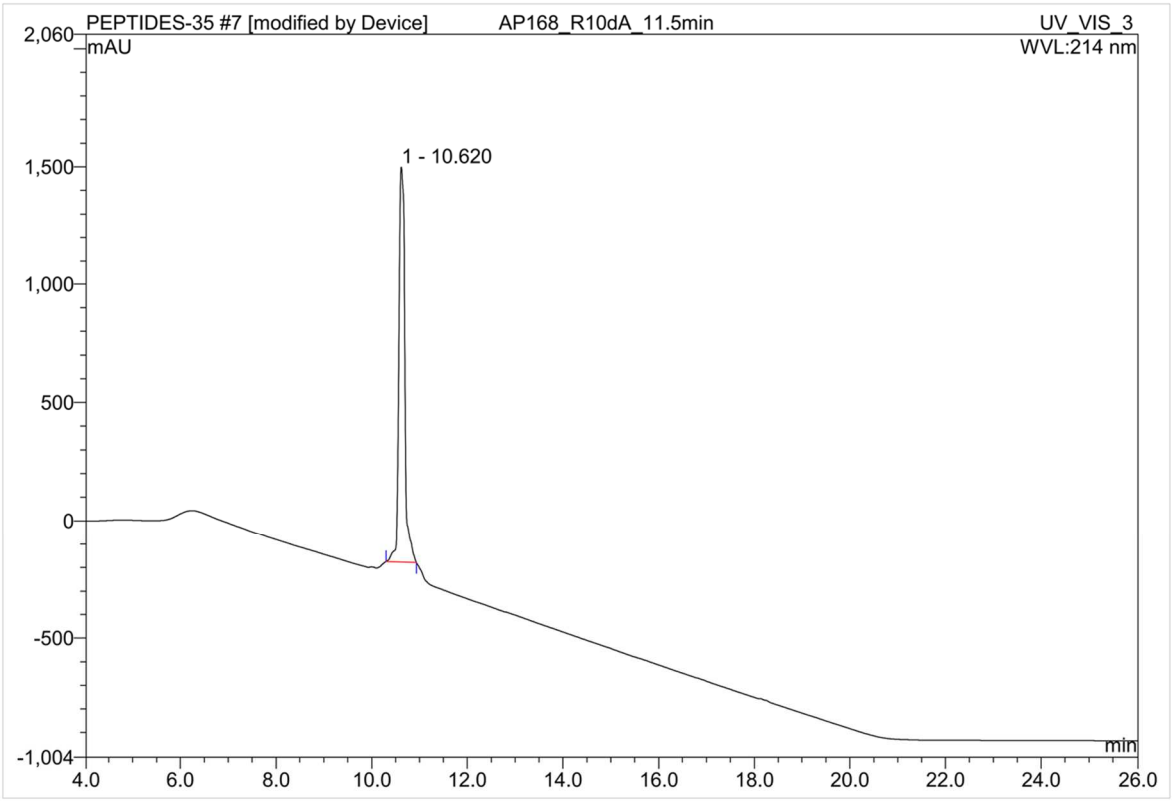

Figure S5.36: HPLC trace of HPLC purified teixobactin analogue **5.9** (gradient: 5-95% ACN in 25 min using A: 0.1% HCOOH in water, B: ACN)

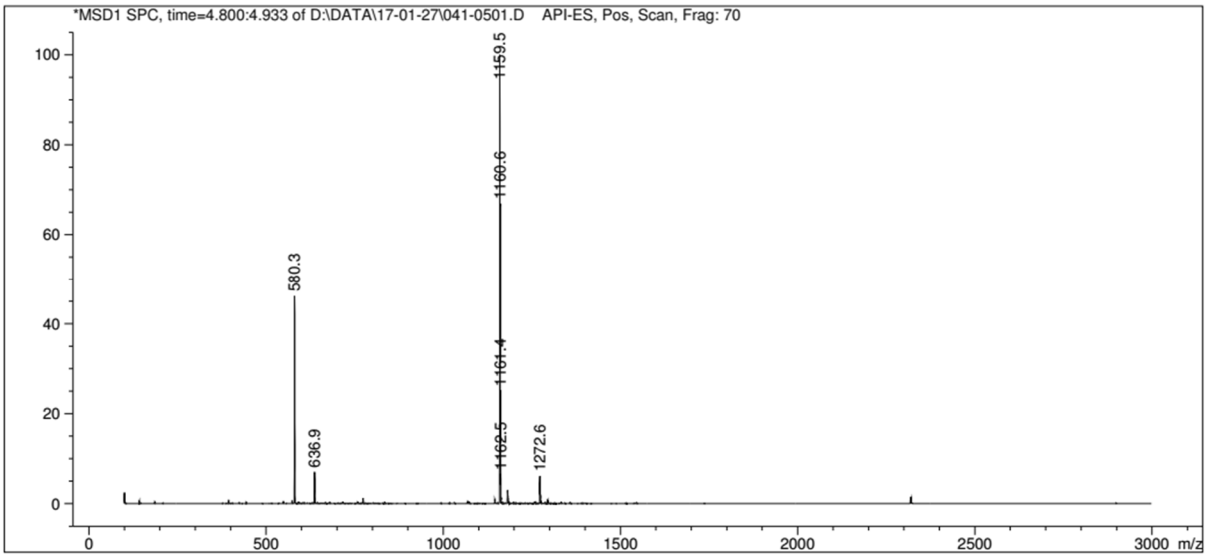

Figure S5.37: ESI-MS from LC-MS of HPLC purified teixobactin analogue **5.9**. Exact mass calcd. for $C_{55}H_{90}N_{12}O_{15}$ = 1158.66, found M + H^+ = 1159.5, M/2 + H^+ = 580.3.

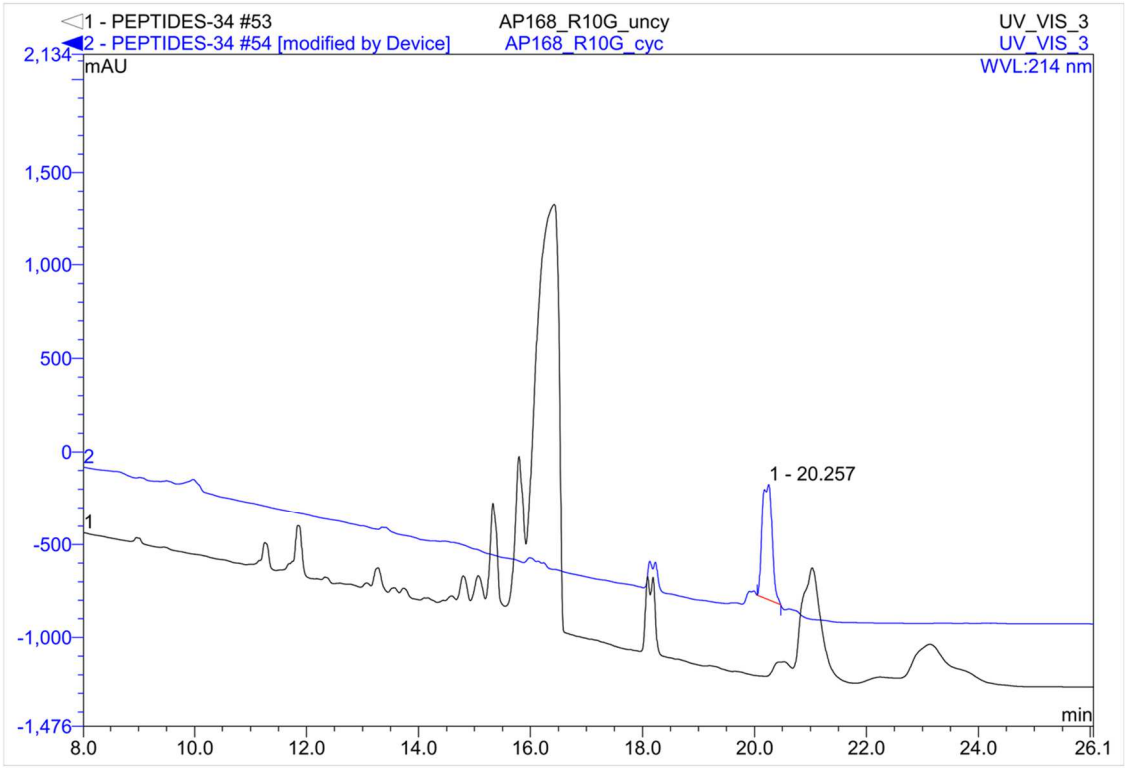

Figure S5.38: HPLC trace showing the progress of cyclisation reaction for the synthesis of analogue **5.10** (i): conversion of the uncyclized protected teixobactin analogue t_R= 16.423 min (shown in black) to the cyclized protected teixobactin analogue t_R = 20.257 min (shown in blue) (Gradient: 5-95% in 25 min)

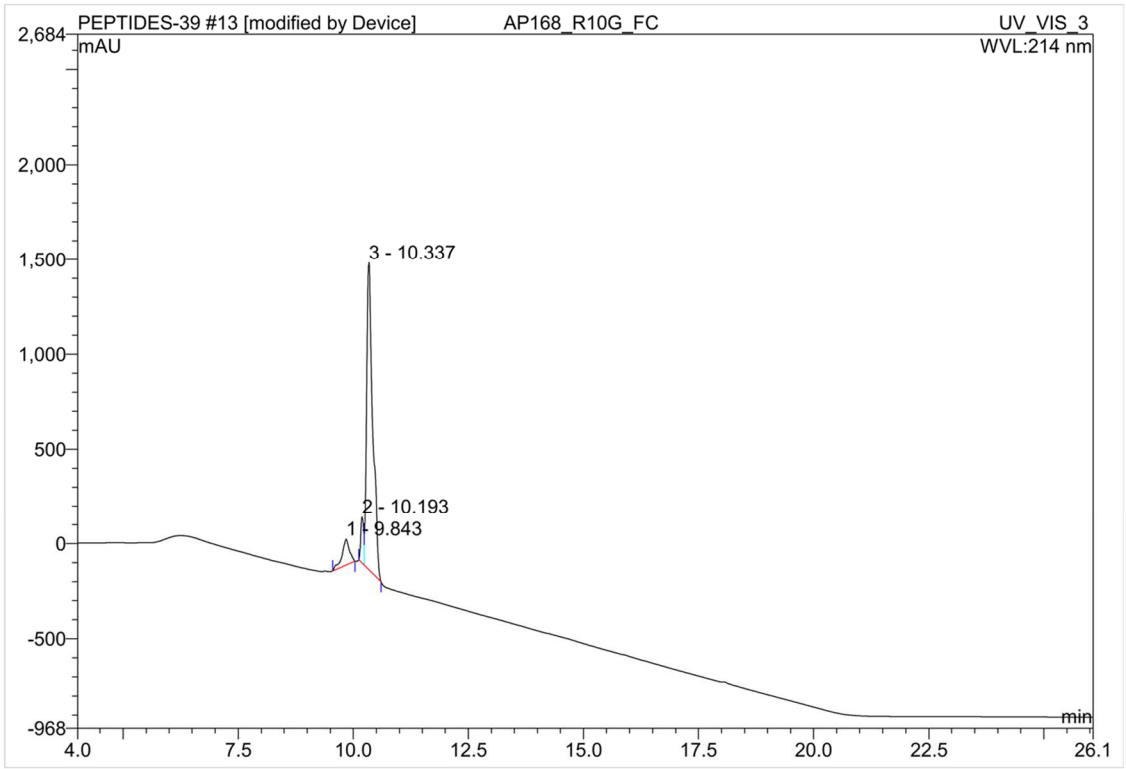

Figure S5.39: HPLC trace of crude teixobactin analogue **5.10** t_R = 10.373 min (gradient: 5-95% ACN in 25 min using A: 0.1% HCOOH in water, B: ACN)

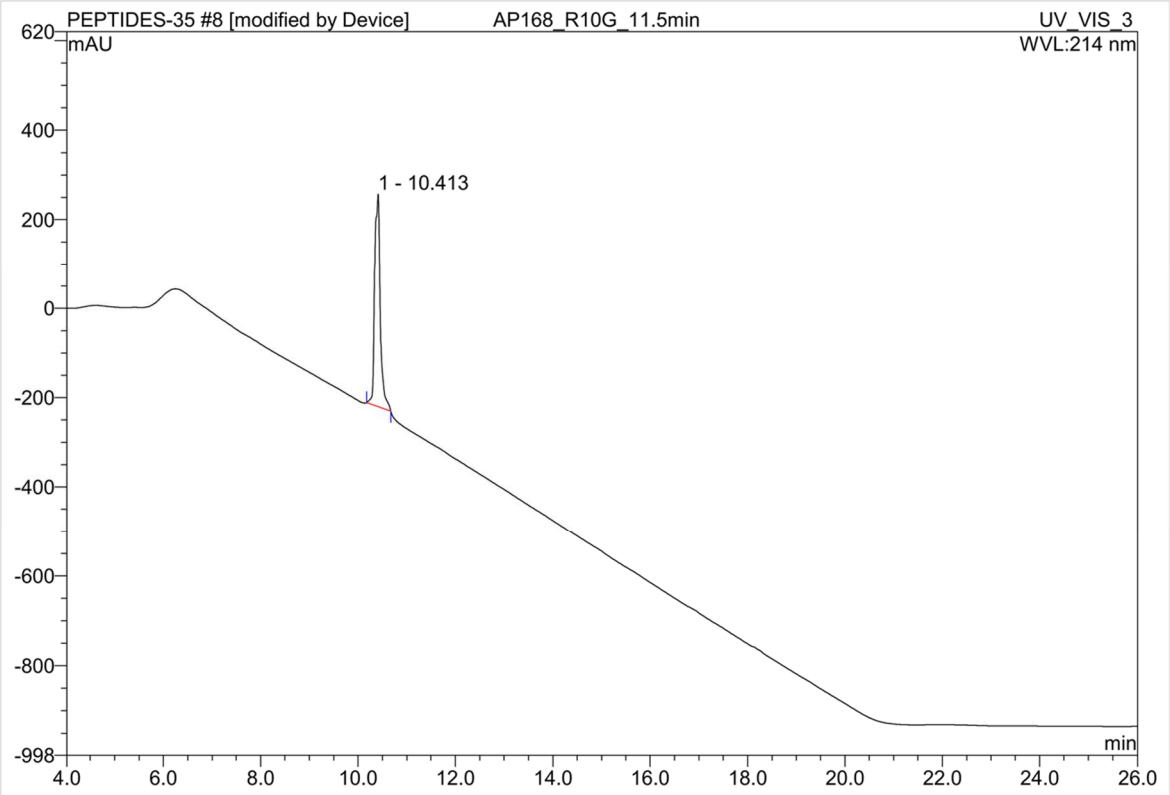

Figure S5.40: HPLC trace of HPLC purified teixobactin analogue **5.10** (gradient: 5-95% ACN in 25 min using A: 0.1% HCOOH in water, B: ACN)

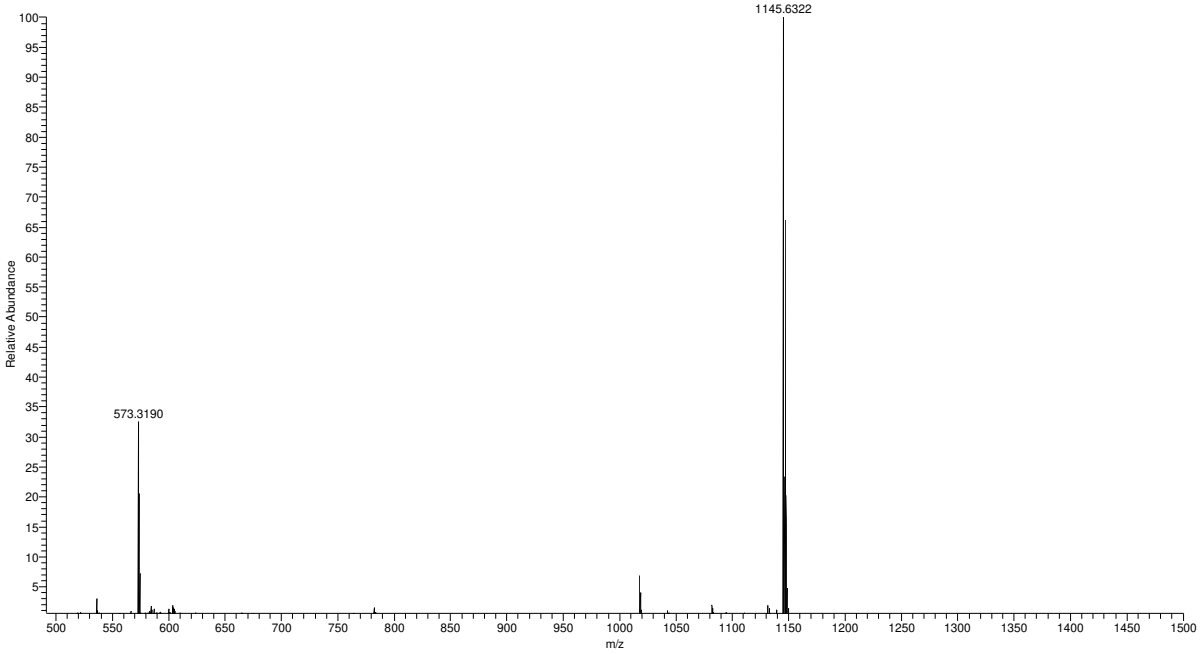

Figure S5.41: HRMS of HPLC purified teixobactin analogue **5.10**. Exact mass calcd. for $C_{54}H_{88}N_{12}O_{15}$ = 1144.6492, found M + H^+ = 1145.6322, M/2 + H^+ = 573.3190.

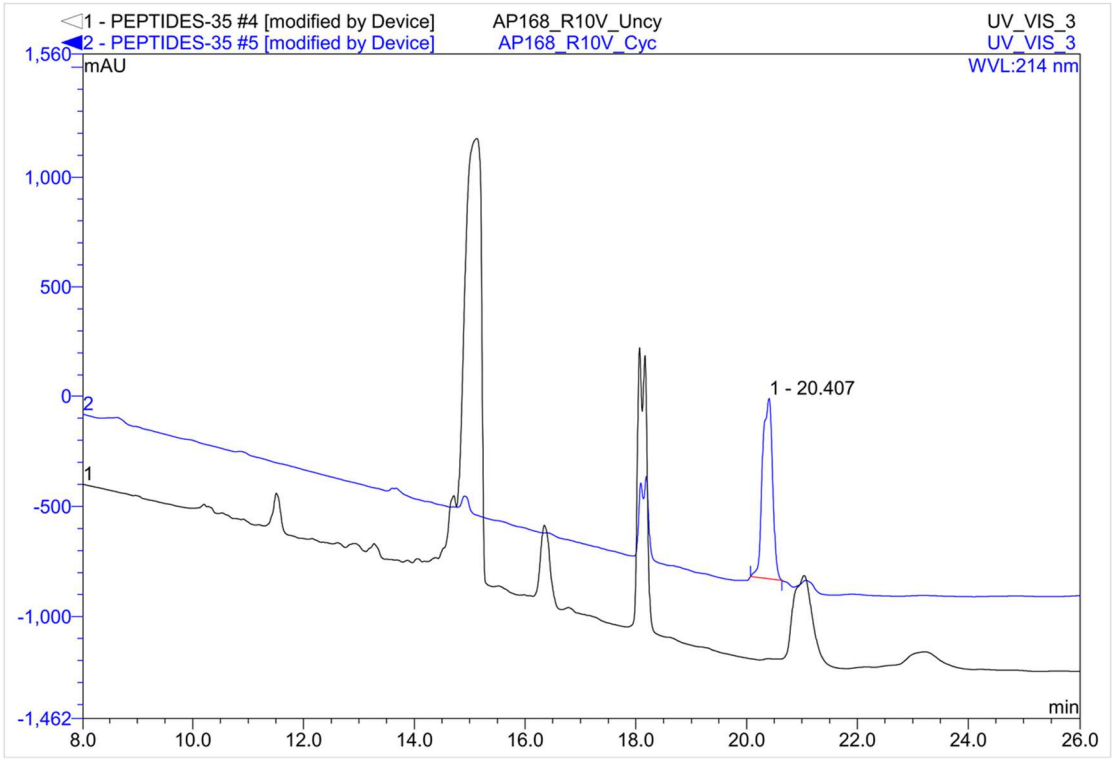

Figure S5.42: HPLC trace showing the progress of cyclisation reaction for the synthesis of analogue **5.11** (i): conversion of the uncyclized protected teixobactin analogue t_R= 15.130 min (shown in black) to the cyclized protected teixobactin analogue t_R = 20.407 min (shown in blue) (Gradient: 5-95% in 25 min)

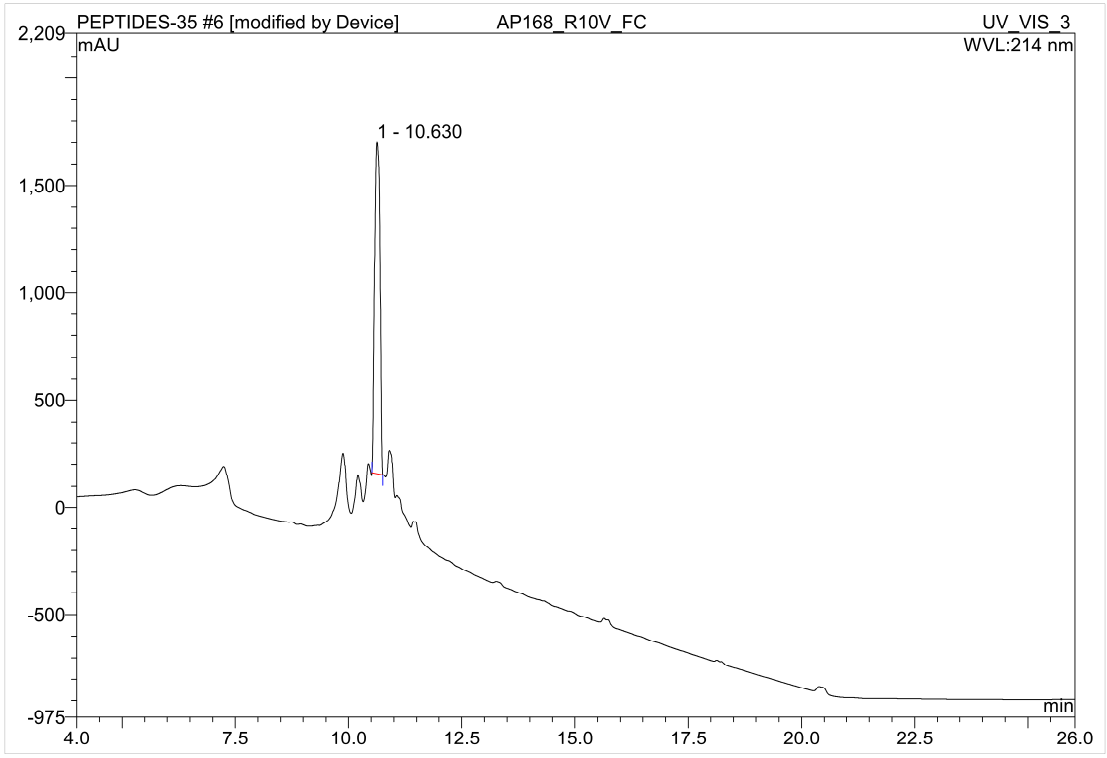

Figure S5.43: HPLC trace of crude teixobactin analogue **5.11** t_R = 10.630 min (gradient: 5-95% ACN in 25 min using A: 0.1% HCOOH in water, B: ACN)

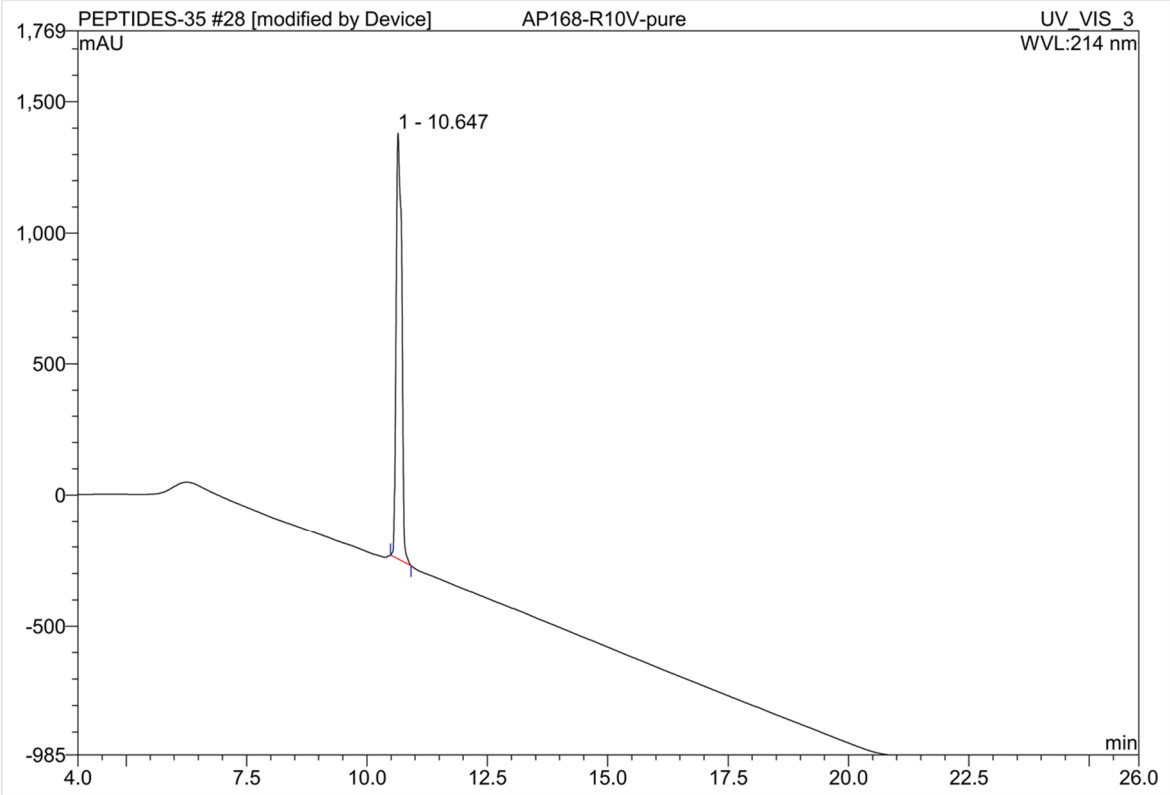

Figure S5.44: HPLC trace of HPLC purified teixobactin analogue **5.11** (gradient: 5-95% ACN in 25 min using A: 0.1% HCOOH in water, B: ACN)

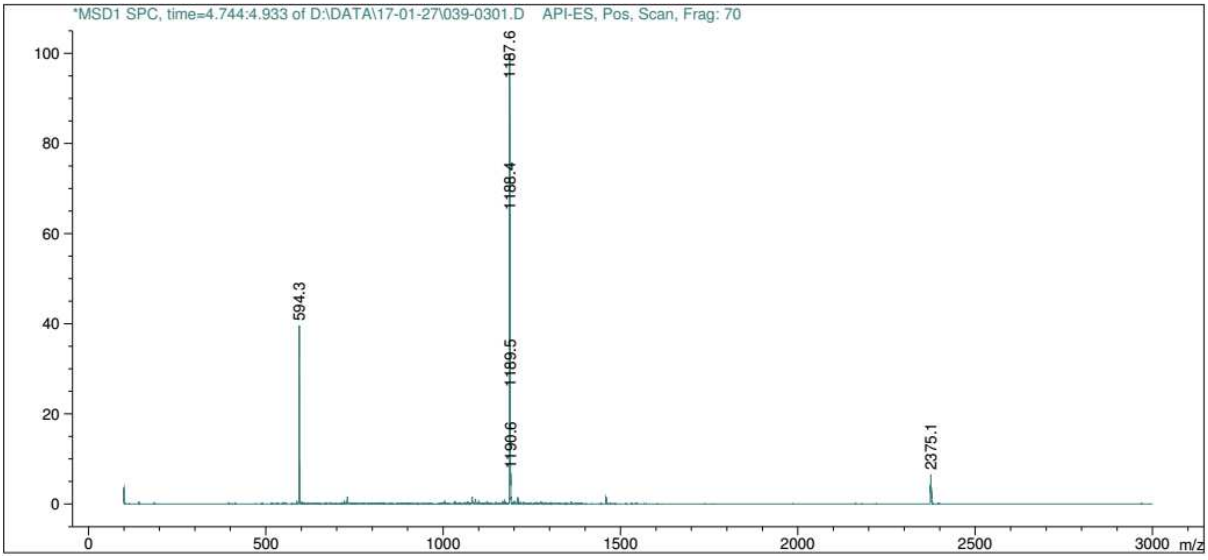

Figure S5.45: ESI-MS from LC-MS of HPLC purified teixobactin analogue **5.11**. Exact mass calcd. for $C_{57}H_{94}N_{12}O_{15}$ = 1186.7, found M + H^+ = 1187.6, M/2 + H^+ = 594.3.

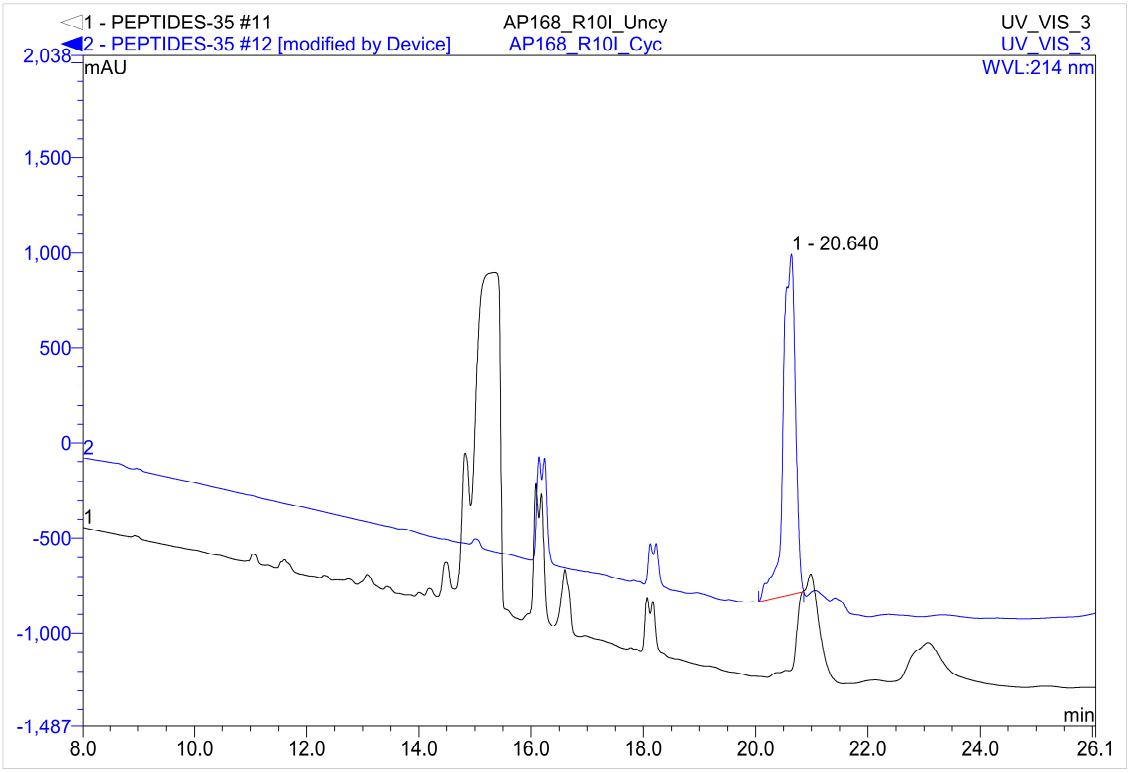

Figure S5.46: HPLC trace showing the progress of cyclisation reaction for the synthesis of analogue **5.12** (i): conversion of the uncyclized protected teixobactin analogue t_R= 15.353 min (shown in black) to the cyclized protected teixobactin analogue t_R = 20.640 min (shown in blue) (Gradient: 5-95% in 25 min)

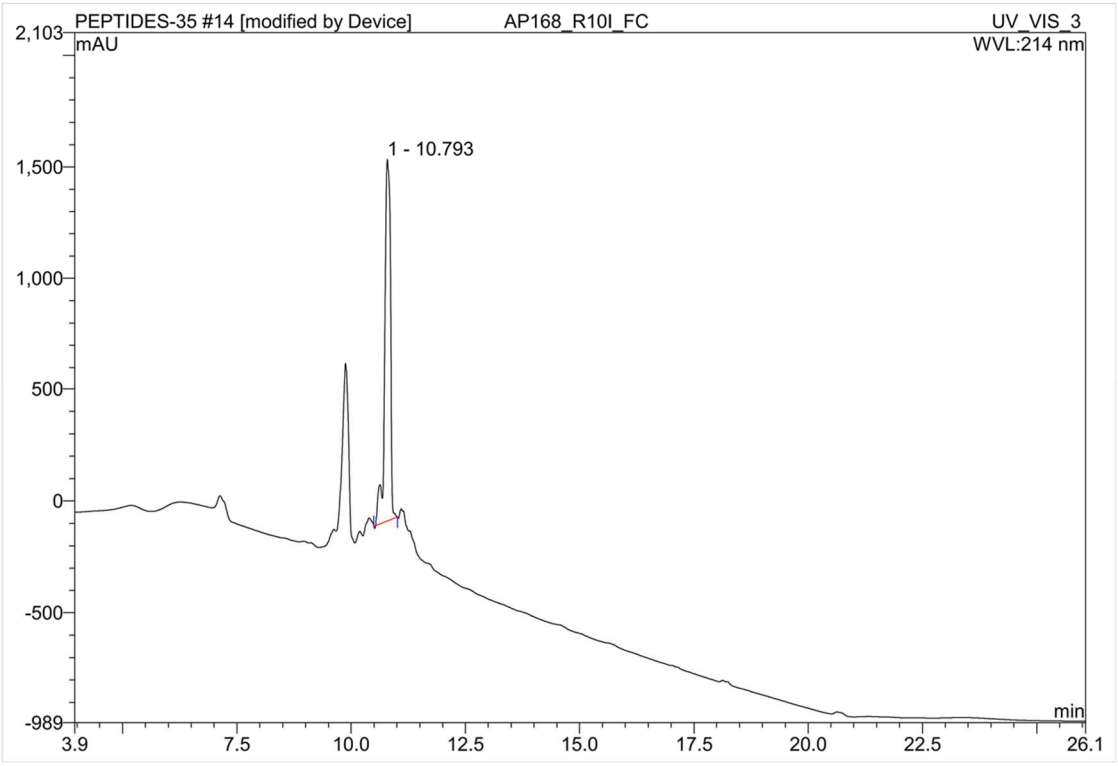

Figure S5.47: HPLC trace of crude teixobactin analogue **5.12** t_R = 10.793 min (gradient: 5-95% ACN in 25 min using A: 0.1% HCOOH in water, B: ACN)

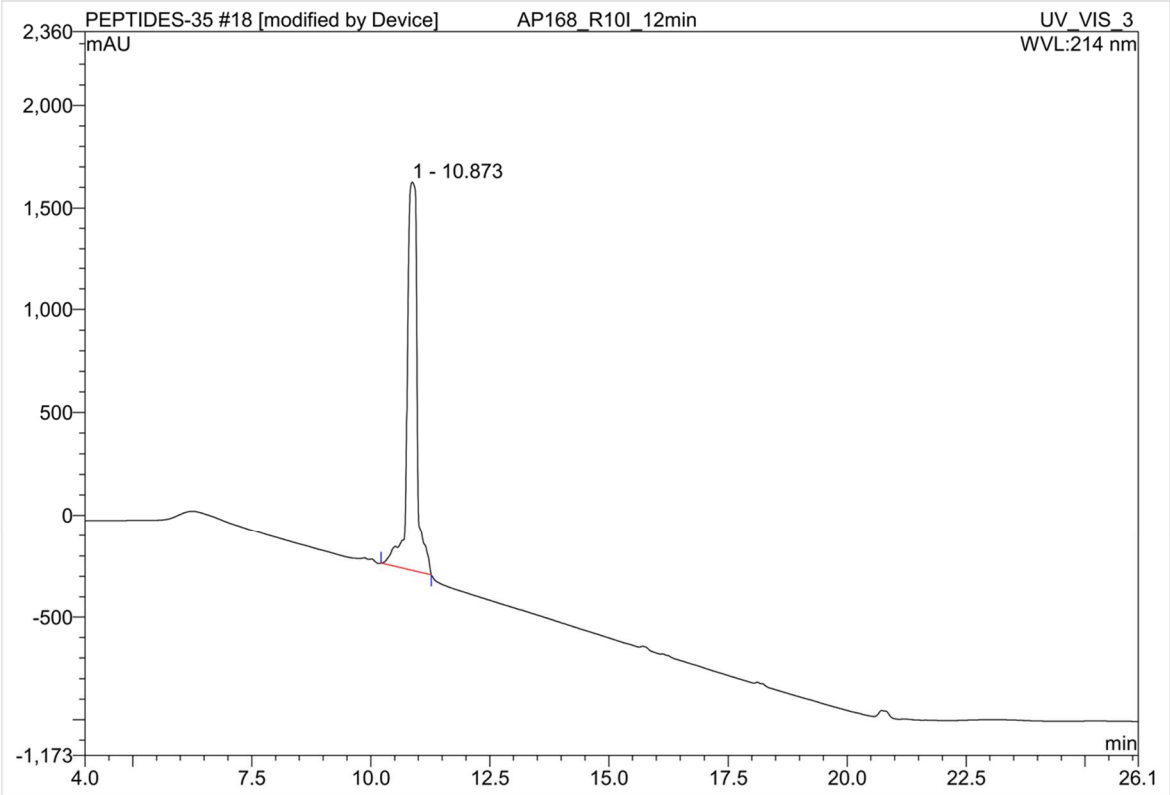

Figure S5.48: HPLC trace of HPLC purified teixobactin analogue **5.12** (gradient: 5-95% ACN in 25 min using A: 0.1% HCOOH in water, B: ACN)

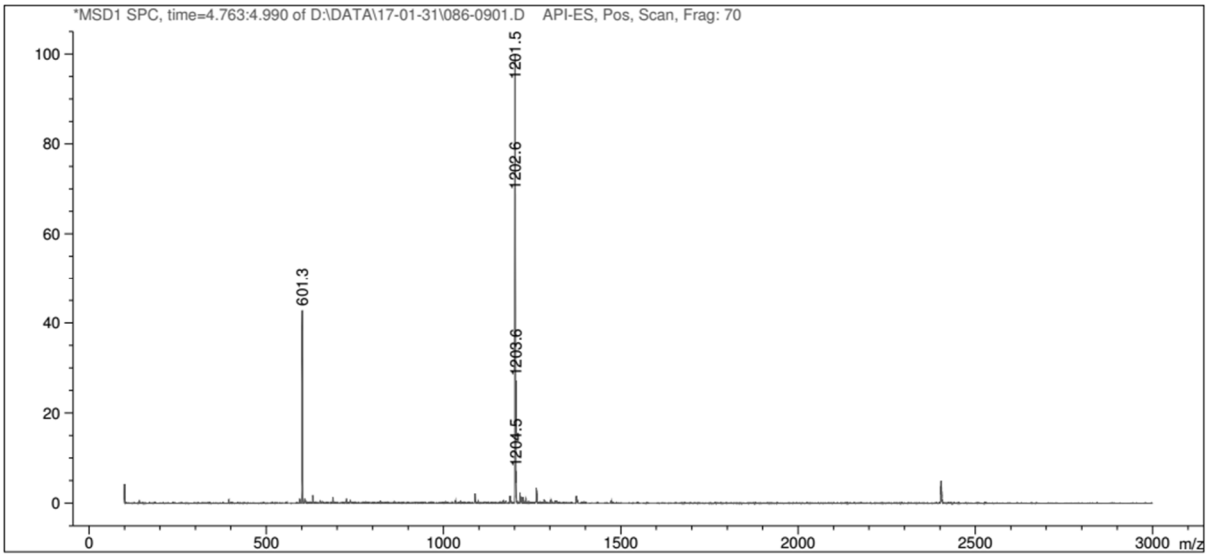

Figure S5.49: ESI-MS from LC-MS of HPLC purified teixobactin analogue **5.12**. Exact mass calcd. for $C_{58}H_{96}N_{12}O_{15}$ = 1200.71, found M + H^+ = 1201.5, M/2 + H^+ = 601.3.

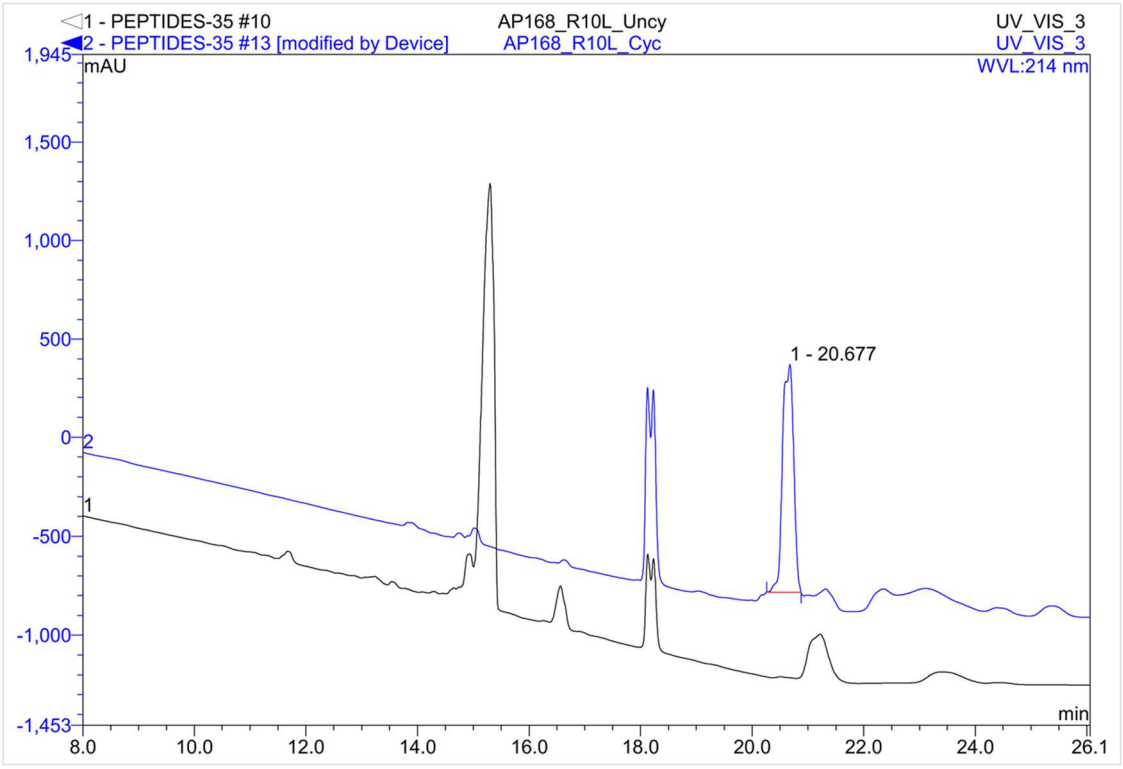

Figure S5.50: HPLC trace showing the progress of cyclisation reaction for the synthesis of analogue **5.13** (i): conversion of the uncyclized protected teixobactin analogue t_R= 15.303 min (shown in black) to the cyclized protected teixobactin analogue t_R = 20.677 min (shown in blue) (Gradient: 5-95% in 25 min)

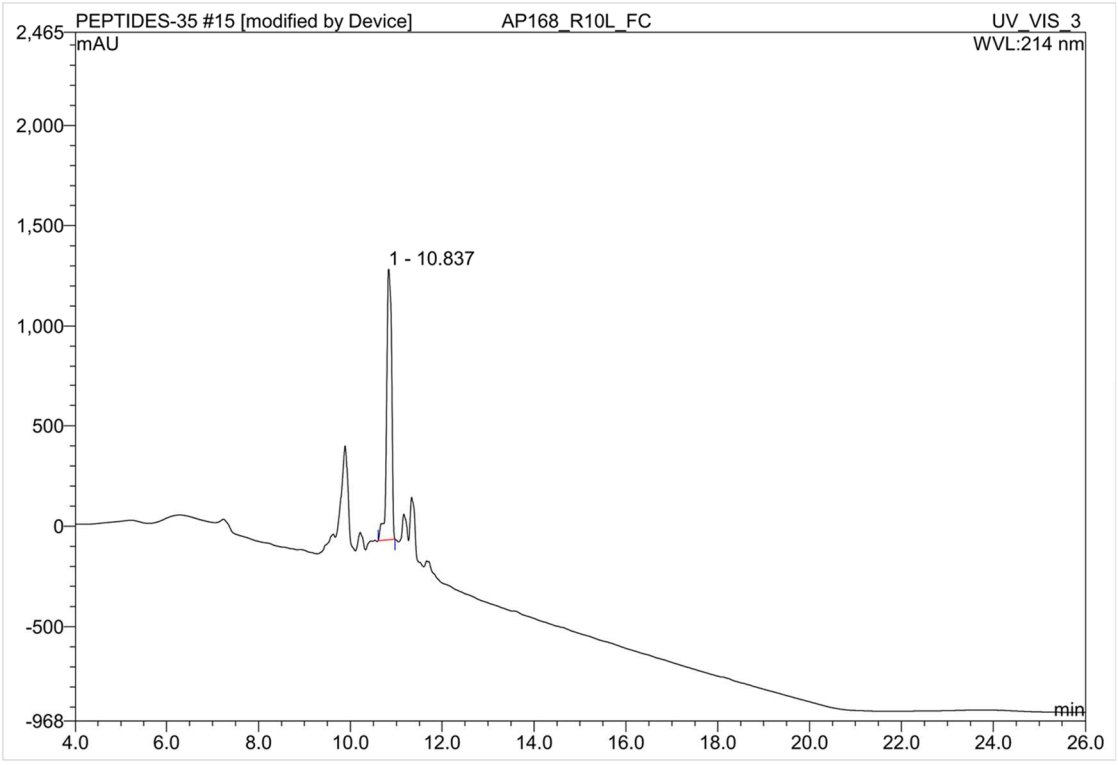

Figure S5.51: HPLC trace of crude teixobactin analogue **5.13** t_R = 10.837 min (gradient: 5-95% ACN in 25 min using A: 0.1% HCOOH in water, B: ACN)

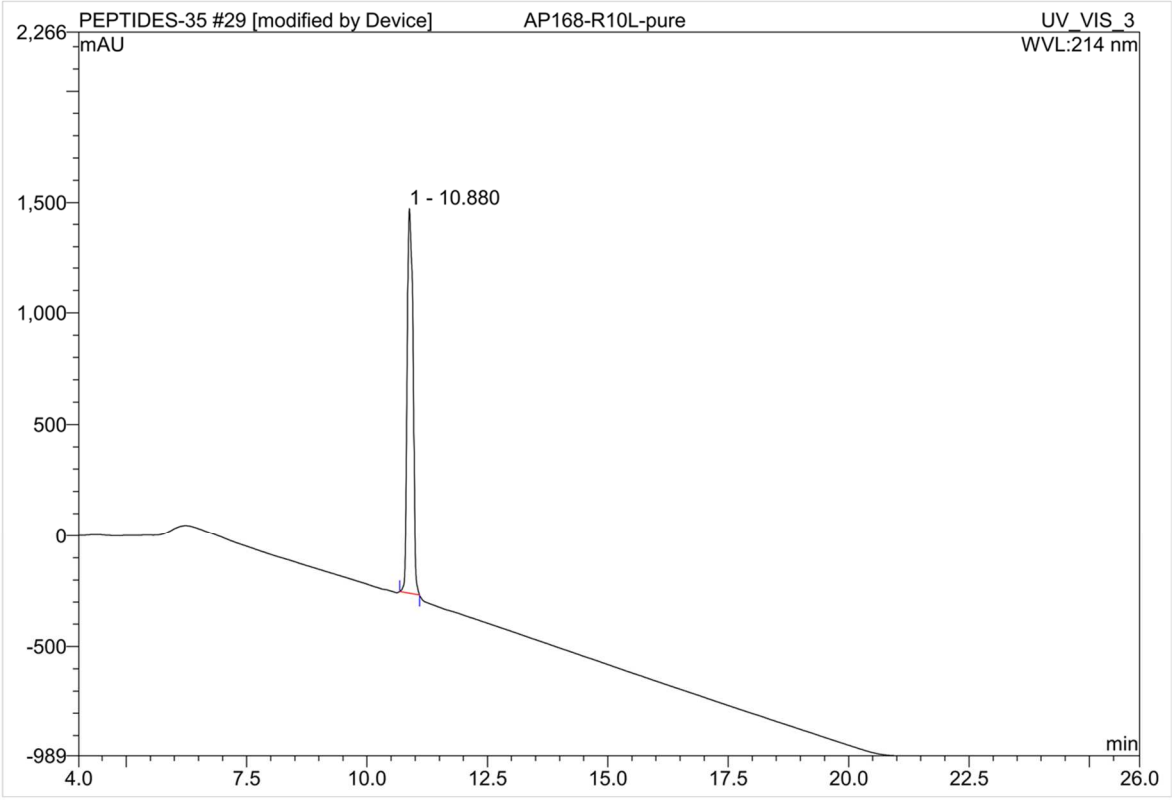

Figure S5.52: HPLC trace of HPLC purified teixobactin analogue **5.13** (gradient: 5-95% ACN in 25 min using A: 0.1% HCOOH in water, B: ACN)

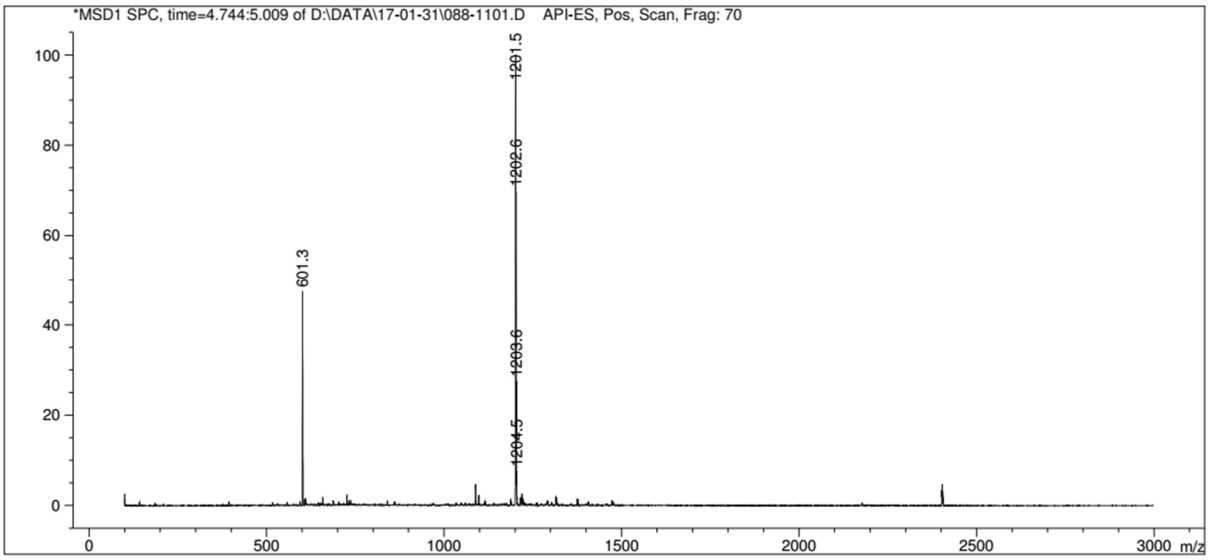

Figure S5.53: ESI-MS from LC-MS of HPLC purified teixobactin analogue **5.13**. Exact mass calcd. for $C_{58}H_{96}N_{12}O_{15}$ = 1200.71, found $M + H^+$ = 1201.5, $M/2 + H^+$ = 601.3.

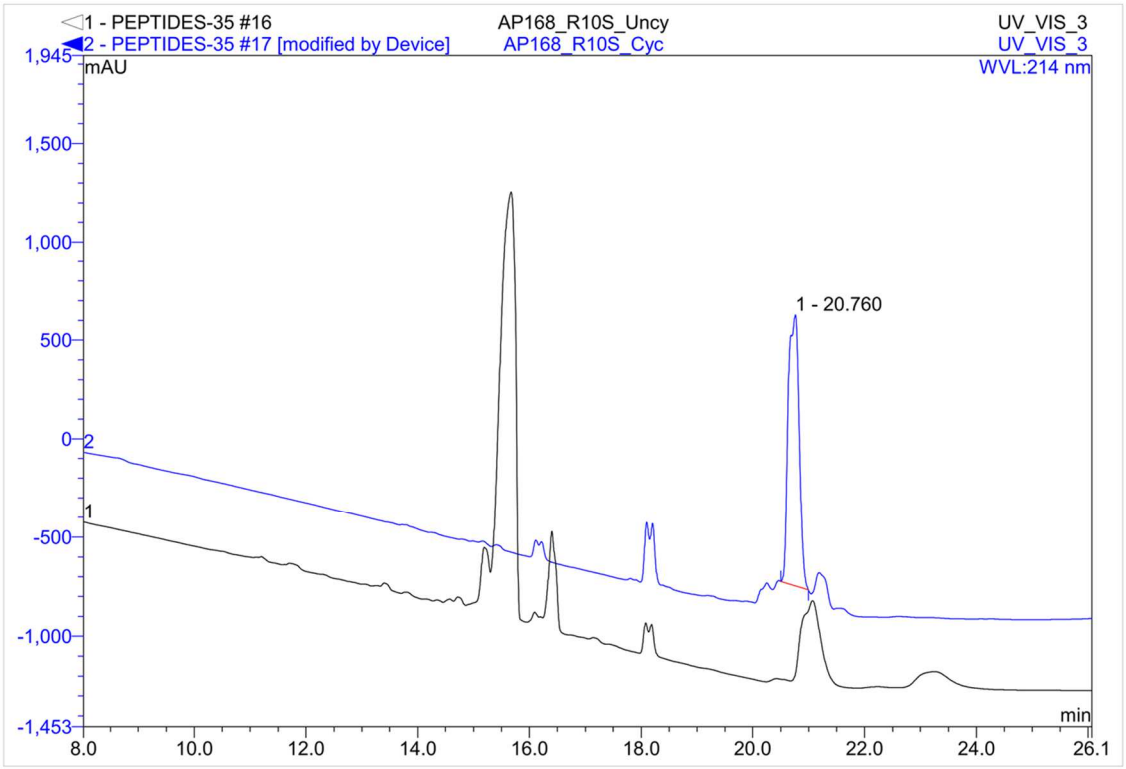

Figure S5.54: HPLC trace showing the progress of cyclisation reaction for the synthesis of analogue **5.14** (i): conversion of the uncyclized protected teixobactin analogue t_R= 15.673 min (shown in black) to the cyclized protected teixobactin analogue t_R = 20.760 min (shown in blue) (Gradient: 5-95% in 25 min)

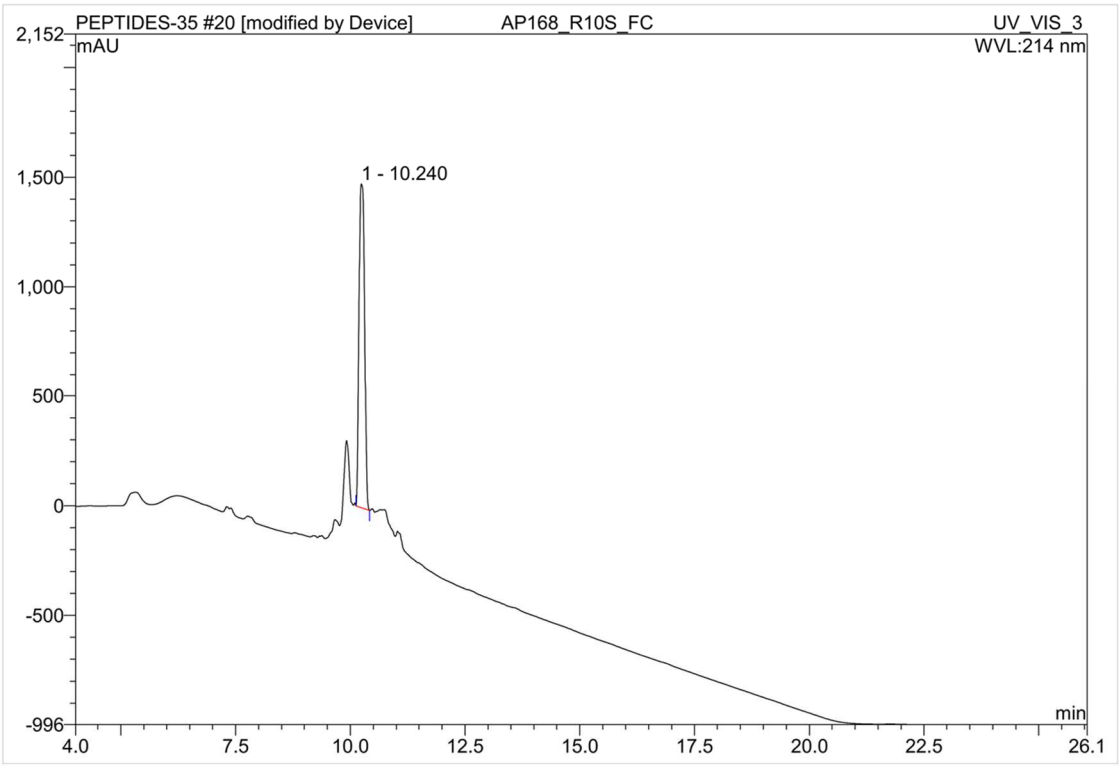

Figure S5.55: HPLC trace of crude teixobactin analogue **5.14** t_R = 10.630 min (gradient: 5-95% ACN in 25 min using A: 0.1% HCOOH in water, B: ACN)

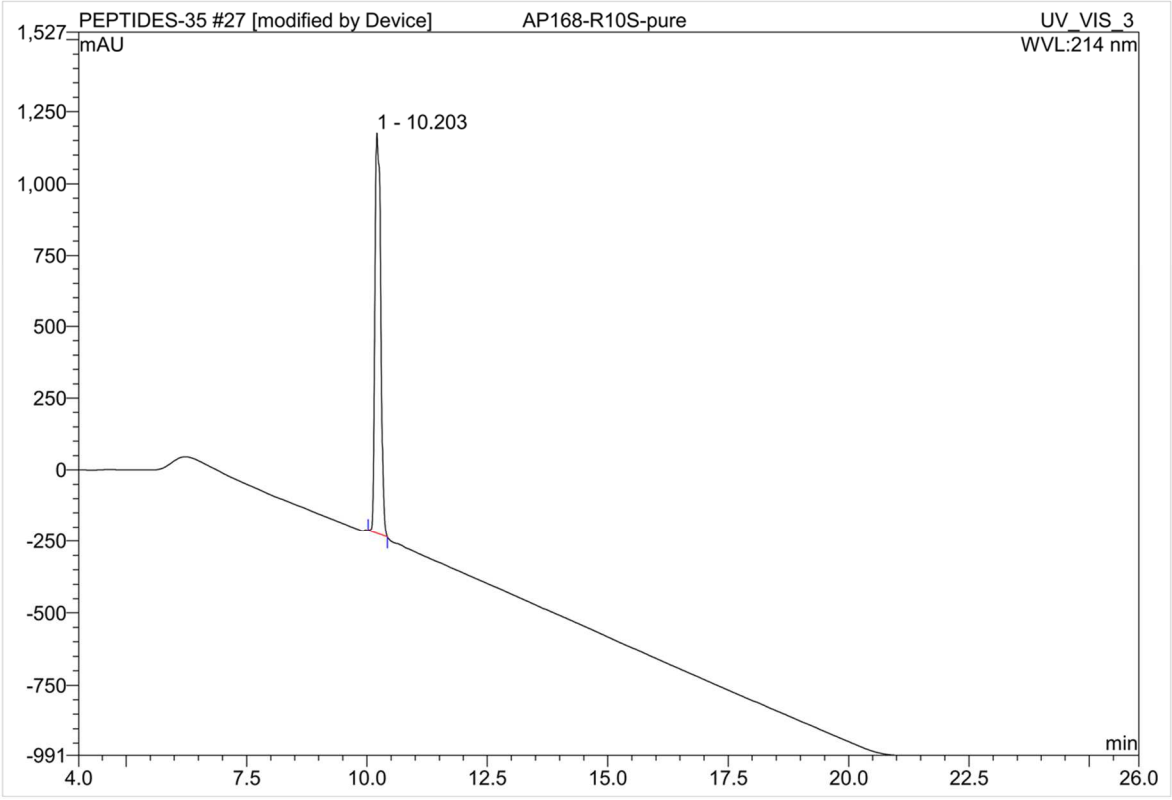

Figure S5.56: HPLC trace of HPLC purified teixobactin analogue **5.14** (gradient: 5-95% ACN in 25 min using A: 0.1% HCOOH in water, B: ACN)

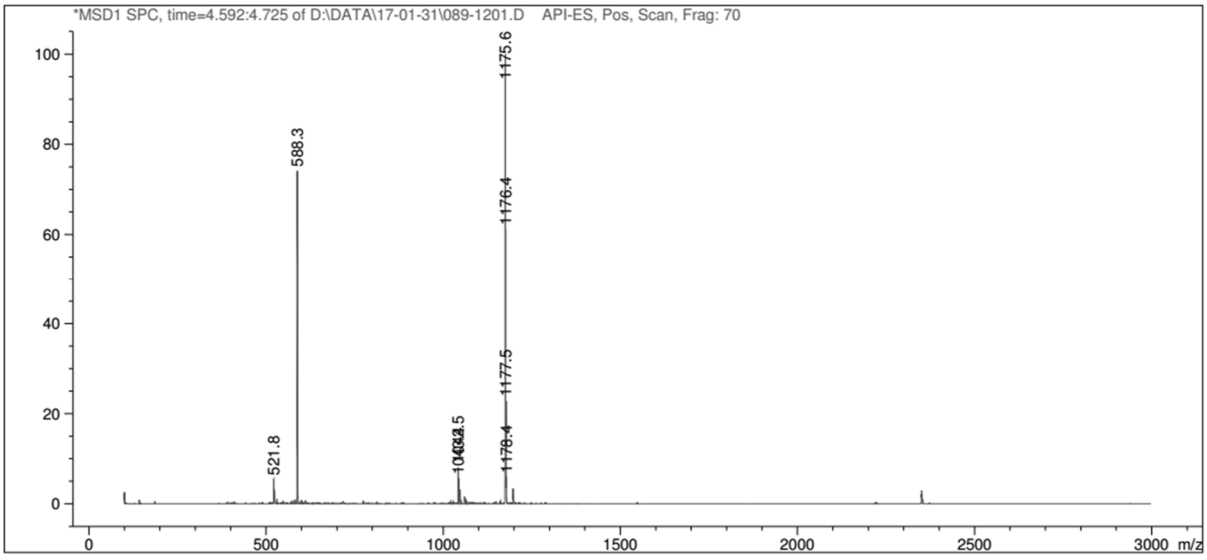

Figure S5.57: ESI-MS from LC-MS of HPLC purified teixobactin analogue **5.14**. Exact mass calcd. for $C_{55}H_{90}N_{12}O_{16}$ = 1174.66, found M + H^+ = 1175.6, M/2 + H^+ = 588.3.

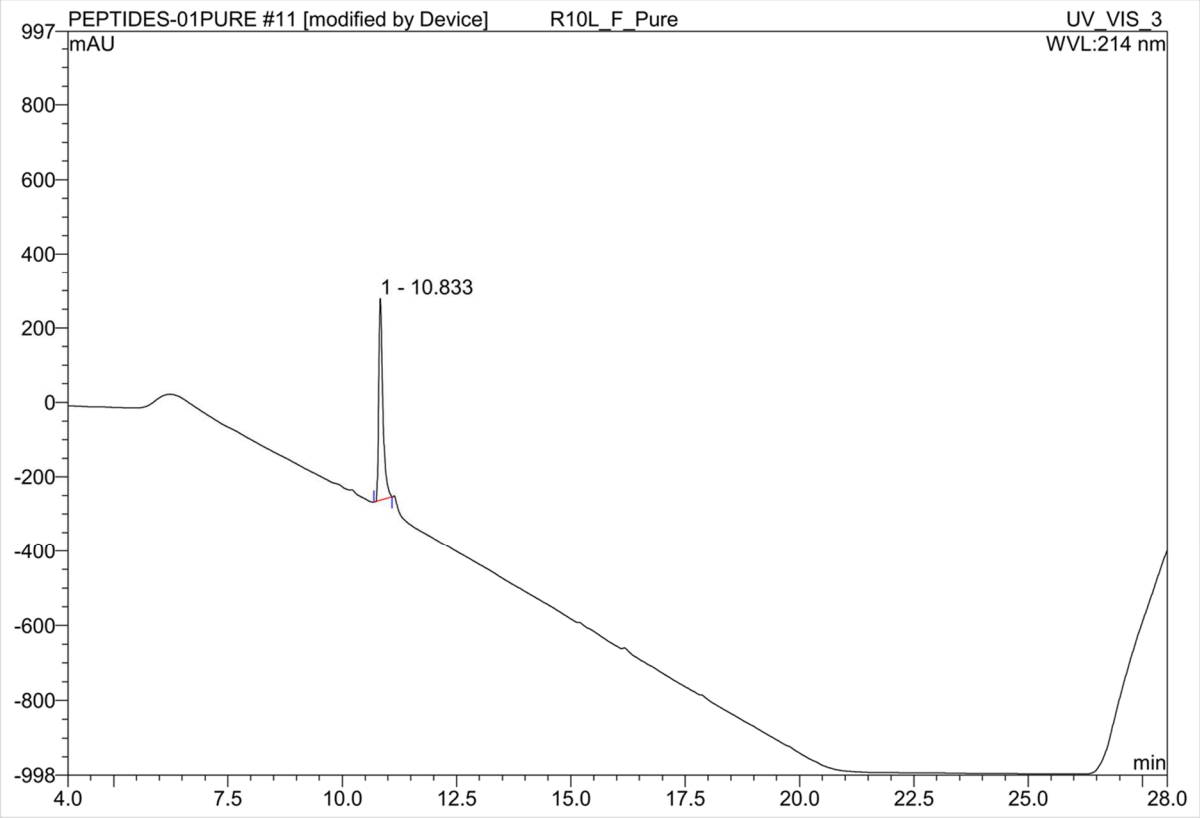

Figure S5.58: HPLC trace of HPLC purified teixobactin analogue **5.15** (gradient: 5-95% ACN in 25 min using A: 0.1% HCOOH in water, B: ACN)

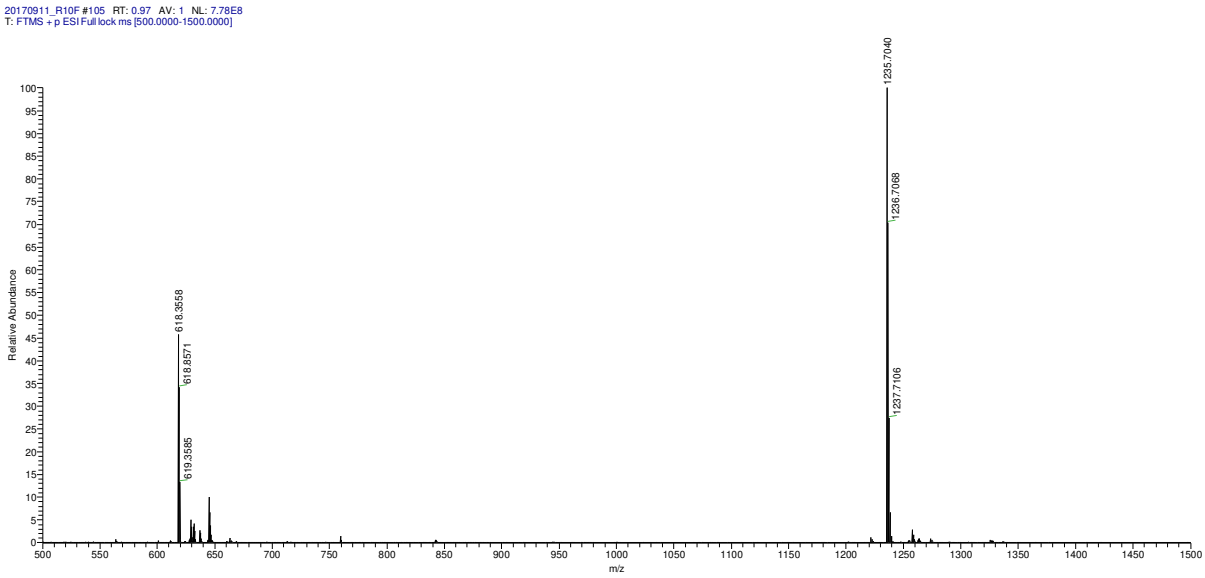

Figure S5.59: HRMS of HPLC purified teixobactin analogue **5.15**. Exact mass calcd. for $C_{61}H_{94}N_{12}O_{15}$ = 1235.6962, found M = 1235.7040, M/2 + H^+ = 618.3558.

V. NMR Analysis

All NMR was carried out in DMSO-d_6 at 27°C on a Bruker Avance III HD 500 MHz spectrometer equipped with a room-temperature broadband probe. The following spectra were utilised in the assignment of 1 mM solutions of the teixobactin mutants: ^{1}H (128k points, 16 scans); ^{13}C{1H} (64k points, 1024 scans); ^{1}H- ^{13}C HSQC (2k and 256 points in the direct and indirect dimensions, 4 scans); ^{1}H- ^{13}C HMBC (2k and 512 points, 8 scans); ^{1}H- ^{1}H TOCSY (2k and 192 points; 32 scans); and ^{1}H- ^{1}H NOESY (2k and 192 points, 48 scans). Spectral analysis was carried out using CCPNMR Analysis.[2] NOE-derived distance restraints obtained from the NOESY spectra were used in structural calculations using Cyana 2.1[3] prior to energy minimisation using Gromacs 5.1[4] and RSFF2 forcefield.[5] Geranyl pyrophosphate titrations were carried out using 0.5 mM teixobactin mutants and the following molar equivalents of geranyl pyrophosphate: 0.0, 0.1, 0.2, 0.4, 0.6, 0.8, 1.0, 1.25 and 1.5. Geranyl pyrophosphate was freeze-dried and dissolved in MeOH:D_2O (7:3, 1 mM concentration) for the titration experiments. ^{1}H- ^{1}H TOCSY spectra were acquired and assigned at each titration point to yield accurate chemical shift perturbations (CSPs). Residue-specific binding isotherms obtained from Hα CSPs were fit using the Hill equation with a Hill coefficient of 1.0 or > 1.0 in the case of sigmoidal curves. (Hα resonances were chosen for CSP analysis because they are common to each residue and because they were resolved for the majority of residues.) Full spectrum analysis of the titration was carried out using TREND[6], which uses principal component analysis (PCA) to give an overall binding isotherm free from the influence of intermediate exchange.

			5.1	**5.2**	**5.3**	**5.4**	**5.5**	**5.6**	**5.7**	**5.8**
1	D-NmPhe	HNm								2.165
1	D -NmPhe	H	8.103							
1	D -NmPhe	Hα	4.339	3.184	3.244	3.259	3.258	3.262	3.264	3.278
1	D -NmPhe	Hβ	**1.190**	2.680 2.805	2.693 2.775	2.690 2.782	2.690 2.786	2.692 2.791	2.690 2.789	2.711 2.782
1	D -NmPhe	Hδ*			7.190	7.180				7.184
1	D -NmPhe	Hε*								7.240
1	D -NmPhe	Hζ								7.175
2	Ile	H	8.045	8.046	7.898	7.943	7.933	7.946	7.944	7.950
2	Ile	Hα	4.215	4.313	4.146	4.215	4.185	4.199	4.197	4.198
2	Ile	Hβ	1.798	**1.123**	1.648	1.686	1.675	1.679	1.679	1.664
2	Ile	Hγ1	1.109 1.390		0.901 1.226	0.913 1.237	0.902 1.243	0.907 1.250	0.906 1.250	0.907 1.234
2	Ile	Hγ2*	0.832		0.735	0.745	0.739	0.734	0.736	0.733
2	Ile	Hδ1*	0.832		0.735	0.745	0.739	0.734	0.736	0.733
3	Ser	H	7.968	7.964	8.017	7.971	7.974	7.946	7.949	7.918

3	Ser	Hα	4.286	4.276	4.309	4.284	4.293	4.305	4.299	4.316
3	Ser	Hβ	3.588 3.862	3.566 3.614	**1.218**	3.534 3.604	3.542 3.627	3.534 3.608	3.534 3.606	3.544 3.598
3	Ser	Hγ	5.003	5.022		4.987	5.020	4.999	5.039	4.958
4	$_D$ -Gln	H	7.820	8.025	7.989	7.884	7.938	7.922	7.966	7.958
4	$_D$ -Gln	Hα	4.287	4.290	4.313	4.332	4.270	4.292	4.299	4.306
4	$_D$ -Gln	Hβ	2.050 2.119	2.093 2.093	2.072 2.072	**1.182**	2.087 2.087	2.068 2.068	2.086 2.086	2.087 2.094
4	$_D$ -Gln	Hγ	1.712 1.888	1.734 1.898	1.694 1.871		1.699 1.898	1.688 1.858	1.687 1.869	1.704 1.872
4	$_D$ -Gln	Hε2	6.782 7.214	6.783 7.220	6.760 7.260		6.760 7.219	6.747 7.204	6.798 7.235	6.789 7.247
5	$_D$ -Ile	H	7.710	7.680	7.749	7.766	8.015	7.801	7.824	7.712
5	D-Ile	Hα	4.379	4.400	4.380	4.265	4.326	4.193	4.244	4.367
5	D-Ile	Hβ	1.779	1.788	1.783	1.728	**1.209**	1.690	1.721	1.772
5	D-Ile	Hγ1	1.062 1.327	1.074 1.295	1.073 1.299	1.051 1.396		1.037 1.404	1.045 1.409	1.074 1.317
5	D-Ile	Hγ2*	0.774	0.765	0.775	0.806		0.787	0.804	0.782
5	D-Ile	Hδ1*	0.774	0.765	0.775	0.806		0.787	0.804	0.784
6	Ile	H	7.957	7.929	7.918	7.889	7.807	8.074	7.992	7.970
6	Ile	Hα	4.269	4.286	4.292	4.280	4.314	4.405	4.191	4.160
6	Ile	Hβ	1.780	1.776	1.776	1.759	1.747	**1.232**	1.778	1.757
6	Ile	Hγ1	1.104 1.418	1.090 1.408	1.092 1.411	1.087 1.408	1.072 1.402		1.135 1.414	1.150 1.416
6	Ile	Hγ2*	0.821	0.816	0.824	0.815	0.810		0.814	0.822
6	Ile	Hδ1*	0.821	0.816	0.819	0.815	0.810		0.814	0.822
7	Ser	H	9.087	9.207	9.188	9.149	9.282	9.565	8.521	8.607
7	Ser	Hα	4.385	4.404	4.402	4.394	4.413	4.279	4.336	4.233
7	Ser	Hβ	3.706 3.768	3.703 3.775	3.701 3.775	3.694 3.767	3.711 3.773	3.783 3.820	**1.335**	3.693 3.694
7	Ser	Hγ	5.652	5.671	5.674	5.665	5.646	5.718		
8	D-Thr	H	8.717	8.856	8.865	8.897	8.847	8.679	8.905	7.987
8	D-Thr	Hα	4.639	4.655	4.650	4.642	4.649	4.647	4.554	4.568
8	D-Thr	Hβ	5.363	5.366	5.362	5.360	5.363	5.351	5.330	5.355
8	D-Thr	Hγ2*	1.105	1.097	1.097	1.094	1.097	1.059	1.112	1.136
9	Ala	H	8.217	8.203	8.210	8.210	8.193	8.103	8.204	8.101

9	Ala	Ha	3.932	3.931	3.933	3.933	3.931	3.908	3.992	3.950
9	Ala	Hβ*	1.294	1.280	1.283	1.282	1.286	1.248	1.351	1.340
10	Arg	H	8.156	8.219	8.235	8.233	8.206	8.349	8.274	7.687
10	Arg	Hα	4.275	4.274	4.280	4.273	4.285	4.271	4.265	4.395
10	Arg	Hβ	1.633 1.767	1.640 1.762	1.641 1.798	1.647 1.765	1.623 1.766	1.585 1.740	1.722 1.795	**1.336**
10	Arg	Hγ	1.429 1.493	1.418 1.487	1.420 1.488	1.416 1.490	1.420 1.484	1.406 1.479	1.438 1.500	
10	Arg	Hδ	3.124 3.124	3.115 3.115	3.127 3.127	3.109 3.109	3.119 3.119	3.112 3.112	3.117 3.117	
10	Arg	Hε	7.693	7.733	7.735	7.750	7.745	7.634	7.911	
10	Arg	Hη1			7.115 7.115	7.125 7.125				
10	Arg	Hη2			7.248 7.248	7.125 7.125				
11	Ile	H	8.390	8.499	8.502	8.495	8.48	8.495	8.104	7.562
11	Ile	Hα	4.033	4.030	4.033	4.033	4.033	4.036	4.054	4.027
11	Ile	Hβ	1.686	1.681	1.675	1.668	1.682	1.609	1.712	1.680
11	Ile	Hγ1	1.092 1.434	1.086 1.423	1.093 1.414	1.091 1.422	1.103 1.432	1.071 1.406	1.113 1.416	1.100 1.448
11	Ile	Hγ2*	0.811	0.798	0.806	0.814	0.800	0.763	0.814	0.829
11	Ile	Hδ1*	0.811	0.798	0.806	0.814	0.800	0.763	0.814	0.830

Table S5.2: Proton chemical shifts obtained from the mutants used in this study. The residue replaced by alanine is shown with a grey background, with the introduced methyl group shown in bold.

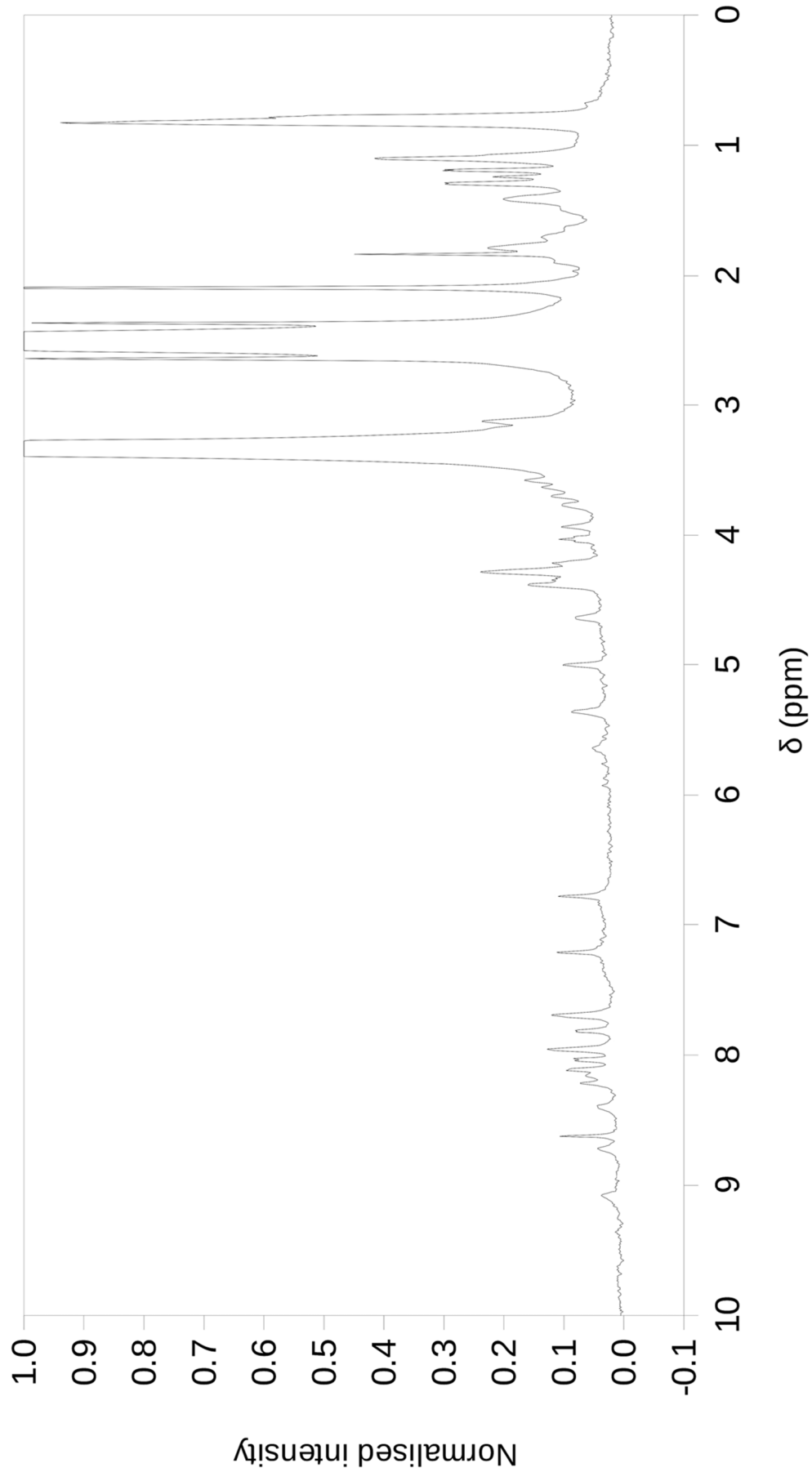

Figure S5.60: 1H NMR spectra obtained from compound **5.1**

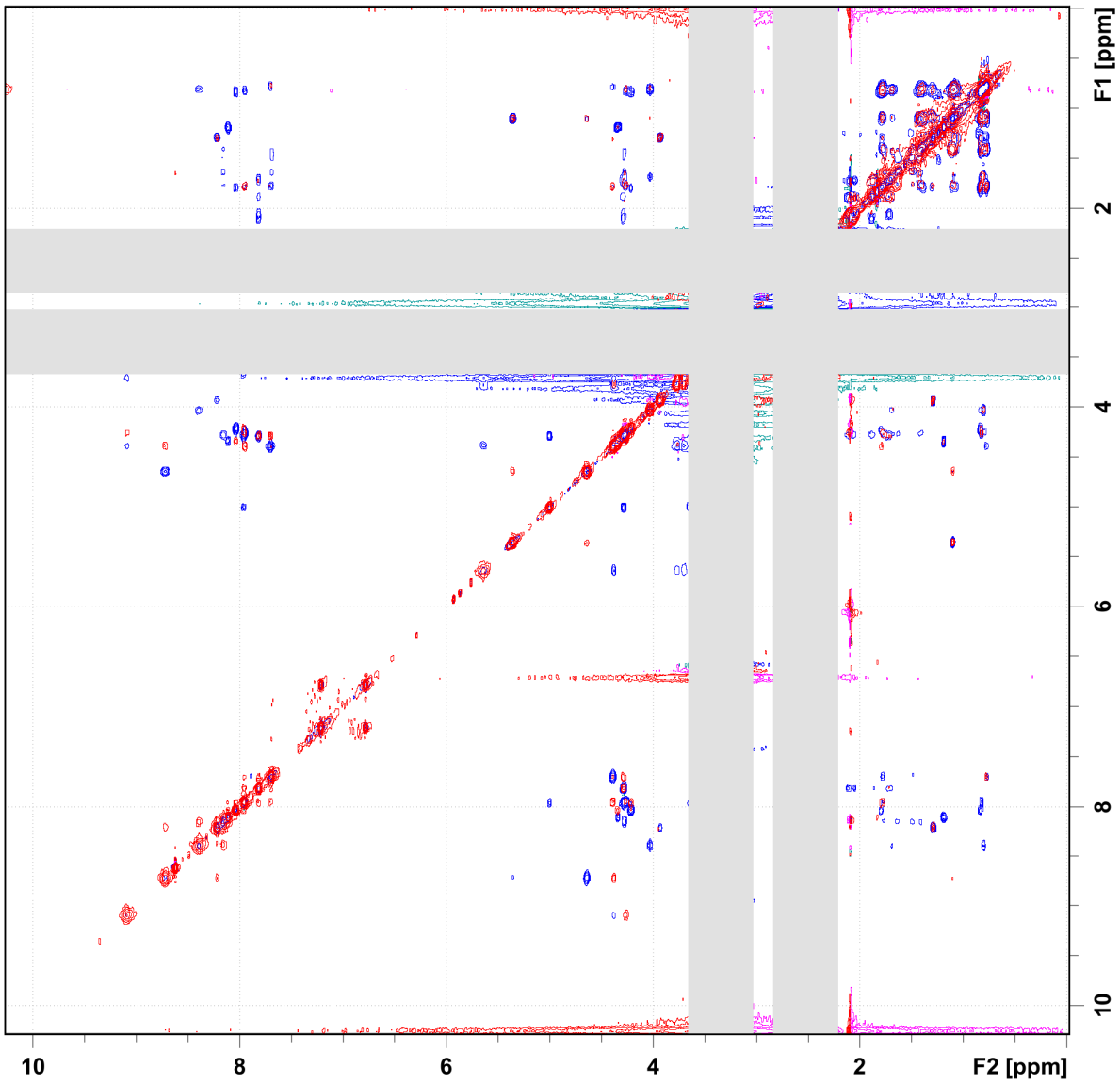

Figure S5.61: ^{1}H-^{1}H TOCSY (blue) and ^{1}H-^{1}H NOESY (red) spectra obtained from compound **5.1**. For clarity, grey boxes obscure solvent signals.

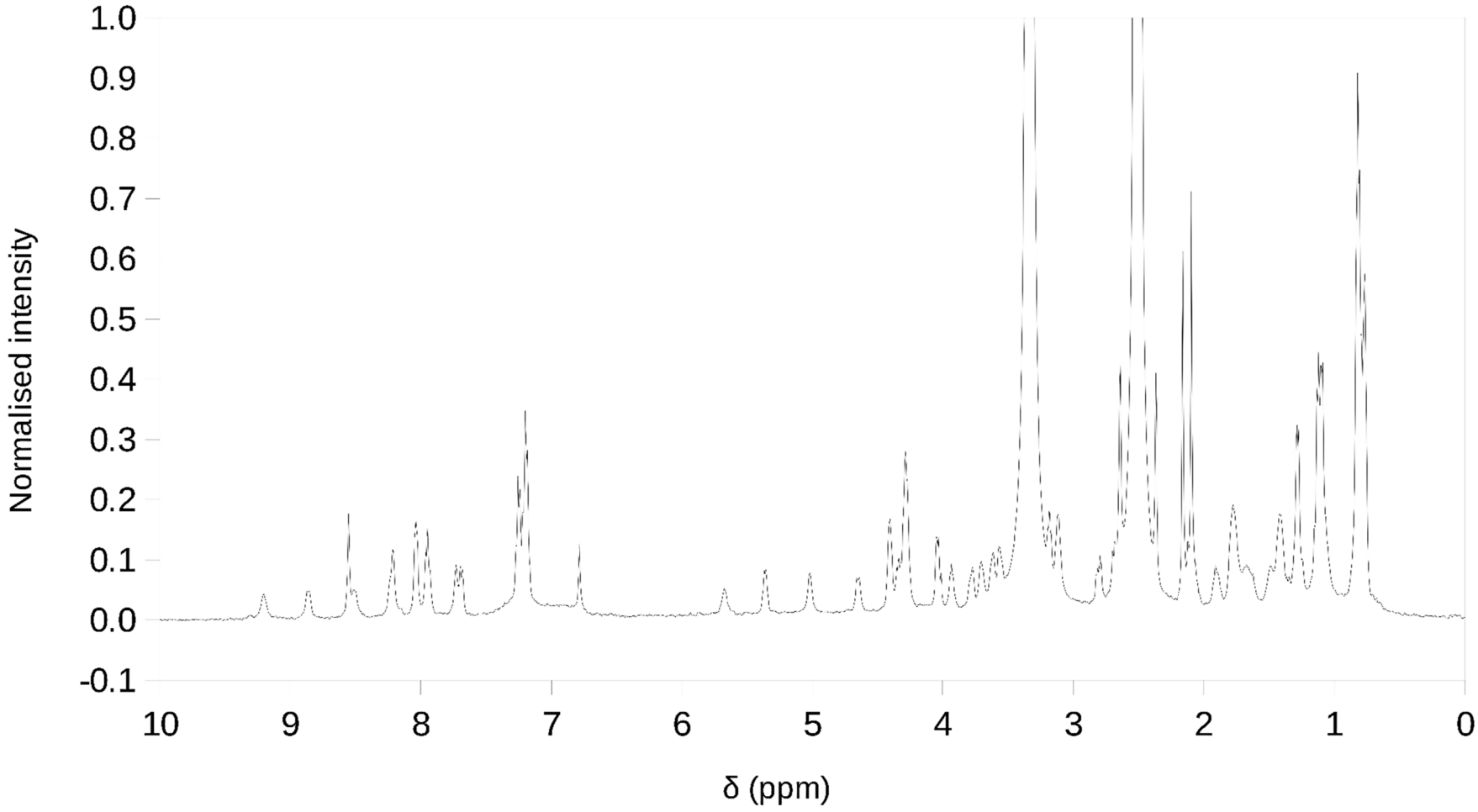

Figure S5.62: 1H NMR spectra obtained from compound **5.2**

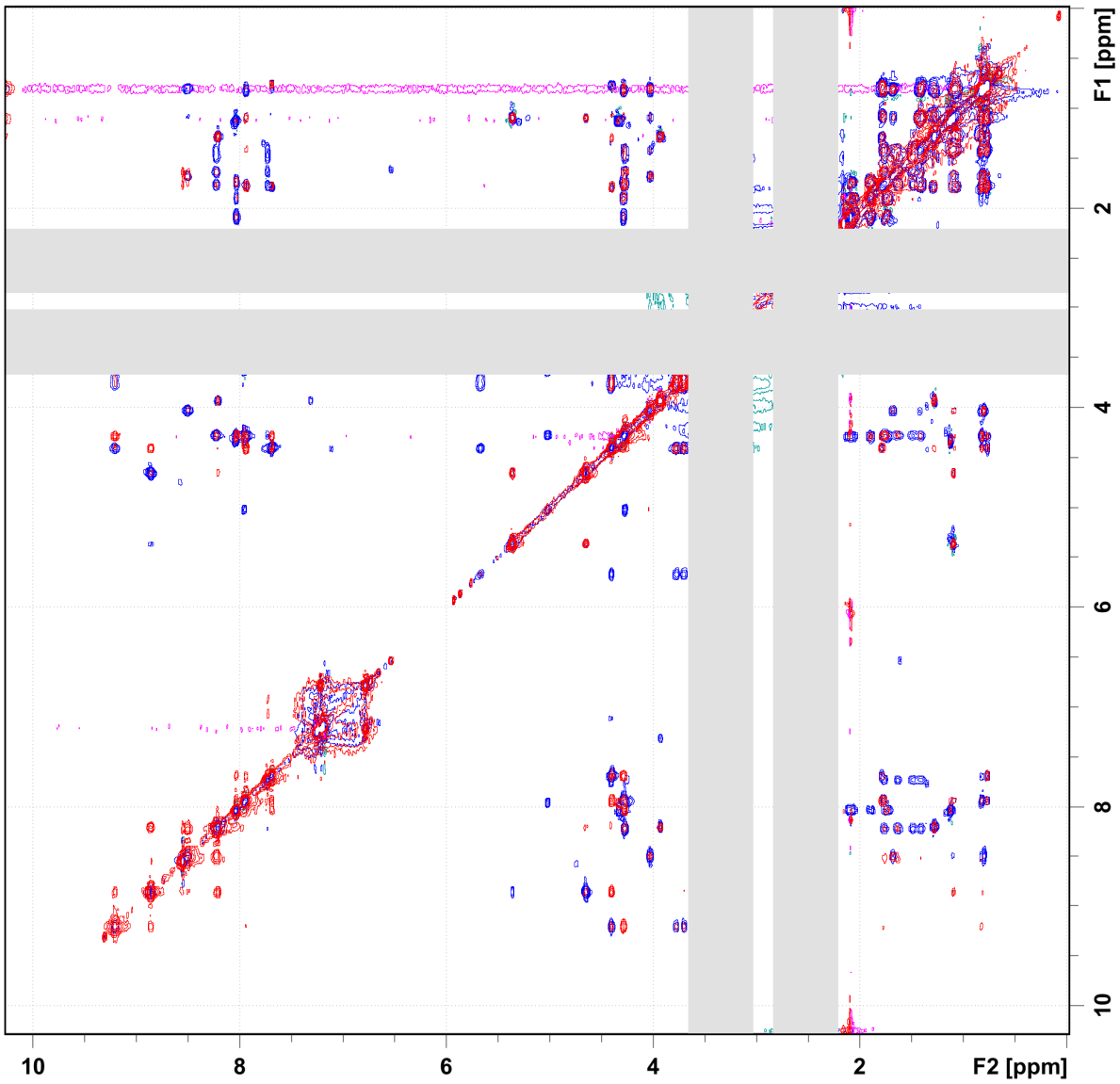

Figure S5.63: ^{1}H-^{1}H TOCSY (blue) and ^{1}H-^{1}H NOESY (red) spectra obtained from compound **5.2**. For clarity, grey boxes obscure solvent signals.

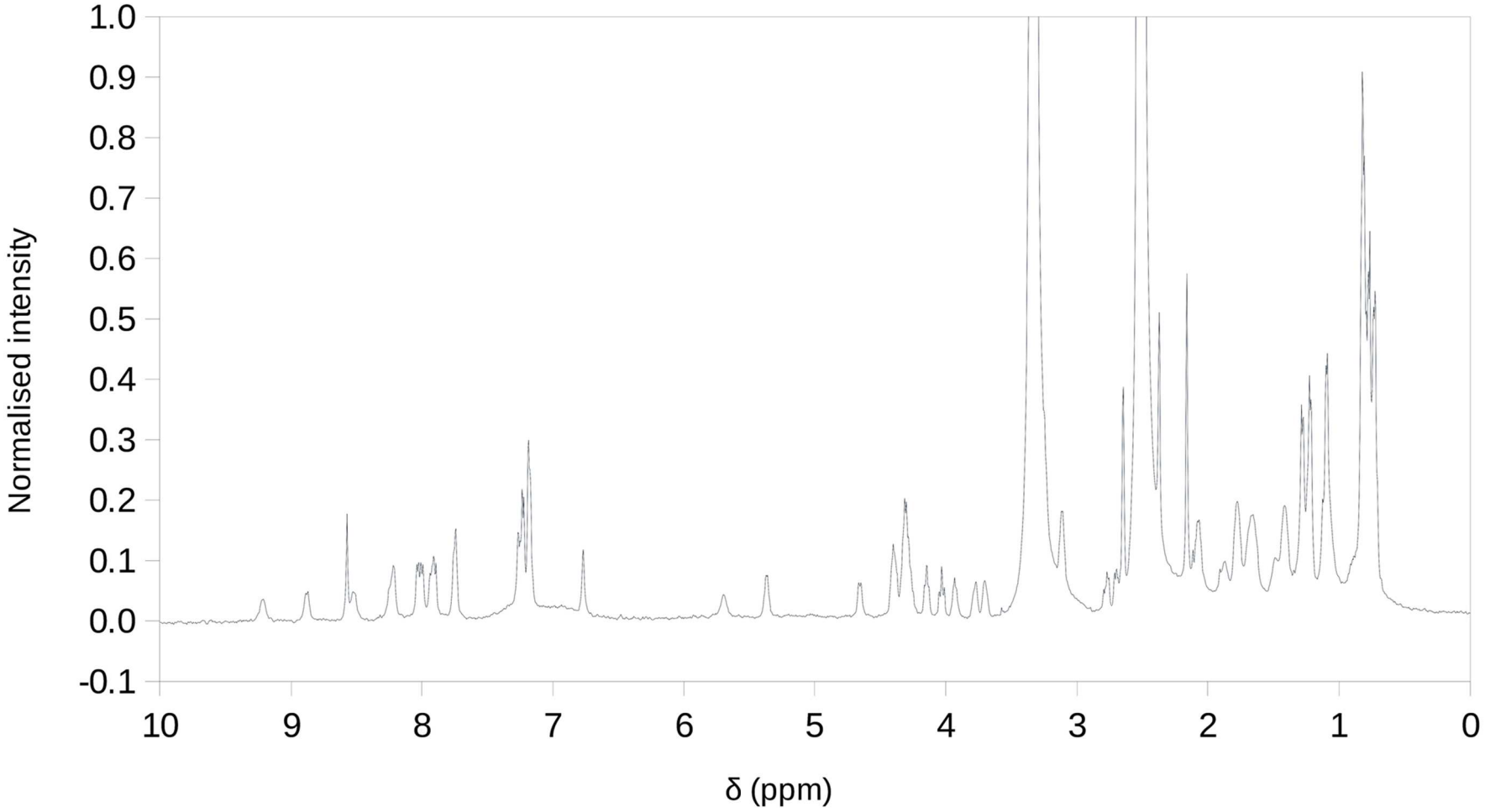

Figure S5.64: 1H NMR spectra obtained from compound **5.3**

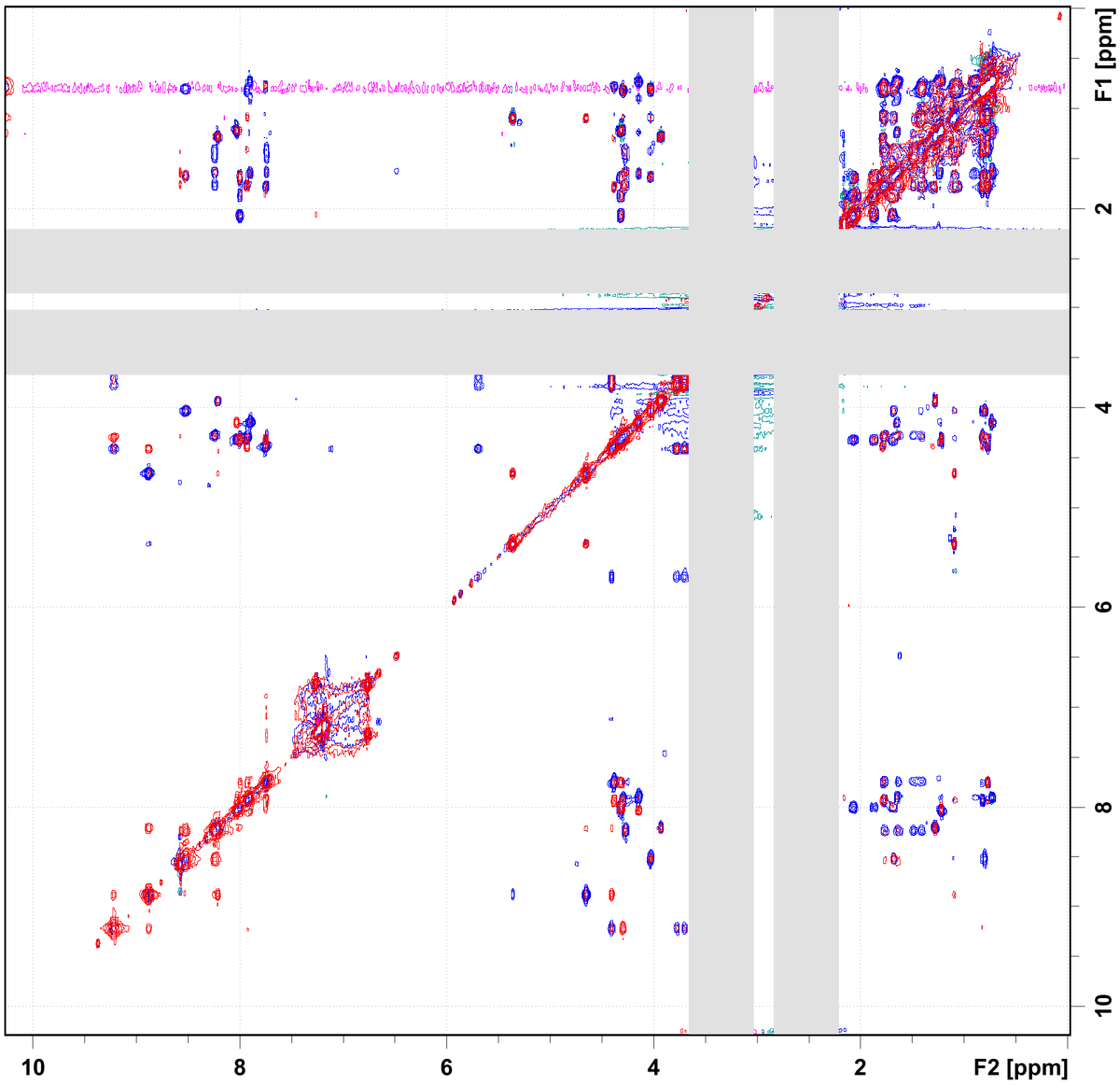

Figure S5.65: ^{1}H-^{1}H TOCSY (blue) and ^{1}H-^{1}H NOESY (red) spectra obtained from compound **5.3**. For clarity, grey boxes obscure solvent signals.

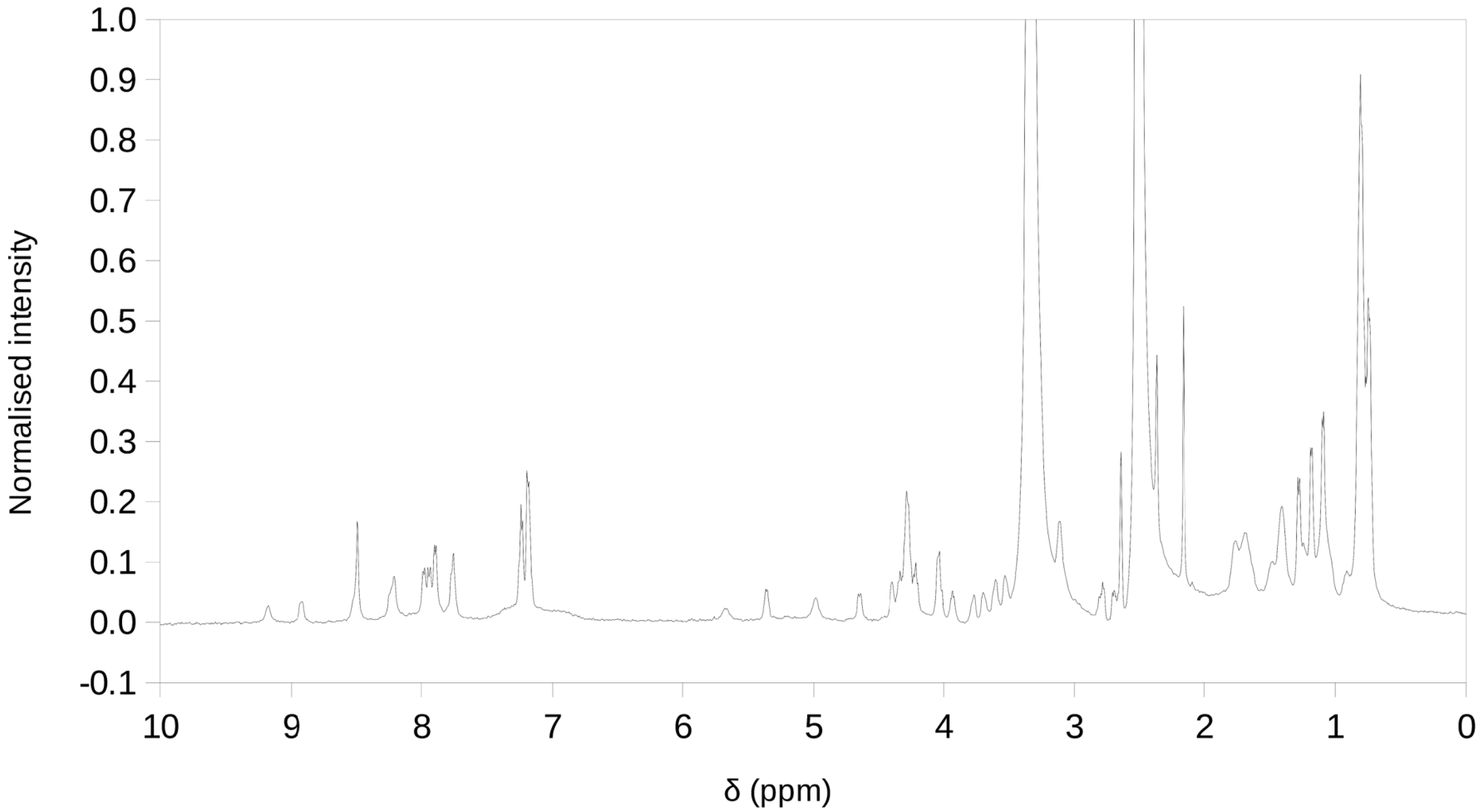

Figure S5.66: ^{1}H NMR spectra obtained from compound **5.4**

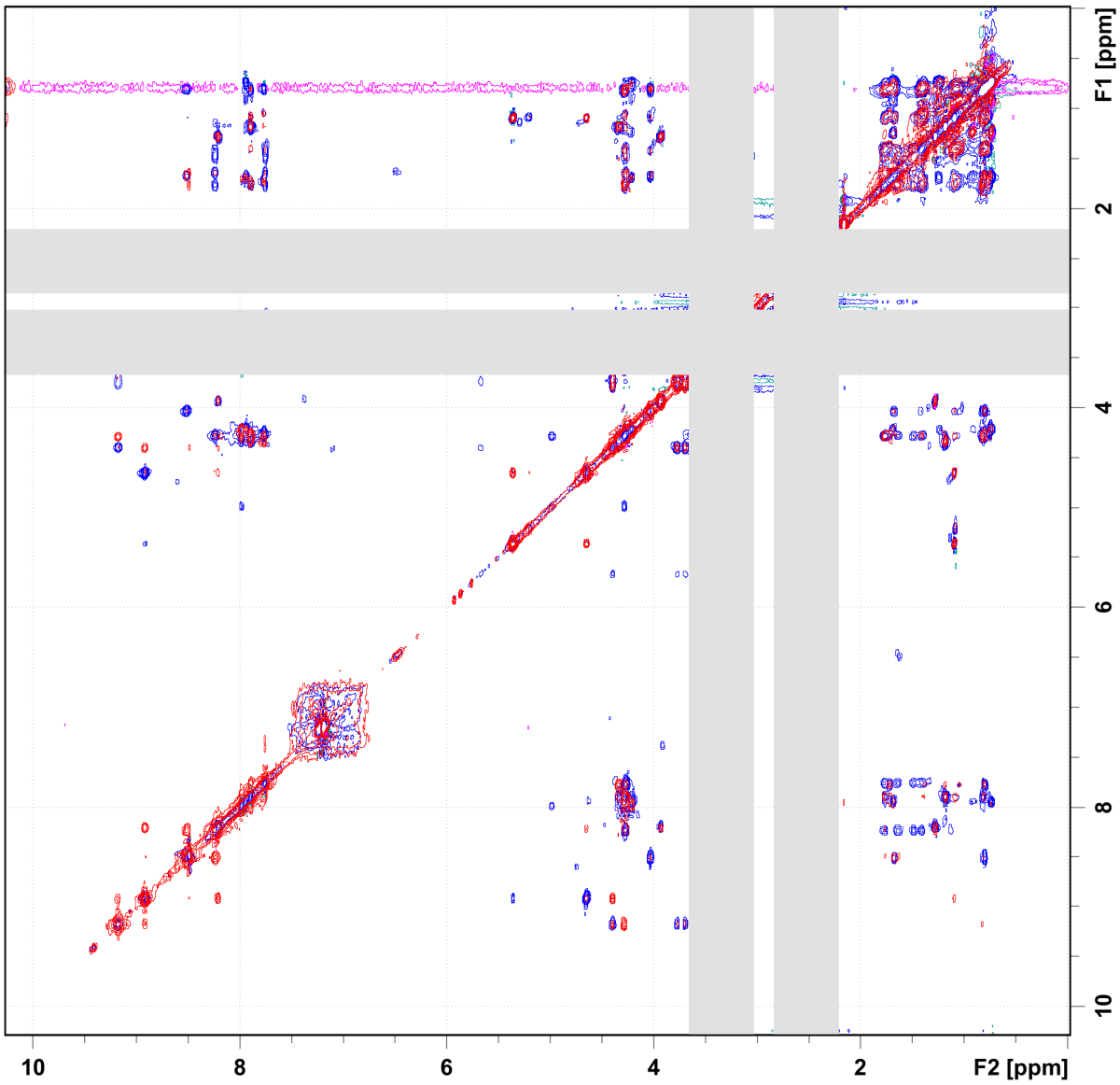

Figure S5.67: ^{1}H-^{1}H TOCSY (blue) and ^{1}H-^{1}H NOESY (red) spectra obtained from compound **5.4**. For clarity, grey boxes obscure solvent signals.

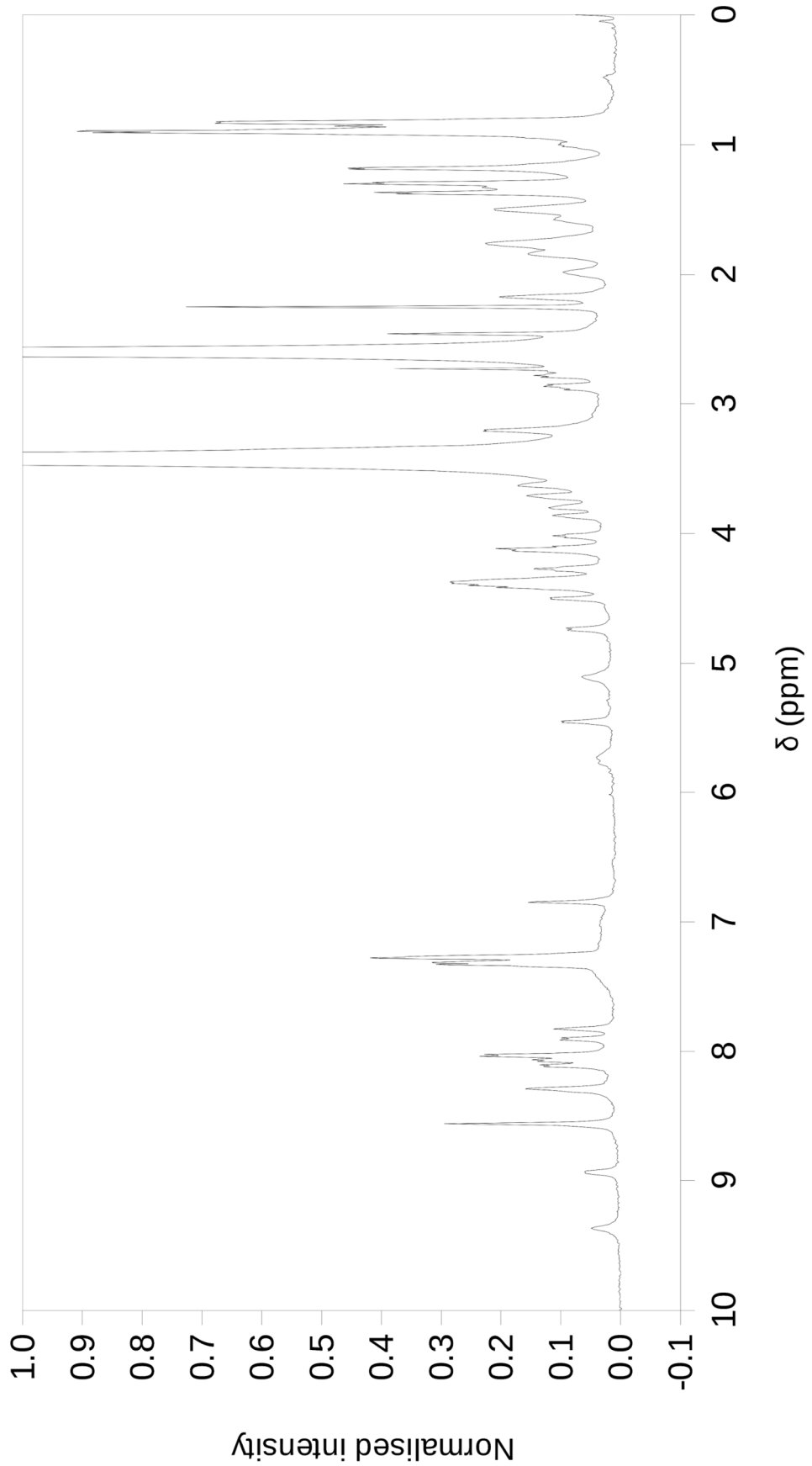

Figure S5.68: ^{1}H NMR spectra obtained from compound **5.5**

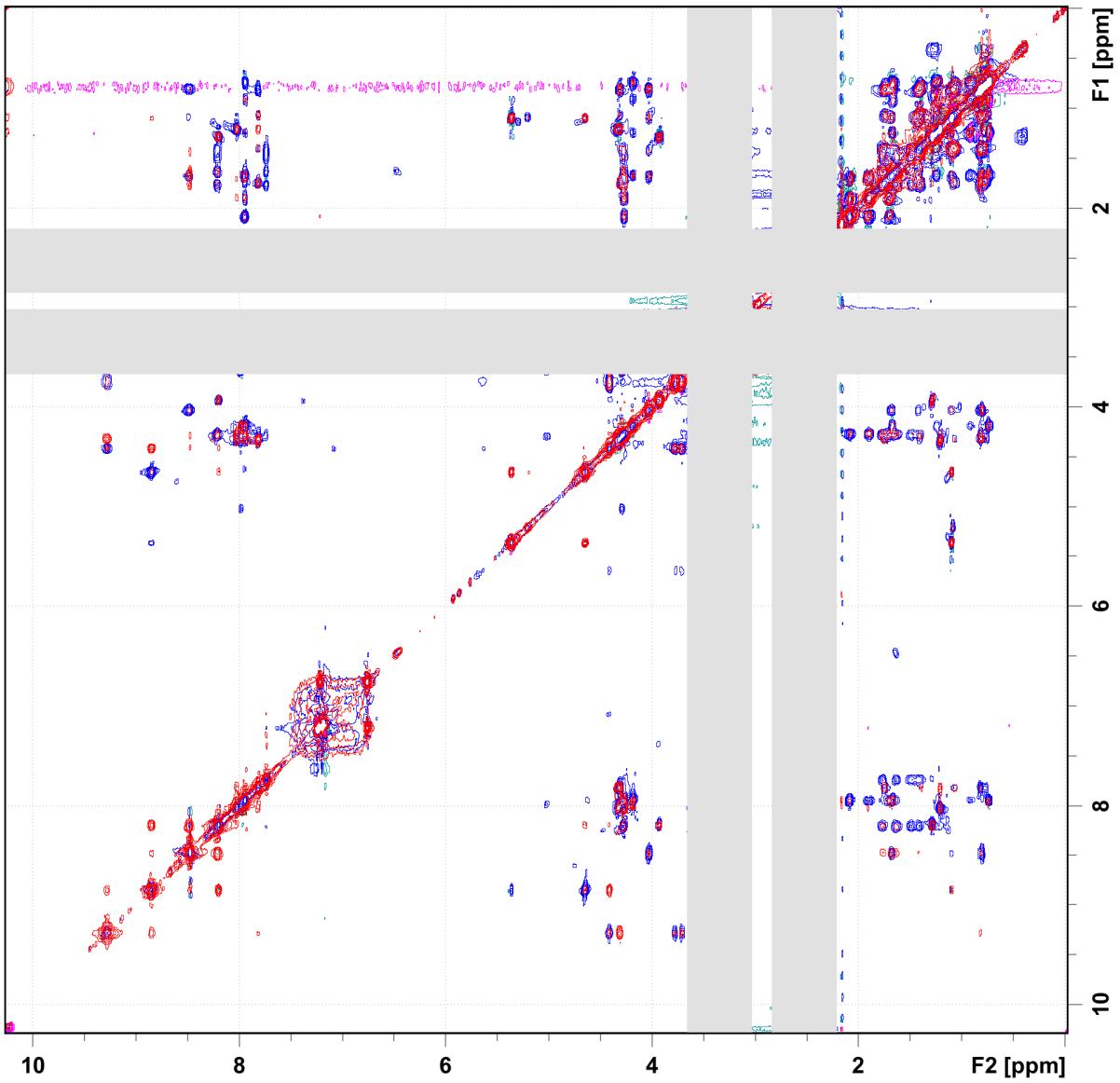

Figure S5.69: ^{1}H-^{1}H TOCSY (blue) and ^{1}H-^{1}H NOESY (red) spectra obtained from compound **5.5**. For clarity, grey boxes obscure solvent signals.

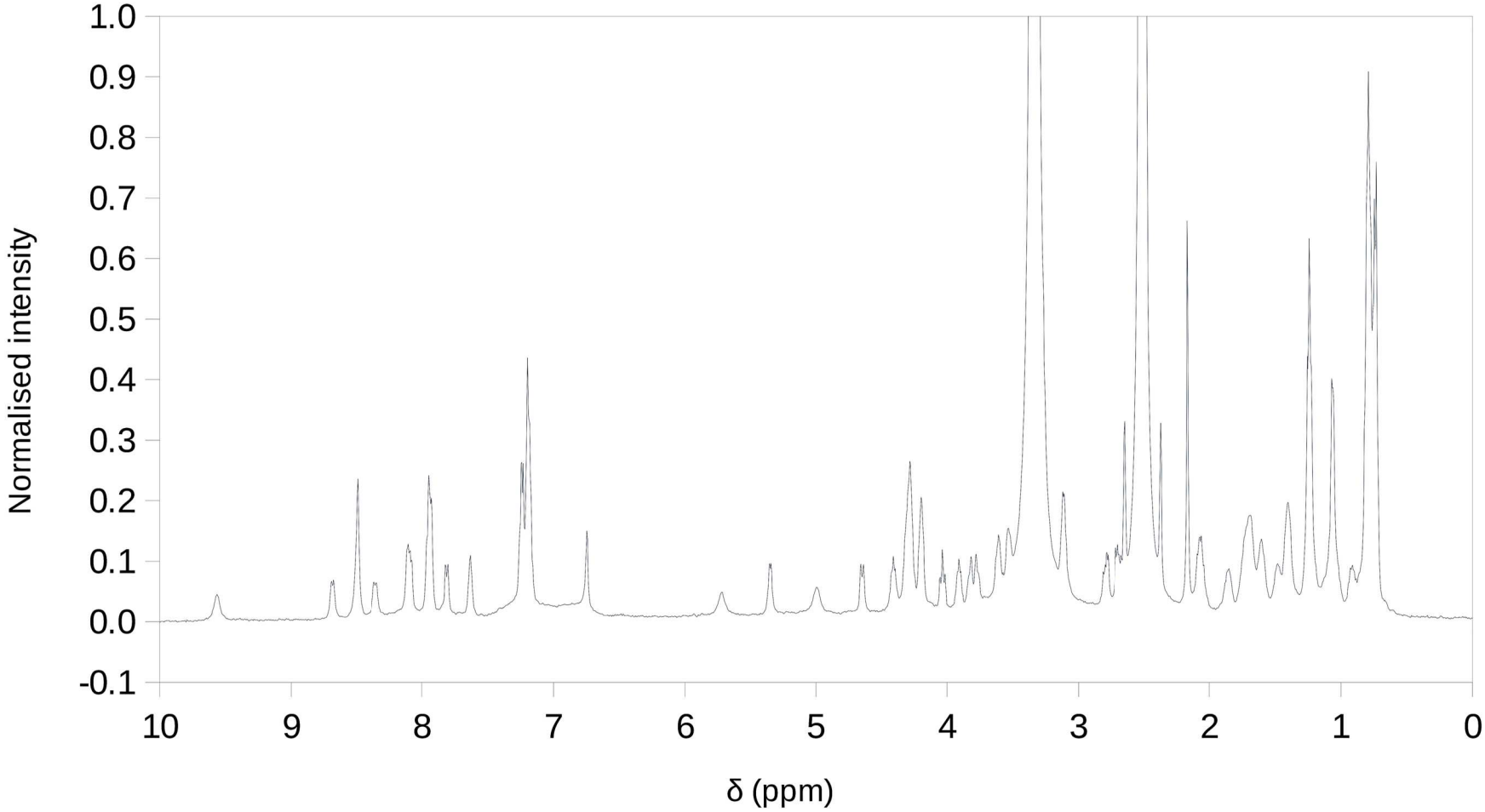

Figure S5.70: ^{1}H NMR spectra obtained from compound **5.6**

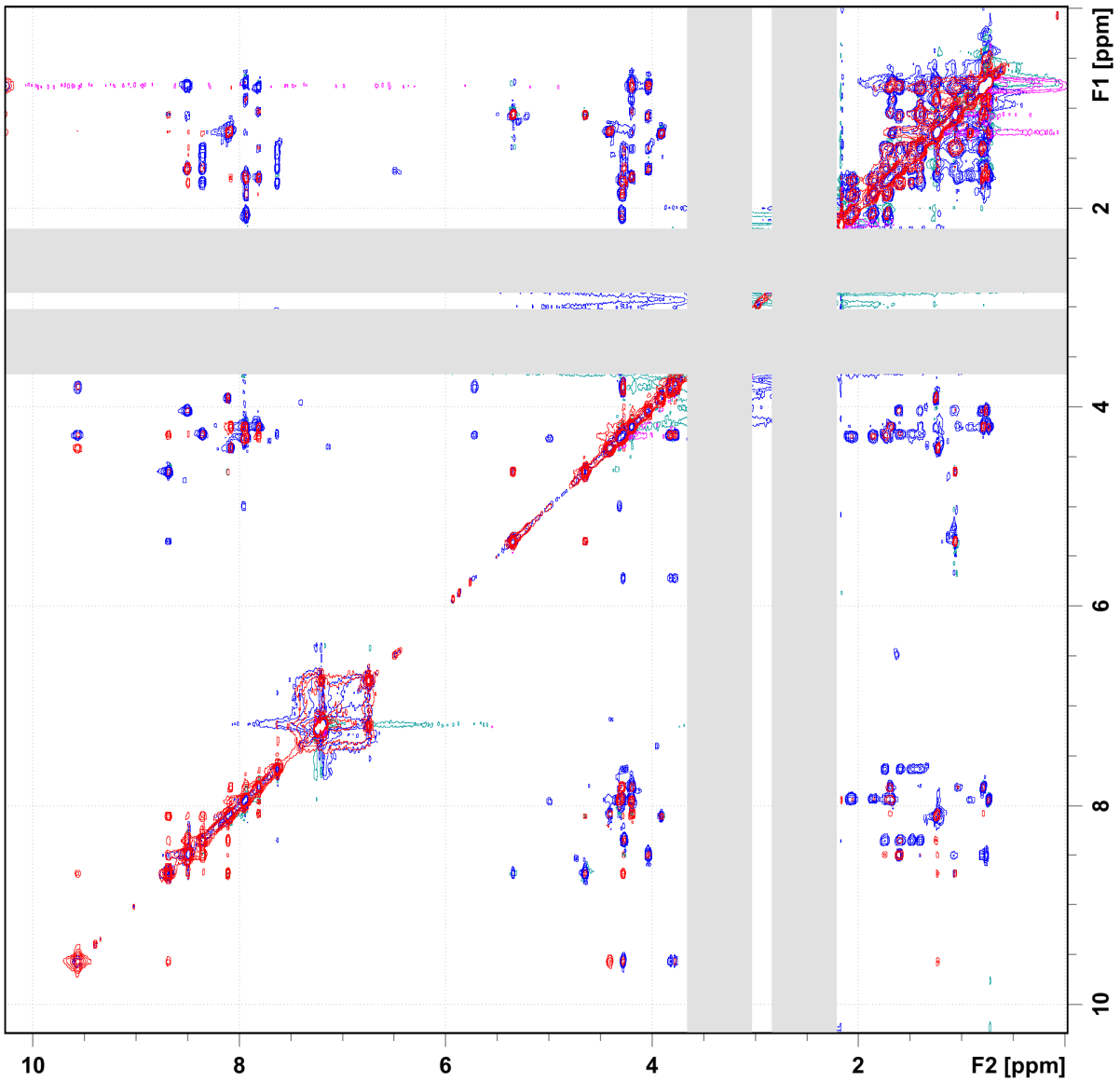

Figure S5.71: ^{1}H-^{1}H TOCSY (blue) and ^{1}H-^{1}H NOESY (red) spectra obtained from compound **5.6**. For clarity, grey boxes obscure solvent signals.

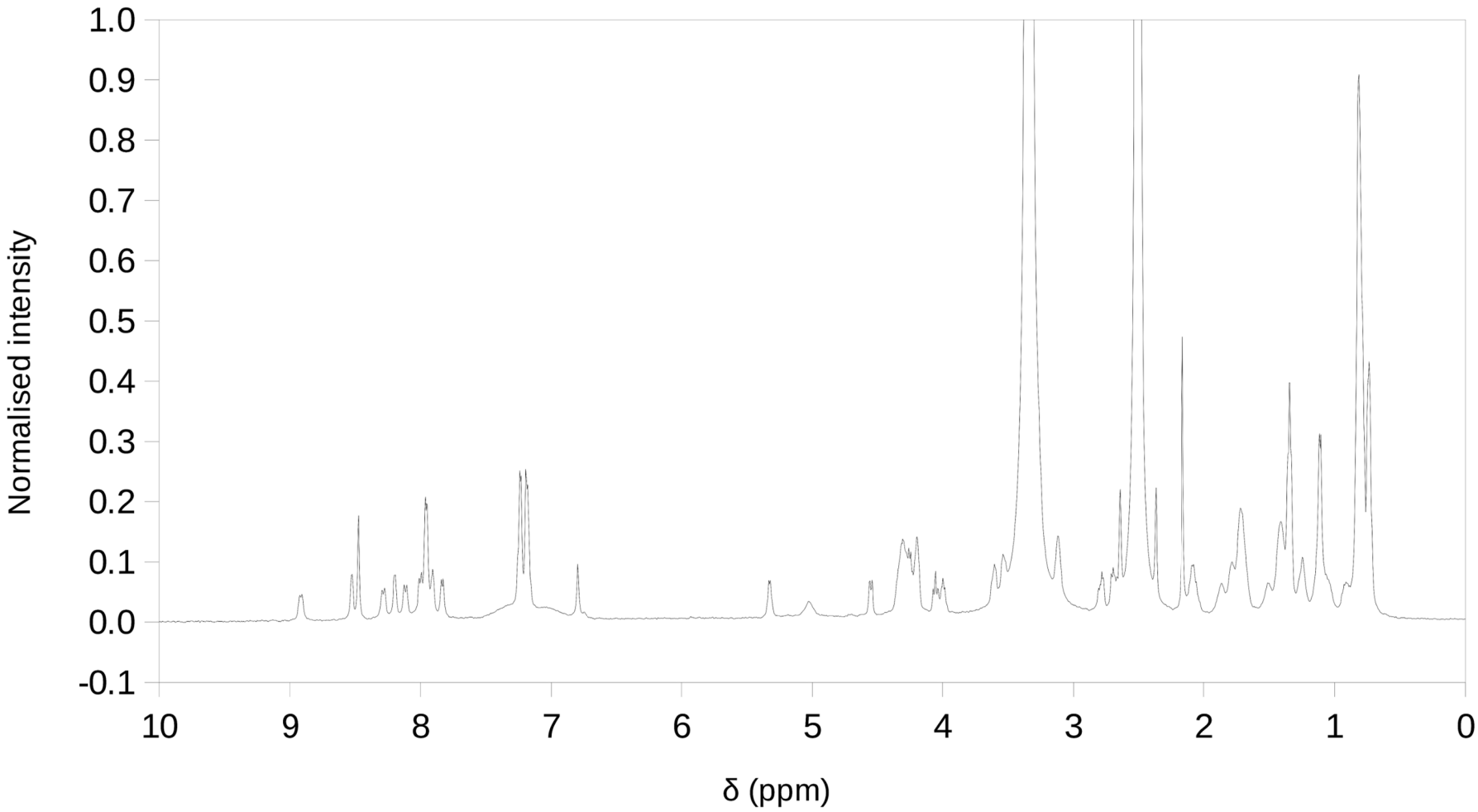

Figure S5. 72: ^{1}H NMR spectra obtained from compound **5.7**

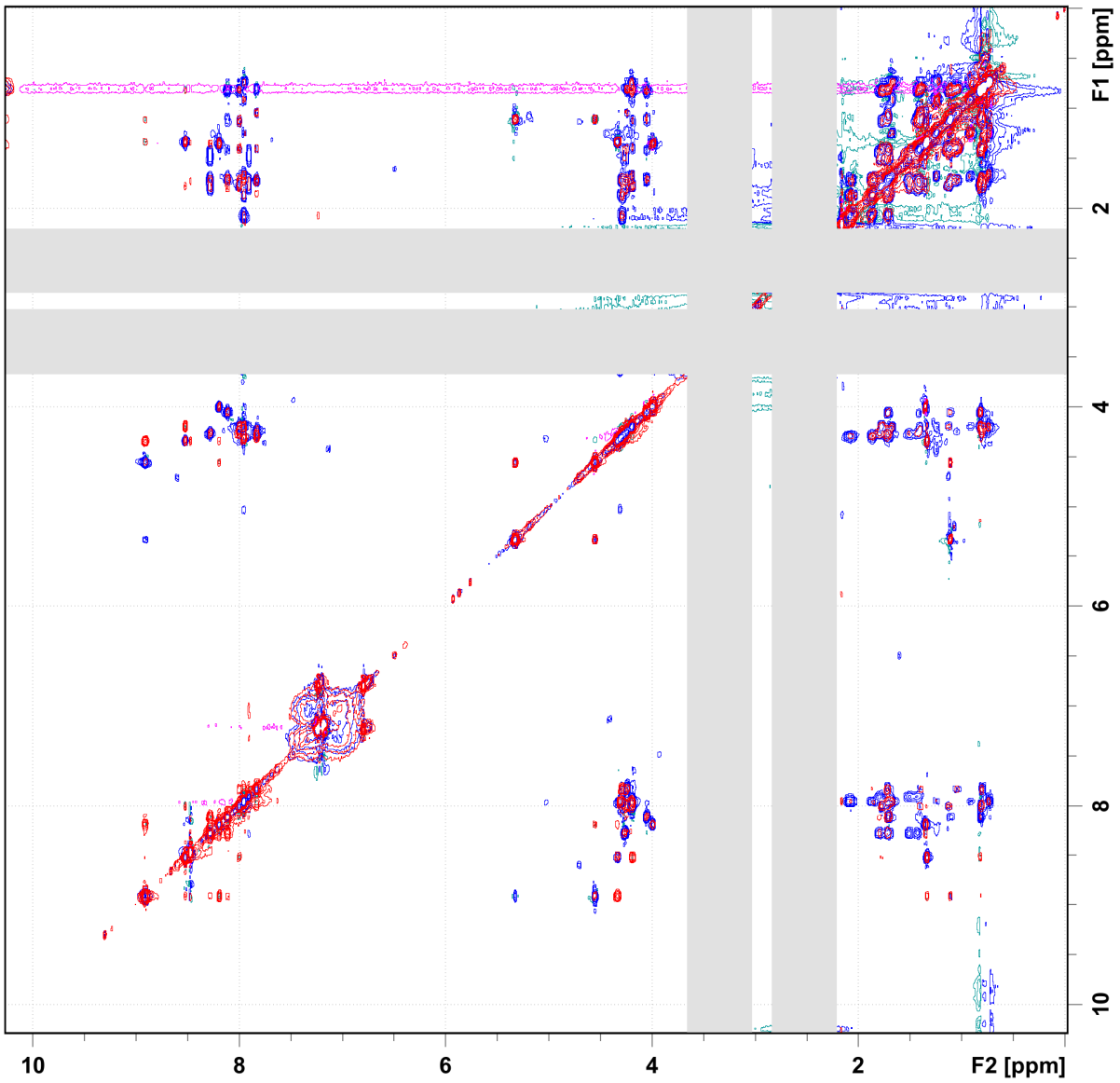

Figure S5.73: ^{1}H-^{1}H TOCSY (blue) and ^{1}H-^{1}H NOESY (red) spectra obtained from compound **5.7**. For clarity, grey boxes obscure solvent signals.

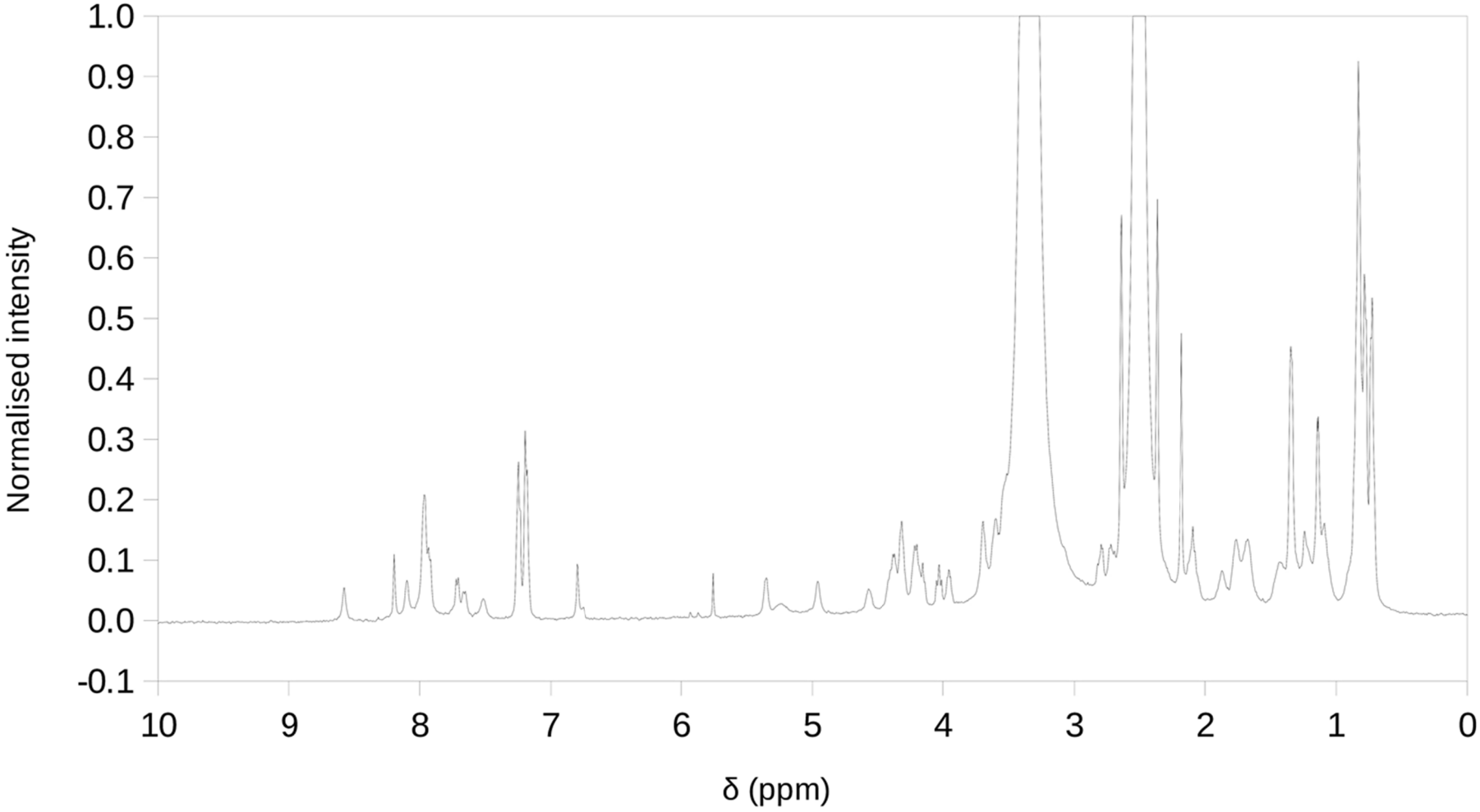

Figure S5. 74: ^{1}H NMR spectra obtained from compound **5.8**

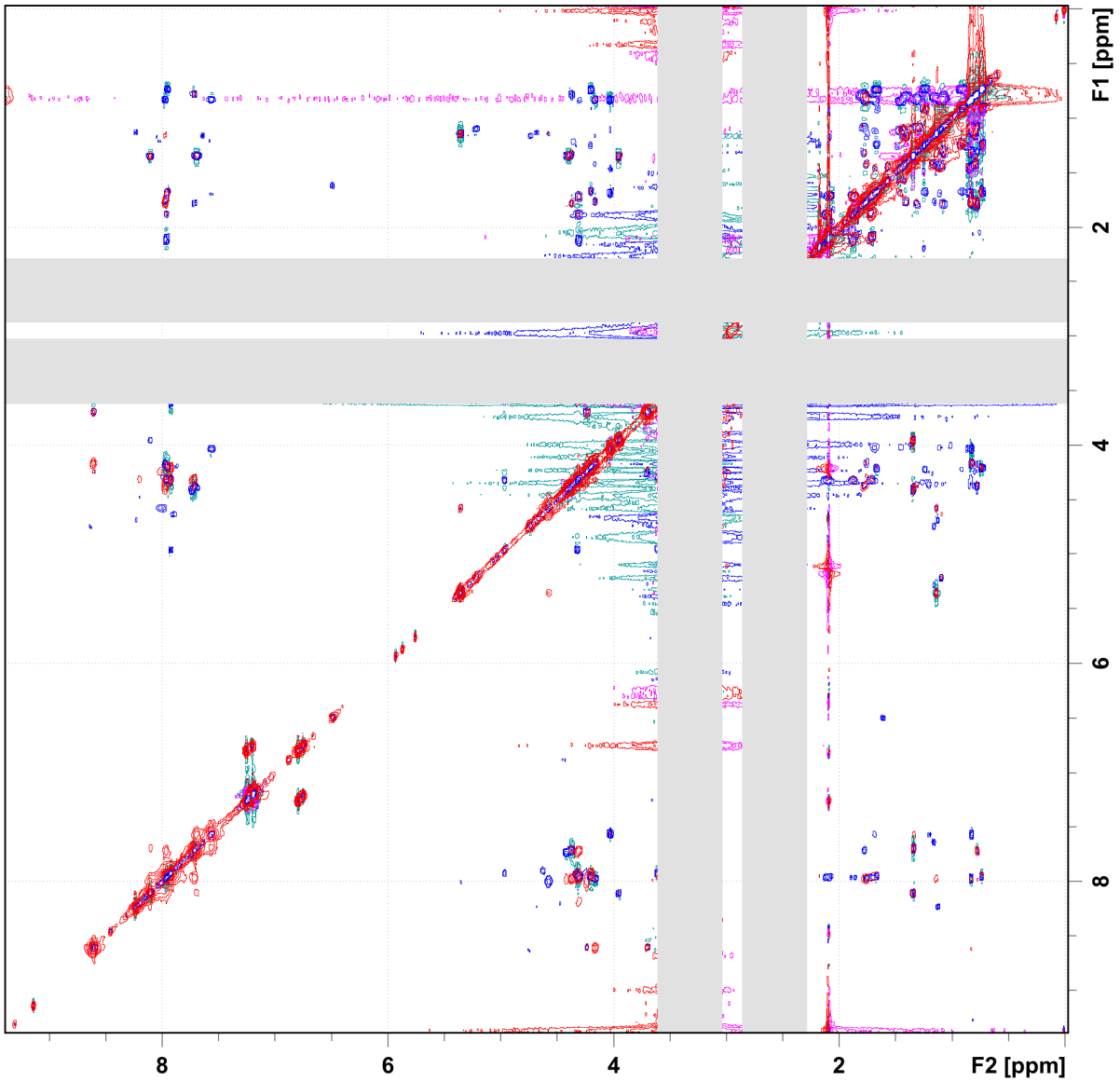

Figure S5.75: ^{1}H-^{1}H TOCSY (blue) and ^{1}H-^{1}H NOESY (red) spectra obtained from compound **5.8**. For clarity, grey boxes obscure solvent signals.

^{1}H NMR spectra were from 1mM compounds 1-8 dissolved in DMSO-d_6. 128K complex points acquired at 300°C with 16 scans.

^{1}H-^{1}H TOCSY (blue) and ^{1}H-^{1}H NOESY (red) spectra were acquired from 1 mM compounds **5.1-5.8** dissolved in DMSO-d_6 at 300°C on a Bruker Avance III HD 500 MHz equipped with a room-temperature broadband probe. Spectra were 2048 and 192 complex points in the direct and indirect dimensions, respectively. For clarity, grey boxes obscure solvent signals.

VI. MIC testing (screening)

For MIC assays all peptides were dissolved in DMSO containing 0.002% polysorbate 80[7]. All bacteria were grown in Mueller Hinton broth (Oxoid) in triplicate. All incubations were at 37°C. Dilutions were carried out in triplicate. 100 µl of autoclaved Mueller Hinton broth was added to wells 2-12 in a 96-well plate. 200 µl of the peptide was added to well one at a concentration of 256 µg/mL. 100µl of peptide in well one was taken up and pipetted into well two. The mixture was then mixed via pipetting before 100µl was taken up and pipetted into well three. This process was repeated up to well 11. Once peptide was added to well 11 100 µl was taken up and then discarded ensuring the well 12 had no peptide present. Thus, the concentrations (in µg/mL) were: 256, 128, 64, 32, 16, 8, 4, 2, 1, 0.5, 0.25 and no peptide present. Each well was then inoculated with 100µl of bacteria that had been diluted to an OD600nm of 0.1. This was repeated three times. The 96-well plates were then incubated at 37°C for 24 hours. The MIC was determined to be the lowest concentration at which there was no growth visible.

For all the compounds in which the MIC lower than 1 µg/ml for the initial test, the above procedure was repeated at an altered initial concentration of 64 µg/ml. Therefore, the new concentrations for MIC were: 64, 32, 16, 8, 4, 2, 1, 0.5, 0.25, 0.125, 0.0625 and no peptide present. Vancomycin was used as a control.

To determine the MIC of *M. smegmatis* ATCC 607 an inoculum was shaken at 140rpm, 37°C in 5ml Middlebrook 7H9 broth (SIGMA) supplemented to 5% Middlebrook ADC (SIGMA) growth supplement for 3-4 days and harvested mid-late exponential phase (OD ~0.6). The harvested cells were washed once in fresh media and diluted 10-fold from the original volume. Then plated out in a 96-well plate as previously described, incubated at 37°C 140RPM with MIC readings taken after 72 hours.

To determine the effect of serum on antibacterial activity, the MIC of compounds **5.12** and **5.13** were measured in presence of 10% human serum using the above protocols. Both the compounds were pre-treated with 10% human serum (Sigma, H4522) for 30 mins and 2 hours. These pre-treated samples were used for MIC determination using Mueller Hinton Broth supplemented with 10% human serum.

VII. Antagonization assay

An antagonization assay was performed using Leu_{10}-teixobactin (**5.13**) and Lipid II as reported in literature.[7] MIC was tested using the protocols described in section VI.

Precursor	Molar ratio of precursor to Leu_{10}-teixobactin				
	0x	0.5x	1x	2x	5x
Lipid II	-	+	+	+	+

Table S5.3: Leu_{10}-teixobactin at 8x MIC exposed to increasing concentrations of lipid II. MIC was tested against the strain reported in ref 7. *S. aureus ATCC 29213.* Experiments were performed in triplicate.

VIII. MIC testing (extended panel)

Bacterial cultures were grown overnight in Mueller-Hinton Agar (MHA) plates and adjusted to a final concentration of 10^5 – 10^6 CFU/ml. 100 µl of inoculum in Meuller-Hinton broth (MHB) was mixed with equal volume of peptides (dissolved in MHB) at 2x their concentration in a 96 well plate. In parallel experiments, MIC values were determined in the media containing polysorbate 80 (0.002%, v/v) to prevent non-specific adsorption of the peptides to plastic surfaces. The final peptides concentrations ranged from 0.0625 – 32 µg/ml. Positive and negative controls contained 200 µl of inoculum without any peptide dissolved in broth, respectively. The 96 well plates were then incubated at 37 °C for 24 h. All the experiments were performed in two independent duplicates and the MIC was determined as the lowest concentration in which no visible growth was observed. Minimum bactericidal concentration (MBC) was determined by plating out the dilution representing the MIC and concentrations up to 16x MIC on MHA plates kept at 37 °C for 24 h. The lowest concentration in which no visible colonies could be detected was taken as the MBC.

Compound➔ Strain ↓		**5.8**	**5.11**	**5.12**	**5.13**	**2.1**	Vancomycin **1.12**	Daptomycin **1.13**
MRSA 1	MIC (with polysorbate 80)	4	1	0.25	0.25	1	1	0.5
	MIC (without polysorbate 80)	8	4	2	2	4	2	-
	MBC	16	4	1	2	2	-	-
MRSA 2	MIC (with polysorbate 80)	1	0.5	≤ 0.0625	≤ 0.0625	0.125	1	0.5
	MIC (without polysorbate 80)	4	2	2	2	2	2	-
	MBC	4	4	≤ 0.0625	≤ 0.0625	0.5	-	-
MRSA 3	MIC (with polysorbate 80)	1	0.25	≤ 0.0625	≤ 0.0625	0.5	1	0.5
	MIC (without polysorbate 80)	4	4	2	2	4	2	-
	MBC	2	2	0.125	≤ 0.0625	1	-	-
S. aureus	MIC (with polysorbate 80)	1	0.25	≤ 0.0625	≤ 0.0625	0.25	2	0.25
	MIC (without polysorbate 80)	4	2	1	1	2	4	-
	MBC	2	1	0.125	0.125	1	-	-
VRE 1	MIC (with polysorbate 80)	4	0.5	≤ 0.0625	0.25	2	>4	0.5
	MIC (without polysorbate 80)	8	4	1	2	4	>4	-
VRE 2	MIC (with polysorbate 80)	4	0.5	≤ 0.0625	0.25	2	>4	0.5
	MIC (without polysorbate 80)	8	4	1	2	4	>4	-

Table S5.4: MIC and MBC (in µg/mL) of the lead teixobactin analogues **5.8**, **5.11**-**5.13**, **2.1** and Daptomycin control against an extended panel of Gram positive bacteria in the presence and absence of polysorbate 80. Strain information: MRSA 1: MRSA ATCC 700699, MRSA 2: MRSA DR 42412 (sputum), MRSA 3: MRSA DM21455 (eye). MRSA 2 and MRSA 3 are clinical isolates. *Staphylococcus aureus ATCC 29213, Enterococcus faecalis,* (VRE 1: VRE ATCC 700802, VRE 2: VRE ATCC 29212).

IX. Time-dependent killing of bacteria by teixobactin analogues 5.12 and 5.13

Time-kill kinetics against MRSA DM21455 strains (clinical isolates from patients) was carried out in MHB. Cultures were grown overnight in MHA plates and adjusted to a final inoculum of 10^5 – 10^6 CFU/ml in MHB (containing 0.002% v/v, polysorbate 80) with teixobactin analogues **5.12** and **5.13** maintained at a final concentration of 0.5 µg/ml. For vancomycin, the concentration was varied from 0.5 – 16 µg/ml without polysorbate 80. The tubes were then incubated at 37 °C. 100 µl of cell suspension was withdrawn at various time points (0, 2, 4, 8, 24 h), serially diluted (10^1-10^5 fold dilutions) and plated onto a MHA plates and incubated for 24 h at 37 °C. Colonies were then enumerated using a haemocytometer. Colony counting too numerous to count (>300 colonies) was taken as 10^{10} CFU. Average values from two independent experiments are reported.

X. Complex formation of teixobactin with lipid II and geranyl pyrophosphate

Complex formation of teixobactin analogues **5.8** (Ala_{10}-teixobactin) and **2.1** (Arg_{10}-teixobactin) with lipid II and geranyl pyrophosphate was performed using TLC as described previously.[7] Binding of teixobactin to lipid II and geranyl pyrophosphate was analysed by incubating 30 µL of 2 nmol of each precursor with 2 or 4 nmoles of teixobactin in 50 mM Tris/HCl, pH 7.5, for 30 min at room temperature. Complex formation was analysed by extracting unbound precursors from the reaction mixture with 30 µL n- butanol/6M pyridine acetate (pH 4.2) (2:1; vol/vol) followed by TLC analysis of the organic layer using chloroform/methanol/water/ammonia (88:48:10:1, v/v/v/v) as the solvent and detection of lipid/phosphate containing precursors by phosphomolybdic acid staining. The TLC figures represent the results obtained through three independent experiments.

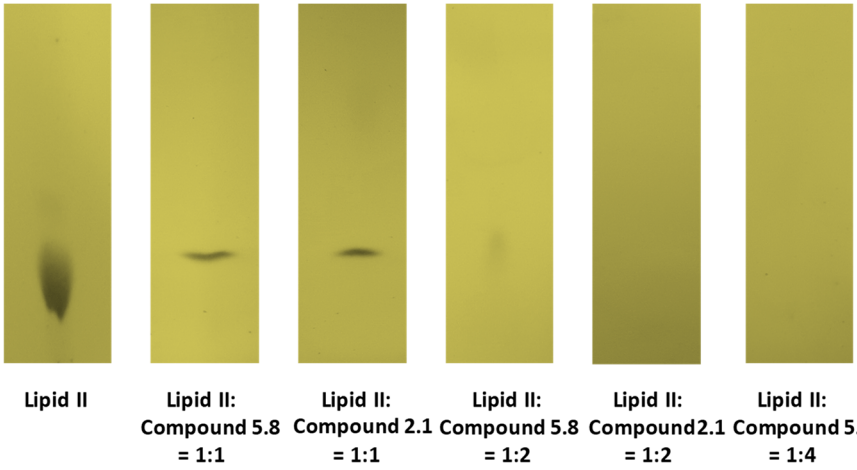

Figure S5.76: Binding of teixobactin analogues **5.8** (Ala_{10}-teixobactin) and **2.1** (Arg_{10}-teixobactin) with lipid II using the protocols described in literature.[7] Partial binding is observed when the ratio of lipid II to the analogue is 1:1 (indicated by lighter spots on the TLC) and complete binding is observed when the ratio of lipid II to the analogue is 1:2 in case of analogue **5.8** and 1:4 in case of analogue **2.1** (indicated by no spots on TLC).

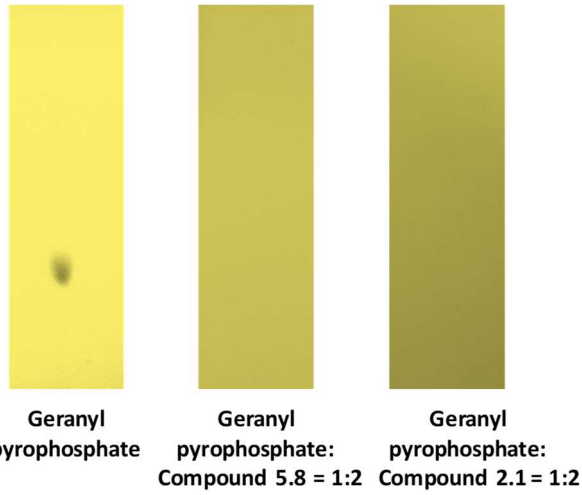

Figure S5.77: Binding of teixobactin analogues **5.8** (Ala_{10}-teixobactin) and **2.1** (Arg_{10}-teixobactin) with geranyl pyrophosphate using the protocols described in literature.[7] complete binding is observed when the ratio of the phosphate to the analogue is 1:2 (indicated by no spots on the TLC).

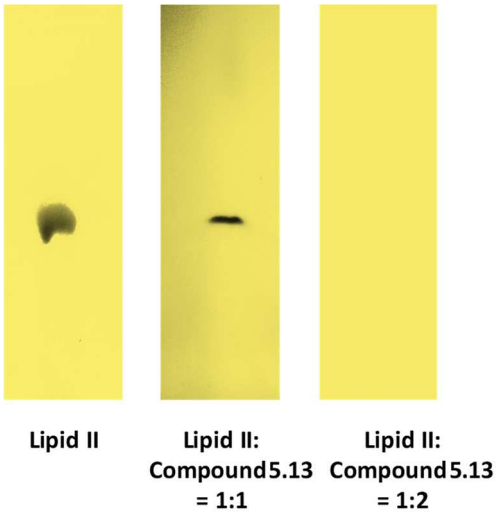

Figure S5.78: Binding of teixobactin analogue **5.13** (Leu_{10}-teixobactin) with lipid II using the protocols described in literature.[7] Partial binding is observed when the ratio of lipid II to the analogue is 1:1 (indicated by lighter spots on the TLC) and complete binding is observed when the ratio of lipid II to the analogue is 1:2 (indicated by no spots on TLC).

XI. Cytotoxicity assay

a) Cytotoxicity assay by Formazan bioreduction

HeLa cells were seeded in a 96-well plate at 10^4 cells/cm^2 density in Dulbecco's Modified Eagles Medium (DMEM) supplemented with 10% serum. The cells were repeatedly rinsed with Hank's Balanced Salt Solution (HBSS) prior to be exposed to different peptides in the range of 0.5 – 100 µM in HBSS 24 hrs post-seeding. Following 6 hrs of exposure to the teixobactin analogue, CellTiter 96 AQueous Nonradioactive Cell Proliferation Assay (Promega) was used according to the manufacturer's instructions.[8] Not ingested teixobactin analogue was removed by repeated washings with fresh medium. 20 µL of the combined MTS/PMS solution was added to 100 µL fresh medium in each well and plates were incubated for 3 hrs at 37°C. Absorbance was measured at 490 nm on Tecan Infinite M200 PRO plate reader with i-control 1.10 software (Molecular Devices).

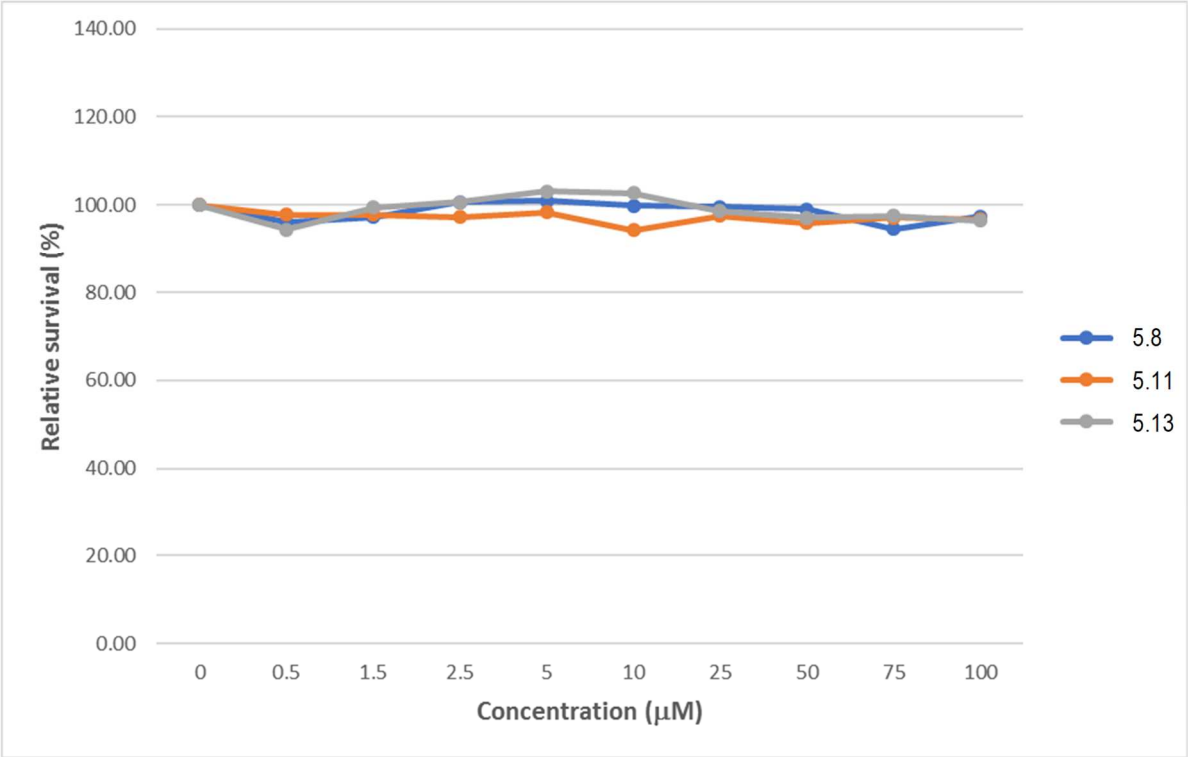

Figure S5.79: Toxicity results showing relative survival vs. Concentration (in µM) in HeLa cells for teixobactin analogues **5.8** (Ala_{10}-teixobactin), **5.11** (Val_{10}-teixobactin) and **5.13** (Leu_{10}-teixobactin).

b) Haemolytic Assay Protocol

This assay was done at Singapore Eye Research Institute, Singapore. Hemolytic assay was performed on rabbit red blood cells (RBCs) immediately after collecting the blood samples from adult rabbits. All procedures for isolating blood from rabbits were approved by IACUC Singhealth and performed according to the standards of the Association for the Research in Vision and Ophthalmology.

Haemolytic activity of peptides was determined for rabbit red blood cells (rRBC), as reported before.[9] Rabbit erythrocytes were isolated from freshly collected blood samples and washed twice with sterile

PBS. Two-fold serial dilutions of peptides (0.195 – 250 µg/ml) was mixed with rRBC (final concentration 4% v/v), incubated at 37ºC for 1h and centrifuged at 3000 rpm for 5 minutes. The release of hemoglobin in the supernatant was monitored by measuring the hemoglobin absorbance at 576nm. The readings from negative control (PBS and rRBC without any additives) and positive control (2% Triton-X100 and rRBC) were used as 0% and 100% haemolysis, respectively. Prolific pore forming and haemolytic melittin was used as comparator peptide. The data represents average value from triplicates experiments.

XII. References:

1. A. Parmar, A. Iyer, C. S. Vincent, D. Van Lysebetten, S. H. Prior, A. Madder, E. J. Taylor, I. Singh, Efficient total syntheses and biological activities of two teixobactin analogues. *Chem. Commun.* **52**, 6060–6063 (2016).

2. W. F. Vranken, W. Boucher, T. J. Stevens, R. H. Fogh, A. Pajon, M. Llinas, E. L. Ulrich, J. L. Markley, J. Ionides, E. D. Laue, The CCPN data model for NMR spectroscopy: Development of a software pipeline. *Proteins: Structure, Function and Genetics*. **59**, 687–696 (2005).

3. T. Herrmann, P. Güntert, K. Wüthrich, Protein NMR structure determination with automated NOE assignment using the new software CANDID and the torsion angle dynamics algorithm DYANA. *Journal of molecular biology*. **319**, 209–27 (2002).

4. M. J. Abraham, T. Murtola, R. Schulz, S. Pall, J. C. Smith, B. Hess, E. Lindah, Gromacs: High performance molecular simulations through multi-level parallelism from laptops to supercomputers. *SoftwareX*. **1–2**, 19–25 (2015).

5. S. Li, A. H. Elcock, Residue-Specific Force Field (RSFF2) Improves the Modeling of Conformational Behavior of Peptides and Proteins. *The Journal of Physical Chemistry Letters*. **13**, 2127–2133 (2015).

6. J. Xu, D. Van, Tracking Equilibrium and Nonequilibrium Shifts in Data with TREND. *Biophysical Journal*. **112**, 224–233 (2017).

7. L. L. Ling, T. Schneider, A. J. Peoples, A. L. Spoering, I. Engels, B. P. Conlon, A. Mueller, D. E. Hughes, S. Epstein, M. Jones, L. Lazarides, V. a Steadman, D. R. Cohen, C. R. Felix, K. A. Fetterman, W. P. Millett, A. G. Nitti, A. M. Zullo, C. Chen, K. Lewis, A new antibiotic kills pathogens without detectable resistance. *Nature*. **517**, 455–459 (2015).

8. A. H. Cory, T. C. Owen, J. A. Barltrop, J. G. Cory, Use of an aqueous soluble tetrazolium/formazan assay for cell growth assays in culture. *Cancer communications*. **3**,

207–12 (1991).

9. R. Lakshminarayanan, S. Liu, J. Li, M. Nandhakumar, T. T. Aung, E. Goh, J. Y. T. Chang, P. Saraswathi, C. Tang, S. R. B. Safie, L. Y. Lin, H. Riezman, Z. Lei, C. S. Verma, R. W. Beuerman, Synthetic Multivalent Antifungal Peptides Effective against Fungi. *PLoS ONE*. **9**, e87730 (2014).

EXPERIMENTAL SECTION FOR CHAPTER 6

I. Materials

All L amino acids, Fmoc-$_D$-Arg(pbf)-OH, Fmoc-$_D$-Gln(Trt)-OH, Boc-N-methyl-$_D$-phenylalanine, 1 [Bis(dimethylamino)methylene]-1H-1,2,3-triazolo[4,5-b]pyridinium3-oxidhexafluorophosphate (HATU), Phenylsilane ($PhSiH_3$), Tetrakis(triphenylphosphine)palladium(0) [$Pd(PPh_3)$], Diisoproplycarbodiimide (DIC) and Triisopropylsilane (TIS) were purchased from Fluorochem, UK. Fmoc-$_D$-*allo*-Ile-OH and oxyma pure were purchased from Merck Millipore. The side chain protecting

groups for the amino acids are *t*Bu for Ser, Pbf for Arg and Trt for Gln and Thr unless specified otherwise. Diisopropylethylamine (DIPEA), supplied as extra dry, redistilled, 99.5 % pure, Acetic anhydride, allyl chloroformate, $CDCl_3$ and polysorbate 80 and were purchased from Sigma Aldrich. Tritylchloride and 4-(Dimethylamino)pyridine were purchased from Alfa Aesar. Dimmethylformamide (DMF) peptide synthesis grade was purchased from Rathburn chemicals. Triethylamine, Diethyl ether (Et_2O), Dimethylsulfoxide (DMSO), Dichloromethane (DCM), Tetrahydrofuran (extra dry with molecular sieves), Formic acid 98-100% purity and Acetonitrile (HPLC grade) were purchased from Fisher Scientific. Water with the Milli-Q grade standard was obtained in-house from an ELGA Purelab Flex system. 2-Chlorotritylchloride resin (manufacturer's loading: 1.20 mmol/g) was purchased from Fluorochem. All chemicals were used without further purification.

II. Equipment used for the analysis and purification of compounds

All peptides were analysed on a Thermo Scientific Dionex Ultimate 3000 RP-HPLC equipped with a Phenomenex Gemini NX C18 110 Å (150 x 4.6 mm) column using the following buffer systems: A: 0.1% HCOOH in milliQ water. B: ACN using a flow rate of 1 ml/min. The column was flushed with 95% A for 5 min prior to an injection and was flushed for 5 min with 95% B and 5% A after the run was finished. Peptides were dissolved in (1:1) 0.1% HCOOH buffer in water and acetonitrile (ACN) and analysed using the following gradient: 95% A for 2 min. 5-95% B in 25 min. 95% B for 5 min. 5% A for 4 min. Peptides were dissolved in 0.1% HCOOH buffer in water and in ACN (10-30% ACN) and purified using the same gradient as mentioned above, on a Thermo Scientific Dionex Ultimate 3000 RP-HPLC with a flow rate of 5 mL/min using a Phenomenex Gemini NX C18 110 Å (150 x 10 mm) semi-prep column.

HRMS spectra were recorded on a Thermo

Scientific Q Exactive Plus Orbitrap Mass Spectrometer in the positive ion mode.

III. Syntheses of teixobactin analogues

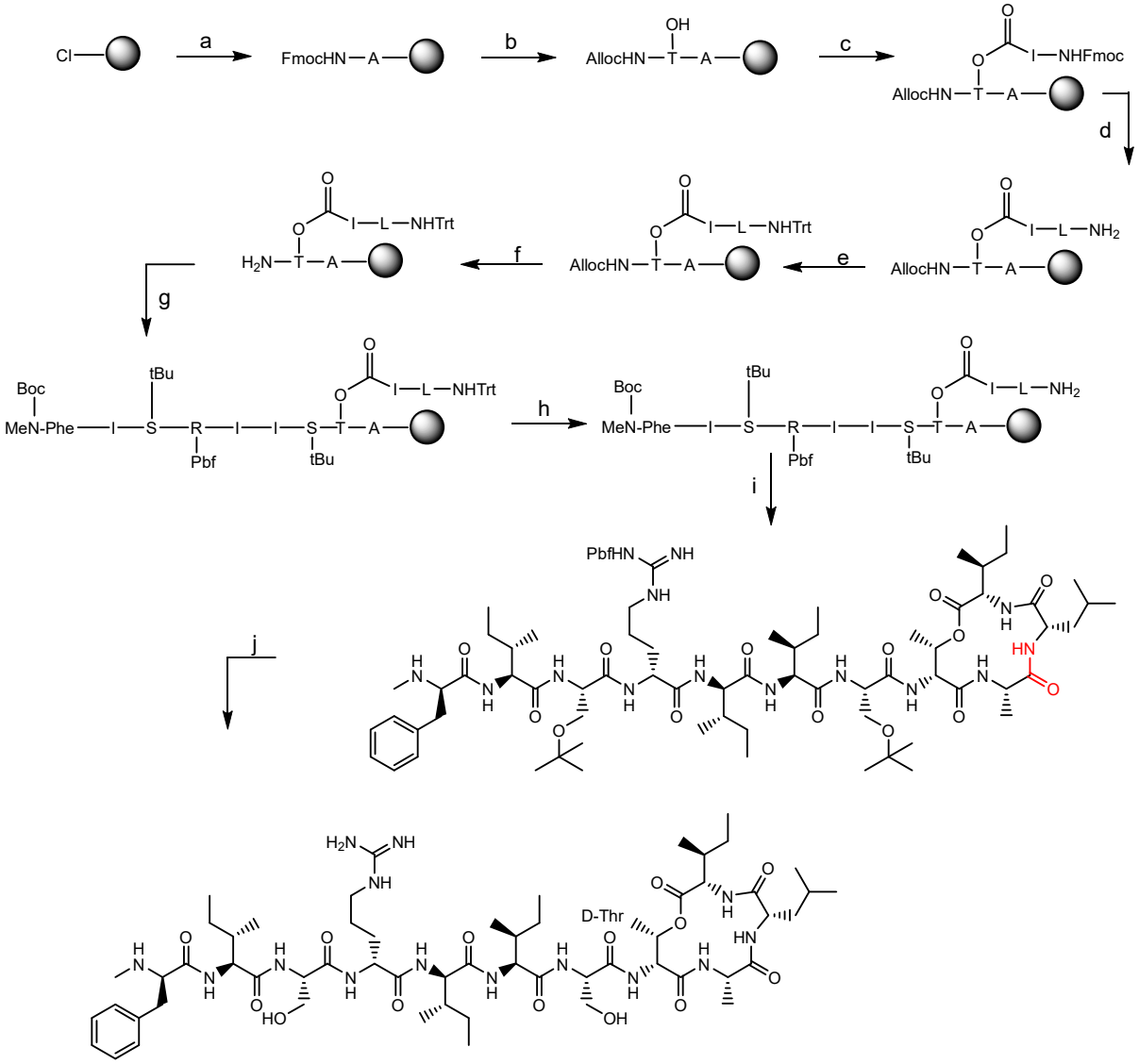

Scheme S6.1: Synthesis of $_{D}$-Arg$_4$-Leu$_{10}$-teixobactin (**6.2**)

(step a) Commercially available 2-Chlorotrityl chloride resin (manufacturer's loading = 1.2 mmol/g, 170 mg resin) was swelled in DCM in a reactor. To this resin was added 4 eq. Fmoc-Ala-OH/8 eq. DIPEA in DCM and the reactor was shaken for 3h. The loading determined by UV absorption of the piperidine-dibenzofulvene adduct was calculated to be 0.6 mmol/g, (170mg resin, 0.102 mmol). Any unreacted resin was capped with MeOH:DIPEA:DCM = 1:2:7 by shaking for 1h. (step b) The Fmoc protecting group was deprotected using 20% piperdine in DMF by shaking for 3 min, followed by draining and shaking again with 20% piperidine in DMF for 10 min. AllocHN-D-Thr-OH was then coupled to the resin by adding 3 eq. of the AA, 3 eq. HATU and 6 eq. DIPEA in DMF and shaking for 1.5h at room temperature. (step c) Esterification was performed using 10 eq. of Fmoc-Ile-OH, 10 eq. DIC and 5 mol% DMAP in DCM and shaking the reaction for 2h. This was followed by capping the unreacted alcohol using 10% Ac_2O/DIPEA in DMF shaking for 30 min and Fmoc was removed

using protocol described earlier in step (b). (step d) Fmoc-Leu-OH was coupled using 4 eq. of AA, 4 eq. HATU and 8 eq. DIPEA in DMF and shaking for 1h followed by Fmoc deprotection using 20% piperidine in DMF as described earlier. (step e) The N terminus of Leu was protected using 10 eq. Trt-Cl and 15% Et_3N in DCM and shaking for 1h. The protection was verified by the Ninhydrin colour test. (step f) The Alloc protecting group of $_D$-Thr was removed using 0.2 eq. $[Pd(PPh^3)]^0$ and 24 eq. $PhSiH_3$ in dry DCM under argon for 20 min. This procedure was repeated increasing the time to 45 min and the resin was washed thoroughly with DCM and DMF to remove any Pd stuck to the resin. (step g) All amino acids were coupled using 4 eq. Amino Acid, 4 eq. DIC/Oxyma using a microwave peptide synthesizer. Coupling time was 10 min. Deprotection cycles were performed as described earlier. (step h) The peptide was cleaved from the resin without cleaving off the protecting groups of the amino acid side chains using TFA:TIS:DCM = 2:5:93 and shaking for 1h. (step i) The solvent was evaporated and the peptide was redissolved in DMF to which 1 eq. HATU and 10 eq. DIPEA were added and the reaction was stirred for 30 min to perform the cyclization. (step j) The side-chain protecting groups were then cleaved off using TFA:TIS:H_2O = 95:2.5:2.5 by stirring for 1h. The peptide was precipitated using cold Et_2O (-20°C) and centrifuging at 7000 rpm to obtain a white solid. This solid was further purified using RP-HPLC using the protocols described previously.

[§]Teixobactin analogues were synthesised by using our previously reported protocols.

Coumpound Number	Name	Chemical formula	Mass Calcd (Da)	Mass obsd (Da)
6.1	Arg_3-Leu_{10}-teixobactin	$C_{61}H_{104}N_{15}O_{14}$	1270.7887	1270.7913
6.2	$_D$-Arg_4-Leu_{10}-teixobactin	$C_{59}H_{101}N_{14}O_{14}$	1229.7622	1229.7650
6.3	Arg_9-Leu_{10}-teixobactin	$C_{61}H_{104}N_{15}O_{15}$	1286.7836	1286.7843
6.4	Arg_3-$_D$-Arg_4-Leu_{10}-teixobactin	$C_{62}H_{108}N_{17}O_{13}$	1298.8313	1298.8325
6.5	Arg_3-Arg_9-Leu_{10}-teixobactin	$C_{64}H_{111}N_{18}O_{14}$	1355.8527	1355.8606
6.6	$_D$-Arg_4-Arg_9-Leu_{10}-teixobactin	$C_{62}H_{108}N_{17}O_{14}$	1314.8262	1314.8263
6.7	Arg_3-$_D$-Arg_4-Arg_9-Leu_{10}-teixobactin	$C_{65}H_{115}N_{20}O_{13}$	1383.8952	1383.8943
6.8	Arg_3-Ile_{10}-teixobactin	$C_{61}H_{104}N_{15}O_{14}$	1270.7887	1270.7896
6.9	$_D$-Arg_4-Ile_{10}-teixobactin	$C_{59}H_{101}N_{14}O_{14}$	1229.7622	1229.7607
6.10	Arg_9-Ile_{10}-teixobactin	$C_{61}H_{104}N_{15}O_{15}$	1286.7836	1286.7780

Table S6.1: Compound number, name, chemical formula, mass calculated and mass observed for compounds **6.1-6.10**. The overall yields were typically in the range of 13-22%.

[§] Parmar, A. *et al.* Teixobactin analogues reveal enduracididine to be non-essential for highly potent antibacterial activity and lipid II binding. *Chemical Science* **8**, 8183–8192 (2017)

IV. HPLC/MS analysis

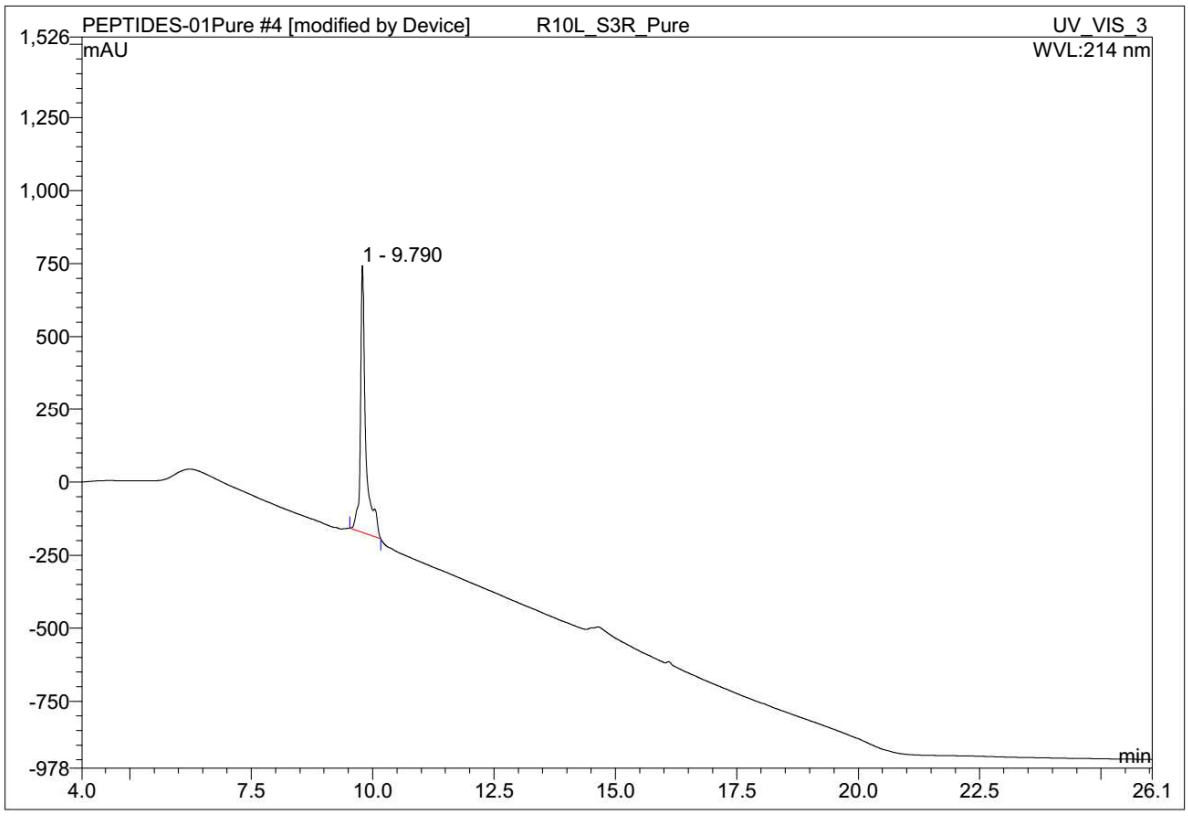

Figure S6.1: HPLC trace of HPLC purified teixobactin analogue **6.1** (gradient: 5-95% ACN in 25 min using A: 0.1% HCOOH in water, B: ACN)

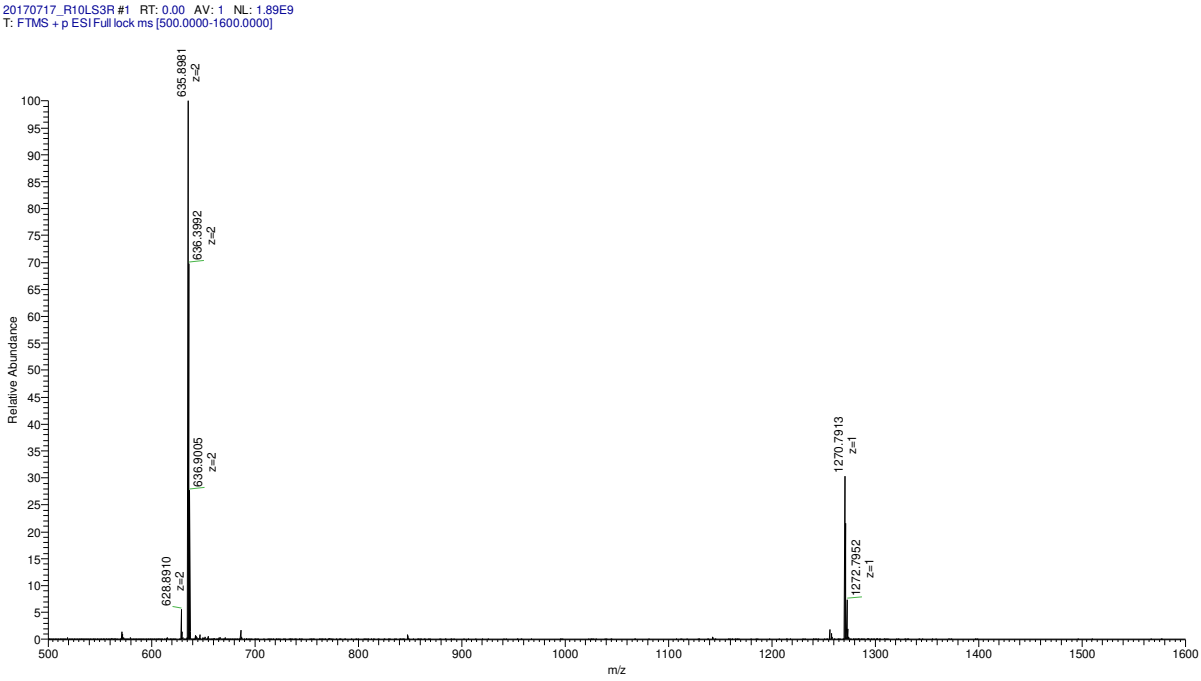

Figure S6.2: HRMS of HPLC purified teixobactin analogue **6.1**. Mass calcd. for $C_{61}H_{104}N_{15}O_{14}$ = 1270.7887, found M + H^+ = 1270.7913, M/2 + H^+ = 635.8981.

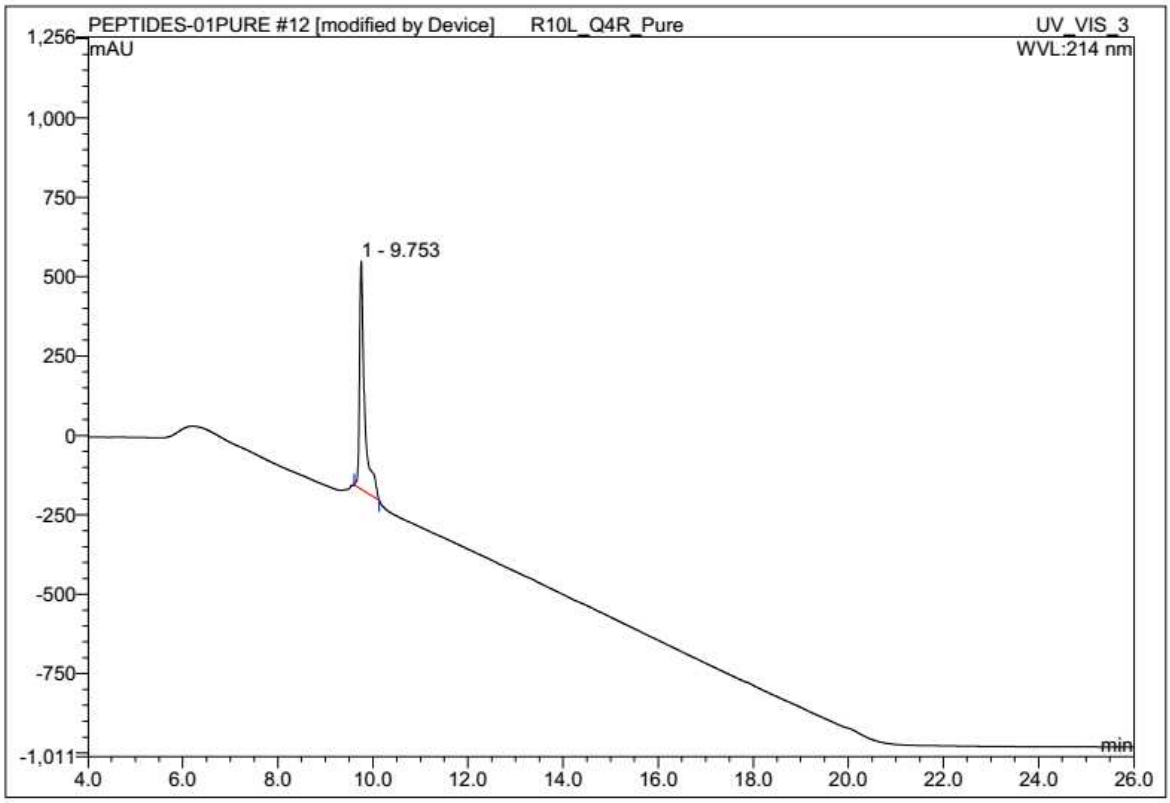

Figure S6.3: HPLC trace of HPLC purified teixobactin analogue **6.2** (gradient: 5-95% ACN in 25 min using A: 0.1% HCOOH in water, B: ACN)

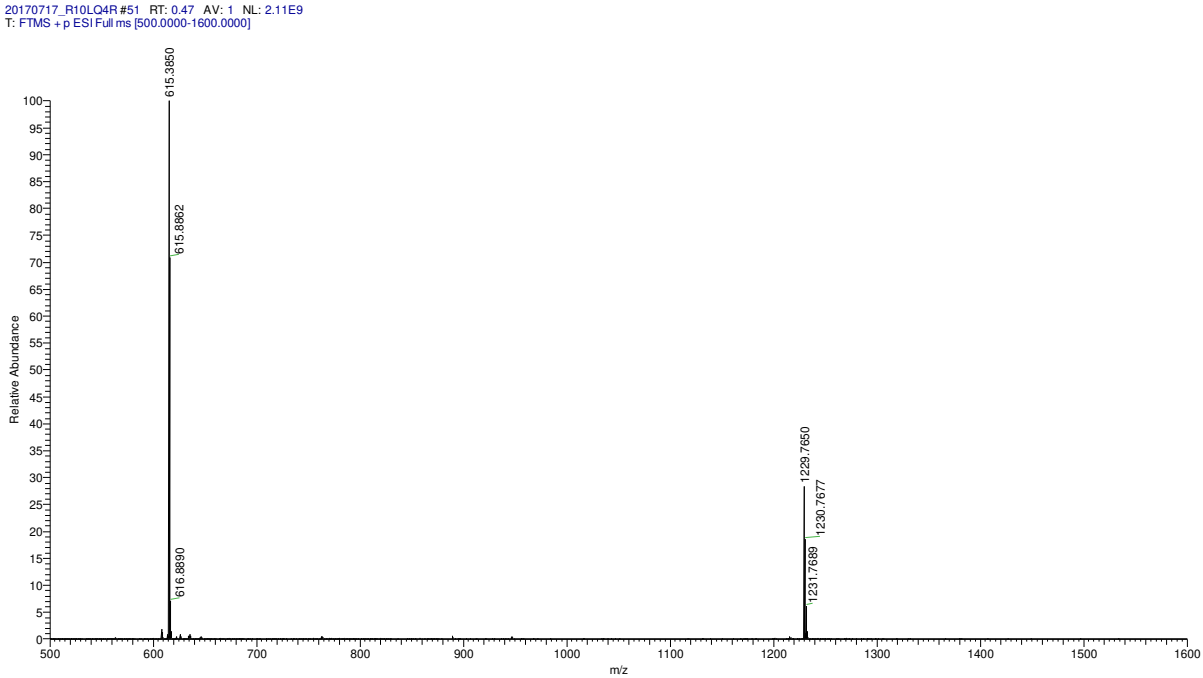

Figure S6.4: HRMS of HPLC purified teixobactin analogue **6.2**. Mass calcd. for $C_{59}H_{101}N_{14}O_{14}$ = 1229.7622, found M + H^+ = 1229.7650, M/2 + H^+ = 615.8850.

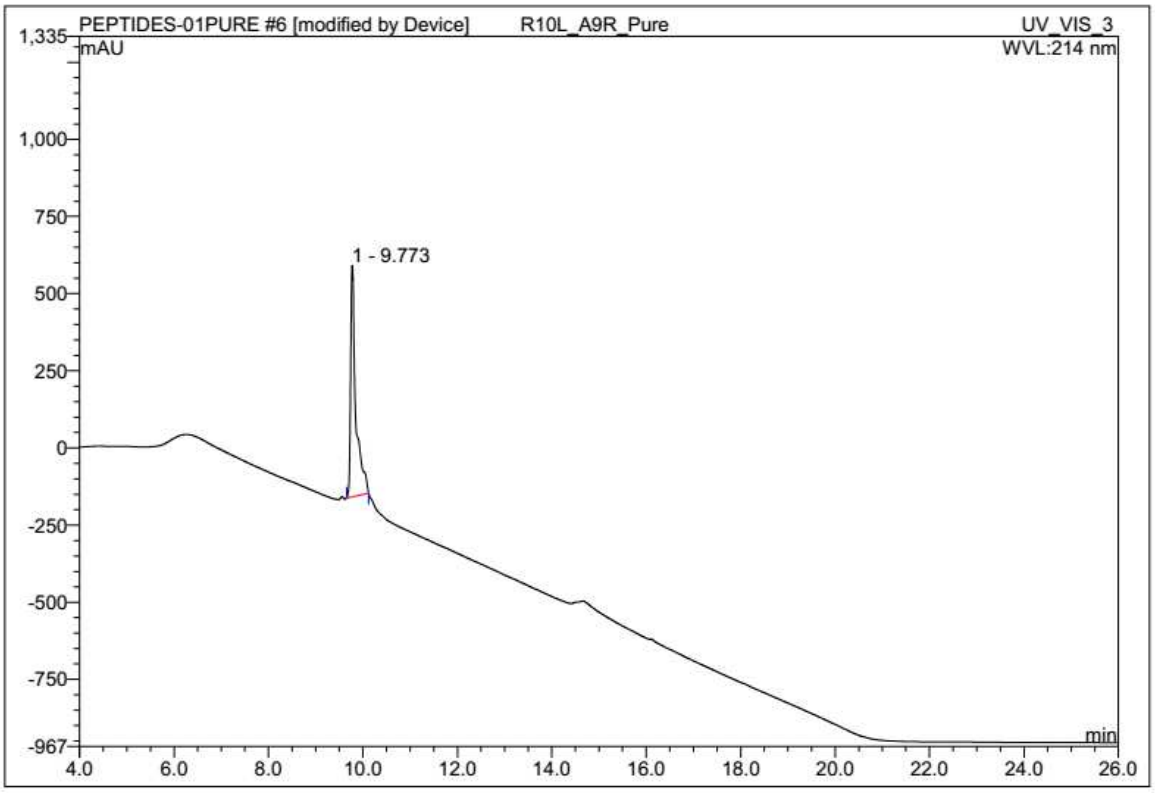

Figure S6.5: HPLC trace of HPLC purified teixobactin analogue **6.3** (gradient: 5-95% ACN in 25 min using A: 0.1% HCOOH in water, B: ACN)

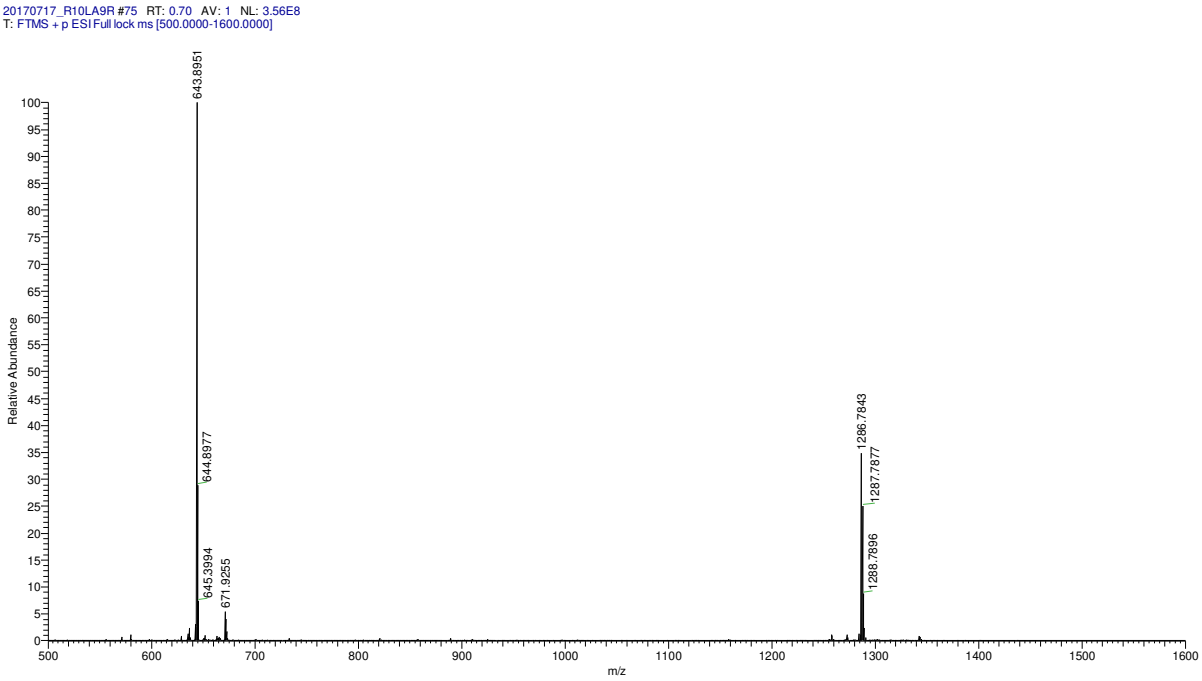

Figure S6.6: HRMS of HPLC purified teixobactin analogue **6.3**. Mass calcd. for $C_{61}H_{104}N_{15}O_{15}$ = 1286.7836, found M + H^+ = 1286.7843, M/2 + H^+ = 643.8951.

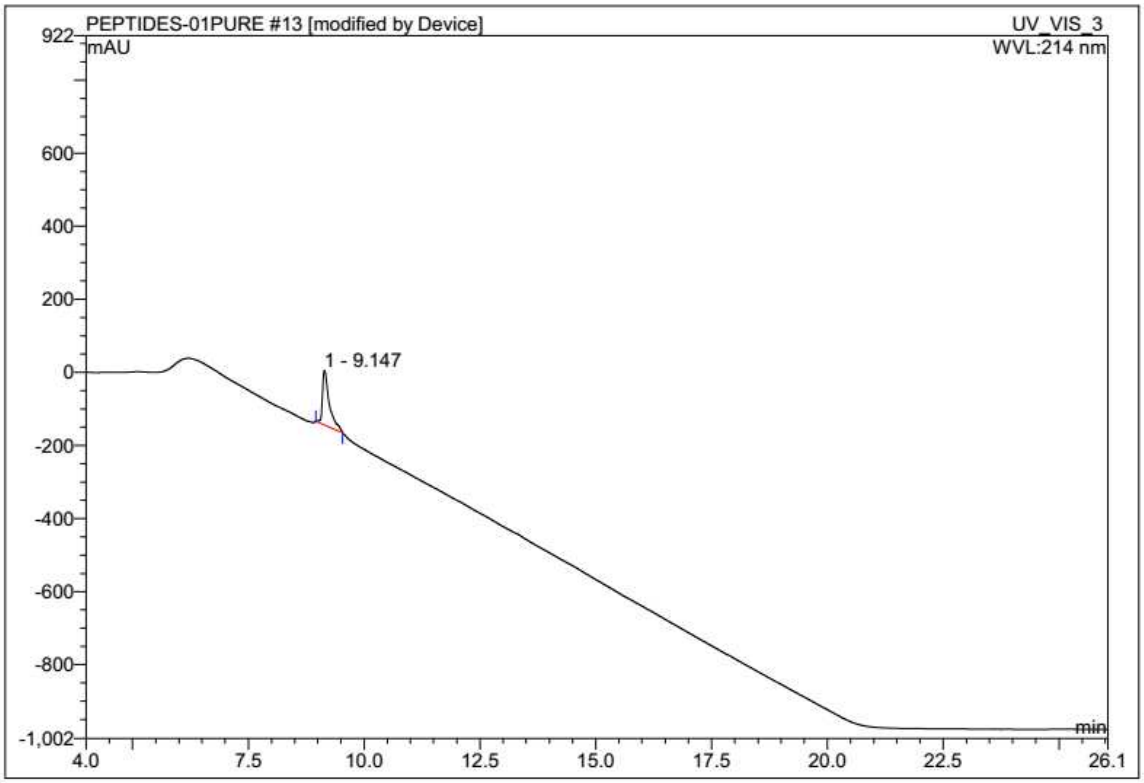

Figure S6.7: HPLC trace of HPLC purified teixobactin analogue **6.4** (gradient: 5-95% ACN in 25 min using A: 0.1% HCOOH in water, B: ACN)

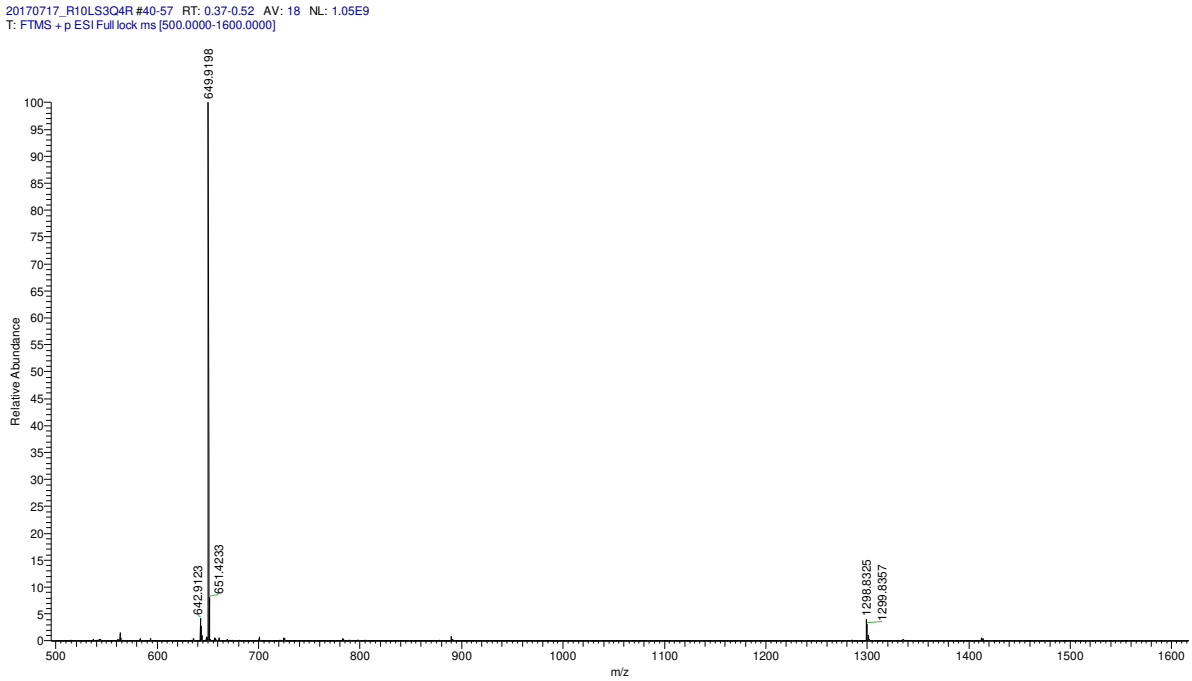

Figure S6.8: HRMS of HPLC purified teixobactin analogue **6.4**. Mass calcd. for $C_{62}H_{108}N_{17}O_{13}$ = 1298.8313, found M + H^+ = 1298.8325, M/2 + H^+ = 649.9198.

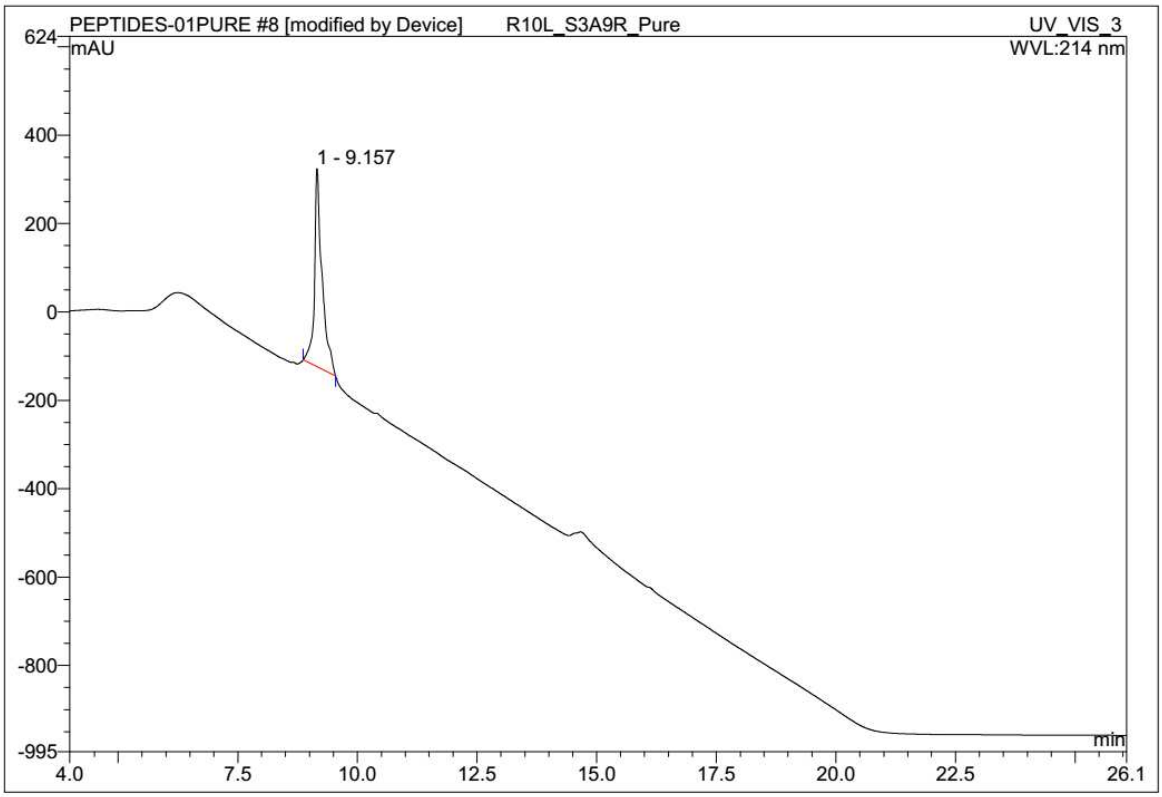

Figure S6.9: HPLC trace of HPLC purified teixobactin analogue **6.5** (gradient: 5-95% ACN in 25 min using A: 0.1% HCOOH in water, B: ACN)

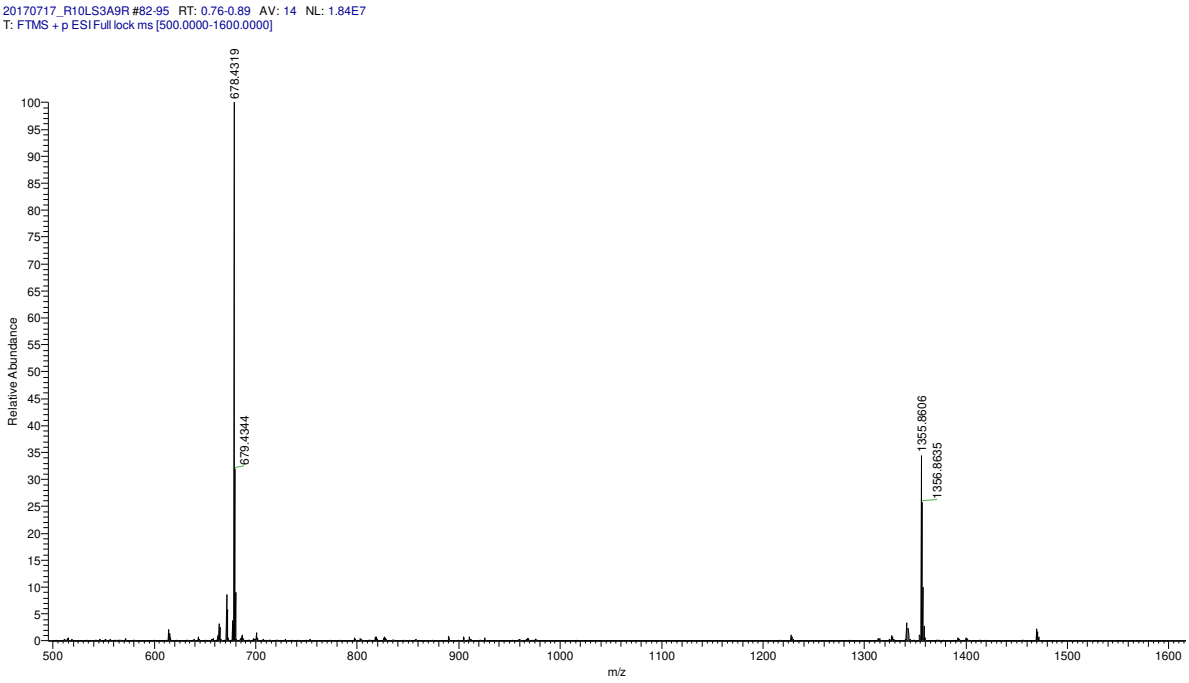

Figure S6.10: HRMS of HPLC purified teixobactin analogue **6.5**. Mass calcd. for $C_{64}H_{111}N_{18}O_{14}$ = 1355.8527, found M + H^+ = 1355.8606, M/2 + H^+ = 678.4319.

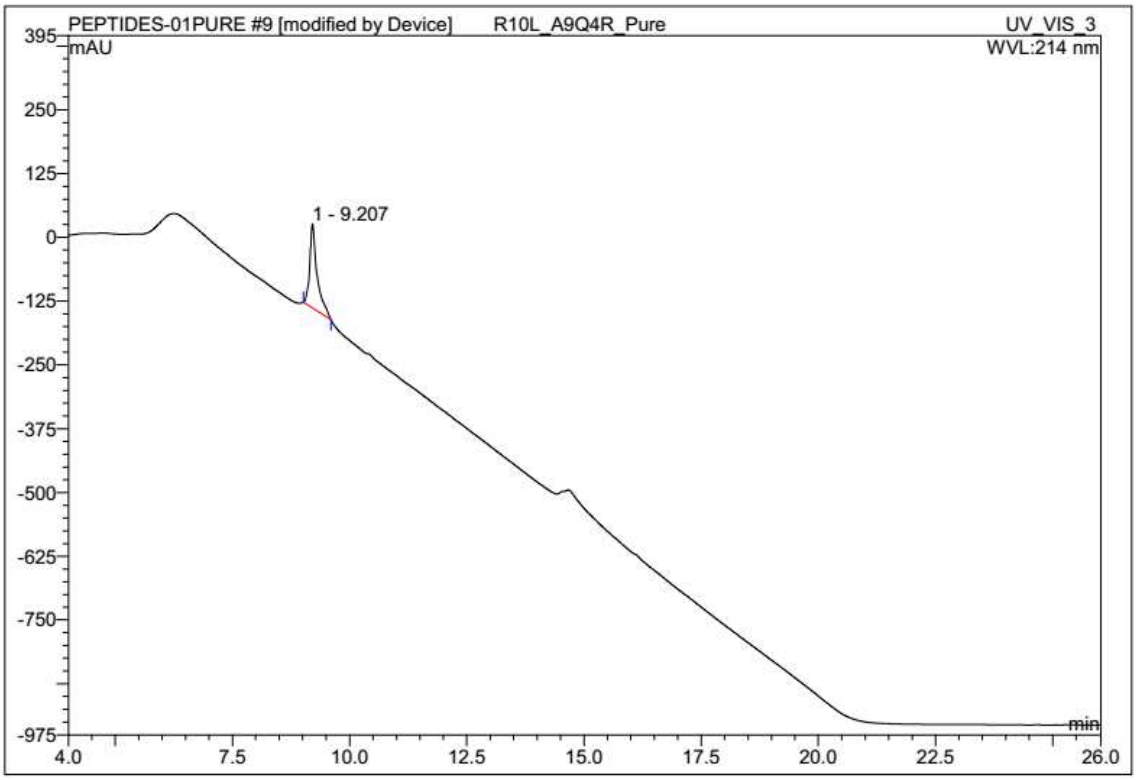

Figure S6.11: HPLC trace of HPLC purified teixobactin analogue **6.6** (gradient: 5-95% ACN in 25 min using A: 0.1% HCOOH in water, B: ACN)

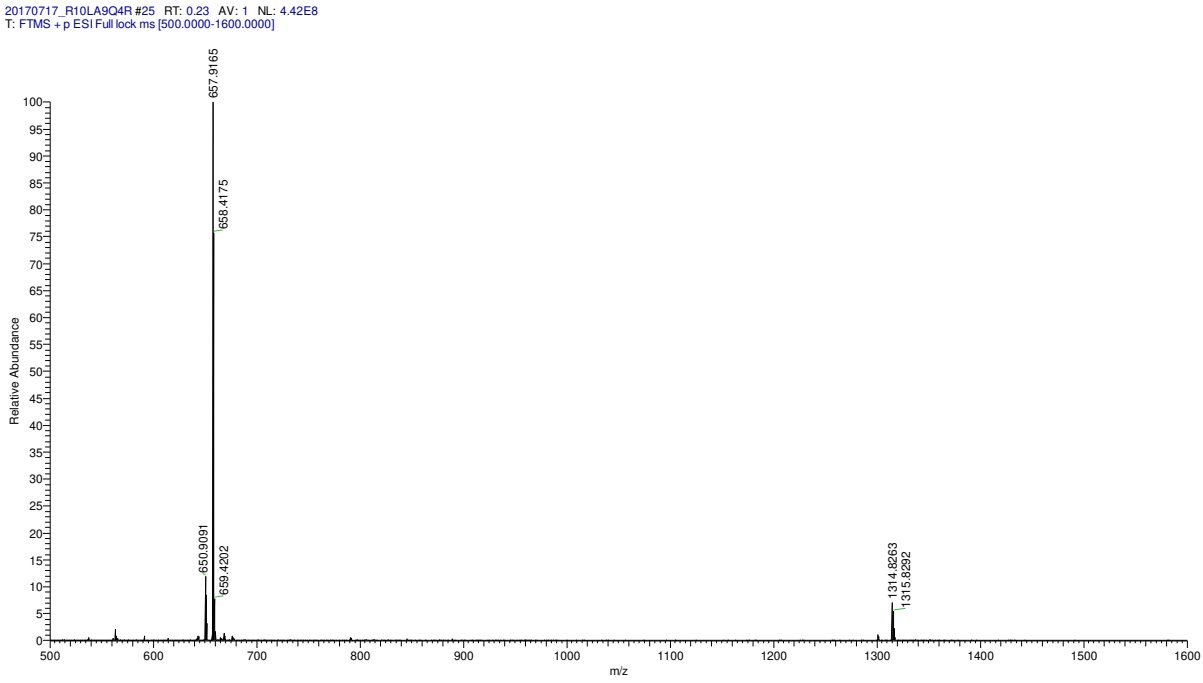

Figure S6.12: HRMS of HPLC purified teixobactin analogue **6.6**. Mass calcd. for $C_{62}H_{108}N_{17}O_{14}$ = 1314.8262, found M + H^+ = 1314.8263, M/2 + H^+ = 657.9165.

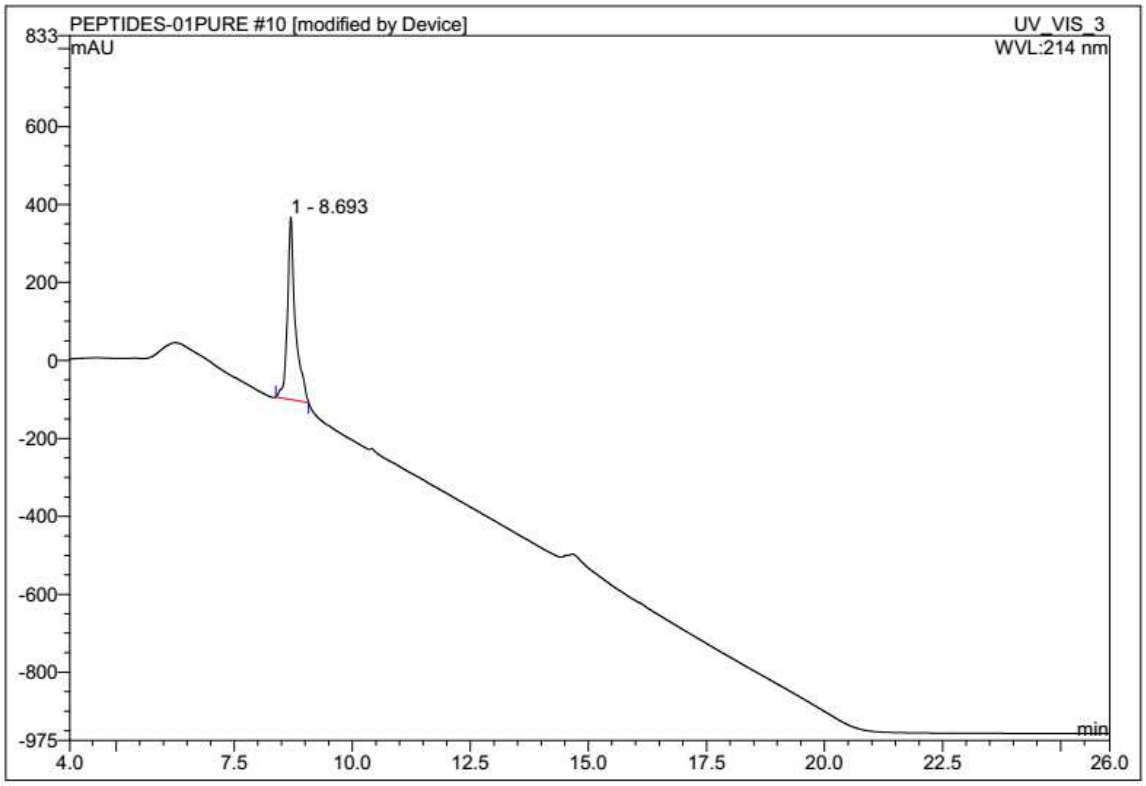

Figure S6.13: HPLC trace of HPLC purified teixobactin analogue **6.7** (gradient: 5-95% ACN in 25 min using A: 0.1% HCOOH in water, B: ACN)

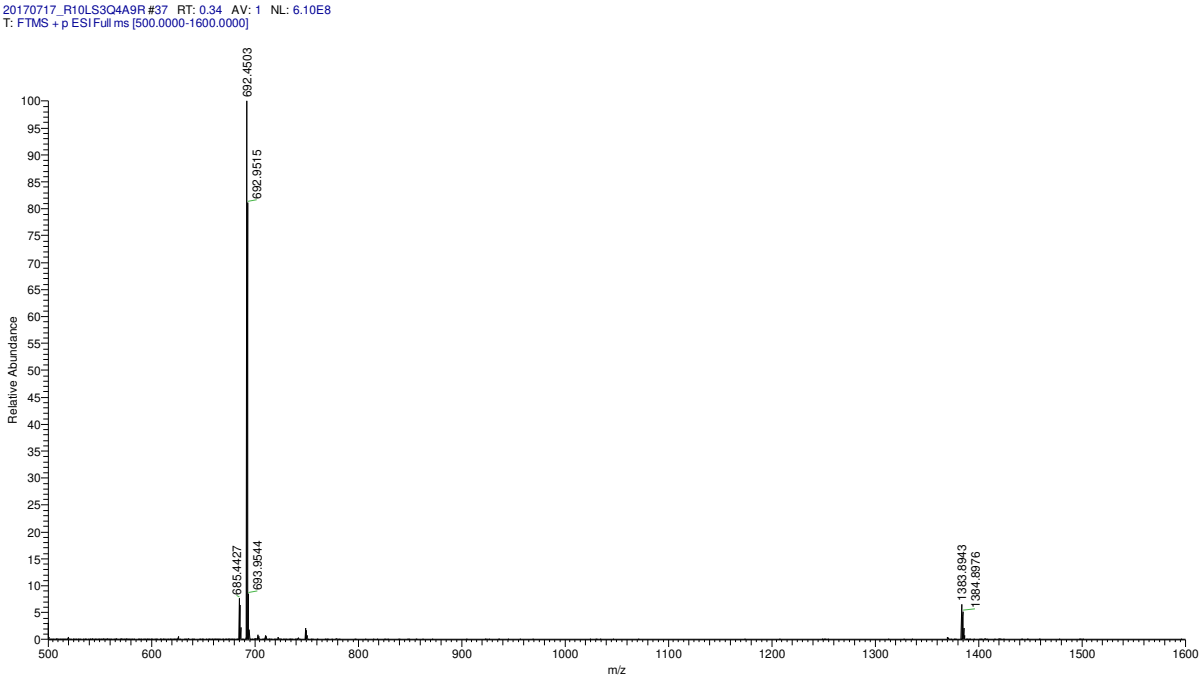

Figure S6.14: HRMS of HPLC purified teixobactin analogue **6.7**. Mass calcd. For $C_{65}H_{115}N_{20}O_{13}$ = 1383.8952, found M + H^+ = 1383.8943, M/2 + H^+ = 692.4503.

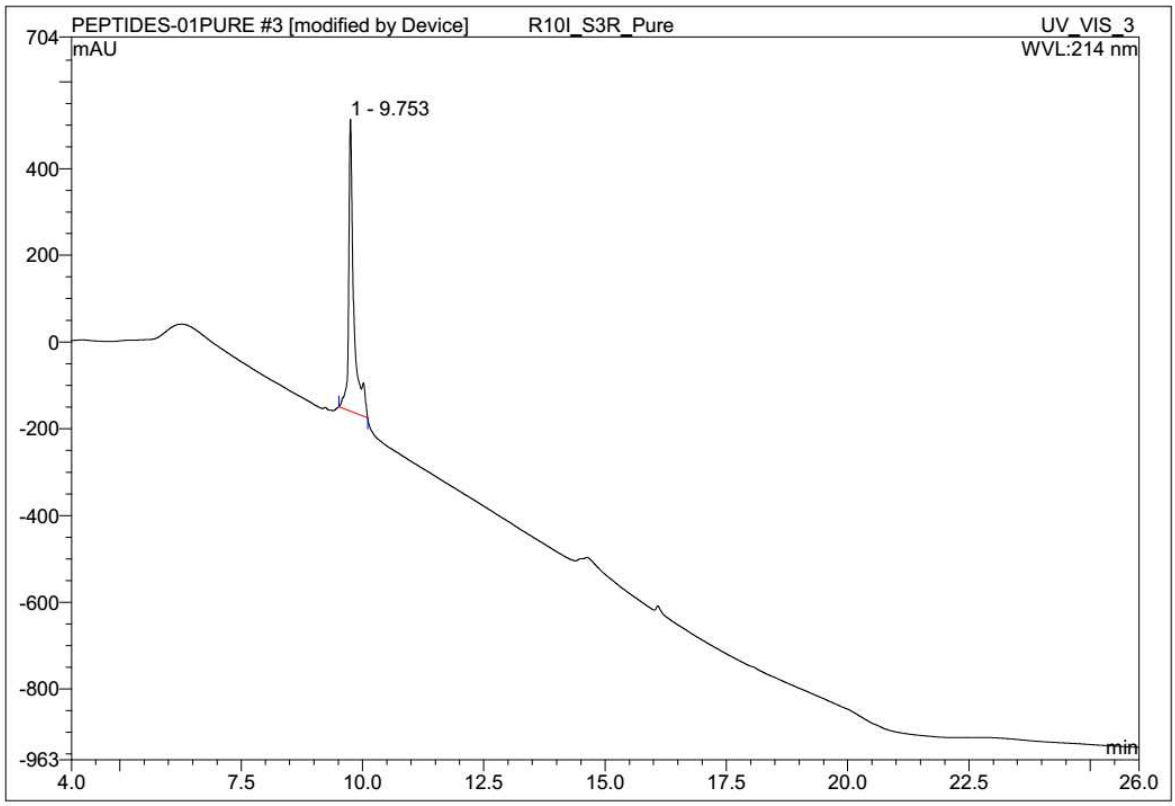

Figure S6.15: HPLC trace of HPLC purified teixobactin analogue **6.8** (gradient: 5-95% ACN in 25 min using A: 0.1% HCOOH in water, B: ACN)

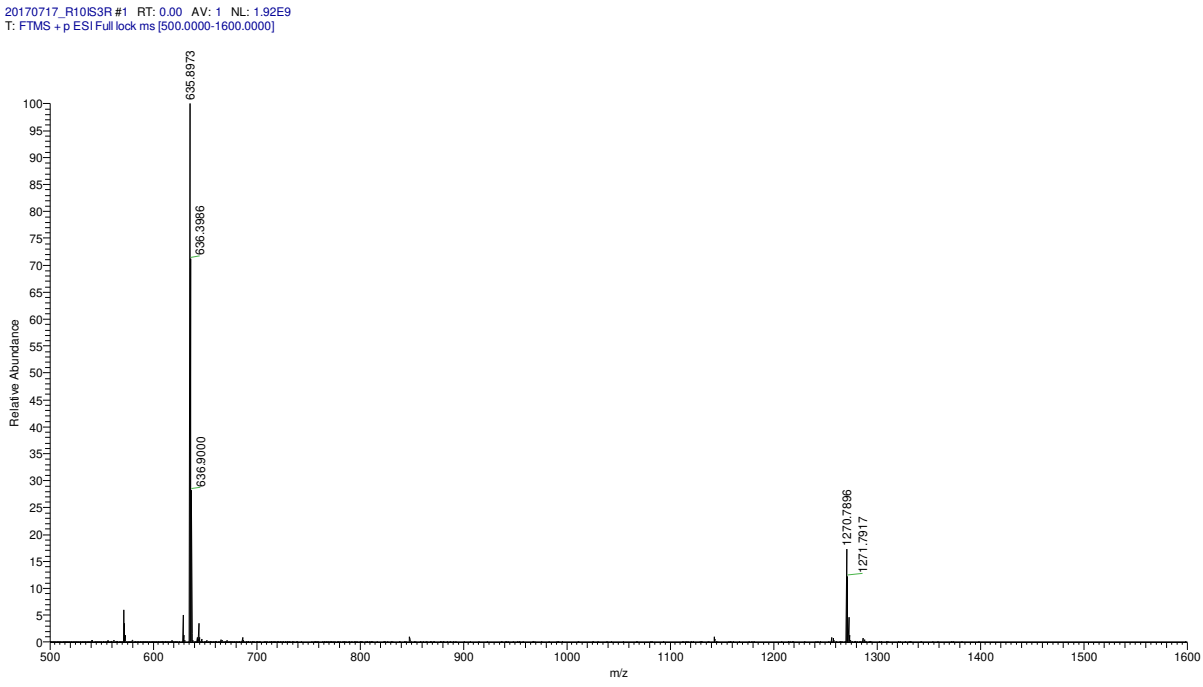

Figure S6.16: HRMS of HPLC purified teixobactin analogue **6.8**. Mass calcd. For $C_{61}H_{104}N_{15}O_{14}$ = 1270.7887, found M + H^+ = 1270.7896, M/2 + H^+ = 635.8973.

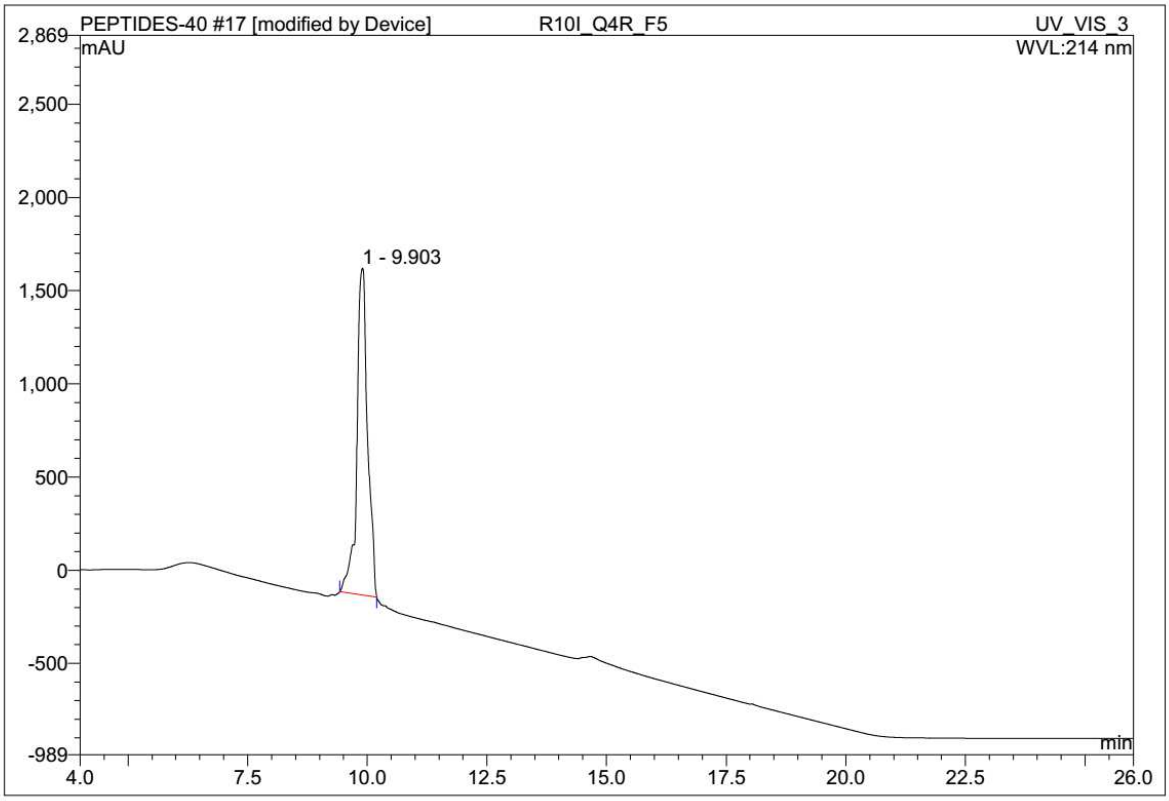

Figure S6.17: HPLC trace of HPLC purified teixobactin analogue **6.9** (gradient: 5-95% ACN in 25 min using A: 0.1% HCOOH in water, B: ACN)

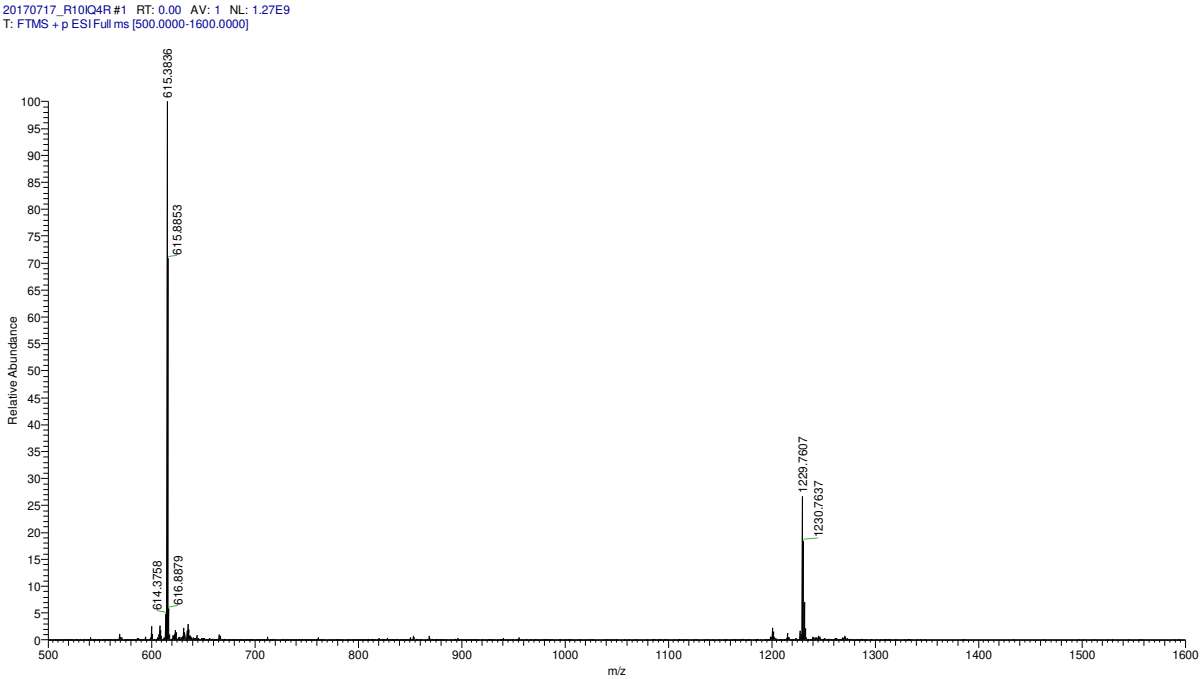

Figure S6.18: HRMS of HPLC purified teixobactin analogue **6.9**. Mass calcd. for $C_{59}H_{101}N_{14}O_{14}$ = 1229.7622, found M + H^+ = 1229.7607, M/2 + H^+ = 615.3836.

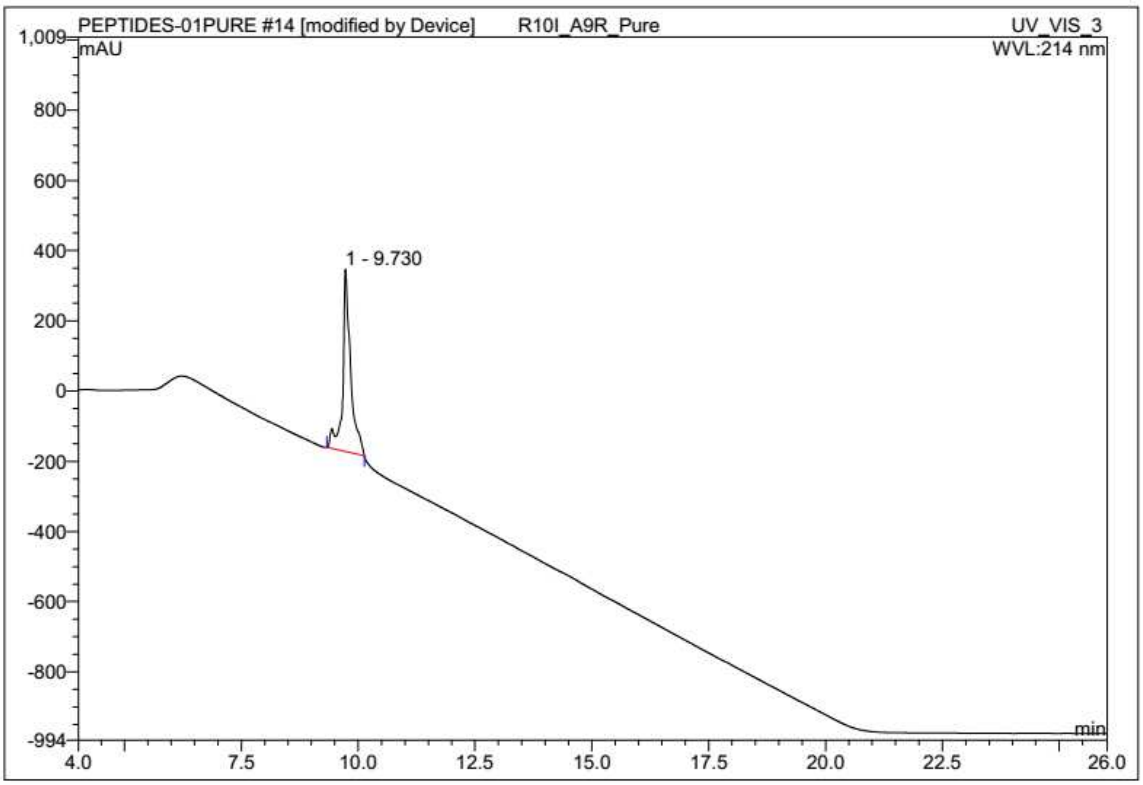

Figure S6.19: HPLC trace of HPLC purified teixobactin analogue **6.10** (gradient: 5-95% ACN in 25 min using A: 0.1% HCOOH in water, B: ACN)

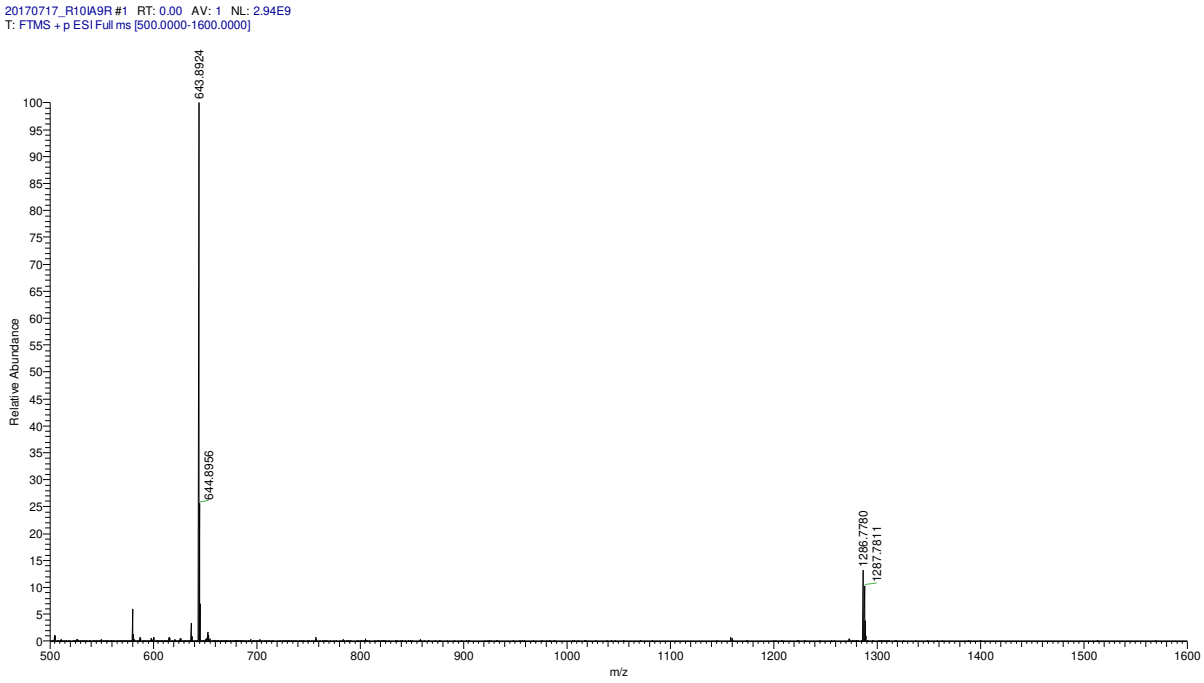

Figure S6.20: HRMS of HPLC purified teixobactin analogue **6.10**. Mass calcd. For $C_{61}H_{104}N_{15}O_{15}$ = 1286.7836, found M + H^+ = 1286.7780, M/2 + H^+ = 643.8924.

V. NMR analysis

All NMR was carried out in DMSO-d_6 at 27°C on a Bruker Avance III HD 500 MHz spectrometer equipped with a room-temperature broadband probe. The following spectra were utilised in the assignment of 1 mM solution of the teixobactin analogue **6.2**: ^{1}H (128k points, 16 scans); ^{13}C{1H} (64k points, 1024 scans); ^{1}H- ^{13}C HSQC (2k and 256 points in the direct and indirect dimensions, 4 scans.

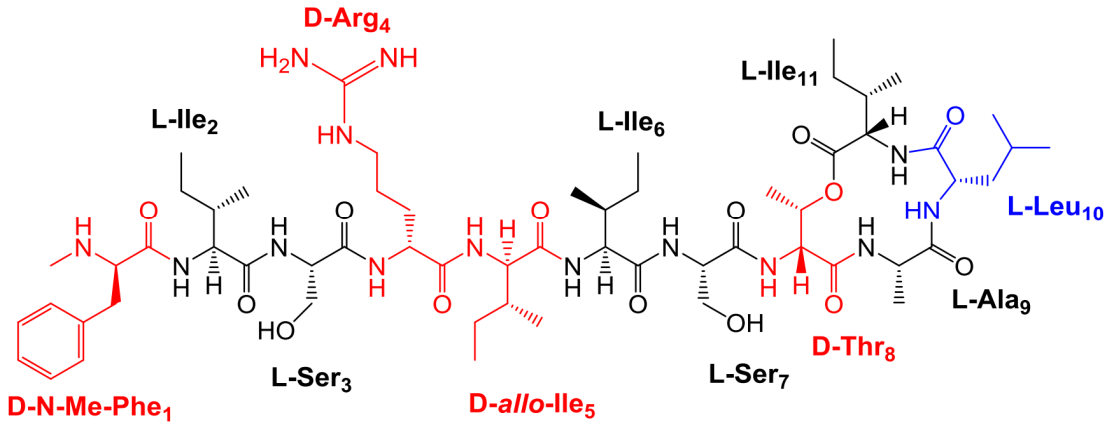

D-Arg$_4$-Leu$_{10}$-Teixobactin 6.2

	H	Hα	Cα	
1 Nm-Phe		3.272	68.12	H_3: 2.170 H_b: 2.795,2.694 H_{d*}: 7.186 H_{e*}: 7.239 H_z: 7.171 C_3: 37.43 C_b: 42.27 C_{d*}: 132.27 C_{e*}: 131.13 C_z: 129.19
2 Ile	7.945	4.193	59.70	H_b: 1.676 H_{g1}: 0.919,1.262 H_{g2*}: 0.746 H_{d1*}: 0.742 C_b: 39.43 C_{g1}: 27.31 C_{g2}: 18.39 C_{d1}: 14.01
3 Ser	7.962	4.323	58.23	H_b: 3.609,3.543 H_g: 4.991 C_b: 64.90
4 Arg	7.923	4.355	32.15	H_b: 1.710,1.494 H_g: 1.476,1.476 H_d: 3.075 H_e: 7.537 C_b: 27.90 C_d: 43.59
5 Ile	7.707	4.391	58.96	H_b: 1.785 H_{g1}: 1.076,1.302 H_{g2*}: 0.781 H_{d1*}: 0.779 C_b: 40.06 C_{g1}: 28.89 C_{g2}: 17.41 C_{d1}: 13.79
6 Ile	7.956	4.264	59.57	H_b: 1.782 H_{g1}: 1.109,1.413 H_{g2*}: 0.831 H_{d1*}: 0.831 C_b: 39.36 C_{g1}: 27.46 C_{g2}: 18.47
7 Ser	9.040	4.376	58.96	H_b: 3.687,3.770 C_b: 64.99
8 Thr	8.546	4.634		H_b: 5.367 H_{g2*}: 1.104 C_b: 73.43 C_{g2}: 18.77
9 Ala	8.151	3.922	54.89	H_{b*}: 1.287 C_b: 20.12
10 Leu	7.908	4.364	55.27	H_b: 1.534,1.534 H_g: 1.535 H_{d*}: 0.881,0.906 C_b: 44.18 C_g: 27.67 C_d: 24.80,25.69
11 Ile	8.111	4.028	60.09	H_b: 1.678 H_{g1}: 1.419,1.098 H_{g2*}: 0.809 H_{d1*}: 0.807 C_b: 39.43 C_{g1}: 27.46 C_{g2}: 18.36

Table S6.2: NMR Assignments of teixobactin analogue **6.2**.

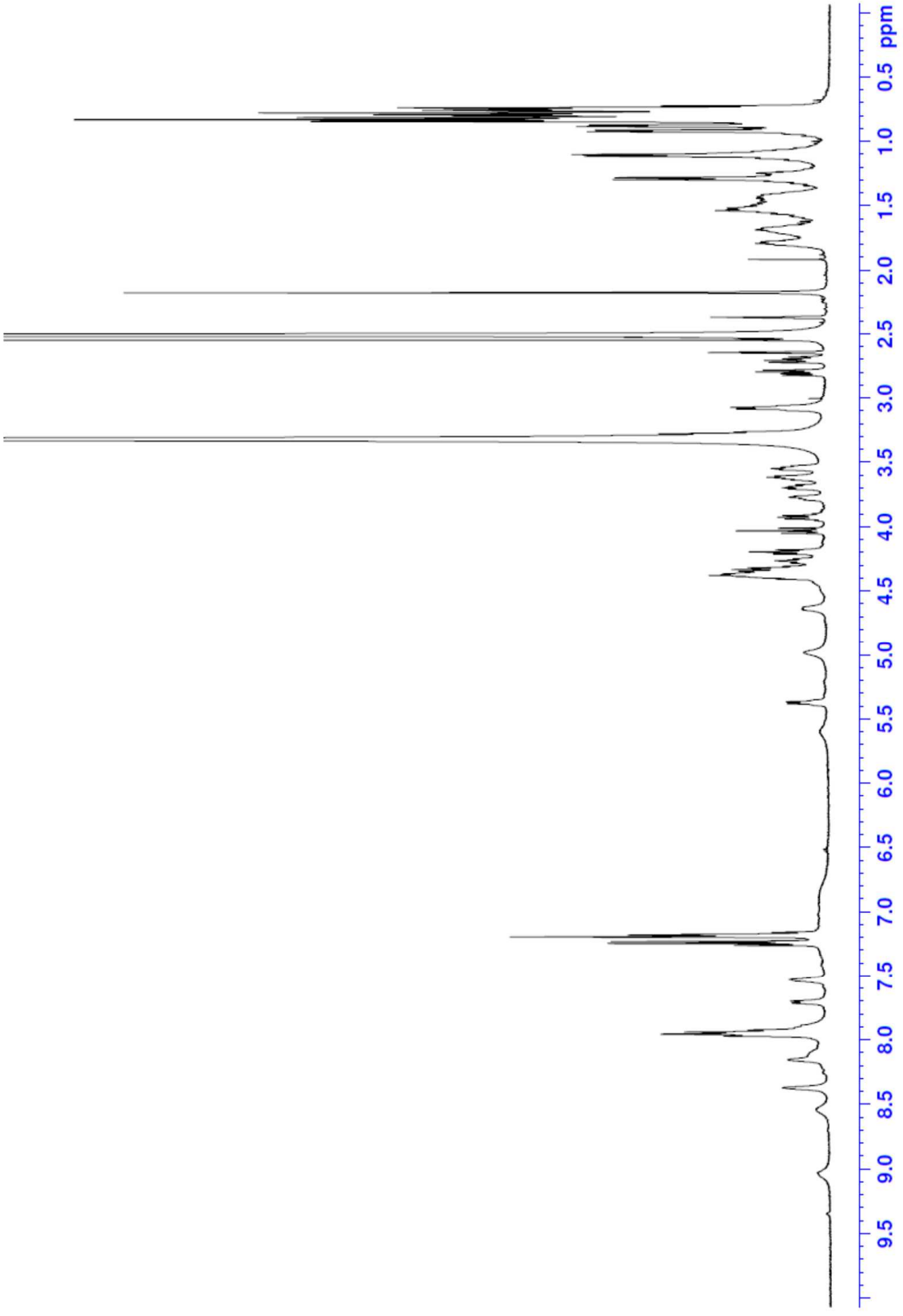

Figure S6.21: ^{1}H NMR Spectrum of teixobactin analogue **6.2**.

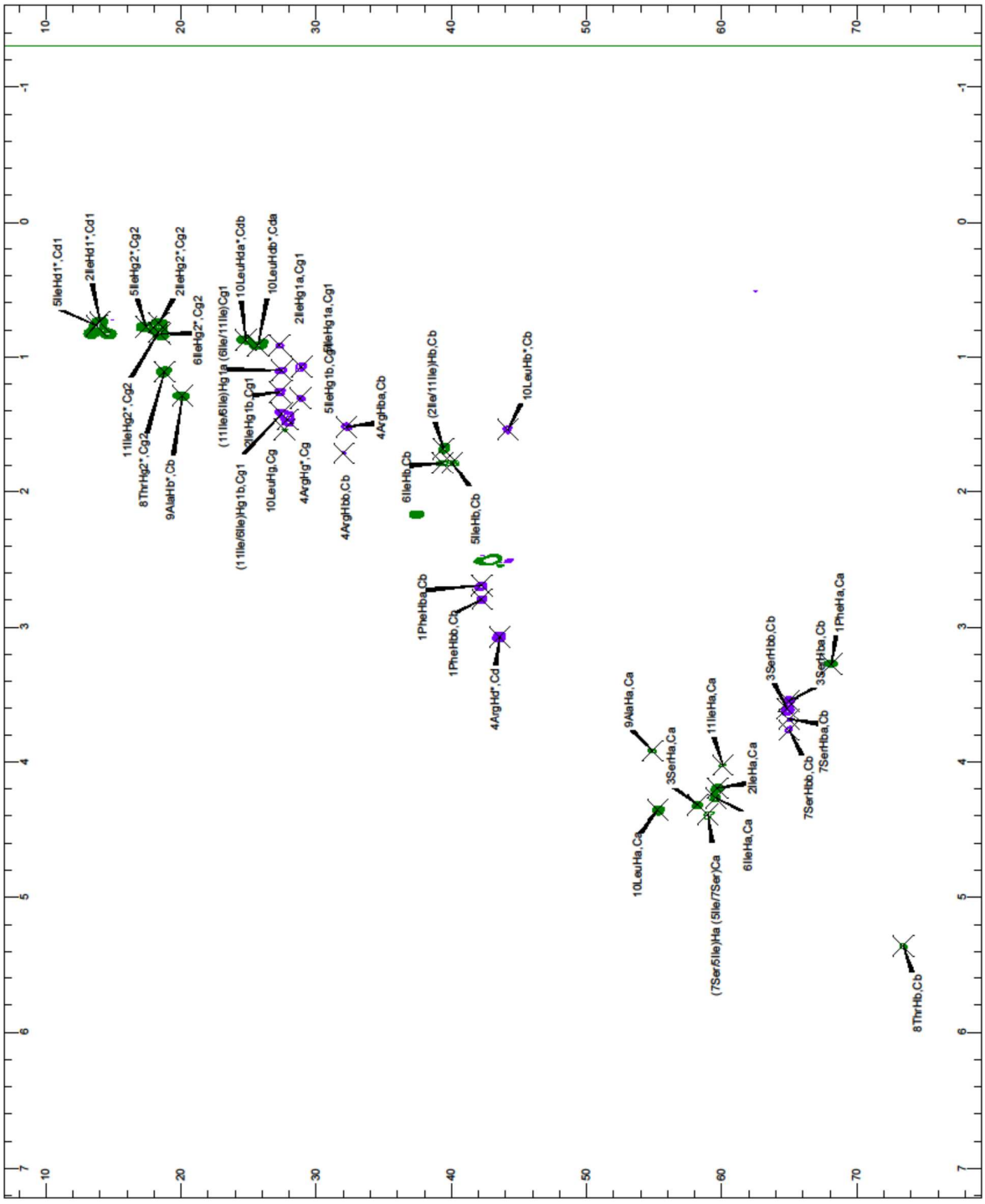

Figure S6.22: ^{1}H-^{13}C HSQC spectrum of teixobactin analogues **6.2**, showing assignment.

VI. MIC & MBC testing

For MRSA ATCC 33591: For MIC assays all peptides were dissolved in DMSO containing 0.002% polysorbate 80. MRSA ATCC 33591 was grown in Mueller Hinton broth (Oxoid) in triplicate. All incubations were at 37°C. Dilutions were carried out in triplicate. 100 µl of autoclaved Mueller Hinton broth was added to wells 2-12 in a 96-well plate. 200 µl of the peptide was added to well one at a concentration of 256 µg/mL. 100µl of peptide in well one was taken up and pipetted into well two. The mixture was then mixed via pipetting before 100µl was taken up and pipetted into well three. This process was repeated up to well 11. Once peptide was added to well 11 100 µl was taken up and then discarded ensuring the well 12 had no peptide present. Thus, the concentrations (in µg/mL) were: 256, 128, 64, 32, 16, 8, 4, 2, 1, 0.5, 0.25 and no peptide present. Each well was then inoculated with 100µl of bacteria that had been diluted to an OD600nm of 0.1. This was repeated three times. The 96-well plates were then incubated at 37°C for 24 hours. The MIC was determined to be the lowest concentration at which there was no growth visible.

For all the compounds in which the MIC lower than 1 µg/ml for the initial test, the above procedure was repeated at an altered initial concentration of 64 µg/ml. Therefore, the new concentrations for MIC were: 64, 32, 16, 8, 4, 2, 1, 0.5, 0.25, 0.125, 0.0625 and no peptide present.

(Extended panel)

Bacterial cultures were grown overnight in Mueller-Hinton Agar (MHA) plates and adjusted to a final
concentration of $10^5 – 10^6$ CFU/ml. 100 µl of inoculum in Meuller-Hinton broth (MHB) was mixed with equal volume of peptides (dissolved in MHB) at 2x their concentration in a 96 well plate. In parallel experiments, MIC values were determined in the media containing polysorbate 80 (0.002%, v/v) to prevent non-specific adsorption of the peptides to plastic surfaces. The final peptides concentrations ranged from 0.0625 – 32 µg/ml (for lower range 0.031 – 16 µg/ml was used). Positive and negative controls contained 200 µl of inoculum without any peptide dissolved in broth, respectively. The 96 well plates were then incubated at 37 °C for 24 h. All the experiments were performed in two independent duplicates and the MIC was determined as the lowest concentration in which no visible growth was observed. Minimum bactericidal concentration (MBC) was determined by plating out the dilution representing the MIC and concentrations up to 16x MIC on MHA plates kept at 37 °C for 24 h. The lowest concentration in which no visible colonies could be detected was taken as the MBC.

Resistance studies: For single step resistance, 100µl *S. aureus* ATCC 29213 or MRSA ATCC 33591 at 10^{10} c.f.u./ml were plated onto MHB containing 20 x MIC of teixobactin analogues **6.2**. Agarose was used as a solidifying agent. After 24 h of incubation at 37º C, no resistant colonies were detected, giving the calculated frequency of resistance to teixobactin analogues **6.2** of $<10^{-10}$.

Strain ↓	Compd 6.1	Compd 6.2	Compd 6.3	Compd 6.4	Compd 6.5	Compd 6.6	Compd 6.7	Compd 6.8	Compd 6.9	Compd 6.10	Daptomycin 1.13
Staphylococcus saprophyticus ATCC BAA 750	<0.0625	<0.0625	<0.0625	<0.0625	<0.0625	<0.0625	<0.0625	<0.0625	<0.0625	<0.0625	0.125
Staphylococcus saprophyticus ATCC 15305	<0.0625	<0.0625	<0.0625	<0.0625	<0.0625	<0.0625	0.25	<0.0625	<0.0625	<0.0625	0.125
Staphylococcus saprophyticus ATCC 49453	<0.0625	<0.0625	<0.0625	<0.0625	<0.0625	<0.0625	<0.0625	<0.0625	<0.0625	<0.0625	0.125
Staphylococcus saprophyticus ATCC 49907	<0.0625	<0.0625	<0.0625	<0.0625	<0.0625	<0.0625	<0.0625	<0.0625	<0.0625	<0.0625	0.125
VRE 1001	0.25	0.5	0.5	1	0.5	1	2	1	0.5	1	2
VRE 1002	0.5	1	1	1	1	1	8	1	1	1	4
VRE 1004	<0.0625	0.25	0.25	0.5	0.5	1	4	1	0.5	1	1
VRE 1008	0.125	0.5	0.25	0.5	0.5	1	8	1	0.5	1	4
VRE ATCC 700802	0.5	0.5	0.5	2	1	1	4	1	0.25	1	0.25
VRE ATCC 29212	0.5	0.5	1	1	1	1	4	1	0.25	1	0.25
MRSA ATCC 700699	0.5	0.25	0.5	0.5	1	1	2	1	0.25	1	1
MRSA 42412	<0.0625	0.0313	<0.0625	0.25	0.25	1	2	0.125	<0.0625	0.125	0.5
MRSA 21455	0.03125	0.0313	0.25	0.5	1	1	2	0.25	0.03125	0.5	0.5
MRSA 1003	<0.0625	0.5	0.25	1	2	0.5	2	0.125	<0.0625	0.5	0.5
S. aureus 29213	0.25	<0.0625	0.5	0.25	1	1	1	0.5	0.0625	1	0.5
S. aureus 4299	0.125	-	0.25	0.25	0.5	0.5	1	0.125	<0.0625	1	0.5
S. epidermidis 12228	<0.0625	<0.0625	<0.0625	<0.0625	<0.0625	<0.0625	<0.0625	<0.0625	<0.0625	<0.0625	0.125
Bacillus Cereus ATCC 11788	<0.0625	0.5	0.25	1	1	1	1	0.125	<0.0625	0.5	0.25
Bacillus Subtilis ATCC 6633	<0.0625	0.125	<0.0625	<0.0625	<0.0625	<0.0625	<0.0625	<0.0625	<0.0625	0.125	0.125
P.aeruginosa ATCC 27853	-	>64	-	-	-	-	-	-	-	-	-

Table S6.3: MIC (in µg/mL) of the teixobactin analogues **6.1-6.10** and Daptomycin control against an extended panel of Gram-positive bacteria in the presence of polysorbate 80.

Peptides	Minimum Bactericidal Concentration (in µg/ml) against			
	***S. aureus* 29213**	***S. aureus* 4299**	**MRSA 700699**	**MRSA 21455**
6.1	>2 (8×)	1 (>8×)	2 (4×)	0.0625 (2×)
6.2	0.125 (1×)	≤0.0625 (1×)	2 (4×)	≤0.0625 (1×)
6.3	>4 (8×)	2 (8)	>4 (>8×)	>2 (>8×)
6.4	>2 (>8×)	>2 (>8×)	>4 (>8×)	1 (2×)
6.5	2 (2×)	4 (8×)	2 (2×)	1 (2×)
6.6	4 (4×)	2 (4×)	8 (8×)	2 (2×)
6.7	2 (2×)	1 (1×)	>8 (>4×)	2 (1×)
6.8	4 (8×)	1 (8×)	2 (2×)	0.5 (2×)
6.9	>0.5 (>8×)	>0.5 (>8×)	0.5 (2×)	0.25 (8×)
6.10	8 (8×)	8 (8×)	1 (1×)	2 (4×)

Table S6.4: Minimum bactericidal concentrations of teixobactin peptides against *S. aureus* and MRSA strains MBC (in µg/mL) of the teixobactin analogues **6.1-6.10**.

VII. Time-dependent killing of bacteria by teixobactin analogue 6.2

Time-kill kinetics against *S. aureus* ATCC 29213 was carried out in MHB. Cultures were grown overnight in MHA plates and adjusted to a final inoculum of 10^5 – 10^6 CFU/ml in MHB (containing 0.002% v/v, polysorbate 80) with teixobactin analogue 2 maintained at a final concentration of 0.5 and 1 µg/ml. The tubes were then incubated at 37 °C. 100 µl of cell suspension was withdrawn at various time points (0, 2, 4, 8h), serially diluted (10^1-10^5 fold dilutions) and plated onto a MHA plates and incubated for 24 h at 37 °C. Colonies were then enumerated using a haemocytometer. Colony counting too numerous to count (>300 colonies) was taken as 10^{10} CFU. Average values from two independent experiments are reported.

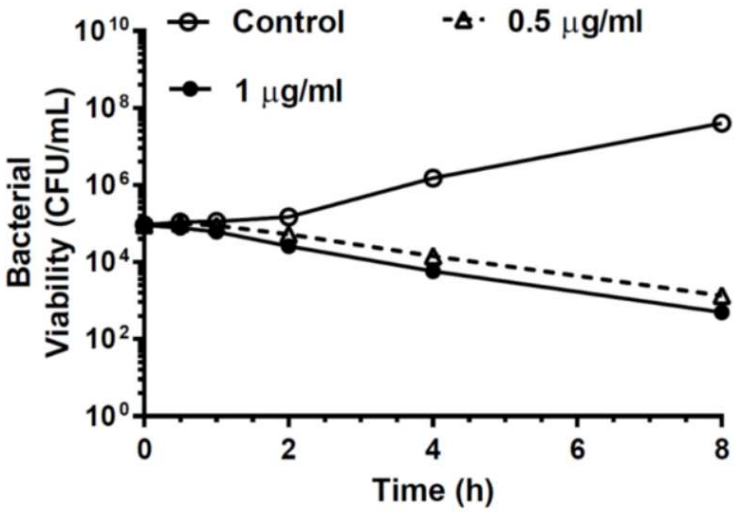

Figure S6.23: Time-kill kinetics of teixobactin analogue **6.2** against *S. aureus* ATCC 29213. The concentration of teixobactin analogue **6.2** was maintained at 0.5 and 1 µg/ml.

VIII. Cytocompatibility of 6.2 for mammalian cells

Cytocompatibility assessment of **6.2** for A549 lung adenocarcinoma cell line and primary human dermal fibroblasts (hDF) were determined by MTS ((3-(4,5-dimethylthiazol-2-yl)-5-(3-carboxymethoxyphenyl)-2-(4-sulfophenyl)-2H-tetrazolium)) assay and high content analysis (HCA). Both A549 or hDF cells (2 X 10^3 cells/well) seeded on 96-well plates were treated with various concentrations of peptide (15.625 – 250 mg/ml) and incubated for 24 h at 37 °C and 5% CO_2. The stock solution of 2 (500µg/ml) was prepared fresh by directly dissolving 2 in cell culture medium (Dulbecco's Modified Eagle Medium, Gibco®) and used. The metabolic activity was determined using CellTier 96® Aqueous One solution cell proliferation assay kit according to the manufacturer's instruction (Promega Corporation, Madison, WI). The relative cell viability was determined from UV readings of untreated control cells. The antineoplastic agent, nocodazole (5 µg/ml dissolved in DMSO) served as the negative control. Data represents mean ± standard error of the mean of three

independent triplicate experiments. For HCA, cells treated with peptide **6.2** were washed with PBS and fixed in 3% paraformaldehyde. A549/hDF cells were fluorescently stained with Alex Fluor 488 anti-α-tubulin (green), Hoechst 33342 (blue) and Rhodamine-Phalloidin (red) to visualize cellular morphologies and imaged by IN Cell Analyzer 2200 automated microscope.

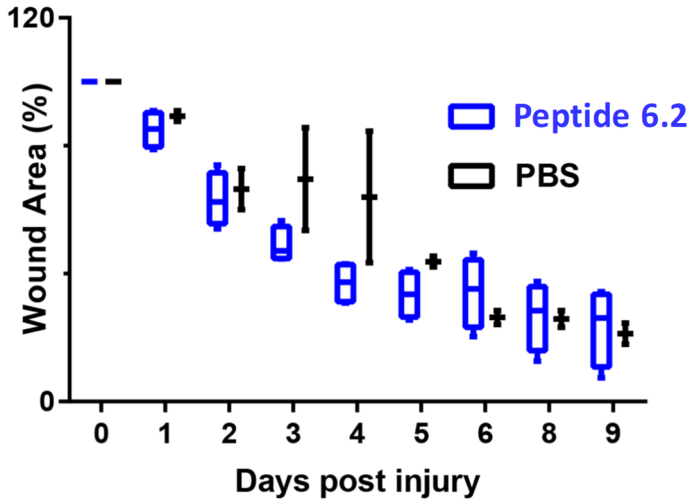

Figure S6.24: Quantitative determination of corneal wound healing after topical instillation of PBS or peptide **6.2** after corneal injury in rabbits. The re-establishment of corneal epithelium after injury confirm that peptide **6.2** does not interfere with regular wound healing process, thus establishing its safety for topical applications.

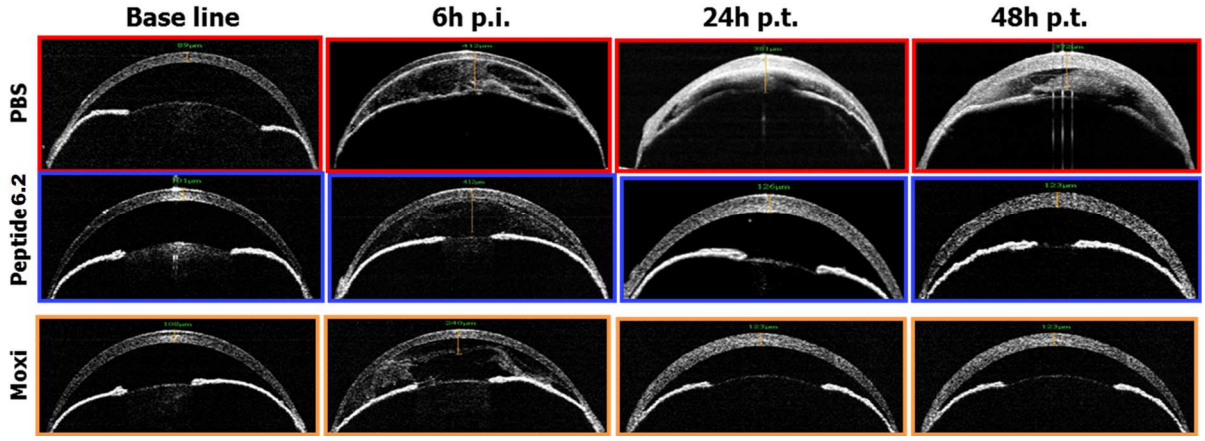

Figure S6.25: Representative AS-OCT images showing the changes in corneal thickness before and after infections or Treatment with various groups. Note the significant presence of corneal edema and hyper reflective materials throughout the cornea in the case of PBS treated groups but were minimized in peptide **6.2** or moxifloxacin treated groups.

IX. The *in vivo* toxicity in a rabbit model of corneal epithelium-injured

All the animals used in this study were treated in accordance to the tenets of the Association for Research in Vision and Ophthalmology (ARVO) statement, and the protocol was approved by SingHealth Institutional Animal Care and Use Committee (IACUC) (AALAC accredited; protocol number 2012/SHS/775 for wound healing). Six New Zealand White rabbits, aged 8 months old and

body weight 3-3.5 kg were used for the study. Prior to the creation of corneal wound, all the rabbit eyes were examined by slit-lamp photography to ensure absence of any ocular defects. The rabbits were anesthetized and a 7.5-mm-diameter region of the corneal surface was de-epithelialized with a sterile mini blade (BD Beaver, MA, USA) and divided into two groups. Rabbits received a 50 µl topical instillation of peptide **6.2** (0.3% w/v in PBS) (4 eyes) or PBS (2 eyes) 4 times/day for ten days. The corneal epithelial wound healing was visualized using 2% w/v fluorescein sodium (Bausch & Lomb) staining. The progression of wound healing was examined by illumination with cobalt blue light with a digital camera. The area of corneal abrassion was quantified using Image J software.

X. *In vivo* efficacy of peptide in a mice model of infectious keratitis

We have used eighteen pathogen free 6-8 weeks old Female mice (wild type C57BL/6). As per the Sing- Health Institutional Animal Care and Use Committee (IACUC) guidelines, all the animals were handled, and for the animal experimentation, the guidelines of Association for Research in Vision and Ophthalmology (ARVO) were followed. The designated groups, with six mice each were categorized as *group I* treated with PBS, *group II* treated with 0.3% of moxifloxacin Hydrochloride, *group III* treated with 0.3% of peptide **6.2**. *Staphylococcus aureus* ATCC 29213 strains were grown overnight in Tryptic Soy Agar (TSA) plates at 35°C. Isolated single bacterial colonies were identified and suspended in sterile PBS at a final inoculum concentration of 3 x 10^6 CFU/mL. Slit-lamp biomicroscopy (FS-3V Zoom Photo Slit Lamp, Nikon, Tokyo, Japan) and AS-OCT (RTvue, Optovue, Fremont, CA) were carried out on the days before bacterial inoculation (Baseline), and 6 h post infection (p.i.), 24 h and 48 post treatment (p.t.).

Prior to infection all the mice eyes were examined by slit-lamp photography and AS-OCT to make sure that there was no corneal aberration, such as vascularization or any other ocular defects. Mice were anesthetized by an intraperitoneal injection of xylazine (10 mg/kg, Troy Laboratories, Smithfield, Australia) and ketamine (80 mg/kg, Ketamine, Parnell Laboratories, Australia) under the dissecting microscope (Zeiss, Stemi-2000C). The mice corneal epithelium were then scratched and removed using a sterile Beaver 6400 Mini-Blade to create a superficial wound without damaging the stroma and one drop of 1-5% lignocaine hydrochloride were used as topical anesthesia instilled before corneal wounding and then the cornea was irrigated with sterile saline to wash away any debris and residual topical anesthetic agent. Immediately following this procedure, 15µL of bacterial suspension containing 3 x 10^6 CFU/mL of *Staphylococcus aureus* ATCC 29213 was applied topically on the corneal surface. After 6 h post infection, mice were treated with peptide **6.2**, Moxifloxacin and PBS topically (15µL).

The dosage regimen are two times on Day 1 (2:30PM; 5:30PM), four times (8AM; 11AM; 2PM; 5PM) on day 2 and two times on day 3. The eyes were examined daily by slit lamp and OCT, sacrificed at 48 hr post-treatment (day 3) for evaluation of bacteria quantification analysis.

After treatment with various groups, the mice corneas were dissected and homogenized in sterile PBS by using Pellet pestles cordless motor (Z359971, Sigma) with sterile plastic pestles followed by fine homogenization with bead beating using sterile glass beads (2 mm). The homogenates were vortexed and 10-fold serial dilutions were prepared using sterile PBS to give 10^2 to 10^4 dilutions. A 0.1 mL of each suspension was inoculated onto Tryptic Soy Agar (TSA) plates in duplicate and incubated at 35°C for 48 h. The numbers of colonies were enumerated, and the results were expressed as the $\log_{10}$ number of CFU/cornea.